Investigating group III metabotropic glutamate receptors as novel therapeutic targets in Parkinson's disease and Levodopa-induced dyskinesia

Finlay, Clare Judith

Awarding institution:
King's College London

Investigating group III metabotropic glutamate receptors as novel therapeutic targets in Parkinson's disease and Levodopa-induced dyskinesia

Clare Judith Finlay

Submitted for the degree of

Doctor of Philosophy

Wolfson Centre for Age-Related Disease

King's College London

Abstract

The loss of nigrostriatal dopamine neurones in Parkinson's disease causes characteristic motor symptoms resulting from signalling alterations in the basal ganglia. An important consequence of this is increased firing of the glutamatergic subthalamic nucleus (STN). Since the STN innervates dopaminergic neurones in the substantia nigra pars compacta (SNc), any increased firing could perpetuate degeneration of these cells by promoting excitotoxicity. Activation of group III mGlu receptors reportedly reduces glutamatergic transmission at the subthalamonigral synapse suggesting activation of these receptors might provide neuroprotection in PD.

The results reported in this thesis support site-directed targeting of the group III receptor subtype $mGlu_4$ in the SNc as a neuroprotective approach in the 6-hydroxydopamine lesioned rat; however while one $mGlu_4$ positive allosteric modulator tested was successful another was not, highlighting several future considerations for the use of these agents. Unexpectedly, activation of group III and $mGlu_4$ receptors *increased*, rather than reduced glutamate release in the intact SNc. However, this effect was lost in the 6-hydroxydopamine lesioned SNc, reassuring us that in the parkinsonian state activation of these receptors should not exacerbate excitotoxicity. Further experiments are required to define the mechanisms by which the $mGlu_4$-mediated protection is afforded. Additional studies are also required to shed light on why these protective effects were lost in a subsequent study following systemic injection of an $mGlu_4$ PAM (LuAF21934); might this relate to severity of lesion, or a detrimental effect of activating $mGlu_4$ receptors outside the SNc, for example? The lack of protective efficacy subsequently found with a systemically administered $mGlu_7$ agonist (AMN082) against a severe 6-hydroxydopamine lesion also points towards partial lesion models for future testing.

Finally, since other antiglutamatergic strategies have proven successful, we investigated $mGlu_4$ activation as a means to inhibit L-DOPA-induced dyskinesia expression or development in rodents. While this approach was ineffective at reversing established dyskinesia there was a hint that it might be efficacious at delaying the onset of this complication that will be worth investigating further.

In conclusion, targeting the $mGlu_4$ receptor has shown some beneficial effects in relation to Parkinson's disease but much remains to be discovered about the actions of these agents both within and outside of the basal ganglia before any clear potential is revealed.

Acknowledgements

The completion of this thesis has been possible thanks to the support and dedication of my supervisors Dr. Susan Duty and Dr. Mike O'Neill. With your expert help and guidance I have hopefully come out of the other end of these past four years a more rounded, critical and skilled scientist! I can't thank you enough for believing in me and supporting me both in the lab and in pursuit of my future endeavours.

I'd also like to thank the many other lab members, both at King's and at Lilly, for their help and for providing some much-needed laughter, tea and cake along the way. At the King's end: Matt and Eugene – cheers for settling me in and showing me the ropes, not to mention optimising all the protocols! To Ed, our most recent addition – thanks for the weekend drug blinding, wrapping up rat tails in plasters and most importantly Vitamin T. And lastly to our honorary laboratory adviser Martin – I appreciate you listening patiently to all my many questions and misfortunes and offering advice. At the Lilly end: cheers to Tracey and Mike for giving me the opportunity to get into all this in the first place during my extramural year! Many thanks are also due to Jane and Sandra for their tireless practical help when the world of bioanalysis turned against me – and to Ellen, Claire, Mark, Kayta and Marie for keeping me sane with tea and cake when it did.

In addition to this I would like to thank our collaborators at Lundbeck and within King's, particularly Dario, Christoffer, and Sarah for their assistance with the design and implementation of the dyskinesia studies and to Anthony Vernon for throwing an enthusiastic amount of time and funding into an ongoing MRI project! Last but not least, I'd like to thank Atsuko for going above and beyond to assist me with dopamine HPLC to ensure I got my final results in time for my write-up.

To my office buddies without whose chatter I might have finished in 2 years (not really!). Talisia, Nisha, Chancie and Clive – I'll miss spinning round on a Friday afternoon to have a gossip with you all. Good luck Talisia in your upcoming viva – eek, can't believe we made it!

I would like to thank my family: my parents Lydia and John who have always supported me in whatever I have set my mind to, and my sisters Rebecca and Nicola for their encouragement and wine when I needed reminding that it would all be OK in the end! And finally I would like to give a special mention to Chris. You've stuck with me through the busiest and most stressful times I've yet had to contend with and kept me smiling all the way – I love you so much and I look forward to finally spending weekends with you again!

List of Abbreviations

5-HIAA – 5-hydroxyindoleacetic acid

5-HT – 5-hydroxytryptamine

6-OHDA – 6-hydroxydopamine

AADC – amino acid decarboxylase

AIM(s) – abnormal involuntary movement(s)

AMPA – α-Amino-3-hydroxy-5-methyl-4-isoxazolepropionic acid, activates a subset of ionotropic glutamate receptors

AP – anteroposterior (front to back [of the brain])

ATP – adenosine triphosphate

BBB – blood-brain barrier

BG – basal ganglia

COMT – catechol-*O*-methyl transferase

CPu – caudate-putamen (dorsal striatum in rodents)

DA – dopamine

DBS – deep brain stimulation

DOPAC – 3,4-dihydroxyphenylacetic acid

DV – dorsoventral (top to bottom [of the brain])

EC_{50} – half the maximal effective concentration (measure of agonist/PAM potency)

EPN – entopeduncular nucleus (rodent equivalent of the GPi)

EPSC/EPSP – excitatory post-synaptic current/potential

GPCR – G-protein coupled receptor

GPe – globus pallidus externus

GPi – globus pallidus internus

GRK – G-protein receptor kinase

HVA – homovanillic acid

IC_{50} – half the maximal inhibitory concentration (measure of antagonist/NAM potency)

i.c. – intracerebral

i.c.v. – intracerebroventricular

i.p. – intraperitoneal

IPSC/IPSP – inhibitory post-synaptic current/potential

KA – kainic acid, activates a subset of ionotropic glutamate receptors

LB – Lewy bodies

L-DOPA/Levodopa – L-3,4-dihydroxyphenylalanine

LID – Levodopa-induced dyskinesia

MAO-A – monoamine oxidase A

MAO-B – monoamine oxidase B

MFB – medial forebrain bundle

$mGlu_x$ – metabotropic glutamate receptor (x)

ML – mediolateral (middle to edge [of the brain])

MT – medial terminal nucleus

NAc – nucleus accumbens

NADH – nicotinamide adenine dinucleotide

NAM – negative allosteric modulator

NMDA – N-methyl-D-aspartate, activates a subset of ionotropic glutamate receptors

PAM – positive allosteric modulator

PD – Parkinson's disease

PPN – pedunculopontine nucleus

p.o. – per os (oral dose)

RNS – reactive nitrogen species

ROS – reactive oxygen species

s.c. – subcutaneous

SNc – substantia nigra pars compacta

SNr – substantia nigra pars reticulata

STN – subthalamic nucleus

TH – tyrosine hydroxylase

VFD – venus flytrap domain

VL/VM thalamus – ventral lateral and ventral medial thalamic nuclei

VMAT-2 – vesicular monoamine transporter 2

VTA – ventral tegmental area

Drug abbreviations

AMPA receptor ligands

CNQX	7-nitro-2,3-dioxo-1,4- dihydroquinoxaline-6-carbonitrile
CX516	6-(piperidin-1-ylcarbonyl)quinoxaline
LY503430	4'-{(1*S*)-1-fluoro-2-[(isopropylsulfonyl)amino]-1-methylethyl}*N*-methylbiphenyl-4-carboxamide
LY404187	*N*-[2-(4'-cyanobiphenyl-4-yl)propyl]propane-2-sulfonamide
NBQX	2,3-Dioxo-6-nitro-1,2,3,4-tetrahydrobenzo[f]quinoxaline -7-sulfonamide
Talampanel	(8*R*)-7-Acetyl-5-(4-aminophenyl)-8,9-dihydro-8-methyl-7*H*-1,3-dioxolo[4,5-h] [2,3]benzodiazepine (a.k.a. GYKI 537773, LY300164)

NMDA receptor ligands

(R)-HA-966	(*R*)-(+)-3-Amino-1-hydroxypyrrolidin-2-one
Amantadine	adamantan-1-amine
AP7	2-amino-7-phosphonoheptanoic acid
CPP	3-(2-Carboxypiperazin-4-yl)propyl-1-phosphonic acid
MK-801	[5R,10S]-[+]-5-methyl-10,11-dihydro-5*H*-dibenzo[*a*,*d*]cyclohepten-5,10-imine (a.k.a. Dizocilpine)
SDZ 220-581	(S)-alpha-amino 2'chloro-5-(phosphonomethyl)[1,1'-biphenyl]-3-propanoic acid

GluN2 subunit-specific ligands

BZAD01	4-trifluoromethoxy-N-(2-trifluoromethyl-benzyl)-benzamidine
CP-101,606	(1*S*,2*S*)-1-(4-hydroxyphenyl)-2-(4-hydroxy-4-phenylpiperidino)-1-propanol (a.k.a. Traxoprodil)
Eliprodil	1-(4-chlorophenyl)-2-[4-[(4-fluorophenyl)methyl]piperidin-1-yl]ethanol
Ifenprodil	4-[2-(4-benzylpiperidin-1-yl)-1-hydroxypropyl]phenol

MK-0657	(3S,4R)-4-methylbenzyl-3-fluoro-4-((pyrimidin-2ylamino)methyl)piperidine-1-carboxylate
Ro 25-6981	(aR,bS)-a-(4-hydroxyphenyl)-bmethyl-4-(phenylmethyl)-1-piperidinepropanol

Kainate receptor ligands

CNQX	7-nitro-2,3-dioxo-1,4- dihydroquinoxaline-6-carbonitrile
DNQX	6,7-Dinitroquinoxaline-2,3-dione
LY377770	(3*SR*,4*aR*,6*R*,8*aR*)-6[2-(1(2)*H*-tetrazole-5yl)ethyl]decahydroisoquinoline-3-carboxylic acid
NS102	5-Nitro-6,7,8,9-tetrahydro-1*H*-benzo[*g*]indole-2,3-dione 3-oxime

Group I mGlu receptor ligands

$mGlu_1$

LY367385	(*S*)-(+)-α-Amino-4-carboxy-2-methylbenzeneacetic acid

$mGlu_5$

AFQ056	Methyl (3a*R*,4*S*,7a*R*)-4-hydroxy-4-[(3-methylphenyl)ethynyl]octahydro-1*H*-indole-1-carboxylate (a.k.a. Mavoglurant)
Dipraglurant	2-(4-{6-fluoroimidazo[1,2-a]pyridin-2-yl}but-1-yn-1-yl)pyridine
MPEP	2-Methyl-6-(phenylethynyl)pyridine
MTEP	3-[(2-methyl-1,3-thiazol-4-yl)ethynyl]pyridine

Group II mGlu receptor ligands

2R,4R-APDC	(2*R*,4*R*)-4-Aminopyrrolidine-2,4-dicarboxylate
4C3HPG	RS-4-carboxy-3-hydroxyphenylglycine
DCG-IV	(1R,2R)-3-[(1S)-1-amino-2-hydroxy-2-oxoethyl]cyclopropane-1,2-dicarboxylic acid
L-CCG-I	(2*S*,1'*S*,2'*S*)-2-(Carboxycyclopropyl)glycine

LY379268	(1S,2R,5R,6R)-2-amino-4-oxabicyclo[3.1.0]hexane-2,6-dicarboxylic acid

Group III mGlu receptor ligands

(R,S)-PPG	(*RS*)-4-Phosphonophenylglycine
ACPT-I	(1*S*,3*R*,4*S*)-1-Aminocyclopentane-1,3,4-tricarboxylic acid
L-AP4	L-(+)-2-Amino-4-phosphonobutyric acid
L-SOP	L-Serine-*O*-phosphate
$mGlu_4$	
ADX88178	5-Methyl-N-(4-methylpyrimidin-2-yl)-4-(1H-pyrazol-4-yl)thiazol-2-amine (a.k.a. AF42744)
Compound 11	4-((E)-styryl)-pyrimidin-2-ylamine
LSP1-2111	(2S)-2-amino-4-(hydroxyl(hydroxyl(4-hydroxy-3-methoxy-5-nitrophenyl)-methyl)phosphoryl)butanoic acid
LuAF21934	(1S,2R)-2-[(aminooxy) methyl]-N-(3,4-dichlorophenyl)cyclohexane-1-carboxamide
(-)PHCCC	(-)-N-phenyl-7-(hydroxyimino) cyclopropa[b]chromen-1a-carboxamide
VU0155041	cis-2-[[(3,5-dichlorophenyl)amino]carbonyl]cyclohexanecarboxylic acid
VU0364770	*N*-(3-Chlorophenyl)-2-pyridinecarboxamide
$mGlu_7$	
AMN082	N,N'-dibenzhydrylethane-1,2-diamine dihydrochloride
MMPIP	6-(4-methoxyphenyl)-5-methyl-3-pyridin-4-ylisoxazolo[4,5-c]pyridin-4(5H)-one
$mGlu_8$	
(S)-3,4-DCPG	(S)-3,4,-dicarboxyphenylglycine
AZ12216052	2-(4-bromobenzylthio)-N-(4-sec-butylphenyl)acetamide

Table of Contents

Table of Figures

Table of Tables

1 Introduction

1.1 What is Parkinson's disease?

1.1.1 Prevalence and pathology

Parkinson's disease (PD) is the second most prevalent neurological disorder in the world after Alzheimer's disease, and was named in recognition of Dr. James Parkinson after he described the condition in his 'Essay on the Shaking Palsy' (Parkinson, 2002 (orig. 1817)). The cardinal motor symptoms of the disease include bradykinesia, rigidity and a resting tremor, alongside other non-motor symptoms such as depression, autonomic dysfunction and sleep disturbances (discussed further in section 1.5.2). PD affects 1.8% of the European population over the age of 65 (de Rijk *et al.*, 2000) but estimates of overall worldwide incidences vary, probably as a result of differences in genetic susceptibility and exposure to environmental risk factors (Twelves *et al.*, 2003).

PD results from the degeneration of the so-called nigrostriatal pathway; dopaminergic cells that project from the substantia nigra pars compacta (SNc) to the caudate nucleus and putamen (collectively the dorsal striatum). Dopamine acts in the striatum to balance the activation of two opposing efferent pathways, the striatonigral 'direct' pathway and the striatopallidal 'indirect' pathway (see section 1.3.2). The motor symptoms of PD present when the striatal dopamine content is reduced by 50-66% (Kordower *et al.*, 2013; Riederer *et al.*, 1976) and nigral cell loss is >50% (Kordower *et al.*, 2013), at which point this critical balance between the pathways is lost.

Along with degeneration of the nigrostriatal tract, the other pathological hallmark of PD is the presence of intraneuronal 8-30µm diameter protein inclusions called Lewy bodies (LB), mainly composed of fibrillar α-synuclein and ubiquitin (Spillantini *et al.*, 1997). Whether LBs are intrinsically neurotoxic or merely symptomatic of neuronal malfunction is unknown, since on the one hand they stain positive for aggresome markers such as γ-tubulin and pericentrin (Olanow *et al.*, 2004), which suggests they form as a cytoprotective measure, but on the other hand misfolded α-synuclein is thought to propagate PD pathology between cells (Luk *et al.*, 2014; Masuda-Suzukake *et al.*, 2013), implicating them in the progression of the disease. Nevertheless, the spread of LB into specific areas of the brain has been linked to the progressive worsening of PD (Braak *et al.*, 2003) and has also been suggested to underlie the varied non-levodopa responsive non-motor symptoms of PD (Dickson *et al.*, 2009). The link between spreading LB pathology and the development of

motor and non-motor symptoms led to the development of Braak staging for classification of the progression of PD (Braak *et al.*, 2002).

1.1.2 Aetiology

1.1.2.1 Genetic factors

Mutations in several genes are associated with increased risk of developing PD, though familial forms of the disease account for <5% of total PD cases. A brief summary of the functions of some of the genes implicated in monogenic forms of familial PD is shown in Table 1.

Table 1: A selection of genes implicated in monogenic forms of familial parkinsonism. Information on gene function was obtained from Genetics Home Reference (GHR, 2014) at http://ghr.nlm.nih.gov on 6/8/14.

Gene	Protein	Function
SYNA (PARK1/4)	α-synuclein (α-syn)	This protein is located presynaptically and is thought to be involved in vesicle trafficking. It is a major component of Lewy bodies.
Parkin (PARK2)	Parkin	Parkin is part of the E3 ubiquitin ligase complex that is involved in tagging damaged or excess proteins for degradation by the proteasome.
PINK1 (PARK6)	PTEN-induced putative kinase 1	This serine/threonine kinase causes the binding of parkin to damaged mitochondria, leading to mitophagy.
DJ-1 (PARK7)	Daisuki-Junko-1	This protein has putative roles as a sensor to oxidative stress and as a chaperone involved in protein folding and degradation.
LRRK2 (PARK8)	Dardarin (Leucine-rich repeat kinase 2)	A mitochondrial-associated protein that interacts with parkin. Likely involved in the cellular response to oxidative stress.

Unsurprisingly given its presence in LB, at least 18 mutations in *SYNA*, the gene encoding α-synuclein, are associated with the development of autosomal dominant forms of parkinsonism. Alongside these missense mutations, notably A53T, *SYNA* can also undergo gene duplication, which proportionately increases the production of the α-synuclein protein within cells. *SYNA*-linked parkinsonism tends to be early-onset (~50y) and includes extensive Lewy body pathology. Symptoms range from the classical motor features to more severe features such as dementias and myoclonus, and in the case of gene multiplications the severity is linked to the gene dose (Bonifati, 2014).

Autosomal dominant mutations in LRRK2, encoding the protein Dardarin, account for around 10% of cases of familial parkinsonism (Spatola *et al.*, 2014). This multicatalytic kinase/GTPase is ubiquitously expressed and has diverse functions including immune regulation, endocytosis and autophagy (Cookson, 2012). Importantly from the point of view of PD, Dardarin is involved in mitochondrial dynamics (Wang *et al.*, 2012b) and mutations in this protein lead to enhanced vulnerability to excitotoxic stress (Plowey *et al.*, 2014).

Mutations in several other mitochondrially-associated proteins are also responsible for a proportion of cases of autosomal recessive familial PD, including PINK1 and Parkin. These proteins act in conjunction to facilitate the degradation of damaged mitochondria (Narendra *et al.*, 2012), and mutations in either one of them leads to mitochondrial dysfunction *in vitro* and *in vivo* (Burman *et al.*, 2012; Grunewald *et al.*, 2010; Marongiu *et al.*, 2009; Moisoi *et al.*, 2014).

The function of DJ-1 is not well-defined but an acidic form of this protein accumulates under conditions of oxidative stress, and this shift appears to be part of a neuroprotective function (Canet-Aviles *et al.*, 2004). Mutations in this protein enhance susceptibility to oxidative stress *in vivo* (Kim *et al.*, 2005), perhaps by inhibiting the protective acidification at a key residue, cysteine 106. DJ-1 may also form a complex with Parkin and PINK1 to promote degradation of unfolded proteins, therefore mutations in any of these components could promote the accumulation of damaged proteins (Xiong *et al.*, 2009).

While cases of familial parkinsonism are rare, the study of these genes has helped to identify pathways and cellular processes that are likely to also be disrupted in idiopathic PD. Indeed polymorphisms in these genes and others may enhance susceptibility to PD in patients in whom the disease is of otherwise unknown aetiology.

1.1.2.2 Environmental factors

Alongside genetic factors, exposure to exogenous agents may promote the development of PD. One major risk factor that has been associated with PD is increased exposure to pesticides (Kamel *et al.*, 2007; Priyadarshi *et al.*, 2001). Several of these, such as rotenone, pyridaben and fenpyroximate, have been shown to be mitochondrial complex I inhibitors (Sherer *et al.*, 2007), and dopaminergic neurones have been shown to exhibit enhanced susceptibility to degeneration following exposure to pesticides with complex I inhibiting properties (Bywood *et al.*, 2003). As well as inducing oxidative stress by inhibition of mitochondrial function, widely-used pesticides, herbicides and fungicides including rotenone, DDT, paraquat and maneb, may co-operate with metal ions to cause a

conformational change in α-synuclein to a shape that promotes the formation of fibrillar α-synuclein, the main component of LB (Uversky *et al.*, 2002). This suggests that pesticides may promote more than one pathological mechanism associated with PD.

Secondly, there is evidence that exposure to heavy metals, particularly manganese, iron and copper, is also associated with increased risk of idiopathic PD (Coon *et al.*, 2006; Fukushima *et al.*, 2010; Rybicki *et al.*, 1993). The mechanism by which heavy metals are thought to promote degeneration is by catalysing the formation of free radicals and depleting intracellular antioxidant stores (Ercal *et al.*, 1991), putting cells under additional oxidative stress.

Finally, there is evidence that external causes of inflammation, including infection and head trauma, are associated with increased risk of PD. Regarding infection, several studies report that agents such as *Streptococcus* species, influenza and herpes simplex increase risk of PD (Fang *et al.*, 2012; Vlajinac *et al.*, 2013). The variety of infectious agents involved suggests that rather than these viruses or bacteria being uniquely causative, future PD susceptibility is increased by infection-related inflammation (Liu *et al.*, 2003). Similarly, increased susceptibility to idiopathic PD has been associated with various sources of head trauma (Friedman, 1989; Goldman *et al.*, 2006), notably boxing, leading to the term 'pugilistic parkinsonism'. Again, this is likely due to a general increase in inflammation in the CNS secondary to traumatic injury.

1.2 What Mechanisms Contribute to the Degeneration of the Nigrostriatal Pathway?

Several mechanisms are believed to contribute to the degeneration of dopaminergic neurones in PD, either related to the innate properties of these neurones or initiated by genetic susceptibility and/or exposure to environmental risk factors. Interactions between these mechanisms help to propagate cell loss once it has been initiated.

1.2.1 Innate sensitivity

Dopaminergic cells may be more vulnerable to ROS-mediated degeneration than other cell types due to the inherent instability of dopamine, which can spontaneously oxidise to form H_2O_2 , superoxide ($\cdot O_2^-$) and dopamine-*o*-quinone free radicals (Hastings, 2009). Quinone autoxidation products of dopamine can impair mitochondrial function, leading to disruption of mitochondrial membrane potential and apoptotic-like cell death (Jana *et al.*,

2011). However this does not explain why other dopaminergic cell populations, such as the A10 projection from the VTA to the NAc, are relatively spared in PD while the A9 nigrostriatal projection degenerates. The difference is likely due to increased energy requirement of A9 cells versus other dopaminergic cells, meaning an increased reliance on mitochondria and therefore an increased vulnerability to anything that compromises their function (Neuhaus *et al.*, 2014; Surmeier *et al.*, 2012).

1.2.2 Mitochondrial dysfunction and oxidative stress

Given the particular reliance of nigrostriatal dopaminergic neurones on optimal mitochondrial function, any factor that inhibits this may contribute to the degeneration found in PD. This assertion is further supported by the existence of familial forms of parkinsonism that are caused by mutations in genes that regulate mitochondrial turnover and the response to oxidative stress (section 1.1.2.1).

Mitochondria are double-membraned organelles that generate energy in the form of adenosine triphosphate (ATP) via the electron transport chain (ETC). The ETC is composed of a series of redox proteins located on the inner mitochondrial membrane (Figure 1). Electrons from the metabolic intermediates nicotinamide adenine dinucleotide (NADH) and succinate are cycled through the various complexes (complex I-IV), eventually joining with molecular oxygen and protons to form water.

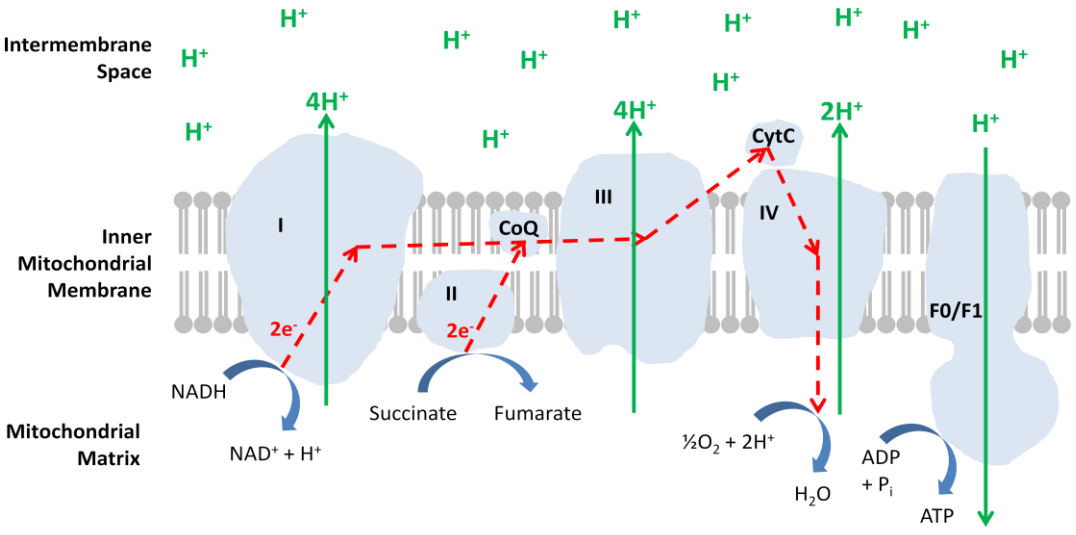

Figure 1: The complexes of the electron transport chain. The passage of electrons through complexes I-IV (red dashed arrows) releases Gibb's free energy, which drives protons into the intermembrane space creating a gradient (solid green arrows). Re-entry of protons into the matrix via the F0/F1 ATP synthase pump drives the production of ATP. CoQ = coenzyme Q; CytC = cytochrome C; P_i = inorganic phosphate

The passage of these electrons releases Gibb's free energy, which drives the accumulation of protons in the intermembrane space. These protons re-enter the mitochondrial matrix via the F0/F1 ATP synthase complex, driving the generation of ATP from adenosine diphosphate (ADP) and inorganic phosphate.

Several factors have been suggested to contribute to mitochondrial dysfunction in PD. Complexes I-IV are encoded not by chromosomal DNA but by mitochondrial DNA (mtDNA). The accumulation of mutations in mtDNA is thought to lead to impaired ETC complex function, especially at complex I (Parker *et al.*, 1989; Swerdlow *et al.*, 1996). Complex I activity is known to be reduced in patients compared to healthy controls in a variety of neuronal and non-neuronal cell types (Haas *et al.*, 1995; Keeney *et al.*, 2006; Schapira *et al.*, 1990), though not all of these cell types degenerate in PD. Dopaminergic neurones seem to be selectively vulnerable to the deleterious effects of widespread complex I deficits in PD, which is supported by a recent study showing that catecholaminergic neurones are more vulnerable than other neurones to equivalent mutation rates in mtDNA (Neuhaus *et al.*, 2014).

Reduced activity or inhibition of ETC complexes can cause 'leakage' of electrons, which readily join with surrounding molecules leading to the formation of free radical species such as superoxide. Mitochondrial dysfunction is therefore deleterious to cells not only through ATP depletion but also through the generation of free radicals and reactive oxygen species (ROS) from the electron transport chain. Increased ROS production that is not counteracted by antioxidant mechanisms results in a state known as oxidative stress. ROS and reactive nitrogen species (RNS) are highly reactive and cause oxidative damage to biomolecules, triggering apoptosis and thereby degeneration. There is extensive evidence for the involvement of oxidative/nitrosative stress in the aetiology of idiopathic PD, including the presence of the protein nitration product 3-nitrotyrosine in LBs (Good *et al.*, 1998) and increases in the SNc of protein oxidation products such as protein carbonyls (Alam *et al.*, 1997; Yoritaka *et al.*, 1996), lipid peroxidation products such as malondialdehyde (Dexter *et al.*, 1989), and DNA oxidation products such as 8-hydroxyguanosine (Zhang *et al.*, 1999) in PD patients compared with age-matched healthy controls.

The normal cellular defence against oxidative stress includes enzymes such as superoxide dismutase (SOD) and antioxidant molecules such as glutathione that neutralise oxidising species. Impaired functioning of antioxidant enzymes or depleted levels of antioxidant

molecules in cells can predispose them to oxidative stress. Dopamine quinones have been shown to reduce the activity of the mitochondrial antioxidant enzyme SOD2 *in vitro* (Belluzzi *et al.*, 2012), however studies of antioxidant enzymes in PD patients have variously shown them to have reduced (Abraham *et al.*, 2005; Ambani *et al.*, 1975; Kish *et al.*, 1985) or increased activity (Kalra *et al.*, 1992; Saggu *et al.*, 1989), perhaps depending on the specific enzyme measured, region of interest or disease duration. With regard to molecular antioxidants, decreased amounts of the reduced form of glutathione (GSH) have consistently been found in the SN of PD patients (Pearce *et al.*, 1997; Riederer *et al.*, 1989; Sian *et al.*, 1994), reflecting a general increase in oxidative stress. Interestingly, glutathione deficiency has been shown to be sufficient to initiate degeneration of dopaminergic neurones in rats (Garrido *et al.*, 2010).

1.2.3 Proteasomal dysfunction

The ubiquitin-proteasome system (UPS) consists of a series of enzymes which label (ubiquitinate) and ATP-dependently degrade excess or non-functional proteins. If these proteins are not degraded and recycled they form aggregates within cells that can interfere with cell function, and this is believed to underlie the proposed neurotoxic effects of LBs. The presence of LBs and increased oxidatively damaged proteins in PD led to speculation that the disease may be the result of deficiencies within the UPS. In addition, mutations in the genes encoding the aforementioned E3 ubiquitin ligase Parkin and the enzyme ubiquitin carboxy-terminal hydrolase L1 (UCH-L1) have also been associated with monogenic forms of familial parkinsonism (Dawson *et al.*, 2010; Leroy *et al.*, 1998), further supporting proteasomal dysfunction as a pathogenic mechanism.

Indeed there have been several reports of impaired 20/26S proteasomal activity in *post mortem* PD brains, associated with structural abnormalities such as loss of the α subunit of the proteasome complex (McNaught *et al.*, 2003; McNaught *et al.*, 2001). This would lead to incomplete degradation of abnormally folded or damaged proteins, which would then accumulate in the cytoplasm and interfere with normal functioning. The reason for impaired proteasomal function in idiopathic PD is uncertain, however proteasomal function has been shown to be inhibited *in vitro* by hydrogen peroxide and by peroxynitrite and hypochlorite radicals (Reinheckel *et al.*, 1998), therefore the oxidative stress that has been described to contribute to neurodegeneration in PD by damage to biomolecules and ATP depletion could further enhance neurodegeneration by interfering with protein degradation.

1.2.4 Inflammation

The brain contains resident immune cells called microglia that can be activated by inflammatory stimuli such as the bacterial endotoxin lipopolysaccharide (LPS) or by cellular contents released during necrosis. Astrocytes can also become activated by exposure to these stimuli. Once activated, these immune cells release a series of inflammatory mediators such as nitric oxide and superoxide (which directly damage cells) along with cytokines such as tumour necrosis factor-α, and interleukins -1β and -6, which have been implicated in neurotoxicity when present at high concentrations (reviewed by Liu *et al.*, 2003; McGeer *et al.*, 2004).

Inflammation is implicated in the pathogenesis of PD by *post mortem* studies in humans that have identified increased glial activation and cytokine production in and around the SN (Boka *et al.*, 1994; Hunot *et al.*, 1999; Imamura *et al.*, 2003; McGeer *et al.*, 1988; Mogi *et al.*, 1996). However the question of whether this is a cause or effect of the degeneration of the dopaminergic cells originating in this nucleus is up for debate (Teismann *et al.*, 2003). It is likely that both scenarios occur in tandem, such that an initial toxic stimulus (such as an environmental toxin or infectious agent) causes the initial glial activation and as the neurones are overwhelmed, either by the stimulus or by the chronic exposure to inflammatory mediators, and cell death begins to occur this damage will drive reactive gliosis (Burda *et al.*, 2014). The selective loss of dopaminergic neurones in an inflammatory situation could be explained by a further innate vulnerability of these cells; the SN is particularly rich in microglia, meaning that dopaminergic neurones are more susceptible than other neurones to neurodegeneration following an inflammatory stimulus (Kim *et al.*, 2000).

Inflammation could interact with other potential mechanisms of cell loss, for example there is a suggestion that neuroinflammation and α-synuclein aggregation potentiate each other (Gao *et al.*, 2011). In addition, inflammation causes export of glutamate from microglia (McMullan *et al.*, 2012), thereby increasing the risk of initiating excitotoxicity (expanded below).

1.2.5 Glutamate-mediated excitotoxicity

Increases in glutamate concentration in the SNc may increase the risk of neurodegeneration via a process called excitotoxicity. This can result from increased release of glutamate from overactive subthalamic nucleus terminals or from reduced glutamate clearance from the synaptic cleft, both of which mechanisms have been

demonstrated in Parkinson's disease (Ferrarese *et al.*, 1999; Remple *et al.*, 2011). This mode of degeneration is also thought to play a role in preclinical models of neurodegeneration such as 6-hydroxydopamine (6-OHDA)-lesioned rats, where downregulation of glial glutamate transporters (Chung *et al.*, 2008) and loss of inhibitory control over the subthalamic nucleus have been reported (Fernandez-Suarez *et al.*, 2012).

Excessive stimulation of neurones by excitatory amino acids (mainly glutamate) causes cell death. While normal stimulation of NMDA receptors on the post-synaptic membrane is associated with neuroprotective effects, when glutamate release is sufficiently high for it to overspill from the synaptic cleft it activates extrasynaptic NMDA receptors. Activation of these receptors causes downstream activation of multiple pathways, mainly mediated by increases in intracellular free Ca^{2+}, that promote cell death (Hardingham *et al.*, 2010; MacDermott *et al.*, 1986).

Increases in intracellular Ca^{2+} activate neuronal nitric oxide synthase (nNOS), which catalyses the transformation of arginine and NADPH to citrulline and $NADP^{+}$, with the release of nitric oxide (NO). NO can react with superoxide in the cytoplasm to produce the highly reactive oxidant peroxynitrite ($ONOO^{-}$), which causes oxidative damage to biomolecules such as DNA and proteins. Calcium can also accumulate in the mitochondria, where it causes depolarisation of the mitochondrial membrane and subsequent opening of the permeability transition pore (PTP), releasing pro-apoptotic molecules and initiating apoptosis (reviewed by Rasola *et al.*, 2011).

In a healthy cell, with adequate stores of antioxidant molecules (such as glutathione) and antioxidant enzymes (such as SOD and catalase), the effects of glutamate overstimulation would be counteracted. However a cell that may already be under a degree of oxidative stress is more easily overwhelmed by an excitotoxic insult (see sections 1.2.1 and 1.2.2 for more detail about the selective vulnerability of dopaminergic neurones and oxidative stress in PD). In support of this, exposure of dopaminergic neurones *in vitro* to a normally non-noxious glutamate insult can cause degeneration if these neurones have been rendered more vulnerable by inducing a low level mitochondrial dysfunction (Marey-Semper et al., 1995). There also seems to be cross-talk between excitotoxicity and neuroinflammation (Chang *et al.*, 2008; Ossola *et al.*, 2011), which has also been demonstrated in PD (see section 1.2.4).

An additional glutamate-mediated mechanism of cell death involves inhibition of L-cystine uptake into cells as excess glutamate inhibits the transporter (Bannai *et al.*, 1980). Once inside cells, cystine is reduced to cysteine, one of the trio of amino acids that comprise the antioxidant molecule glutathione. Therefore inhibition of cystine uptake will decrease cellular glutathione production, rendering the cell more vulnerable to oxidative stress.

Though not demonstrated in the human disease, there is evidence from animal models of PD that excitotoxicity might be involved in dopaminergic neurodegeneration. This includes the finding that disinhibition of the STN via lesioning of the GP can cause SNc degeneration in rats, suggestive of an excitotoxic mechanism of cell loss (Wright *et al.*, 2004). In addition, an MPTP-induced lesion can be exacerbated by nigral infusion of glutamate (Kucheryanu *et al.*, 2000). The main evidence for a role of excitotoxicity in PD comes from preclinical PD models, where inhibition of glutamate signalling has been shown to be neuroprotective. This is discussed in detail in section 1.6.

1.3 Symptom Generation: Structure and Function of the Basal Ganglia

The degeneration of dopaminergic neurones via the mechanisms described leads to altered signalling in the basal ganglia (BG), a series of nuclei in the midbrain that receive cortical input, integrate the information and feed back again to the cortex to either promote or inhibit motor function. It is this altered BG functioning that underlies the generation of bradykinetic motor symptoms in patients with Parkinson's disease.

1.3.1 Anatomy of the basal ganglia

The BG comprise several nuclei; the SNc, caudate nucleus and putamen (while these nuclei are anatomically distinct in the human and primate BG, they are fused in rodents to form a single structure called the CPu that is commonly referred to as the dorsal striatum or simply the striatum), globus pallidus externus (GPe), subthalamic nucleus (STN), substantia nigra pars reticulata (SNr) and the globus pallidus internus (GPi; this is called the entopeduncular nucleus or EPN in rodents). The connectivity between these nuclei is explored below; much of the work on both the anatomical and functional connectivity described in this section was performed in rodents and primates, which are also the most commonly used species for modelling PD.

Striatal connectivity

The major neuronal input to the striatum is a glutamatergic projection originating in lamina V and lamina III of various cortical regions, which project to defined but overlapping regions within the striatum (McGeorge *et al.*, 1989). These afferents form asymmetric contacts on the dendritic spines of GABAergic medium spiny neurones (MSNs), which make up the vast majority, ~95%, of the neuronal population within the striatum. It is widely accepted that there are two distinct main types of MSN; striatonigral MSNs, which express dopamine D1 receptors (D1R), substance P and dynorphin and project to the SNr and EPN/GPi, and striatopallidal MSNs, which express dopamine D2 receptors (D2R) and enkephalin and project to the GP(e) (Bertran-Gonzalez *et al.*, 2010; Gerfen *et al.*, 1990). Immunolabelling studies in rats have shown that distinct populations of cortical neurones innervate striatonigral MSNs compared with striatopallidal MSNs (Lei *et al.*, 2004), supporting the functional segregation of these two striatal cell populations. It is this segregation that underlies the idea of a 'direct' and an 'indirect' pathway in the BG, which will be described in more detail later. More recent studies have also identified a small population of D1R and D2R-expressing MSNs projecting to multiple nuclei within the BG but their function has not yet been elucidated (Perreault *et al.*, 2011).

Another important striatal input from the point of view of PD is the dopaminergic nigrostriatal projection, originating in the SNc. It is the differential actions of dopamine at D1R and D2R on MSNs that balances the activation of these opposing neuronal populations in response to corticostriatal input, exerting opposite effects on D1 and D2 receptors (Surmeier *et al.*, 2007; West *et al.*, 2002). The binding of dopamine at D1R leads to $G\alpha_{s/olf}$-coupled activation of adenylate cyclase and enhancement of L-type Ca^{2+} currents, increasing neuronal excitability in the presence of corticostriatal glutamatergic input (Hernandez-Lopez *et al.*, 1997; Nishi *et al.*, 2011). Conversely, the binding of dopamine at D2R leads to $G\alpha_i$-coupled inhibition of adenylate cyclase, Gβγ-mediated activation of phospholipase C, and inhibition of L-type Ca^{2+} currents (Hernandez-Lopez *et al.*, 2000). Hence the actions of dopamine in the striatum are to promote the activation of striatonigral MSNs and inhibit the activation of striatopallidal MSNs. In addition to this dopaminergic influence, other neurotransmitters are released into the striatum, including serotonin from the dorsal raphe nucleus and noradrenaline from the locus coeruleus.

The remaining 5% of cells present in the striatum are GABAergic and cholinergic interneurones, which are mainly activated by glutamatergic afferents originating in the

thalamus. Large aspiny cholinergic interneurones are tonically active and inhibit glutamate release from corticostriatal terminals via muscarinic M2 and M3 receptors, thereby inhibiting MSN activation (Pakhotin *et al.*, 2007). Fast-spiking GABAergic interneurones mediate feedforward inhibition of MSNs and are thought to be responsible for lateral inhibition, such that only a specific pool of MSNs is activated at any one time and surrounding MSNs are inhibited. This leads to a pattern of activation that is task-specific and avoids excessive 'noise' in the BG output (Tepper *et al.*, 2004). These interneurones are additionally activated by dopamine (Bracci *et al.*, 2002), meaning that reduced dopaminergic input might be expected to decrease the extent of lateral inhibition and lead to dysregulated striatal output.

GP connectivity

The GP is the first relay nucleus in the classical 'indirect' pathway. The main inputs to the GP are a GABAergic projection from the striatum (via D2R/enkephalin-expressing MSNs, as described above), inhibiting GP efferent neurones, and a glutamatergic projection from the STN, which will activate them (Parent *et al.*, 1995b).

GP efferent neurones are GABAergic and highly collateralised, mainly projecting to the subthalamic nucleus, where they form synapses with proximal and distal dendrites and soma of neurones in the rostrolateral regions of the STN, and the GPi/EPN, where they form synapses overwhelmingly at soma and proximal dendrites of target neurones (Parent *et al.*, 1995b). Additional targets have also been described following anterograde tracing studies, including the SNr, SNc and pedunculopontine nucleus (PPN) as well as feedback targeting of striatal interneurones by parvalbumin-negative neurones (Billings *et al.*, 2004; Bolam *et al.*, 2000; Parent *et al.*, 1995b).

While the GP was originally considered to be a simple relay with a main role in the inhibitory control of the glutamatergic STN, the discovery of efferents from the GP to the output nuclei of the BG, the SNr and EPN/GPi, along with a range of other BG nuclei has led to an increasingly important role being assigned to this region as an integrator of striatal and subthalamic inputs. This role is supported by the convergence of subthalamopallidal and striatopallidal inputs on single pallidal neurones, as has been described in primates (Parent *et al.*, 1995b).

STN connectivity

The STN is the second relay nucleus in the classical 'indirect' pathway and is the only glutamatergic nucleus within the basal ganglia. The major inhibitory input to the STN is the GABAergic projection originating in the GP, causing a direct inhibition of subthalamic excitatory output. The STN also receives glutamatergic input from the cortex, along with the thalamic parafascicular nucleus and PPN (Canteras *et al.*, 1990). The corticosubthalamic projection is of particular interest as it forms part of the third pathway within the BG, the 'hyperdirect' pathway. This pathway is unique in that it bypasses the striatum, allowing a direct cortico-STN connection, subsequent increased output from the STN, and thereby increased output from the EPN/SNr. Activation of the hyperdirect pathway therefore inhibits motor function. The cortico-STN connection arises in the primary motor cortex and supplementary motor area, projecting to the lateral and medial STN respectively, and is somatotopically arranged, suggesting that it is composed of parallel connections that are each specific to a particular movement (Nambu *et al.*, 1996). The corticosubthalamic connection has been demonstrated in multiple species (Bosch *et al.*, 2012; Brunenberg *et al.*, 2012; Nambu *et al.*, 1996) and it is currently understood to play a role in termination of an ongoing movement and impulsivity (Obeso *et al.*, 2008).

Another important input to the STN in the context of Parkinson's disease is a dopaminergic projection from the SNc, which modulates the various other neuronal inputs to this nucleus thereby affecting STN output (Hassani *et al.*, 1996; Hassani *et al.*, 1997). In addition the subthalamic nucleus is innervated by thalamic nuclei, the dorsal raphe nucleus and the PPN (Parent *et al.*, 1995b).

The excitatory glutamatergic efferents of the STN project primarily from the lateral portion of this nucleus to the EPN/GPi and SNr, the output nuclei of the BG, and also to the GP, with which it makes a reciprocal connection (Parent *et al.*, 1995b). The importance of this reciprocal relationship between the GP and STN in normal function and in pathological conditions has been of particular recent interest with regard to synchronisation of activity within the BG network and will be discussed in section 1.3.3.5. The subthalamo-SNr/EPN projection completes the classical 'indirect' pathway from the striatum to the output nuclei.

In addition the STN sends lesser projections to the SNc, striatum, cortex and PPN (Parent *et al.*, 1995b). As is the case for the GP, the STN and SNc form a reciprocal connection.

Subthalamonigral glutamate release into the pars compacta is of particular interest in this thesis, as excessive glutamate levels can trigger degeneration of cells by excitotoxicity (section 1.2.5) and this is the cell population that degenerates in Parkinson's disease.

EPN/SNr connectivity

The EPN and SNr collectively form the output nuclei of the BG, sharing similar afferent and efferent neurones, and therefore they are considered together in this section.

The main glutamatergic input to the EPN and SNr originates in the STN. Subthalamic afferents form asymmetrical synapses, predominantly with dendritic shafts of SNr neurones (Parent *et al.*, 1995b), and make up ~10% of total boutons in the SNr. An additional minor glutamatergic input originates in the prefrontal cortex (Naito *et al.*, 1994).

This glutamatergic input from the 'indirect' pathway is counterbalanced by the main GABAergic input to the EPN and SNr, the striatonigral MSNs that form the 'direct' pathway. Additionally the output nuclei receive considerable GABAergic innervation from the GP as described above (Smith *et al.*, 1989). Further minor GABAergic afferents originate in the nucleus accumbens and ventral pallidum (Blandini, 2000).

The EPN and SNr send highly collateralised GABAergic efferents primarily to the small dendrites of the ventral anterior (VA) and ventral lateral (VL) motor thalamus, and also send more minor projections/collaterals to the parafascicular thalamic nucleus, superior colliculus and PPN (Parent *et al.*, 1995a). A glutamatergic nigrothalamic connection has also recently been described, though its function is as yet unknown (Antal *et al.*, 2014). Inhibition of the VA and VL thalamus by activation of the BG output nuclei leads to inhibition of thalamocortical feedback and reduces motor function, whereas reduced BG output disinhibits thalamocortical feedback and facilitates motor function. Therefore regulation of this output by striatonigral GABAergic efferents and subthalamonigral glutamatergic afferents is of utmost importance for motor function.

Thalamocortical feedback

The VA and VL thalamic nuclei receive GABAergic inputs from the EPN and SNr and provide feedback to the premotor, primary, cingulate and supplementary motor areas of the cortex via glutamatergic efferents (McFarland *et al.*, 2002; Schell *et al.*, 1984). While VL efferents tend to target caudal motor cortical areas involved with execution of movements, VA efferents tend to target rostral motor cortical areas that are involved in cognitive aspects of

movement such as motor learning (Haber *et al.*, 2001). The thalamic nuclei (centromedian and parafascicular nuclei in this case) additionally innervate the striatum, providing the second largest glutamatergic input to this nucleus after the cortex. This feedback is thought to help prepare the striatum for subsequent cortical input or modulation of activity that might result from the thalamocortical feedback (Groenewegen *et al.*, 1994).

As well as projecting to the cortex, the VA and VL thalamic nuclei receive reciprocal and non-reciprocal glutamatergic corticothalamic innervation (Fonnum *et al.*, 1981), which relays information between areas of the cortex from limbic to cognitive to motor regions (McFarland *et al.*, 2002).

Thus when the output nuclei of the BG, the EPN/SNr, are activated they inhibit thalamocortical neurones from providing feedback to the cortex. Conversely when the output nuclei of the BG are inhibited they disinhibit thalamocortical neurones and thereby increase activity in the cortex, which promotes motor function.

SNc connectivity

Located in the dorsal part of the substantia nigra, the pars compacta is made up of melanin-containing dopaminergic neurones. These are the cells that degenerate in PD.

Several afferent neurones innervate the SNc, including GABAergic neurones from the striatum and GP and glutamatergic neurones from the STN, PPN and prefrontal cortex (Kanazawa *et al.*, 1976; Parent *et al.*, 1999). In addition, the SNc receives cholinergic projections from the PPN and serotonergic projections from the raphe nuclei (Blandini, 2000).

Dopaminergic efferents from the SNc terminate largely in the striatum, but also in the STN and GP (Guyenet *et al.*, 1978; Hassani *et al.*, 1997). In the striatum, the nigral projection neurones converge with corticostriatal inputs to form symmetrical synapses with spines and dendrites of MSNs (Smith *et al.*, 2000); dopamine released from these terminals acts on post-synaptic D1R and D2R on striatonigral and striatopallidal MSNs respectively, modulating excitability of these neurones as described earlier. In the STN, dopamine acts on both D1-type and D2-type receptors, with activation of either receptor subtype eliciting similar effects of depolarisation and increased firing rate of STN neurones and reduction of the impact of competing GABAergic inputs (Cragg *et al.*, 2004; Mintz *et al.*, 1986a; Ni *et al.*, 2001; Zhu *et al.*, 2002). The functionality of the dopaminergic nigropallidal connection has not been fully clarified, however experiments in rats have shown that intrapallidal

administration of both D1 and D2 receptor antagonists cause catalepsy, highlighting an important role for dopamine in this nucleus in motor function (Hauber *et al.*, 1999).

1.3.1.1 Working model of the BG

Given the complex connectivity between the BG nuclei, simplified working models have been developed in order to explain its functionality. In the basic, canonical model of the BG (Albin et al., 1989) these structures are arranged into two functionally discrete pathways that respond with opposite effects to corticostriatal input (Figure 2).

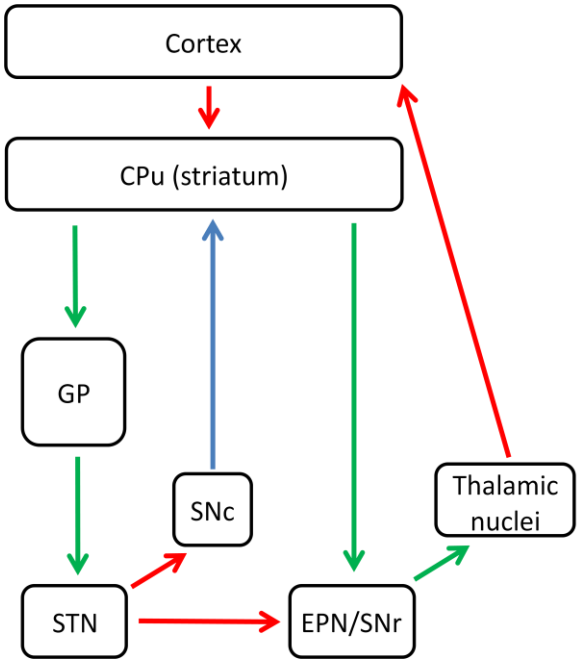

Figure 2: Classical model of the basal ganglia as described by Albin *et al.* (1989). Glutamatergic neurones are shown in red, GABAergic neurones are shown in green and dopaminergic neurones are shown in blue. CPu = caudate-putamen; EPN = entopeduncular nucleus; GP = globus pallidus; SNc/SNr = substantia nigra pars compacta/reticulata; STN = subthalamic nucleus.

The 'direct' pathway is a monosynaptic GABAergic connection of the striatum to the EPN/SNr, which are the output nuclei of the basal ganglia. The net output of activation of this pathway is the disinhibition of thalamocortical feedback, which promotes movement.

The 'indirect' pathway is a multisynaptic connection between the striatum and EPN/SNr, via the GP and STN. The net effect of activation of this pathway is the inhibition of thalamocortical feedback, and thus the inhibition of movement.

In simple terms, the role of dopamine in the BG is to balance the activation of these opposing pathways. Dopamine in the striatum activates dopamine D1 receptors (D1R)

present on striatonigral 'direct' medium spiny neurones (MSN) to facilitate signalling in this pathway, whilst simultaneously activating D2 receptors (D2R) present on striatopallidal 'indirect' MSNs to inhibit signalling in this pathway (explained in greater detail earlier).

Since this model was proposed in the late 1980s it has been considerably updated to include additional connections (Blandini, 2000; Wichmann *et al.*, 2011), namely the corticosubthalamic glutamatergic connection, the pallido-EPN/SNr connection, the subthalamopallidal glutamatergic connection and the nigrosubthalamic dopaminergic connection. The updated model as detailed by Blandini *et al.* (2000) is shown in Figure 3, and places the STN in a more central role than the classical model. This newer model also brings into play the 'hyperdirect' pathway, connecting the cortex to the STN to the EPN/SNr, allowing additional and more rapid excitation of BG output (and thus inhibition of motor function) than that afforded by the 'indirect' pathway.

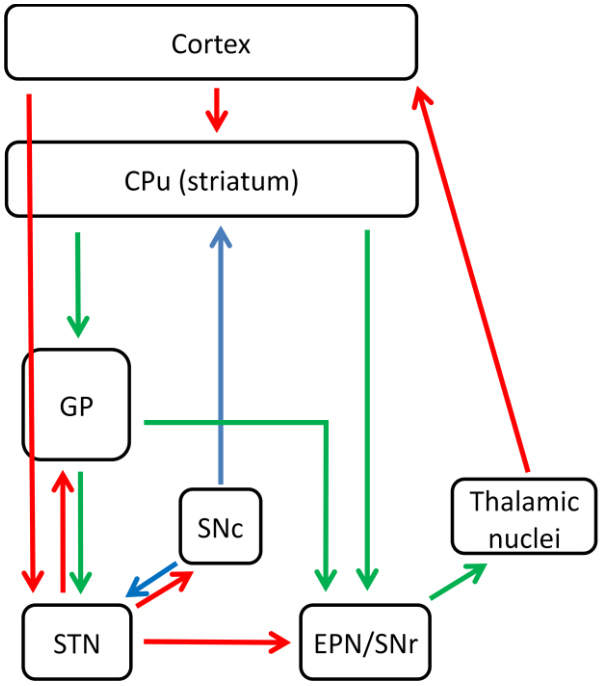

Figure 3: Updated model of the basal ganglia as described by Blandini *et al.* (2000). Glutamatergic neurones are shown in red, GABAergic neurones are shown in green and dopaminergic neurones are shown in blue. CPu = caudate-putamen; EPN = entopeduncular nucleus; GP = globus pallidus; SNc/SNr = substantia nigra pars compacta/reticulata; STN = subthalamic nucleus.

Of course, all of these models are simplifications of the anatomically defined neuronal populations within the BG. While the models shown in Figure 2 and Figure 3 are useful to explain the generation of motor symptoms in PD, and have been informative in defining targets for surgical intervention, the connectivity within this network is significantly more

complicated, as is clear from the connectivity of the individual nuclei detailed earlier, and these models also fail to account for neuromodulatory influences from cholinergic and noradrenergic inputs.

In addition to the highly complex connectivity within the BG, yet more complicated models have also been proposed that encompass areas beyond the BG. Notably one model incorporates the lower brainstem nuclei that are affected by Lewy body pathology prior to the onset of parkinsonian motor symptoms, placing the pedunculopontine nucleus in a bridging role between these nuclei and the BG nuclei (Braak *et al.*, 2008). Further connections between the BG and the cerebellum, which is highly involved in motor function, have also been demonstrated using neuronal tracing studies (Bostan *et al.*, 2010) so it is clear that the field has moved on considerably from the original model detailed by Albin *et al.* (1989).

1.3.2 Functioning of the healthy basal ganglia

At rest, striatal MSNs are predominantly silent and the BG output nuclei exert tonic inhibitory control over the thalamic nuclei, inhibiting their activation of the cortex (Chevalier *et al.*, 1990).

The prevailing view of signalling in the BG is that during initiation of movement a corticostriatal signal activates MSNs in the direct pathway. The MSNs activated are thought to be specific to the particular movement; target MSNs are activated at the expense of surrounding MSNs, which are inhibited by striatal interneurones (Tepper *et al.*, 2004), ensuring that the outcome is a pattern of neuronal activation that is specific to the action being performed. The activated pool of striatonigral MSNs inhibits a corresponding pool of output neurones in the EPN/SNr, causing a phasic gap in their tonic inhibition of thalamocortical neurones, which are thus activated to feed back to the cortex. Following the initiation of a movement by activation of the direct pathway, the indirect pathway is then activated, enhancing the inhibitory control of certain sets of neurones in the output nuclei over thalamocortical feedback. This aids in focusing the desired movement and inhibiting unwanted movement (Haber *et al.*, 2001; Sano *et al.*, 2013).

The role of the hyperdirect pathway is less certain, but due to its net inhibitory effect on motor function it has been suggested that it plays a similar role to the indirect pathway (Obeso *et al.*, 2008). Therefore activation of the STN in turn activates populations of output neurones in the EPN/SNr that are distinct from the target population that are inhibited by the striatonigral MSNs. In this way the activation of these potentially 'noise creating'

populations would maintain the inhibition of their corresponding thalamocortical feedback neurones, meaning that they do not interfere with the specific feedback activated via the direct pathway. In addition, the activation of the STN by the cortex could lead to activation of the GP via subthalamopallidal neurones. The GP could then exert further inhibitory control over the population of output neurones targeted by the striatonigral MSNs, enhancing the actions of the direct pathway.

1.3.3 Functioning of the parkinsonian basal ganglia

According to the classical model, motor symptoms such as bradykinesia in Parkinson's disease arise from increased signalling in the hyperdirect and indirect pathways and decreased signalling in the direct pathway (Figure 4). This is due to the loss of the actions of dopamine, which normally inhibits indirect pathway activity via activation of D2R and promotes direct pathway activity via activation of D1R. In simple terms, when the striatal dopamine concentration is too low, such as in Parkinson's disease, signalling in the indirect pathway predominates, leading to an overall inhibition of thalamocortical feedback and therefore an inhibition of motor function.

As was the case for the anatomical studies, much of the evidence of altered firing in the parkinsonian BG presented in this section was obtained from experiments in animal models.

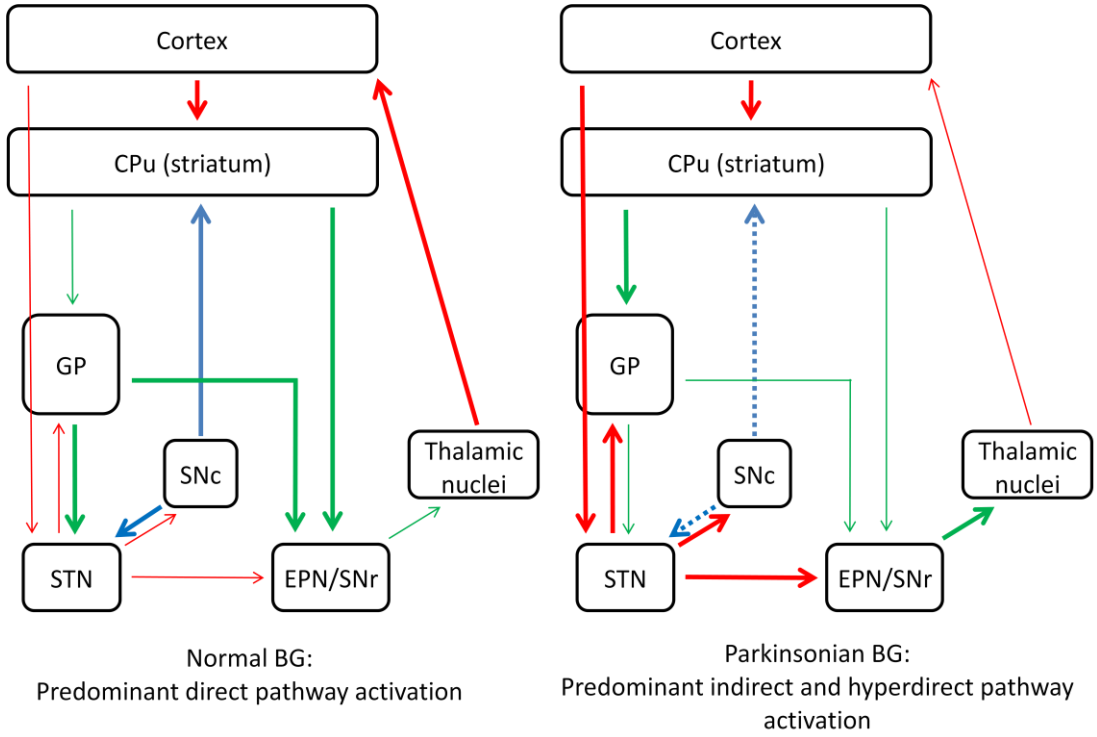

Figure 4: Model of motor symptom generation in the BG in Parkinson's disease. Degeneration of the nigrostriatal dopaminergic neurones leads to reduced striatal dopamine release. In the normal, intact BG, dopamine in the striatum acts on D1 and D2 receptors to respectively promote signalling in the 'direct' (CPu → EPN/SNr) pathway and inhibit signalling in the 'indirect' (CPu → GP → STN → EPN/SNr) pathway. In the PD brain, dopamine levels are insufficient to elicit its usual D1- and D2-mediated effects, leading to a pathological overactivation of the indirect pathway. In addition there is also evidence that the hyperdirect pathway (cortex → STN → EPN/SNr) is overactive in the parkinsonian BG, further enhancing the effects of increased activation of the indirect pathway. The net effect of this is an increase in basal ganglia output to the ventral anterior and ventral lateral thalamic nuclei, inhibiting thalamocortical feedback and thus reducing motor function.

1.3.3.1 Altered corticostriatal input

Input into the BG is altered in the parkinsonian state, and striatal spine loss has been consistently shown in 6-OHDA-lesioned rats, MPTP-treated primates and also in PD patients (Day *et al.*, 2006; Ingham *et al.*, 1993; Stephens *et al.*, 2005). Despite this spine loss, the morphology of remaining spines is altered in ways that are suggestive of *enhanced* transmission, for example in MPTP-treated primates there is evidence of increased spine volume and more extensive and complex post-synaptic densities at corticostriatal synapses (Smith *et al.*, 2009). A similar increase in post-synaptic density has also been demonstrated in PD patients (Anglade *et al.*, 1996).

The specificity of this plasticity to striatonigral, striatopallidal, or both types of striatal projection neurones is controversial, and may depend on the species being examined

(Smith *et al.*, 2009). Overall though, there seems to be an increase in corticostriatal input in the parkinsonian BG.

1.3.3.2 Reduced activity in the direct pathway

There is some evidence for reduced activity of striatonigral neurones in the parkinsonian BG, such as reduced expression of the direct pathway-specific opioid precursor PPE-B in dopamine denervated rats (Gerfen *et al.*, 1991; Henry *et al.*, 1999). In addition to this there is some indirect evidence, for example in 6-OHDA-lesioned rats corticostriatal input is altered such that the corticostriatal neurones that activate striatonigral MSNs show decreased activity (Mallet *et al.*, 2006), which together with the decreased dopamine concentration would reduce the excitability of these neurones compared with striatopallidal neurones. In addition to this, destruction of the nigrostriatal pathway causes an increase in $GABA_A$ receptor expression in the SNr and EPN of rats, suggesting a compensatory upregulation in response to reduced activation of striatonigral neurones (Yu *et al.*, 2001).

1.3.3.3 Overactivation of the indirect pathway

The predominant activation of the indirect pathway following nigrostriatal degeneration has been demonstrated by microdialysis (Bianchi *et al.*, 2003) and electrophysiology (Mallet *et al.*, 2006) in 6-OHDA-lesioned rats.

Indicators of increased activity in striatopallidal MSNs, the first step in the indirect circuit, have been demonstrated in MPTP-treated primate and 6-OHDA-lesioned rodent models of PD. These include increases in D2R, enkephalin and glutamic acid decarboxylase 67 (GAD67; GABA synthesising enzyme) expression (Betarbet *et al.*, 2004; Soghomonian *et al.*, 1997).

The next stage in this pathway, the pallidosubthalamic connection, is also affected by dopamine depletion. The overactivity in the inhibitory striatopallidal connection would be expected to reduce activity of pallidosubthalamic neurones, and such an effect has been shown in MPTP-treated primates (Fillion *et al.*, 1991) and 6-OHDA-lesioned rats (Pan *et al.*, 1988). Additionally, there is evidence from both of these models that suggests that in the dopamine denervated state there is a specific loss of cells in the GP that innervate the STN and the EPN/GPi (Fernandez-Suarez *et al.*, 2012). This would disinhibit not only the STN but also the output nucleus efferents that target the VA/VL thalamus, causing an additive enhancement of the inhibition of thalamocortical feedback that underlies parkinsonian motor symptoms. Despite this cell loss, experiments in 6-OHDA-lesioned rats have shown a

proliferation of synapses in pallidosubthalamic neurones that might be a response to this cell loss (Fan *et al.*, 2012), however this could also serve to enhance the reciprocal connection between the GP and STN, which could have important implications regarding the generation of abnormal electrical activity within the parkinsonian BG (section 1.3.3.5).

There is abundant evidence for an increase in activity of the STN in the parkinsonian state, not only in MPTP-treated primates (Bergman *et al.*, 1994b) and 6-OHDA-lesioned rats (Breit *et al.*, 2005; Breit *et al.*, 2006; Kreiss *et al.*, 1997) but also in human PD (Remple *et al.*, 2011; Yokoyama *et al.*, 1998). This activity involves an increase in abnormal bursty firing (Hassani *et al.*, 1996; Tai *et al.*, 2012), which has been linked to abnormal activity throughout the BG network (section 1.3.3.5).

The hyperactivity in the STN, combined with a reduced inhibitory input from the GP, leads to increased GABAergic signalling from the EPN/GPi and SNr to the thalamus. This has been demonstrated in 6-OHDA-lesioned rats, where the metabolic activity of these nuclei was increased following the lesion but this effect could be reversed by ablation of the STN (Blandini *et al.*, 1997).

As well as the reduction in inhibitory pallidosubthalamic signalling increasing STN activity, the degeneration of dopaminergic neurones in the SNc could also contribute to hyperactivity of this nucleus. Somatodendritic dopamine released in the SNc acts to reduce subthalamonigral glutamate release via activation of presynaptic D2R (Campbell *et al.*, 1985; Hatzipetros *et al.*, 2006). Reduced dopamine in PD would therefore increase glutamate release into the SNc, driving further degeneration of these neurones via an excitotoxic mechanism, and also into the SNr, driving the increase in inhibitory BG output. However, the actions of DA on presynaptic D1R have the opposite effect (Ibanez-Sandoval *et al.*, 2006), so further experiments to determine the net effect of loss of dopamine in PD on control of subthalamonigral glutamate release need to be completed.

1.3.3.4 Overactivation of the hyperdirect pathway

Increased STN activity, if only controlled by reduced GP activity, would be expected to stabilise due to the reciprocal connections between these nuclei, however in the parkinsonian BG the STN is consistently found to be hyperactive. As well as the neuronal loss from the GP to the STN, which would reduce the capacity of the GP to exert its inhibitory effect on the STN in response to increased subthalamopallidal firing, enhanced activity in the hyperdirect pathway might additionally explain this lack of a self-corrective effect.

Increased activation of the hyperdirect pathway has been demonstrated following nigrostriatal denervation in the 6-OHDA-lesioned rat (Dejean *et al.*, 2008), though this is at odds with a previous report which found *reduced* activity of corticosubthalamic neurones in the same model (Orieux *et al.*, 2002). Hyperactivity in this pathway would be expected to further enhance activation of the STN, promoting the inhibition of thalamocortical feedback by the EPN/SNr. This would therefore contribute to the reduced motor function in PD.

1.3.3.5 Synchronous and oscillatory activity

One of the most interesting recent developments in the analysis of BG activity in the parkinsonian state is the discovery that there is an increase in synchronised oscillatory activity in the network. In the dopamine-depleted state, the firing patterns of BG neurones become less regular and more bursty (Bergman *et al.*, 1994b; Fillion *et al.*, 1991), and the local field potential tends to oscillate at a frequency of 13-35 Hz, corresponding to the β frequency range (Kühn *et al.*, 2008; Weinberger *et al.*, 2006). The origin of this abnormal activity is still being debated. The STN has been strongly implicated in the generation of this increased bursting (Ammari *et al.*, 2011) and oscillatory activity, especially via its reciprocal connection with the GP (Gillies *et al.*, 2002; Holt *et al.*, 2014; Tachibana *et al.*, 2011), and a role for the hyperdirect pathway has also been suggested based on computational modelling of connectivity in the parkinsonian BG (Moran *et al.*, 2011).

Synchronised oscillatory activity between the cortex, GP, STN and EPN/GPi is correlated with motor dysfunction. Further to this, both β-oscillatory activity and motor symptoms (bradykinesia and akinesia, but not tremor) are suppressed by L-DOPA (Kühn *et al.*, 2006) or high frequency stimulation of the STN (Ray *et al.*, 2008). These results highlight the involvement of this abnormal synchronous and oscillatory neuronal activity in the generation of motor deficits.

1.4 Current Treatment

Most current treatments for PD aim to correct the unbalanced signalling in the BG by replacement of the dopaminergic regulation of the activation of the direct and indirect pathways. Several alternative strategies target other neurotransmitter systems that are perturbed in the parkinsonian BG but these are less well-established.

1.4.1 Dopamine replacement strategies

Dopamine replacement strategies are the first-line treatment in PD. They involve replacement of the actions of dopamine either by administration of the dopamine precursor 3,4-L-dihydroxyphenylalanine (Levodopa or L-DOPA) or using agonists of dopamine receptors.

1.4.1.1 L-DOPA

L-DOPA is a brain-penetrant precursor of dopamine that is taken up into nerve terminals and converted into dopamine by aromatic amino acid decarboxylase (AADC). To help minimise the necessary therapeutic dose and avoid side effects associated with the peripheral actions of dopamine, such as hypotension, L-DOPA is administered alongside a peripheral AADC inhibitor such as carbidopa or benserazide to prevent its conversion into dopamine outside the brain. In addition to this, inhibitors of monoamine oxidase B (MAO-B) and catechol-*O*-methyl transferase (COMT), enzymes that respectively metabolise dopamine (centrally) and L-DOPA (peripherally), can also be given alongside L-DOPA in order to prolong its central effects and minimise the necessary therapeutic dose; in fact MAO-B inhibitors have been shown to be efficacious as a monotherapy in early PD and significantly delay the requirement for L-DOPA (Myllyla *et al.*, 1993). Commonly prescribed MAO-B inhibitors include selegiline and rasagiline. Examples of COMT inhibitors include entacapone and tolcapone; though tolcapone has a longer half life and shows more potent inhibition of COMT (Forsberg *et al.*, 2003), due to hepatotoxicity issues it is generally only prescribed for patients in whom entacapone is ineffective (Lees, 2008).

L-DOPA significantly improves the cardinal motor symptoms of PD and is considered the gold standard treatment for the disease (Barbeau, 1969; Fahn, 2004; Godwin-Austen *et al.*, 1969; Vu *et al.*, 2012). However this treatment is not without side effects. In the short term these can include nausea and hypotension, which tend to be dose-related (Godwin-Austen *et al.*, 1969), but in the long term patients can develop debilitating involuntary movements that may overtake the therapeutic actions of L-DOPA. This is termed L-DOPA-Induced Dyskinesia (LID) and is explored later in this chapter (section 1.5.1). In addition there is some controversy regarding whether L-DOPA could have a toxic effect via its autoxidation into reactive derivatives, similarly to dopamine (described in section 1.2.1). However this toxicity was observed only *in vitro* (Basma *et al.*, 1995; Jin *et al.*, 2010), whereas experiments in preclinical models and clinical trials have found no evidence for a neurotoxic effect of L-DOPA *in vivo* (Datla *et al.*, 2001; Parkkinen *et al.*, 2011; Rajput, 2001).

1.4.1.2 Dopamine receptor agonists

The second dopamine replacement strategy used for treatment of PD symptoms is dopamine receptor agonists, which can be prescribed as monotherapy to delay the introduction of L-DOPA or as an adjunct to allow reduction of the necessary dose of L-DOPA. These mainly act at D2-like receptors, though mixed D1-like/D2-like receptor agonists such as pergolide and apomorphine are occasionally prescribed. Commonly prescribed D2-like dopamine receptor agonists include pramipexole, bromocriptine and ropinirole. Stimulation of D2-like receptors inhibits activation of striatopallidal neurones in the overactive indirect pathway, correcting basal ganglia output (the pathways of the BG and the roles of D1 and D2 receptors were described in more detail in section 1.3). Receptor agonists do not rely on enzymatic activity within, or storage and release by existing dopaminergic cells, so bypass problems such as reduced AADC levels and reduced numbers of dopaminergic neurones. They may also reduce the risk of developing dyskinesia, as has been demonstrated in both animal models (Bédard *et al.*, 1986; Peace *et al.*, 1998) and clinical trials (Holloway *et al.*, 2004; Rascol *et al.*, 2000). This is believed to result from their longer half life in comparison with L-DOPA, which provides a more continuous dopaminergic stimulus. However, dopamine agonists carry a higher risk than L-DOPA of side effects such as impulse control disorders (e.g. hypersexuality, pathological gambling) and hallucinations, so are not suitable for all patients (Antonini *et al.*, 2009).

1.4.2 Non-dopaminergic strategies

Along with degeneration of the nigrostriatal tract, PD involves changes in other neurotransmitter systems, including noradrenaline (norepinephrine), glutamate and acetylcholine. Several drugs that target these systems are also in use as antiparkinsonian therapies, usually as an adjunct to dopamine replacement strategies, or are currently in clinical trials.

Although more commonly prescribed for LID, there is evidence that the partial NMDA receptor antagonist amantadine also has antiparkinsonian actions (Brenner *et al.*, 1989; Pinter *et al.*, 1999; Schwab *et al.*, 1969). In addition, the NMDA receptor antagonist memantine has shown efficacy against axial motor symptoms in a recent clinical trial (Moreau *et al.*, 2013). Another antiglutamatergic strategy that has shown some benefit is the glutamate release inhibitor safinamide (Stocchi *et al.*, 2004; Stocchi *et al.*, 2012), though this drug has other potential antiparkinsonian mechanisms such as MAO-B inhibition and inhibition of dopamine reuptake that could also contribute to this effect (Caccia *et al.*, 2006).

Given the negative correlation between smoking and incidence of PD (Gorell *et al.*, 1999; Hernán *et al.*, 2001), and the close association between the dopaminergic and cholinergic systems (Quik *et al.*, 2011), it is not surprising that cholinergic signalling has also been investigated with regard to PD. Indeed the first antiparkinsonian medications to be prescribed were anticholinergics, though they are efficacious mainly against tremor and do not ameliorate akinesia and rigidity as well as dopamine replacement strategies (Schrag *et al.*, 1999). Though clinical trials have not consistently found an antiparkinsonian benefit for nicotine (reviewed by Quik *et al.*, 2011), the antiparkinsonian potential of targeting cholinergic signalling is still being investigated, especially for problems with posture and gait (Gurevich *et al.*, 2014; Henderson *et al.*, 2013).

1.4.3 Surgical strategies

Along with pharmacological therapies, there are also surgical options for the alleviation of PD symptoms. Due to the high costs and specialised training associated with surgery, as well as the risk of haemorrhage and infection for the patient, these options are often a last resort for patients that are refractory to alternative treatments.

Initially, surgical ablation of the thalamic nuclei, GPi or STN was carried out and found to have symptomatic benefits in patients, with thalamotomy mainly ameliorating tremor (Duval *et al.*, 2006; Friehs *et al.*, 1995) and subthalamotomy and pallidotomy ameliorating all motor symptoms (Alvarez *et al.*, 2009; Baron *et al.*, 1996; Çoban *et al.*, 2009; Lozano *et al.*, 1995).

The accidental discovery in 1987 that a similar, reversible effect could be achieved by high frequency (≥100 Hz) electrical stimulation of the thalamus, GPi or STN (Benabid *et al.*, 1991; Limousin *et al.*, 1995) led to deep brain stimulation (DBS) largely supplanting irreversible ablation surgery as a means of treating PD symptoms. DBS of the STN or GPi gives long-lasting improvements in bradykinesia, rigidity, tremor and gait, along with alleviating motor complications such as dyskinesia (Benabid *et al.*, 2009; Rodriguez-Oroz *et al.*, 2012). Bilateral stimulation of the STN is generally believed to give the most reliable motor improvements and allow the largest reduction in L-DOPA dose (Anderson *et al.*, 2005; DBS For Parkinson's Disease Study Group, 2001). However recent evidence suggests that stimulation of the two nuclei gives a similar antiparkinsonian benefit but can elicit worsening or improvement of different non-motor symptoms (Follett *et al.*, 2010),therefore this may prove to be a deciding factor for some patients.

Initially, due to the similar clinical outcome, it was believed that DBS had a similar effect to lesioning on neuronal signalling in these nuclei, i.e. inhibition, via local depolarisation block (Beurrier *et al.*, 2001). However over recent years a paradoxical activation of subthalamic neurones has been reported following STN-DBS (Hashimoto *et al.*, 2003; Stefani *et al.*, 2005; Windels *et al.*, 2000), raising the question of how two seemingly opposing mechanisms can have the same clinical effects. Current understanding leans towards the interruption by the electrical stimulation of the pathological synchronous β-oscillatory activity (13-30 Hz) in the BG that is associated with PD (Kang *et al.*, 2013; Moran *et al.*, 2011). This mechanism was mentioned in the previous section (1.3.3.5) and is reviewed in detail elsewhere (Deniau *et al.*, 2010; Hammond *et al.*, 2008).

1.5 Unmet Clinical Needs

The major unmet clinical need with the current pharmacological therapies used for treatment of PD is that they do not address the continuing degeneration of the nigrostriatal tract, although there is some suggestion that disease progression is delayed by dopamine agonists when compared with levodopa (ParkinsonStudyGroup, 2002; Whone *et al.*, 2003). Providing a means to protect the neurones that remain in the SNc at the time of diagnosis is a central objective in the PD field, as it would allow the prevention or slowing down of the loss of dopaminergic terminals that leads to both progressive worsening of PD symptoms and an increased likelihood of developing L-DOPA-related complications. As such, the hunt for neuroprotective therapies has been the focus of extensive preclinical research, including testing of antioxidant therapies and growth factors among many others, however as yet none of these therapies has successfully been approved for use in man. The use of antiglutamatergic strategies as a potential neuroprotective strategy is one of the major focuses of this thesis.

Similarly, the therapies currently used for treatment of PD do not aid regeneration of the nigrostriatal pathway and this is another area of intensive research. Indeed while several attempts to treat PD using embryonic dopaminergic grafts in the striatum have been reported to be successful up to 5 years after transplantation, especially in younger patients (Freed *et al.*, 2001; López-Lozano *et al.*, 1997; Ma *et al.*, 2010), due to the mixed reports of success and the development of side effects such as graft-induced dyskinesia the widespread clinical utility of this approach is still a long way off (Brundin *et al.*, 2010).

As mentioned earlier, the PD therapies that are currently available also have limitations in terms of the side effects they elicit. While issues such as addictive behaviours (dopamine agonists) and nausea (L-DOPA) can often be alleviated by changing to a different treatment strategy, adding in adjuvant therapies or altering the dose, long-term treatment with L-DOPA can have much more long-lasting detrimental side effects, namely the development of dyskinesia.

In addition to this, current treatments do not address the variety of levodopa-unresponsive non-motor symptoms that can both precede and occur simultaneously with PD. These are often the symptoms that are the most detrimental to patient quality of life, especially while dopamine replacement strategies are still efficacious against motor symptoms (Martinez-Martin, 2011).

1.5.1 Levodopa-induced dyskinesia

Levodopa-induced dyskinesia (LID) is a phenomenon that affects around 40% of Parkinson's disease patients within 5 years of starting treatment with L-DOPA (Ahlskog *et al.*, 2001). It represents a major limiting factor in treatment of the symptoms and therefore efforts are being made to develop treatments that can reduce its incidence or severity.

LID manifests in patients as involuntary dystonic and/or choreic movements of the trunk, limbs and face, most commonly when the plasma concentration of dopamine is high ('peak dose' dyskinesia). Though this 'peak-dose dyskinesia' is the most common, it is also the least disabling of the types of dyskinesia related to levodopa use. 'Off-period dyskinesia' (when no drug is in the patient's system) and 'diphasic dyskinesia' (which manifests upon the rise and fall of L-DOPA concentration at the start and end of a dose) often involve painful dystonia of the lower limbs and feet, whereas peak dose dyskinesia is more frequently of the choreic form (reviewed by Fabbrini *et al.*, 2007). However, as PD progresses the severity of peak dose dyskinesia can increase and has a significant detrimental effect on quality of life (Chapuis *et al.*, 2005; Péchevis *et al.*, 2005).

Along with the self-evident exposure-related risk factors such as longer duration of L-DOPA treatment and increased daily dose, there are several other factors that have been reported to be associated with the development of LID. These include dopamine D2 receptor polymorphisms (Oliveri *et al.*, 1999; Rieck *et al.*, 2012), presence or absence of resting tremor (Kipfer *et al.*, 2011), and smoking status (Strong *et al.*, 2006). While these may help identify susceptible patients, allowing delay of L-DOPA administration in favour of alternative antiparkinsonian agents such as dopamine agonists, eventually most patients

will require L-DOPA to control their symptoms and will therefore be at risk of developing LID.

L-DOPA-associated motor complications became apparent soon after its approval for treatment of PD symptoms (Cotzias *et al.*, 1969) but the underlying mechanisms are complex and are still not fully understood some 45 years later. Once established, LID does not reverse and although reducing the L-DOPA dose can alleviate the severity of dyskinesia it is often at the expense of the antiparkinsonian benefits. There is inconsistent evidence on the efficacy of an L-DOPA 'holiday' for amelioration of existing dyskinesia (Rascol, 2000), which at best has a transient effect (Koller *et al.*, 1981; Weiner *et al.*, 1980). The causes of dyskinesia seem to vary depending on what type a patient has (reviewed by Brotchie, 2005) but given the nature of the experiments performed in this thesis I will focus only on peak-dose dyskinesia.

There are two main requirements for the development of LID in PD patients: severe dopamine denervation and pulsatile exposure to dopaminergic medication. As the nigrostriatal degeneration underlying PD progresses, the patient will have a diminishing number of dopaminergic terminals in the striatum, and thus a diminishing capacity to buffer the sudden influx of L-DOPA associated with an acute dose. Consequently striatal dopamine receptor activation will no longer be determined by physiological release from nigrostriatal neurones, but will more closely reflect the drug bioavailability and pharmacokinetics. In addition to this, serotonergic and noradrenergic terminals also possess the necessary AADC to convert L-DOPA into dopamine, so when dopaminergic terminals are lost the L-DOPA is taken up, converted into dopamine and released by these neurones instead as a 'false neurotransmitter' (Tanaka *et al.*, 1999). Indeed increased integrity of the serotonergic system has been shown to be associated with increased incidence of LID in patients (Politis *et al.*, 2014). This nonphysiological and pulsatile exposure to dopamine leads to alterations in the signalling of a variety of other neurotransmitter systems within the BG motor loop, and this combination of erratic dopamine release and dysregulated dopamine response is believed to underlie dyskinesiogenesis (Lindgren *et al.*, 2010). The cellular and molecular mechanisms underlying the development and expression of peak-dose dyskinesia are explored in detail in Chapter 6.

Current treatments focus on reduction of the erratic exposure of the striatum to dopamine, often by fragmentation of L-DOPA doses, use of sustained release formulas, or continuous

drug infusion (for example Duodopa®). These methods aim to prevent the induction or delay the worsening of early dyskinesia, as per the continuous dopaminergic stimulation concept (Stocchi, 2009). This approach is not always successful. There are data suggesting that sustained release formulations of L-DOPA do not significantly reduce peak dose dyskinesia in preclinical models (Papathanou *et al.*, 2012) or patients (Jensen *et al.*, 1988), however other studies have shown reduced LID severity preclinically using L-DOPA-loaded nanoparticles or microspheres (Yang *et al.*, 2012a; Yang *et al.*, 2012b). There is also clinical evidence that L-DOPA infusion (Nyholm *et al.*, 2003) or slow release preparations (Ghika *et al.*, 1997) reduce dyskinesia, and a novel approach reducing phasic dopamine release by depletion of vesicular dopamine storage also reduced severity of LIDs (Brusa *et al.*, 2013). A potential alternative way of prolonging the effect of L-DOPA was recently demonstrated in a rodent model of dyskinesia, whereby administration of a more potent, deuterated form of L-DOPA that is more resistant to enzymatic breakdown reduced the required dosage and thereby reduced the risk of dyskinesia in these rats (Malmlöf *et al.*, 2010).

Amantadine, a weak NMDA receptor antagonist, is the only commonly prescribed antidyskinetic drug at present, suggesting that targeting glutamate signalling is clinically efficacious. However its duration of effect has been questioned and therefore there is a clear need for the development of new therapies that can either delay the onset, or suppress the expression of LID.

1.5.2 Non-motor symptoms

Parkinson's disease is associated with an array of non-motor symptoms that are not alleviated by dopamine replacement strategies and can have a severe impact on the patient's quality of life. These affect up to 90% of PD patients (McDowell *et al.*, 2012) and include sleep disorders such as Rapid Eye Movement (REM) Sleep Behaviour Disorder (RBD), daytime somnolence and restless leg syndrome; neuropsychiatric disorders such as depression, anxiety, apathy, cognitive impairment and dementia; autonomic disturbances such as constipation, urinary incontinence and orthostatic hypertension; and pain (Chaudhuri *et al.*, 2006).

Currently, non-motor symptoms are treated using drugs developed for these conditions in the absence of comorbid PD (e.g. selective serotonin reuptake inhibitors for depression, anticholinergics for urinary incontinence; Lees *et al.*, 2009), however extrapyramidal PD pathology may underlie several of these symptoms and little work has been done to ascertain the aetiology of these symptoms specifically in PD patients. There is considerable

evidence that non-motor symptoms including hyposmia, anxiety, RBD and autonomic dysfunction result from PD-related degeneration or LB pathology in non-dopaminergic systems, such as the serotonergic dorsal raphe nucleus, noradrenergic locus coeruleus and cholinergic nucleus basalis of Meynert (Dickson *et al.*, 2009; Doty, 2012; McCarter *et al.*, 2012; Prediger *et al.*, 2012). As such, it is perhaps not surprising that these symptoms are not alleviated by dopaminergic treatments.

One of the difficulties in ascertaining whether a common pathophysiological mechanism underlies each of these non-motor symptoms in PD compared with the non-PD population is the lack of preclinical models that display these symptoms, or the difficulty in identifying and quantifying their presence. However, in recent years genetic models have provided some insights into the development of non-motor symptoms. For example, cognitive impairment that precedes motor dysfunction has been identified in Mitopark® mice (Li *et al.*, 2013), sleep abnormalities have been described in α-synuclein over-expressing mice (Kudo *et al.*, 2011), and gastrointestinal dysfunction has been noted in A53T α-synuclein transgenic mice (Noorian *et al.*, 2012) and also LRRK2 transgenic mice (Bichler *et al.*, 2013). Another paper reported that vesicular monoamine transporter 2 (VMAT-2)-deficient mice develop a PD phenotype with multiple non-motor manifestations such as anxiety, constipation and sleep disturbances (Taylor *et al.*, 2009). In addition to transgenic models, non-motor symptoms are increasingly being recognised in classical models of PD, for example sleep disorders have been noted in MPTP-treated marmosets (Verhave *et al.*, 2011) and gastrointestinal dysfunction, cognitive abnormalities and depressive-like symptoms have been described in 6-OHDA-lesioned rats (Casas *et al.*, 2011; Colucci *et al.*, 2012). These studies provide hope that the specific aetiologies of these symptoms on a background of PD can now be better investigated, along with identification of the most effective treatments.

1.6 Role of Glutamate in PD

Glutamate is the most abundant excitatory neurotransmitter in the mammalian central nervous system and plays a key role in the BG. As previously noted in section 1.3.1, the only glutamatergic nucleus within the BG is the STN, but alongside this the main inputs into the BG from the cortex are also glutamatergic, as well as some afferents originating in the PPN. Hyperactivity of the STN has been consistently shown in the parkinsonian state, along with enhanced corticostriatal signalling (Anglade *et al.*, 1996; Smith *et al.*, 2009), enhanced

corticosubthalamic signalling (Dejean *et al.*, 2008) and increased activity in the PPN (Breit *et al.*, 2006), therefore a global attenuation of glutamatergic signalling might be beneficial in PD.

Given the target nuclei of the STN in the model of the basal ganglia described in section 1.3.3, attenuation of glutamatergic signalling at the subthalamonigral synapse might particularly be expected to have antiparkinsonian effects. Reduced subthalamo-SNr activity would in turn reduce the inhibitory output of the SNr/EPN on thalamocortical feedback, and would therefore be expected to promote motor function. Indeed, interruption of activity within the hyperactive STN via surgical ablation or high frequency stimulation successfully ameliorates motor symptoms (section 1.4.3). Given the risk of infection, haemorrhage and incorrect lesion/electrode placement associated with these techniques, as well as the associated training and procedure costs, attenuation of glutamatergic signalling via pharmacological means would be a preferable way of achieving this result.

As well as symptomatic improvements, attenuation of glutamate release from the STN into the SNc might potentially slow the ongoing degeneration of dopaminergic cells in the nigrostriatal projection by inhibiting glutamate excitotoxicity (see section 1.2.5 for a detailed explanation of this process), thereby delaying the progression of the disease. Excessive subthalamonigral excitatory signalling is sufficient to cause degeneration of SNc neurones *in vivo* (Assous *et al.*, 2014), so it is likely that the overactivity of this synapse in PD also contributes to the ongoing degeneration in the human brain. Evidence for targeting glutamate release from the hyperactive STN as a neuroprotective strategy includes the findings that lesioning or high-frequency deep brain stimulation of the STN is neuroprotective in both the 6-OHDA rat model (Carvalho *et al.*, 2001; Maesawa *et al.*, 2004; Piallat *et al.*, 1996; Temel *et al.*, 2006) and the MPTP primate model (Wallace *et al.*, 2007). However, evidence for a neuroprotective or disease stabilising effect of this strategy in humans in inconsistent (Hilker *et al.*, 2005; Krack *et al.*, 2003; Østergaard *et al.*, 2006; Visser-Vandewalle *et al.*, 2005).

Glutamate signalling occurs via two groups of receptors: the fast-conducting ionotropic glutamate receptors and the slower G-protein coupled metabotropic glutamate receptors, which modulate the excitability of pre- and post-synaptic neurones. In this section these receptor types are explored in relation to their signalling, their location in the BG and their potential as targets for antiparkinsonian/neuroprotective therapies. Their potential as

targets for antidyskinetic therapies is explored in Chapter 6 and is therefore not introduced here.

1.6.1 Ionotropic glutamate receptors

Ionotropic glutamate receptors are (generally) post-synaptic ligand-gated ion channels and are subdivided into three groups defined by their preferred agonists: α-amino-3-hydroxy-5-methyl-4-isoxazolepropionic acid (AMPA), *N*-methyl-D-aspartate (NMDA) and kainate. All ionotropic receptor types mediate rapid excitation of the postsynaptic neurone in response to glutamate, therefore antagonists or negative allosteric modulators at these receptors are of therapeutic interest in the parkinsonian situation, where glutamatergic activity is increased.

All ionotropic glutamate receptors are composed of multiple subunits, each with three transmembrane domains (M1, M3, M4) and one re-entrant membrane loop (M2) on the cytoplasmic side. The M2 loop forms part of the ion pore, and amino acid residues within this region determine ion permeability, especially that of calcium. Ligand binding occurs at sites within the external segments S1 and S2, bringing the extracellular loops together and opening the ion pore (Kew *et al.*, 2005).

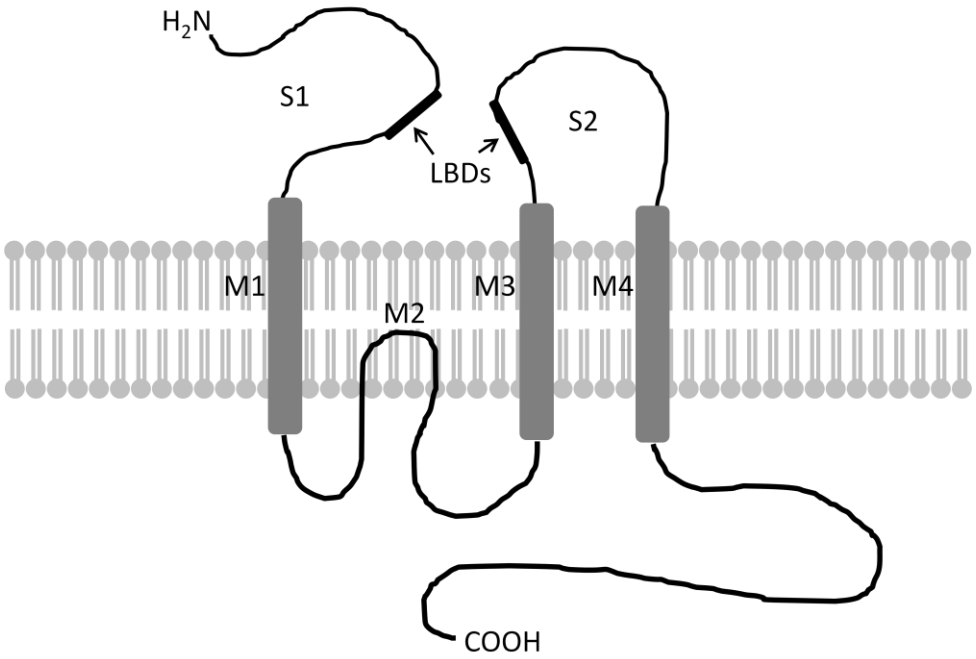

Figure 5: General structure of an ionotropic glutamate receptor subunit. The final receptor is a tetramer of these subunits. Binding of the ligand (glutamate/glycine) at the ligand binding domains (LBDs) of external segments S1 and S2 causes a conformational change in the receptor that leads to opening of the cation pore formed by the re-entrant membrane loop M2. The specific amino acids within this loop in different subunits alter the permeability of the ion channel to calcium.

1.6.1.1 AMPA receptors

Structure and signalling:

AMPA receptors are tetrameric receptors composed of GluR1-4 subunits. They are often composed of a 'dimer of dimers', with a GluR2 dimer and a second homodimer of another subunit type (Tichelaar *et al.*, 2004). AMPA receptor tetramers form an ion-permeable pore in the post-synaptic membrane and, upon activation by ligand binding, facilitate rapid depolarisation via influx of cations. Conductance through the AMPA receptor pore is dependent on the degree of ligand binding, requiring a minimum of 2 occupied sites and increasing up to 4 occupied sites (Rosenmund *et al.*, 1998).

Variations in subunit composition confer specific properties on AMPA receptors, for example receptors that lack GluR2 subunits are permeable to sodium (Na^+), potassium (K^+) and calcium (Ca^{2+}) ions, whereas the presence of GluR2 renders a receptor impermeable to Ca^{2+} and therefore may protect against excitotoxicity (Kim *et al.*, 2001). The calcium impermeability property of GluR2 is due to a substitution of an arginine residue in the M2 domain where in other subunits this amino acid is a glutamine. In addition to this, a further level of diversity is added by the alternative splicing of 'flip' and 'flop' variants in the extracellular domain of each subunit between M3 and M4, which affects receptor channel opening and closing kinetics (Pei *et al.*, 2009). Like many receptors, phosphorylation of AMPA subunits also represents an important means of regulation (Wang *et al.*, 2005).

Expression in the BG:

The expression of AMPA receptor subunits varies throughout the BG, with GluR1-3 expressed in striatal MSNs, the EPN/GPi and the SNc and GluR1 and/or GluR4 expressed in the STN, EPN/GPi and SNr. Additionally GluR4 is expressed by glial cells (Greenamyre, 2001). With particular regard to glutamatergic signalling in the SNc, rat nigral dopaminergic neurones primarily express GluR2/3 subunits, with a heterogeneous expression of GluR1 subunits that is higher in the ventral tier of the SNc than the dorsal tier (Albers *et al.*, 1999).

Antiparkinsonian potential:

As mentioned above, antagonists of AMPA receptors might be expected to have an antiparkinsonian effect, however evidence for the efficacy of targeting AMPA receptors in PD is inconsistent. Symptomatic relief has been demonstrated using the AMPA receptor antagonist NBQX in rodent and primate models of PD (Klockgether *et al.*, 1991), while others reported no symptomatic improvements using the same compound (Luquin *et al.*,

1993). In several cases (using NBQX and CX516), a symptomatic improvement was found that acted synergistically with dopamine replacement therapies (Konitsiotis *et al.*, 2000; Loschmann *et al.*, 1991; Wachtel *et al.*, 1992), suggesting that AMPA ligands may work well as adjunct therapies.

The neuroprotective efficacy of the AMPA antagonist Talampanel has been demonstrated in rodent models of ischemic stroke (Denes *et al.*, 2006; Erdo *et al.*, 2005), however when the AMPA/kainate dual antagonist CNQX and AMPA antagonist NBQX were tested against MPP^+ toxicity in the rat they showed no neuroprotective effect (Turski *et al.*, 1991), and a similar lack of protection was found for NBQX in the 6-OHDA-lesioned rat (Blandini *et al.*, 2001). Interestingly, AMPA receptor potentiators such as LY503430 and LY404187 *do* show a neuroprotective effect in the 6-OHDA-lesioned rat model of PD (Murray *et al.*, 2003b; O'Neill *et al.*, 2004). This seemingly paradoxical protection brought about by potentiation of glutamatergic signalling is thought to involve increases in brain-derived neurotrophic factor production and cell proliferation.

Thus from the preclinical data the most promising use for AMPA antagonists in PD was as an adjunct therapy alongside dopamine replacement strategies. Unfortunately this did not translate into the human disease, as when the AMPA antagonist Perampanel was tested in the clinic there was no improvement in motor scores during L-DOPA-related 'on' time in Perampanel-treated patients versus placebo (Lees *et al.*, 2012). As such, AMPA antagonists are no longer being actively pursued as potential therapeutic targets in PD.

1.6.1.2 NMDA receptors

Structure and signalling:

NMDA receptors are heterotetrameric and are generally composed of two GluN1 and two GluN2 subunits, usually as a dimer of dimers. GluN1 (NR1) is encoded by a single gene but there are eight functional splice variants of this receptor subunit; GluN2 is encoded by a family of four genes, GluN2A-D (NR2A-D). Of the GluN2 subunits the most highly expressed in the mammalian forebrain are GluN2A and GluN2B, with GluN2A largely present in synaptic NMDA receptors and GluN2B largely present in extrasynaptic NMDA receptors, though this segregated distribution is not absolute (Groc *et al.*, 2009). NMDA receptors containing GluN2A have higher opening probability and faster deactivation kinetics than receptors containing GluN2B, but GluN2B has the higher affinity for glutamate of the two (Sanz-Clemente *et al.*, 2013). The differential spatial distribution, ligand affinity and kinetics

of these receptor subunits might have important consequences for excitotoxicity. Activation of NMDA receptors requires the binding of glycine to both GluN1 subunits and glutamate to both GluN2 subunits. It also requires depolarisation of the membrane in order to relieve the magnesium ion (Mg^{2+}) block, a process that is mediated by antecedent AMPA receptor activation. When all of these conditions are met, the ion channel opens to allow Ca^{2+} and Na^{+} influx and K^{+} efflux. In NMDA receptors the permeability to Ca^{2+} is determined by the presence of asparagine or glutamine residue within the M2 region (Burnashev *et al.*, 1992).

In addition to the five genes encoding GluN1 and GluN2A-D, there are two genes encoding GluN3A and GluN3B subunits (NR3A-B) which can assemble alongside these subunits. While GluN3 subunits were previously thought to only act as dominant negative regulators of GluN1 and GluN2 subunits, a specific developmental role for these receptors is currently being elucidated. GluN3A subunits are also proposed to be involved in synaptic plasticity and can additionally form an excitatory glycine-activated receptor in combination with GluN1, with reduced Ca^{2+} permeability that is insensitive to Mg^{2+} block (reviewed by Kehoe *et al.*, 2013).

Expression in the BG:

GluN1 subunits are expressed throughout all nuclei of the BG, as would be expected given their requirement for the formation of functional receptors, alongside GluN2D. GluN2A and GluN2B are expressed mainly in the striatum and GluN2C is restricted to the SNc (Greenamyre, 2001). The strong expression of GluN2C/D in the dopaminergic neurones of the SNc, compared with weaker expression of GluN2A/B (Albers *et al.*, 1999), is particularly interesting due to the unique properties of NMDA receptors containing the 2C/2D subunits; namely a less potent Mg^{2+} block that is rapidly overcome compared with GluN2A and GluN2B subunits (Clarke *et al.*, 2013), meaning that these receptors might not rely on concomitant depolarisation alongside ligand binding for activation. Previous studies have suggested that the majority of NMDA receptors present on dopaminergic SNc neurones are GluN1/GluN2B/GluN2D triheteromers (Brothwell *et al.*, 2008; Jones *et al.*, 2005), suggesting that inhibitors of any of these subunits might inhibit excitotoxic cell loss in the context of Parkinson's disease.

Antiparkinsonian potential:

Given that glutamatergic neurotransmission is increased in the parkinsonian situation, it is expected that antagonists of NMDA-mediated signalling would have an antiparkinsonian

effect. Indeed, inhibition of NMDA-mediated glutamatergic transmission using systemically-administered antagonists such as MK-801, amantadine and SDZ 220-581 successfully reverses motor dysfunction in preclinical symptomatic models of PD including reserpine-induced akinesia (Carlsson *et al.*, 1988; Danysz *et al.*, 1994) and haloperidol-induced catalepsy (Danysz *et al.*, 1994; Hauber *et al.*, 1990; McAllister, 1996). Based on a local administration study using CPP, the sites of action of NMDA antagonists within the BG are the STN, EPN/GPi and SNr (Klockgether *et al.*, 1990).

NMDA receptor inhibition also shows neuroprotective potential, as has been demonstrated in 6-OHDA-lesioned rats using MK-801 infused into the STN (Blandini *et al.*, 2001), in MPTP-treated rodents following systemic administration of (R)-HA-966 or MK-801 or local nigral injection of AP7, CPP or MK-801 (Brouillet *et al.*, 1993; Kanthasamy *et al.*, 1997; Turski *et al.*, 1991), and in primates when MPTP was coadministered with MK-801 or CPP (Lange *et al.*, 1993; Zuddas *et al.*, 1992). All of these compounds non-specifically inhibit signalling via GluN1/GluN2 receptors, for example MK-801 inhibits ion flow through the ion channel, amantadine accelerates ion channel closing, (R)-HA-966 is a competitive inhibitor of the glycine site on GluN1, and SDZ 220-581, and AP7 and CPP are competitive inhibitors of the glutamate binding site on GluN2. However, the adverse effects relating to widespread inhibition of NMDA-mediated signalling, such as the development of schizophrenia-like cognitive dysfunction (Krystal *et al.*, 2005), mean that this is not a viable therapeutic option for patients.

In an attempt to avoid these side effects, recent attention has turned to inhibiting specific NMDA receptor subunits, most often GluN2B (NR2B). GluN2B subunits have a higher affinity for glutamate than GluN2A subunits and are generally found in extrasynaptic NMDA receptors, which are associated with excitotoxicity. Importantly from the point of view of neuroprotection in parkinsonism, GluN2B subunits form part of the triheteromeric NMDA receptors found on SNc neurones and therefore inhibition of signalling at receptors containing this subunit could also reduce excitotoxic cell loss. The GluN2B-specific antagonists Ro 25-6981, Ifenprodil, Eliprodil and CP-101,606 have been shown to reduce parkinsonian symptoms in a variety of rodent and primate models (Loschmann *et al.*, 2004; Nash *et al.*, 2000; Nash *et al.*, 1999; Steece-Collier *et al.*, 2000). In addition to symptomatic improvements, neuroprotective effects have been reported following systemic administration of the GluN2B-specific antagonists BZAD01 (Leaver *et al.*, 2008) and Ifenprodil (Riquelme *et al.*, 2012) in the 6-OHDA-lesioned rat. Unfortunately the positive

preclinical data has not thus far translated into a positive clinical outcome in PD patients, for example no motor improvements were found following acute treatment with MK-0657 (Addy *et al.*, 2009). In addition, it seems that GluN2B-specific antagonists can also cause cognitive adverse events in patients, for example when the GluN2B-specific inhibitor CP-101,606 was tested in clinical trials against L-DOPA-induced dyskinesia it elicited unwanted side effects such as dissociation and amnesia (Nutt *et al.*, 2008). This might mean that GluN2B-specific antagonists also prove unsuitable as antiparkinsonian therapies.

1.6.1.3 Kainate receptors

Structure and signalling:

Kainate receptors are the least well characterised of the ionotropic glutamate receptors. Kainate receptors are tetrameric and composed of GluK1-3 (GluR5-7), and GluK4-5 (KA-1 and KA-2) subunits. GluK1-3 subunits can form functional homomeric receptors but GluK4-5 subunits need to combine with GluK1-3 subunits in heteromeric assemblies in order to function (Kew *et al.*, 2005). Alternative splicing and RNA editing of these subunits adds further diversity to the mature receptors.

Similarly to AMPA receptors, kainate receptors are permeable primarily to Na^+ and K^+ but less so to Ca^{2+} (Huettner, 2003). They are predominantly located post-synaptically, where they depolarise and activate the neurone on which they reside, mediating excitatory neurotransmission. In addition, kainate receptors have been localised to presynaptic sites, where their stimulation reduces neurotransmitter release at both glutamatergic and GABAergic synapses; however the mechanism behind this has not been elucidated and it is possible that the effect is indirect, involving kainate-induced release of endogenous neurotransmitters such as glutamate under experimental conditions where this has not been controlled for (Huettner, 2003). GluK1 and GluK2 can be edited at the RNA stage, leading to the presence of an arginine residue within the M2 region in place of a glutamine residue, thus reducing the permeability of the ion channel to Ca^{2+} (Burnashev *et al.*, 1995).

Expression in the BG:

Within the rodent BG, mRNA for kainate receptor subunits is expressed in all regions of the basal ganglia, though GluK1 and GluK4 are less widely distributed (Bischoff *et al.*, 1997; Wullner *et al.*, 1997). Within the SNc in particular there is moderate to high expression of GluK1-3 and GluK5, which colocalises with TH, suggesting that kainate receptors are expressed in dopaminergic neurones. Whether these receptors are located pre- or post-

synaptically in these regions is not known. Additionally, kainate receptors are located in the cortex, where they contribute to thalamocortical transmission (Huettner, 2003), so there is a clear role for these receptors in BG function.

Antiparkinsonian potential:

As in the case for the other ionotropic glutamate receptors, antagonists of kainate receptors might be expected to have an antiparkinsonian effect, however there are few kainate receptor-specific antagonists available, and commonly-used antagonists such as CNQX and DNQX are also antagonists at AMPA receptors, meaning that a specific role for kainate receptors cannot be elucidated. A novel antagonist that preferentially inhibits kainate receptors over AMPA receptors is NS102 (Johansen *et al.*, 1993), however there are no published reports into the use of this compound in parkinsonian symptomatic or neurodegenerative models. An alternative kainate-specific antagonist is LY377770, which acts at GluK1 (previously known as GluR5). Though it has not been tested in a model of parkinsonism there is a published report showing neuroprotection when LY377770 was administered in a model of ischaemic stroke, which was associated with improvements in locomotor performance (O'Neill *et al.*, 2000). Therefore there is potential that with further development of kainate receptor-specific ligands, the potential antiparkinsonian and neuroprotective effects of targeting signalling at these receptors could be examined.

1.6.2 Metabotropic glutamate receptors

Metabotropic glutamate receptors (mGlu receptors) are a family of eight Class C G-protein coupled receptors (GPCRs). Unlike ionotropic glutamate receptors, which mediate fast excitatory neurotransmission, mGlu receptors play a modulatory role in both excitatory and inhibitory neurotransmission via regulation of neuronal excitability and neurotransmitter release. mGlu receptors are divided into three groups on the basis of sequence homology, downstream signalling and pharmacology; group I mGlu receptors ($mGlu_1$, $mGlu_5$), group II mGlu receptors ($mGlu_2$, $mGlu_3$) and group III mGlu receptors ($mGlu_4$, $mGlu_6$, $mGlu_7$, $mGlu_8$).

Structurally, mGlu receptors have seven α-helical transmembrane domains (TM1-7) along with a hinged globular 'venus fly trap' ligand binding domain (VFD) at the N terminus (Figure 6). Ligand binding at the VFD causes a conformational change and this triggers activation of the intracellular heterotrimeric guanosine nucleotide binding proteins (G proteins) with which the receptor is coupled (Kunishima *et al.*, 2000). G proteins are located at the inside of the cell membrane and are thought to associate with the second intracellular loop of the receptor (Gomeza *et al.*, 1996). Upon GPCR activation, the receptor

becomes a guanine nucleotide exchange factor, exchanging the guanosine diphosphate on the Gα subunit for a guanosine triphosphate. When this happens it causes the dissociation of the GTP-Gα complex from the Gβγ complex, and both of these complexes then go on to activate downstream effectors to initiate intracellular signalling cascades (reviewed by Oldham *et al.*, 2008).

Functional mGlu receptors exist in the cell membrane as dimers, linked via disulphide bonds in the cysteine rich region between the VFD and TM1 (Romano *et al.*, 1996). In general these dimers are homomeric, however the formation of heterodimeric mGlu receptors has also been described *in vitro* within group I receptor subtypes and within or between group II and group III receptor subtypes (Doumazane *et al.*, 2011). Further to this, functional $mGlu_2/mGlu_4$ heteromers have very recently been reported *in vivo* in the rodent striatum, with important impacts on pharmacological response to modulation (Yin *et al.*, 2014) due to the necessity of coactivation with ligands at each receptor subtype (Kammermeier, 2012). This added level of complexity is yet to be investigated in detail and will certainly be of interest when it is.

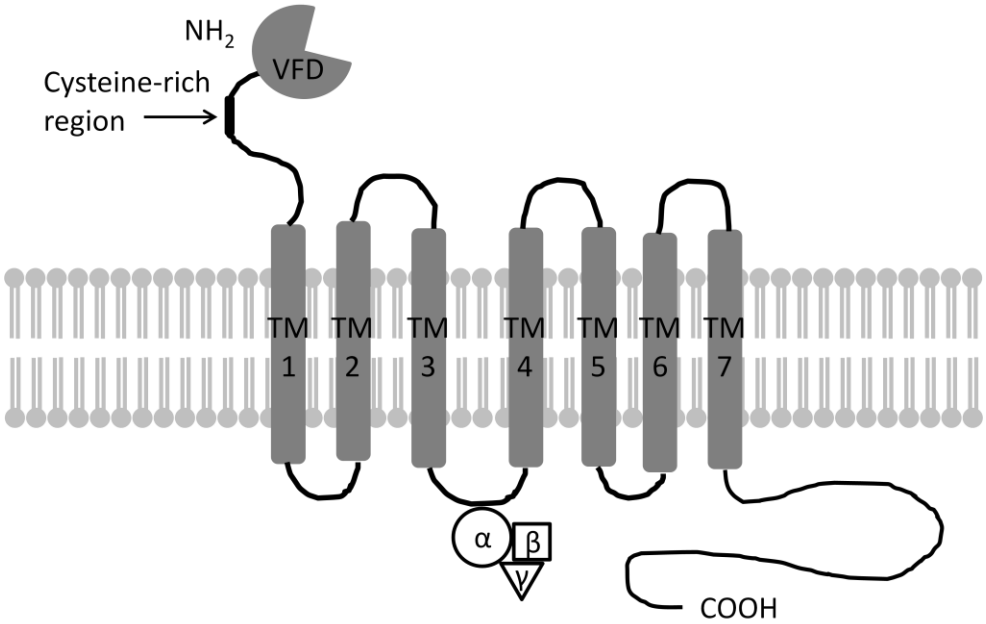

Figure 6: General structure of a metabotropic glutamate receptor monomer. Glutamate and other orthosteric ligands bind within the venus flytrap domain (VFD) at the N terminus of the receptor while allosteric ligands bind within the 7 transmembrane domains. Glutamate/agonist binding causes a conformational change in the receptor that activates the intracellular G protein trimer (α, β, γ) with which the receptor is coupled. mGlu receptors are present in the cell membrane as dimers that are linked by disulphide bridges in the cysteine-rich region between the VFD and TM1.

Activity of mGlu receptors is limited by GPCR kinases (GRKs), which phosphorylate the activated receptor and cause it to associate with β-arrestin proteins, inhibiting its availability to further interact with the G-protein heterotrimer (Gurevich *et al.*, 2012). In addition, certain mGlu receptor subtypes can be post-translationally modified in other ways, including sumoylation and ubiquitination, often with as yet unidentified effects on physiological function (reviewed by Mao *et al.*, 2011).

1.6.2.1 Group I mGlu receptors

Structure and signalling:

Group I mGlu receptors comprise $mGlu_1$ (6 splice variants $mGlu_1$a-f) and $mGlu_5$ (2 splice variants, $mGlu_5$a-b) and are predominantly located at the post-synaptic membrane (Niswender *et al.*, 2010; Shigemoto *et al.*, 1997). Upon ligand binding, this group of receptors couples through $G\alpha_q$, leading to activation of phospholipase C (PLC), which hydrolyses the phosphoinositide phosphatidylinositol-4,5-bisphosphate (PIP_2) that is present within the cytosolic side of the cell membrane, generating diacyl glycerol (DAG) and inositol-1,4,5-trisphosphate (IP_3). IP_3 diffuses into the cytoplasm where it binds to receptors on the endoplasmic reticulum, causing the release of Ca^{2+} into the cytoplasm and thereby generating a slow excitatory post synaptic potential (EPSP) (Congar *et al.*, 1997). In addition, the Ca^{2+} and DAG together activate protein kinase C (PKC), a key regulator of many intracellular cascades (Tanaka *et al.*, 1994) that importantly potentiates the NMDA response by reduction of Mg^{2+} block (Chen *et al.*, 1992). Activation of group I mGlu receptors also regulates ion channel conductance, suppressing M-type K^+ conductance and activating non-specific cation conductances, with the effect of enhancing neuronal excitability (Chuang *et al.*, 2000; Gee *et al.*, 2002; Ikeda *et al.*, 1995). Alongside G proteins, group I mGlu receptors also interact with other intracellular proteins such as Homer proteins and arrestins, which can lead to activation of cascades such as the mitogen-activated protein kinase (MAPK) pathway that influence transcription and are involved in synaptic plasticity (reviewed by Gerber *et al.*, 2007; Hermans *et al.*, 2001).

Expression in the BG:

Group I mGlu receptors are widely expressed in the rodent BG, with a relatively higher expression of mRNA for $mGlu_5$ compared with $mGlu_1$ in most regions (Messenger *et al.*, 2002; Testa *et al.*, 1994), suggesting that $mGlu_5$ would be a good target for normalisation of signalling. Within the SNc there is a higher expression of $mGlu_1$ than $mGlu_5$, suggesting that inhibition of $mGlu_1$ might have neuroprotective effects, and activation of these receptors

causes a Ca^{2+}-independent and Na^{+}-dependent inward current in dopaminergic neurones (Guatteo *et al.*, 1999). In addition to their postsynaptic role, group I mGlu receptors are also thought to be present presynaptically where their activation moderately inhibits neurotransmitter release. Indeed, a reduction of EPSCs/EPSPs has been demonstrated in SNc dopamine neurones upon application of a group I mGlu receptor agonist (Bonci *et al.*, 1997; Wigmore *et al.*, 1998) and also in the striatum, where group I mGlu receptors on nigrostriatal terminals can be activated by glutamate spillover to inhibit dopamine release (Zhang *et al.*, 2003). The mechanism by which this counterintuitive group I-mediated inhibition of neurotransmission occurs has not been confirmed, however in the nigra it has been suggested that it might be an indirect effect attributable to the release of an NMDA receptor-dependent inhibitory retrograde messenger (Wigmore *et al.*, 1998) or secondary to an increased release of GABA (Bonci *et al.*, 1997). In the striatum, the inhibition of dopamine release is likely mediated by $mGlu_1$ and might involve activation of Ca^{2+}-dependent K^{+} channels (Zhang *et al.*, 2003).

Antiparkinsonian potential:

Since group I mGlu receptors predominantly facilitate glutamatergic signalling there has been much interest in the potential antiparkinsonian effects of inhibiting these receptor subtypes using antagonists or negative allosteric modulators. In general it seems that targeting of $mGlu_5$ is a more successful antiparkinsonian and neuroprotective strategy than targeting $mGlu_1$ (Dekundy *et al.*, 2006; Ossowska *et al.*, 2007; Szydlowska *et al.*, 2007). Nevertheless there are reports of neuroprotection at the nigral level with local intracerebral infusion of the $mGlu_1$ antagonist LY367385 in 6-OHDA-lesioned rats (Vernon *et al.*, 2007), which is not unexpected given the abundant $mGlu_1$ expression in the SNc. Reversal of parkinsonian symptoms has been demonstrated using the $mGlu_5$ allosteric antagonists MPEP and MTEP in the haloperidol-induced catalepsy model (Dekundy *et al.*, 2006; Ossowska *et al.*, 2001) and in 6-OHDA-lesioned rats (Ambrosi *et al.*, 2010; Breysse *et al.*, 2002). While this symptomatic relief did not translate into the MPTP-treated primate model using MTEP as a monotherapy (Johnston *et al.*, 2010), there is evidence that a negative allosteric modulator (NAM) of $mGlu_5$, AFQ056, can potentiate the antiparkinsonian effects of a low dose of L-DOPA in this model (Grégoire *et al.*, 2011).

In addition to symptomatic improvements there is a wealth of evidence for a neuroprotective effect of the $mGlu_5$ antagonist MPEP in PD models such as 6-OHDA-lesioned rats (Armentero *et al.*, 2006; Vernon *et al.*, 2005) and MPTP-treated rodents

(Aguirre *et al.*, 2005; Battaglia *et al.*, 2004; Hsieh *et al.*, 2012). Interestingly, Ambrosi *et al.* (2010) reported that in rats with a partial 6-OHDA lesion, chronic treatment with MPEP had a symptomatic effect but did not provide neuroprotection, in contrast to another study using the same model where MPEP was reported to reverse STN hyperactivity and protect against cell loss (Chen *et al.*, 2012).

Though $mGlu_5$ antagonists/NAMs have not been tested in clinical trials for their effects on PD motor function, two NAMs, AFQ056 and dipraglurant, are currently in development as potential antidyskinetic therapies for patients suffering from L-DOPA-induced dyskinesia (Berg *et al.*, 2011; Kumar *et al.*, 2013; Maggos, 2012; Stocchi *et al.*, 2013).

1.6.2.2 Group II mGlu receptors

Structure and signalling:

Group II mGlu receptors comprise $mGlu_2$ (only one form) and $mGlu_3$ (4 splice variants, $mGlu_3$, Δ2, Δ4, Δ2Δ3) and are located predominantly presynaptically in the peri-synaptic zone, though they have also been localised postsynaptically (Niswender *et al.*, 2010; Shigemoto *et al.*, 1997). This group of receptors couples through $G\alpha_{i/o}$, negatively regulating the enzyme adenylate cyclase (AC) and thus reducing the production of the cellular second messenger cyclic adenosine monophosphate (cAMP). This in turn reduces the activity of cAMP-dependent protein kinase A (PKA), reducing phosphorylation of K^+ channels and thereby increasing their activity (Cain *et al.*, 2008; Lesage *et al.*, 2000). In addition, the liberation of Gβγ via $G\alpha_i$ activation leads to inhibition of L-type and N-type Ca^{2+} channels (Chavis *et al.*, 1994; Ikeda *et al.*, 1995; McCool *et al.*, 1996), restricting the entry of calcium into the cell and therefore inhibiting depolarisation and neurotransmitter release (Zamponi *et al.*, 2013). Group II mGlu receptors can act as autoreceptors on glutamatergic terminals and also as heteroreceptors at inhibitory (GABAergic) or neuromodulatory (e.g. noradrenaline) terminals to negatively regulate neurotransmitter release (Lorrain *et al.*, 2003; Salt *et al.*, 1995; Xi *et al.*, 2002).

Expression in the BG:

Group II receptors are widely expressed in the BG, with a preference towards $mGlu_3$ over $mGlu_2$. mRNA expression studies have identified $mGlu_2$ in the STN and cortex, with maybe some weak expression in the SNr, GP and VM thalamus (Messenger *et al.*, 2002; Ohishi *et al.*, 1993a; Testa *et al.*, 1994). On the other hand $mGlu_3$ was found to be expressed in every nucleus in the BG and additionally in glia, though in contrast to Messenger *et al.*, Testa *et*

al. suggested that the expression found in the GP and EPN is attributable to glial and not neuronal expression, and Ohishi *et al.* reported no expression in the STN and SN (Messenger *et al.*, 2002; Ohishi *et al.*, 1993b; Tanabe *et al.*, 1993; Testa *et al.*, 1994). With regard to subthalamonigral signalling, the fact that $mGlu_2$ and $mGlu_3$ are generally found to be expressed by the STN might mean that group II mGlu receptors function as autoreceptors at these synapses, and in fact dense staining for group II mGlu receptor protein has been found in the SNc (Petralia *et al.*, 1996). In addition, group II receptors have been localised to the presynaptic membrane, at least at the subthalamonigral synapse targeting the SNr (Bradley *et al.*, 1999a), and accordingly activation of these receptors inhibits glutamate release into the SNc and SNr (Bradley *et al.*, 2000; Wigmore *et al.*, 1998).

Antiparkinsonian potential:

Given their negative regulation of glutamate release, activation of group II mGlu receptors has been investigated as a potential antiparkinsonian strategy. Broad spectrum group II agonists such as DCG-IV and LY379268 have shown efficacy in symptomatic models of PD such as reserpine-induced akinesia when administered intracerebrally (Dawson *et al.*, 2000; Murray *et al.*, 2002). Neuroprotective effects have also been reported following systemic or intracerebral treatment with the group II agonists DCG-IV, LY379268 and 2R,4R-APDC in the 6-OHDA-lesioned rat (Chan *et al.*, 2010; Murray *et al.*, 2002; Vernon *et al.*, 2005) and MPTP-treated rodent (Battaglia *et al.*, 2003; Matarredona *et al.*, 2001).

Additionally, neuroprotection has been shown against excitotoxic insults both *in vitro* using DCG-IV, 4C3HPG and L-CCG-I (Bruno *et al.*, 1997) and *in vivo* using LY379268 (Corti *et al.*, 2007), an effect that is seemingly dependent on activation of astrocytic $mGlu_3$ and might involve the subsequent release of nerve growth factors from these cells (Ciccarelli *et al.*, 1999). In fact, activation of group II mGlu receptors induces release of multiple growth factors, including glial derived neurotrophic factor (GDNF) in striatal neurones (Battaglia *et al.*, 2009) and brain-derived neurotrophic factor (BDNF) in the cortex and hippocampus (Di Liberto *et al.*, 2010), which likely contribute to the protective effect of activating these receptors.

1.6.2.3 Group III mGlu receptors

Structure and signalling:

There are four receptor subtypes within the group III mGlu receptors; $mGlu_4$ (only one form), $mGlu_6$ (3 splice variants, $mGlu_6$a-c), $mGlu_7$ (5 splice variants, $mGlu_7$a-e) and $mGlu_8$ (3

splice variants, $mGlu_8$a-c) (Niswender *et al.*, 2010). Group III mGlu receptors are predominantly presynaptically located and reside in the active zone (Shigemoto *et al.*, 1997), where they act as autoreceptors on glutamatergic terminals and also as heteroreceptors on GABAergic terminals (Salt *et al.*, 1995; Turner *et al.*, 1999). They are thought to be endogenously activated by glutamate spillover (Mitchell *et al.*, 2000; Scanziani *et al.*, 1997; Vera *et al.*, 2012), which implies that they may play an important role where glutamate transmission is pathologically hyperactive such as in the case of Parkinson's disease.

Similarly to group II, group III mGlu receptors are negatively coupled via $G\alpha_{i/o}$ to AC, decreasing the production of cAMP and thus deactivating PKA. The inhibition of PKA leads to reduced phosphorylation and hence increased activation of two-pore K^+ channels, and in addition the release of the Gβγ complex is also known to activate K^+ ion channels (Cain *et al.*, 2008; Niswender *et al.*, 2008a; Saugstad *et al.*, 1997), thereby altering neuronal excitability. Activation of group III mGlu receptors also leads to inhibition of N-type and/or P/Q-type Ca^{2+} channels, decreasing the probability of neurotransmitter release (Martín *et al.*, 2007; Millán *et al.*, 2002; Stefani *et al.*, 1999; Trombley *et al.*, 1992).

In addition to their classical signal transduction pathways, group III mGlu receptors also interact with a variety of other proteins and signalling cascades. For example, the neuroprotective effect of group III mGlu receptor activation in cultured cerebellar granule cells was produced via G-protein-mediated activation of both the MAPK and phosphoinositide-3-kinase (PI-3-K) pathways (Iacovelli *et al.*, 2002). Further C-terminal interactions are found within group III receptor subtypes and splice variants for multiple scaffolding, signalling and cytoplasmic proteins (reviewed in detail by Enz, 2007). Briefly these include:

- The scaffolding proteins **GRIP** and **PICK1** (which additionally interact with ionotropic glutamate receptors) and **Syntenin** (which interacts with PICK1).
- The signalling proteins **PKA** and **PKC** (which phosphorylate the mGlu receptor and inhibit calmodulin binding), **Calmodulin** (which inhibits PKC-mediated receptor phosphorylation and displaces Gβγ to initiate its signalling cascade), **Gβγ** (which inhibits P/Q-type Ca^{2+} ion channel conductance), **Pias1** (part of the sumoylation cascade) and protein phosphatase γ1 (**PPγ1**).

- The cytoplasmic proteins **Filamin A** (which crosslinks receptors to actin in the absence of Calmodulin) and **α-tubulin** (which affects vesicle trafficking and endo/exocytosis).

Therefore it is clear that on top of the classical effects of activation of group III mGlu receptors of reducing cAMP production and altering ionic conductance, many complex signalling interactions may also be activated depending on which receptor subtype and/or splice variant is expressed by the particular neurone.

Expression in the BG:

The expression of $mGlu_6$ is restricted to the retina (Nakajima *et al.*, 1993) therefore it will not be considered further in this thesis. The expression of mRNA for $mGlu_4$, $mGlu_7$ and $mGlu_8$ in the BG, cortex and thalamus as reported by Messenger *et al.* (2002) is shown in Table 2.

Table 2: Relative expression of mRNA for group III mGlu receptors in the rat basal ganglia as reported by Messenger *et al.* (2002). + to +++++ denotes mild to strong expression.

BG region	$mGlu_4$	$mGlu_7$	$mGlu_8$
Premotor cortex	++	+++++	++++
Striatum (CPu)	+++	++++	++
GP(e)	+	+	+
STN	++	++	++
EPN (GPi)	+	+	+
SNr	+	+	+
SNc	+	+	++
Thalamus (VM / VL)	+++++	+++	+

A fuller analysis of $mGlu_4$ mRNA and protein expression in the rodent BG is given in Chapter 4. Briefly, $mGlu_4$ is widely expressed within the BG, particularly in the striatum, STN and VM and VL thalamic output nuclei (Messenger *et al.*, 2002; Ohishi *et al.*, 1995; Testa *et al.*, 1994). $mGlu_4$ protein has been identified at high levels in the GP, moderate levels in the SNr and EPN, low to moderate levels in the striatum and cortex, and not at all in the STN (Bradley *et al.*, 1999b; Bradley *et al.*, 1999c; Broadstock *et al.*, 2012; Corti *et al.*, 2002). Electron microscopy studies have localised this protein to the presynaptic membrane in the majority of instances, and at both inhibitory and excitatory synapses, suggesting that $mGlu_4$

acts as an autoreceptor and heteroreceptor in the BG (Bradley *et al.*, 1999c; Corti *et al.*, 2002). In particular it appears to modulate striatopallidal, striatonigral and subthalamonigral signalling.

An analysis of $mGlu_7$ mRNA and protein expression in the rodent BG is given in Chapter 5. Briefly, mRNA for $mGlu_7$ is expressed throughout the BG at low levels, with slightly higher levels in the STN and more intense expression in the striatum, VM and VL thalamic nuclei and premotor cortex (Messenger *et al.*, 2002; Ohishi *et al.*, 1995). Electron microscopic studies have identified $mGlu_7$ receptor protein located presynaptically in the CPu, GP, EPN and SNr (Bradley *et al.*, 1999b; Kosinski *et al.*, 1999), suggesting that it plays a role in modulation of corticostriatal, striatopallidal, and striatonigral signalling. The presence of $mGlu_7$ receptors on presynaptic terminals of subthalamonigral neurones has not been investigated, however given the expression of $mGlu_7$ mRNA in the STN and the intense immunohistochemical staining for $mGlu_7$ in the SNr and EPN it is plausible that these receptors are also present presynaptically at this synapse.

Compared with the other group III receptor subtypes, $mGlu_8$ has not been well-characterised with regard to its expression within the BG. Like $mGlu_4$ and $mGlu_7$, it is expressed at low levels by the GP, EPN and SNr, and at moderately low levels in the STN. Compared with the other group III receptor subtypes, $mGlu_8$ expression in the striatum is lower, however it has increased relative expression in the SNc (Messenger *et al.*, 2002; Robbins *et al.*, 2007). At the protein level, $mGlu_8$ has been described in the striatum (CPu and NAc; Broadstock *et al.*, 2012; Zhang *et al.*, 2009), SNc (Gu, 2003), and at low levels in the SNr (Broadstock *et al.*, 2012) but has neither been investigated in other regions nor its pre- or postsynaptic localisation ascertained within the BG. On the other hand, it has been localised both pre- and postsynaptically in the dentate gyrus and also on astrocytes (Tang *et al.*, 2001), suggesting that in other brain regions it functions as an autoreceptor as well as having postsynaptic functions and a possible role in neuroinflammation. Experimental investigation of the location and targetability of $mGlu_8$ might also give us some clues about its localisation and function. For example, the selective $mGlu_8$ agonist (S)-3,4-DCPG failed to inhibit release of the glutamate analogue [^{3}H]-D-aspartate from nigral prisms, suggesting that it is not present and/or functional at the subthalamonigral synapse as an autoreceptor (Broadstock *et al.*, 2012), however *in vitro* evidence showed that both (S)-3,4-DCPG and an $mGlu_8$ PAM (AZ12216052) were able to protect retinoic acid-differentiated SH-SY5Y dopaminergic cells from MPP^+-induced degeneration (Jantas *et al.*, 2014), suggesting that

activation of postsynaptic $mGlu_8$ receptors on dopaminergic neurones may have a neuroprotective effect in the absence of attenuation of glutamate release.

Antiparkinsonian potential:

Electrophysiological and microdialysis studies have shown that activation of group III mGlu receptors modulates signalling at multiple synapses within the BG:

- **In the striatum:** L-AP4 and L-SOP depress corticostriatal EPSPs and intrastriatal IPSPs (Cuomo *et al.*, 2009; Pisani *et al.*, 1997).
- **In the GP:** L-AP4 and L-SOP reduce GABA release in the GP *in vivo* (MacInnes *et al.*, 2008) and reduce $GABA_A$-mediated IPSCs at the striatopallidal synapse in brain slices (Matsui *et al.*, 2003; Valenti *et al.*, 2003). In addition group III mGlu receptors also function as autoreceptors on the glutamatergic subthalamopallidal projection. Activation of these receptors by L-AP4 reduces subthalamopallidal EPSCs in rat GP (Matsui *et al.*, 2003).
- **In the SNr:** L-SOP and L-AP4 can reduce glutamate release into the SNr, likely as a result of inhibiting release at the subthalamonigral synapse (Austin *et al.*, 2010; Wittmann *et al.*, 2001). The direct pathway synapse onto the SNr is a GABAergic projection originating in the striatum, and both L-AP4 and L-SOP reduce GABA release from these striatonigral neurones (Wittmann *et al.*, 2001).
- **In the SNc:** L-AP4 was found to reduce EPSCs in the SNc, suggesting a reduction of glutamate release from subthalamonigral neurones (Valenti *et al.*, 2005; Wigmore *et al.*, 1998). This inhibition of EPSCs is more efficient than the inhibition of IPSCs that has also been described in the SNc, suggesting that group III mGlu receptors preferentially regulate excitatory transmission in this region (Bonci *et al.*, 1997).

The balance between inhibition of signalling at the striatopallidal and the striatonigral synapses will have an important effect on the antiparkinsonian efficacy of targeting group III mGlu receptors, as each effect will oppositely modulate the net output of the BG from the EPN/SNr. Evidence from PD models where group III mGlu receptor agonists have been administered systemically or intracerebroventricularly (i.c.v.) supports the idea that the net effect of activation of these receptors within the parkinsonian BG is therapeutically beneficial.

The antiparkinsonian potential of targeting group III mGlu receptors has been demonstrated in a variety of models of PD. For example, haloperidol-induced catalepsy can

be reversed by administration of ACPT-I, either locally into the striatum, GP or SNr (Konieczny *et al.*, 2007; Lopez *et al.*, 2007) or systemically (Lopez *et al.*, 2012), or by i.c.v. administration of L-AP4 (Valenti *et al.*, 2003). Similarly, reserpine-induced akinesia is reversed by intranigral injection of L-SOP or L-AP4 (Austin *et al.*, 2010), intrapallidal injection of L-SOP, or i.c.v. injection of either agent (MacInnes *et al.*, 2004; Valenti *et al.*, 2003). Relief of akinesia and forelimb impairments have also been reported in rats with 6-OHDA-induced nigrostriatal degeneration following systemic treatment with ACPT-I, or intrastriatal or i.c.v. infusion of L-AP4 (Cuomo *et al.*, 2009; Lopez *et al.*, 2012; Valenti *et al.*, 2003).

As well as providing symptomatic relief, the broad spectrum group III mGlu receptor agonist L-AP4 has also shown neuroprotective potential when administered locally to the SNc in 6-OHDA-lesioned rats (Austin *et al.*, 2010; Vernon *et al.*, 2005; Vernon *et al.*, 2006), and both i.c.v. (R,S)-PPG and intrahippocampal ACPT-I have been demonstrated to protect against other forms of excitotoxic injury *in vivo* (Domin *et al.*, 2014; Gasparini *et al.*, 1999).

Identification of the key receptor subtypes involved:

The success of widespread targeting of group III mGlu receptors led to attempts to dissect out which particular receptor subtype was responsible for the antiparkinsonian and neuroprotective actions elicited by these broad spectrum agonists.

With regard to antiparkinsonian actions, which are thought to result from suppression of the increased activity in the indirect pathway, studies in $mGlu_4$ knock-out mice implicated this receptor subtype in the effects of L-AP4 of reducing transmission at the striatopallidal synapse (Valenti *et al.*, 2003). In addition, $mGlu_4$ appears to play an important role in the neuroprotective actions of broad spectrum group III mGlu receptor agonists. For example, *in vitro* studies using cortical cultures prepared from wild type and $mGlu_4^{-/-}$ mice found that the neuroprotection afforded by the broad spectrum agonists L-AP4, (R,S)-PPG and L-SOP against NMDA-mediated toxicity in wild-type cultures was lost in $mGlu_4^{-/-}$ cultures, implicating $mGlu_4$ in the protective effect. What's more, (R,S)-PPG was protective against striatal NMDA infusion in wild type but not $mGlu_4^{-/-}$ mice (Bruno *et al.*, 2000), lending further support to the importance of this receptor subtype in mediating protection against excitotoxicity. With respect to protection of dopaminergic neurones, $mGlu_4$ was also implicated in L-AP4-mediated inhibition of excitatory signalling in the rat SNc (Valenti *et al.*, 2005). These findings led to speculation that the selective targeting of this receptor subtype might offer similar effects; the specific antiparkinsonian and neuroprotective

potential of selectively targeting $mGlu_4$ is explored further in Chapter 2 (section 2.1.3) and Chapter 4 (section 4.1.3).

In addition to the strong evidence for the involvement of $mGlu_4$ in the antiparkinsonian and neuroprotective effects of broad spectrum group III agonists, in the experiment by Bruno *et al.* (2000) even $mGlu_4^{-/-}$ mice were partially protected against excitotoxic cell loss by high doses of (R,S)-PPG. The authors suggest that this is due to activation of $mGlu_7$ receptors, therefore activation of this subtype might also be expected to be a useful strategy in the development of neuroprotective therapies. The specific antiparkinsonian and neuroprotective potential of selectively targeting $mGlu_7$ is explored in Chapter 5 (section 5.1.2).

$mGlu_8$ has not been widely investigated as a potential target for antiparkinsonian/neuroprotective therapies. Though (S)-3,4-DCPG has been reported in conference proceedings to provide functional neuroprotection in a lactacystin-infused rat model of PD, possibly involving attenuation of inflammation (Williams *et al.*, 2010), no further publications have followed this report and thus it is possible that the findings could not be reproduced. Instead, this receptor subtype has predominantly been studied as a potential target in schizophrenia, seizures and anxiety disorders (Duvoisin *et al.*, 2010; Lee *et al.*, 2003; Robbins *et al.*, 2007).

Overall the best candidate for subtype-specific modulation within the group III mGlu receptors in order to obtain an antiparkinsonian and/or neuroprotective effect appears to be $mGlu_4$, followed by $mGlu_7$ and then $mGlu_8$. When targeting these receptors with subtype specific ligands it would be preferable to use positive allosteric modulators rather than orthosteric or allosteric agonists, for reasons that are explained in the following section.

1.6.3 Orthosteric versus allosteric modulation

Receptor activation can be achieved directly using an orthosteric or allosteric agonist, or the probability of physiological activation enhanced using a positive allosteric modulator (PAM). Orthosteric or allosteric agonists directly activate the receptor upon binding, whereas PAMs increase the probability of activation of the receptor but require simultaneous binding of endogenous ligand for receptor activation.

Allosteric ligands are preferable to orthosteric ligands from the point of view of group III receptor subtype specificity. Orthosteric ligands bind at the glutamate binding site in the VFD and are therefore difficult to design to be subtype-specific due to the evolutionary

conservation of this region. Allosteric ligands, on the other hand, generally bind within the heptahelical (7TM) domain, which tends to have more variability between receptor subtypes, giving greater scope for designing subtype-specific molecules.

Within allosteric ligands, there are several advantages to using allosteric modulators rather than agonists, which have been reviewed in more detail elsewhere (Engers *et al.*, 2012; Flor *et al.*, 2012) and are briefly presented here. Using a positive allosteric modulator rather than an allosteric or orthosteric agonist at group III mGlu receptor subtypes might be expected to produce a more physiological means of modulation of signalling, since allosteric modulators rely on the binding of endogenous ligand for receptor activation. This should mean that only those receptors that are present in areas of pathologically increased extracellular glutamate concentration would be expected to be affected, and the activity of these receptors would be altered in a phasic rather than a tonic fashion due to the reliance on glutamate release. This should limit receptor desensitisation compared with using an agonist, and therefore increase the therapeutic dosing range of the compound. In addition, the specific modulation only where glutamate signalling is pathologically increased should minimise adverse events that might be caused by indiscriminate targeting of glutamatergic and GABAergic signalling. The higher potency of glutamate at $mGlu_4$ (EC_{50} = 3-38 μM) and $mGlu_8$ (EC_{50} = 3-11 μM) compared with $mGlu_7$ (EC_{50} >1000 μM) makes the former receptors preferable targets for allosteric modulation than the latter due to this reliance on co-stimulation with endogenous glutamate (Cartmell *et al.*, 2000).

A final advantage of allosteric over orthosteric ligands is that due to their tendency to be hydrophobic molecules (rather than hydrophilic amino acid analogues as is the case for many orthosteric ligands) they have increased blood-brain barrier penetrance. This is a significant obstacle in the research and development of therapeutics targeted at the central nervous system, and is important because by increasing the brain penetrance of a compound the therapeutic dose can be reduced, which will minimise peripheral activation of target receptors that could cause adverse events.

However, a downside of this hydrophobicity is that it limits solubility in biocompatible vehicles, thus making the formulation of a homogenous and stable dosing solution more complicated. In addition, due to their enhanced binding with biomolecules, hydrophobic compounds tend to be less bioavailable (reduced free fraction) and are more likely to exhibit off-target effects by non-specifically binding to non-target receptors.

1.7 Modelling Parkinson's disease

During the early stages of research into PD, whether it be defining mechanisms or testing novel therapeutics, it is necessary to use animal models. In this section I will concentrate on mammalian models of PD as they are the best-characterised and are also the most utilised for testing of potential treatments, however increasing amounts of research in to the genetics of PD and mechanisms of degeneration is carried out in transgenic *D. melanogaster* and *C. elegans* models, and these models can also be used for simple drug screens (Lim, 2010).

Parkinson's disease can be modelled preclinically in mammals using a variety of protein inhibitors, neurotoxins and genetic modifications. The ideal model would reproduce both the hallmark pathology of PD (nigrostriatal – and some extrapyramidal – degeneration and the presence of LBs), so-called construct validity, and the symptomatology of PD (bradykinesia, rigidity, tremor and perhaps non-motor symptoms), so-called face validity. The L-DOPA-responsiveness of these motor symptoms is also often used to determine the predictive validity of preclinical models of PD, given that this is the gold-standard treatment in humans to which all new therapies would be compared. Ideally, the mechanisms of degeneration would also be relevant to the human disease, and this is especially important when choosing a model for testing neuroprotective strategies.

1.7.1 Symptomatic models of PD

1.7.1.1 Reserpine

Reserpine is an irreversible inhibitor of VMAT-2, which causes a severe depletion of central and peripheral catecholamines. Behaviourally this results in abnormal posture, tremor, rigidity and hypokinesia in rodents that persists for approximately 72 hours if untreated (Glow, 1959), but which can be reversed by administration of catecholamine precursors (Carlsson *et al.*, 1957). It is a crude model of Parkinson's disease since it does not selectively deplete dopamine but also serotonin and noradrenaline. In addition, it does not reproduce either of the neuropathological hallmarks of Parkinson's disease, namely nigrostriatal degeneration and the presence of Lewy bodies. Nevertheless despite this poor construct validity it has a good degree of predictive validity for drugs with antiparkinsonian efficacy (see Duty *et al.*, 2011), and may even be predictive of drugs with antidyskinetic potential (Johnston *et al.*, 2005).

1.7.1.2 Haloperidol

The neuroleptic drug haloperidol is a dopamine receptor antagonist, acting on post-synaptic D1 and D2 receptors (Sanberg, 1980). The resulting alterations in activity of striatal medium spiny neurones lead to rigidity and catalepsy that persists for 1-2 hours after a single administration in rats (Hillegaart *et al.*, 1986). Similarly to the reserpine model, this model fails to recapitulate the nigrostriatal degeneration or Lewy body pathology associated with PD. Nevertheless this model has likewise shown a moderate to high degree of predictive validity for symptomatic effects (see Duty *et al.*, 2011) and is an inexpensive and straightforward test that is regularly carried out for novel compounds.

1.7.2 Toxin-based models of PD

PD can be modelled in rodents and non-human primates by toxin-mediated destruction of the nigrostriatal pathway. The main toxins used in preclinical research are 6-hydroxydopamine (6-OHDA) and 1-methyl-4-phenyl-1,2,3,6-tetrahydropyridine (MPTP). Administration of these toxins, either by direct infusion into the brain or by systemic injection, causes selective degeneration of dopaminergic cells that mimics the degeneration seen in Parkinson's disease patients. In addition to these classical models, the link between pesticide exposure and increased risk of developing PD (section 1.1.2.2) led to investigation of pesticides as neurotoxic agents.

1.7.2.1 6-hydroxydopamine

The 6-OHDA-lesioned rat is one of the most common animal models of PD used in preclinical research, and was first described in 1968 by Urban Ungerstedt. He noted that rats given a unilateral intranigral infusion of 6-OHDA displayed marked motor asymmetry. Similar motor asymmetry was also noticeable in rats given a unilateral intrastriatal infusion of 6-OHDA, but was less severe. Analysis of the brains revealed loss of dopaminergic cell bodies in the SNc and dopaminergic terminals in the striatum (Ungerstedt, 1968).

6-OHDA enters dopaminergic neurones via the dopamine transporter (DAT), however it also has affinity for other catecholamine transporters, notably the norepinephrine transporter (NET), and is therefore commonly given alongside a NET inhibitor such as desipramine to enhance dopaminergic specificity. Once inside the cell, 6-OHDA causes rapid and irreversible disturbances in intracellular Ca^{2+} homeostasis and alterations in neuronal firing and membrane properties (Berretta *et al.*, 2005). Neurodegeneration results from the ability of 6-OHDA to elicit oxidative stress by autoxidation and generation of reactive oxygen species such as the superoxide ($\cdot O_2^-$) and hydroxyl ($\cdot OH$) radicals (Cohen

et al., 1974; Saner *et al.*, 1970; Soto-Otero *et al.*, 2010). 6-OHDA-induced neurodegeneration is also associated with neuroinflammation (Henning *et al.*, 2008; Maia *et al.*, 2012; Marinova-Mutafchieva *et al.*, 2009; Walsh *et al.*, 2011) and inhibition of mitochondrial function (Kupsch *et al.*, 2014), both of which are mechanisms thought to contribute to human PD pathology (Keeney *et al.*, 2006; McGeer *et al.*, 1988; Mirza *et al.*, 2000; Schapira *et al.*, 1990). Also in common with the human disease, the 6-OHDA model of PD is additionally associated with increased oxidation of biomolecules (Kikuchi *et al.*, 2011; Sanchez-Iglesias *et al.*, 2007) and 6-OHDA has been reported to inhibit proteasomal function *in vitro* (Elkon *et al.*, 2004). Along with mechanistic similarities to the human disease regarding neurodegeneration, the generation of motor symptoms within the 6-OHDA-lesioned BG also reflects the pathological state in humans, for example the development of motor deficits in 6-OHDA-lesioned rats is associated with increased striatopallidal transmission (Bianchi *et al.*, 2003; Jian *et al.*, 1993) and increased STN signalling (Breit *et al.*, 2005; Breit *et al.*, 2006; Kreiss *et al.*, 1997), demonstrating a pathological overactivation of the indirect pathway and hence an increase in BG output from the SNr/EPN.

The site of 6-OHDA administration (Francardo *et al.*, 2011; Yuan *et al.*, 2005) as well as the dose used (Baluchnejadmojarad *et al.*, 2004; Truong *et al.*, 2006; van Oosten *et al.*, 2002) results in variable severity of behavioural measures and cell loss, and this variability is exploited in order to model different stages of PD.

When 6-OHDA is infused into the SNc, where the A9 dopaminergic cell bodies reside, the lesion is severe, with a typical TH-positive cell loss of ≥80% that is mostly complete within 4-5 days (Hanrott *et al.*, 2008; Maler *et al.*, 1973). Similarly, infusion of a high dose of 6-OHDA into the medial forebrain bundle (MFB), where the A9 axons pass between the substantia nigra and the striatum, also causes a severe loss of TH-positive cells, typically ≥90% (Grealish *et al.*, 2008; Truong *et al.*, 2006). The toxin is taken up into the axon and travels to the cell bodies in the SNc by retrograde transport, therefore the lesion takes longer to reach its stable end-point compared with SNc infusion, typically 14 days (Walsh *et al.*, 2011). Due to the presence of A10 as well as A9 dopaminergic fibres in the MFB, these lesions also typically result in loss of cell bodies in the ventral tegmental area and dopaminergic terminals in the nucleus accumbens (Grealish *et al.*, 2008). Both SNc and MFB infusions model the extensive nigrostriatal denervation of end-stage PD, with a predominant necrotic mode of cell death (Hanrott *et al.*, 2008; Jeon *et al.*, 1995; Maler *et*

al., 1973), though some apoptotic features have been noted following MFB lesioning (He *et al.*, 2000). Due to the severity of the lesion produced following MFB administration of 6-OHDA, rats with these lesions quickly develop motor complications reminiscent of LID when repeatedly exposed to levodopa. This model is discussed in more detail in Chapter 6 section 6.1.1. The severity of SNc or MFB lesions also means that they are almost exclusively performed unilaterally (i.e. one side of the brain) to avoid the high mortality and intensive care required with complete bilateral lesions (Paillé *et al.*, 2007; Ungerstedt, 1971a). This has the advantage that the intact hemisphere acts as an internal control, and therefore allows for comparison of functional performance between the healthy and impaired sides of the body as well as neurological comparisons between the intact and lesioned nigrostriatal tracts. When a lesion is performed unilaterally, parkinsonian symptoms are apparent only on the contralateral side of the body, comprising postural, sensorimotor, reaction time and fine motor control deficits (Cenci *et al.*, 2002).

When 6-OHDA is infused into the dorsal striatum (a single structure in the rat, referred to as the caudate-putamen or CPu) the degree of cell loss is more variable, tending to be between 50 and 80% (Blandini *et al.*, 2007; Branchi *et al.*, 2008; Roedter *et al.*, 2001), though this is highly dependent on the dose and site of injection. Although not technically a progressive model, the degeneration occurs more slowly following striatal infusion of 6-OHDA compared with MFB or SNc due to the time taken for the toxin to be retrogradely transported to the cell body. The site of injection within the CPu has an important influence over the behavioural characteristics resulting from the lesion, as particular areas are more or less innervated by the A9 and A10 projections (Kirik *et al.*, 1998). The partial and slower-developing nature of striatal lesions more closely mimics the pre- and early symptomatic phases of PD, eliciting an apoptotic mode of cell death (Ariano *et al.*, 2005; Hanrott *et al.*, 2008). Though most often performed unilaterally as in the case of SNc and MFB lesions, the reduced severity of degeneration associated with striatal lesions mean that they can also be performed bilaterally, resulting in a more accurate representation of the human condition. Bilateral lesions are reflected behaviourally with symptoms reminiscent of classical PD symptoms; akinesia, rigidity and tremor (Lindner *et al.*, 1999).

Overall, the 6-OHDA model reproduces the selective degeneration of dopaminergic cells, recapitulating the main pathological hallmark of PD, and the mechanisms of degeneration are also similar to those in the human disease. The model is extensively characterised, both with regard to the degenerative characteristics and the associated behavioural changes,

which are driven by comparable changes in basal ganglia signalling as in human PD and for which many robust tests have been devised. On the other hand, this model fails to reproduce the α-synuclein-related Lewy body pathology that is characteristic of the human disease (though there is a single report of increased formation of PINK-1/parkin-positive inclusions in 6-OHDA lesioned rats; Um *et al.*, 2010) and also shows none of the extrapyramidal degeneration encountered in human idiopathic PD.

1.7.2.2 MPTP

This neurotoxin was discovered by accident when drug users in the late 1970s and early 1980s were exposed to batches of 1-methyl-4-phenyl-4-propionoxypiperidine (MPPP) that had been contaminated with the by-product 1-methyl-4-phenyl-1,2,3,6-tetrahydropyridine (MPTP), causing them to develop severe and irreversible symptoms reminiscent of idiopathic Parkinson's disease (Langston *et al.*, 1983a). The *post mortem* analysis of one of these sufferers revealed monoaminergic cell loss that was mostly restricted to the SNc and also the presence of a Lewy-like inclusion (Davis *et al.*, 1979). MPTP causes neurodegeneration via its active metabolite MPP^+, which is formed when MPTP is metabolised by MAO B in glial cells (Chiba *et al.*, 1984), and acts as a complex I inhibitor (Nicklas *et al.*, 1985). This causes mitochondrial dysfunction, generation of ROS and eventual cell death as outlined in section 1.2.1. It is particularly damaging to dopaminergic neurones as MPP^+ is a substrate for the DAT, leading to its accumulation in these cells (Gainetdinov *et al.*, 1997; Javitch *et al.*, 1985).

These findings led researchers to generate a new primate model of PD by repeated intravenous administration of MPTP, resulting in a parkinsonian motor phenotype including akinesia, rigidity, hunched posture and tremor that was reversible with L-DOPA. When examined *post mortem*, parkinsonian histopathological features were evident, including selective loss of nigrostriatal neurones and infiltration of the SNc with immune cells (Burns *et al.*, 1983; Langston *et al.*, 1983b), along with a single report of eosinophilic inclusions in the locus coeruleus of MPTP-treated squirrel monkeys (Forno *et al.*, 1986). As in the human disease, the development of parkinsonian symptoms in MPTP-treated primates has been linked to increased activity in the indirect pathway, with increased activity of striatopallidal neurones (Robertson *et al.*, 1990), increased firing of the STN (Bergman *et al.*, 1994a) and increased output from the GPi (Bergman *et al.*, 1994a) all described in MPTP-treated primates. There are also reports of synchronous oscillatory activity driven by the GPe-STN in the parkinsonian primate BG (Raz *et al.*, 2000; Tachibana *et al.*, 2011) that is akin to what has been found in human PD. Accordingly, transient inactivation, lesioning or high

frequency stimulation of the STN of GPi has an antiparkinsonian effect in MPTP-treated primates (Baron *et al.*, 2002; Benazzouz *et al.*, 1993; Bergman *et al.*, 1990; Boraud *et al.*, 1996; Wichmann *et al.*, 1994).

Though the MPTP-treated non-human primate is the gold standard PD model due to its similarities to the human disease, both symptomatically and pathophysiologically, it is an exceptionally expensive model and is thus generally reserved for later stages of drug development. At earlier stages of preclinical research, the rodent MPTP model may be used instead. MPTP is significantly less effective in rats due to increased sequestration of MPP^+ in vesicles (Staal *et al.*, 2000) but is commonly used in mice to generate a similar bilateral parkinsonian phenotype to that seen in non-human primates. The relative resistance to MPTP toxicity of mice compared with primates means that the MPTP dosing schedule greatly affects the neurodegenerative outcome (Schmidt *et al.*, 2001), however with chronic or sub-chronic systemic dosing mice develop partial or full dopaminergic lesions respectively (Jackson-Lewis *et al.*, 2007; Tatton *et al.*, 1997), with the presence of nigral inflammation (Kohutnicka *et al.*, 1998). Alongside degeneration of dopaminergic neurones, one paper reported Lewy-like inclusions and extrapyramidal cell loss, such as degeneration in the locus coeruleus, following continuous 30-day infusion with MPTP in mice (Fornai *et al.*, 2005), which better recapitulates the idiopathic human disease, though this is by no means a robust finding. Behaviourally, MPTP-treated mice show rigidity, akinesia, tremor and gait disturbances, which can be measured using behavioural tests such as open field locomotor activity and rotarod performance (reviewed by Sedelis *et al.*, 2001). However, the assessment of MPTP-induced behavioural deficits has yielded inconsistent results that vary depending on the MPTP dosing regimen employed for the induction of the lesion, which could make assessment of the functional effects of neuroprotective therapies problematic (Duty *et al.*, 2011).

The MPTP mouse model is widely used, however there are important practical considerations concerning dosing regimen, systemic toxicity that varies depending on mouse strain and gender, behavioural assessment, and importantly the safety of the investigator, since the effects of MPTP in humans are well-established and irreversible.

1.7.2.3 Rotenone and other pesticides

Following the link between pesticide exposure and incidence of parkinsonism, several labs investigated the use of complex I-inhibiting pesticides to model the disease in rats. In addition to their actions as complex I inhibitors, several pesticides have also been shown to

have proteasome inhibiting effects in vitro (Wang *et al.*, 2006), which means that they could enhance more than one potential neurotoxic mechanism.

The most studied of these is the insecticide rotenone. In 2000, Betarbet *et al.* reported that exposing rats to chronic systemic intravenous rotenone via an osmotic minipump reproduced the pattern of degeneration and inclusion bodies typical of PD in around 50% of rats, along with hypokinesia, rigidity and a tremor-like phenotype (Betarbet *et al.*, 2000). These findings have been replicated by some (Alam *et al.*, 2009; Cannon *et al.*, 2009; Sherer *et al.*, 2003), but not all other laboratories that have attempted to characterise this model. Among the problems that have been encountered with this model by those labs that have failed to replicate the original findings are a high degree of systemic toxicity in liver and muscles (Hoglinger *et al.*, 2003; Lapointe *et al.*, 2004), which has been suggested to underlie to postural abnormalities, inconsistent loss of TH-positive cells (Lapointe *et al.*, 2004), and non-specific degeneration of multiple neuronal populations (Hoglinger *et al.*, 2003). In addition, it has been suggested that the symptoms displayed by rotenone-infused animals of postural instability and dystonia, but not often tremor or rigidity, make the rotenone model more similar to atypical parkinsonism than idiopathic PD (Hoglinger *et al.*, 2006). The hepatotoxicity and inconsistent lesioning effect make systemic rotenone administration an unreliable model, however there have been subsequent reports that local infusion of rotenone into the striatum or MFB also produces a parkinsonian syndrome in rats, both biochemically and behaviourally (Saravanan *et al.*, 2005; Sindhu *et al.*, 2005), so this approach might be more successfully employed in preclinical research.

The herbicide paraquat is a structural analogue of MPP^+ and has also been investigated as a potential toxic agent for modelling PD. Paraquat induces the formation of ROS (Chang *et al.*, 2013) and has also been linked to enhancement of α-synuclein fibrillation (Uversky *et al.*, 2001), which are two of the potential mechanisms thought to underlie neurodegeneration in idiopathic PD. Accordingly, systemic injection of paraquat in mice has been demonstrated to cause selective degeneration of nigral dopaminergic cell bodies with an inflammatory component (McCormack *et al.*, 2002), however striatal dopamine was largely preserved, possibly reflecting compensatory mechanisms. A further study by the same group reported the presence of this compensation in younger, but not aged mice when exposed to paraquat, the complex III-inhibiting fungicide maneb, or both in combination, and this ageing effect was also noted with regard to locomotor deficits (Thiruchelvam *et al.*, 2003). In addition to the compensatory mechanisms that may

confound interpretation of neuroprotection or behavioural studies, the selectivity of paraquat toxicity to dopaminergic neurones has also been questioned (Calò *et al.*, 1990), therefore this model is not widely used in preclinical research.

1.7.3 Proteasomal inhibition to model PD

Decreased proteasomal activity has been demonstrated in the SNc of idiopathic PD patients *post mortem* (McNaught *et al.*, 2001) and the accumulation of damaged proteins is proposed to contribute to neuronal degeneration in this condition. In light of this finding, a new rodent model was developed in an attempt to reproduce both neurodegeneration *and* protein pathology, the latter of which is not consistently obtained in either the 6-OHDA or MPTP models. Inhibition of the 26/20S proteasome with several different compounds was demonstrated to cause protein aggregation and dopaminergic neurotoxicity *in vitro* (Mytilineou *et al.*, 2004; Rideout *et al.*, 2005; Rideout *et al.*, 2001), therefore attempts were made to reproduce these results *in vivo* by administration of proteasome inhibitors in rodents with the aim of producing a more partial and gradual model of nigrostriatal degeneration with the presence of LB-like pathology. The main proteasome inhibition models of PD involve systemic administration of Z-lle-Glu(O*t*Bu)-Ala-Leu-al (PSI) or intracerebral infusion of lactacystin.

In a landmark paper in 2004, McNaught *et al.* reported that repeated systemic injection of PSI in rats caused a delayed degeneration of the nigrostriatal tract, along with extrapyramidal degeneration in areas typically affected in idiopathic PD such as the locus coeruleus and nucleus basalis of Meynert. This degeneration was associated with α-synuclein-positive Lewy-like inclusions and a motor phenotype comprising bradykinesia, rigidity and abnormal posture (McNaught *et al.*, 2004). At first glance, this seems like an almost-perfect model of PD, however over the subsequent few years other groups attempted to replicate these results with mixed success. While some groups reported similar results (Schapira *et al.*, 2006; Zeng *et al.*, 2006), others could not reproduce the model in rats, mice or non-human primates (Bové *et al.*, 2006; Kadoguchi *et al.*, 2008; Kordower *et al.*, 2006; Manning-Boğ *et al.*, 2006). In an examination of possible reasons for the difficulties in reproducing the results, the original authors suggested that batch variability of the PSI between and within suppliers might be the explanation, since this peptide aldehyde is hard to keep in stable solution (McNaught *et al.*, 2006). As a result the PSI model is not widely used for preclinical modelling of PD.

Another proteasome inhibitor that has been tested as a potential agent for modelling PD is lactacystin, which is naturally produced by the *Streptomyces* genus of bacteria (Omura *et al.*, 1991). Injection of lactacystin into the nigrostriatal tract causes selective nigrostriatal degeneration with induction of oxidative stress and the formation of Lewy-like inclusions (Fornai *et al.*, 2003; Lorenc-Koci *et al.*, 2011; Miwa *et al.*, 2005; Xie *et al.*, 2010). Behavioural deficits in unilaterally lactacystin-infused rats can be alleviated by L-DOPA, which suggests that it has good predictive validity (Konieczny *et al.*, 2014). This model is expected to be used increasingly in PD research moving forward, though further characterisation of the model is still required.

1.7.4 Genetic models of PD

Following the rare cases of familial parkinsonism, attempts have been made to recreate the pathology by mutating or knocking out the corresponding genes in mice.

The most commonly used α-synuclein transgenic models are mice that over-express human α-synuclein or mice that express human A53T or A30P mutant α-synuclein proteins under neuronal-specific or monoamine-specific promoters. The pattern of degeneration and behavioural phenotypes vary between these models, but in general these transgenic animals exhibit a moderate behavioural phenotype but with little or no loss of nigrostriatal neurones and varying degrees of α-synuclein aggregation (reviewed by Chesselet *et al.*, 2011). Improved results have been reported using adeno-associated virus (AAV)-mediated delivery of WT or A53T human α-synuclein into the region of the SN, including Lewy-like inclusions, striatal dopamine loss and a reduction in the number of TH-positive cells in the SN from 3 weeks post-injection, with corresponding behavioural deficits (Kirik *et al.*, 2002). A recent comparison between the AAV-mediated α-synuclein model and the 6-OHDA lesion model concluded that the AAV α-synuclein model recapitulated idiopathic PD more closely, given the larger behavioural deficits recorded with smaller degrees of cell loss (Decressac *et al.*, 2012). Nevertheless, much work still needs to be done to characterise this model before it can be employed more widely in preclinical research.

LRRK2 mutations, which like α-synuclein mutations cause an autosomal dominant parkinsonian phenotype in humans, have also been modelled in mice. Mutant R1441G LRRK2 transgenic mice showed an L-DOPA-responsive hypokinetic/akinetic phenotype with reduced dopamine release, however the morphology and number of dopaminergic cell bodies in the SNc was unaffected, suggesting a functional rather than a degenerative impairment (Li *et al.*, 2009). Similar abnormalities in dopamine release were described with

a different mutant LRRK2, R1441C, again in the absence of nigrostriatal neurodegeneration (Tong *et al.*, 2009). Similarly to the α-synuclein model, viral-mediated local delivery of the mutant gene gives a more valid model than the transgenic animal, for example Adenoviral-mediated delivery of G2019S mutant LRRK has been reported to cause dopaminergic dysfunction and nigrostriatal degeneration in rats (Dusonchet *et al.*, 2011). In both examples this might be explained by possible compensatory mechanisms in congenital mutants that are not in place in naive animals where the mutant protein is expressed at a later time point. This is supported by a conditional mutant where induced short-term, but not developmental, expression of a LRRK2 G2019S mutant caused impaired dopamine reuptake, though this was not associated in either case with neurodegeneration (Zhou *et al.*, 2011).

Transgenic models have also been made to reflect the autosomal recessive monogenic familial forms of parkinsonism, including parkin, DJ-1 and PINK1 mutants. These mutations are thought to exert their deleterious effects via mitochondrial dysfunction, however while these models had evidence of increased oxidative stress, they failed to elicit any nigrostriatal cell loss or cause the development of parkinsonian behavioural deficits (reviewed by Harvey *et al.*, 2008). Indeed, even a triple knockout of all three of these mitochondrial-associated genes is insufficient to cause degeneration (Kitada *et al.*, 2009), leading the authors to suggest that these genes are protective but not essential for dopaminergic neurone survival.

Alongside recapitulation of the mutations identified in familial parkinsonism, several other novel genetic models of PD have been developed. One example of this is the Mitopark® mouse, which has a conditional knockout of the mitochondrial transcription factor Tfam in dopaminergic neurones, causing a general mitochondrial dysfunction in these cells. The Mitopark® model causes an age-related progressive decline in midbrain dopaminergic neurones and striatal dopamine content along with the formation of protein inclusions, though these do not stain positive for α-synuclein (Ekstrand *et al.*, 2007). This is associated with progressive locomotor deficits that are L-DOPA responsive (Ekstrand *et al.*, 2007; Galter *et al.*, 2010). The delayed onset and progressive pathology of this model make it an exciting prospect for testing neuroprotective therapies in the future.

1.7.5 Comparing rodent models

A summary of the characteristics of the rodent versions of the models described in this section are shown in Table 3. Further details can be found in the relevant section above.

Table 3: Comparison of rodent models of PD as described in this section.

Model	SNc neurone loss?	Striatal DA loss?	Mechanisms involved	LB pathology	Behavioural outcomes?
Reserpine	x	✔	Global loss of catecholamines for 72 hours	x	Akinesia, rigidity
Haloperidol	x	x	Dopamine receptor antagonist, 1-2 hours	x	Catalepsy
6-OHDA	✔	✔	ROS generation, inflammation, excitotoxicity?	x	Bilateral: akinesia rigidity and tremor. Unilateral: limb use deficits and stimulant-induced rotation
MPTP mouse	✔	✔	Mitochondrial dysfunction, ROS generation, inflammation	✔ with continuous infusion	Akinesia, rigidity, tremor, gait disturbance but can be highly variable
Rotenone	✔/x but non-specific cell loss reported	✔/x	Mitochondrial dysfunction, ROS generation, inflammation	✔/x	Hypokinesia, rigidity, tremor. May result from systemic toxicity?
PSI	✔/x	✔/x	Proteasome inhibition	✔	Bradykinesia, rigidity, postural abnormality
Lactacystin	✔	✔	Proteasome inhibition, oxidative stress	✔	Unilateral: catalepsy and limb use deficits and stimulant-induced rotation
PARK gene transgenics	Little or none	Little or none	Various: protein aggregation, mitochondrial dysfunction	✔ particularly α-synuclein transgenics	Hypokinesia or akinesia, generally with vector-mediated delivery of transgene
Mitopark mouse	✔	✔	Mitochondrial dysfunction	✔ but not α-synuclein positive	Progressive akinesia

Based on this information the best model for my neuroprotection studies is the 6-OHDA-lesioned rat, as it shows robust, reproducible degeneration that occurs by similar

mechanisms to those encountered in human PD, namely oxidative stress and inflammation. In addition, the alterations in signalling in the BG following 6-OHDA lesioning are also similar to those encountered in the human parkinsonian BG, particularly with regard to the increased activity of the glutamatergic subthalamic nucleus, suggesting that excitotoxicity could play a role in this model as well as human PD. In contrast to MPTP-treated mice, the behavioural deficits caused by unilateral 6-OHDA-induced lesions are robust and well-characterised, meaning that functional assessment of neuroprotection will also be possible in my experiments. This is important for evaluation of the potential clinical benefits of any neuroprotection achieved.

1.8 General Aims and Hypothesis for this Thesis

As noted earlier in this introduction, the unmet clinical needs that remain to be addressed with respect to treatment of Parkinson's disease include, but are not restricted to:

1. **Neurodegeneration** - The inability of current treatments to address the continuing degeneration of dopaminergic neurones that underlies the motor symptoms of the disease.
2. **Levodopa-induced dyskinesia** - The motor fluctuations and LID associated with >5 years of treatment with L-DOPA is not adequately controlled and therapies that can suppress or inhibit the development of LID are required.
3. **Non-motor symptoms** - The often overlooked non-motor symptoms of PD are often inadequately controlled or treated by currently available therapies.

The current use of the weak NMDA receptor antagonist amantadine as an antiparkinsonian and an antidyskinetic agent supports the idea of attenuating glutamate transmission as a therapeutic strategy in PD and LID, therefore we hope to demonstrate similar efficacy using a group III mGlu receptor-targeted approach. Non-motor symptoms of PD are not addressed in this thesis, largely as a result of the lack of well-characterised and validated preclinical models of PD-related non-motor symptoms, however the utility of targeting glutamate receptors for the treatment of non-motor symptoms has recently been reviewed (Finlay *et al.*, 2014) and may be an interesting outcome to measure in future studies.

Neurodegeneration:

The preclinical data using antagonists at ionotropic glutamate transporters was promising in the case of NMDA antagonists, however the non-selective antagonism of NMDA

receptors is associated with psychiatric adverse events and is therefore not suitable for widespread clinical use. Alternative strategies of negatively modulating glutamate signalling have been explored via inhibition of signalling by group I mGlu receptors, or by activation of group II and group III mGlu receptors.

Based on the evidence outlined in section 1.6.2.3, activation of group III mGlu receptors has shown promise as an antiparkinsonian and neuroprotective strategy. Non-subtype-specific activation of these receptors provides not only symptomatic relief, by correcting aberrant signalling in the BG via reduction of indirect pathway activity, but also corrects subthalamonigral hyperactivation, which could in turn reduce excitotoxic degeneration of dopaminergic neurones in the SNc. In addition to potentially reducing excitotoxicity, activation of group III mGlu receptors has been shown to reduce inflammation, which could also help protect against continuing degeneration of the nigrostriatal tract due to release of inflammatory mediators and ROS by activated microglia (Taylor *et al.*, 2003).

In particular, selective activation of $mGlu_4$ is a promising strategy because it seems to be the principal receptor subtype involved in modulation of signalling at key synapses within the indirect pathway (striatopallidal and subthalamonigral). This receptor subtype also underlies the protective effects of broad spectrum group III agonists against excitotoxic neurodegeneration in non PD-related models. Alongside $mGlu_4$, $mGlu_7$ is also a potential target given its presynaptic localisation in the GP, suggesting that it could modulate signalling at the overactive GABAergic striatopallidal synapse. This might be expected to indirectly reduce glutamate release from the subthalamic nucleus and thus could exert a neuroprotective effect.

Levodopa-induced dyskinesia:

Inhibition of glutamatergic signalling has shown promise both preclinically and clinically as a means to suppress the expression of established LID. Additionally, there is preclinical evidence that inhibition of glutamate signalling can inhibit LID development in *de novo* L-DOPA-treated parkinsonian models (evidence for this is explored in Chapter 6).

Therefore testing group III mGlu receptor subtype-targeted compounds in dyskinesia is another interesting avenue of investigation.

1.8.1 Aims

In light of the unmet clinical needs of PD patients, the broad aims of this thesis are to:

- Investigate the neuroprotective potential of selectively targeting $mGlu_4$ and $mGlu_7$ in the 6-OHDA-lesioned hemiparkinsonian rat, and also to investigate potential mechanisms by which this might occur.

  Studies relating to targeting of $mGlu_4$ are described in Chapters 2 and 4, studies relating to targeting of $mGlu_7$ are described in Chapter 5, and investigation of one potential mechanism is described in Chapter 3.
- Investigate the ability of selective activation of $mGlu_4$ to suppress the expression of established dyskinesia in 6-OHDA-lesioned L-DOPA-primed rats.

  These studies are reported in Chapter 6.
- Investigate the ability of selective activation of $mGlu_4$ to inhibit the development of dyskinesia in 6-OHDA-lesioned rats when administered alongside *de novo* L-DOPA treatment.

  These studies are reported in Chapter 6.

1.8.2 Hypotheses

Our general hypotheses are as follows:

Selective activation of $mGlu_4$ or $mGlu_7$ using allosteric ligands will provide protection against a 6-OHDA-induced nigral lesion in rats.

Selective positive allosteric modulation of $mGlu_4$ will both suppress the expression of established dyskinesia, and inhibit the development of dyskinesia, in 6-OHDA-lesioned rats treated sub-chronically with L-DOPA.

2 Targeting $mGlu_4$ locally as a potential neuroprotective approach in a hemiparkinsonian rat model

2.1 Introduction

$mGlu_4$ is the most extensively studied receptor subtype in group III with respect to Parkinson's disease. This is partly due to the range of subtype-specific tool compounds that are commercially available and also because many of the antiparkinsonian effects seen with broad spectrum group III mGlu receptor agonists were attributed to actions at $mGlu_4$ based on the concentration of agonist applied and through $mGlu_4$ knock-out studies.

In the studies reported in this chapter we used two $mGlu_4$ positive allosteric modulators (PAMs) in a model of end-stage Parkinson's disease to test for neuroprotective efficacy. One of these PAMs, Compound 11, had only just been reported in the literature when the study was carried out (East *et al.*, 2010). The other, VU0155041, had already been shown by a previous researcher in our laboratory to have a neuroprotective effect in the 6-OHDA model of PD (Betts *et al.*, 2012), so this study acted to verify that these results could be repeated by an independent researcher.

2.1.1 Neuroprotective strategies in PD

Several neuroprotective and neuroregenerative strategies have been suggested on the basis of the proposed degenerative mechanisms identified in PD outlined in section 1.2. These include antioxidant therapies (Cadet *et al.*, 1989; Chan *et al.*, 2013; Fahn, 1991; Shults *et al.*, 2002), chelation of catalysing transition metal ions (Dexter *et al.*, 2010), nitric oxide synthase inhibitors (Broom *et al.*, 2011) and administration of growth factors (Kirik *et al.*, 2001; Sleeman *et al.*, 2012). These novel therapies mainly target the oxidative stress and inflammatory responses thought to perpetuate the degeneration of neurones, but an alternative strategy could be to target the overactivity of glutamate in the basal ganglia that contributes to the generation of this oxidative stress and excitotoxicity.

2.1.2 Targeting group III mGlu receptors as an antiparkinsonian or neuroprotective strategy

Given the model of the basal ganglia described in section 1.3, attenuation of glutamatergic signalling at several key synapses, particularly the subthalamonigral synapse, might be expected to have antiparkinsonian effects.

Drugs targeting ionotropic glutamate receptors have been reported to have antiparkinsonian and/or neuroprotective effects in preclinical models, as have therapies

targeting group I, group II and group III mGlu receptors. This is described in more detail in section 1.6.2 of the Introduction. This thesis concentrates on the potential of targeting group III mGlu receptors, and a brief summary of the early work on this group of receptors using broad spectrum agonists to investigate antiparkinsonian and neuroprotective potential of group III mGlu receptors is given below.

Broad spectrum group III mGlu receptor agonists such as L-AP4, L-SOP and ACPT-I have shown antiparkinsonian efficacy in the haloperidol (Konieczny *et al.*, 2007; Lopez *et al.*, 2012; Lopez *et al.*, 2007) and reserpine (Austin *et al.*, 2010; Valenti *et al.*, 2003) models of PD. They have also demonstrated neuroprotective and behavioural benefits in lesion models of PD, such as 6-OHDA-lesioned rats (Austin *et al.*, 2010; Cuomo *et al.*, 2009; Lopez *et al.*, 2012; Valenti *et al.*, 2003; Vernon *et al.*, 2005; Vernon *et al.*, 2006).

Therefore the obvious next step was to test the neuroprotective effects of selective activation of the receptor subtypes within group III. Given the enhanced potency of these broad spectrum agonists at $mGlu_4$ and $mGlu_8$ compared with $mGlu_7$ (Conn et al., 1997), these subtypes seem to represent a good target.

2.1.3 Symptomatic and neuroprotective efficacy of pharmacological targeting of $mGlu_4$ receptors *in vivo*

Building on previous work with broad spectrum group III mGlu receptor agonists, subtype-specific activation of $mGlu_4$ using PAMs has shown efficacy in several rodent models of PD. For example haloperidol-induced catalepsy can be reversed by the $mGlu_4$ agonist LSP1-2111 (Beurrier *et al.*, 2009) and $mGlu_4$ PAMs including Compound 11 (East *et al.*, 2010), VU0155041 (Niswender *et al.*, 2008b), VU0364770 (Jones *et al.*, 2012), ADX88178 (referred to in this thesis as AF42744; Le Poul *et al.*, 2012) and LuAF21934 (Bennouar *et al.*, 2013). Reserpine-induced akinesia is similarly reversed by PHCCC (Battaglia *et al.*, 2006; Broadstock *et al.*, 2012; Marino *et al.*, 2003) and VU0155041 (Niswender *et al.*, 2008b). In addition to symptomatic improvements, neuroprotection has also been recently observed when VU0155041 was given supranigrally in 6-hydroxydopamine-lesioned rats (Betts *et al.*, 2012) and when PHCCC was given systemically in MPTP-treated mice (Battaglia *et al.*, 2006).

2.1.4 Potential mechanisms of neuroprotection

$mGlu_4$ activation plays an important role in resistance to excitotoxicity *in vitro* and *in vivo* in cortical and striatal neurones (Bruno *et al.*, 2000; Maj *et al.*, 2003). There is evidence from *in vitro* studies that the $mGlu_4$ PAM PHCCC can inhibit the release of a glutamate analogue

in nigral prisms (Broadstock *et al.*, 2012) and in addition, though not demonstrated for $mGlu_4$ specifically, activation of group III mGlu receptors is known to attenuate subthalamonigral excitatory neurotransmission (Valenti *et al.*, 2005). Though not all studies are in agreement (Ohishi *et al.*, 1995), low-level expression of $mGlu_4$ has been localised to the STN at the mRNA level (Messenger *et al.*, 2002; Testa *et al.*, 1994) and in the SNc at the protein level (Gu, 2003). This suggests that this receptor might function as an autoreceptor to reduce glutamate release into the SNc from subthalamonigral terminals and thereby reduce excitotoxic cell death, therefore it is a promising target for neuroprotection studies.

In addition to the potential involvement of reduced glutamate release, $mGlu_4$ activation has been shown to mediate several additional mechanisms, including microtubule stabilisation (Jiang *et al.*, 2006) and attenuation of inflammation (Besong *et al.*, 2002; Betts *et al.*, 2012; Fallarino *et al.*, 2010). Along with the STN as described above, $mGlu_4$ mRNA has also been demonstrated in the SNc in some (Messenger *et al.*, 2002; Testa *et al.*, 1994) but not all (Ohishi *et al.*, 1995) reports. Combined with the evidence of $mGlu_4$ protein expression in this nucleus (Gu, 2003) this might suggest that there are some post-synaptic receptors in this region, which might underlie a microtubule stabilisation response. Alternatively both the mRNA and protein expression in the SNc might in fact be localised to non-neuronal cells; indeed $mGlu_4$ expression has been demonstrated in several non-neuronal cell types such as microglia (Besong *et al.*, 2002; Taylor *et al.*, 2003), and activation of $mGlu_4$ receptors on these cells is postulated to underlie the *in vitro* and *in vivo* anti-inflammatory effects that have previously been demonstrated (Besong *et al.*, 2002; Betts *et al.*, 2012).

Along with the mechanisms mentioned above, $mGlu_4$ PAMs may also increase cell viability and proliferation via activation of ERK1/2 (Jantas *et al.*, 2014). Therefore there are multiple mechanisms by which $mGlu_4$ activation could offer neuroprotective potential.

2.1.5 6-OHDA SNc-lesioned rat

Since only one previous study had shown neuroprotective potential in the 6-OHDA-lesioned rat using an $mGlu_4$ PAM (Betts *et al.*, 2012), the present studies were conducted to further support targeting of this receptor in PD. In the studies reported in this chapter we tested two $mGlu_4$ PAMs for neuroprotective efficacy, firstly a novel $mGlu_4$ PAM that had only recently been described in the literature (Compound 11; East *et al.*, 2010) and secondly we repeated the study using VU0155041 in order to verify that the same effect that had been described previously by Betts *et al.* (2012) could be replicated by an independent

researcher. Both compounds were tested for their ability to protect against the nigrostriatal degeneration associated with a unilateral nigral infusion of 6-OHDA.

The 6-OHDA-lesioned rat model of hemiparkinsonism was introduced in section 1.7.2.1. Direct infusion of 6-OHDA into the SNc causes rapid cell degeneration with a necrotic phenotype (Hanrott *et al.*, 2008; Maler *et al.*, 1973), and due to the severity of cell loss it is considered to best reflect late-stage Parkinson's disease. Unlike in Parkinson's disease itself, the cell death does not happen progressively but occurs within hours of 6-OHDA injection and is complete within 4-5 days. Nonetheless the selective and permanent degeneration of the nigrostriatal tract that is achieved by 6-OHDA recapitulates the degeneration seen in Parkinson's disease, meaning that the construct validity of this model is good and will allow us to test our $mGlu_4$ PAMs for their ability to provide protection against this cell loss. What's more, the overactivity in the subthalamic nucleus that has been described in patients (Remple *et al.*, 2011; Yokoyama *et al.*, 1998) is also found in this model (Breit *et al.*, 2006; Kreiss *et al.*, 1997) and 6-OHDA-induced degeneration is coincident with neuroinflammation (Henning *et al.*, 2008; Maia *et al.*, 2012; Marinova-Mutafchieva *et al.*, 2009; Walsh *et al.*, 2011). This means that the postulated neuroprotective effects of $mGlu_4$ activation via reduction of subthalamonigral glutamate release and reduction of inflammation may both play a role in any neuroprotective effects observed.

The face validity of this model is good with respect to the motor symptoms, and a large variety of behavioural tests have been devised for quantification of parkinsonian impairments in this model. The main test performed is drug-induced rotometry, where asymmetrical turning is measured in response to drugs such as amphetamine and apomorphine. This test has been used as a screen for antiparkinsonian drugs with a high level of predictive validity (Duty *et al.*, 2011). In addition there are many drug-free behavioural tests that have been described in this model. These include tests of paw preference such as the cylinder test (Schallert *et al.*, 2000a), assessments of fine motor co-ordination such as the staircase test (Montoya *et al.*, 1991), measures of more general co-ordination such as the rotarod (Rozas *et al.*, 1997), and tests of akinesia and impairments in movement initiation such as forelimb placement (Schallert *et al.*, 2000a) and stepping tests (Olsson *et al.*, 1995). Each test has been designed to quantify a specific aspect of the behavioural phenotype following a 6-OHDA lesion, but their usefulness may vary according to the extent of lesion. This is discussed in more detail in sections 2.2.3.3 and 2.4.2.1 with

regard to the cylinder test, adjusted steps test and drug-induced rotometry. In our studies the behavioural outcomes are designed to reflect the degree of dopaminergic cell loss induced by the lesion and any degree of neuroprotection provided by the tested $mGlu_4$ PAMs.

2.1.6 Hypothesis and aims

Given the pattern of expression within the rat BG, $mGlu_4$ is an attractive target for potential antiparkinsonian therapies. Localisation of mRNA for $mGlu_4$ in the STN and of $mGlu_4$ receptor protein in the SNc suggests that it is expressed on subthalamonigral terminals, where its activation might be expected to reduce presynaptic glutamate release. If so, this could reduce excitotoxic cell loss secondary to infusion of the neurotoxin 6-OHDA. Therefore we hypothesise that:

Activation of $mGlu_4$ locally within the SNc will provide neuroprotection in the 6-OHDA-lesioned rat.

The experiments described in this chapter sought to assess the neuroprotective efficacy of two $mGlu_4$ PAMs – Compound 11 and VU0155041 – when given sub-chronically in rats with a nigral infusion of 6-OHDA. This was carried out by assessing:

- Survival of TH-positive neurones in the SNc.
- Preservation of striatal dopamine content.
- Functional effects of neuroprotection, as assessed by the cylinder test, adjusted steps test and amphetamine- or apomorphine-induced rotometry.

Both Compound 11 and VU0155041 were administered supranigrally to circumvent permeability issues at the blood-brain barrier.

2.2 Materials and Methods

2.2.1 Compounds tested

Table 4 shows the structures of the $mGlu_4$ PAMs tested for neuroprotective efficacy in the 6-OHDA SNc-lesioned rat model of Parkinson's disease.

Table 4: The chemical structures of the $mGlu_4$ PAMs tested for neuroprotective efficacy in the hemiparkinsonian rat.

Structure	Name	Target
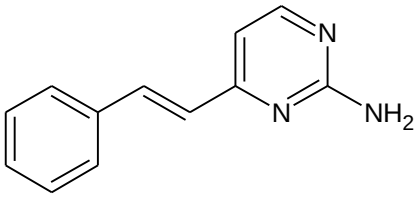	'Compound 11' *4-((E)-styryl)-pyrimidin-2-ylamine)*	$mGlu_4$ Positive Allosteric Modulator
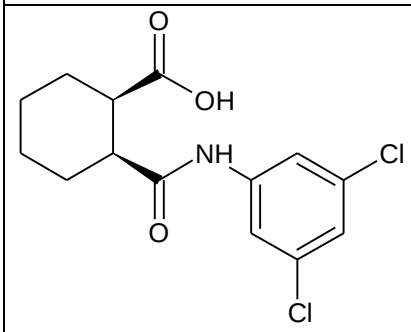	VU0155041 *cis-2-[[(3,5-Dichlorophenyl) amino]carbonyl] cyclohexanecarboxylic acid*	$mGlu_4$ Positive Allosteric Modulator

Compound 11 was developed at Evotec/Boehringer Ingelheim and acts as a PAM at human or rat $mGlu_4$ (EC_{50} = 1.0µM). It is reported to show good oral bioavailability, with anticataleptic efficacy in the haloperidol model following an oral dose (East *et al.*, 2010). However the *in vivo* clearance rate of this molecule in rats is high so we chose to administer Compound 11 directly into the brain in this neuroprotection study. The neuroprotective potential of this compound has not yet been examined.

VU0155041 was discovered via a high-throughput screen at Vanderbilt University. It acts as a PAM at human $mGlu_4$ (EC_{50} = 750nM) and rat $mGlu_4$ (EC_{50} = 560nM) and reverses catalepsy and akinesia in the haloperidol and reserpine models respectively following intracerebroventricular administration (Niswender *et al.*, 2008b). This compound has also been reported in previous work from our lab to exert neuroprotective effects following subchronic supranigral infusion in the 6-OHDA lesioned rat (Betts *et al.*, 2012) and therefore the purpose of this study was to confirm that these results could be repeated by an independent investigator. Previous work has shown poor brain penetrance of

VU0155041 following systemic administration (Doller *et al.*, 2010) and therefore it was administered intracerebrally in this study.

2.2.1.1 Drug formulation

Compound 11 was synthesised and characterised by Eli Lilly and Company (LSN3030797). It was dissolved in a vehicle comprising 10:45:45 v/v/v DMSO/PEG-200/sterile water. DMSO (dimethylsulfoxide) and PEG-200 (polyethylene glycol, average molecular weight 200) were obtained from Sigma Aldrich (Poole, UK).

VU0155041 sodium salt was obtained from Tocris Bioscience (Bristol, UK) and was dissolved in phosphate buffered saline (PBS) which was made up in distilled water and then sterilised in an autoclave. PBS tablets were obtained from Sigma Aldrich (Poole, UK).

2.2.2 Other materials

2.2.2.1 Experimental materials

6-hydroxydopamine hydrochloride, ascorbic acid, desipramine hydrochloride and pargyline hydrochloride were obtained from Sigma Aldrich (Poole, UK). Peri-operative analgesia was provided using bupivicaine (Marcain; Astra Zeneca, UK) and post-operative analgesia with buprenorphine (Vetergesic; (Alstoe/Sovegal) York, UK). All drugs were formulated uncorrected for salt weight.

D-Amphetamine hemisulfate and R-(−)-Apomorphine hydrochloride hemihydrate were obtained from Sigma Aldrich (Poole, UK) and dissolved in sterile saline (Aquapharm) before use.

10% buffered formalin for fixing of the midbrain for histology *post mortem* was obtained from Sigma Aldrich (Poole, UK).

2.2.2.2 Analytical materials

Tissue processing for immunohistochemistry: Solvents for tissue processing (industrial methylated spirits (IMS) and xylene) were obtained from VWR International (Lutterworth, UK). Paraffin wax was obtained from Fisher Scientific (Loughborough, UK).

TH Immunohistochemistry:

King's College London: SuperFrost Plus° slides, xylene and IMS were obtained from VWR International (Lutterworth, UK). 10% buffered formalin solution, hydrogen peroxide (H_2O_2), citric acid, bovine serum albumin (BSA), sodium azide (NaN_3), Trizma® base, sodium

chloride, 3,3-diaminobenzidine (DAB) and DPX mountant were obtained from Sigma Aldrich (Poole, UK). Polyclonal anti-tyrosine hydroxylase primary antibody was obtained from Chemicon via Millipore (AB152; Watford, UK). Biotinylated secondary antibody (goat-anti-rabbit, BA-1000) and StreptABC (PK-4000) were obtained from Vector Laboratories (Peterborough, UK).

Eli Lilly: SuperFrost Plus® slides were obtained from Thermo Fisher (Loughborough, UK). Xylene and (IMS) were obtained from Fisher Scientific (Loughborough, UK). PBS tablets were obtained from Sigma Aldrich (Poole, UK). Anti-tyrosine hydroxylase (TH) primary antibody (rabbit polyclonal) was obtained from Chemicon via Millipore (AB152; Watford, UK)). Normal goat serum, biotinylated secondary antibody and StreptABC were part of a kit supplied by Vector Laboratories UK (PK-6101; Peterborough, UK) and DAB (SK-4100) was also obtained from the same supplier.

HPLC for dopamine and its metabolites: Dopamine, DOPAC, HVA, perchloric acid (PCA), EDTA, ascorbic acid, sodium dihydrogen phosphate and octane sulfonic acid were all obtained from Sigma Aldrich (Poole, UK). HPLC grade methanol was obtained from Fisher Scientific (Loughborough, UK). HPLC grade water was obtained using the ELGA LabWater system (Veolia Water Technologies, High Wycombe, UK).

2.2.3 Neuroprotection study methods

All procedures were performed in accordance with the U.K. Animals (Scientific Procedures) Act, 1986. Unless otherwise stated, all experimental procedures and analysis described below were carried out at King's College London.

2.2.3.1 Lesioning and treatment

Male Sprague-Dawley (SD) rats (270-300g, Harlan, UK) were maintained in a temperature- and humidity-controlled environment with a 12-hour light-dark cycle and ad libitum access to chow and tap water.

For all studies, rats were pre-treated 30 minutes before lesioning with 5mg/kg pargyline and 25mg/kg desipramine (i.p.) to inhibit extracellular metabolism of 6-OHDA by monoamine oxidase B and to block the norepinephrine transporter to ensure selective uptake of the toxin into dopaminergic cells respectively.

The $mGlu_4$ PAMs Compound 11 and VU0155041 were delivered by direct intracerebral infusion in the region above the SNc due to poor blood-brain barrier penetrance. 12.0mm 23G stainless steel guide cannulae (Coopers Needleworks; Birmingham, UK) were stereotaxically implanted under isoflurane anaesthesia (5% induction, 2% maintenance) so as to be 2mm above the substantia nigra, and were secured using screws and dental cement (Rapid Repair, Dentsply; Surrey, UK). Bilateral implantation was carried out to improve the probability of at least one cannula remaining patent during recovery, thereby minimising animal use. For testing of Compound 11 the cannulae were implanted at AP -4.8mm, ML ±2.0mm, DV -6.3mm relative to bregma and for the VU0155041 study they were implanted at AP +3.7mm, ML +2.0mm, DV +4.2mm relative to the interaural line (ML calculated from the midline). The co-ordinates were altered for the VU0155041 study due to the significant differences between anteroposterior levels with respect to loss of TH-positive cells in the Compound 11 study. We wanted to lose this effect, so rather than aiming the lesion in the anterior region of the SNc (-4.8mm from bregma) we tried some co-ordinates that aimed more centrally in the SNc (-5.3mm from bregma). These co-ordinates had been used successfully by another researcher in our laboratory.

Rats were allowed to recover for a minimum of five days before baseline behavioural assessments were carried out. A minimum of seven days after implantation rats underwent unilateral nigral lesioning with 6-OHDA. 12µg 6-OHDA.HCl in 2.5µl 0.2% ascorbate in 0.9% saline was infused directly into the SNc at a rate of 1.25µl/min under brief isoflurane anaesthesia, using a 30G infusion needle with a 2mm overhang to the guide cannula.

Following infusion the needle was allowed to remain in place for a further 2 minutes to prevent reflux by allowing the solution to diffuse away from the tip of the needle.

Figure 7 depicts the cannula placement and lesioning co-ordinates for each of these studies in schematic form.

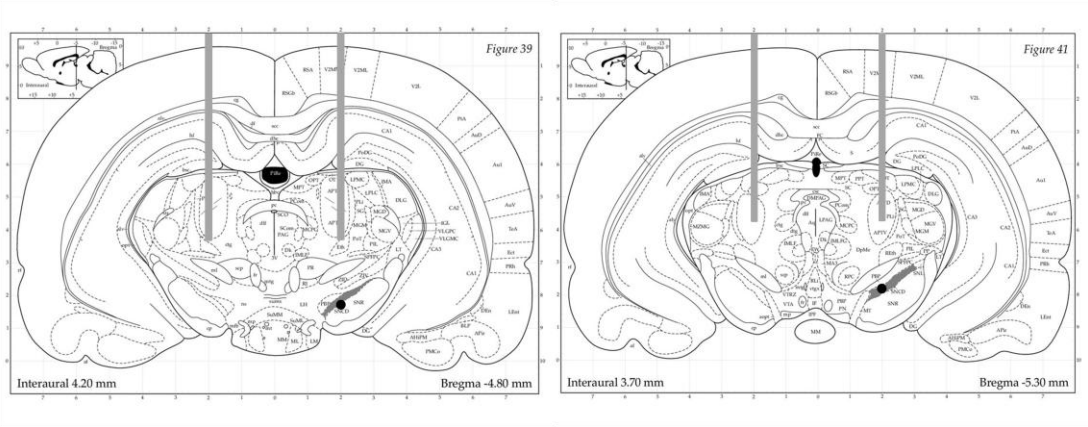

Figure 7: Cannula implantation and lesion location for $mGlu_4$ PAM neuroprotection studies. The left hand panel shows the cannula and lesion co-ordinates used in the Compound 11 neuroprotection study. The right hand panel shows the cannula and lesion co-ordinates for the VU0155041 neuroprotection study. The grey bars show the location of the bilaterally implanted 23G cannulae; the grey shaded region in each image is the SNc; the black spots represent the location of 6-OHDA infusion. Diagrams of coronal sections were obtained from The Rat Brain in Stereotaxic Coordinates (Paxinos *et al.*, 1998).

Animals were randomly assigned to vehicle and treatment groups (each group n=8) following implantation surgery. All $mGlu_4$ PAMs were made up fresh daily and 4µl volume was administered supranigrally at a rate of 2.0µl/min using a 30G needle that protruded 1mm below the guide cannula, resting 1mm above the SNc to avoid causing unnecessary mechanical damage to the SNc. The injection needle was allowed to remain in place for a further 2 minutes after infusion to prevent reflux. Treatment was administered 1 hour prior to lesioning and once daily between 09:00 and 12:00 for a further 7 days (total of 8 doses) in conscious animals. Both $mGlu_4$ PAMs were tested at three doses against a vehicle control: Compound 11 was tested at 20, 100 and 200nmol/day and VU0155041 was tested at 50, 100 and 200nmol/day. Figure 8 and Figure 9 show the study designs for testing of these $mGlu_4$ PAMs.

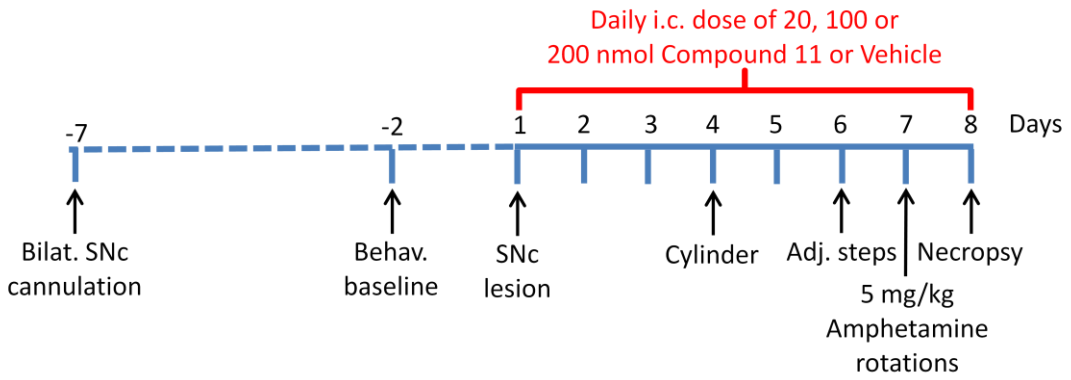

Figure 8: Experimental protocol for the Compound 11 (Cpd 11) neuroprotection study. Rats were bilaterally cannulated above the SNc and behavioural baselines for the cylinder and adjusted steps measured following recovery. On the day of lesioning, rats were treated with Cpd 11 or vehicle (i.c.) one hour prior to lesioning of the SNc with 6-OHDA, and then daily after lesioning for a further 7 days. Behavioural testing was carried out at intervals during the treatment period and following the final dose rats were killed by CO_2 asphyxiation and their brains removed for analysis.

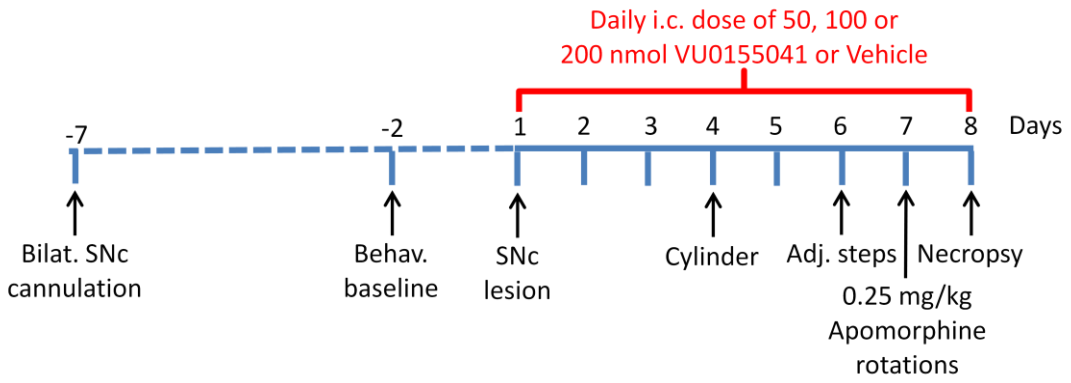

Figure 9: Experimental protocol for the VU0155041 neuroprotection study. Rats were bilaterally cannulated above the SNc and behavioural baselines for the cylinder and adjusted steps measured following recovery. On the day of lesioning, rats were treated with VU0155041 or vehicle (i.c.) one hour prior to lesioning of the SNc with 6-OHDA, and then daily after lesioning for a further 7 days. Behavioural testing was carried out at intervals during the treatment period and following the final dose rats were killed by CO_2 asphyxiation and their brains removed for analysis.

2.2.3.2 Assessment of lesion size

At the completion of each study rats were killed by CO_2 asphyxiation followed by decapitation, and the brain removed. The striatum was dissected out on an ice-cold platform and snap-frozen on dry ice for HPLC analysis of dopamine, while a coronal block containing the midbrain was post-fixed for a minimum of 72 hours in 10% buffered formalin before being processed and paraffin embedded for immunohistochemical analysis.

Immunohistochemistry

In order to assess the effect of lesioning/treatment on the number of dopaminergic cell bodies in the SNc, brain sections were stained for tyrosine hydroxylase (TH), the rate-limiting enzyme in the dopamine synthetic pathway.

Formalin-fixed coronal brain tissue blocks (6-7mm thick) were processed using a TP1020 tissue processor (Leica), which dehydrates and de-fats tissue samples by progressing them through timed immersions in the following solvents; 1 x 4 hours in 90% IMS, 3 x 4 hours in 100% IMS, 3 x 4 hours in xylene, 3 x 4 hours in paraffin wax at 60°C. The processed brain blocks were then embedded in paraffin wax for sectioning.

7µm coronal sections were cut throughout the substantia nigra and mounted in triplicate on SuperFrost Plus® slides. Slides were picked for immunostaining at 3 anteroposterior levels of the SNc: -4.8mm, -5.3mm and -5.8mm from Bregma (Paxinos et al., 1998), giving a total of 9 sections per animal.

For the Compound 11 study: Slides were dewaxed in xylene and IMS and then incubated for 10 minutes in 3% H_2O_2 to quench endogenous peroxidases. After antigen retrieval in boiling 1mM citric acid (pH 6) slides were blocked with blocking buffer (1% BSA in 0.1M TBS and 0.1% NaN_3, pH 7.6) for a minimum of 10 minutes, then each section incubated overnight in 50µl primary antibody solution (1:1000 to 1:500 rabbit polyclonal anti-tyrosine hydroxylase antibody (AB152) in blocking buffer; dilution was dependent on batch but was consistent within studies). The following day, sections were incubated with 50µl secondary antibody (1:200 biotinylated goat-anti-rabbit IgG in blocking buffer) for 1 hour, then for 30 minutes in 50µl StreptABC/HRP conjugate, before developing in 0.05% DAB in TBS for 10 minutes. Unless otherwise stated all steps were carried out at room temperature.

Stained sections were cover-slipped manually using DPX mountant and viewed using the Zeiss Axioskop brightfield microscope. Images were captured at 100x magnification using Axiovision release 4.6 software (Zeiss) and cells counted manually at using Image J software (publically accessible software developed by the National Institutes of Health).

For the VU0155041 study: Immunohistochemical staining and analysis were carried out at Eli Lilly while on placement. The protocol used is similar but was carried out using an automated immunostainer (Lab Vision). The de-waxing and citrate antigen retrieval steps were also automated, and carried out in a single step using a PT module and the supplied reagent (Lab Vision). Thereafter sections were incubated with 0.3% H_2O_2 for 30 minutes,

blocked with normal goat serum in PBS for 20 minutes, incubated with anti-TH AB152 primary antibody in PBS at 1:500 for 1 hour, followed by biotinylated goat-anti-rabbit secondary antibody in block at 1:200 for 30 minutes, StreptABC/HRP for 30 minutes and finally DAB for 5 minutes. All steps were carried out at room temperature and all reagents were applied at 200µl per section, with PBS rinsing between reagents. After cover-slipping, the slides were scanned at high resolution using an Aperio ScanScope (Leica Biosystems). Cells were counted from these images at 100x magnification.

Cell counts were all performed manually, and viable cells were defined as being rounded, densely TH-stained cells with a clear nucleus (Figure 10). Though stereological analysis is generally considered to be the most accurate way to quantify cells, sampling of multiple sections throughout the SNc has been shown to be a valid alternative (Iczkiewicz *et al.*, 2010).

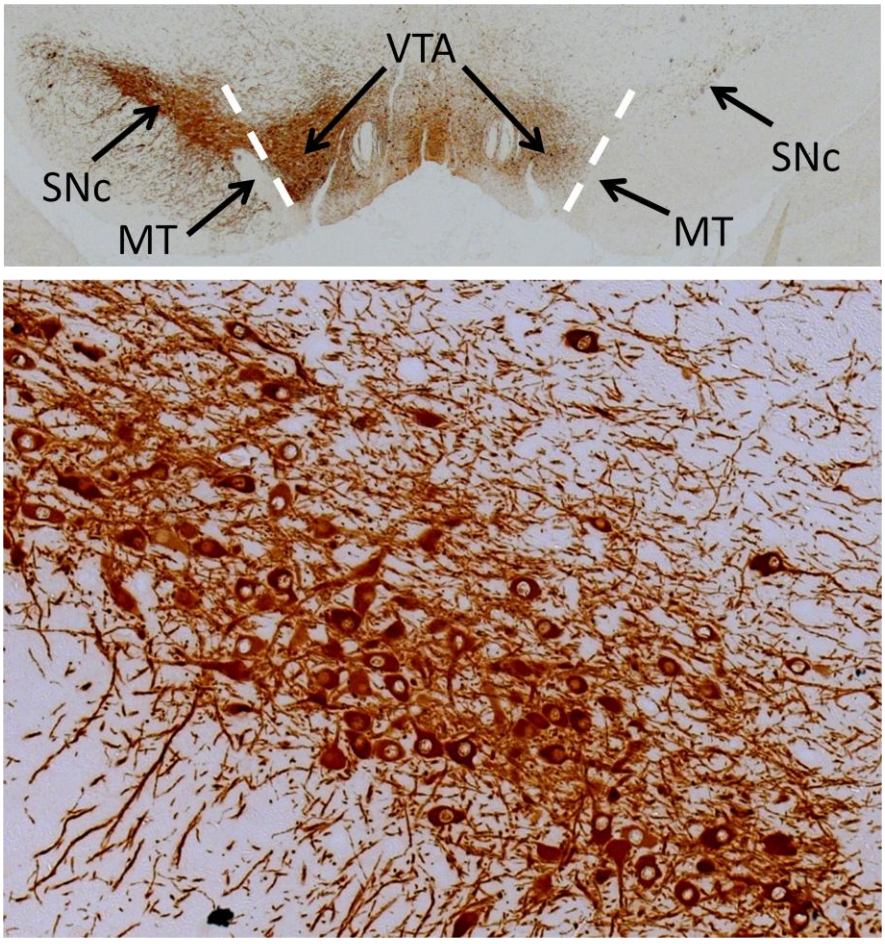

Figure 10: Cell counting methodology. The top panel shows the delineation of TH-positive cells in the substantia nigra pars compacta (SNc) and those in the ventral tegmental area (VTA) at the -5.3mm level where the two regions are divided by the medial terminal nucleus accessory optic tract (MT). The bottom panel shows a 200x magnified image of TH-positive cells in the intact SNc. Viable cells can be identified by a densely stained cytoplasm with a clear intact nucleus.

Neurochemical analysis by HPLC

To confirm the effect of the nigrostriatal lesion and different treatments on striatal dopamine content, the left and right striata analysed for their monoamine content by High Performance Liquid Chromatography (HPLC), which was carried out either by Jane Cooper or by me at Eli Lilly.

For sample preparation, tissue samples were placed on ice and 0.5ml homogenising buffer (0.1M PCA, 0.1mM EDTA, 2.5mg/l ascorbate) was immediately added. The samples were homogenised by sonication with a Vibra-cell sonic disruptor, then centrifuged at 20000 x g for 15 minutes at 8°C. The supernatant was removed and filtered, then immediately assayed.

Samples were loaded into an autosampler maintained at 8°C. HPLC with electrochemical detection was performed using a BDS Hypersil 150x3mm C18 (3µm particle size) column (Thermo Scientific, UK) with mobile phase (100mM NaH_2PO_4, 1.6mM octanesulfonic acid, 14% methanol; pH 3.2) running at 400µl/min with recycling. The dopamine metabolites 3,4-dihydroxyphenylacetic acid and homovanillic acid (DOPAC and HVA) were detected at the oxidation electrode at 50nA/V sensitivity, and dopamine was detected at the reduction electrode, also at 50nA/V sensitivity.

Peak areas of samples and standards were defined using Empower 2 software (Waters Ltd., UK) and further analysed using JMP 8.0 (SAS Institute Inc.) to enable use of the 4-parameter least-squares fit for the standard curve. This allows loss of peak area between standards the start and end of the run to be accounted for and defines the limits of quantification. The lower limit and upper limit of quantification (LLOQ and ULOQ) for each run was determined by the presence of visible peaks with <20% area difference between pre- and post- run standards. The LLOQ and ULOQ for dopamine were 1ng/ml and 1500ng/ml respectively, for DOPAC were 0.5ng/ml and 750ng/ml respectively, and for HVA were 0.5ng/ml and 750ng/ml respectively, as determined by the linear range of mixed standards ranging from 0.5-1500ng/ml.

All analyte concentrations were corrected for tissue weight. An example chromatogram for the 1500ng/ml mixed standard at the reduction electrode and an example standard curve for dopamine are shown in Figure 11 (both from Empower).

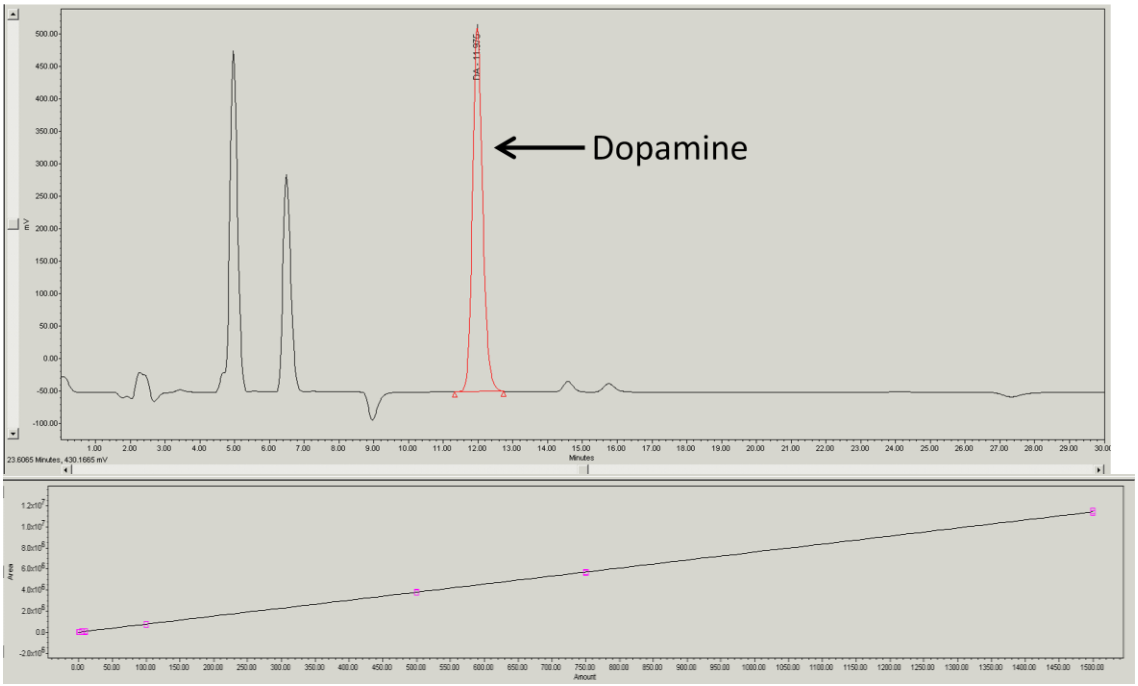

Figure 11: HPLC to analyse dopamine concentrations in the lesioned and intact striata following 6-OHDA lesioning of the MFB. The upper panel shows an example chromatogram obtained at the reduction electrode with a 1500ng/ml mixed standard. The lower panel shows an example dopamine standard curve constructed from duplicate sets of standards that are analysed at the beginning and end of each sample set.

2.2.3.3 Behavioural assessment

Three behavioural tests were performed to assess the functional outcome of the lesioning and $mGlu_4$ PAM or vehicle treatment: the cylinder test, the adjusted stepping test and rotational asymmetry. Timings of these tests varied by study and details can be found in the study plans in Figure 8 and Figure 9. Testing was carried out from 3 hours after dosing, between 12:00 and 15:00.

Cylinder test

The cylinder test was first described by Schallert *et al.* (2000) and exploits the natural exploratory behaviour of rodents when placed in a novel environment in order to define bias in use of the forelimbs following induction of unilateral injury. This test has been shown to be sensitive to nigrostriatal degeneration, leading to a clear bias towards use of the ipsilateral paw of 80-90% in rats or mice with a 'full' lesion (Glajch *et al.*, 2012; Kirik *et al.*, 2000; Lundblad *et al.*, 2002; Schallert *et al.*, 2000a) and a significant positive correlation between post-lesion forelimb use and striatal dopamine content or TH-positive cell survival (Iancu *et al.*, 2005; Schallert *et al.*, 2000a). This ipsilateral bias is reversed by known human antiparkinsonian therapies such as L-DOPA and bromocriptine (Lundblad *et al.*, 2002) along

with diverse novel neuroprotective agents such as growth factors (Kirik *et al.*, 2000) and antioxidants (de Araujo *et al.*, 2013), and neuroreplacement strategies (Haas *et al.*, 2007). This test can therefore detect both short-term pharmacological and longer-term neuroprotective/neuroregenerative antiparkinsonian effects.

For testing, rats were placed in a clear Perspex cylinder of 21cm diameter and 34cm height with a mirror behind to allow a 360° view, then video-recorded for 5 minutes (Figure 12). Supporting paw touches during exploratory rearing were scored from the video according to whether they involved the ipsilateral, contralateral or both paws, as outlined for vertical behaviour (Schallert *et al.*, 2000b) – landing behaviour was not scored. Some rats showed reduced spontaneous exploration post-lesion, probably in part because the environment was no longer novel. In these cases increased exploration was encouraged by flicking the main lights in the testing room off and on up to 3 times during the recording period.

Touches were counted by a non-blinded experimenter throughout the whole 5-minute period, or until 10 touches had been made if this was not achieved in the first 5 minutes. The number of touches involving both paws was divided equally between the ipsilateral and contralateral paws and the overall percent use of ipsilateral and contralateral paws calculated as the number of touches involving that paw divided by the total number of touches. Percentage use of each paw was compared between groups at baseline and post-lesion.

Figure 12: Rats performing the cylinder test. Rats are placed in a clear Plexiglas® cylinder of 21cm diameter and 34cm height and video-recorded for 5 minutes. The number of exploratory forepaw contacts made on the sides of the cylinder is counted for ipsilateral, contralateral and both paws together. Forelimb bias is assessed by calculating the percentage of touches involving either the ipsilateral or contralateral paws (touches using both paws are divided equally between sides).

Adjusted steps test

Several variants of stepping tests were described by Olsson *et al.* (1995) in rats with full (>98%) lesions. The one used in these studies was the adjusted steps test, whereby rats are held by the tester such that they are resting their weight on a single forepaw on the edge of a table (Figure 13). The rat is then moved laterally over a fixed distance and the number of adjusting steps taken in both the forehand (forward) and backhand (reverse) directions counted. Rats with a nigrostriatal lesion show rigidity and a greater latency to initiation of movement on the affected side, and will therefore take fewer adjusting steps post-lesion compared with pre-lesion (Lindner *et al.*, 1999; Olsson *et al.*, 1995).

Contralateral paw stepping deficits can be improved by pharmacological interventions such as L-DOPA (Winkler *et al.*, 2002), dopamine receptor agonists (Olsson *et al.*, 1995) and NMDA antagonists (Kelsey *et al.*, 2004). Improvements in the stepping test have also been reported for neuroprotective/neuroregenerative studies using growth factors (Kirik *et al.*, 2001) and dopaminergic grafts (Mukhida *et al.*, 2001).

The sensitivity of this test, i.e. the ability to predict nigrostriatal integrity on the basis of the adjusted stepping score, is unclear. In one particular study experimenters were able to detect a significant stepping difference between a 38% lesion and a 55% lesion (Kirik *et al.*, 2001), but this has not been widely replicated. These same authors had earlier described a significant positive correlation between improved stepping performance and increased survival of SNc TH-positive cells and striatal dopamine in partial to full lesions (50-98%) by linear regression (Kirik *et al.*, 1998). However several other studies have failed to reproduce a linear correlation, reporting an 'all-or nothing' effect with a threshold loss of striatal dopamine or TH-positive cells of 65%, 80% or ~98% DA loss depending on the paper (Barnéoud *et al.*, 2001; Chang *et al.*, 1999; Tseng *et al.*, 2005). Similarly a deficit in adjusted stepping has been described in MPTP mice with ~65% lesion, that is improved by L-DOPA, but not linearly correlated (Blume *et al.*, 2009). In some (Blume *et al.*, 2009; Tseng *et al.*, 2005) but not all (Barnéoud *et al.*, 2001; Chang *et al.*, 1999) of these studies there could be a linear relationship above the lesion threshold given, but this is not always investigated. Further studies report measurable but equal deficits in adjusted stepping for cell losses ranging from 20-98% (Fang *et al.*, 2006; Sun *et al.*, 2013).

For all the neuroprotection studies reported in this thesis, rats were moved along a 90cm distance over 5 seconds and the number of adjusting steps taken counted in triplicate for each paw in the forward and reverse directions. The test was performed by an

experimenter who was blinded to the treatment received by each subject. Post-lesion performance (number of steps) is expressed as a percentage of pre-lesion performance for both the ipsilateral and contralateral paws, and was compared between groups for each paw and each direction.

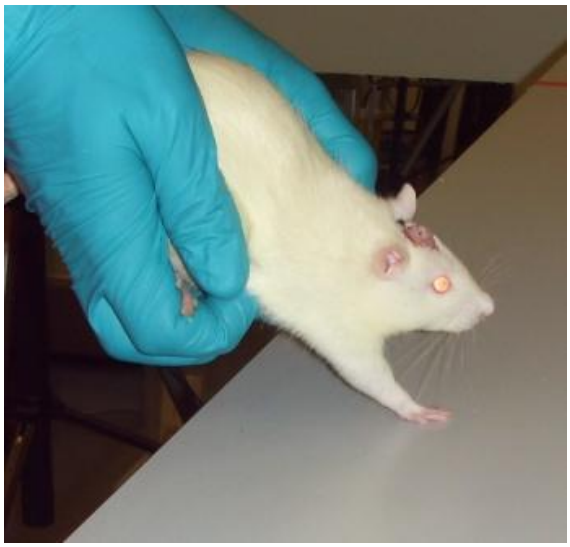

Figure 13: A rat performing the adjusted steps test. Rats are held with their weight supported on one forelimb and moved laterally over a 90cm distance in 5 seconds in forward and reverse directions. The number of adjusting steps taken is counted in triplicate for each paw in each direction.

Rotational asymmetry

Drug-induced rotational asymmetry is a standard method of assessing the extent of the lesion in a hemiparkinsonian model by measuring the imbalance in activation between the lesioned and intact hemispheres in the presence of stimulant drugs (Figure 14).

Amphetamine is a dopamine-releasing agent, therefore in the unilaterally lesioned animal amphetamine will lead to a greater release of dopamine from the intact nigrostriatal pathway compared with the lesioned nigrostriatal pathway. This imbalance leads to ipsiversive (towards the side of the lesion) turning (Ungerstedt, 1971b) assuming that the striatal dopamine in the lesioned striatum is depleted by >50% (Hefti *et al.*, 1980).

Apomorphine is a mixed D1 and D2 receptor agonist. In rats with a severe lesion, typically greater than 90% loss of nigrostriatal integrity (Hefti *et al.*, 1980), the reduced dopamine concentration in the striatum leads to upregulation of dopamine receptors. This process is called supersensitisation. Therefore administration of apomorphine in an animal with a

severe unilateral lesion causes enhanced activation in the lesioned striatum compared with the intact striatum, leading to contraversive (away from the side of the lesion) turning.

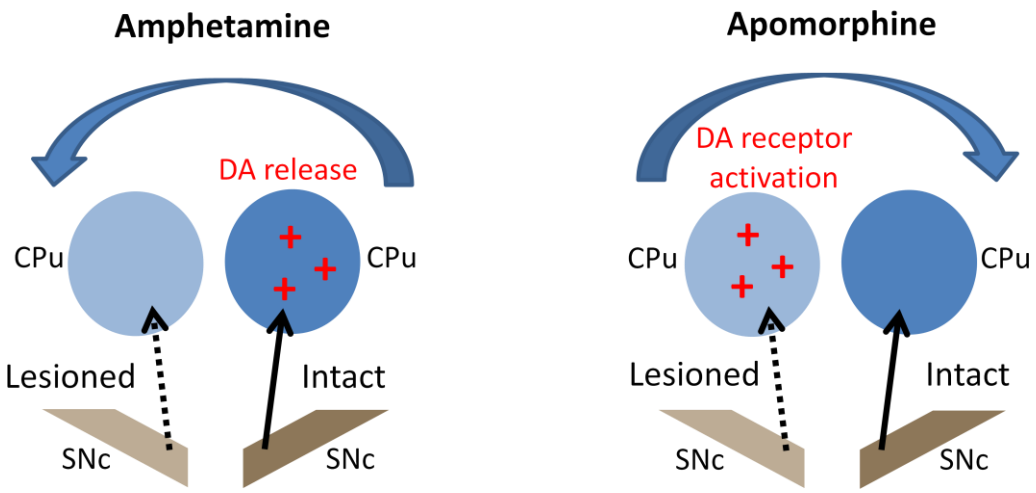

Figure 14: Diagram showing the mechanisms behind amphetamine- and apomorphine-induced rotational asymmetry in unilaterally lesioned animals. Left panel: Amphetamine causes release of dopamine from intact terminals, causing a greater activation on the intact side. This results in ipsiversive (towards the lesioned side) rotation. Right panel: Apomorphine is a dopamine receptor agonist. Where >90% striatal dopamine is lost there is receptor upregulation, leading to supersensitisation. This results in a greater activation on the lesioned side and therefore in contraversive (away from the lesioned side) rotation.

The degree of amphetamine-induced rotational asymmetry is assumed to reflect the degree of degeneration of the nigrostriatal pathway and was assessed when testing Compound 11. For this test, rats were tethered to rotational encoders in automated rotometry testing chambers (MedAssociates Inc.) and habituated for 10-30 minutes to establish baseline asymmetry before being injected with 2.5 or 5mg/kg amphetamine (intraperitoneally). Rotational behaviour was assessed automatically using Rotorat software (Med Associates Inc.) to measure full rotations in 5-minute time intervals for a total of 60-120 minutes. The total net number of ipsiversive turns over the testing period was compared between groups in the Compound 11 study.

In the VU0155041 study apomorphine-induced rotations were measured instead of amphetamine-induced rotations. This was due to the large degree of variability and also paradoxical contraversive rotations that had been measured in response to amphetamine in the Compound 11 study. Additionally, Betts *et al.* (2012) had already shown an effect of VU0155041 treatment on amphetamine-induced rotations in this model so we thought that it would be interesting to see if a similar reversal of rotational response would be elicited

when apomorphine was used instead. Rats were habituated to the rotometry apparatus for 40 minutes and then injected with 0.25mg/kg apomorphine (subcutaneously) and recorded for 90 minutes, using the same software and parameters as for amphetamine testing. The total net number of contraversive turns over the testing period was compared between groups.

2.2.3.4 Statistical analysis

Normally distributed data are reported as mean ± s.e.m and are presented as bar charts, where the bar height represents the mean and the error bars represent the s.e.m.

Nonparametric data are presented as median ± interquartile range (IQR) and are presented as box and whisker plots, where the box represents the IQR, the line within the box represents the median and the whiskers represent the minimum and maximum values obtained.

Statistical analysis was carried out using GraphPad Prism version 5.

Neuroprotective outcomes: Neuroprotection was assessed at the level of the substantia nigra by comparing cell counts in the lesioned SNc, expressed as a percent of the intact SNc, using a Kruskal-Wallis test with Dunn's *post-hoc* (for non-parametric data) or a one-way ANOVA with Dunnett's *post-hoc* (for normally-distributed data). In each group the percent of cells remaining at each anteroposterior level counted (-4.8mm, -5.3mm and -5.8mm relative to bregma) was compared using a one-way ANOVA with Bonferroni *post-hoc* test; if significant differences between percent survival was found between levels, each level was analysed separately, but if no significant difference was found between levels the data were pooled in order to calculate an overall percent survival in the lesioned SNc. Where within-group comparisons between intact and lesioned SNc cell counts were made, a t-test was used.

The effect of lesion on striatal markers of dopamine and its turnover was compared within groups using Mann-Whitney U tests (for non-parametric data) or t-tests (for normally-distributed data). Neuroprotection in the striatum was assessed by comparing the concentration of dopamine and its metabolites DOPAC and HVA remaining in the lesioned striatum, expressed as percentages of the concentrations in the intact striatum. Dopamine turnover is increased in the caudate, putamen and nucleus accumbens in PD patients (Rabey *et al.*, 2008), therefore the dopamine turnover in each rat was calculated from the measured concentrations of dopamine and its metabolites using the formula

(DOPAC+HVA)/DA. The turnover in the lesioned striatum, expressed as a percentage of the turnover in the intact striatum, was compared between treatment groups. Normally distributed striatal data were analysed using a one-way ANOVA with Dunnett's *post-hoc* test. Nonparametric striatal data were analysed using a Kruskal-Wallis with a Dunn's *post-hoc* test.

Behavioural tests: The cylinder test was analysed using a 2-way repeated measures ANOVA with Bonferroni *post-hoc* analysis to assess the effects of both lesion and treatment on paw use. Adjusted steps and rotometry data and were analysed using a one-way ANOVA with a Dunnett's *post-hoc*. Where pre- vs. post-lesion performance in the adjusted steps test was compared within a group, a paired t-test was used to compare the absolute number of steps taken.

For all tests, the outcome was considered significant where $P<0.05$.

2.3 Results

2.3.1 Compound 11 (Cpd11)

2.3.1.1 General observations

One rat died in the 200nmol-treated group, leaving n=7. For all other treatment groups n=8.

No acute- or sub-chronic adverse effects of dosing with vehicle or Cpd 11 were noted on animal health or wellbeing.

2.3.1.2 Compound 11 did not protect against nigrostriatal degeneration

TH-positive cells in the SNc

Intranigral infusion of 6-OHDA was expected to result in a large loss of TH-positive cells in the lesioned SNc, with cells in the intact SNc unaffected. Representative nigral images from each treatment group at -5.3mm from bregma and the results of the TH-positive cell counts are shown in Figure 15. There was a significant difference in the vehicle-treated and 20nmol Cpd 11-treated rats with regard to the percent of cells remaining at the different anteroposterior levels of the SNc, therefore each level was analysed separately.

-4.8mm: At this level, closest to the lesion site, vehicle-treated rats had a mean of 26 ± 7% TH-positive cells remaining in the lesioned SNc. Within the Cpd 11-treated rats the 20nmol group had 12 ± 3% survival, the 100nmol group had 25 ± 5% survival and the 200nmol group had 22 ± 10% survival, meaning that there was no significant effect of treatment on TH-positive cell survival at this level (P=0.3574, one-way ANOVA with Dunnett's *post-hoc*).

-5.3mm: At this level, vehicle-treated rats had a mean of 38 ± 5% TH-positive cells remaining in the lesioned SNc. Within the Cpd 11-treated rats the 20nmol group had 27 ± 4% survival, the 100nmol group had 38 ± 4% survival and the 200nmol group had 28 ± 5% survival. Again there was no significant effect of treatment on TH-positive cell survival at this level (P=0.1736, one-way ANOVA with Dunnett's *post-hoc*).

-5.3mm: At this level, vehicle-treated rats had a mean of 39 ± 3% TH-positive cells remaining in the lesioned SNc. Within the Cpd 11-treated rats the 20nmol group had 37 ± 5% survival, the 100nmol group had 36 ± 3% survival and the 200nmol group had 37 ± 8% survival. Again there was no significant effect of treatment on TH-positive cell survival at this level (P=0.9738, one-way ANOVA with Dunnett's *post-hoc*).

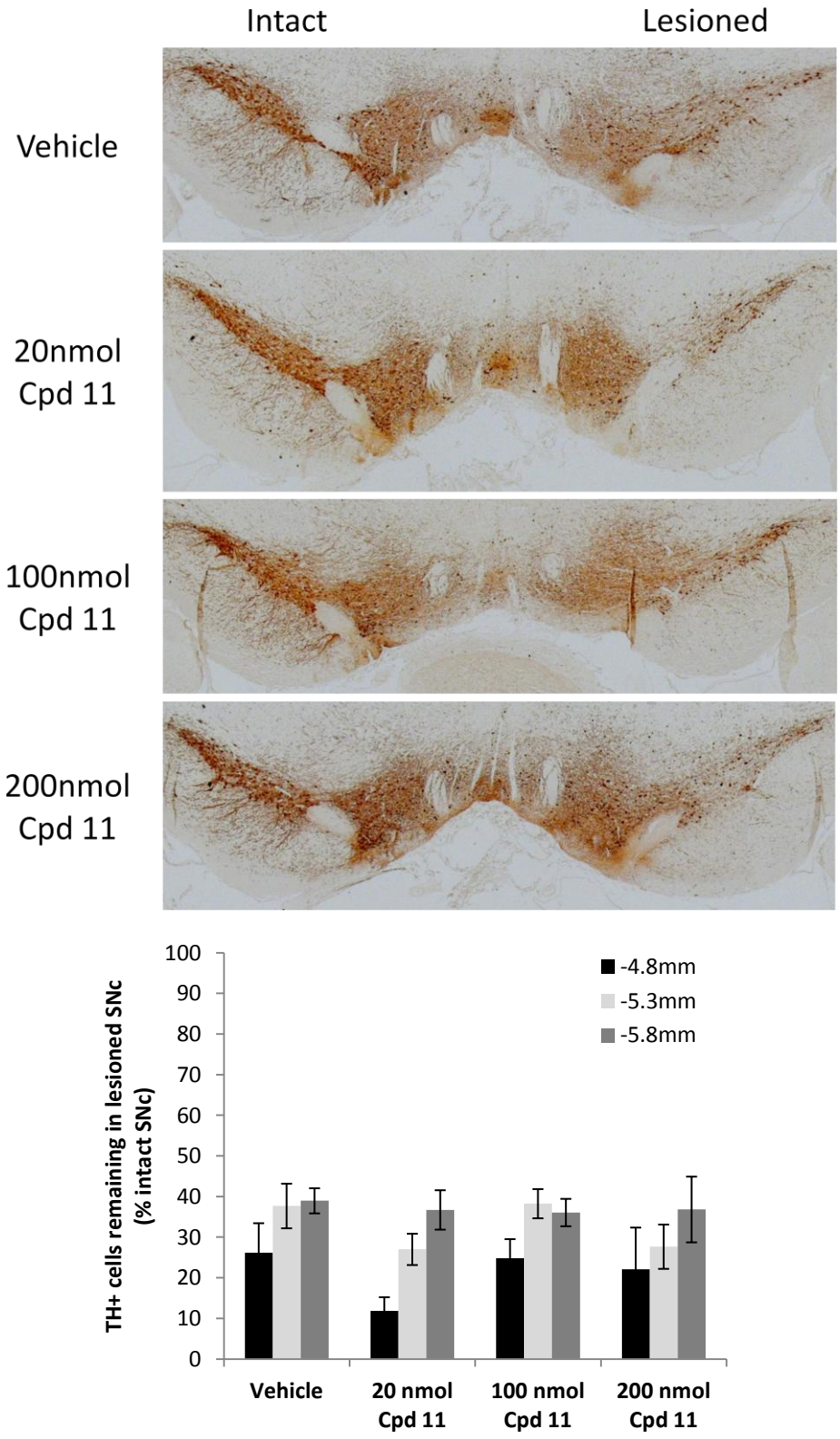

Figure 15: TH-positive cells remaining in rats with a nigral 6-OHDA lesion, sub-chronically treated with vehicle or Cpd 11. The upper panels show representative nigral images comparing TH-positive cells in the intact and 6-OHDA-lesioned SNc in each treatment group at -5.3mm from bregma. The graph shows the mean number of TH-positive cells in the lesioned SNc as a percent of the intact SNc at each anteroposterior level. There was no significant effect of treatment on the percent of surviving TH-positive cells at any level. Data are presented as mean ± s.e.m. (n = 7-8).

Striatal dopamine content

Upon induction of a lesion of the nigrostriatal pathway dopaminergic neurochemical parameters are subject to change. As A9 cells degenerate, the total striatal dopamine content decreases and dopamine turnover, measured as the ratio of dopamine metabolites to dopamine, increases as remaining dopaminergic terminals adapt to try to maintain normal extracellular levels of dopamine. The following data were non-parametric and are therefore reported as median ± interquartile range, with non-parametric statistical analysis.

The median concentrations of dopamine and its metabolites in the intact and lesioned striatum are shown in Table 5. In all groups, nigral infusion of 6-OHDA led to significant reductions of dopamine, DOPAC and HVA ($P<0.01$; Mann-Whitney U test) and significant increases in dopamine turnover ($P<0.05$; Mann-Whitney U test) in the lesioned striatum compared with the intact striatum.

Table 5: Striatal concentrations of dopamine and its metabolites in the intact and lesioned striatum following a 6-OHDA nigral lesion and treatment with vehicle or Cpd 11. Data reported are median concentrations in ng/g (nearest whole number), except for the dopamine turnover ratio (n = 7-8) *P<0.05, **P<0.01, ***P<0.001 (Mann-Whitney U test versus intact).

	Dopamine (DA)		DOPAC		HVA		(DOPAC+HVA)/DA	
	Intact	**Lesioned**	**Intact**	**Lesioned**	**Intact**	**Lesioned**	**Intact**	**Lesioned**
Vehicle	12003	221***	1061	10***	597	45***	0.14	0.34***
20nmol Cpd 11	13467	184***	1332	8***	632	35***	0.16	0.32*
100nmol Cpd 11	13223	285***	1318	9***	717	46***	0.16	0.27*
200nmol Cpd 11	11830	145**	1258	8**	675	39**	0.16	0.36*

Vehicle-treated rats showed a decrease of striatal dopamine content in the lesioned striatum to 1.83 ± 0.67% of the intact concentration (Figure 16). Dopamine metabolites were similarly reduced, to 0.74 ± 1.67% for DOPAC and to 8.69 ± 6.57% for HVA.

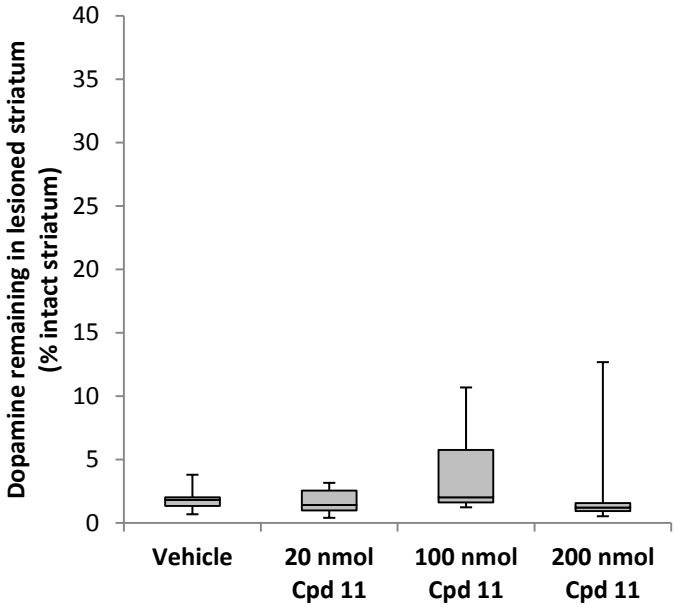

Figure 16: Striatal dopamine content in the lesioned striatum of rats with a nigral 6-OHDA lesion, sub-chronically treated with vehicle or Cpd 11. Treatment with Cpd 11 did not provide significant preservation of striatal dopamine content at any of the doses tested. Data are presented as median ± IQR (n = 7-8).

Treatment with Cpd 11 did not provide significant preservation of striatal dopamine or its metabolites at any of the doses tested. 20nmol Cpd 11-treated rats retained 1.43 ± 1.57% dopamine, 0.62 ± 1.16% DOPAC and 5.91 ± 3.70% HVA; 100nmol Cpd 11-treated rats retained 2.02 ± 4.14% dopamine, 0.63 ± 10.39% DOPAC and 5.53 ± 16.69% HVA; and 200nmol Cpd-11 treated rats retained 1.22 ± 0.61% dopamine, 0.60 ± 0.04% DOPAC and 4.98 ± 1.26% HVA. There was no significant effect of treatment on percent dopamine content (P=0.2816; Kruskal-Wallis test with Dunn's *post-hoc*), percent DOPAC content (P=0.7869; Kruskal-Wallis test with Dunn's *post-hoc*, data not shown) or percent HVA content (P=0.6722; Kruskal-Wallis test with Dunn's *post-hoc*, data not shown).

Dopamine turnover was significantly affected by the lesion in all groups (data not shown). Vehicle-treated rats had an increase in turnover from 0.14 ± 0.01 in the intact striatum to 0.34±0.21 in the lesioned striatum, an increase of 222 ± 143%. Rats treated with 20nmol Cpd 11 showed a similar increase in dopamine turnover in the lesioned striatum, to 218 ± 132% of the turnover measured in the intact striatum, and likewise 100nmol Cpd 11-treated rats showed a 163 ± 100% increase and 200nmol Cpd 11-treated rats showed a 217 ± 46% increase. Dopamine turnover was not significantly different between vehicle and treated rats (P=0.6293; Kruskal-Wallis test with Dunn's *post-hoc*).

2.3.1.3 Compound 11 did not show consistent preservation of functional outcomes

Cylinder test

Pre-lesion and post-lesion use of the ipsilateral and contralateral forelimbs during the cylinder test is shown in Figure 17. At baseline (Figure 17a) there was no significant difference between groups with respect to either forelimb use (P=0.5888; two-way RM ANOVA with Bonferroni *post-hoc*), with all groups using each forelimb for approximately 50% of touches.

Lesioned rats that were vehicle-treated showed a significant decrease in use of the contralateral forelimb during exploratory reaching in the cylinder test, from a mean of 46 ± 4% touches to 8 ± 4% touches (Figure 17b; P<0.0001; two-way RM ANOVA with Bonferroni *post-hoc*). This result shows that a measurable deficit was caused by the lesion induced in these rats. Groups treated with 20-200nmol Cpd 11 also showed significantly decreased use of the contralateral forelimb post-lesion (P<0.0033; two-way RM ANOVA with Bonferroni *post-hoc*).

This two-way comparison also revealed an overall effect of treatment that was approaching significance (P=0.0807; two-way RM ANOVA with Bonferroni *post-hoc*). The Bonferroni *post-hoc* test revealed a significant effect of treatment between the vehicle-treated group and the 20nmol Cpd 11-treated group regarding post-lesion contralateral forelimb use, with only 8 ± 4% touches in the vehicle group and 24±5% touches in the 20nmol Cpd 11 group (P<0.01; two-way RM ANOVA with Bonferroni *post-hoc*). This suggests that there was partial preservation of contralateral forelimb function in the cylinder test at this dose, although it still represents a significant deficit compared with pre-lesion (P=0.0033; two-way RM ANOVA with Bonferroni *post-hoc*).

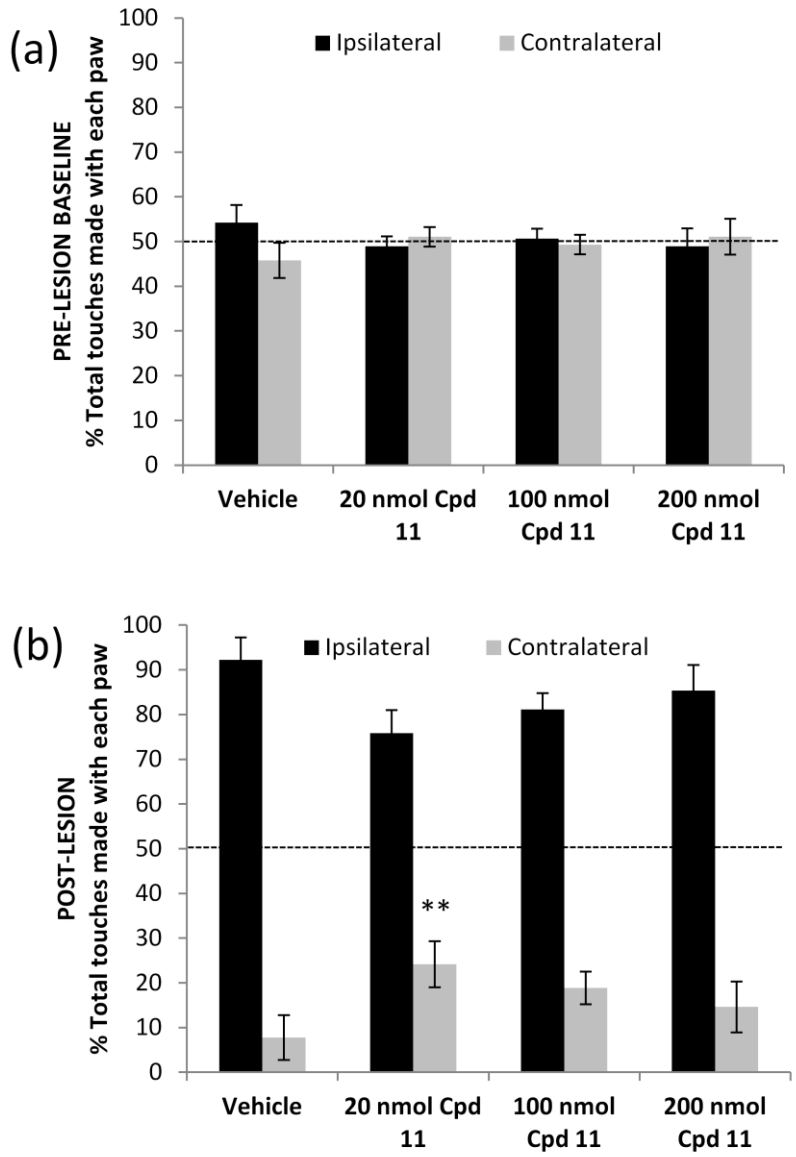

Figure 17: Forelimb use in the cylinder test in rats with a nigral 6-OHDA lesion, sub-chronically treated with vehicle or Cpd 11. The dashed line shows the expected use of each paw in intact rats. Baseline forelimb use is shown in graph (a), indicating no significant bias towards either limb in any group. Post-lesion results are shown in (b), indicating that all groups showed a clear bias towards use of the ipsilateral paw following nigral 6-OHDA infusion. Daily treatment with 20nmol Cpd 11 significantly preserved contralateral forelimb use compared with vehicle-treated rats, though this was still significantly reduced compared with pre-lesion use. Data are presented as mean ± s.e.m. (n = 7-8) **P<0.01 versus Vehicle (two-way ANOVA with Bonferroni *post-hoc*).

Adjusted steps test

In the adjusted steps test (Figure 18), vehicle-treated animals took a reduced number of adjusting steps with the contralateral forelimb post-lesion, achieving only 59 ± 4% baseline forward steps and 64 ± 6% baseline reverse steps. When the numbers of contralateral steps taken pre- and post-lesion in this group were compared these percentages represented a significant decrease in both the forward (P=0.0003; paired t-test) and reverse (P=0.0010;

paired t-test) directions. These results show that a unilateral deficit was measurable in fully-lesioned rats using this test.

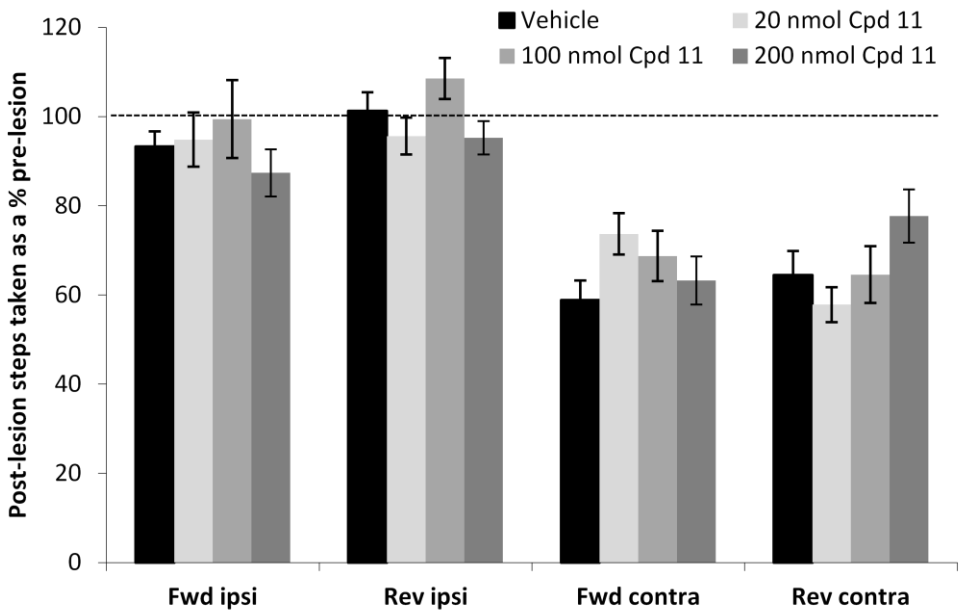

Figure 18: Adjusted stepping test performance in rats with a nigral 6-OHDA lesion, sub-chronically treated with vehicle or Cpd 11. The dashed line shows the expected performance in intact rats (100% baseline). Contralateral paw performance was decreased post-lesion in all groups, and there was no significant effect of treatment with Cpd 11 on post-lesion use of this forelimb in either the forward or reverse directions. As expected, ipsilateral paw performance was not significantly affected by the lesion. Data are presented as mean ± s.e.m. (n = 7-8). Fwd = forward direction; Rev = reverse direction; Ipsi = ipsilateral forelimb; Contra = contralateral forelimb.

The contralateral limb performance of rats (compared with pre-lesion) treated with 20nmol Cpd 11 was reduced to 74 ± 5% forward and 58 ± 4% in reverse, with 100nmol Cpd 11 to 69 ± 6 forward and 65 ± 6% in reverse and with 200nmol Cpd 11 to 63 ± 5% forward and 78 ± 6% in reverse. When the percentage performance was compared between Cpd 11-treated groups and vehicle for the contralateral limb there was no significant effect of treatment on stepping in either the forward (P=0.1860; one-way ANOVA with Dunnett's *post-hoc*) or reverse (P=0.1294; one way ANOVA with Dunnett's *post-hoc*) directions.

There was also no significant effect of treatment with Cpd 11 on the post-lesion performance of the ipsilateral paw, which was unaffected in both the forward (P=0.6448; one-way ANOVA) and reverse (P=0.1168; one-way ANOVA with Dunnett's *post-hoc*) directions compared with the vehicle-treated group.

As would be expected with a unilateral lesion, there was no effect of lesion on adjusted stepping performance of the ipsilateral forelimb in any group in either the forward (P>0.3153; paired t-tests) or reverse (P>0.1447; paired t-tests) directions.

Amphetamine-induced rotational asymmetry

Unilaterally lesioned animals are expected to turn in an ipsiversive direction following administration of amphetamine, as mentioned in section 2.2.3.3, and the imbalance is expected to be greatest in untreated animals, resulting in a high degree of net ipsiversive asymmetry. However, the results of the response to 5mg/kg i.p. D-amphetamine sulfate in this study were so variable within each group as to render them inconclusive. The time course and total net ipsiversive rotations over 60 minutes are shown in Figure 19.

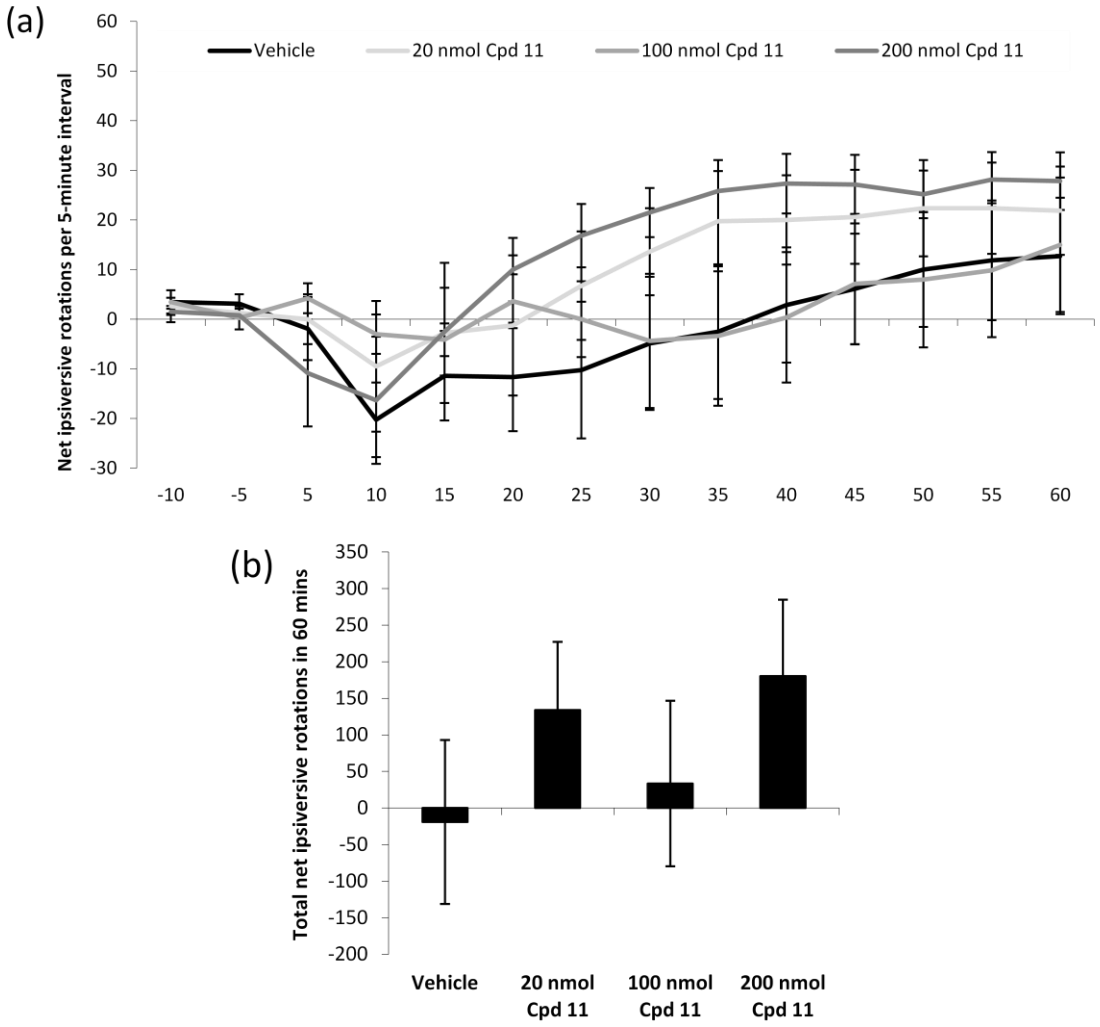

Figure 19: Amphetamine-induced rotational asymmetry in rats with a nigral 6-OHDA lesion, sub-chronically treated with vehicle or Cpd 11. The time course of rotations is shown in graph (a) and the total net number of full ipsiversive rotations over 60 minutes is shown in graph (b). There was no significant effect of treatment with Cpd11 on net rotational asymmetry. Data are presented as mean ± s.e.m. (n = 7-8 per group).

Contrary to expectations the vehicle-treated animals showed net contraversive turning during the 60 minute testing period (-19.1 ± 112 net ipsi turns per 60 mins), however this is likely due to a large variability between animals in this group, where many rats rotated strongly in a contraversive direction in the initial stages after the injection.

The net ipsiversive turns in 60 minutes for the Cpd 11-treated groups were 134 ± 113 at 20nmol, 33 ± 105 at 100nmol and 180 ± 48 at 200nmol. Although 20-200nmol Cpd 11-treated animals had net ipsiversive asymmetry as would be expected following amphetamine, the time course shows that several rats within these groups also demonstrated contraversive turning following the injection, before switching to the expected ipsiversive turning.

The variability in the responses of the rats within all groups means that the standard errors of the mean are extremely large both throughout the time course and for the total net ipsiversive rotations over 60 minutes. There were no significant differences between groups with respect to the total net rotational asymmetry over the 60 minute testing period (P=0.5393; one-way ANOVA with Dunnett's *post-hoc*).

2.3.2 VU0155041

2.3.2.1 General observations

One rat each in the 200nmol-treated group and the vehicle-treated group were excluded from analysis on the basis that their lesions were incomplete (reflux of 6-OHDA solution was noted in both rats during infusion, reflected in <50% loss of TH-positive cells). For these groups therefore n=7. For all other treatment groups n=8.

No acute- or sub-chronic effects of dosing with vehicle or VU0155041 were noted on animal health or wellbeing..

2.3.2.2 VU0155041 provides significant protection of nigrostriatal integrity

TH-positive cells in the SNc

Though cells were counted at 3 anteroposterior levels of the substantia nigra (-4.8mm, -5.3mm and -5.8mm relative to bregma), there were no significant differences between the levels regarding the percent of cells remaining in any group (P>0.2734; one-way ANOVAs with Bonferroni *post-hoc* test) and therefore the data was pooled to calculate overall percent cell survival.

The lesioned SNc of vehicle-treated rats contained a mean of 3.6 ± 0.8 TH-positive cells compared with 101.5 ± 3.8 in the intact SNc, meaning that only 3.6 ± 0.9% dopaminergic cells survived the lesion (Figure 20). Treatment with VU0155041 offered some degree of neuroprotection, with 50nmol VU0155041-treated rats retaining 21.0 ± 10.2% cells, 100nmol VU0155041-treated rats retaining 27.6 ± 7.6% cells and 200nmol VU0155041-treated rats retaining 11.2 ± 4.0% cells. Analysis revealed that there was a significant effect of 100nmol VU0155041 compared with vehicle with respect to the percentage of cells surviving in the lesioned SNc compared with the intact SNc (P=0.0199; one-way ANOVA with Dunnett's *post-hoc*).

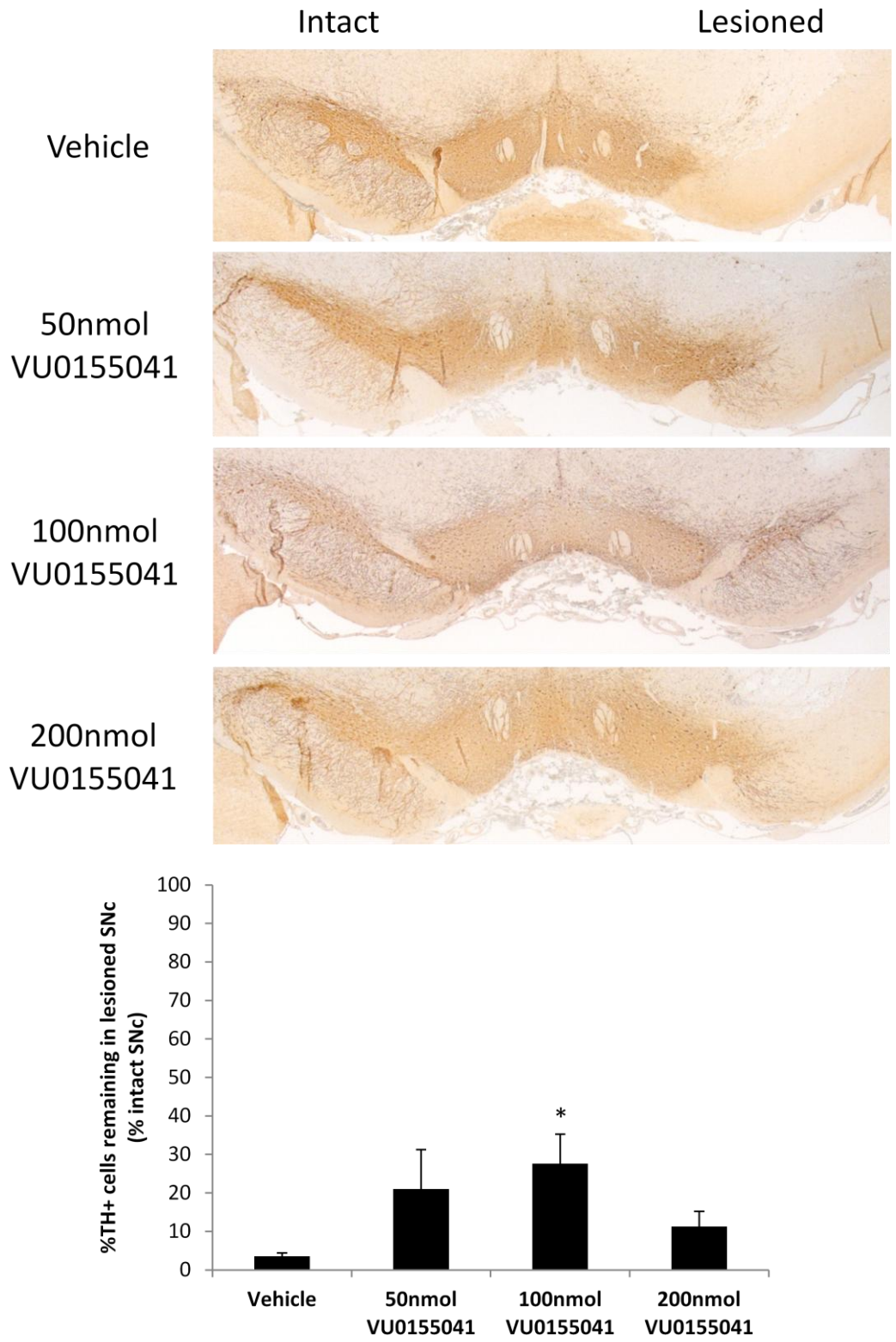

Figure 20: TH-positive cells remaining in rats with a nigral 6-OHDA lesion, sub-chronically treated with vehicle or VU0155041. The upper panels show representative nigral images comparing TH-positive cells in the intact and 6-OHDA-lesioned SNc in each treatment group. The graph shows the mean number of TH-positive cells in the lesioned SNc as a percent of the intact SNc. Sub-chronic treatment with 100nmol VU0155041 significantly increased the percent of surviving TH-positive cells compared with vehicle-treated rats. Data are presented as mean ± s.e.m. (n = 7-8) *P<0.05 versus vehicle (one-way ANOVA with Dunnett's *post-hoc*)

Striatal dopamine content

The mean concentrations of dopamine, DOPAC and HVA measured by HPLC in the intact and lesioned striatum are shown in Table 6 along with the dopamine turnover. 6-OHDA lesioning led to a significant reduction in dopamine, DOPAC and HVA in the lesioned striatum in all groups (P<0.01; t-tests) along with a significant increase in dopamine turnover (P<0.01; t-tests).

Table 6: Striatal concentrations of dopamine and its metabolites in the intact and lesioned striatum following a 6-OHDA nigral lesion and treatment with vehicle or VU0155041. Data reported are mean concentrations in ng/g (nearest whole number), except for the dopamine turnover ratio (n = 7-8) **P<0.01, ***P<0.001 (t-test versus intact).

	Dopamine (DA)		**DOPAC**		**HVA**		**(DOPAC+HVA)/DA**	
	Intact	**Lesioned**	**Intact**	**Lesioned**	**Intact**	**Lesioned**	**Intact**	**Lesioned**
Vehicle	14128	748***	1488	139***	705	96***	0.16	0.33**
50nmol VU0155041	14298	4077***	1614	492***	819	285***	0.17	0.30**
100nmol VU0155041	15664	5845***	1639	785***	722	383**	0.15	0.22**
200nmol VU0155041	14126	2289***	1576	423***	673	217***	0.16	0.34**

In vehicle-treated animals, 6-OHDA lesioning of the SN led to a large depletion of striatal dopamine and its metabolites in the lesioned striatum, such that the lesioned striatum contained only 5.2 ± 1.2% of the dopamine measured in the intact striatum (Figure 21).

Treatment with VU0155041 preserved the dopamine content in the lesioned striatum, retaining 25.6 ± 11.3% in the 50nmol group, 38.1 ± 9.7% in the 100nmol group and 16.1 ± 4.5% in the 200nmol group. There was a significant effect of 100nmol VU0155041 compared with vehicle on the percent of striatal dopamine remaining (P<0.05; one-way ANOVA with Dunnett's *post-hoc*). The mean of 38% striatal dopamine remaining in the 100nmol group is tantalisingly close to the 40% threshold at which motor symptoms of Parkinson's disease are said to become apparent, meaning that this level of protection would likely be associated with clinical improvements.

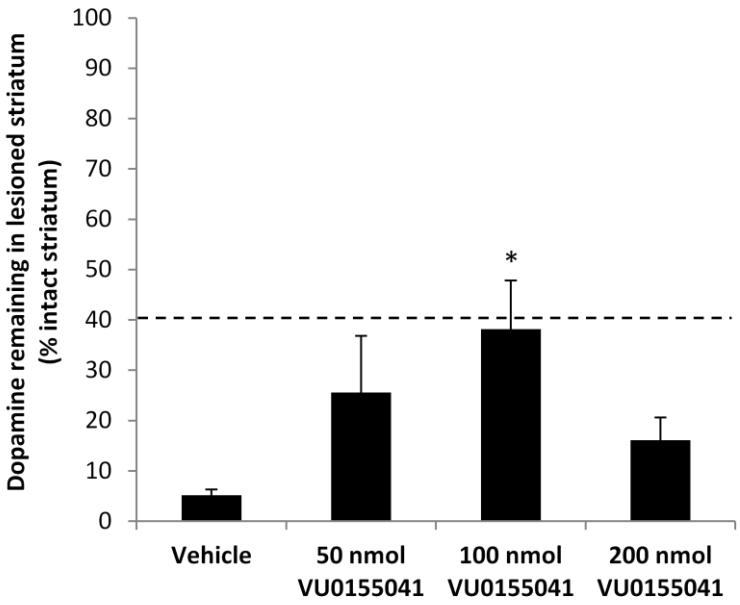

Figure 21: Striatal dopamine content in the lesioned striatum of rats with a nigral 6-OHDA lesion, sub-chronically treated with vehicle or VU0155041. Treatment with 100nmol VU0155041 led to significant preservation of striatal dopamine content compared with rats treated with vehicle. The dashed line shows 40% striatal dopamine preservation, the threshold at which motor symptoms are said to become apparent in human PD. Data are presented as mean ± s.e.m. (n = 7-8) *P<0.05 versus Vehicle (one-way ANOVA with Dunnett's *post-hoc*).

Along with significant preservation of striatal dopamine in the 100nmol VU1055041-treated group, the same effect was found for the percent DOPAC and HVA concentrations. Vehicle-treated rats had a mean of 9.0 ± 2.5% DOPAC and 13.4 ± 1.3% HVA preserved in the lesioned striatum whereas the 100nmol VU0155041-treated group had 47.7 ± 10.2% DOPAC and 52.1 ± 9.8% HVA remaining in the lesioned striatum (both P<0.05; one-way ANOVAs with Dunnett's *post-hoc*).

As would be expected following a lesion, dopamine turnover in the vehicle-treated group was increased in the lesioned striatum compared with the intact striatum, with (DOPAC+HVA)/DA ratios of 0.33 and 0.16 respectively (Table 6), representing a 210 ± 19% increase (Figure 22). Dopamine turnover rates were reduced by treatment with VU0155041, with an inverse bell-shaped dose response, with the effect approaching significance (P=0.0855; one-way ANOVA with Dunnett's *post-hoc*).

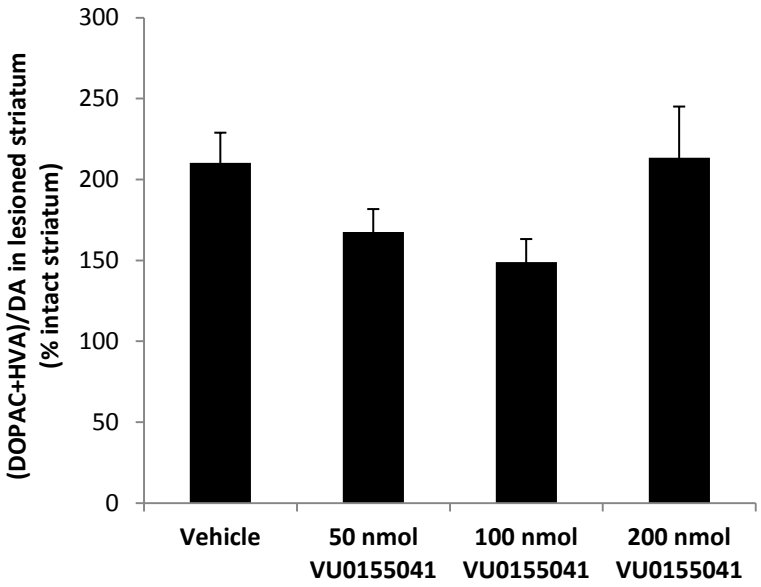

Figure 22: Dopamine turnover rate in the lesioned striatum of rats with a nigral 6-OHDA lesion, sub-chronically treated with vehicle or VU0155041. The increase in dopamine turnover induced by the lesion in vehicle-treated rats was partially reversed in rats treated with 50nmol or 100nmol VU0155041, an effect which approached significance (P=0.086; one-way ANOVA with Dunnett's *post-hoc*). Data are displayed as mean ± s.e.m. (n = 7-8).

2.3.2.3 VU0155041 provided significant preservation of functional outcomes

Cylinder test

Pre-lesion and post-lesion use of the ipsilateral and contralateral forelimbs during the cylinder test is shown in Figure 23. At baseline (Figure 23a) there was no significant difference between groups with respect to either forelimb use (P=0.9337; two-way RM ANOVA with Bonferroni *post-hoc*), with all groups using each forelimb for approximately 50% of touches.

Vehicle-treated 6-OHDA-lesioned rats showed a marked reduction in use of the contralateral paw in the cylinder test post-lesion (Figure 23b), from a mean of 50 ± 3% touches to a mean of 5 ± 2% touches (P<0.0001; two-way RM ANOVA with Bonferroni *post-hoc*).

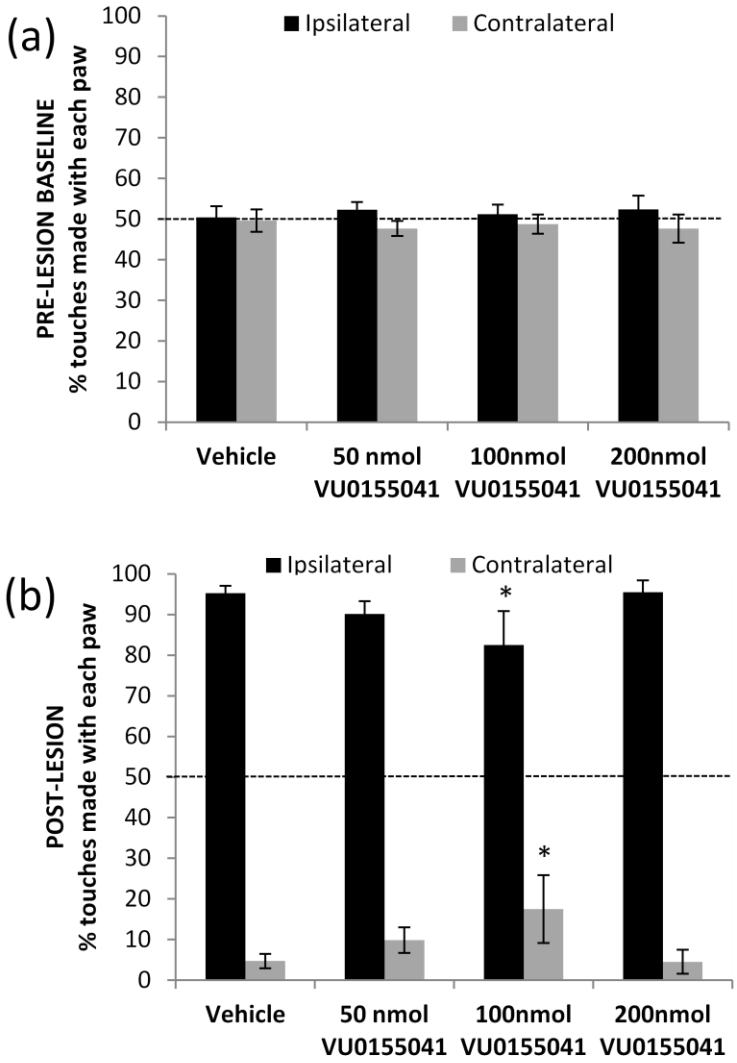

Figure 23: Forelimb use in the cylinder test in rats with a nigral 6-OHDA lesion, sub-chronically treated with vehicle or VU0155041. The dashed line shows the expected use of each paw in intact rats. Baseline forelimb use is shown in graph (a), indicating no significant bias towards either limb in any group. Post-lesion results are shown in (b), indicating that all groups showed a clear bias towards use of the ipsilateral paw following nigral 6-OHDA infusion. Daily treatment with 100nmol VU0155041 significantly preserved contralateral forelimb use compared with vehicle-treated rats, though this was still significantly reduced compared with pre-lesion use. Data are presented as mean ± s.e.m. (n = 7-8) *P<0.05 versus Vehicle (two-way ANOVA with Bonferroni *post-hoc*).

Treatment with increasing doses of VU0155051 produced a bell-shaped effect on contralateral paw reaching, such that the 50nmol group used the contralateral paw in 10 ± 3% of touches, the 100nmol group in 18 ± 8% of touches and the 200nmol group in 5 ± 3% touches. The 100nmol group had significantly increased post-lesion use of the contralateral paw compared to vehicle (P<0.05; two-way RM ANOVA with Bonferroni *post-hoc*). While significantly higher than the vehicle-treated group, this still represented a significant

decrease compared with pre-lesion performance (P=0.0054; two-way RM ANOVA with Bonferroni *post-hoc*).

Adjusted steps test

Vehicle-treated 6-OHDA lesioned animals showed a decrease in number of steps taken in both the forward (P=0.0006; paired t-test) and reverse (P=0.0024; paired t-test) directions post-lesion compared with pre-lesion. This corresponded to a reduction in performance to 58 ± 4% of pre-lesion in the forward direction and 63 ± 6% in the reverse direction (Figure 24).

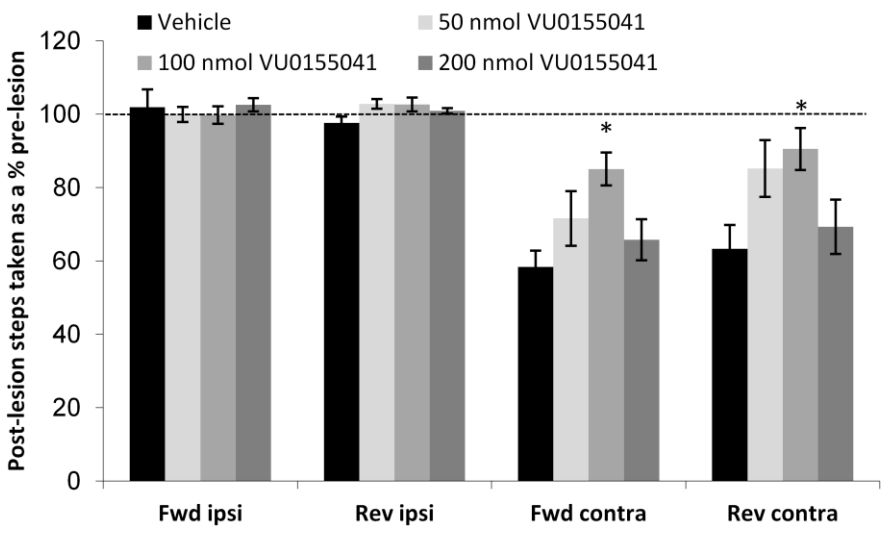

Figure 24: Adjusted stepping test performance in rats with a nigral 6-OHDA lesion, sub-chronically treated with vehicle or VU0155041. The dashed line shows the expected performance in intact rats (100% baseline). Contralateral paw performance was decreased post-lesion in all groups, however treatment with 100nmol VU0155041 significantly preserved stepping performance in this paw in both the forward and reverse directions. Data are presented as mean ± s.e.m. (n=7-8). Fwd = forward direction; Rev = reverse direction; Ipsi = ipsilateral forelimb; Contra = contralateral forelimb.*P<0.05 versus Vehicle (one-way ANOVA with Dunnett's *post-hoc*).

Treatment with VU0155041 preserved the function of this paw as demonstrated by the increased stepping in VU-treated animals. In the forward direction, contralateral stepping performance was 72 ± 7% in the 50nmol group, 85 ± 4% in the 100nmol group and 66 ± 6% in the 200nmol group compared. This increase was significant in the 100nmol group (P=0.0247; one-way ANOVA with Dunnett's *post-hoc*). In the reverse direction, contralateral stepping performance was 85 ± 8% in the 50nmol group, 90 ± 6% in the

100nmol group and 69 ± 7% in the 200nmol group. Again, this increase in stepping was significant in the 100nmol group (P=0.0351; one-way ANOVA with Dunnett's *post-hoc*).

As would be expected with a unilateral lesion, there was no effect of lesion on the number of adjusted steps taken by the ipsilateral forelimb in any group in either the forward (P>0.1761; paired t-tests) or reverse (P>0.2031; paired t-tests) directions.

Apomorphine-induced rotational asymmetry

The time course of rotations before and following 0.25mg/kg s.c. apomorphine is shown in Figure 25. Apomorphine acts on post-synaptic dopamine receptors, and elicits contraversive rotations in rodents with a full unilateral lesion due to supersensitisation of these receptors. This was the case for the vehicle-treated group, where baseline spontaneous ipsiversive rotations (net ipsiversive turns over 40 minutes = 7.7 ± 2.4) gave way to contraversive rotations following injection of apomorphine (net contraversive turns over 90 minutes = 44.0 ± 27.3).

Following injection of apomorphine, rats treated with 50nmol VU0155041 showed overall contraversive asymmetry (19.6 ± 14.2 turns over 90 minutes), as did rats treated with 200nmol VU0155041 (21.1 ±1 0.7 turns over 90 minutes), though to a lesser degree than vehicle-treated animals. On the other hand, rats treated with 100nmol VU0155041 showed no overall contraversive asymmetry in response to apomorphine, with a net rotational asymmetry of 4.1 ± 10.5 ipsiversive rotations over 90 minutes.

When net contraversive rotations were compared between groups there was no significant effect of treatment with VU0155041 on apomorphine-induced asymmetry (P=0.2396; one-way ANOVA with Dunnett's *post-hoc*), despite a clear trend towards reduced contraversive turning in VU0155041-treated groups compared with the vehicle-treated group. This is likely explained by the high degree of variability in rotational response within groups, with some rats showing very little asymmetry following apomorphine injection and at least one animal from each VU0155041-treated group having a net ipsiversive response to apomorphine. This will be addressed in the discussion.

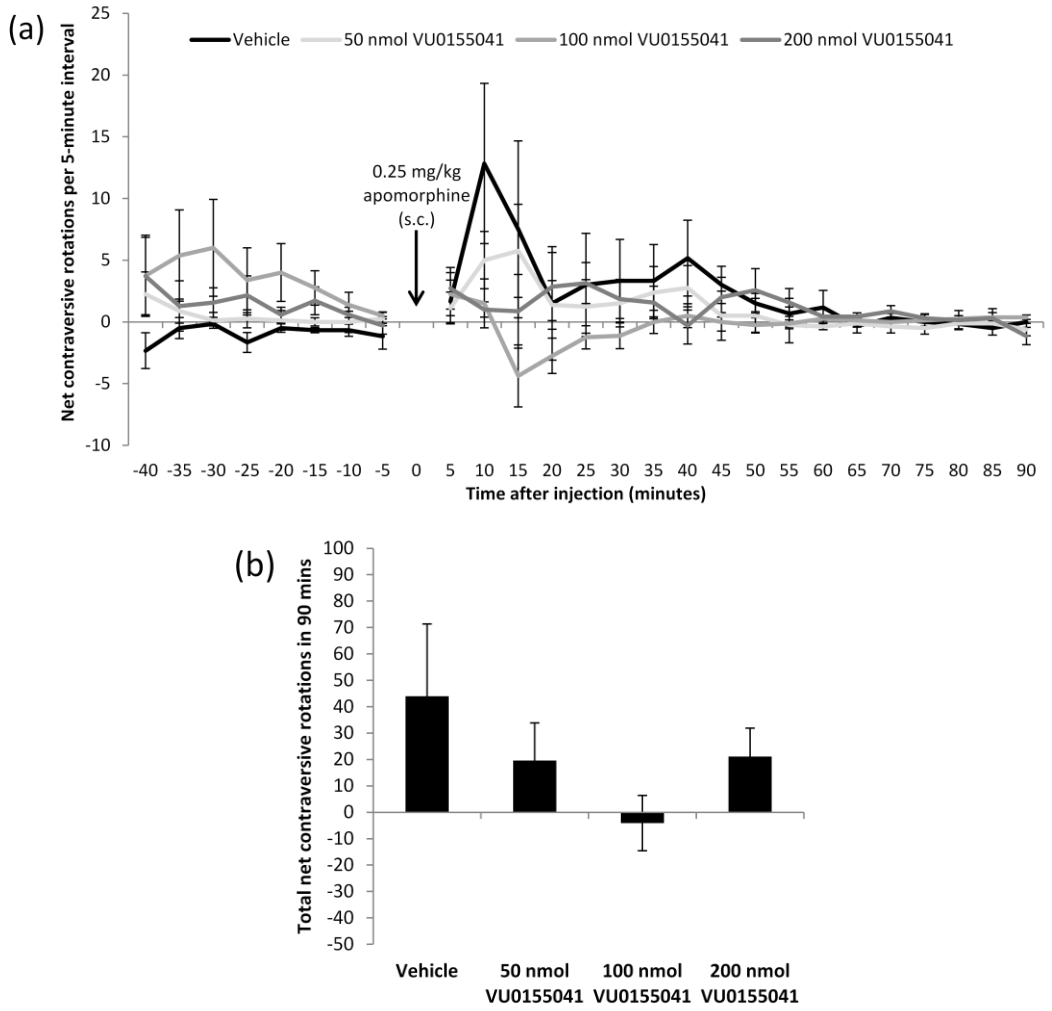

Figure 25: Apomorphine-induced rotational asymmetry in rats with a nigral 6-OHDA lesion, sub-chronically treated with vehicle or VU0155041. The time course of rotations is shown in graph (a) and the total net number of full ipsiversive rotations over 90 minutes is shown in graph (b). There was no significant effect of treatment with VU0155041 on net rotational asymmetry. Data are presented as mean ± s.e.m. (n = 7-8 per group).

2.4 Discussion

These studies set out to ascertain whether selective activation of $mGlu_4$ in the SNc by sub-chronic supranigral infusion of two novel $mGlu_4$ PAMs could provide neuroprotection following nigral infusion of 6-OHDA in the rat.

Contrary to our hypothesis, Compound 11 failed to provide a significant degree of neuroprotection at either the nigral or striatal level. This was largely reflected in the functional assessments, with the exception of a significant improvement in the cylinder test in rats treated with 20nmol Cpd 11. The loss of TH-positive cells in this study was not equivalent to the loss of striatal dopamine, such that vehicle-treated rats retained around 33% TH-positive neurones overall throughout the SNc but only 2% of striatal dopamine content. The reason for this is unknown but could relate to the possible antioxidant/neuroprotective effects of DMSO (Di Giorgio *et al.*, 2008; Sanmartín-Suárez *et al.*, 2011), which composed 10% of the vehicle used in this study. This might have partially protected against the physical loss of TH-positive cells without preserving their function, which would explain why striatal dopamine was more severely depleted than the number of cell bodies. Additionally, the injection of 6-OHDA in the anterior region of the SNc led to a non-uniform cell loss between the levels that were assessed in this study. The majority of dopaminergic cell bodies reside in this anterior portion of the SNc (Paillé *et al.*, 2007) so cell loss here might be more likely to impact on striatal dopamine content than cell loss at more posterior levels, therefore the enhanced survival of TH-positive neurones at -5.3mm and -5.8mm might not have contributed as much to the residual dopamine concentration in the lesioned striatum, which was more reflective of cell loss at the -4.8mm level. The variation in cell loss between anteroposterior levels in this study led us to change our lesioning and treatment co-ordinates when we carried out the repeat of the VU0155041 study. For this study we used co-ordinates that aim closer to the centre of the SNc, which resulted in no significant degree of variability from front-to-back.

VU0155041 on the other hand *did* provide a significant degree of neuroprotection, in accordance with our hypothesis. The results of this study closely replicate a previous report from our lab demonstrating a similar degree of neuroprotection with sub-chronic supranigral administration of VU0155041 (Betts *et al.*, 2012). Neuroprotection was observed at both the nigral and the striatal levels, and was significantly different from vehicle-treated rats in the 100nmol-treated group. Moreover, the preservation of striatal dopamine observed in this group approached the critical threshold of 40% at which the

symptoms of PD in humans first become apparent, meaning that this level of protection is likely to be clinically important. This was reflected in significant functional preservation in both the cylinder test and the adjusted steps test in this group, and a trend towards reversal of the apomorphine-induced rotational response.

The bell-shaped dose-dependency exhibited by VU0155041 is typical of agonist dose response curves, where higher doses of compound lead to desensitisation of the target receptor and therefore a loss of therapeutic effect. Desensitisation is brought about by prolonged stimulation by agonists and may involve internalisation of the receptor, or uncoupling of the receptor from its downstream effectors by receptor phosphorylation. Although use of allosteric modulators rather than agonists has been suggested to avoid these desensitisation effects, VU0155041 is not only a PAM at $mGlu_4$ but also shows allosteric agonist activity (Niswender *et al.*, 2008b). Therefore at high concentrations it might be expected that VU0155041 would cause desensitisation of $mGlu_4$ and this could underlie the loss of efficacy of VU0155041 at higher doses.

2.4.1 Differing abilities of $mGlu_4$ PAMs to provide neuroprotection

Despite both of these compounds acting as positive allosteric modulators at the same receptor, they showed differing abilities to elicit neuroprotection against nigral infusion of 6-OHDA in the rat. There are several possible reasons that may help explain this:

- **Differences in the clearance rates of these drugs following intracerebral injection.** No pharmacokinetic parameters for either Cpd 11 or VU0155041 have been reported following intracerebral injection, so until this has been defined this is purely speculative. Certainly the neuroprotection observed in the VU0155041 study suggests that this $mGlu_4$ PAM was present in the brain for a sufficient duration to partially counteract the toxic effects of the 6-OHDA lesion, however this might not have been the case for Compound 11. Even if Compound 11 exerted short-term effects, as might have underpinned the improved performance of 20nmol-treated rats in the cylinder test, it is possible that its pharmacological activity is short-lived overall and therefore the once-daily dosing regimen used in this study might not have provided continuous enough $mGlu_4$ modulation to exert a neuroprotective effect in a lesion model of this severity. Some pharmacokinetic data have been reported for Compound 11 in rats by East *et al.* (2010), including its rapid metabolism when administered systemically (which led to us choosing to dose intracerebrally in this study) and a short mean residence time (0.6h) following

intravenous delivery. These results point to rapid *in vivo* clearance in the rat following systemic administration that might also be the case following local administration. It might be interesting to investigate Compound 11 further with more frequent or even continuous delivery, allowing for more consistent activation of $mGlu_4$ and circumventing clearance issues that might be hindering a protective effect.

- **Differing potencies of the PAMs at $mGlu_4$**

  VU0155041 is twice as potent at $mGlu_4$ *in vitro* as Compound 11. However given that VU0155041 gave significant protection at 100nmol but a similar degree of protection was not observed when Cpd 11 was given at 200nmol this is unlikely to underlie the difference.

- **PAM versus agonist activity**

  As well as acting as a PAM, VU0155041 is known to be a partial agonist of $mGlu_4$ at high concentrations (a so-called ago-PAM), and the bell-shaped curve of the dose response in the neuroprotection study reported in this chapter supports this. It could be that the protective effect of VU0155041 was driven by its activity as a partial agonist rather than as a PAM, and perhaps the pure allosteric modulation afforded by Cpd 11 was insufficient to protect against 6-OHDA-induced degeneration.

- **Presence of $mGlu_{2/4}$ heterodimers at subthalamonigral synapse**

  Though previously thought to mainly exist as homodimers, there is evidence that mGlu receptors can also heterodimerise with other subtypes that share a common G protein, particularly $mGlu_{2/4}$ (Doumazane *et al.*, 2011). Though $mGlu_{2/4}$ heterodimers have not been demonstrated *in vivo* at the subthalamonigral synapse they have been demonstrated in the rat striatum (Yin *et al.*, 2014). In addition the subthalamic nucleus expresses mRNA for both $mGlu_2$ and $mGlu_4$ at comparable levels (Messenger *et al.*, 2002), which suggests that these heterodimers *could* also form at the subthalamonigral synapse. When in the form of a heterodimer it was originally thought that activation of both subunits was necessary for receptor activation (Kammermeier, 2012), however further investigation has revealed that depending on the allosteric site at which they bind, certain positive allosteric modulators of $mGlu_4$ are *unable* to potentiate the effects of orthosteric activation with L-AP4 or glutamate at these heterodimers (e.g. PHCCC, 4PAM-2) while others *are* able to potentiate the actions of orthosteric agonists (e.g. VU0155041,

LuAF21934) (Yin *et al.*, 2014). While the allosteric binding site of Compound 11 has not been reported it is conceivable that if it binds at the same site as PHCCC it will not activate $mGlu_{2/4}$ heterodimers, while we know that due to its allosteric binding site VU0155041 will activate these heterodimers. Differential activation of $mGlu_{2/4}$ heterodimers could therefore underlie the differential abilities of these two compounds to elicit neuroprotection in this model, via the ability of VU0155041 but not Compound 11 to inhibit subthalamonigral glutamate release and therefore excitotoxicity.

2.4.2 General considerations

One of the main caveats of these experiments is the fact that neuroprotection was attempted in a model that replicates very late-stage PD, where the nigrostriatal tract has severely degenerated leading to an almost complete loss of striatal dopamine (even alongside the less severe loss of TH-positive cells in the Compound 11 study). The degeneration following a nigral lesion is rapid, beginning within hours and almost complete after a week, leaving little scope for intervention. Treatment was started prior to lesioning in an attempt to counteract this, however it cannot be discounted that the failure of Compound 11 to elicit neuroprotection was due to the very severe functional lesion that it would have had to overcome. In support of this, a previous study investigating the neuroprotective effect of nicotine in the 6-OHDA rat showed that significant protection was observed in a partial lesion model but that this effect was lost in the full lesion model (Costa *et al.*, 2001). Nevertheless it does seem that certain drugs do have sufficient activity to partially protect against even this very severe lesion, as was shown in this chapter and by Betts *et al.* (2012) to be the case for VU0155041, and has also been shown in a previous study using the broad spectrum group III mGlu receptor agonist L-AP4 (Austin *et al.*, 2010).

Since PD symptoms appear when striatal dopamine is depleted to around 60% of normal it would perhaps be more realistic to attempt neuroprotection in a model of degeneration approximating this stage of the disease. This could be achieved using the same toxin by using a smaller dose of 6-OHDA in the nigra (Carman *et al.*, 1991; Costa *et al.*, 2001; van Oosten *et al.*, 2002) or MFB (Datla *et al.*, 2001; Murray *et al.*, 2003a; Truong *et al.*, 2006), or by infusion of 6-OHDA into the striatum (Kirik *et al.*, 1998; Li *et al.*, 2010b; Przedborski *et al.*, 1995). Alternatively, use of the dopamine-selective systemically active toxin MPTP at a dose that causes a partial lesion could also be considered (in mice, as it is ineffective in rats). This would allow for treatment with $mGlu_4$ PAMs either alongside the toxin or starting at a time when the lesion is only partial, which would more accurately reflect the

clinical situation as drugs would not be given to PD patients until after striatal dopamine depletion had reached 60% and symptoms had become apparent. However different behavioural tests would need to be employed as the degeneration induced by systemic MPTP is bilateral.

2.4.2.1 Behavioural tests

Short-term pharmacological effects: Another consideration when interpreting the data is that behavioural testing was carried out from 3 hours after supranigral infusion of the drug in both studies. No studies were carried out to determine the half life of the drugs in the brain when administered locally and so it is impossible to know for sure whether or not the behavioural results collected in these studies are a reflection of neuroprotective efficacy (as was seemingly the case for VU0155041) or an acute pharmacological effect (as might have been the case for the significant effect of 20nmol Cpd11 in the cylinder test, where no neuroprotection was observed).

In the Compound 11 study we found a significant effect of treatment with 20nmol Cpd 11 on contralateral paw use in the cylinder test post-lesion, in the absence of a significant neuroprotective effect. One possible explanation for this apparent functional improvement in the absence of neuroprotection is that Cpd 11 exerted a short-term partial correction in BG signalling that was sufficient to provide some relief from the effects of the lesion as measured in this test. Certainly this drug has previously been shown to provide symptomatic relief in the haloperidol model of catalepsy, though the construct validity of this model is poor. Since the behavioural testing was carried out around 3 hours after dosing it is possible that there was still a sufficient concentration of the drug in the brain to modulate signalling in the nigra.

Predictive validity: In addition to the possibility of confounding acute pharmacological effects, the validity of the behavioural data may be questionable with regard to its correlation with neuroprotection. This not only might have affected the results measured in these studies but would be even more pertinent if the study were to be repeated using a unilateral partial lesion model.

For example a previous study found no difference in performance in the cylinder test between mice with an intermediate (80% striatal TH loss) and a severe lesion (94% striatal TH loss) (Grealish *et al.*, 2010). In addition, I know from my own experience that up to 30% use of the contralateral forelimb can be observed in rats with >98% TH-positive cell loss in

the lesioned SNc. Therefore the significant effect found in the Cps 11 study may have been a false positive.

We also noted unusual responses when testing both amphetamine-induced rotations in the Compound 11 study and in apomorphine-induced rotations in the VU0155041 study. With regard to amphetamine, the correlation between amphetamine-induced rotations and nigrostriatal degeneration has been queried (Carman *et al.*, 1991; Dolleman-van der Weel *et al.*, 1993; Fang *et al.*, 2006) and may depend on the extent of VTA lesion (Thomas *et al.*, 1994), however in the Compound 11 study it was not the degree of turning that was unusual but the directionality. Amphetamine causes dopamine release, and as such should cause a greater activation of the striatum in the intact hemisphere, leading to ipsiversive rotation. However several animals in this study exhibited an initial vigorous contraversive response to the drug which cancelled out the later switch to ipsiversive turning. This so-called 'paradoxical' turning behaviour has been previously noted in rats up to ~6 days post-lesion (Carey, 1992; Robinson *et al.*, 1994) and even beyond (Mintz *et al.*, 1986b), and within our 60-minute testing period some animals switched from one turning behaviour to the other, some remained contraversive, and others only turned in the expected ipsiversive direction. In order to overcome this effect we tested amphetamine-induced rotations at later time points post-lesion in subsequent studies (day 12 in both LuAF21934 and AMN082 neuroprotection studies, Chapters 4 and 5 respectively).

With regard to the apomorphine-induced asymmetry in the VU0155041 study, while the results were in line with the functional effects seen in the cylinder and adjusted steps tests, this effect failed to reach significance despite a clear abolition of the contraversive turning observed in the vehicle-treated group in the 100nmol VU0155041-treated group. The high degree of variability in the net turning response probably underlies this, since several VU0155041-treated rats displayed ipsiversive turning in response to apomorphine while others showed contraversive turning as would be expected. The ipsiversive turning in response to apomorphine that was observed in these rats could be explained by the fact that despite the canonical model, apomorphine can elicit ipsiversive rotations in rats with 'medium-size' (25-50%) lesions such as were obtained in several rats due to the neuroprotective effect of VU0155041 (Da Cunha *et al.*, 2008).

Nevertheless, the tests used in these studies have been used and shown to be effective in similar studies to the ones reported here (and indeed picked up the neuroprotection observed in the VU0155041 study reported in this chapter), and all studies are powered in

order to be able to detect differences using these measurements. Behavioural analysis carries with it an inherently high risk of variability and therefore alternative behavioural tests would likely experience similar caveats.

2.5 Conclusion

Local activation of $mGlu_4$ in the SNc using the $mGlu_4$ PAM VU0155041 provided a statistically significant and clinically relevant degree of neuroprotection in rats following nigral infusion of 6-OHDA, lending further support to the idea of targeting these receptors as a neuroprotective strategy in Parkinson's disease.

The lack of a protective effect observed when another $mGlu_4$ PAM, Compound 11, was tested in the same model suggests that differences in drug properties such as half life and bioavailability may well determine whether or not these compounds are efficacious against the severe lesion that is induced by nigral infusion of 6-OHDA. However the significant effect of treatment in the cylinder test in this study, along with the antiparkinsonian efficacy that has been reported for Compound 11 in the haloperidol model of catalepsy, does at least suggest that this compound has an acute antiparkinsonian effect that is likely due to a partial correction in signalling in the SNc. Further testing of this compound in partial lesion models, possibly also using continuous drug delivery, would give a more definitive answer as to whether Compound 11 provides only acute pharmacological relief from symptoms or if it can also provide neuroprotection in a more clinically relevant situation.

Overall the neuroprotection observed with VU0155041 in the 6-OHDA model in this study and in a previous study from our lab, along with the neuroprotection that has been observed with systemic administration of the $mGlu_4$ PAM PHCCC in the MPTP mouse model of PD, strongly supports the targeting of $mGlu_4$ as a neuroprotective strategy in Parkinson's disease.

3 Investigating the effects of group III mGlu receptor agonists on glutamate and GABA release in the substantia nigra

3.1 Introduction

Having demonstrated neuroprotection following local infusion of VU0155041 into the SNc both in the previous chapter and also by previous researchers in our lab (Betts *et al.*, 2012), and following other studies that have used the same experimental design to demonstrate a neuroprotective effect of broad spectrum group III agonists (Austin *et al.*, 2010; Vernon *et al.*, 2005; Vernon *et al.*, 2006), we next wanted to discover whether inhibition of glutamate release in the SNc could underlie this protective effect.

3.1.1 Potential mechanisms of antiparkinsonian effects

More than one mechanism has been proposed to explain the antiparkinsonian and/or neuroprotective effects of activation of group III mGlu receptors in the SNc.

The first is the inhibition of glutamate release into the SNc from subthalamic efferent neurones, which are hyperactive in the parkinsonian state and could contribute to degeneration by enhancing excitotoxicity. Activation of group III mGlu receptors with L-AP4 was found to reduce EPSCs in the SNc, suggesting a reduction of glutamate release from subthalamonigral neurones (Valenti *et al.*, 2005). This is a promising result from the point of view of neuroprotection, and is what we investigated in the studies in this chapter.

The second mechanism is suppression of inflammation; anti-inflammatory effects have been shown *in vitro* following pan group III activation (Besong *et al.*, 2002; Taylor *et al.*, 2003) and *in vivo* following $mGlu_4$ activation (Betts *et al.*, 2012). This effect is presumably mediated by non-neuronal cells, for example activation of group III receptors expressed on microglia has been shown to reduce their neurotoxic effects following stimulation with the bacterial toxin lipopolysaccharide (LPS) (Taylor *et al.*, 2003).

There may be some cross-talk between excitotoxicity and inflammation (Chang *et al.*, 2008) and accordingly group III mGlu receptor agonists can inhibit LPS-evoked glutamate export from microglia, and may thus reduce excitotoxicity (McMullan *et al.*, 2012). In addition, activation of astroglial group III mGlu receptors may similarly modulate excitotoxicity secondary to toxic (MPP^+) or inflammatory (LPS) stimuli, via enhancement of glutamate reuptake (Yao *et al.*, 2005; Zhou *et al.*, 2006).

Overall, these mechanisms could potentially lead to neuroprotection by reduction of excitotoxic and inflammation-mediated cell loss. In line with this theory, group III mGlu receptor activation has shown protective effects in models of inflammatory (Zhou *et al.*, 2006) and excitotoxic (Domin *et al.*, 2014; Gasparini *et al.*, 1999; Vera *et al.*, 2012) neurodegeneration.

3.1.2 Glutamate, GABA and group III mGlu receptors in the SN

Given the neuroprotective effect observed in the 6-OHDA rat model of PD following sub-chronic supranigral injection of the $mGlu_4$ PAM VU0155041, we were interested to see if we could demonstrate an effect of either broad spectrum group III mGlu receptor activation or $mGlu_4$-specific activation on glutamate release into the SNc in order to ascertain if this mechanism contributed to the protection. The distribution of group III receptors in the substantia nigra certainly suggests that activation of these receptors could modulate both glutamatergic and GABAergic signalling.

The main glutamatergic input to the SNc is from subthalamonigral neurones, but there are additional afferents originating in the pedunculopontine nucleus (PPN), cortex and amygdala (Chatha *et al.*, 2000). There are also several GABAergic afferents that innervate the SNc, predominantly originating in the striatum (the 'direct' striatonigral medium spiny neurones) but also from the GP and SNr collaterals (Fujiyama *et al.*, 2002).

The antiparkinsonian effects of group III mGlu receptor agonists when administered into the SN, along with evidence that they can reduce subthalamonigral glutamatergic signalling, demonstrate the presence of these receptors at this synapse. Given the differences in potency of broad spectrum agonists at each receptor subtype it is useful to know their relative abundances to try to ascertain which might be the most important receptor in mediating these effects.

3.1.2.1 Intact SNc

Receptor protein for both $mGlu_4$ and $mGlu_8$ has been identified in the SN (likely the SNc though this is not made clear in the paper), with moderate and low relative expressions respectively (Gu, 2003). $mGlu_7$ was not examined in this paper, however another study found no evidence for $mGlu_7$ protein expression in the SNc (Kinoshita *et al.*, 1998).

Regarding glutamatergic afferents, mRNA for $mGlu_4$, $mGlu_7$ and $mGlu_8$ has been detected at moderate levels in the STN and at moderate to high levels in the cortex (Messenger *et al.*, 2002). Along with the protein expression information, this suggests that $mGlu_4$ and

$mGlu_8$ might be present presynaptically at the subthalamonigral synapse. In addition, mRNA for $mGlu_7$ but not $mGlu_4$ has been detected at moderate levels in the PPN, and mRNA for both these receptors has also been detected at low to moderate levels in various areas of the amygdala (Ohishi *et al.*, 1995), therefore group III mGlu receptor agonists might also modulate signalling at these synapses.

Regarding GABAergic afferents, mRNA for $mGlu_4$, $mGlu_7$ and $mGlu_8$ has been detected at moderate to high levels in the striatum and at low levels in the GP and SNr (Messenger *et al.*, 2002; Testa *et al.*, 1994). Another report detected both $mGlu_4$ and $mGlu_7$ in the striatum, but only $mGlu_7$ in the GP and SNr (Ohishi *et al.*, 1995). The increased abundance of mRNA in the striatum compared with the GP and SNr might suggest that the majority of group III heteroreceptors in the SNc modulate signalling at striatonigral neurones.

In addition, mRNA for all three group III mGlu receptors that are expressed in the brain has been identified in the SNc of naive rats. In one study that looked at all group III receptor subtypes, $mGlu_4$ and $mGlu_7$ were equivalently expressed at relatively low levels, whereas $mGlu_8$ was expressed at moderate levels (Messenger *et al.*, 2002). Other studies support some, but not all, of these findings, for example when only $mGlu_4$ was investigated it was found to have low level expression in the SNc by one group (Testa *et al.*, 1994) but where both $mGlu_4$ and $mGlu_7$ were investigated by another group, only $mGlu_7$ mRNA was localised to the SNc (Ohishi *et al.*, 1995). Since the pre- or post-synaptic localisation of group III mGlu receptors in the SNc has not been elucidated it is possible that mRNA expression in this region could lead to either local or distal group III mGlu receptor expression.

3.1.2.2 6-OHDA-lesioned SNc

The reported effects of 6-OHDA-induced nigrostriatal degeneration on group III mGlu receptor expression in the SNc are inconsistent, with one study reporting no change in any receptor subtype at the level of mRNA (Messenger *et al.*, 2002) and another reporting that both $mGlu_4$ and $mGlu_8$ receptor proteins were reduced in SN (likely SNc, see above) after lesioning ($mGlu_7$ was not examined) (Gu, 2003).

3.1.3 Using microdialysis to determine neurotransmitter release

Microdialysis is a technique that involves the sampling of molecules across a partially permeable membrane. Membranes are designed with a specific size cut-off that generally allows the passage of small molecules such as steroid hormones and neurotransmitters but not large molecules such as proteins. This membrane is on the end of a flexible probe, which is perfused continuously with an isotonic perfusate (e.g. artificial cerebrospinal fluid

(aCSF), 0.9% saline or another isotonic solution) and acts like an artificial capillary (Figure 26).

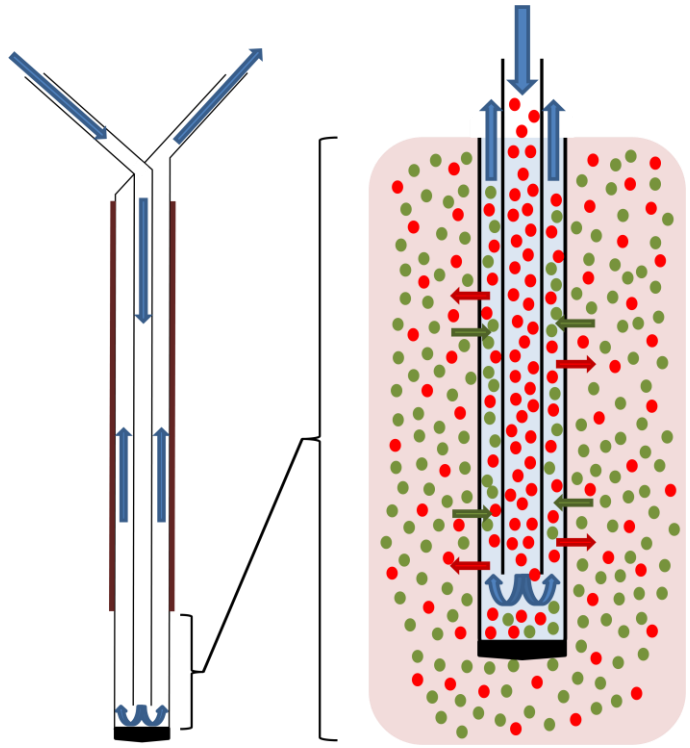

Figure 26: Schematic showing the technique of microdialysis using a concentric probe. Perfusate (e.g. aCSF) flows continuously through the probe (blue arrows) at a slow rate, usually 0.1-3µl/min. The membrane allows diffusion of small molecules into the aCSF within the probe from the extracellular environment (green circles and arrows). This technique also allows delivery of small molecules into the extracellular environment by retrograde dialysis (red circles and arrows).

As the aCSF flows past the membrane, molecules that are in the extracellular milieu surrounding the probe tip diffuse across the membrane into the probe along their concentration gradients. The flow of perfusate then carries these molecules out of the probe and they are collected in a dialysate fraction. This is how neurotransmitters or other small molecules are sampled.

Microdialysis can also be used for local delivery of small molecules into the region of interest by a process called retrograde dialysis. This is simply where a drug is delivered via the perfusate flowing through the probe. As the drug molecules pass the membrane they will diffuse out into the extracellular milieu along their concentration gradient.

Microdialysis is increasingly employed to measure free drug concentrations within discrete brain regions in pharmacokinetic studies, however it is still most often used to measure

neurotransmitter concentrations, both basal and also depolarisation-evoked exocytotic release by exposure of the sampled region to a high concentration of potassium ions (high K^+).

3.1.4 Considerations for microdialysis

The recovery of the analyte of interest is dependent on several factors, including:

- **Membrane length/diameter.** In general, the larger the membrane area, the better the analyte recovery (Kendrick, 1989). However this parameter is usually limited by the size of the region of interest.
- **Membrane material.** Examples of membrane materials include cellulose or regenerated cellulose (e.g. cuprophane), polyacrylonitrile, polycarbonate ether and polyethersulfone. These membranes have different properties with regard to size exclusion, binding and stability and must be chosen according to the analyte that is to be sampled.
- **Perfusate (e.g. aCSF) flow rate.** In general, the slower the flow rate the higher the relative recovery of analyte, but having said that it is important to also bear in mind the sample volume that is required for analysis, and also the reduced temporal resolution with very slow flow rates. Use of a very low flow rate such as <0.1µl/min can result in almost 100% analyte recovery (Smith *et al.*, 1992), however common flow rates used in microdialysis are 1-3µl/min, where relative recovery is typically 10-30% (Kendrick, 1989).
- **Perfusate composition.** The perfusate flowing through the probe should be as close to a physiological solution as possible. aCSF is commonly used, but it is important to get the composition correct, as efflux of Na^+ and Ca^{2+} ions especially could influence normal neuronal signalling.
- **Analyte properties.** Properties such as molecular weight and charge of certain analytes can make them incompatible with certain membranes – proteins in particular can be 'sticky'. Amino acids and monoamines generally have the highest recovery of all neurotransmitters, likely due to their low molecular weight (Kendrick, 1989).

3.1.5 Pros and cons of microdialysis

As with all techniques, microdialysis has pros and cons. The pros include the fact that the procedure is relatively simple and has minimal physical impact on the brain insofar as the flow of perfusate is kept separate from brain tissue by the membrane. Physical damage to

the brain can be minimised by using flexible concentric microdialysis probes instead of rigid U-shaped probes. This technique also allows localised administration of drugs or altered perfusate components (such as high K^+) by retrograde dialysis.

The cons of this technique include the poor temporal resolution versus some other techniques (typically ≥10 minutes, versus real-time second/millisecond resolution using alternative analyte detection techniques such as fast-scan cyclic voltammetry (FSCV; Stamford, 1990), due to the need to balance slow flow rates and the collection of adequate sample volumes for analysis. The spatial resolution is also poor, since the membrane is not within the synaptic cleft, and it has been suggested that some neurotransmitters such as GABA and glutamate signal over too short a distance to create overflow that would reach a dialysis probe (reviewed in Del Arco *et al.*, 2003).

Other concerns depend on the dialysis method used and the outcomes being measured. For example microdialysis can be performed on anaesthetised or freely-moving animals, but anaesthesia is known to influence neurotransmitter concentrations to varying degrees depending on the anaesthetic used (de Souza Silva *et al.*, 2007). In addition, relative recovery of analytes can be low due to incomplete sampling across membrane. It is not always easy to relate dialysate concentrations to actual extracellular concentrations, and the *in vitro* recoveries that used to be typically employed for calculating the extracellular fluid/dialysate ratio have been shown to be inaccurate due to the impaired movement of analytes in the extracellular space compared with in solution (Glick *et al.*, 1994; Nicholson *et al.*, 1986). Accurate calculation of extracellular analyte concentrations are particularly important in pharmacokinetic studies, however it is not always necessary in the case of experiments that are looking at relative changes (e.g. calculating a ratio between responses) as relative recovery is assumed to be constant *in vivo* as it has been shown to be *in vitro* (Kendrick, 1989).

3.1.6 Hypothesis and aims

Previous studies have shown that broad spectrum group III mGlu receptor agonists can reduce glutamate release in the SNr (Austin *et al.*, 2010) but this has not been tested in the SNc in either the intact or lesioned BG. Neither has the effect of group III agonists been tested on GABA release into the SNc. Unravelling how transmitter release is affected in the SNc will help to predict the likely therapeutic benefits of targeting these receptors. In addition, such knowledge may help to provide an explanation for the previously reported neuroprotective effects of supranigral infusion of broad spectrum group III mGlu receptor agonists and subtype-selective $mGlu_4$ PAMs. We hypothesise that:

The broad spectrum group III mGlu receptor agonist L-AP4 will inhibit evoked glutamate and GABA release in the naive rat SNc.

In addition, the effects of $mGlu_4$ subtype-specific positive allosteric modulators on glutamate and GABA release in the SNc have not been tested, even though many of the effects of group III agonists have been attributed to this receptor subtype (Lopez *et al.*, 2007; Valenti *et al.*, 2005; Wittmann *et al.*, 2001). Therefore we also tested the effect of VU0155041 on evoked glutamate and GABA release in the SNc, where we hypothesise that

The $mGlu_4$ selective PAM VU0155041 will have similar effects to L-AP4, inhibiting evoked release of both glutamate and GABA release in the naive SNc.

Since there is some evidence that 6-OHDA lesioning reduces the expression of $mGlu_4$ and $mGlu_7$ receptor proteins in this region (Gu, 2003), this effect may be altered in the lesioned SNc. Given previous electrophysiological data that have demonstrated that in the dopamine-depleted state (acute reserpinisation) group III activation retains its ability to inhibit glutamatergic transmission but loses its ability to inhibit GABAergic transmission in the SNr (Wittmann *et al.*, 2002), along with the finding that subthalamonigral neurotransmission is enhanced in the SNc in the parkinsonian state (Guridi *et al.*, 1996; Remple *et al.*, 2011), we might expect that in the lesioned SNc:

The broad spectrum group III mGlu receptor agonist L-AP4 will inhibit evoked glutamate release but have a lesser or no effect on evoked GABA release in the 6-OHDA-lesioned rat SNc.

We expect the intact SNc of these rats to retain the decrease in both GABA and glutamate release in the presence of L-AP4 that we hypothesise to occur in the naive SNc.

A set of experiments was therefore carried out to test:

- The effects of L-AP4 on K^+-evoked glutamate and GABA release in the SNc of anaesthetised naive rats.
- The effects of VU0155041 on K^+-evoked glutamate and GABA release in the SNc of anaesthetised naive rats.
- The effects of L-AP4 on K^+-evoked glutamate and GABA release in the intact vs. lesioned SNc of anaesthetised rats with a unilateral 6-OHDA lesion of the MFB.

3.2 Materials and Methods

All of the studies outlined in this chapter were carried out at Eli Lilly and Co. Ltd., Windlesham, Surrey, U.K. All procedures were performed in accordance with the U.K. Animals (Scientific Procedures) Act, 1986.

3.2.1 Compounds tested

These experiments tested the broad spectrum group III agonist L-AP4 and the $mGlu_4$ PAM VU0155041, shown in Table 7.

Table 7: Structures of the compounds tested in the microdialysis studies.

Structure	Name	Target
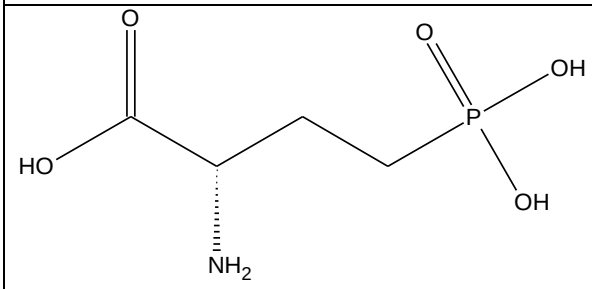	L-AP4 *(2S)-2-amino-4-phosphonobutanoic acid*	Broad spectrum group III mGlu receptor agonist
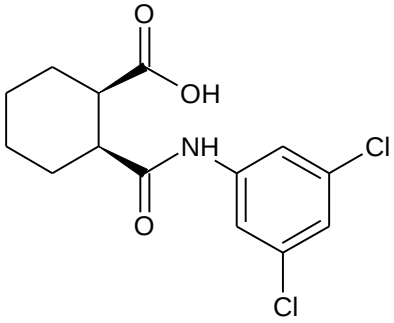	VU0155041 *cis-2-[[(3,5-Dichlorophenyl) amino]carbonyl] cyclohexanecarboxylic acid*	$mGlu_4$ Positive Allosteric Modulator

L-AP4 is a broad spectrum agonist of group III receptors, displaying activity at all three receptor subtypes that are expressed in the brain: EC_{50} = 0.43µM at $mGlu_4$, 160µM at $mGlu_7$ and 0.67µM at $mGlu_8$. It has been demonstrated to have antiparkinsonian efficacy as described in the Introduction.

VU0155041 was discovered at Vanderbilt University and acts as a PAM at human $mGlu_4$ (EC_{50} = 0.75µM) and rat $mGlu_4$ (EC_{50} = 0.56µM). Similarly to L-AP4, this molecule has shown antiparkinsonian efficacy in acute models of PD including the haloperidol and reserpine models when administered into the third ventricle (Niswender *et al.*, 2008b).

3.2.1.1 Drug formulation

L-AP4 and VU0155041 sodium salt were obtained from Tocris Biochemicals, Bristol UK. Drugs stocks were made up in sterile distilled water and made up to their final concentration in aCSF (141mM NaCl, 5mM KCl, 1.5mM $CaCl_2$, 0.8mM $MgCl_2$ in dH_2O) or high K^+ aCSF (46mM NaCl, 100mM KCl, 1.5mM $CaCl_2$, 0.8mM $MgCl_2$) as appropriate.

3.2.2 Other materials

3.2.2.1 Experimental materials

Microdialysis: Urethane and the aCSF / 100mM K^+ aCSF components NaCl, KCl, $CaCl_2.2H_20$ and $MgCl_2$ were obtained from Sigma Aldrich (Poole, UK).

6-OHDA lesioning: 6-OHDA.HCl, Pargyline.HCl and Desipramine.HCl were obtained from Sigma Aldrich (Poole, UK).

3.2.2.2 Analytical materials

LC-MS/MS (liquid chromatography with tandem mass spectrometry): Glutamate, GABA, benzoyl chloride, acetonitrile (ACN), borax (sodium tetraborate decahydrate), LC-MS grade methanol and formic acid (FA) were obtained from Sigma Aldrich (Poole, UK). The internal standards D5-Glutamate and D6-GABA were obtained from CDN isotopes (Pointe-Claire, Quebec, Canada).

HPLC (high pressure/performance liquid chromatography) for GABA and glutamate: O-phthaldehyde (OPA), sodium sulphite, boric acid, ethylenediaminetetraacetic acid (EDTA) and citric acid monohydrate were obtained from Sigma Aldrich (Poole, UK). LC-MS grade methanol was obtained from Fisher Scientific (Loughborough, UK). 85% phosphoric acid and 50% sodium hydroxide solutions were obtained from Acros Organics (via Fisher Scientific, Loughborough, UK).

HPLC for dopamine: As described in section 2.2.2.2.

3.2.3 General methods: microdialysis procedure

3.2.3.1 Probe implantation

Male Charles River-derived rats (CD; derived from Sprague-Dawley (SD) rats – Charles River, UK) between 280-330g were anaesthetised with urethane (2.5g/kg i.p. initial bolus with maintenance doses given as required) and placed in a stereotaxic frame with the toothbar set at -3.3mm. A 15mm concentric microdialysis probe with a 1mm active membrane length (MAB 4.15.1.Cu; Royem Scientific Ltd., Luton, UK) was implanted into the SNc at co-ordinates AP -5.0mm; ML -2.0mm; DV -8.6mm from bregma (Figure 27). The dialysis membrane used was a cuprophane membrane with a size cut-off of 6kDa.

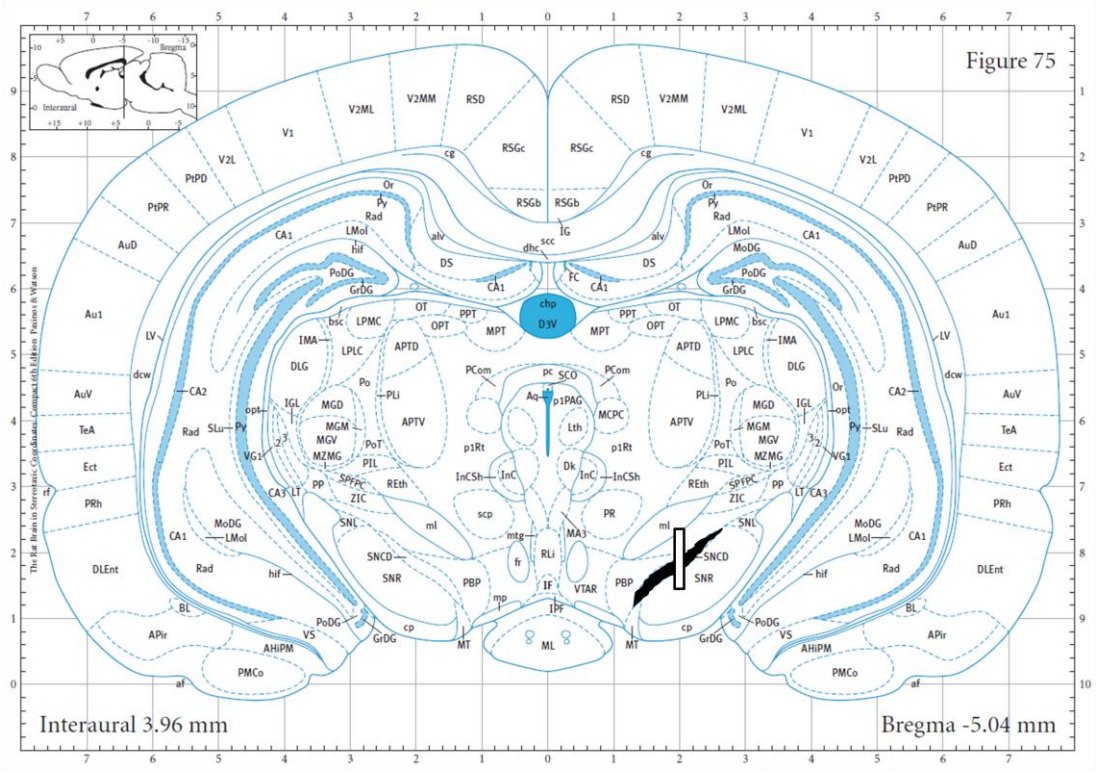

Figure 27: Implantation location of microdialysis probe within the SNc. The 1mm probe membrane would be expected to lie within the SNc 5.0mm posterior of bregma, as shown in the diagram above. The outlined box shows the positioning of the probe tip in relation to the SNc (shaded black). The brain diagram was obtained from the Rat Brain in Stereotaxic Co-ordinates (Paxinos *et al.*, 1998).

3.2.3.2 Microdialysis

For all microdialysis studies we used a dual-stimulation protocol. This was to correct for inter-animal variation in the degree of glutamate and GABA release evoked by K^+ stimulation that was noted in preliminary studies where only a single stimulus was assessed. This is a similar protocol to that utilised by Austin et al. (2010).

The microdialysis probe was perfused with aCSF (141mM NaCl, 5mM KCl, 1.5mM $CaCl_2$, 0.8mM $MgCl_2$) at a flow rate of 1.2µl/min, and sampling started after a 90-minute pre-sample to allow for stabilisation of the baseline. After four 20-minute baseline samples, the perfusate was switched for 10 minutes to a high K^+ aCSF (46mM NaCl, 100mM KCl, 1.5mM $CaCl_2$, 0.8mM $MgCl_2$) to evoke depolarisation and neurotransmitter release, before being switched back to aCSF for a further four baseline samples. This gave the control K^+-evoked response for each animal (S1).

Following this, animals were exposed firstly for 10 minutes with either vehicle (dH_20) or drug in aCSF as a pre-treatment, then for 10 minutes with the same vehicle or drug in high K^+ aCSF, before being returned to aCSF for a further four baseline samples. This provided the response to high K^+ in the presence of the test drug (S2).

The difference between these two responses was the major outcome being measured. 20-minute fractions (24µl) were frozen on dry ice immediately following collection and kept at -80°C until analysis.

3.2.3.3 Probe positioning

In order to verify the probe positioning, a 1% solution of trypan blue in aCSF was perfused for 20 minutes at 1.2µl/min after the experiment. The brain was removed and fresh frozen in cooled isopentane and stored at -80°C until analysis. Brains were brought up to -20°C for 30 minutes, then mounted using OCT (Tissue-Tek) and 30µm sections cut coronally on a cryostat (Leica) until the dye was visible. Sections were mounted and inspected using a brightfield microscope to confirm that the blue dyed area bisected the SNc.

Only samples collected from animals with correctly positioned probes were analysed in these studies. The positioning success rate was 80% for the unilateral L-AP4 and VU0155041 studies (Figure 28).

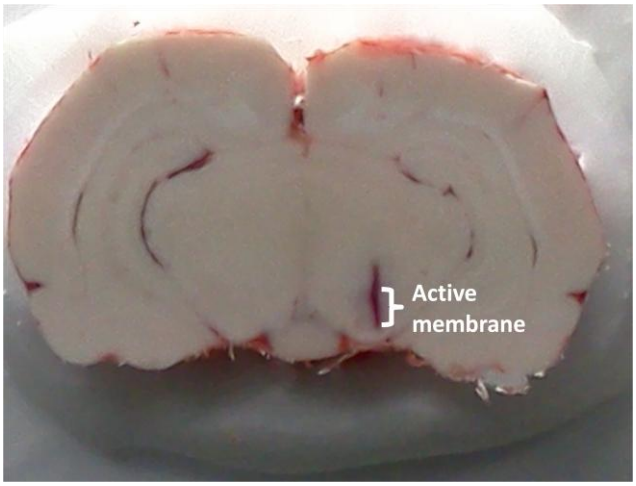

Figure 28: Probe positioning within the SNc for unilateral microdialysis. The membrane length was 1mm, therefore only the bottom 1mm of blue staining shows the sampled region (marked on diagram).

For the bilateral dialysis study the success rate was 92% (Figure 29).

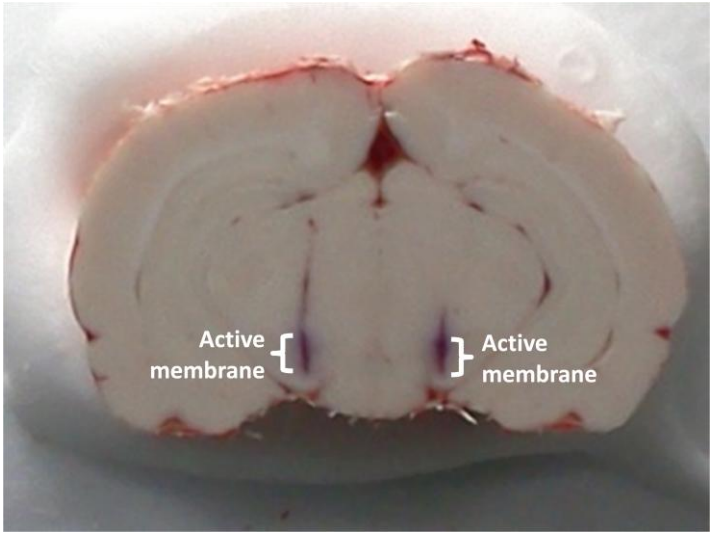

Figure 29: Probe positioning within the SNc for bilateral microdialysis. The nigrostriatal tract was lesioned (MFB infusion of 6-OHDA) on the left hand side of the brain and microdialysis performed in both the intact and lesioned SNc to ascertain the effect of lesioning on L-AP4 response. The active membrane length was 1mm (marked on diagram).

The group sizes quoted in the results section only refer to animals with correctly-placed probes.

3.2.4 Methods specific to Experiment 1: Effect of L-AP4 on glutamate and GABA release in the naive SNc

3.2.4.1 Microdialysis

Naive male CD rats were implanted with microdialysis probes into the SNc under urethane anaesthesia as described in the general methods.

Groups (all n=6) were exposed to high K^+ aCSF for the first evoked release (S1, control) and vehicle, 100µM or 300µM L-AP4 in aCSF or high K^+ aCSF was infused before and during the second evoked release (S2, test).

The doses of L-AP4 used were chosen to reflect a previous microdialysis experiment performed in the SNr, where 300µM L-SOP significantly reduced K^+-evoked glutamate release (Austin *et al.*, 2010).

3.2.4.2 LC-MS/MS analysis of glutamate and GABA in the dialysate

Dialysate samples were analysed using LC-MS/MS as we had encountered problems with the HPLC (high performance liquid chromatography) system with regard to peak separation on the glutamate chromatograms. The methodology involves derivatisation of samples with benzoyl chloride to yield molecules of sufficient size for accurate identification by mass spectrometry.

Samples were prepared by mixing 8µl dialysate (thawed from storage at -80°C) with 4µl 100mM borax and 4µl of internal standard (either 10µM D5-glutamate or 1µM D6-GABA). While mixing, 4µl 2% benzoyl chloride in ACN was added to each sample. Samples were vortexed thoroughly and then diluted with 90µl of 50:50:0.05 MeOH:H_2O:FA to minimise the introduction of borate into the HPLC column. Standards containing equimolar concentrations of glutamate and GABA were prepared in aCSF and derivatised in the same way, covering a concentration range of 2.5-1000nM.

Each derivatised sample or standard was first separated at room temperature by gradient HPLC (mobile phase A: 0.1% FA in H_2O; mobile phase B: 100% LC-MS grade MeOH; flow rate 200µl/min) on a Phenomenex ACE C18-PFP 50 x 2mm 3µm particle size column fitted with a javelin prefilter. The analytes were then ionised by atmospheric pressure ionisation (API) and identified by mass spectrometry using an API4000 triple quadropole (MMSP606) mass spectrometer (Applied Biosystems).

3.2.4.3 LC-MS/MS data analysis

Calibration curves were generated within Analyst software (v 1.4.2) from the GABA and glutamate standards. Concentrations were calculated for each sample from these standard curves.

3.2.4.4 Statistical analysis

The data in this study were normally distributed; therefore the results quoted are mean ± standard error of the mean (s.e.m.). The data are presented as bar charts or line graphs, where the bar height/plotted point represent the mean and the error bars represent the s.e.m.

The sizes of the glutamate and GABA release responses at S1 (control) and S2 (with L-AP4/vehicle) were determined using area-under-curve (AUC) analysis in SigmaPlot (v. 12.5). The sizes of the S1 and S2 responses were compared within groups using a paired t-test.

In addition, the S2/S1 ratios for glutamate and GABA responses were compared between vehicle and L-AP4-treated groups using a one-way ANOVA with Dunnett's *post-hoc*.

Results were considered to be statistically significant where $P<0.05$.

3.2.5 Methods specific to Experiment 2: Effect of VU0155041 on glutamate and GABA release in the naive SNc

This experiment investigated the effect of subtype-selective activation of $mGlu_4$ on glutamate and GABA release by using the positive allosteric modulator VU0155041. Parallel experiments were performed using equimolar concentrations of L-AP4 for comparison, lower than the concentrations tested in experiment 1, since VU0155041 and L-AP4 have similar potencies at $mGlu_4$ (EC_{50} = 0.56µM for VU0155041 or 0.43µM for L-AP4).

3.2.5.1 Microdialysis

Naive male CD rats were implanted with microdialysis probes into the SNc under urethane anaesthesia as described in the general methods.

Groups were exposed to high K^+ aCSF for the first evoked release (S1, control) and either vehicle (n=6), 3µM L-AP4 (n=8), 30µM (n=7) L-AP4, 3µM VU0155041 (n=8) or 30µM (n=7) VU0155041 in aCSF or high K^+ aCSF was infused before and during the second evoked release (S2, test).

3.2.5.2 HPLC analysis of glutamate and GABA in the dialysate

Dialysate samples were analysed for GABA content using a reverse-phase HPLC system with electrochemical detection, the Alexys GABA-Glu Analyzer (Antec, Netherlands). This system switches between two columns of different lengths to provide two chromatograms, one for the glutamate and one for the GABA (Figure 30).

The mobile phase consisted of 50mM phosphate, 50mM citrate 0.5mM EDTA and 5% methanol (pH 3.70) and was pumped without recycling at 200µl/minute. The stationary phase in the columns consists of C-18-linked silica of particle size 3µm. Derivatisation of samples with OPA-sulfite (37mM OPA, 50mM sodium sulphite, 90mM boric acid, 5% methanol; pH 10.4) was performed by the autosampler, and the electroactive reaction products of glutamate and GABA were detected at 2nA/V and 10nA/V respectively.

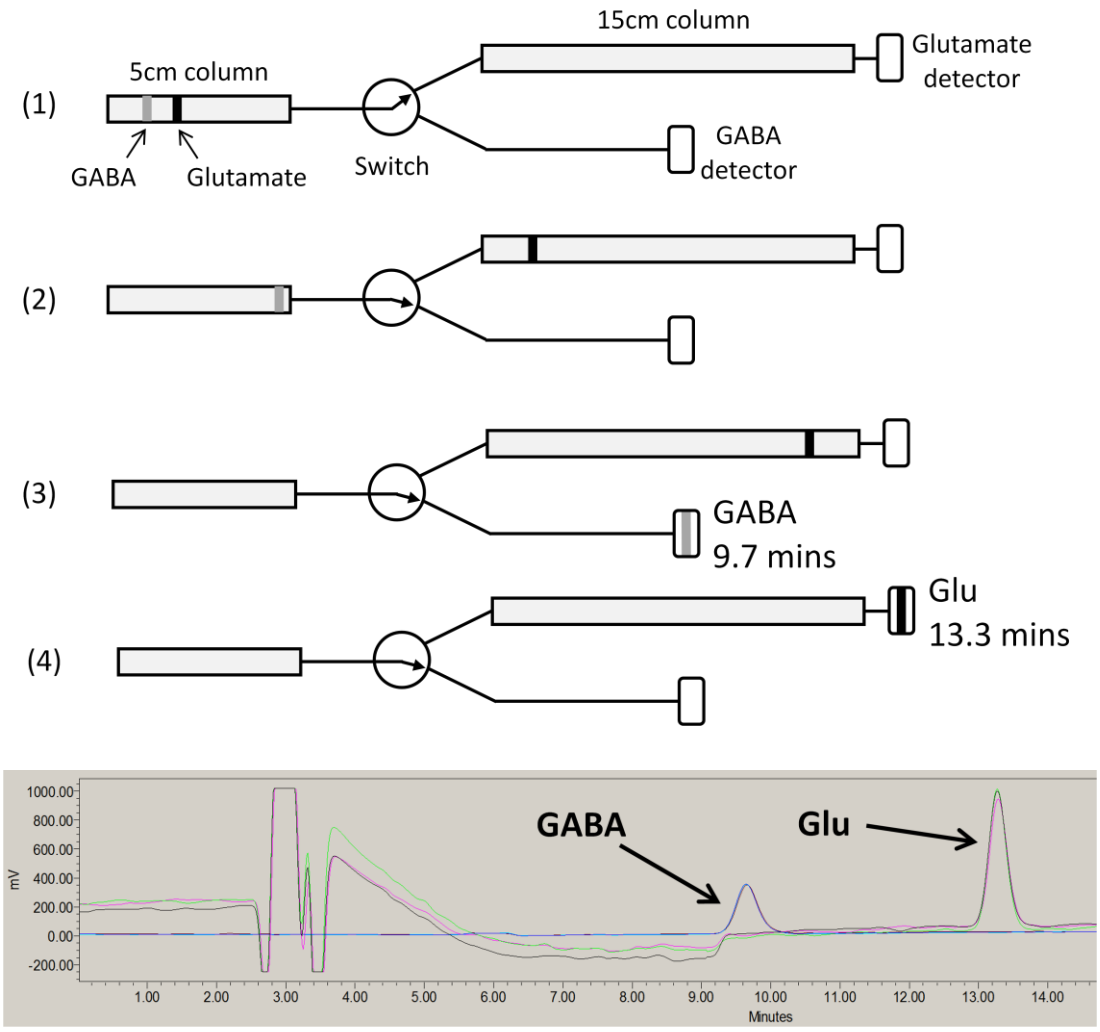

Figure 30: Column switching for dual analysis of GABA and glutamate. The upper panel shows a schematic of the column switching process used by the Alexys GABA-Glu analyser: The OPA-sulfite-derivatised sample undergoes preliminary separation on a 5cm column (1). The fraction containing the glutamate (black) is further separated on a 15cm column (2), while the fraction containing the GABA (grey) is switched straight onto its detector, arriving at about 9.7 minutes (3). The glutamate is detected at a separate detector after around 13.3 minutes (4). The lower panel shows an overlaid chromatogram of a 700nM standard run in triplicate. The peaks for GABA and glutamate are clearly visible at their respective retention times.

3.2.5.3 Data analysis

Peak areas were measured on Empower 3 software (Waters Corp.) and the areas of the standards and samples were analysed using JMP v. 8.0 (SAS Software). For each run the standard curve was determined using a 4-parameter logistic fit to account for loss of peak area in the standards between the start and end of the run. The individual lower limit and upper limit of quantification (LLOQ and ULOQ) for each run was determined by the presence of visible peaks with <20% area difference between pre- and post- run standards. The LLOQ and ULOQ for glutamate were 10nM and 500nM respectively, and for GABA were

5nM and 1000nM respectively, as determined by the linear range of mixed glutamate and GABA standards ranging from 3-3000nM.

3.2.5.4 Statistical analysis

The data in this study were normally distributed; therefore the results quoted are mean ± standard error of the mean (s.e.m.). The data are presented as bar charts or line graphs, where the bar height/plotted point represent the mean and the error bars represent the s.e.m.

The sizes of the GABA release responses at S1 (control) and S2 (with L-AP4/VU0155041/vehicle) were determined using AUC analysis in SigmaPlot (v. 12.5). The sizes of the S1 and S2 responses were compared within groups using a paired t-test.

In addition, the S2/S1 ratios for the GABA response were compared between vehicle- and L-AP4-treated and between vehicle- and VU0155041-treated groups using a one-way ANOVA with Dunnett's *post-hoc*.

Results were considered to be statistically significant where $P<0.05$.

3.2.6 Methods specific to Experiment 3: Comparing the effect of L-AP4 on glutamate and GABA release in the intact and 6-OHDA-lesioned SNc

As mentioned in the hypothesis for this experiment, dopamine denervation has been shown to alter both subthalamonigral transmission (glutamatergic) and the expression of $mGlu_4$ and $mGlu_7$ receptor proteins. Therefore this experiment sought to investigate whether or not a full unilateral lesion of the nigrostriatal tract would alter the effect of L-AP4 on GABA and glutamate release in the SNc. The highest dose of L-AP4 was chosen in this experiment to maximise the chance of activating all group III receptor subtypes, and because an effect on glutamate release had previously been demonstrated in the SNr for the same concentration of L-SOP, another broad spectrum group III mGlu receptor agonist with comparable potencies at $mGlu_4$ and $mGlu_7$ (Austin *et al.*, 2010). 6-OHDA lesioning of the MFB was carried out two weeks prior to microdialysis.

3.2.6.1 Lesioning

Male CD rats (250-270g) were pre-treated 30 minutes prior to lesioning with 5 mg/kg pargyline and 25 mg/kg desipramine (i.p.) to inhibit MAO-B and prevent extracellular metabolism of the 6-OHDA, and to prevent uptake of toxin into noradrenergic neurones respectively. Following this rats were anaesthetised with isoflurane (5% induction and 2-3% maintenance) and placed in a stereotaxic frame with the toothbar set at -4.5mm from the interaural line. The scalp was excised and bregma identified using a surgical microscope. The location of the MFB was defined as -4.0mm AP, -1.3mm ML from bregma, and -7.0mm ventral of dura mater. These co-ordinates were chosen as the animals used were at the lower end of the weight range covered by Paxinos and Watson's Rat Brain in Stereotaxic Co-ordinates (Paxinos *et al.*, 1998), and in smaller animals these co-ordinates were found to have a greater efficacy than those classically used for MFB lesions (Torres et al., 2011).

A hole was drilled in the skull and a 28G injection cannula was lowered into position. Using a Hamilton syringe and CMA pump, 3µl of a 30mM 6-OHDA solution in 0.03% ascorbate was infused at a rate of 1µl/minute for 3 minutes (total 15.42µg 6-OHDA). The cannula was left *in situ* for 2 minutes after infusion to allow the toxin to diffuse away from the site and prevent reflux up the tract upon retraction.

The wound was sutured and the animals given 10ml/kg sterile 0.9% saline (s.c.) and kept in thermostatically-controlled cages to aid recovery. Analgesia was provided by the administration of 0.1ml Vetergesic (Alstoe) following surgery.

3.2.6.2 Microdialysis

14 days post-surgery, when the 6-OHDA-induced lesion was expected to be complete (Labandeira-Garcia *et al.*, 1996; Wang *et al.*, 2004) and the rats were in the weight range 310-350g, they underwent bilateral microdialysis. In order to reflect previous studies this was done under urethane anaesthesia (2.5g/kg i.p. initial bolus with maintenance doses given as required). Microdialysis probes were implanted bilaterally into the SNc, at co-ordinates AP -5.0mm; ML ±2.0mm; DV -8.6mm.

The effect of 300µM L-AP4 on glutamate and GABA release was simultaneously tested in both the lesioned and intact nigra. For the control response, S1, high K^+ aCSF was perfused into the brain for 10 minutes. For the test response, S2, 300µM L-AP4 was infused for 10 minutes before (in aCSF), and during the 10 minute evoked release (in high K^+ aCSF).

3.2.6.3 HPLC analysis of striatal dopamine

To confirm the success of the nigrostriatal lesion, following microdialysis the left and right striata were dissected, weighed and snap frozen for analysis of monoamines by HPLC as described in section 2.2.3.2.

3.2.6.4 LC-MS/MS analysis of dialysate

Dialysate samples were analysed using LC-MS/MS as detailed for experiment 1.

3.2.6.5 Statistical analysis

The data in this study were normally distributed; therefore the results quoted are mean ± standard error of the mean (s.e.m.). The data are presented as bar charts or line graphs, where the bar height/plotted point represent the mean and the error bars represent the s.e.m.

Lesion-induced changes in striatal dopamine and its metabolites were compared between lesioned and intact sides using t-tests.

Baseline glutamate and GABA concentrations were measured as an average of the concentrations obtained in the first four dialysate samples. These were compared between the intact and lesioned SNc using a t-test.

The sizes of the glutamate and GABA release responses at S1 (control) and S2 (with 300 µM L-AP4) were determined using AUC analysis in SigmaPlot (v. 12.5). The sizes of the S1 and S2 responses were compared within sides using a paired t-test.

The S2/S1 ratios for glutamate were compared between the intact and lesioned SNc using a Mann-Whitney U-test as these data were not normally distributed. The S2/S1 ratios for GABA were compared between the intact and lesioned SNc using a t-test.

Results were considered to be statistically significant where $P<0.05$.

3.3 Results

3.3.1 Experiment 1: Effect of L-AP4 on glutamate and GABA release in the naive SNc

3.3.1.1 L-AP4 increased K⁺-evoked glutamate release in the SNc at S2 compared with S1

A plot of the dialysate concentration of glutamate over the course of experiment 1 is shown in Figure 31. The reason for the dual-release protocol can clearly be seen by the differences between groups in glutamate release at S1, when all rats were exposed to only high K^+ aCSF. This may be caused by inter-individual variation or differences in the exact location of the microdialysis probe within the SNc.

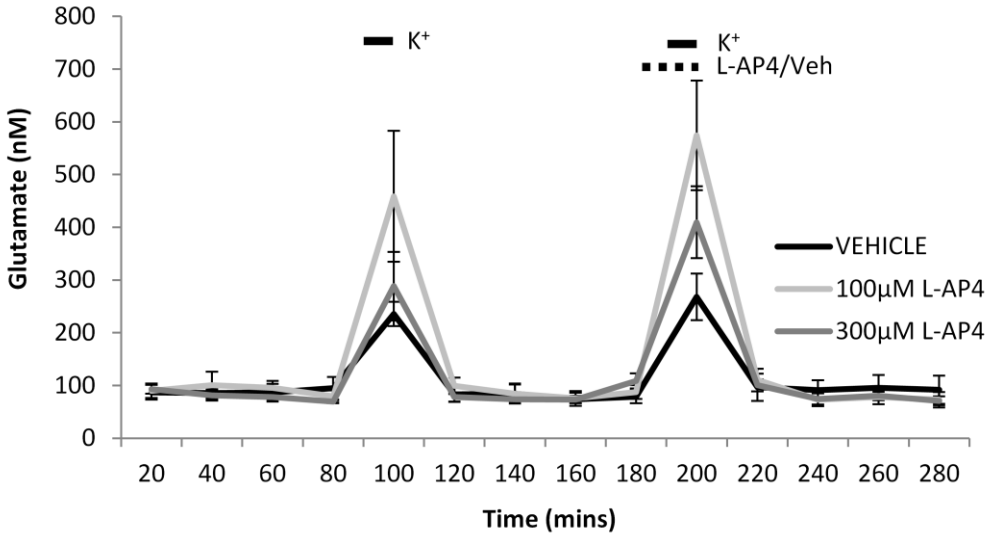

Figure 31: Dialysate glutamate concentrations during unilateral microdialysis in the naive SNc. The two evoked releases, S1 and S2, can clearly be seen at 100 and 200 minutes. The filled bar shows the duration of exposure to high K+ aCSF. The dashed bar shows the duration of exposure to L-AP4 or vehicle. Data are displayed as mean ± s.e.m. (n = 6 per group).

In the vehicle group, the AUC of the control response (S1) was 6498 ± 730 and the AUC of the S2 response (with vehicle) was 7119 ± 1182 (Figure 32a). This increase in glutamate release was not significant (P=0.5572; paired t-test).

In the 100µM L-AP4 group, the AUC of the control response (S1) was 10963 ± 2695 and the AUC of the S2 response (with drug) was 13470 ± 2360 (Figure 32b). This increase in glutamate release in the presence of 100 µM L-AP4 was not significant (P=0.2156; paired t-test).

In the 300µM L-AP4 group, the AUC of the control response (S1) was 7324 ± 1314 and the AUC of the S2 response (with drug) was 10288 ± 1407 (Figure 32c). This represented a significant increase at S2 in the presence of 300 µM L-AP4 compared with S1 (P=0.0001; paired t-test).

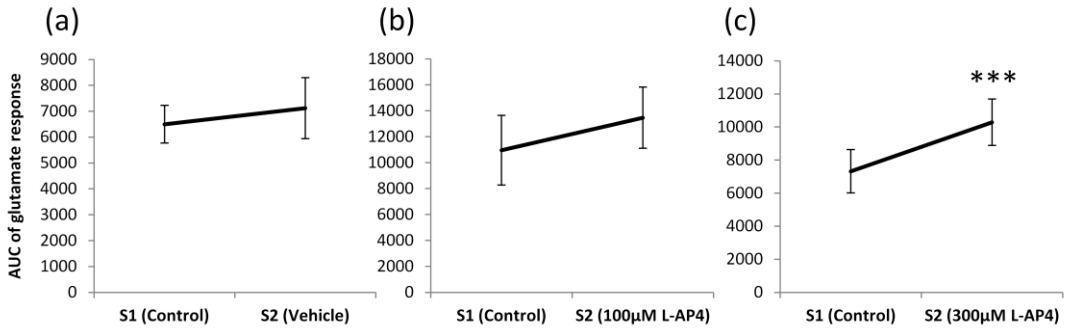

Figure 32: Glutamate S1 vs. S2 response in the SNc of anaesthetised naive rats. The S2 response is significantly increased compared with S1 in the presence of 300µM L-AP4 (c), but not in the presence of either 100µM L-AP4 (b) or vehicle (a). Data are displayed as mean ± s.e.m. (n = 6 per group) ***P<0.001 (paired t-test versus S1).

3.3.1.2 L-AP4 did not affect glutamate S2/S1 ratio

In line with the significant increase in glutamate release at S2 compared with S1 in the 300µM L-AP4 group, the S2/S1 ratio showed a similar trend towards increasing with increasing concentrations of L-AP4; the S2/S1 ratio was 1.10 ± 0.16 in the vehicle group, and increased to 1.34 ± 0.14 in the 100µM L-AP4 group and 1.47 ± 0.10 in the 300µM L-AP4 group. However, despite this trend, when the ratio of S2/S1 response was compared between groups (Figure 33) there was no significant effect of treatment (P=0.2230; one-way ANOVA with Dunnett's *post-hoc*).

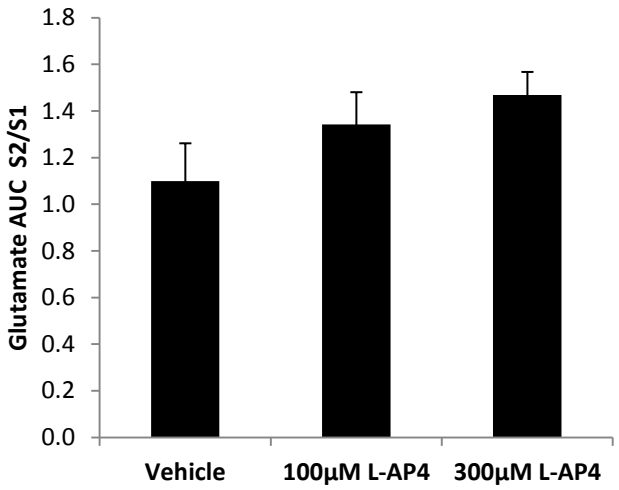

Figure 33: Glutamate S2/S1 ratio in the naive SNc in the presence of L-AP4 or vehicle. The S2/S1 ratio was not significantly altered by exposure to L-AP4 during K^+-evoked glutamate release. Data are displayed as mean ± s.e.m. (n = 6 per group).

3.3.1.3 L-AP4 decreased K^+-evoked GABA release in the SNc at S2 compared with S1

A plot of the dialysate concentration of GABA over the course of experiment 1 is shown in Figure 34.

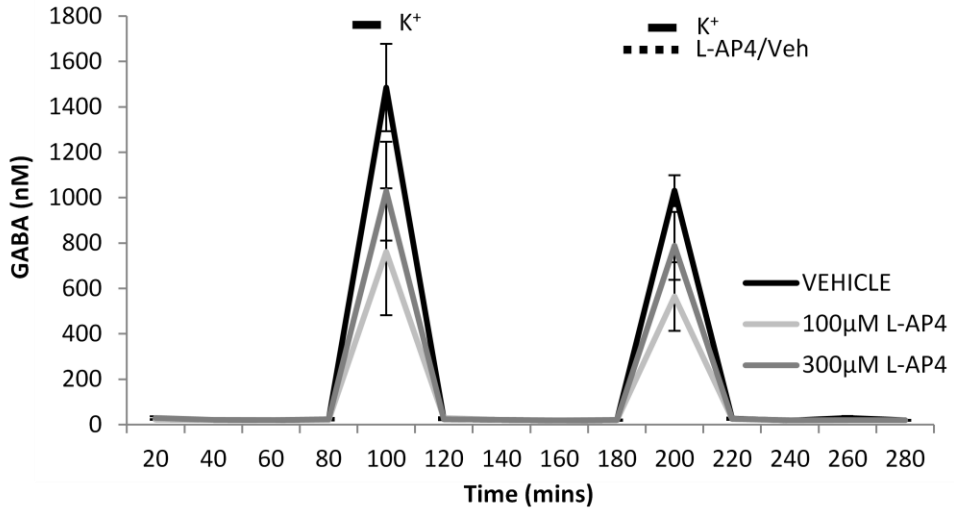

Figure 34: Dialysate GABA concentrations during unilateral microdialysis in the naive SNc. The two evoked releases, S1 and S2, can clearly be seen at 100 and 200 minutes. The filled bar shows the duration of exposure to high K+ aCSF. The dashed bar shows the duration of exposure to L-AP4 or vehicle. Data are displayed as mean ± s.e.m. (n = 6 per group).

In the vehicle group, the AUC of the control response at S1 was 22570 ± 5411 and 16580 ± 3006 at S2 in the presence of vehicle (Figure 35a). There was no significant difference between the S1 and S2 GABA release responses in this group (P=0.1177; paired t-test).

In the 100µM L-AP4 group, the AUC of the control response at S1 was 15731 ± 5636 and 11738 ± 3056 at S2 in the presence of the drug (Figure 35b). This slight decrease was not significant when the S1 and S2 GABA release responses were compared (P=0.1903; paired t-test).

In the 300µM L-AP4 group, the AUC of the control response at S1 was 21079 ± 4385, decreasing to 16218 ± 3000 at S2 in the presence of the drug (Figure 35c). This decrease was found to be significant when the S1 and S2 GABA release responses were compared (P=0.0277; paired t-test).

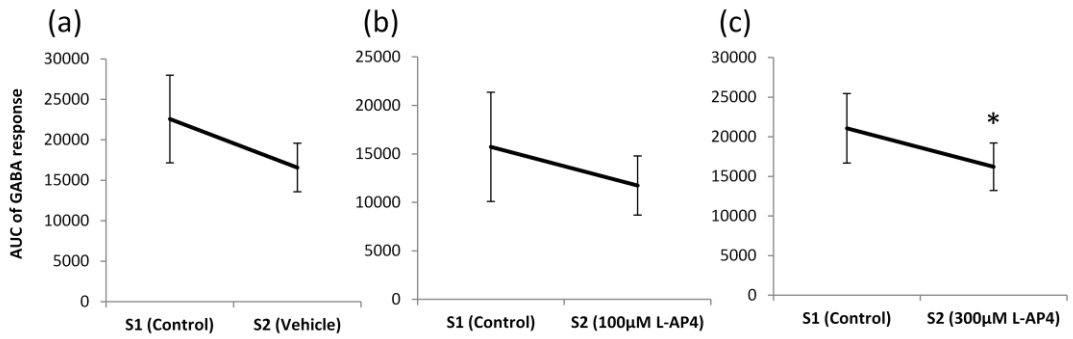

Figure 35: GABA S1 vs. S2 response in the SNc of anaesthetised naive rats. The S2 response is significantly decreased compared with S1 in the presence of 300µM L-AP4 (c), but not in the presence of either 100µM L-AP4 (b) or vehicle (a). Data are displayed as mean ± s.e.m. (n = 6 per group) *P<0.05 (paired t-test versus S1)

3.3.1.4 L-AP4 did not affect GABA S2/S1 ratio

The S2/S1 ratio was 0.84 ± 0.10 in the vehicle group, 0.87 ± 0.07 in the 100µM L-AP4 group and 0.81 ± 0.06 in the 300µM L-AP4 group (Figure 36). Though the within group comparison reported above had shown that the non-significant decrease in GABA release at S2 in the vehicle group was enhanced by L-AP4 such that it became significant in the 300µM group, when the ratio of S2/S1 response was compared between groups there was no significant effect of treatment (P=0.8464; one-way ANOVA with Dunnett's *post-hoc*).

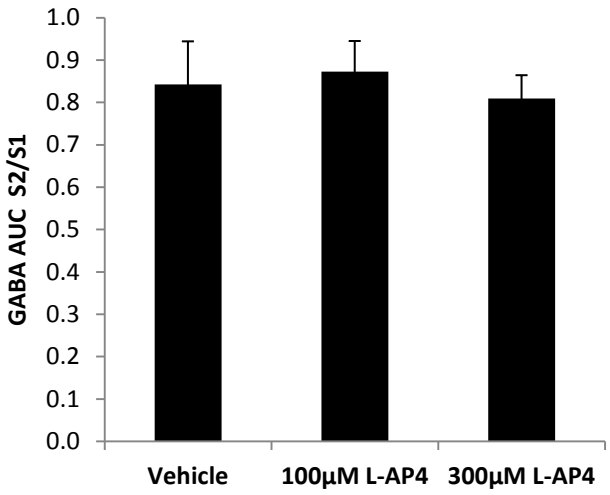

Figure 36: GABA S2/S1 ratio in the naive SNc the in the presence of L-AP4 or vehicle. The S2/S1 ratio was not significantly altered by exposure to L-AP4 during K^+-evoked GABA release. Data are displayed as mean ± s.e.m. (n = 6 per group).

3.3.2 Experiment 2: Effect of VU0155041 on glutamate and GABA release in the naive SNc

3.3.2.1 Effect of L-AP4 and VU0155041 on glutamate release in the SNc

Due to technical issues (see Discussion) the glutamate results from this analysis were unreliable and are therefore not reported.

3.3.2.2 L-AP4 decreased GABA release in the SNc at S2 compared with S1

A plot of the dialysate concentration of GABA over the course of the L-AP4 study is shown in Figure 37.

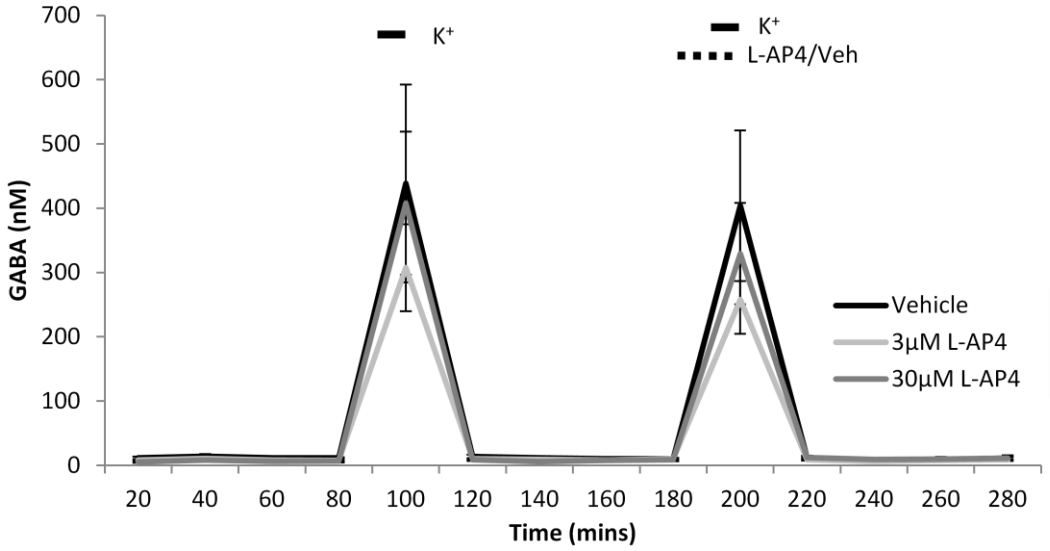

Figure 37: Dialysate GABA concentrations during unilateral microdialysis in the naive SNc. The two evoked releases, S1 and S2, can clearly be seen at 100 and 200 minutes. The filled bar shows the duration of exposure to high K+ aCSF. The dashed bar shows the duration of exposure to L-AP4 or vehicle. Data are displayed as mean ± s.e.m. (n = 6-8 per group).

The AUC for the GABA response in the vehicle group was 9023 ± 2836 at S1 and 8297 ± 2147 at S2 (Figure 38a), which was not significantly different (P=0.5056; paired t-test).

Even with the lower concentrations employed in this study compared with experiment 1, L-AP4 reduced GABA release significantly (Figure 38b), reducing the AUC from 6331 ± 1266 at S1 to 5353 ± 996 at S2 at a concentration of 3µM (P=0.0293; paired t-test).

This effect was lost when L-AP4 was given at 30µM (Figure 38c), with an AUC for the GABA response of 8300 ± 2086 at S1 that was not significantly changed (6757 ± 1489) at S2 (P=0.1091; paired t-test).

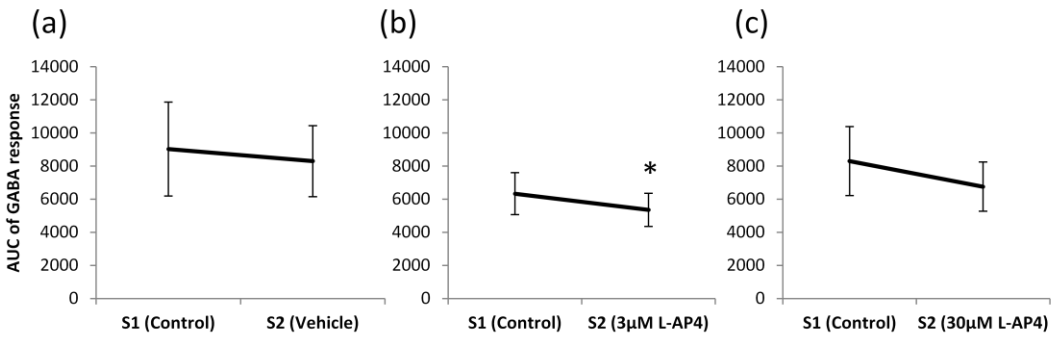

Figure 38: GABA S1 vs. S2 response in the SNc of anaesthetised naive rats. The S2 response is significantly decreased compared with S1 in the presence of 3µM L-AP4 (b), but not in the presence of either 30µM L-AP4 (c) or vehicle (a). Data are displayed as mean ± s.e.m. (n = 6-8 per group) *P<0.05 (paired t-test versus S1)

3.3.2.3 L-AP4 did not affect GABA S2/S1 ratio

Despite the fact that 3µM L-AP4 elicited a significant decrease in evoked GABA release at S2 versus S1 that vehicle treatment did not, there was no significant difference between vehicle and L-AP4-treated groups with regard to the S2/S1 ratio (Figure 39), which was 1.00 ± 0.06 in the vehicle treated group, 0.87 ± 0.04 in the 3µM L-AP4 group and 0.86 ± 0.09 in the 30µM L-AP4 group (P=0.3728; one-way ANOVA with Dunnett's *post-hoc*).

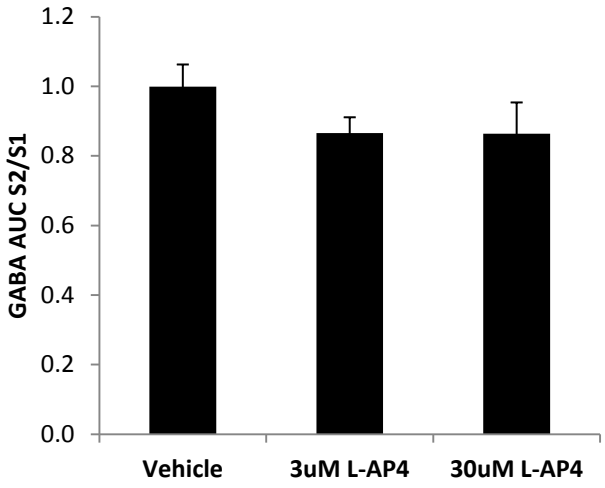

Figure 39: GABA S2/S1 ratio in the naive SNc the in the presence of L-AP4 or vehicle. The S2/S1 ratio was not significantly altered by exposure to L-AP4 during K^+-evoked GABA release. Data are displayed as mean ± s.e.m. (n = 6-8 per group).

3.3.2.4 VU0155041 decreased GABA release in the SNc at S2 compared with S1

A plot of the dialysate concentration of GABA over the course of the VU0155041 study is shown in Figure 40.

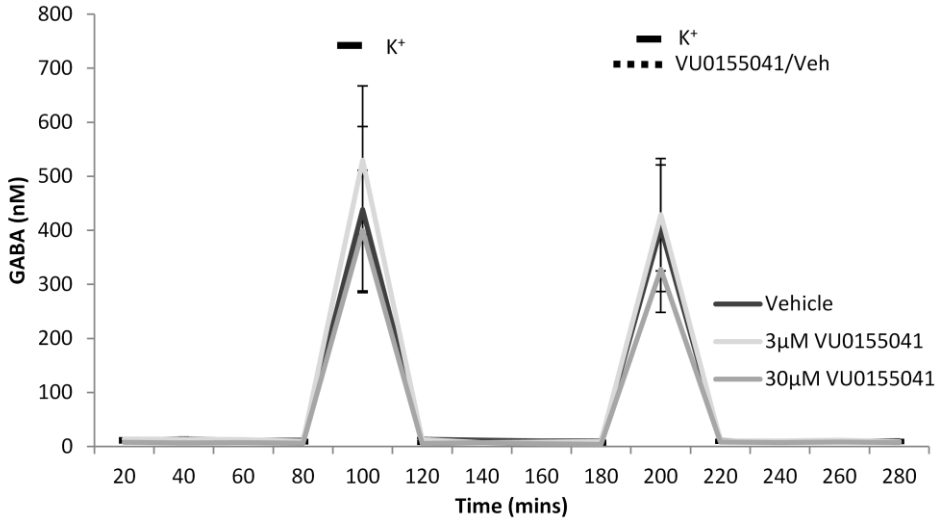

Figure 40: Dialysate GABA concentrations during unilateral microdialysis in the naive SNc. The two evoked releases, S1 and S2, can clearly be seen at 100 and 200 minutes. The filled bar shows the duration of exposure to high K+ aCSF. The dashed bar shows the duration of exposure to VU0155041 or vehicle. Data are displayed as mean ± s.e.m. (n = 6-8 per group).

The AUC for the GABA response in the vehicle group was 9023 ± 2836 at S1 and 8297 ± 2147 at S2 (Figure 41a), which was not significantly different (P=0.5056; paired t-test).

When the SNc was exposed to 3µM VU0155041 during evoked release, the AUC of the GABA response was 10797 ± 2566 for the control response at S1 compared with 8757 ± 1939 for the response in the presence of drug at S2 (Figure 41b). This was a statistically significant decrease (P=0.0371; paired t-test).

When the SNc was exposed to 30µM VU0155041 during evoked release, the AUC of the GABA response 8103 ± 2072 for the control response at S1 compared with 6679 ± 1478 for the response in the presence of drug at S2 (Figure 41c). There was no significant difference between these responses (P=0.1085; paired t-test).

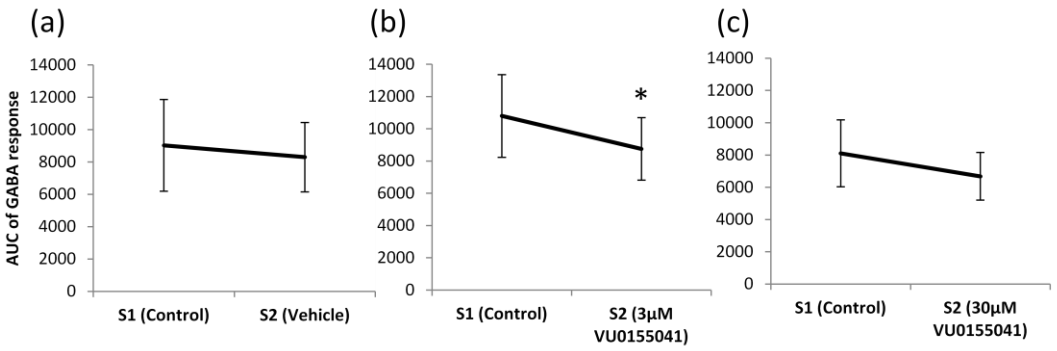

Figure 41: GABA S1 vs. S2 response in the SNc of anaesthetised naive rats. The S2 response is significantly decreased compared with S1 in the presence of 3µM VU0155041 (b), but not in the presence of either 30µM VU0155041 (c) or vehicle (a). Data are displayed as mean ± s.e.m. (n = 6-8 per group) *P<0.05 (paired t-test vs. S1)

3.3.2.5 VU0155041 did not affect GABA S2/S1 ratio

Despite the fact that 3µM VU0155041 elicited a significant decrease in evoked GABA release that vehicle treatment did not, there was no significant difference between vehicle and VU0155041-treated groups with regard to the S2/S1 ratio (Figure 42), which was 1.00 ± 0.06 in the vehicle treated group, 0.87 ± 0.04 in the 3µM VU0155041 group and 0.91 ± 0.07 in the 30µM VU0155041 group (P=0.3466; one-way ANOVA with Dunnett's *post-hoc*).

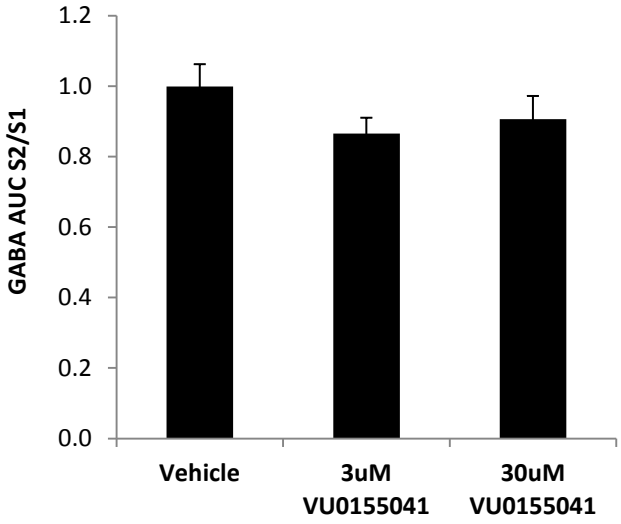

Figure 42: GABA S2/S1 ratio in the naive SNc the in the presence of VU0155041 or vehicle. The S2/S1 ratio was not significantly altered by exposure to VU0155041 during K^+-evoked GABA release. Data are displayed as mean ± s.e.m. (n = 6-8 per group).

3.3.3 Experiment 3: Comparing the effect of L-AP4 on glutamate and GABA release in the 6-OHDA-lesioned and intact SNc

In one rat the probe placement in the intact hemisphere was too medial, therefore for the lesioned SNc (n = 6) and for the intact SNc (n = 5).

3.3.3.1 MFB lesioning significantly reduced striatal dopamine content

MFB lesioning with 6-OHDA caused a severe depletion of striatal dopamine and its metabolites (Figure 43).

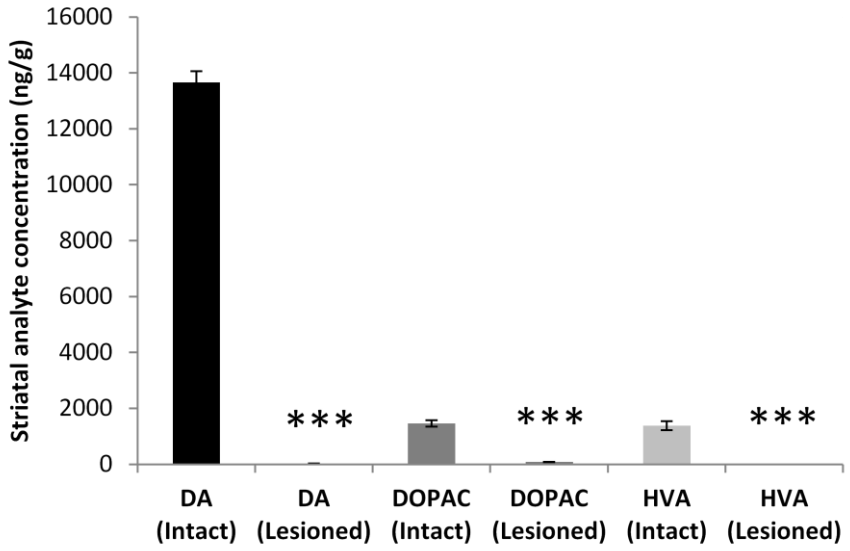

Figure 43: Concentration of dopamine and its metabolites in the intact and lesioned striatum following unilateral 6-OHDA lesioning of the MFB. Data are presented as mean ± s.e.m. (n=6) ***P<0.001 (t-test vs. intact striatum)

The striatal dopamine content in the intact side was 13662 ± 397ng/g, and this was reduced to 22.9 ± 7.4ng/g in the lesioned striatum (P<0.0001; t-test). Similarly, the DOPAC content was reduced from 1460 ± 112ng/g in the intact striatum to 83.1 ± 8.3ng/g in the lesioned striatum (P<0.0001; t-test) and HVA content was reduced from 1378 ± 158ng/g in the intact striatum to 15.1 ± 1.5ng/g in the lesioned striatum (P<0.0001; t-test).

3.3.3.2 6-OHDA lesioning did not affect basal glutamate or GABA concentrations

Plots of the dialysate concentrations of glutamate and GABA over the course of the experiment are shown in Figure 44.

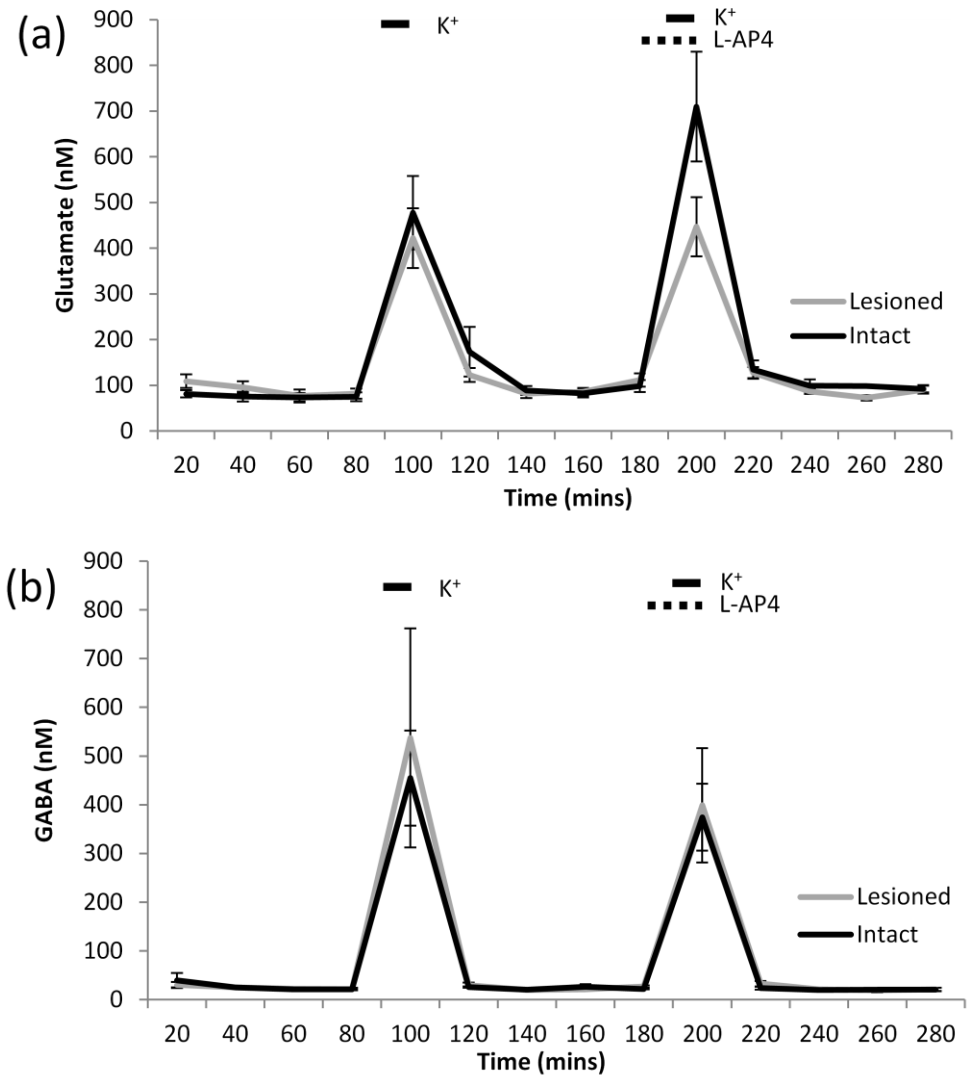

Figure 44: Dialysate glutamate (a) and GABA (b) concentrations during bilateral microdialysis in the intact and lesioned SNc. Neurotransmitter release was evoked by exposure to high K^+ aCSF in the presence of vehicle (100 mins) and 300µM L-AP4 (200 mins). The filled bar shows the duration of exposure to high K+ aCSF. The dashed bar shows the duration of exposure to L-AP4 or vehicle. Data are displayed as mean ± s.e.m. (n = 5-6 per hemisphere).

Basal dialysate glutamate concentrations, as measured between 20 and 80 minutes, were not significantly affected by the lesion, with 76.3 ± 8.7nM measured in the intact SNc and 93.6 ± 14.6nM measured in the lesioned SNc, though there is a trend towards increased basal glutamate levels in the lesioned SNc (P=0.0988; t-test).

Basal dialysate GABA concentrations were also unaffected by the lesion, with 26.8 ± 4.1nM in the intact SNc and 22.3 ± 2.1nM in the lesioned SNc (P=0.7294; t-test).

3.3.3.3 L-AP4 increased K^+-evoked glutamate release in the intact but not lesioned SNc at S2 compared with S1

The effect on glutamate release with L-AP4 exposure in the intact SNc was comparable to the results collected in the naive rats in experiment 2. The AUC for the S2 response was 16522 ± 2661, increased from 11413 ± 1805 at S1 (Figure 45; P=0.0427; paired t-test).

Conversely this effect of L-AP4 was lost in the lesioned SNc, where the AUC for the S2 response was 11265 ± 1448 compared with 10486 ± 1502 at S1. This did not represent a significant increase (P=0.4453; paired t-test).

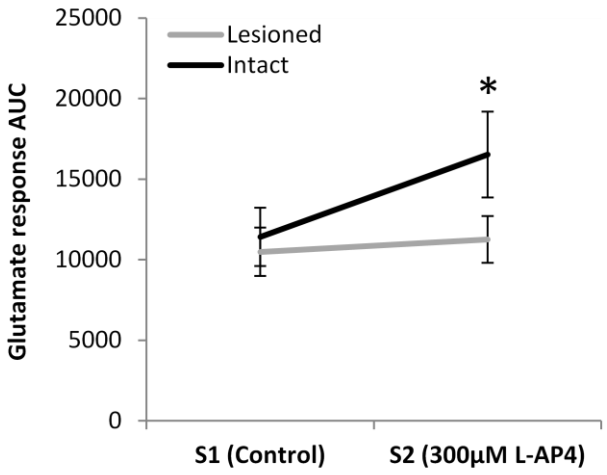

Figure 45: K^+-evoked glutamate release with vehicle (S1) and L-AP4 (S2). Evoked glutamate release was increased at S2 vs. S1 in the intact SNc but this effect was lost in the lesioned SNc. Data are displayed as mean ± s.e.m. (n = 5-6 per hemisphere) *P<0.05 (paired t-test vs. S1)

3.3.3.4 The lesion had no overall effect on glutamate S2/S1 ratio

Despite the presence of an effect of L-AP4 in the intact but not in the lesioned SNc, and a trend when the ratios are compared by eye, the overall glutamate S2/S1 ratio was not significantly affected by treatment (Figure 46), coming out at 1.38 ± 0.17 in the intact SNc and 1.14 ± 0.05 in the lesioned SNc (P=0.1255; Mann-Whitney U test).

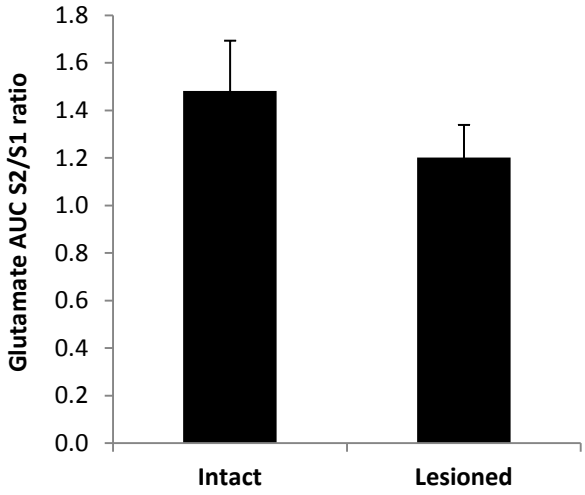

Figure 46: The glutamate S2/S1 ratio in the intact and lesioned SNc the in the presence of L-AP4. The response to L-AP4 as determined by the S2/S1 ratio was not significantly altered by the lesion. Data are displayed as mean ± s.e.m. (n = 5-6).

3.3.3.5 L-AP4 tended to decrease K⁺-evoked GABA release in the intact but not lesioned SNc at S2 compared with S1

The effect on GABA release with L-AP4 exposure in the intact SNc (Figure 47) was also comparable to the results collected in the naive rats in experiment 2, though this time it narrowly missed reaching significance. The AUC for the S2 response was 7947 ± 1358, down from 9565 ± 1971 at S1 (P=0.0758; paired t-test).

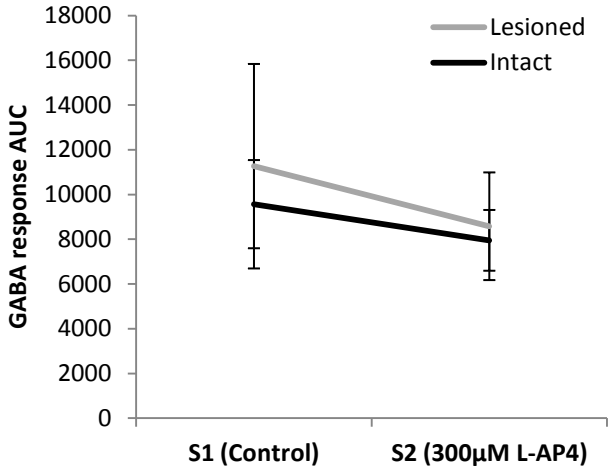

Figure 47: K^+-evoked GABA release with vehicle (S1) and L-AP4 (S2). Evoked GABA release was decreased at S2 vs. S1 in the intact SNc, an effect that approached significance (P=0.076), but there was no significant effect of L-AP4 on GABA release in the lesioned SNc. Data are displayed as mean ± s.e.m. (n = 5-6 per hemisphere).

As was the case for glutamate, L-AP4 had no effect on evoked GABA release in the lesioned SNc. The control response at S1 had an AUC of 11261 ± 4570 and the S2 response in the presence of L-AP4 had an AUC of 8578 ± 2406 (P=0.2800; paired t-test).

3.3.3.6 The lesion had no overall effect on GABA S2/S1 ratio

Unlike the trend towards an effect of L-AP4 in the intact but not in the lesioned SNc, the effect of lesion on GABA S2/S1 ratio was not significant, being 0.86 ± 0.06 in the intact SNc and 0.94 ± 0.05 in the lesioned SNc (Figure 48; P=0.8395; t-test).

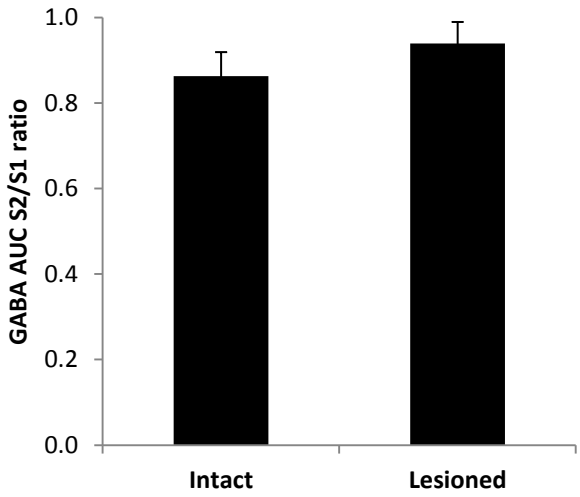

Figure 48: The GABA S2/S1 ratio in the intact and lesioned SNc the in the presence of L-AP4. The response to L-AP4 as determined by the S2/S1 ratio was not significantly altered by the lesion. Data are displayed as mean ± s.e.m. (n = 5).

3.3.4 Summary of results

The results of all the microdialysis studies reported in this chapter are summarised in Table 8. Overall, L-AP4 at high or low, but not intermediate, concentrations causes a reduction in GABA release and an increase in glutamate release in the naive/intact SNc (where measurable). VU0155041 at a low but not an intermediate dose also causes a reduction in GABA release in the naive/intact SNc, though any concurrent effects on glutamate release could not be determined due to technical issues.

The effects of a high dose of L-AP4 on glutamate and GABA release in the intact SNc were lost in the 6-OHDA-lesioned SNc.

Table 8: Summary of the effects of L-AP4 and VU0155041 on K^+-evoked glutamate and GABA release in the intact and lesioned SNc. n.d. = not determined. The arrow in brackets represents a result that approached significance.

Drug	Effect on glutamate at S2 vs. S1 (naive SNc)		Effect on GABA at S2 vs. S1 (naive SNc)	
3µM L-AP4	n.d.		↓	
30µM L-AP4	n.d.		↔	
100µM L-AP4	↔		↔	
300µM L-AP4	↑		↓	
3µM VU0155041	n.d.		↓	
30µM VU0155041	n.d.		↔	
300µM L-AP4	**Intact SNc**	**Lesioned SNc**	**Intact SNc**	**Lesioned SNc**
	↑	↔	(↓)	↔

3.4 Discussion

The hypothesis underlying the execution of these experiments was that activation of group III mGlu receptors would lead to a reduction in neuronal release of glutamate into the SNc, and that a similar effect would be seen with selective activation of $mGlu_4$ due to its implication in the effects mediated by broad spectrum group III agonists. Since group III mGlu receptors are also located on GABAergic terminals in the SNc we also expected that L-AP4 and VU0155041 would reduce GABA release.

Moreover, in light of 6-OHDA lesioning producing changes in group III mGlu receptor expression in the SN in general, we also wanted to confirm whether any beneficial effects of mGlu receptors on decreasing glutamate release were maintained in the parkinsonian state.

3.4.1 Effects of L-AP4 on GABA release in the naive SNc

In experiments 1 and 2, L-AP4 significantly reduced GABA release compared with the control response at the lowest concentration tested (3µM) and at the highest concentration tested (300µM). These results support our hypothesis that activation of group III mGlu receptors in the SNc reduces GABA release.

To our knowledge there are no existing published studies regarding the effects of group III mGlu receptor agonists on GABAergic transmission in the SNc. On the other hand there are several studies that have investigated the effects of broad spectrum group III agonists on GABAergic transmission in the SNr. Given that the microdialysis membrane in the above studies would have been partially located within the SNr due to the small size of the SNc (0.5mm high compared with the 1mm membrane length; technical considerations relating to microdialysis are considered later in the discussion), the decreased GABA and increased glutamate detected in the presence of L-AP4 might therefore have partly originated in the SNr and so previous studies performed in this region might also be relevant to the analysis of the present results. Another factor that might suggest the validity of considering data collected in the SNr when discussing results collected in the SNc is that the main glutamatergic and GABAergic afferents that innervate the SNr and SNc are shared, though of course we cannot be sure that they operate in the same way as the distribution of group III mGlu receptors at the synapses could be different.

The reduction in GABA release described here in the intact SNc in the presence of L-AP4 is concordant with electrophysiological experiments, where L-AP4 and L-SOP inhibited

GABAergic transmission in the SNr (Wittmann *et al.*, 2001). It also reflects published behavioural experiments, where acute SNr infusion of ACPT-I in naive rats caused an akinetic phenotype (likely mediated by $mGlu_8$) and acute or chronic SNr infusion of ACPT-I led to delayed reaction times in a lever-pressing task (Lopez *et al.*, 2007). These effects are recapitulated by acute intra-SNr infusion of the $GABA_A$ antagonist picrotoxin and therefore seem to involve a group III-mediated reduction in GABAergic transmission (Lopez *et al.*, 2007). In turn this would disinhibit SNr neurones and increase the SNr-mediated inhibition of thalamocortical feedback that underlies parkinsonian motor disability.

3.4.2 Effects of L-AP4 on glutamate release in the naive SNc

In experiment 1, where glutamate release was successfully quantified alongside GABA release, the significant reduction in GABA release achieved with 300µM L-AP4 was associated with a concomitant significant *increase* in glutamate release. This finding was contrary to our hypothesis and would lead us to believe that activation of group III receptors in this region, far from having a neuroprotective effect secondary to reduction of glutamate release, could in fact enhance glutamate release and potentially thereby enhance excitotoxic neurodegeneration of SNc neurones.

Group III mGlu receptor agonists have been reported elsewhere to inhibit glutamatergic transmission in the intact SNc *in vitro* (Valenti *et al.*, 2005) and also in the intact SNr *in vivo* (Austin *et al.*, 2010; Wittmann *et al.*, 2001). In addition, *in vitro* results using subtype-specific activators of $mGlu_4$ and $mGlu_7$ have demonstrated decreased release of a glutamate analogue in nigral prisms in the presence of a subthreshold dose of L-AP4 (Broadstock *et al.*, 2012). However the results of our studies suggest that activation of group III receptors with L-AP4 can *increase* glutamate release in the SNc. A possible mechanism that could explain this is that the reduction in GABA release described above causes a secondary increase in glutamate release, as explored below.

GABA has been shown to negatively regulate glutamate release from STN terminals (Hatzipetros *et al.*, 2006). This may either be via a direct effect on $GABA_A$ or $GABA_B$ heteroreceptors on STN terminals (Boyes *et al.*, 2003; Hatzipetros *et al.*, 2006) or via an indirect mechanism involving $GABA_A$–mediated inhibition of dopaminergic neurones in the SNc (Paladini *et al.*, 1999) and subsequent reduction of dopamine release in the nigrosubthalamic pathway, which would usually enhance glutamate release (Cragg *et al.*, 2004). GABA released from co-stimulated striatonigral afferents is also proposed to inhibit glutamate release from subthalamonigral terminals via activation of presynaptic $GABA_B$

receptors during STN-DBS, further supporting a tonic inhibitory effect of GABA on glutamate release in the SN (Dvorzhak *et al.*, 2013).

Logically therefore, a reduction of GABA release into the SN, such as might be brought about by activation of group III mGlu heteroreceptors on GABAergic terminals, would lead to a disinhibition of either or both of the subthalamonigral and nigrosubthalamic neurones, thereby giving rise to increased glutamate release from the subthalamonigral neurones into the SN (Figure 49). Indeed such an effect was borne out in the intact BG by the results of the studies reported here, and therefore we believe that such a mechanism was responsible for the increased evoked glutamate release in the presence of L-AP4, which was only present where GABA release was also significantly affected.

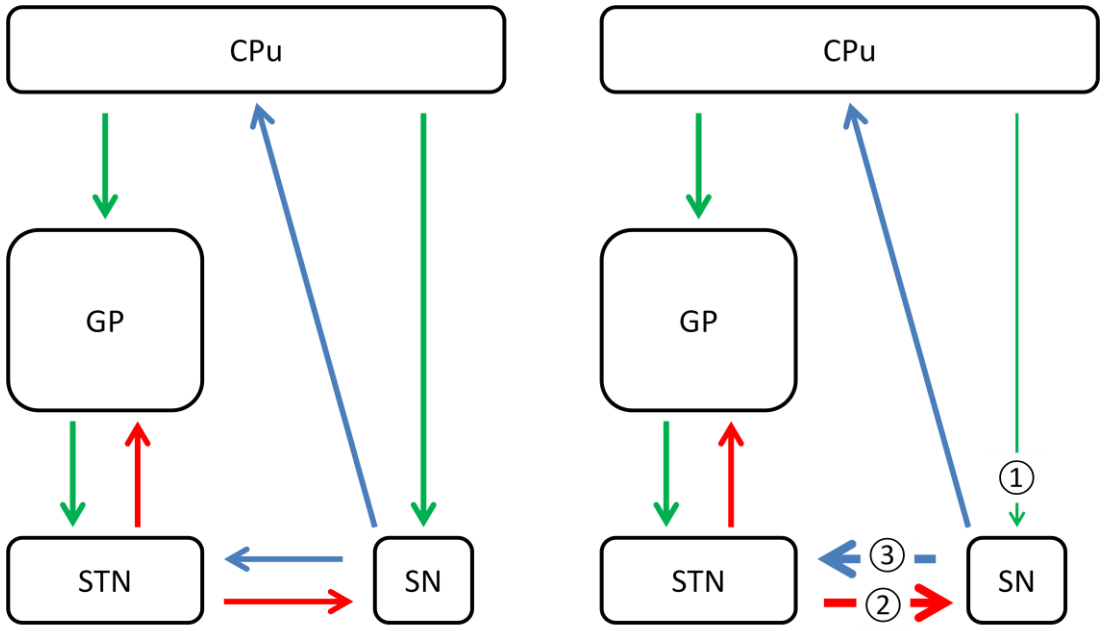

Figure 49: Proposed mechanism of the effect of group III mGlu receptor activation on GABA and glutamate release in the naive/intact SNc. The normal functioning of the BG is shown in the left hand panel, and the proposed functioning in the presence of L-AP4 is shown in the right hand panel. GABAergic connections are denoted by the green arrows, glutamatergic connections by the red arrows and dopaminergic connections by the blue arrows. Upon L-AP4 administration: ① Activation of presynaptic group III mGlu heteroreceptors leads to decreased GABA release into SN (possibly from striatonigral MSNs). ② Reduced GABA release leads to reduced presynaptic $GABA_B$-mediated inhibition of glutamate release from subthalamonigral terminals AND/OR ③Reduced $GABA_A$-mediated inhibition of dopamine release in nigrosubthalamic pathway (dopamine release in the STN enhances glutamate release from STN-SN neurones).

The results of our experiments with L-AP4, and the mechanism we propose to underlie these, would suggest that the affinity of L-AP4 for group III mGlu receptors is higher on

striatonigral (or other GABAergic) terminals than on subthalamonigral (or other glutamatergic) terminals. Alternatively, this effect could be explained by differential expression or distribution of group III mGlu receptors between GABAergic and glutamatergic afferents. Indeed the distribution of presynaptic $mGlu_4$ receptors in the SNr is primarily at inhibitory type II synapses rather than excitatory type I synapses (Corti *et al.*, 2002), suggesting that agonists that target this receptor subtype may preferentially modulate GABA release. Whether this is the case in the SNc as well is unknown, therefore further experiments to test receptor distribution in the SNc would be of value.

3.4.3 Effects of VU0155041 on GABA release in the naive SNc

Since neuroprotective effects have been previously reported following selective allosteric modulation of $mGlu_4$ in the SNc with VU0155041 (Betts *et al.*, 2012) we decided to test this compound to gauge its effects on glutamate and GABA release in the same model, alongside equimolar concentrations of L-AP4 for comparison. As in the case for broad spectrum group III mGlu receptor agonists, we are not aware of any previous studies that have investigated the effects of $mGlu_4$ PAMs on GABAergic transmission in the SNc.

The reduction of GABA release during exposure to VU0155041 was in agreement with our hypothesis that activation of $mGlu_4$ heteroreceptors on GABAergic terminals would reduce neurotransmitter release. The ability of VU0155041 as well as L-AP4 to inhibit GABA release in the SNc implicates the involvement of $mGlu_4$ receptors in this effect. Though not previously demonstrated in the SN, selective $mGlu_4$ receptor activation is known to inhibit GABA release at other locations within the basal ganglia such as the globus pallidus (Valenti *et al.*, 2003) and striatum (Cuomo *et al.*, 2009) so it may well also occur in the SNc.

Unfortunately in this experiment the effects of VU0155041 or equimolar concentrations of L-AP4 on glutamate release could not be ascertained due to technical issues with the HPLC method employed. This included crowding and overlapping of peaks that could not be rectified due, we think, to the progressive degradation of the HPLC columns by the pH 10.3 derivatisation reagent. Though analysed on the same system, the results for GABA were valid as no interfering electroactive products eluted anywhere near the peak of interest and therefore the effect of degradation was simply reflected in an incremental reduction in retention time.

3.4.4 Possible receptor subtype involvement in the GABA response in the naive SNc

Interestingly, 3µM L-AP4 had a similar effect to 300µM L-AP4 on GABA release, causing a significant reduction at S2 compared with S1. The effect of VU0155041 on GABA release was hard to predict, because as a PAM (rather than an orthosteric agonist like L-AP4) stimulation by endogenous glutamate is required for receptor activation. If the VU0155041 were to reduce glutamate release in line with expectations (which could not be tested due to the technical issues mentioned) this might mean that there was insufficient glutamate present to activate $mGlu_4$ heteroreceptors, and therefore the drug would have no effect on GABA release. However when tested, an equimolar dose of the $mGlu_4$ PAM VU0155041 caused a significant decrease in GABA release at S2 versus S1 that was similar to that found for 3µM L-AP4 and was not present in the vehicle group.

The biphasic efficacy of L-AP4 in inhibiting GABA release, such that the reduction at S2 versus S1 was significant at 3µM and 300µM but not at 30µM or 100µM, is of interest. Given that VU0155041 and L-AP4 demonstrate similar potency at $mGlu_4$ (0.43µM and 0.56µM respectively), the effect at 3µM concentration for each of these drugs likely involves activation of the $mGlu_4$ receptor. Activation of $mGlu_8$ may also contribute to this effect in the case of L-AP4 since $mGlu_8$ receptor protein has been detected in the SN (Gu, 2003) and the EC_{50} of L-AP4 at $mGlu_8$ is similar to that at $mGlu_4$. The loss of the effect on GABA release at 30 and 100µM L-AP4 may reflect desensitisation of the $mGlu_4$ and $mGlu_8$ receptors, and its re-emergence at 300µM concentrations may reflect the ability of higher concentrations of L-AP4 to activate $mGlu_7$ receptors (EC_{50} = 160µM). This cannot be stated conclusively though, as despite the known drug concentrations in the perfusate, the actual concentration of drug that diffused across the membrane and into the brain was not determined.

3.4.5 Loss of L-AP4-mediated effects in the lesioned SNc

The results obtained for L-AP4 and VU0155041 in the intact SNc conflicted with our expectations, implying that broad activation of group III mGlu receptors or selective activation of $mGlu_4$ would in fact promote excitotoxic degeneration of dopaminergic neurones in the SNc by increasing glutamate release. The potential mechanism explored above, involving negative regulation of subthalamonigral glutamate release by GABA, stems from experiments performed in naive rodents, and the results I obtained in naive rats in experiments 1 and 2 reflected these findings, but it was not clear if the same mechanism might be functional in the parkinsonian condition. Therefore we set out to

confirm whether or not L-AP4-mediated alterations in evoked glutamate and GABA release were maintained in the SNc following nigrostriatal denervation with 6-OHDA.

Firstly, we found no effect of 6-OHDA lesioning on baseline GABA and glutamate concentrations in the SNc, though there was a trend towards increased basal glutamate concentrations in the lesioned SNc. This trend for enhanced basal glutamate was in line with our expectations, given that glutamatergic transmission in the SNc is enhanced in the dopamine denervated BG by increased subthalamonigral firing (Bergman *et al.*, 1994b; Remple *et al.*, 2011). Although no comparable microdialysis data have been published for the SNc, in previous microdialysis studies performed in the SNr some authors have found no significant difference between intact and lesioned sides with respect to basal GABA or glutamate concentrations (Bianchi *et al.*, 2003) while others reported no difference in GABA but an increase in basal glutamate concentrations in the lesioned SNr (Ochi *et al.*, 2004).

As stated earlier, we used a dual-stimulation protocol for all our studies due to the inter-animal variability that we encountered in pilot studies at S1, and therefore we did not compare the size of the response at S1 between groups in any of our studies. However another group has previously compared K^+-evoked glutamate release in 6-OHDA-lesioned rats and intact rats using microdialysis, and they showed a ~40% decrease in K^+-evoked glutamate release in the SNr of 6-OHDA-lesioned rats compared with control rats with no change in basal glutamate levels (Bianchi *et al.*, 2003). This is interesting as it contradicts the dogmatic expectation of increased signalling in the indirect pathway in the parkinsonian BG (and therefore increased subthalamic nucleus-derived glutamate in the SNr).

The decrease in K^+-evoked GABA release that we described in experiment 1 in the naive SNc in the presence of 300µM L-AP4 was reproduced in the intact SNc in experiment 3, albeit at a level that did not quite attain significance. As in the naive SNc, in the intact SNc the decrease in GABA release was concomitant with a significant increase in glutamate release. Interestingly the effects of 300µM L-AP4 on GABA and glutamate release in the intact SNc were both lost in the lesioned SNc. Therefore our results suggest that the mechanism that underlies the effects of L-AP4 in the intact SNc is altered following a full 6-OHDA lesion of the nigrostriatal pathway such that it is no longer functional (Figure 50).

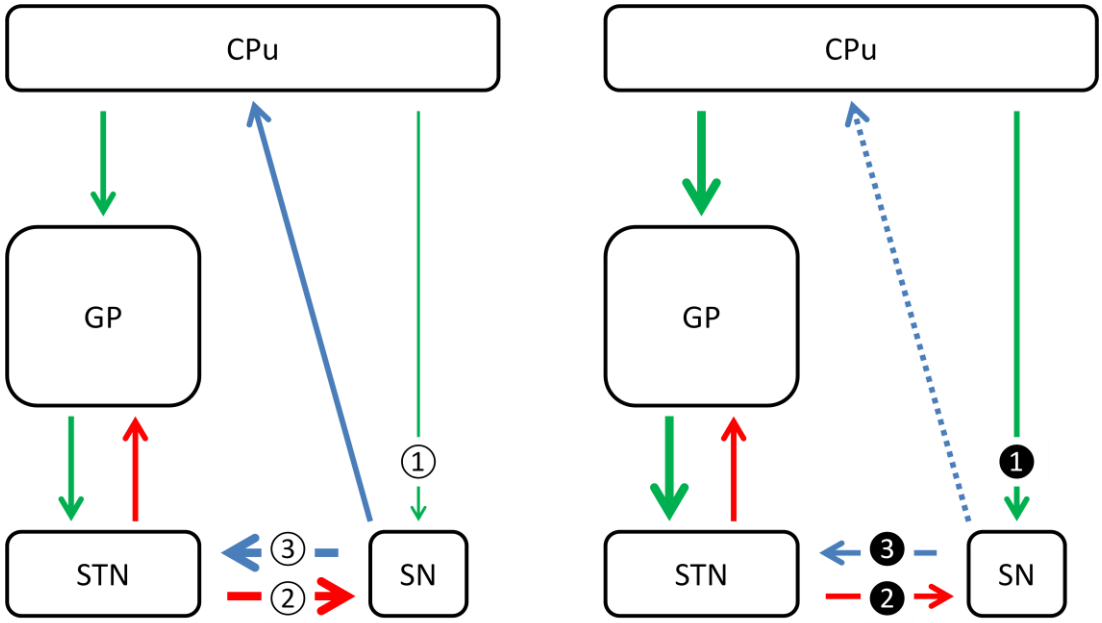

Figure 50: Proposed mechanism of the effect of group III mGlu receptor activation on GABA and glutamate release in the intact and lesioned SNc. The proposed effects of activation of group III mGlu receptors is shown in the left hand panel for the intact SNc, and in the right hand panel for the lesioned SNc. GABAergic connections are denoted by the green arrows, glutamatergic connections by the red arrows and dopaminergic connections by the blue arrows. In the intact SNc: ① Activation of presynaptic group III mGlu heteroreceptors leads to decreased GABA release into SN (possibly from striatonigral MSNs). ② Reduced GABA release leads to reduced presynaptic $GABA_B$-mediated inhibition of glutamate release from subthalamonigral terminals AND/OR ③Reduced $GABA_A$-mediated inhibition of dopamine release in nigrosubthalamic pathway (dopamine release in the STN enhances glutamate release from STN-SN neurones). In the lesioned SNc: ❶ GABA release into SN not affected by L-AP4. In the parkinsonian state signalling in the striatonigral pathway is reduced and this could lead to downregulation of group III mGlu heteroreceptors on these terminals. ❷ GABA can still act on presynaptic $GABA_B$ receptors on STN terminals, preventing the rise in glutamate release seen in the intact SNc AND/OR ❸ GABA can still act on $GABA_A$ receptors on nigrosubthalamic neurones, which inhibits dopamine release into the STN, removing its enhancing effects on glutamate release.

The loss of the effect of L-AP4 on GABA release in the SNc in experiment 3 is in line with a previous study showing that the ability of L-AP4 to inhibit striatonigral IPSCs is reduced in acutely dopamine-depleted rats (Wittmann *et al.*, 2002). However it contradicts the results of behavioural experiments where intra-SNr infusion of the group III agonists ACPT-I and L-AP4 causes reaction time deficits in both naive *and* 6-OHDA lesioned rats, an effect which is mimicked by the $GABA_A$ antagonist picrotoxin in both groups of animals and is therefore likely caused by a reduction in GABA signalling (Lopez *et al.*, 2012; Lopez *et al.*, 2007).

The loss of the effect of L-AP4 on glutamate release in the SNc in experiment 3 is likely secondary to the loss of the effect on GABA via the mechanism explained earlier. In the parkinsonian state, signalling in the BG is increased in the indirect pathway and decreased

in the direct pathway. Decreased direct pathway activity could lead to compensatory downregulation of group III mGlu receptors on striatonigral terminals, possibly explaining the downregulation of $mGlu_4$ and $mGlu_8$ receptor proteins described previously in the SN following a 6-OHDA lesion (Gu, 2003). With reduced receptor expression or function on GABAergic terminals, the decreased GABA release elicited by L-AP4 in the intact SNc would be prevented.

The increase in glutamate release in the intact SNc and lack of change in glutamate release in the lesioned SNc contradict a previous experiment which showed that L-AP4 induced inhibition of glutamate transmission in both intact and acutely dopamine depleted rats *in vitro* (Wittmann *et al.*, 2002). However the acute dopamine depletion that was induced by reserpine in the Wittmann (2002) study (1.5-2 hours) may not have comparable effects on glutamatergic signalling as the chronic dopamine depletion caused by 6-OHDA-induced degeneration of the nigrostriatal tract. Firstly, the duration of dopamine depletion may have affected the results, with chronic depletion allowing time for longer-term alterations in receptor expression and coupling to occur. For example a differential response to $mGlu_8$ activation with DCPG (administered i.c.v.) has been noted following acute (2 hours) or chronic (18 hours) dopamine depletion by reserpine, an effect which may be attributed to time-related alterations in receptor protein expression or trafficking (Johnson *et al.*, 2008). Secondly, the method of dopamine depletion may have played a role, especially as reserpine not only depletes dopamine but also other catecholamines and may therefore have a more complicated effect on signalling within the BG than selective dopaminergic denervation. For example $mGlu_5$ mRNA expression has been shown to be decreased in the striatum 18 hours after reserpine-mediated dopamine depletion (Ismayilova *et al.*, 2006) but is unchanged following a 6-OHDA lesion (Messenger *et al.*, 2002). Though changes in mRNA expression do not necessarily translate to changes at the protein level, these experiments demonstrate that different methods of dopamine depletion may cause different effects on glutamatergic signalling by differentially altering glutamate receptor expression or function.

3.4.6 General considerations

It should be noted that although the within-group S2 versus S1 comparisons mentioned above were significant in the relevant drug-treated groups and were not significant in the vehicle groups, none of the experiments performed gave a significant difference between drug-treated and vehicle groups with respect to the S2/S1 ratio, and therefore they should be interpreted with caution. Nevertheless the clear trends in S2/S1 ratio in certain

experiments, notably experiment 1, certainly lend support to the S2 vs. S1 effects measured in these experiments reflecting a genuine effect of group III mGlu receptor activation on glutamate and GABA release.

There are several technical limitations to the studies reported in this chapter that should also be considered when interpreting the data. The main caveat is that the area targeted for microdialysis is very small. The depth of the SNc from top to bottom at the implantation location is ~0.5mm, meaning that the 1mm membrane used for these studies (the smallest produced by the supplier) protruded beyond the borders of this structure. This means that a proportion of the glutamate and GABA in the dialysates was sampled from areas outside the SNc, likely the SNr. Another feature of the small size of the sampling target is that probe implantation can cause physical damage to the area, resulting in the formation of a 'trauma layer' in which neurotransmission is perturbed (Bungay *et al.*, 2003). Though there is no way to prevent this phenomenon completely, any effects were minimised by the use of a concentric probe design with a small membrane area, which results in reduced tissue damage compared with classical U-shaped dialysis probes (Kendrick, 1989).

In addition, the short membrane length dictated by the size of the SNc would have resulted in reduced analyte recovery than if a larger membrane length could have been used, but this was not important from the point of view of these studies, where a comparison between two responses was the outcome rather than a calculation of the absolute extracellular concentration.

Secondly, microdialysis was performed in anaesthetised rats rather than freely moving rats. Anaesthetics are known to affect GABA and glutamate neurotransmission (Garcia *et al.*, 2010) so this could have affected both basal and evoked release. The anaesthetic used in these studies, urethane, has minimal effects on GABA and glutamate neurotransmission compared with inhalable anaesthetics such as halothane and isoflurane (Larsen *et al.*, 1998; Maclver *et al.*, 1996; Miyazaki *et al.*, 1997; Westphalen *et al.*, 2005), nevertheless it is known to modestly potentiate $GABA_A$ receptor function and inhibit AMPA and NMDA receptor function (Hara *et al.*, 2002) and may also suppress spontaneous glutamate release (Tian *et al.*, 2012) so it is still not ideal. In order to completely remove these effects the studies could be repeated in freely-moving rats to see if comparable results are collected.

Thirdly, the temporal resolution is poor in microdialysis, therefore it cannot be deduced whether the increase in glutamate release is the cause of result of the decrease in GABA

release. There are alternative methods that can be used that have enhanced temporal resolution such as FSCV (Stamford, 1990) or enzyme-based microelectrode arrays (Rutherford *et al.*, 2007) with sub-second acuity.

Finally, though the evoked release that was measured is assumed to reflect neuronal release of glutamate and GABA, there is some disagreement in the literature as to the potential contribution of other pools of GABA and glutamate such as glial cells (reviewed by Westerink *et al.*, 2007). For glutamate especially it has been suggested that none escapes the synaptic cleft and therefore none will reach the microdialysis probe to be sampled (Obrenovitch *et al.*, 2000). Conversely others have suggested that there *is* sufficient overspill from the synaptic cleft to enable sampling of neuronally released GABA and glutamate (Bergles *et al.*, 1999; Isaacson *et al.*, 1993). Classically, testing basal or K^+-evoked neurotransmitter release in the presence of the voltage-dependent sodium channel blocker tetrodotoxin (TTX) or in Ca^{2+}-free conditions is used to verify the neuronal origin of extracellular neurotransmitters. However while this proved straightforward in the case of neurotransmitters such as monoamines (Herrera-Marschitz *et al.*, 1992), when this has been attempted for glutamate it has yielded mixed results, which overall suggest a predominant neuronal origin of glutamate but with complicating factors such as rapid reuptake into glial cells (Herrera-Marschitz *et al.*, 1996; Lada *et al.*, 1998). From the point of view of excitotoxicity, which is the focus of our research into group III mGlu receptors, an increase in the overall extracellular glutamate concentration is likely to be significant regardless of whether it is of neuronal or non-neuronal origin. Its localisation to the synaptic cleft is also unnecessary as activation of extrasynaptic rather than post-synaptic NMDA receptors is believed to underlie excitotoxicity (Hardingham *et al.*, 2010; Stark *et al.*, 2011; Xu *et al.*, 2009).

3.5 Conclusion

Contrary to our hypothesis, administration of L-AP4 in the intact SNc led to a significant increase in glutamate release and a significant decrease in GABA release compared with the control response. When this experiment was repeated using the $mGlu_4$ PAM VU0155041 a similar reduction in GABA release was apparent, although due to technical difficulties the effect of this drug on glutamate release could not be ascertained.

Though the significance of these drug effects could be called into question given the lack of significant differences in the S2/S1 ratio between drug- and vehicle-treated groups, the ability of L-AP4 and VU0155041 to significantly decrease GABA release and (in the case of L-AP4) increase glutamate release compared to the control responses within groups do suggest an effect of group III mGlu receptors, and $mGlu_4$ in particular, in modulating evoked neurotransmitter release *in vivo*.

Whilst these results might discourage the use of group III mGlu receptor agonists as a means to reduce subthalamonigral glutamate release and the possible associated excitotoxicity in Parkinson's disease, these unexpected and potentially damaging effects were not maintained following complete lesioning of the nigrostriatal tract. This gives us hope that even in the absence of a detectable reduction in glutamate release, administration of drugs that activate group III mGlu receptors should at least not worsen any ongoing excitotoxicity in the parkinsonian SNc.

Taken in combination, these experiments do not support the idea of reduced glutamate release at the subthalamonigral synapse as the mechanism underlying the neuroprotective effects of L-AP4 and VU0155041 in the 6-OHDA model of PD. An alternative mechanism that has been suggested to underlie the neuroprotective efficacy of these compounds is the reduction of inflammation, so future studies focusing on the potential anti-inflammatory aspects of group III mGlu receptor targeting would be worthwhile.

4 Targeting $mGlu_4$ systemically as a potential neuroprotective approach in a hemiparkinsonian rat model

4.1 Introduction

The neuroprotection afforded by local supranigral infusion of the $mGlu_4$ PAM VU0155041 points to targeting of this receptor as a promising strategy to promote dopaminergic cell survival in Parkinson's disease. Though the microdialysis studies that were subsequently performed do not point to reduction of glutamate release in the SNc as the protective mechanism, previous studies have suggested that VU0155041 reduces inflammation (Betts *et al.*, 2012), which is known to also be a feature in the human parkinsonian SNc (Teismann *et al.*, 2003), and therefore this could underlie its protective effect.

Regardless of the mechanism, direct targeting of $mGlu_4$ in the SNc by intracerebral injection is not a clinically relevant scenario and therefore the next step is to target the same receptor using a systemically active compound. Following systemic administration we would expect a more widespread activation of $mGlu_4$ receptors throughout the basal ganglia, which could have implications for the efficacy of this therapeutic approach.

4.1.1 Localisation of $mGlu_4$ in the basal ganglia

$mGlu_4$ expression at the mRNA and protein levels has been identified at several locations within the intact rodent basal ganglia (Figure 51).

$mGlu_4$ mRNA is expressed at low to moderate levels in the cortex and striatum, and at very low to low levels in the GP, STN, SNc, SNr and EPN (Messenger *et al.*, 2002; Ohishi *et al.*, 1995; Testa *et al.*, 1994), although in one of these studies it was not detected anywhere in the BG except the cortex and striatum (Ohishi *et al.*, 1995).

$mGlu_{4a}$ protein has been detected at low to moderate levels in the cortex and striatum, very high levels in the GP, moderate levels in the SNr and EPN and not at all in the STN (Bradley *et al.*, 1999b; Bradley *et al.*, 1999c; Broadstock *et al.*, 2012; Corti *et al.*, 2002). There is one report where $mGlu_{4a}$ was detected at moderate levels in the intact SNc (Gu, 2003), in contrast to previous reports where it was not detected (Bradley *et al.*, 1999c; Corti *et al.*, 2002).

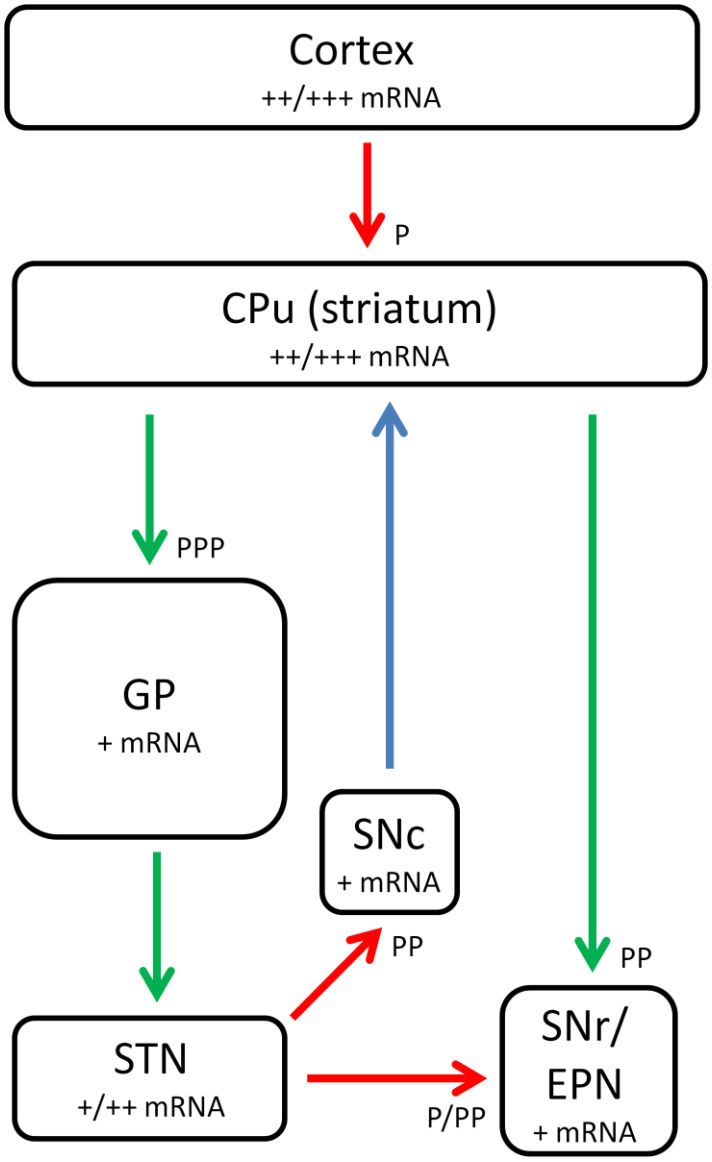

Figure 51: Location of $mGlu_4$ mRNA or receptor protein in the rodent basal ganglia. +, ++ and +++ denote low, moderate and high expression of mRNA respectively. P, PP and PPP denote low, moderate and high expression of $mGlu_{4a}$ protein respectively. Green arrows denote GABAergic neurones, red arrows denote glutamatergic neurones and blue arrows denote dopaminergic neurones.

Where the protein has been identified, electron microscopy studies have shown that it is (mainly) pre-synaptically located, suggesting it is acting in its canonical role as an inhibitor of presynaptic neurotransmitter release:

- In the striatum, though one study found no evidence for somal localisation (Bradley *et al.*, 1999c), another report found that some $mGlu_4$ staining was found in the somata of MSNs but that some was also localised to dendrites and axon terminals at mainly type II (inhibitory) and also type I (excitatory) synapses (Corti *et al.*, 2002).

- In the GP, $mGlu_4$ was localised along dendrites and at axon terminals forming type II synapses, implicating a role in modulation of striatopallidal GABAergic transmission (Bradley *et al.*, 1999c; Corti *et al.*, 2002).
- Finally, in the EPN and SNr $mGlu_4$ was again localised to dendrites, and in the SNr was more commonly identified in axon terminals making type II synapses than type I synapses, suggesting that $mGlu_4$ receptors play a greater role in modulating inhibitory striatonigral neurotransmission compared with excitatory (perhaps subthalamonigral) neurotransmission in the output nuclei of the BG (Bradley *et al.*, 1999c; Corti *et al.*, 2002).

The effect of nigrostriatal denervation on $mGlu_4$ receptor expression in the rat is unclear. In the model that we use, the 6-OHDA-lesioned rat, lesioning has been reported to reduce the expression of $mGlu_4$ mRNA in the striatum (Messenger *et al.*, 2002). At the protein level 6-OHDA lesioning does not alter striatal $mGlu_4$ receptor expression (Picconi *et al.*, 2002), suggesting that the reduction in mRNA expression is either not carried through to the protein level or that the downregulation is restricted to striatofugal terminals. In addition, 6-OHDA lesioning has been reported to reduce $mGlu_4$ receptor expression in the SNc (Gu, 2003).

On the other hand in alternative models of PD, namely the haloperidol-treated mouse (an acute model) and the MPTP-lesioned mouse (a degenerative model), $mGlu_4$ mRNA has been reported to be upregulated in striatal projection neurones, a mechanism that is postulated to underlie the 'compensation' that is thought to occur in early PD (Cannella *et al.*, 2012). However whether this translates to the protein level has not been investigated so the consequences of this upregulation for neurotransmission are unknown.

Finally, in MPTP-lesioned primates no change in $mGlu_4$ expression was noted in any basal ganglia region in lesioned animals compared with control (Bogenpohl *et al.*, 2012). Again, without any information on whether receptor protein levels are affected the impact of MPTP lesioning on $mGlu_4$ activity in primates is unclear.

To our knowledge there are no existing reports examining the effect of 6-OHDA lesioning on $mGlu_4$ receptor protein expression at several of the key synapses that might be targeted for an antiparkinsonian therapy, especially on striatopallidal MSNs in light of the reported reduction in $mGlu_4$ mRNA in the striatum. While it is not clear exactly how and where these receptors might be altered by the lesion, previous behavioural results using $mGlu_4$-specific

compounds in this model have demonstrated antiparkinsonian efficacy in combination with sub-threshold L-DOPA (e.g. Bennouar *et al.*, 2013; Le Poul *et al.*, 2012), supporting the presence and targetability of these receptors in this model.

4.1.2 Potential mechanisms of neuroprotection following $mGlu_4$ activation

Activation of $mGlu_4$ receptors (located presynaptically) leads to inhibition of neurotransmitter release from the presynaptic terminal. Though the microdialysis studies in the previous chapter did not support this mechanism as underlying the protective effect of VU0155041 in the SNc (though this was only tested in the naive SNc; the maintenance of this effect is yet to be verified in the 6-OHDA-lesioned SNc), there are previous reports that activation of group III receptors, or specifically $mGlu_4$ inhibits glutamatergic transmission in the SNc (Broadstock *et al.*, 2012; Valenti *et al.*, 2005; Wittmann *et al.*, 2001). Even in the absence of an effect at the subthalamonigral synapse there are other candidate synapses elsewhere in the BG at which activation of $mGlu_4$ has been shown to alter signalling and at which inhibition of signalling might be predicted to have an antiparkinsonian effect. These are explored below.

The main input to the basal ganglia is the glutamatergic signalling between the cortex and the striatum. The $mGlu_4$ PAM LuAF21934 has been shown to inhibit corticostriatal synaptic transmission in naive rats (Bennouar *et al.*, 2013; Gubellini *et al.*, 2014).

Parkinson's disease symptoms are driven by overactivation of signalling in the indirect pathway (striatum → GPe → STN → SNr/EPN). In addition to the reported ability of $mGlu_4$ activation to inhibit excitatory transmission at the subthalamonigral synapse (above), $mGlu_4$ is also present at the striatopallidal synapse. At this particular synapse, the inhibitory effect of broad spectrum group III mGlu receptor agonists on GABAergic signalling *in vitro* was believed to be contingent on $mGlu_4$ receptors (Valenti *et al.*, 2003). This assertion has since been supported by data showing that the $mGlu_4$ PAMs LuAF21934 and PHCCC inhibit GABA release in the striatopallidal pathway *in vitro* in the presence of co-stimulation of the orthosteric site with either L-AP4 or endogenous glutamate (Gubellini *et al.*, 2014; Marino *et al.*, 2003). In addition, the neuroprotection afforded by systemic administration of PHCCC in MPTP-treated mice was recapitulated in mice where PHCCC was instead administered intrapallidally, implicating the globus pallidus as the primary site of action for this $mGlu_4$ PAM (Battaglia *et al.*, 2006; Fazio *et al.*, 2012).

Therefore activation of $mGlu_4$ at several synapses within the BG might have additive antiparkinsonian effects (demonstrated by the reversal of symptoms and neuroprotection

mentioned with systemic or i.c.v. administration of $mGlu_4$ activators in the previous section). Decreased striatopallidal transmission would lead to increased pallidosubthalamic inhibitory neurotransmission, thereby indirectly decreasing glutamate release into the SNc from subthalamonigral neurones. This indirect inhibition of nigral glutamate release still might lead to a neuroprotective effect even if $mGlu_4$ activation has no *direct* effect on subthalamonigral glutamate release.

4.1.3 Support for an antiparkinsonian or neuroprotective effect of widespread activation of $mGlu_4$ receptors

In the previous section we explored the potential direct and indirect mechanisms via which $mGlu_4$ activation within the BG might normalise signalling in the BG and thereby reduce subthalamonigral glutamate release. This would be expected to have symptomatic and neuroprotective efficacy in PD models, and indeed there is promising evidence that these effects are apparent when subtype-specific compounds are given using routes of administration that will simultaneously activate $mGlu_4$ receptors throughout the BG.

Haloperidol-induced catalepsy can be reversed by systemic or intracerebroventricular (i.c.v.) administration of the $mGlu_4$ agonist LSP1-2111 (Beurrier *et al.*, 2009) or the $mGlu_4$ PAMs Compound 11 (East *et al.*, 2010), VU0155041 (Niswender *et al.*, 2008b), VU0364770 (Jones *et al.*, 2012) ADX88178/AF42744 (Le Poul *et al.*, 2012) and LuAF21934 (Bennouar *et al.*, 2013). Another acute model of PD, reserpine-induced akinesia, is reversed by systemic or i.c.v. administration of PHCCC (Battaglia *et al.*, 2006; Marino *et al.*, 2003) or VU0155041 (Niswender *et al.*, 2008b).

In the context of lesion models of PD, there is so far only a single published report investigating the neuroprotective effect of $mGlu_4$ activation. In this study systemic administration of the $mGlu_4$ PAM PHCCC protected against MPTP-induced nigrostriatal degeneration in mice, preventing loss of both TH-positive cell bodies in the SNc and dopamine in the striatum (Battaglia *et al.*, 2006). This effect was primarily mediated by the actions of PHCCC in the globus pallidus and was proposed by the authors to elicit neuroprotection by reducing the excitotoxic component by reducing downstream subthalamonigral glutamate release. However there remains a possibility that the protection observed in this study was at least partially mediated by the partial antagonist activity of PHCCC at $mGlu_{1b}$ receptors (Maj *et al.*, 2003) and therefore further studies using compounds that are more selective for $mGlu_4$ would be informative.

Taken together this evidence suggests that the net effect of activation of $mGlu_4$ receptors throughout the BG is antiparkinsonian and, on the basis of the single study reported so far, neuroprotective. This gives us a sound basis for investigating the effects of $mGlu_4$ activation in an alternative degenerative model of PD using a different $mGlu_4$ PAM.

4.1.4 Hypothesis and aims

A previous study has shown that systemic administration of the $mGlu_4$ PAM PHCCC has neuroprotective effects in the mouse MPTP model of PD (Battaglia *et al.*, 2006). In light of the neuroprotective effect seen with nigral delivery of the $mGlu_4$ PAM VU0155041 in the 6-OHDA lesioned rat in Chapter 2, the aim of this study was to see if a similar protective effect could be shown in the same model with more clinically-relevant systemic administration of the $mGlu_4$ PAM LuAF21934, where actions will also occur elsewhere in the BG. We hypothesise that:

Widespread activation of $mGlu_4$ receptors in the BG using the positive allosteric modulator LuAF21934 will have a neuroprotective effect in the 6-OHDA model of PD in the rat.

Before commencing this study, the pharmacokinetic (PK) profile for LuAF21934 was defined in naive male Sprague-Dawley rats following an oral dose. A plasma profile was obtained up to 6 hours after dosing and the brain/plasma ratio was measured at 1-hour and 2-hour time points. This study informed the frequency of dosing in the neuroprotection study.
For the neuroprotection study, LuAF21934 was administered twice daily for 3 days preceding and 7 days after intranigral infusion of 6-OHDA in rats. This study assessed the ability of LuAF21934 to:

- Enhance survival of tyrosine hydroxylase (TH)-positive neurones in the SNc.
- Preserve striatal dopamine content.
- Preserve motor function secondary to any measured neuroprotection, as assessed by the cylinder test, adjusted steps test and amphetamine-induced rotometry.

To ensure that any neuroprotective effects observed were mediated by activation of $mGlu_4$, LuAF21934-treated groups were compared with lesioned rats that were treated with vehicle or with 30mg/kg LuAF21935, a negative control compound that is the inactive enantiomer of LuAF21934.

4.2 Materials and Methods

4.2.1 Compounds tested

Table 9 shows the structure of LuAF21934, the $mGlu_4$ PAM tested for neuroprotective efficacy in the 6-OHDA SNc-lesioned rat model of Parkinson's disease, and LuAF21935, the negative control compound used to compare it with. Both LuAF21934 and LuAF21935 were synthesised and characterised at Lundbeck (Copenhagen, Denmark).

Table 9: The chemical structure of the $mGlu_4$ PAM tested for neuroprotective efficacy in the hemiparkinsonian rat following systemic administration. Also shown is the structure of the negative control compound LuAF21934.

Structure	Name	Target
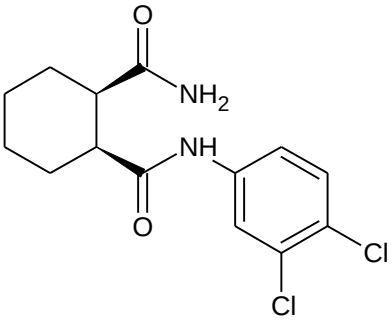	LuAF21934 *(1S, 2R)-N^1-(3,4-dichlorophenyl)-cyclohexane-1,2-dicarboxamide*	$mGlu_4$ Positive Allosteric Modulator
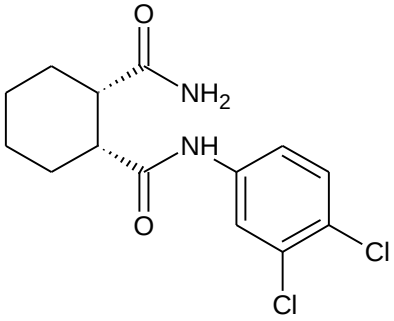	LuAF21935 *Neg Ctrl*	Inactive enantiomer of LuAF21934

LuAF21934 was developed at Lundbeck as a variant on VU0155041 that was designed to have increased brain penetrance following peripheral administration. The EC_{50} of LuAF21934 at human $mGlu_4$ is ~500nM and when given parenterally can reduce both latency in the haloperidol test of catalepsy, and forelimb akinesia in 6-OHDA-lesioned rats (Bennouar *et al.*, 2013; Doller *et al.*, 2010). The neuroprotective potential of this compound has not yet been examined.

LuAF21935 is the inactive enantiomer of LuAF21934 and was used in this study as a negative control compound (Neg Ctrl group).

4.2.1.1 Drug formulation

LuAF21934 and Neg Ctrl were dissolved in PEG-400 (polyethylene glycol, average molecular weight 400), obtained from Sigma Aldrich (Poole, UK).

4.2.2 Other materials

4.2.2.1 Experimental materials

Materials and compound for lesioning surgery and behavioural testing were as described in section 2.2.2.1.

4.2.2.2 Analytical materials

Immunohistochemistry: Tyrosine hydroxylase (TH) immunohistochemistry materials used were as described in section 2.2.2.2. Ionised calcium binding adaptor molecule 1 (Iba-1) primary antibody was obtained from Wako Chemicals (Neuss, Germany).

HPLC analysis of striatal dopamine and its metabolites: High Performance Liquid Chromatography (HPLC) analysis was carried out at King's College London. Dopamine, DOPAC, HVA, 3,4-dihydroxybenzylamine hydrochloride (DHBA), perchloric acid (PCA), EDTA, HPLC grade methanol and HPLC grade water were obtained from Sigma Aldrich (Poole, UK). Sodium dihydrogen phosphate (NaH_2PO_4) was obtained from Fisher Scientific (Loughborough, UK). Sodium metabisulfite and octane sulfonic acid (OSA) were obtained from VWR International (Lutterworth, UK).

UPLC-MS/MS for PK studies: Ultra-high Performance Liquid Chromatography with tandem Mass Spectrometry (UPLC-MS/MS) analysis of brain and plasma samples for the PK studies was carried out at Lundbeck (Copenhagen, Denmark). 2-propanol, acetonitrile (ACN), ammonium hydroxide, dimethylsulfoxide (DMSO) and formic acid used for brain and plasma sample preparation and UPLC-MS/MS were obtained from Sigma Aldrich (Poole, UK or St. Louis, MO).

4.2.3 Pharmacokinetic testing of LuAF21934

All procedures were performed in accordance with the U.K. Animals (Scientific Procedures) Act, 1986.

Two PK studies were carried out in order to decide on a dosing schedule that would result in a reasonable duration of exposure to LuAF21934 during the lesion development period.

- (**PK-A**) a plasma time course of LuAF21934 and AF42744 in naive rats.
- (**PK-B**) 1-hour and 2-hour plasma and brain time points for 30mg/kg LuAF21934 in naive rats to calculate the brain/plasma ratio.

4.2.3.1 Drug formulation and dosing

For PK-A, 10mg/kg and 30mg/kg LuAF21934 were formulated in PEG-400 (5ml/kg) and administered by oral gavage to naive male Sprague-Dawley (SD) rats (n = 3 per dose). Serial blood samples were collected at 5 minutes, 20 minutes, 1, 2, 4 and 6 hours after dosing.

For PK-B, 30mg/kg LuAF21934 was formulated in PEG-400 (2ml/kg) and administered by oral gavage to 6 naive male SD rats within an hour of formulation. The first group of rats was sacrificed 1 hour after dosing (n = 3) and the second group of rats was sacrificed 2 hours after dosing (n = 3). Blood and brain samples were collected for each group.

4.2.3.2 Sample collection

PK-A: Serial blood samples (~200µl/time point) were collected from the tail vein into EDTA-coated tubes. Blood samples were centrifuged at 3300 x g for 10 minutes at 4°C to separate the cells from the plasma, and the plasma was removed and snap-frozen on dry ice to await analysis.

PK-B: Rats were deeply anaesthetised with isoflurane and a blood sample withdrawn by cardiac puncture and placed into a Lithium-heparin coated tube (Sarstedt). Blood samples were centrifuged at 2000 x g for 10 minutes at room temperature to separate the cells from the plasma, and the plasma was removed and snap-frozen on dry ice to await analysis. Immediately following cardiac puncture, rats were decapitated and the brain was removed from the skull, weighed and snap-frozen on dry ice to await analysis.

4.2.3.3 Bioanalysis

Brain samples for PK-B were prepared at King's College London 24 hours after collection. Plasma samples for both studies were prepared for analysis at Lundbeck (Copenhagen, Denmark). All brain and plasma samples were analysed by UPLC-MS/MS at Lundbeck.

Brain sample preparation: Brains were homogenised in 4 volumes of homogenisation buffer comprising a 5:3:2 v/v/v ratio of HPLC water, 2-propanol and DMSO. Homogenates were centrifuged at 2700 x g for 20 minutes at 4°C and the resulting supernatant removed into a 96-well plate for analysis.

Plasma sample preparation: 25µl plasma samples were protein-precipitated with 150µl ACN containing 5ng/ml internal standard (Lundbeck compound LuAE90074). Samples were centrifuged at 6200xg for 20 minutes at 4°C and 100µl supernatant removed. This supernatant was diluted 1:1 with 100µl water containing 0.1% ammonium hydroxide.

Analysis by UPLC-MS/MS: Drug concentrations were determined using UPLC-MS/MS. For all analytes, gradient UPLC was carried out, with a phase 1 to phase 2 transition time of 3 minutes. Mobile phase 1 consisted of water with 0.1% ammonium hydroxide, mobile phase 2 consisted of ACN with 0.1% ammonium hydroxide. Samples were separated on an Acquity UPLC BEH Phenyl column 1.7µm, 2.1 x 30mm (Waters, MA). Detection by mass spectrometry was performed using a Sciex-API 4000 MS (Applied Biosystems, NL) using electrospray with positive ionization mode.

The limit of detection for LuAF21934 was 1ng/ml in plasma and 5ng/g in brain. The peak area correlated linearly with the plasma and brain concentration of the analytes in the range of 1-1000ng/ml plasma and 5–5000ng/g brain (corrected for dilution). If the plasma/brain sample drug concentration was above 1000ng/ml or 5000ng/g, the sample was diluted appropriately in blank plasma/blank brain homogenate before repeat analysis.

4.2.4 Neuroprotection study methods

All procedures were performed in accordance with the U.K. Animals (Scientific Procedures) Act, 1986.

4.2.4.1 Lesioning and treatment

Rats were anaesthetised using isoflurane as described for the neuroprotection studies in Chapter 2, and the same volume and concentration of 6-OHDA.HCl infused directly into the SNc at the following coordinates relative to the interaural line (ML from midline): AP +3.7mm, ML +2.0mm, DV +2.2mm (Figure 52). The toxin solution was infused at a rate of 0.5µl/min via a 25G injection needle, and following infusion the needle was left in place for a further 5 minutes to prevent reflux.

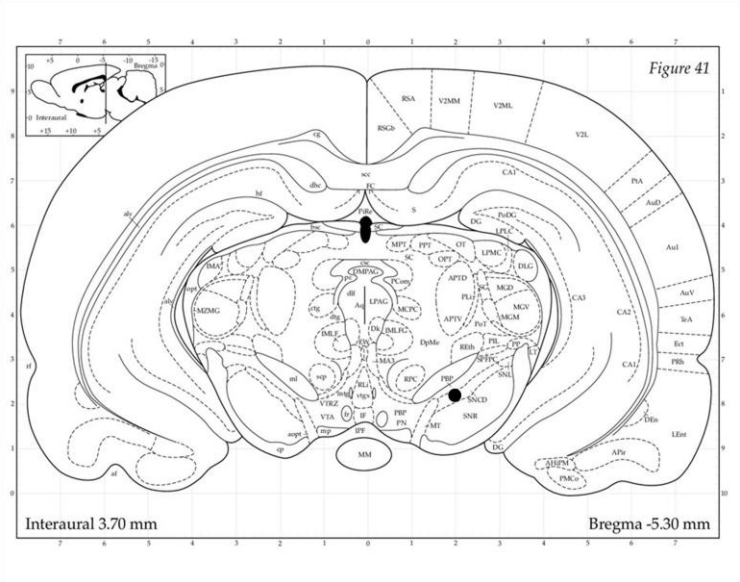

Figure 52: Co-ordinates for unilateral 6-OHDA lesioning of the SNc. The black spot shows the position of the tip of the infusion cannula. The diagram was obtained from The Rat Brain in Stereotaxic Coordinates (Paxinos *et al.*, 1998).

Twice daily treatment at 07:30 and 19:00 with LuAF21934 (10 or 30mg/kg), the negative control LuAF21935 (30 mg/kg) or vehicle (2ml/kg) began three days prior to lesioning. The first dose on the day of 6-OHDA lesioning was administered 1 hour prior to 6-OHDA, the second dose on the day of lesioning at 19.00 and then dosing continued for a further six days at 07:30 and 19:00 as before. This resulted in a total of ten days of twice-daily dosing (the study plan is shown in Figure 53).

Drugs were made up once daily and used for both morning and evening dosing, before being discarded within 24 hours of formulation. Formulations were stored at room

temperature in the dark in between doses. LuAF21934 is known to be stable when formulated in PEG-400 for up to one week (personal communication from Lundbeck).

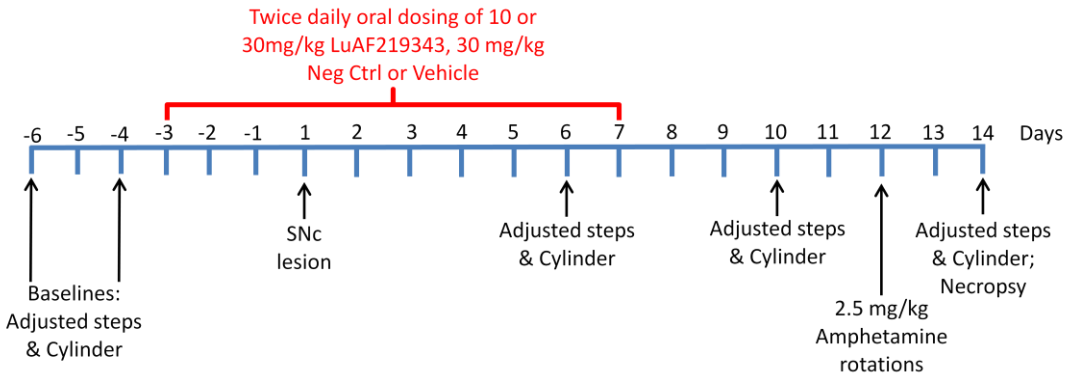

Figure 53: Experimental protocol for the LuAF21934 neuroprotection study. Baseline behaviour in the cylinder and adjusted steps tests was measured in duplicate prior to commencement of the dosing period. Rats were treated twice daily for 3 days prior to lesioning with LuAF21934, vehicle or a negative control compound. On the day of lesioning, rats received their morning dose one hour prior to lesioning of the SNc with 6-OHDA, and the evening dose as usual, then dosing continued daily post-lesion for a further 6 days. Behavioural testing was carried out at intervals during the and after the treatment period (days 6, 10 and 14). 14 days after lesioning, rats were killed by CO_2 asphyxiation and their brains removed for analysis.

4.2.4.2 Assessment of lesion size

At the completion of each study rats were killed by CO_2 asphyxiation followed by decapitation, and the brain removed. The striatum was dissected out on an ice-cold platform, weighed and snap-frozen on dry ice for HPLC analysis of dopamine, while a coronal block containing the midbrain was post-fixed for a minimum of 72 hours in 10% buffered formalin before being processed and paraffin embedded for immunohistochemical analysis.

Immunohistochemistry

In order to assess the effect of lesioning/treatment on the number of dopaminergic cell bodies in the SNc, brain sections were stained for tyrosine hydroxylase, the rate-limiting enzyme in the dopamine synthetic pathway.

Immunohistochemical staining and analysis for this study was carried out at as described for the Compound 11 study in section 2.2.3.2.

Neurochemical analysis by HPLC

In order to assess the effect of lesioning/treatment on the dopamine content of the striatum, the left and right CPu were dissected out at necropsy and analysed by HPLC. Samples were removed from the -80°C freezer and placed on ice. 8 volumes of homogenisation buffer (0.4M perchloric acid, 1mM EDTA, 0.01% $Na_2S_2O_5$) and one volume of 10µM DHBA (internal standard) were added to each sample. Tissue samples were homogenised using a sonic homogeniser for around 5 seconds, then centrifuged at 14000 x g for 10 minutes at 4°C. Supernatant was aliquoted into HPLC vials and then frozen at -80°C to await analysis.

Before analysis, samples were thawed and placed in autosampler trays maintained at 9°C. Mobile phase (0.1M NaH_2PO_4, 1mM EDTA, 0.01% OSA, 12% MeOH, pH 3.2) was recycled at 0.8ml/min and 20µl sample volumes were injected down a Spherisorb ODS(2) 3µm particle size HPLC column (SpheriClone 0.46cm x 15cm; Phenomenex, UK) column maintained at 30°C. The run time for each sample and standard was 20 minutes, and electrochemical detection was performed by an Intro ECD (Antec) at a sensitivity of 50nA/V. An example chromatogram of a 1µM standard is shown in Figure 54.

Chromatograms were analysed using Chromeleon software (Dionex), which automatically assigns peaks and calculates their areas based on a user-defined analysis method. Peaks that were not recognised by the software were manually defined by drawing in a baseline. Sample concentrations were calculated from a linear standard curve constructed from a duplicated set of standards covering a range of 0.01-100µM, followed by correction for sample dilution.

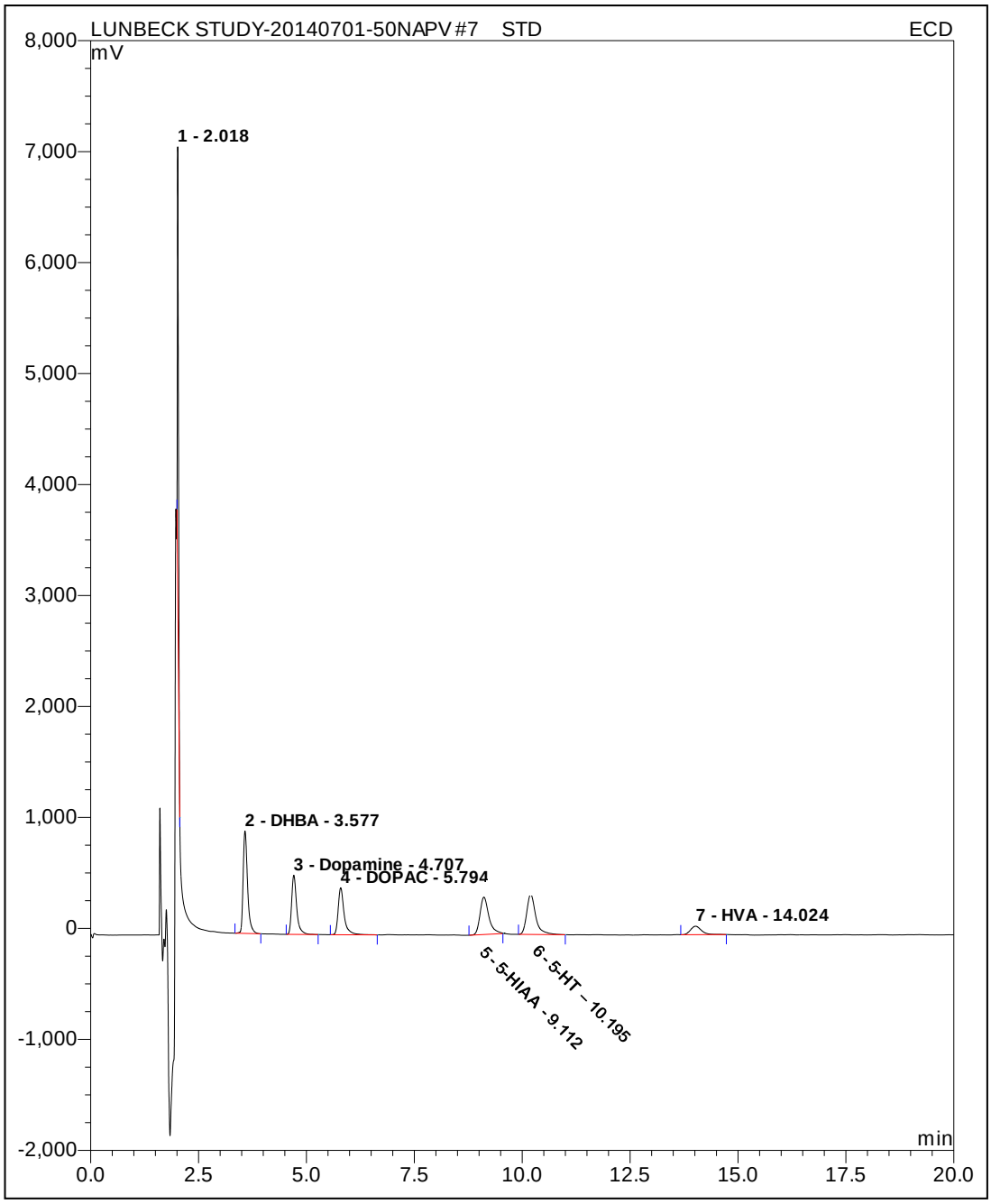

Figure 54: Example chromatogram from a 1µM standard. The standard contains the internal standard DHBA (peak 2), Dopamine (peak 3), DOPAC (peak 4) and HVA (peak 7). Peak areas were quantified and used to construct standard curves from which the analyte concentrations in the striatal homogenates could be calculated.

4.2.4.3 Behavioural assessment

Three behavioural tests were performed to assess the functional outcome of the lesioning and treatment: the cylinder test, the adjusted stepping test and amphetamine-induced rotational asymmetry. The days that these tests were performed are shown in the study

plan (Figure 53) and all behavioural testing was carried out between 10:30 and 13.30. These tests have been discussed in more detail in Chapter 2 (section 2.2.3.3).

4.2.4.4 Assessment of inflammation

At the end of the study an additional analysis was performed investigating inflammatory markers in the SNc of these rats by staining for the microglial marker Ionised calcium binding adaptor molecule 1 (Iba-1). This was done in order to investigate whether we could find evidence for similar anti-inflammatory effects as have been reported in a previous study targeting $mGlu_4$ (Betts *et al.*, 2012).

Nigral sections at -5.3mm and -5.8mm from bregma (adjacent to the sections stained for TH at these levels) were stained in triplicate for Iba-1. The immunohistochemistry protocol used was identical to that used for TH staining (section 2.2.3.2) except for two modifications: 1. The primary antibody used was a 1:2000 dilution of polyclonal rabbit anti-Iba-1 primary antibody and 2. The staining was developed in DAB for 25 minutes.

Due to the damage noted in the nigra close to the injection site (-5.3mm) only sections at -5.8mm were analysed. Slides were imaged at 25x magnification using the Zeiss Axioskop brightfield microscope. Analysis of staining density in the region of the SNc was carried out on greyscale images using Image J (freely available software developed by the National Institutes for Health). Staining density in the lesioned SNc was expressed as a percentage of the staining in the intact SNc.

4.2.4.5 Statistical analysis

Normally distributed data are reported as mean ± s.e.m and are presented as bar charts, where the bar height represents the mean and the error bars represent the s.e.m. Normally distributed data were analysed using t-tests or one-way or two-way ANOVAs.

Nonparametric data are presented as median ± interquartile range (IQR) and are presented as box and whisker plots, where the box represents the IQR, the line within the box represents the median and the whiskers represent the minimum and maximum values obtained. Nonparametric data were compared using Kruskal-Wallis tests with Dunn's *post-hoc* analysis.

Statistical analysis was carried out using GraphPad Prism version 5.

Neuroprotective outcomes: Neuroprotection was assessed at the level of the substantia nigra by comparing the cells remaining in the lesioned SNc as a percent of those remaining

in the intact SNc using a Kruskal-Wallis test with Dunn's *post-hoc* analysis. Where within-group comparisons on absolute cell counts are reported, a t-test was used.

The absolute concentrations of dopamine and its metabolites were compared between the intact and lesioned striatum within treatment groups using t-tests. For comparison between treatment groups the concentration of dopamine and its metabolites DOPAC and HVA in the lesioned striatum were expressed as percentages remaining (lesioned striatal concentration as a percent of intact striatal concentration) and compared where possible using a one-way ANOVA with Bonferroni *post-hoc* test.

Behavioural tests: The cylinder test was analysed using a 2-way repeated measures ANOVA with Bonferroni *post-hoc* analysis to assess the effects of both lesion and treatment on paw use. Adjusted steps and rotometry data and were analysed using a one-way ANOVA with a Bonferroni *post-hoc* to allow for comparison of treated groups with both the vehicle-treated group and the negative control group. Where pre- vs. post-lesion performance was compared within a group for the adjusted steps test, a paired t-test was used to compare the number of steps taken.

Inflammatory marker: The staining density in the lesioned SNc, as a percent of the staining density in the intact SNc, was compared between treatment groups using a one-way ANOVA with Bonferroni *post-hoc* test.

For all tests, the outcome was considered significant where $P<0.05$.

4.3 Results

4.3.1 LuAF21934 PK studies

PK-A: The plasma time course following oral administration of 10mg/kg or 30mg/kg LuAF21934 is shown in Figure 55.

Plasma C_{max} for 10mg/kg LuAF21934 was 869 ± 202ng/ml, achieved 1 hour after dosing with a $t_{½}$ of 1.4 ±0.13 hours.

Plasma C_{max} for 30mg/kg LuAF21934 was 4733 ± 758ng/ml, achieved 1 hour after dosing with a $t_{½}$ of 0.8 ± 0.10 hours.

These data were used to inform the twice-daily dosing regimen that was adopted in the neuroprotection study.

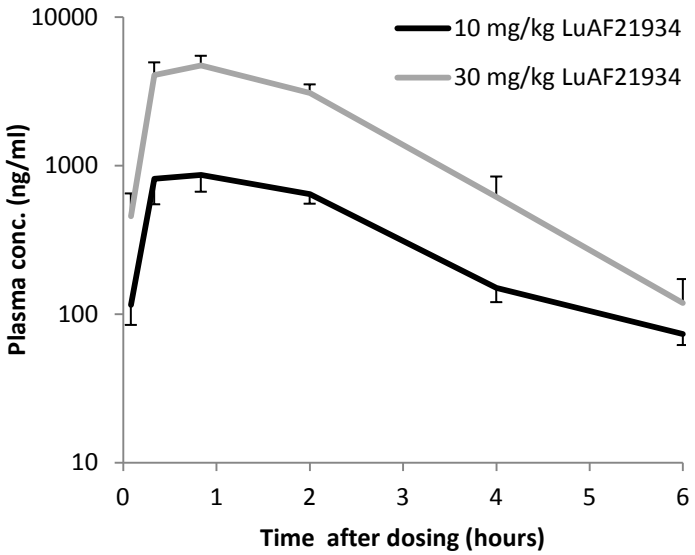

Figure 55: Time course of plasma concentration of LuAF21934. Naive male SD rats were given an oral dose of 10mg/kg or 30mg/kg LuAF21934 in 5ml/kg PEG-400 and serial blood samples collected and analysed by UPLC-MS/MS. Data are shown as mean ± s.e.m. (n = 3 per dose).

PK-B: Brain and plasma samples were analysed at 1 hour and 2 hours following an acute oral dose of 30 mg/kg LuAF21934.

At 1 hour, the plasma concentration of LuAF21934 was 6060 ± 721ng/ml and the brain concentration was 3963 ± 585ng/g, giving a brain/plasma ratio of 0.65. The plasma concentration at this time point is comparable with plasma C_{max} collected for this dose in PK-A (P=0.2737; t-test).

At 2 hours, the plasma concentration of LuAF21934 was 5537 ± 591ng/ml and the brain concentration was 3710 ± 98ng/g, giving a brain/plasma ratio of 0.67. The plasma concentration at this time point is significantly higher than that collected for this dose in PK-A of 3093ng/ml (P=0.0288; t-test) but since the numbers of animals used in each study was low this is likely due to normal variability.

4.3.2 LuAF21934 Neuroprotection study

4.3.2.1 General observations

All rats were included in the analysis, therefore for all groups n=8.

No acute- or sub-chronic adverse effects of dosing with vehicle, LuAF21934 or the negative control compound LuAF21935 were noted on animal health or wellbeing.

4.3.2.2 LuAF21934 did not protect against nigrostriatal degeneration

TH-positive cells in the SNc

There was no significant difference between cell counts at the three levels of the SNc that were analysed (P=0.1249; one-way RM ANOVA with Bonferroni *post-hoc*), therefore the data have been pooled.

The cell counts and corresponding percentage survival in the lesioned SNc compared with the intact SNc are shown in Figure 56 along with representative images from each group. Vehicle-treated rats retained 0.4 ± 0.5 TH-positive cells in the lesioned SNc compared with 109.5 ± 10.2 in the intact SNc, a significant reduction (P<0.0001; t-test) equating to 0.36 ± 0.42% survival.

Rats treated with LuAF21934 retained on average 0.16 ± 0.37% TH-positive cells in the 10mg/kg group and 0.32 ± 0.52% TH-positive cells in the 30mg/kg group. Rats treated with 30mg/kg LuAF21935, the negative control (hereafter referred to as Neg Ctrl), retained 0.34 ± 0.24% TH-positive cells. There were no significant differences between groups regarding the percent of cells remaining (P=0.5578; Kruskal-Wallis test with Dunn's *post-hoc*).

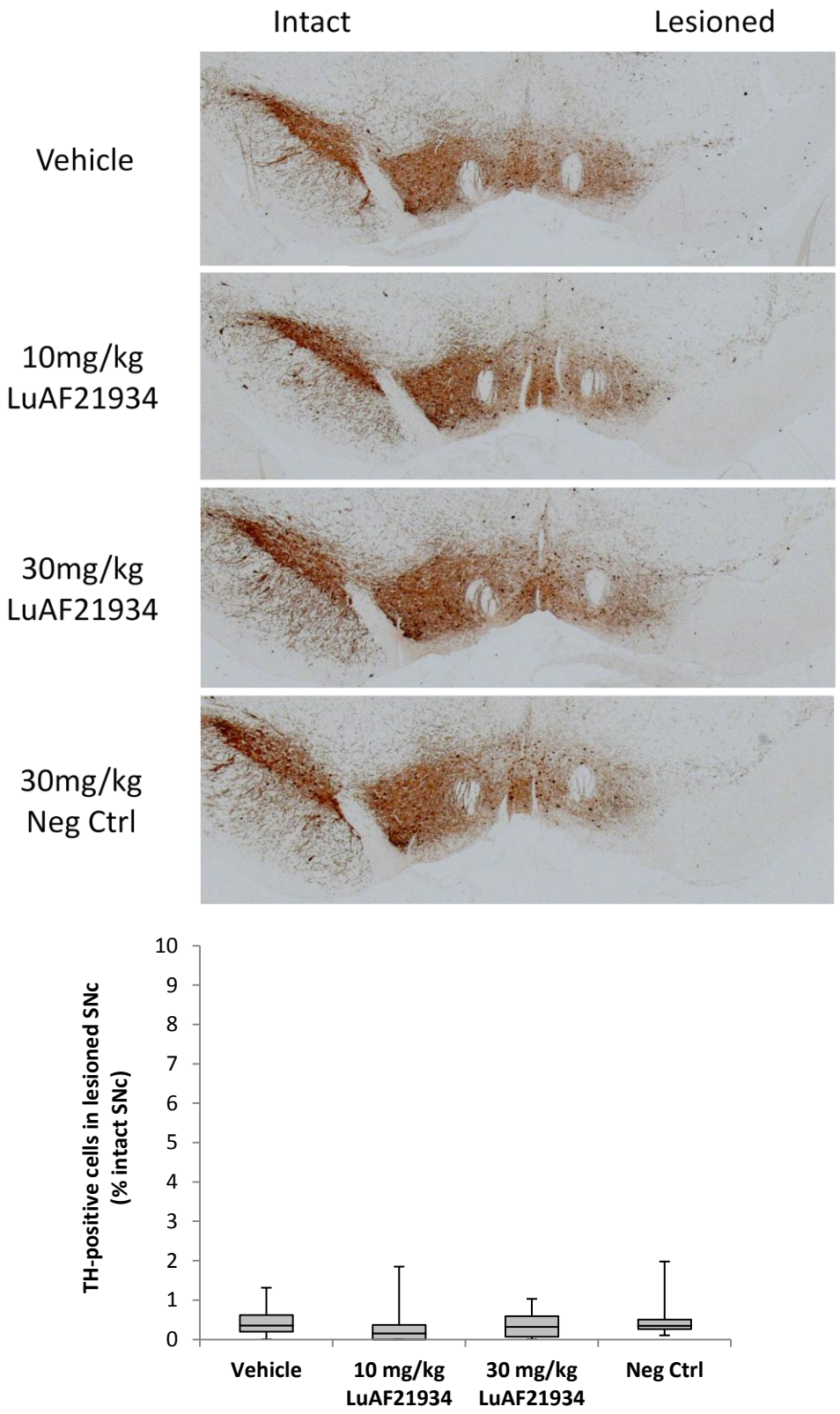

Figure 56: TH-positive cells remaining in the SNc following a 6-OHDA nigral lesion and treatment with vehicle, LuAF21934 or a negative control. Representative images for each treatment group are shown in the upper panels, and the TH-positive cells remaining in the lesioned SNc as a percent of the TH-positive cells in the intact SNc is shown in the graph below the images. There was no effect of treatment on the survival of TH-positive cells in the SNc. Data are presented as median ± IQR (n = 8 per group).

Striatal dopamine content

Striatal dopamine, DOPAC and HVA concentrations in the intact and lesioned striatum are summarised in Table 10.

Table 10: Striatal concentrations of dopamine and its metabolites in the intact and lesioned striatum following a 6-OHDA nigral lesion and treatment with vehicle, LuAF21934 or a negative control. Data reported are mean concentrations in µM (n = 8) ***P<0.001 (t-test versus intact). ND = not detected

	Dopamine		DOPAC		HVA	
	Intact	**Lesioned**	**Intact**	**Lesioned**	**Intact**	**Lesioned**
Vehicle	93.38	0.32***	6.35	0.07***	3.30	ND
10 mg/kg LuAF21934	97.76	0.26***	6.65	0.04***	3.33	ND
30 mg/kg LuAF21934	91.60	0.27***	6.76	0.09***	3.53	ND
Neg Ctrl	98.75	0.35***	6.58	0.07***	3.41	ND

Striatal dopamine content was decreased in vehicle-treated rats from 93.4µM in the intact striatum to 0.32µM in the lesioned striatum (P<0.0001; t-test), meaning that the lesion caused a reduction to 0.37 ± 0.07% of normal levels (Figure 57). DOPAC and HVA were similarly reduced in the lesioned striatum, to 0.65 ± 0.23% and 0.00 ± 0.00% of the intact striatal concentrations respectively (HVA was not detected in any lesioned striatal samples).

Rats treated with LuAF21934 retained on average 0.28 ± 0.05% striatal dopamine in the 10mg/kg group and 0.30 ± 0.04% in the 30mg/kg group. Rats treated with Neg Ctrl retained 0.35 ± 0.07% dopamine. There was no effect of treatment on percent striatal dopamine remaining (P=0.6986; one-way ANOVA with Bonferroni *post-hoc*).

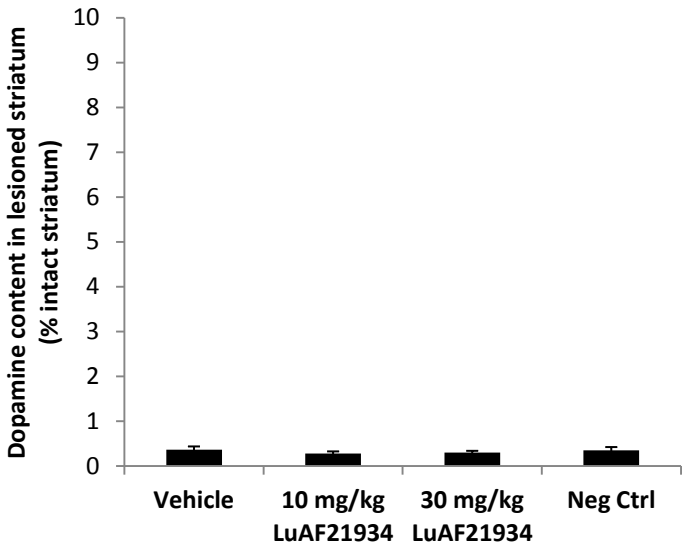

Figure 57: Dopamine content in the lesioned striatum following a 6-OHDA nigral lesion and treatment with vehicle, LuAF21934 or a negative control. Unilateral nigral infusion of 6-OHDA severely depleted dopamine in the ipsilateral striatum, such that less than 1% remained compared with the concentration measured in the intact striatum. Sub-chronic treatment with LuAF21934 or Neg Ctrl had no effect on striatal dopamine content. Data are presented as mean ± s.e.m. (n = 8 per group).

Similarly there was no effect of treatment on the DOPAC remaining in the lesioned striatum as a % of the intact striatum (P=0.3598; one-way ANOVA with Bonferroni *post-hoc*). HVA could not be compared between groups as it was not detected in any lesioned striatum.

Dopamine turnover, normally calculated as (DOPAC+HVA)/DA could therefore not be calculated, and even an alternative measure of DOPAC/DA could only be calculated for 14 of the 32 rats due to non-detectable peaks for DOPAC, therefore this parameter was not reported.

4.3.2.3 LuAF21934 did not preserve functional outcomes

Cylinder test

The cylinder test baseline was the pooled result of two pre-lesion tests, and can be seen in Figure 58. There was no significant differences between groups at baseline regarding use of the ipsilateral or contralateral forelimb (P=0.2923; one-way ANOVA with Bonferroni *post-hoc*).

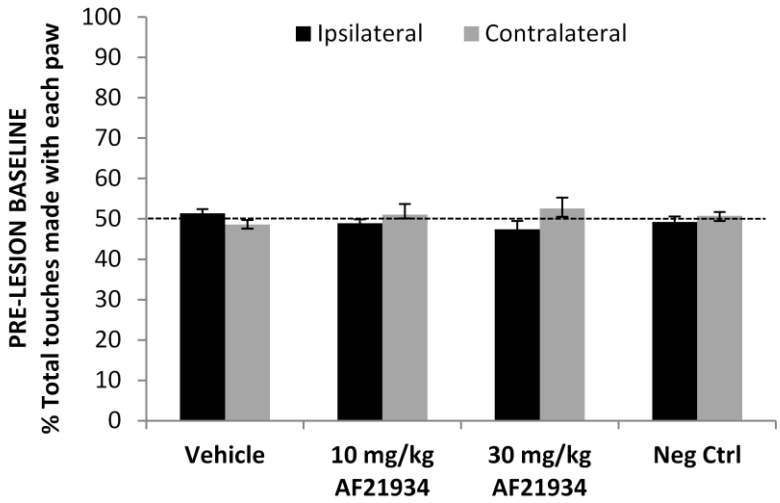

Figure 58: Baseline use of the ipsilateral and contralateral forelimbs during the cylinder test. All groups showed around equal use of each paw before dosing and lesioning, with no significant differences between groups. The dashed line shows the expected use of each paw in intact rats. Data are presented as mean ± s.e.m. (n = 8 per group).

Percent use of the contralateral forelimb in the cylinder test was reduced post-lesion in the vehicle group, from 49 ± 1% at baseline to 6.4 ± 2.2% on day 6, 8.4 ± 3.3% on day 10 and 8.3 ± 3.0% on day 14 (all P<0.0001; two-way RM ANOVAs with Bonferroni *post-hoc* tests), showing that the lesion caused a measurable and sustained deficit (Figure 59).

Day 6 (Figure 59a): Rats treated with 10mg/kg LuAF21934 used the contralateral limb in 6.0 ± 2.1% of touches and those treated with 30mg/kg LuAF21934 in 5.1 ± 1.9% of touches. Rats treated with Neg Ctrl used the contralateral limb for 5.3 ± 2.6% of touches. Compared with baseline there was a significant effect of lesion (P<0.0001) but not treatment group (P=0.8561; two-way RM ANOVA with Bonferroni *post-hoc*) at this time point.

Day 10 (Figure 59b): Rats treated with 10mg/kg LuAF21934 used the contralateral limb in 8.1 ± 2.8% of touches and those treated with 30mg/kg LuAF21934 in 3.6 ± 1.3% of touches. Rats treated with Neg Ctrl used the contralateral limb for 6.6 ± 2.6% of touches. Compared

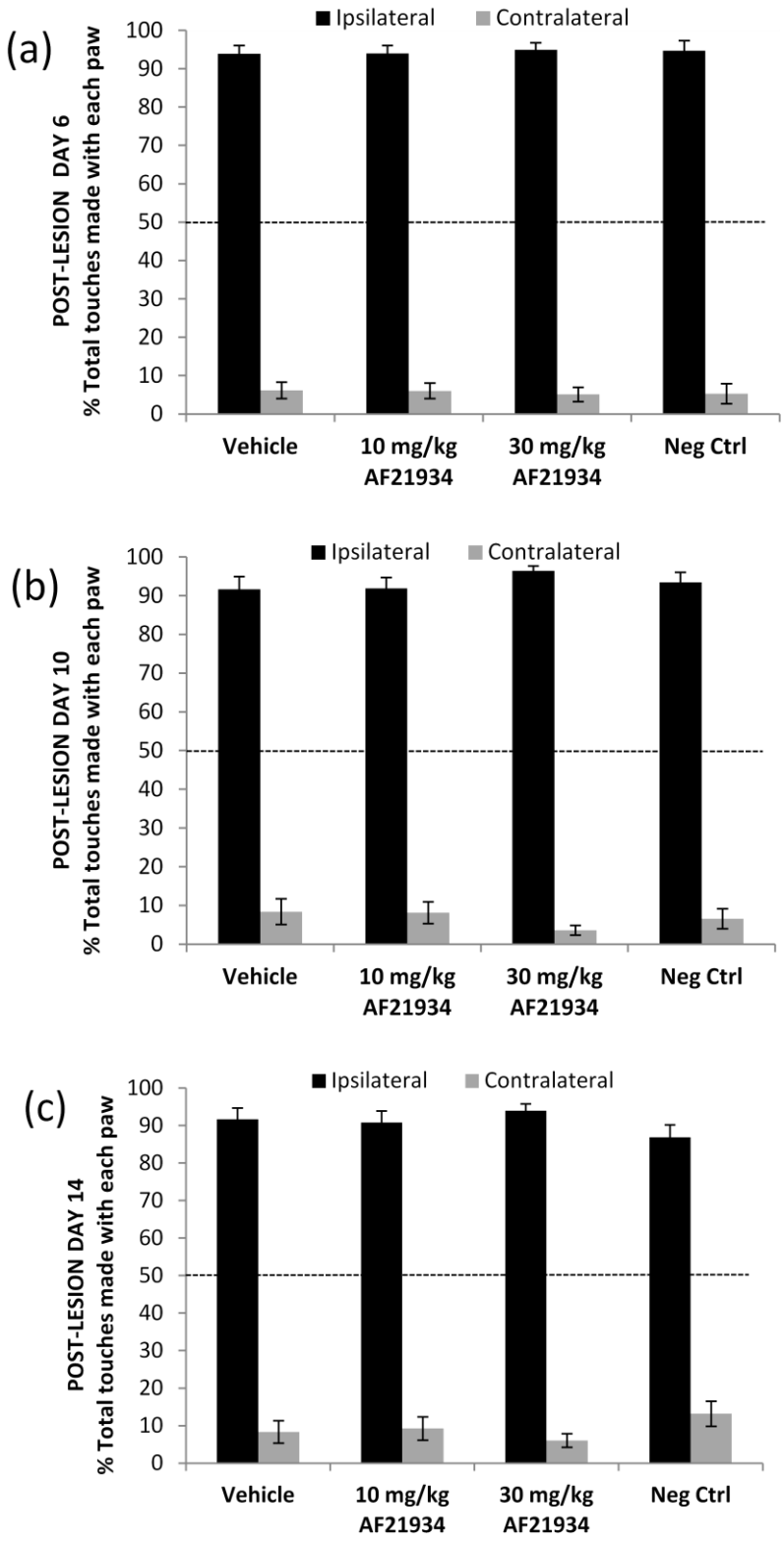

Figure 59: Use of the ipsilateral and contralateral forelimbs during the cylinder test following a nigral 6-OHDA lesion and sub-chronic treatment with vehicle, LuAF21934 or a negative control. The dashed line shows the expected use of each paw in intact rats. All groups showed a similar post-lesion bias towards use of the ipsilateral paw. There was a significant effect of lesion for all groups on all testing days, but no significant effect of treatment at day 6, 10 or 14 post-lesion. Data are presented as mean ± s.e.m. (n = 8 per group).

with baseline there was a significant effect of lesion (P<0.0001) but not treatment group (P=0.9085; two-way RM ANOVA with Bonferroni *post-hoc*) at this time point.

Day 14 (Figure 59c): Rats treated with 10mg/kg LuAF21934 used the contralateral limb in 9.2 ± 3.1% of touches and those treated with 30mg/kg LuAF21934 in 6.1 ± 1.8% of touches. Rats treated with Neg Ctrl used the contralateral limb for 13.2 ± 3.4% of touches. Compared with baseline there was a significant effect of lesion (P<0.0001) but not treatment group (P=0.4500; two-way RM ANOVA with Bonferroni *post-hoc*) at this time point.

Adjusted steps test

The adjusted steps test baseline was the pooled result of two pre-lesion tests, and the post-lesion steps taken on each testing day is expressed as a percentage of this baseline (Figure 60).

As would be expected with a unilateral lesion, there was no deficit detected in the ipsilateral paw in the vehicle-treated group at any time point, with performance >98.8% baseline in the forward direction (P>0.1604; paired t-tests on no. of steps) and >99.8% in the reverse direction (P>0.4957; paired t-tests on no. of steps). There was also no significant effect of treatment with LuAF21934 or negative control on the post-lesion percent performance of the ipsilateral paw, which was unaffected in both the forward (P>0.5126; one-way ANOVAs with Bonferroni *post-hoc* tests) and reverse (P>0.4169; one-way ANOVAs with Bonferroni *post-hoc* tests) directions for every test session.

On the other hand, 6-OHDA lesioning caused a clear deficit in contralateral paw use. Vehicle-treated rats had an average forward-stepping contralateral performance of 50.5 ± 2.0% of baseline on day 6, 53.2 ± 1.2% baseline on day 10 and 52.0±1.5% baseline on day 14 (all P<0.0001; paired t-tests). The average reverse-stepping contralateral performance in this group was reduced to 67.1 ± 1.7% baseline on day 6, 69.5 ± 1.6% of baseline on day 10 and 68.2 ± 1.1% baseline on day 14 (all P<0.0001; paired t-tests).

Day 6 (Figure 60a): The 10mg/kg LuAF21934 group had a forward-stepping contralateral performance of 50.4 ± 4.0% baseline, the 30mg/kg LuAF21934 group performance was 56.7 ± 1.7% baseline and rats treated with Neg Ctrl made 54.4 ± 1.6% baseline steps. There was no significant effect of treatment on contralateral forward-stepping performance (P=0.2468, one-way ANOVA with Bonferroni *post-hoc*).

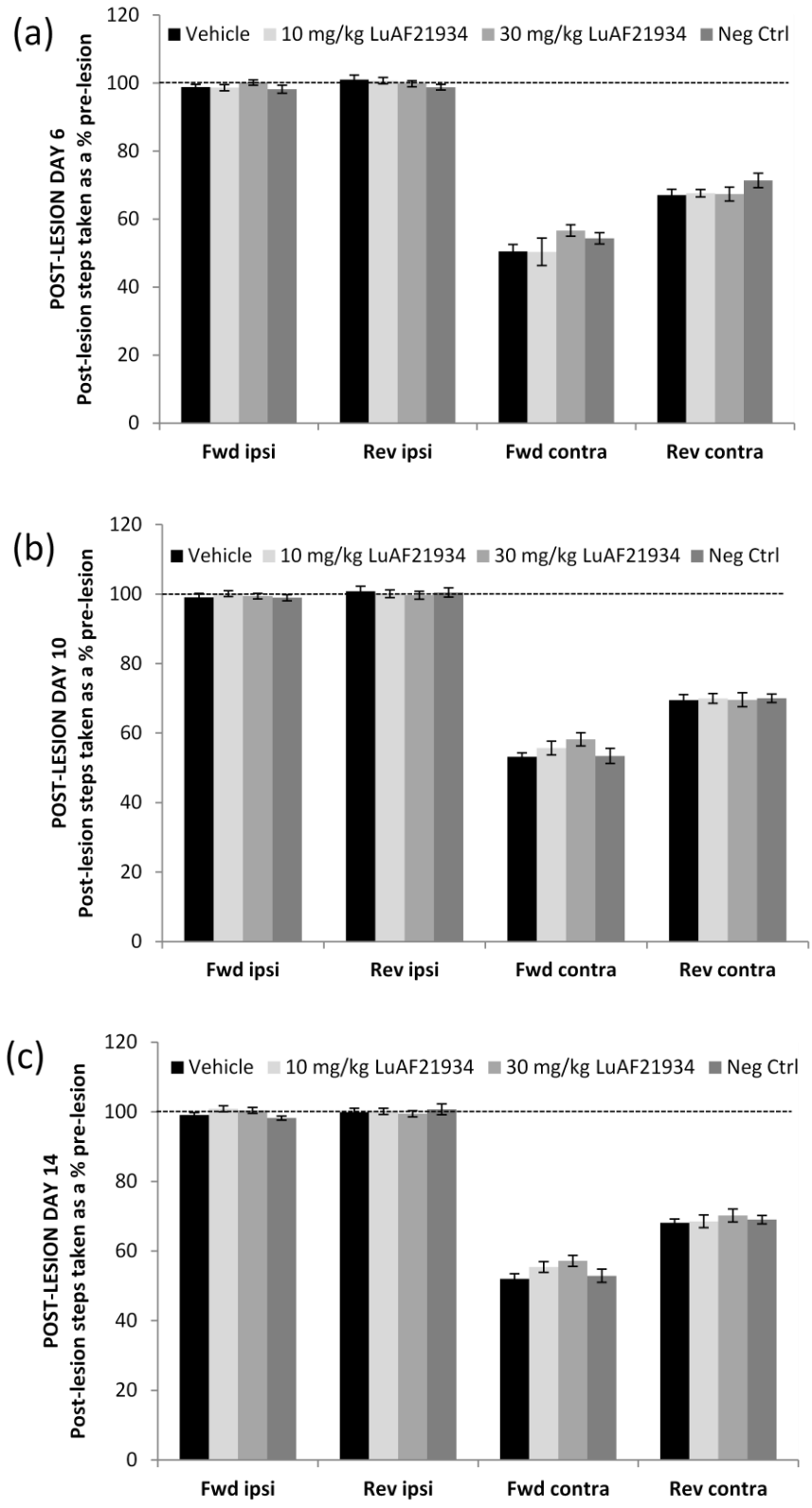

Figure 60: Adjusted stepping test performance following a nigral 6-OHDA lesion and sub-chronic treatment with vehicle, LuAF21934 or a negative control. The dashed line shows the expected performance in intact rats (100% baseline). There was no significant effect of treatment on use of the contralateral paw in either direction at day 6, 10 or 14 post-lesion. Data are presented as mean ± s.e.m. (n = 8 per group). Fwd = forward direction; Rev = reverse direction; Ipsi = ipsilateral forelimb; Contra = contralateral forelimb.

Contralateral reverse-stepping showed a similar pattern, with the 10mg/kg LuAF21934 group at 67.6 ± 1.1% baseline, the 30mg/kg LuAF21934 group at 67.4 ± 2.0% baseline and the Neg Ctrl group at 71.4 ± 2.1% baseline. There was no significant effect of treatment on contralateral reverse-stepping performance (P=0.2946, one-way ANOVA with Bonferroni *post-hoc*).

Day 10 (Figure 60b): The 10mg/kg LuAF21934 group had a forward-stepping contralateral performance of 55.7 ± 0.0% baseline, the 30mg/kg LuAF21934 group performance was 58.2 ± 1.9% baseline and rats treated with Neg Ctrl made 53.4 ± 2.2% baseline steps. There was no significant effect of treatment on contralateral forward-stepping performance (P=0.2188, one-way ANOVA with Bonferroni *post-hoc*).

Contralateral reverse-stepping showed a similar pattern, with the 10mg/kg LuAF21934 group at 70.0 ± 1.5% baseline, the 30mg/kg LuAF21934 group at 69.6 ± 2.1% baseline and the Neg Ctrl group at 70.0 ± 1.2% baseline. There was no significant effect of treatment on contralateral reverse-stepping performance (P=0.9938, one-way ANOVA with Bonferroni *post-hoc*).

Day 14 (Figure 60c): The 10mg/kg LuAF21934 group had a forward-stepping contralateral performance of 55.4 ± 1.5% baseline, the 30mg/kg LuAF21934 group performance was 57.2 ± 1.6% baseline and rats treated with Neg Ctrl made 52.9 ± 1.9% baseline steps. There was no significant effect of treatment on contralateral forward-stepping performance (P=0.1189, one-way ANOVA with Bonferroni *post-hoc*).

Contralateral reverse-stepping showed a similar pattern, with the 10mg/kg LuAF21934 group at 68.5 ± 1.8% baseline, the 30mg/kg LuAF21934 group at 70.2 ± 1.9% baseline and the Neg Ctrl group at 69.0 ± 1.2% baseline. There was no significant effect of treatment on contralateral reverse-stepping performance (P=0.8008, one-way ANOVA with Bonferroni *post-hoc*).

Amphetamine-induced rotational asymmetry

The time-course and overall net ipsiversive rotations in response to 2.5mg/kg amphetamine are shown in Figure 61.

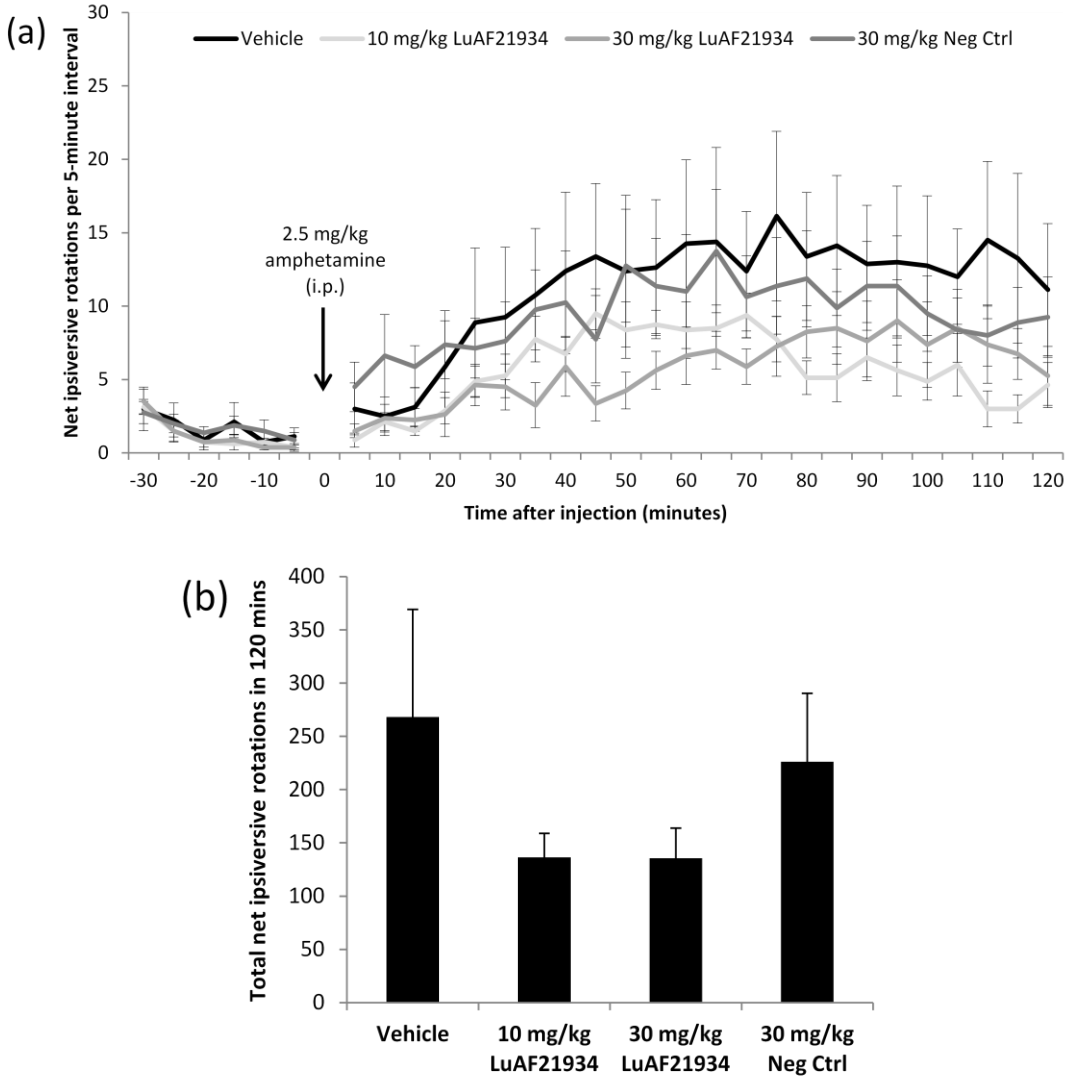

Figure 61: Amphetamine-induced rotational asymmetry in rats with a 6-OHDA nigral lesion treated sub-chronically with vehicle, LuAF21934 or a negative control. The time course of rotations is shown in graph (a) and the total net number of full ipsiversive rotations over 120 minutes is shown in graph (b). Despite a trend towards a reduction in rotational asymmetry in LuAF21934-treated rats there was no significant effect of treatment on net rotational asymmetry. Data are presented as mean ± s.e.m. (n = 8 per group).

Vehicle-treated animals displayed a net ipsiversive rotational asymmetry over 90 minutes of 268 ± 101 turns (Figure 61b). Rats treated with 10mg/kg LuAF21934 had a reduced net asymmetry of 137 ± 22 turns, and a similar reduction was seen in the 30mg/kg LuAF21934-treated group, which made 136 ± 28 turns in the same time. Rats treated with Neg Ctrl

displayed a similar rotational response to the vehicle-treated group, making 226 ± 64 turns in 90 minutes. Despite the reduced turning in the LuAF21934-treated groups, when all groups were compared there was no significant effect of treatment on total net rotational asymmetry over the time tested (P=0.3534; one-way ANOVA with Bonferroni *post-hoc*).

4.3.2.4 LuAF21934 did not reduce microglial activation in the lesioned SNc

Iba-1 is a marker of microglial activation. Previous reports have suggested a role for $mGlu_4$ activation in attenuating inflammation, and this might potentially play a role in neuroprotection. Due to the physical damage that was encountered at the -5.3mm level (see Discussion), Iba-1 staining was only assessed at -5.8mm from bregma. Two rats from the 30mg/kg LuAF21934 and one rat from the Neg Ctrl group were excluded from analysis as a moderate to high degree of physical damage was still evident at this level in these animals.

The results of the Iba-1 staining are shown in Figure 62. The images in the upper panels show representative images to compare the Iba-1 staining in vehicle-treated and 30mg/kg LuAF21934-treated groups. The graph below shows these results as the staining density in the lesioned SNc expressed as a percentage of the staining density in the intact SNc. Vehicle-treated rats showed a slight increase in Iba-1 staining in the lesioned SNc, equivalent to 109 ± 1% that in the intact SNc. Similar results were found in LuAF21934-treated groups, where the 10mg/kg group showed 109 ± 1% staining and the 30mg/kg group showed 109 ± 2% staining. Negative control-treated rats also showed a comparable degree of increased inflammation, with 111 ± 2% staining in the lesioned SNc. There was no significant effect of treatment on microglial activation as assessed by Iba-1 immunohistochemistry (P=0.7079; one-way ANOVA with Bonferroni *post-hoc* test).

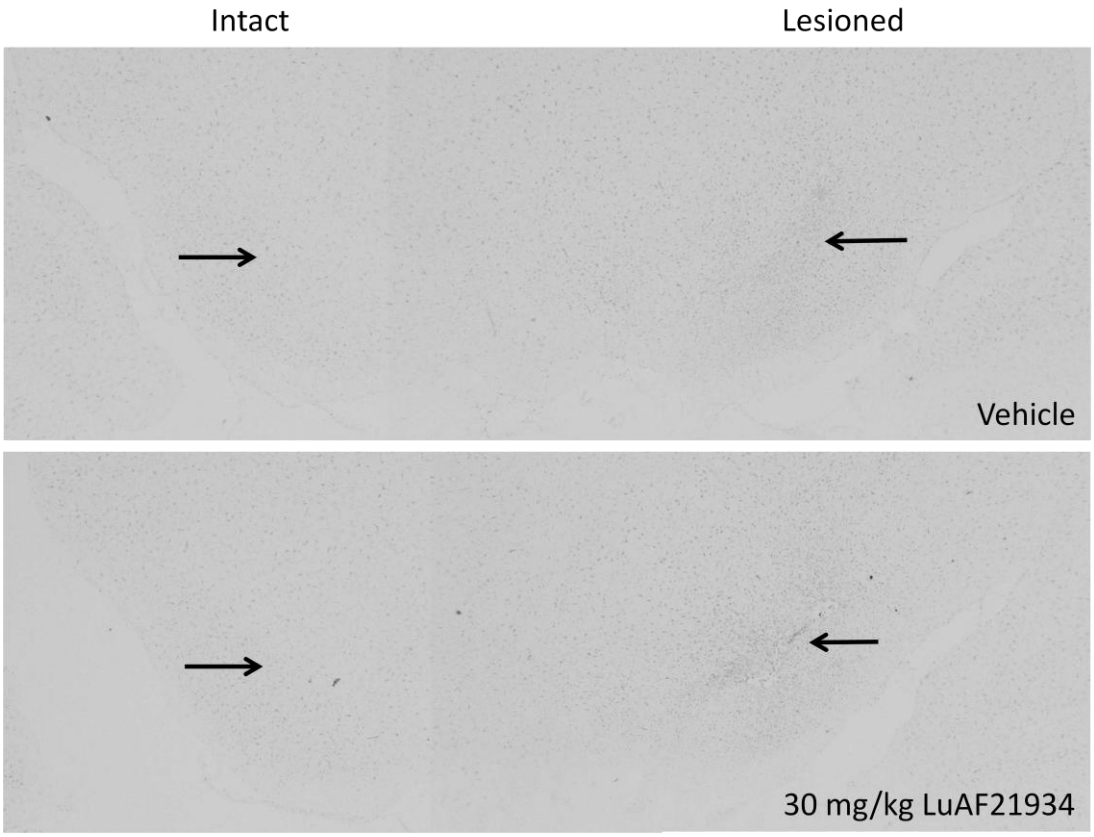

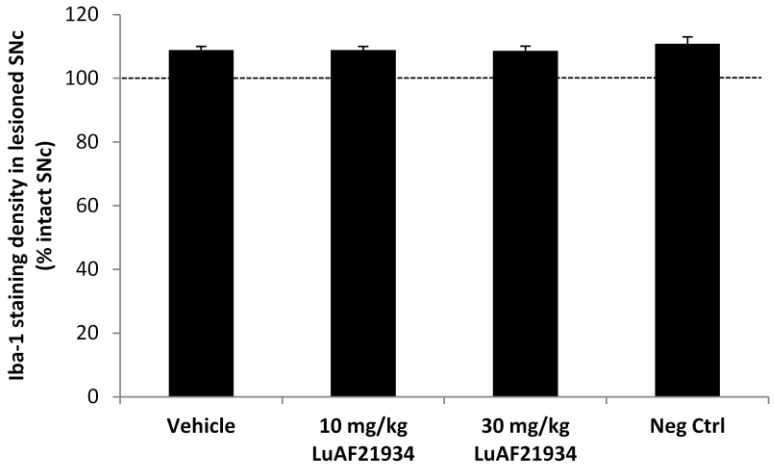

Figure 62: Iba-1 staining density at -5.8mm from bregma in rats with a 6-OHDA nigral lesion treated sub-chronically with vehicle, LuAF21934 or a negative control. The top panels show the degree of Iba-1 staining in the SNc at -5.8mm from bregma. The arrows denote the location of the SNc. The graph below the images shows the Iba-1 staining in the lesioned SNc as a percent of that in the intact SNc following densitometric quantification. The dashed line shows the staining density in the intact SNc, which was defined at 100%. Microglial activation was slightly increased in the lesioned SNc compared with the intact SNc in all groups, but there was no effect of treatment on staining for this inflammatory marker (n = 6-8).

4.4 Discussion

This study sought to identify whether systemic administration of the $mGlu_4$ PAM LuAF21934 could provide neuroprotection in the 6-OHDA rat model of Parkinson's disease.

4.4.1 PK studies

From the PK study we have a good idea of the brain concentrations that were achieved during LuAF21934 dosing. The plasma profile obtained in PK-A led us to dose twice a day with this compound rather than the once-daily used in previous studies where drug was applied intracerebrally, resulting in improved drug exposure during the treatment period while the lesion was developing. In addition, the specific drug concentrations in the plasma and brain were analysed at 1-hour and 2-hour time points after dosing, revealing in a brain/plasma ratio of 0.66, which is in line with previous in-house data from Lundbeck. The 1-hour time point is particularly critical as it reflects the brain concentration at the time of 6-OHDA infusion. The brain concentration at 1 hour was 3963 ± 585ng/g, equivalent to 12.6µM, of which 3% is believed to be unbound in the rat brain (Bennouar *et al.*, 2013). This means that LuAF21934 was present in the brain at a free concentration of around 119ng/g at 1 hour after the highest dose that was used in these studies, which at ~0.38µM is a little below its EC_{50} concentration at $mGlu_4$ (0.5µM). However EC_{50} concentrations are measured *in vitro* and the translatability of potencies between *in vitro* and *in vivo* systems is likely to be imperfect. Certainly the total brain concentration of LuAF21934 measured in PK-B 1 hour after dosing of 30mg/kg LuAF21934 is in the range where pharmacological effects have been noted in other *in vivo* experiments (e.g. haloperidol-induced catalepsy; Bennouar *et al.*, 2013) and therefore it is likely that the maximum brain concentrations that will have been achieved following oral administration of LuAF21934 in the neuroprotection study were sufficient to activate $mGlu_4$ receptors in the BG in this neuroprotection study.

4.4.2 Neuroprotection study

Even with good brain levels achieved, this study did not provide any evidence of LuAF21934 eliciting neuroprotection in this model. This was reflected in the lack of any preservation of motor function as measured by the cylinder test, adjusted steps test or amphetamine-induced rotations. In addition we found no evidence for decreased inflammation following treatment with LuAF21934, however the degree of inflammation overall was extremely low, ~10% increased in the lesioned SNc compared with the intact SNc in this study compared with a 300% increase in a study where the $mGlu_4$ PAM/vehicle were delivered

supranigrally (Betts *et al.*, 2012). It is possible that measuring inflammatory markers 2 weeks after an acute nigral lesion misses the majority of the inflammatory response, since cell loss is usually complete within the first week (Hanrott *et al.*, 2008; Maler *et al.*, 1973). Significant increases in activation of microglia have previously been reported for up to 3 week following lesioning of the MFB or striatum (Maia *et al.*, 2012; Marinova-Mutafchieva *et al.*, 2009; Walsh *et al.*, 2011), however similar experiments have not been reported following nigral infusion of 6-OHDA and it could be that the more rapid completion of the lesion after nigral lesioning compared with MFB or striatal lesioning leads to an earlier abatement of the acute inflammatory response.

The repeat behavioural testing, both during and after the treatment period, was carried out in order to detect both short term (acute pharmacological) and long term (likely neuroprotective) effects of LuAF21934 in this model. The behavioural testing on day 6 was carried out 3 hours after dosing, when according to PK-A we might expect plasma concentrations of up to 1854ng/ml; therefore any improvement in behaviour at this time point could reflect a combination of acute pharmacological benefits and neuroprotective benefits. The fact that no effects of treatment group were found at the day 6 behavioural time point suggests that 3 hours after dosing LuAF21934 does not exert a pharmacological effect that results in a measurable change in limb use bias or function in the cylinder test or adjusted steps test. On the other hand the behavioural testing on days 10 and 14 was carried out between 3 and 7 days after the last dose of LuAF21934, when the drug is no longer present in the brain; therefore any improvement in behaviour at these time points would be expected to reflect neuroprotective effects of this $mGlu_4$ PAM, where preservation of neurones results in improved motor function. The lack of an effect of sub-chronic LuAF21934 treatment on behavioural tests at these later time points clearly suggested that LuAF21934 had not had a neuroprotective effect, and this negative outcome was indeed confirmed *post mortem* by analysis of TH-positive cells and striatal dopamine content.

4.4.3 Possible reasons for the lack of neuroprotection

One possible explanation for the lack of a neuroprotective effect in this model is that physical damage to the SNc was noted in the vicinity of the 6-OHDA injection site when immunohistochemical staining was performed. The degree of damage varied from none to severe and was importantly equally distributed between groups. In some cases the physical damage merely reflected the penetrance of the tip of the injection needle into the SNc and was therefore minimal, however in several rats it was more widespread and included loss

of tissue in a diffuse area around the injection site. This would mean that for neuroprotection to have occurred in this study, LuAF21934 would not only have had to counteract the toxic effects of the 6-OHDA but also, in a number of rats, the physical damage caused by the injection process, which perhaps underlies the lack of a protective effect noted in the study reported here. The varying degree of damage in rats that were lesioned on the same day does not support a definite physically damaging effect of the toxin solution itself (e.g. osmotic damage), and indeed the same batch of 6-OHDA and ascorbate have been used in multiple previous studies without such an effect being noted. The presence/extent of physical damage is also roughly equal between groups, suggesting that it is not related to LuAF21934 or LuAF21935 administration. However for unknown reasons the same toxin solution and same injection conditions (needle diameter, flow rate etc.) caused more widespread damage in some rats than others. Certainly the presence of this damage could have confounded any neuroprotective properties of LuAF21934; nonetheless the degree of TH-positive cell loss was comparable in all rats regardless of the presence and degree of physical damage that was noted in the SNc so other factors likely played a role in the failure of LuAF21934 to provide neuroprotection in this experiment.

In addition to the physical damage, the severity of the lesion induced by nigral infusion of a large dose of 6-OHDA is likely difficult to overcome due to the rapid induction of widespread cell death. The administration of LuAF21934 prior to the lesion gave us the best chance to have the drug in the correct place at the correct time to maximise the chances of a protective effect, however this is not a clinically relevant scenario and also proved unsuccessful in this study anyhow. A repeat of this study is warranted and several improvements to the study design could be made to improve the chances of a neuroprotective effect, for example using a partial rather than a full lesion model and inducing a nigrostriatal lesion without damaging areas that will be subsequently analysed. A partial lesion that leads to around 60% loss of striatal dopamine would more accurately reflect the clinical situation, since patients present with motor symptoms when their dopamine is depleted by around this amount. This could be achieved by using lower doses of 6-OHDA that are infused into the nigrostriatal tract outwith the SNc such as into the MFB or striatum (Datla *et al.*, 2001; Kirik *et al.*, 1998; Li *et al.*, 2010b; Murray *et al.*, 2003a; Przedborski *et al.*, 1995; Truong *et al.*, 2006); this would not only reduce the severity of the lesion (giving the LuAF21934 something to actually protect) but would also remove the confounding influence of physical damage from the infusion of the toxin directly into the site of analysis. Alternatively, a partial lesion induced by systemic administration of MPTP

would be ideal, since it causes incomplete loss of dopaminergic neurones and obviates any physical damage that may be caused by direct infusion of neurotoxin into the nigrostriatal tract. Indeed the MPTP mouse model has already been used to demonstrate the neuroprotective effect of systemic administration of another $mGlu_4$ PAM, PHCCC (Battaglia *et al.*, 2006).

Aside from the effects of the physical damage and the size of the lesion, other factors might explain the lack of neuroprotection in this experiment. One possibility is that activation of $mGlu_4$ receptors throughout the basal ganglia, as would be expected following systemic administration, rather than selectively in the SNc following local administration as in previous studies, could have resulted in the effects at individual synapses cancelling each other out. This would mean that there would be no net effect on signalling in the relevant regions of the BG for neuroprotection (i.e. the subthalamonigral projection) and/or no net change in the BG and therefore motor output. Considering the localisation of $mGlu_4$ within the rodent BG, inhibition of GABA release from striatonigral neurones could lead to inhibition of signalling in the direct pathway that might counteract the effects of $mGlu_4$ at inhibiting signalling in the indirect pathway (acting at the striatopallidal and/or subthalamonigral projections). However this possibility might only be expected to inhibit symptomatic relief rather than neuroprotection, and additionally it is at odds with the wealth of published reports showing that systemic or i.c.v. administration of $mGlu_4$-targeted therapies has an antiparkinsonian and/or neuroprotective effect (Battaglia *et al.*, 2006; Bennouar *et al.*, 2013; Beurrier *et al.*, 2009; East *et al.*, 2010; Jones *et al.*, 2012; Le Poul *et al.*, 2012; Marino *et al.*, 2003; Niswender *et al.*, 2008b). Inhibition of signalling at all other synapses within the BG where $mGlu_4$ has been localised would be expected to reduce subthalamonigral output, however it is possible that the effects of activation of $mGlu_4$ in brain regions outside the BG may also influence activity in this region and this could explain the lack of a protective effect when $mGlu_4$ PAMs are administered systemically versus supranigrally.

Another possibility is that LuAF21934 was not present at sufficient concentrations to activate $mGlu_4$ receptors and therefore did not inhibit signalling at the desired synapses. We are confident from the PK studies reported in this chapter that the brain drug concentrations achieved at 1 hour after dosing were adequate to have a pharmacological effect. However, the lack of behavioural benefits observed 3 hours after dosing of LuAF21934 on day 6 might suggest that by this time after dosing there was insufficient drug

present to exert these effects. While previous studies in this model have shown successful neuroprotection with once-daily local administration for some compounds targeting group III or $mGlu_4$ receptors (VU0155041 study in Chapter 2 and also Austin *et al.*, 2010; Betts *et al.*, 2012; Vernon *et al.*, 2005; Vernon *et al.*, 2006), this dosing regimen has proved unsuccessful for other $mGlu_4$ PAMs, for example Compound 11 (Chapter 2). Therefore these 'gaps' in exposure between doses might underlie the lack of a protective effect of LuAF21934 in this study. In a repeat study, the dosing regimen could be improved further to maximise and stabilise exposure to LuAF21934 during the lesion development period. In this study we dosed twice daily, which likely improved drug exposure during lesion development compared with earlier studies where $mGlu_4$ PAMs were administered only once a day, but given the ~1 hour half life of the drug this still would not have provided complete coverage. In future studies the use of continuous dosing via minipumps might be considered to overcome this problem, especially since LuAF21934 is soluble in a non-toxic vehicle (PEG-400) and is stable for up to a week in non-aqueous solutions (Lundbeck, personal communication).

4.5 Conclusion

The results of this study did not show a protective effect of LuAF21934 against a 6-OHDA lesion of the SNc when administered systemically. However the presence of physical damage within the SNc related to the infusion of the neurotoxin would likely have precluded any protective effect that might have been exerted by LuAF21934 and therefore the results of this study are far from conclusive.

While we are confident that the $mGlu_4$ PAM achieved good brain exposure, leading to at least intermittent receptor activation, a combination of physical damage and the severity of the 6-OHDA lesion noted in this study may have been too drastic for any agent to protect against.

Further studies are required using systemically active $mGlu_4$ PAMs such as LuAF21934, preferably using partial nigrostriatal lesion models, in order to support or discount widespread activation of this receptor within the BG as a neuroprotective strategy in Parkinson's disease.

5 Targeting $mGlu_7$ as a potential neuroprotective approach in a hemiparkinsonian rat model

5.1 Introduction

5.1.1 The role of $mGlu_7$ in the basal ganglia

The group III receptor $mGlu_7$ is highly expressed in many areas of the rat brain (Bradley *et al.*, 1998; Kinoshita *et al.*, 1998; Kinzie *et al.*, 1995). Pertinently for Parkinson's disease it is found in all regions of the rat basal ganglia, with mRNA expression found at particularly high levels in the nucleus accumbens, premotor cortex, striatum, GP, SNr and thalamus (Messenger *et al.*, 2002; Ohishi *et al.*, 1995). Electron microscopic studies have identified $mGlu_7$ receptors located presynaptically in the CPu, GP, EPN and SNr (Bradley *et al.*, 1999b; Kosinski *et al.*, 1999), where they could alter glutamate and GABA release via their role as auto- and heteroreceptors respectively.

As yet, studies have found no evidence suggesting alterations in expression of $mGlu_7$ in the ageing rat (Simonyi *et al.*, 2000) or following 6-OHDA lesioning of the MFB (Kosinski *et al.*, 1999; Messenger *et al.*, 2002). Assuming this situation was reflected in human ageing and PD, $mGlu_7$ receptors would be expected to be present and targetable following nigrostriatal degeneration.

5.1.2 Targeting $mGlu_7$ receptors in PD

Due to the high levels of $mGlu_7$ expression in associated brain areas such as the hippocampus and amygdala (Felix-Ortiz *et al.*, 2013; Kinoshita *et al.*, 1998), this receptor has predominantly been investigated as a potential anxiolytic or antidepressant target (Kalinichev *et al.*, 2013; O'Connor *et al.*, 2013; Palucha-Poniewiera *et al.*, 2013; Palucha *et al.*, 2007). It has also been investigated in relation to addiction (Bahi *et al.*, 2011; Li *et al.*, 2010a) and schizophrenia (Wierońska *et al.*, 2011) due to its expression in the nucleus accumbens. However given its widespread expression in the BG it might also be expected to play a role in motor function, and as such there is evidence that it may be a useful therapeutic target in PD.

As discussed in Chapter 2, there is a wealth of evidence for the symptomatic and neuroprotective potential of activation of $mGlu_4$ receptors. A similar degree of evidence had been lacking for $mGlu_7$, likely resulting from a paucity of tool compounds specifically targeting this receptor subtype. The 2005 discovery of a selective allosteric agonist for $mGlu_7$, N,N'-dibenzhydrylethane-1,2-diamine dihydrochloride, also known as AMN082

(Mitsukawa *et al.*, 2005), has since aided our understanding of the potential role of this receptor in PD.

An acute dose of AMN082 can reverse haloperidol-induced catalepsy in rats when administered systemically or centrally into the striatum or SNr (Greco *et al.*, 2010; Konieczny *et al.*, 2013). AMN082 also reverses reserpine-induced akinesia in rats when administered acutely into the SN (Broadstock *et al.*, 2012), though this result was not replicated when the drug was acutely administered systemically (Konieczny *et al.*, 2013). Importantly from the point of view of models involving nigrostriatal degeneration, acute oral administration of AMN082 showed antiparkinsonian efficacy in two models; it reduced apomorphine-induced rotational asymmetry in rats with a unilateral nigral 6-OHDA lesion when given 30 days post-lesion, and improved reaction time in rats with bilateral striatal 6-OHDA lesions when given between 3 and 4 weeks post-lesion (Greco *et al.*, 2010). Although no neurochemical or histological endpoints were evaluated in these studies it is unlikely that these functional improvements were underpinned by a degree of neuroprotection due to the fact that the drug was administered acutely in both instances and at a stage after the lesion had been fully established.

There is, on the other hand, *in vitro* evidence for $mGlu_7$ activation as a neuroprotective strategy. In cerebellar granule cell cultures a dose of L-AP4 that is sufficient to activate $mGlu_7$ provided neuroprotection against NMDA-mediated toxicity (Lafon-Cazal *et al.*, 1999) and further to this AMN082 has been demonstrated to protect hippocampal cell cultures against toxicity induced by exposure to the inhalable anaesthetic sevoflurane (Wang *et al.*, 2012a).

5.1.3 Potential mechanisms of neuroprotection

From the point of view of protecting against excitotoxicity in the parkinsonian condition, the desired effect of $mGlu_7$ activation in PD is the reduction of the overactive glutamatergic transmission within the SNc (as described in section 1.3.3.3), however the effect of AMN082 seems to be location-dependent. For example it has been shown to reduce glutamatergic transmission/excitatory post-synaptic currents (EPSCs) in the VTA (de Rover *et al.*, 2008), spinal cord (Cui *et al.*, 2011) and the basolateral amygdala (Ugolini *et al.*, 2008), suggesting that it is acting at $mGlu_7$ autoreceptors at these locations. The ability of AMN082 to reduce GABA release from mouse hippocampal synaptosomes (Summa *et al.*, 2013) suggests that it is also functional at $mGlu_7$ heteroreceptors. Conversely AMN082 *increases* glutamate release/EPSCs in other locations such as the retina (Guimarães-Souza

et al., 2012), amygdala (Ren *et al.*, 2011) and nucleus accumbens (Li *et al.*, 2008), believed to result from indirect mechanisms. The mechanisms suggested by the authors above are (1) GABA transporter-mediated GABA release secondary to an $mGlu_7$-mediated increase in Ca^{2+}-dependent glutamate release (Guimarães-Souza *et al.*, 2012) and (2) an AMN082-mediated increase in sEPSCs driven by disinhibition of glutamatergic neurones secondary to inhibition of GABA release (Li *et al.*, 2008; Ren *et al.*, 2011). Increase of glutamate release is the opposite effect to what might be desired for a potential neuroprotective agent. The only report of the effects of $mGlu_7$ activation on neurotransmission at BG synapses is a reduction in [^{3}H]-D-aspartate (glutamate analogue) release from rat nigral prisms with AMN082 in the presence of L-AP4 (Broadstock *et al.*, 2012), which is promising from the point of view of reducing glutamate release into the SNc/SNr. However AMN082 is also pharmacologically active when locally administered into the striatum (Konieczny *et al.*, 2013) and $mGlu_7$ has additionally been localised to presynaptic striatopallidal and striatonigral terminals (Kosinski *et al.*, 1999); therefore the net effect of $mGlu_7$ activation throughout the BG on thalamocortical output is hard to predict.

The published example of *in vitro* neuroprotection by AMN082 points to reduction of apoptosis as the protective mechanism, potentially involving signalling through the MAP kinase pathway and reduction of caspase-3 activation (Wang *et al.*, 2012a), though this may not be applicable to all toxins or indeed all cell types.

Finally, $mGlu_7$ activation with AMN082 may promote proliferation and differentiation of cortical neural progenitor cells into neurones, which could have implications for CNS repair (Tian *et al.*, 2010). However, a different study using clonal human ventral mesencephalic neural stem/progenitor cells contradicts this result, instead suggesting that $mGlu_7$ activation reduces proliferation and favours an astrocytic differentiation (Vernon *et al.*, 2011). This suggests that the effects of $mGlu_7$ activation on cell fate are dependent on cell population.

5.1.4 Hypothesis and aims

Activation of group III mGlu receptors with broad spectrum agonists at several locations within the BG has shown antiparkinsonian effects in various rodent models of PD (Austin *et al.*, 2010; Valenti *et al.*, 2003), making this group of receptors an attractive target for normalising abnormal transmission in the parkinsonian condition. Despite the reduced potency of broad spectrum agonists such as L-AP4 and L-SOP at $mGlu_7$ versus $mGlu_4$ and $mGlu_8$ (Conn *et al.*, 1997), due to the widespread expression of $mGlu_7$ in the basal ganglia it is worthy of investigation with a subtype-selective agonist or modulator, of which AMN082 is currently the only example.

Though alleviation of parkinsonian symptoms has been demonstrated for this compound, potentially by correction of signalling at several points within the basal ganglia, no neuroprotective effect has yet been investigated. Therefore the aim of this study was to investigate whether activation of $mGlu_7$ using the systemically active allosteric agonist AMN082 could provide functional neuroprotection against a 6-OHDA-induced lesion of the SNc when dosed sub-chronically. The finding that AMN082 in conjunction with L-AP4 can reduce release of a glutamate analogue in the SN *in vitro* (Broadstock *et al.*, 2012) supports the targeting of this receptor as a potential neuroprotective therapy, and therefore we hypothesise that:

Activation of $mGlu_7$ *in vivo* will provide neuroprotection in the 6-hydroxydopamine lesioned rat.

The neuroprotection study reported in this chapter assessed the ability of AMN082 to:

- Enhance survival of TH-positive neurones in the SNc.
- Preserve striatal dopamine content.
- Preserve motor function secondary to any measured neuroprotection, as assessed by the cylinder test, adjusted steps test and amphetamine-induced rotometry.

In order to test for the presence of a central action of AMN082 an additional behavioural assessment was carried out during the course of the neuroprotection study. As mentioned in the introduction to this chapter, AMN082 has been widely reported to have anxiolytic effects, and therefore we used a test of anxiety as a positive control for central actions of AMN082. The following parameters were measured:

- Time spent in the central vs. outer zone in the open field test.
- Number of faecal pellets produced during the open field test.

Subsequent to the main study, we also carried out a pharmacokinetic (PK) study to investigate the brain penetrance and metabolism of AMN082 when administered intraperitoneally in 8% DMSO vehicle.

5.2 Materials and Methods

5.2.1 Compound tested

The compound used for the studies reported in this chapter was AMN082, an allosteric agonist of $mGlu_7$. The structure and full IUPAC name of this drug is shown in Table 11. The structure of its primary metabolite as defined by Sukoff-Rizzo et al. (2011) is also shown, as the plasma and brain concentrations of this metabolite were measured in the PK study alongside that of AMN082.

Table 11: The chemical structures of AMN082 and its primary metabolite Met-1. AMN082 was tested for plasma and brain pharmacokinetics in naive rats and neuroprotective efficacy in the hemiparkinsonian rat.

Structure	Name	Target
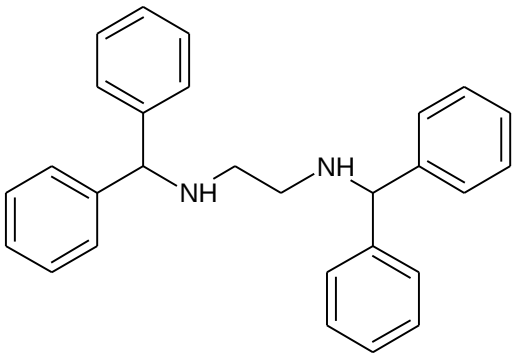	AMN082 *N,N'-dibenzhydrylethane-1,2-diamine dihydrochloride*	$mGlu_7$ allosteric agonist
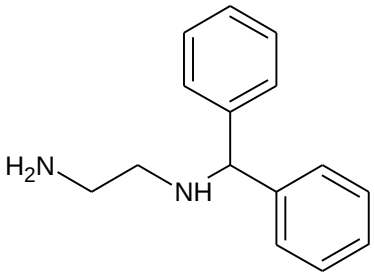	Met-1 *N-(diphenylmethyl)ethane-1,2-diamine*	Primary metabolite of AMN082

AMN082 is a brain-penetrant molecule that was discovered at Novartis via a high-throughput random screen and first described in a paper by Mitsukawa et al. in 2005. It has an agonist action at $mGlu_7$ (EC_{50} = 260nM) at a site independent of the glutamate binding site and is selective for $mGlu_7$ compared with all other metabotropic and three ionotropic glutamate receptors at concentrations ≤10µM (Mitsukawa *et al.*, 2005).

5.2.1.1 Drug formulation

AMN082 was obtained from Abcam Biochemicals (Cambridge, UK) and was dissolved in an 8% solution of dimethylsulfoxide (DMSO; Sigma Aldrich, Poole UK) in sterile water.

5.2.2 Other materials

5.2.2.1 Experimental materials

Surgery and behavioural testing was carried out at King's College London. The materials used have been described previously in Chapter 2.

5.2.2.2 Analytical materials

TH Immunohistochemistry: Tyrosine hydroxylase (TH) immunohistochemistry was carried out at King's College London as described in section 2.2.3.2.

HPLC for dopamine and its metabolites: High Performance Liquid Chromatography (HPLC) analysis of dopamine and its metabolites was carried out at Eli Lilly as described in section .

LC-MS/MS analysis for PK study: Brain and plasma samples from the pharmacokinetic study were analysed Liquid Chromatography with tandem Mass Spectrometry (LC-MS/MS) by S. Sossick at Eli Lilly and Co. to determine the concentrations of AMN082 and its primary metabolite, Met-1. The compounds used to make the standards were obtained from Tocris (Bristol, UK) (AMN082) or made in-house at Lilly (Met-1), and were spiked into blank brain or plasma samples as appropriate. All other reagents were obtained from Sigma (Poole, UK; Trimipramine, ammonium acetate) or Fisher Scientific (Loughborough, UK; Acetonitrile, ACN; Formic acid, FA).

5.2.3 Neuroprotection study methods

All procedures were performed in accordance with the U.K. Animals (Scientific Procedures) Act, 1986.

A time-line for the AMN082 neuroprotection study is shown in Figure 63.

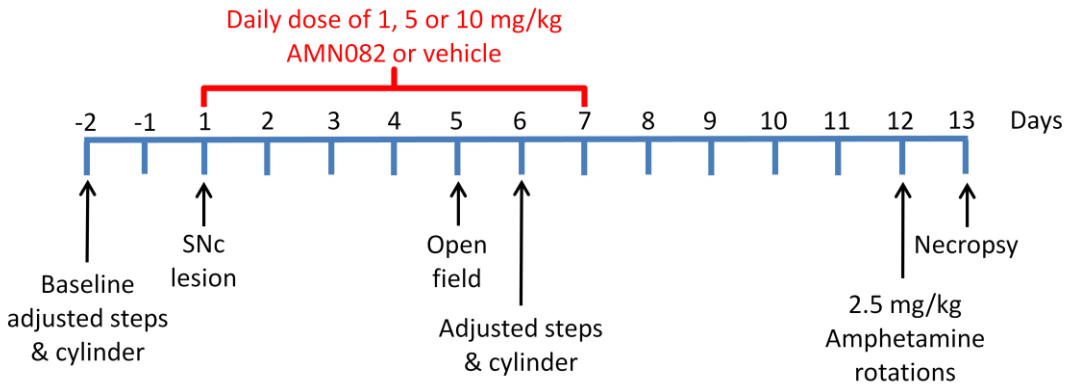

Figure 63: Experimental protocol for AMN082 neuroprotection study. Rats were treated with AMN082 or vehicle (i.p.) one hour prior to lesioning of the SNc with 6-OHDA, and then daily after lesioning for a total of 7 injections. Behavioural testing was carried out at intervals during the treatment period, and after a 5-day wash-out period amphetamine-induced rotations were examined. 24 hours later, rats were killed by CO_2 asphyxiation and their brains removed for analysis.

5.2.3.1 Lesioning and treatment

Male Sprague-Dawley rats (270-300g, Harlan, UK) were maintained in a temperature- and humidity-controlled environment with a 12-hour light-dark cycle and *ad libitum* access to chow and tap water.

Following baseline behavioural measurements, rats were lesioned in the SNc as detailed in section 2.2.3.1. Briefly, rats were pre-treated with 5mg/kg pargyline and 25mg/kg desipramine (i.p.), then 30 minutes later received an infusion of 12µg 6-OHDA.HCl in 2.5µl 0.2% ascorbate in 0.9% saline into the SNc at +3.7mm AP, +2.0mm ML and +2.2mm DV from the interaural line, or midline for ML co-ordinate (Figure 64). The toxin solution was infused at a rate of 1µl/min via a 25G needle, and as in previous studies, the needle was allowed to remain in place for a further 5 minutes following infusion to prevent reflux.

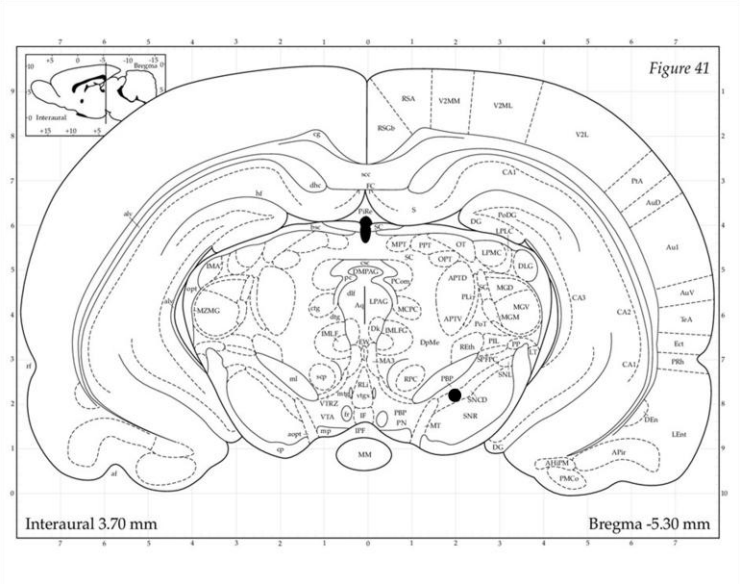

Figure 64: Co-ordinates for 6-OHDA infusion into the SNc during the AMN082 neuroprotection study. The black spot shows the location of the tip of the infusion needle.

One hour prior to lesioning rats received their first dose of AMN082 (1, 5 or 10mg/kg i.p.) or vehicle (2ml/kg 8% DMSO), n=6 per group. Dosing continued daily at 16:00 for a further 6 days post-lesion, alternating injections between the left and right sides of the peritoneal cavity to minimise local reactions or adhesion formation that may be associated with repeat injections (Smith *et al.*, 1967).

5.2.3.2 Assessment of lesion size

Following the one-week dosing regimen, rats were given 6 days' wash-out from AMN082/vehicle and then killed by CO_2 asphyxiation and the brain removed. The striatum was dissected out on an ice-cold platform and snap frozen on dry ice for HPLC analysis, while a coronal block containing the midbrain was post-fixed for a minimum of 24 hours in 10% buffered formalin before being processed and paraffin embedded for immunohistochemical analysis.

Immunohistochemistry

7µm coronal sections were cut throughout the substantia nigra and mounted in triplicate on SuperFrost Plus® slides. Slides were picked at 3 anteroposterior levels of the SNc: -4.8mm, -5.3mm and -5.8mm from Bregma, giving a total of 9 sections per animal. Sections were stained for TH as described for Compound 11 and LuAF21934 in section 2.2.3.2. Slides were viewed using the Axioskop brightfield microscope (Zeiss, UK) and images captured at 100x magnification using Axiovision release 4.6 software (Zeiss, UK). Cells were counted

using Image J software (developed by the NIH) and the number of remaining cells on the lesioned side expressed as a percentage of the intact side.

Neurochemical analysis by HPLC

Dissected striata were analysed at Eli Lilly and Co. using HPLC-ECD as detailed in section 2.2.3.2. Concentrations of dopamine, DOPAC and HVA in the lesioned striatum are expressed as a percent of the concentration measured in the intact striatum. Dopamine turnover was calculated as (DOPAC+HVA)/DA for each side, and expressed as a percentage in the same way.

5.2.3.3 Behavioural assessment

Motor function

Behavioural assessments were carried out at intervals during the treatment period. The same motor tests were carried out in this study as in the other neuroprotection studies reported in Chapter 2, in order to assess the functional outcome of the lesioning and treatment; the cylinder test, adjusted steps test and amphetamine-induced rotometry. Details of these tests can be found in section 2.2.3.3. All of these tests were performed a minimum of 18 hours after dosing, between 10:00 and 16:00, in order to avoid any acute pharmacological effects of AMN082 confounding the results.

Open field test

The open field test was performed as a measure of central activity of peripherally administered AMN082, due to the widely-reported anxiolytic effects of this drug. The open field test was carried out one hour after dosing on day 5 (17:00). The open field test can be used to assess several behaviours depending on the outcome measure. It is most often used as a measure of locomotion/mobility, by assessing the distance travelled by a rat in a given time alongside other features such as rearing (Basso *et al.*, 1995; Walsh *et al.*, 1976), however a variant on this has been designed to measure anxiety. The open field arena is subdivided into central and outer zones and rodent anxiety assessed by measuring the time spent in the centre or at the edge of the open field arena (Kuan *et al.*, 2008; Liebsch *et al.*, 1998). As prey species, rodents generally like to remain close to edges and corners in contact with a wall where the risk of predation is minimised (a phenomenon known as thigmotaxis). An increased proportion of time spent in the outer/peripheral zone is therefore taken to denote anxiety (Liebsch *et al.*, 1998) and an anxiolytic drug would be expected to increase the time spent by a rodent in the central zone (Gentsch *et al.*, 1987).

This test was carried out using automated tracking software; Ethovision XT v.6 (TrackSys). Animals were not habituated to the arenas and no baseline testing was carried out, therefore the post-lesion open field test was completely novel. The open fields used were black low-density polyethylene circular arenas with 30cm high vertical sides. Each arena had a total diameter of 75cm, and the central zone was defined as the area within an 18.75cm radius of the centre of the arena. One hour following treatment with AMN082 or vehicle, rats were placed in the centre of the arena to start. Automated video tracking equipment defined the central point of each rat and recorded the time spent in the central and peripheral zones of the arena in a testing period of 10 minutes.

In addition to this outcome measure, defecation is also a validated measure of anxiety and is increased in anxious compared with non-anxious animals (Kolyaduke *et al.*, 2013). The number of faecal pellets left was counted at the end of the testing period and compared between groups.

5.2.3.4 Statistical analysis

Normally distributed data are reported as mean ± s.e.m and are presented as bar charts or line graphs, where the bar height/plotted point represents the mean and the error bars represent the s.e.m.

Nonparametric data are presented as median ± IQR and are presented as box and whisker plots, where the box represents the IQR, the line within the box represents the median and the whiskers represent the minimum and maximum values obtained.

Statistical analysis was carried out using GraphPad Prism version 5.

For TH-positive cell counts and percent dopamine, DOPAC, HVA and turnover, parametric data were analysed using a one-way ANOVA with a Dunnett's *post-hoc* test. Within-group comparisons on parametric data were made using a t-test. Non-parametric data were analysed using a Kruskal-Wallis test with Dunn's *post-hoc* test. Within-group comparisons on non-parametric data were made using a Mann-Whitney U test.

Cylinder test data were compared using two-way repeated-measures ANOVA with Bonferroni post-hoc, for comparison between treatment groups and pre- and post-lesion performance.

Post-lesion performance as a percent of pre-lesion performance in the adjusted stepping test was compared using a one-way ANOVA with a Dunnett's *post-hoc* (for comparison of all groups to the vehicle group).

Data for total net ipsiversive turns over 90 minutes in the amphetamine-induced rotometry test were also analysed in using a one-way ANOVA with a Dunnett's *post-hoc*.

For the open field test, the time spent in the central zone was calculated as a percentage of the total time spent in the arena. This parameter was compared between groups using a one-way ANOVA with Dunnett's *post-hoc* analysis.

For all tests a result of $P<0.05$ was considered significant.

5.2.4 Pharmacokinetic testing of AMN082

All procedures were performed in accordance with the U.K. Animals (Scientific Procedures) Act, 1986.

5.2.4.1 Sample collection

Male Sprague-Dawley rats (200-220g, Harlan, UK) were maintained in a temperature- and humidity-controlled environment with a 12-hour light-dark cycle and *ad libitum* access to chow and tap water.

AMN082 was prepared on the day of testing as a 5mg/ml solution in 8% DMSO in sterile water. 20 rats received a single dose of 10mg/kg (i.p.) drug solution and were killed at specified times after dosing: 30 minutes (n=4), 1 hour (n=4), 3 hours (n=4), 6 hours (n=4) and 18 hours (n=4). A further group of rats received a single equivalent injection of vehicle (2ml/kg) and were killed after 30 minutes to provide a zero measure.

At the end of the appropriate post-dose interval, rats were exposed to CO_2 until cessation of breathing and a blood sample was then taken by cardiac puncture, transferred into a lithium-heparin-coated tube (Sarstedt) and kept on ice. When all four samples had been collected for a particular time point the blood samples were spun at 2000 x g for 10 minutes at room temperature and the plasma removed and snap frozen on dry ice to await analysis. Immediately following cardiac puncture, rats were killed by cervical dislocation and the brain removed, weighed and snap-frozen on dry ice to await analysis.

5.2.4.2 Analysis of AMN082 and Met-1 by LC-MS/MS

Sample preparation

Brain samples were prepared by addition of 4 volumes of ice-cold 90:10:0.1 ACN:H_2O:FA followed by sonication using the Vibra-cell sonic disruptor (50% amplitude for 20 seconds).

Plasma samples were prepared by taking 25µl of plasma and adding 100µl ice-cold 90:10:0.1 ACN:H_2O:FA.

Both brain and plasma samples were then left to stand for 1 hour at 4°C, after which each tube was mixed and centrifuged at 20,000rpm for 15 minutes at 8°C. After centrifugation, 10µl of the supernatant was mixed with 90µl of 10ng/ml trimiprimine (internal standard) in mobile phase (80:20 ACN:H_2O + 10mM ammonium acetate, unadjusted pH ~7.8). Samples were mixed and loaded into a chilled autosampler (8°C) to await analysis by LC/MS/MS.

LC-MS/MS conditions

Samples (10µl injection volume) were first separated using a 5µm particle size Hichrom Ace C18-300 75 x 2.1mm column with Javelin 2mm pre-filter. The flow rate was 300µl/minute and the mobile phase used was 80:20 ACN:H_2O + 10mM ammonium acetate with an unadjusted pH of ~7.8.

Samples were then electrospray ionised as they eluted the column and the molecules identified using an Applied Biosystems API4000 triple quadropole (MMSP606) mass spectrometer.

An example of the chromatograms produced using this analytical method is shown in Figure 65, in this case showing the chromatogram of a spiked plasma standard.

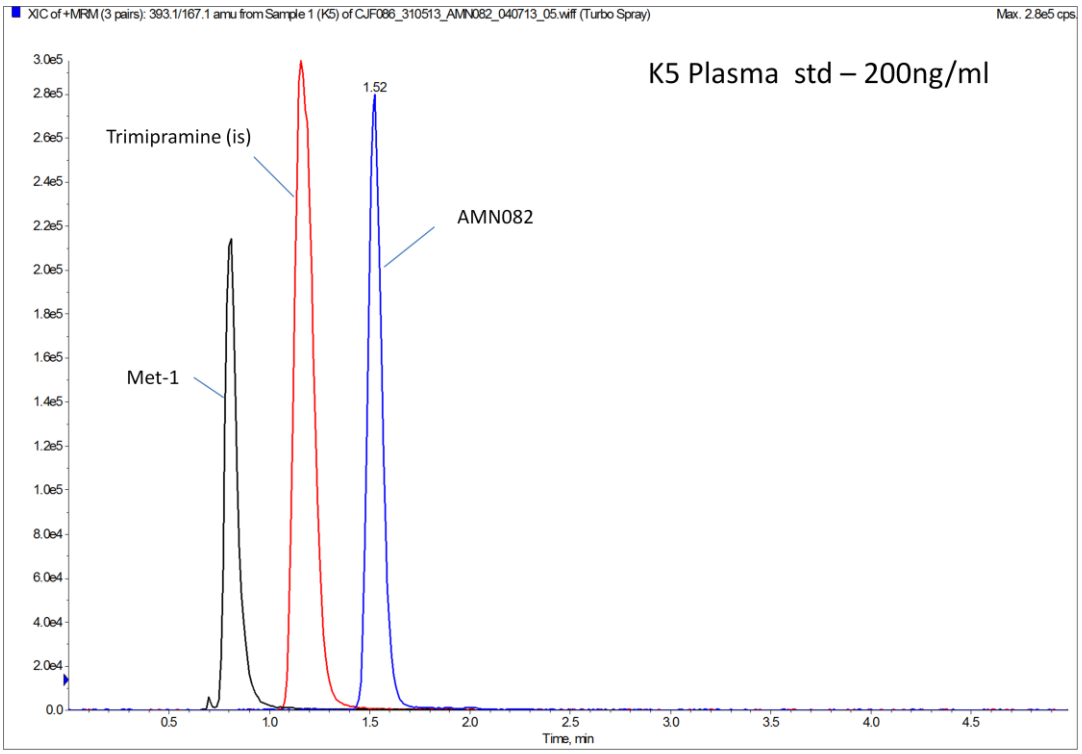

Figure 65: Example chromatogram following LC-MS/MS analysis of a blank plasma sample spiked with 200ng/g AMN082 and 200ng/g Met-1. The peak for the internal standard, trimipramine, is also clearly visible.

LC/MS/MS data analysis

Calibration curves were generated within Analyst software (v 1.4.2) from a set of AMN082 and Met-1 standards (1-5000ng/g for brain samples; 4-8000ng/ml for plasma samples). Analyte concentrations in each sample were calculated from these standard curves;

samples which fell below the bottom standard were recorded as BLLQ (below the lower limit of quantification).

5.2.4.3 PK data analysis

The brain/plasma ratio for AMN082 was calculated by comparison of the corresponding areas under the curve (AUC) for the concentration time courses. AUC was calculated using the relevant macro in SigmaPlot (version 12.5).

5.3 Results

5.3.1 Neuroprotection study

5.3.1.1 General observations

One rat in the 1mg/kg AMN082 group died following lesioning, leaving this group with n=5. For all other groups n=6.

No adverse effects of acute or sub-chronic administration of 8% DMSO vehicle were noted, however in the group administered 10mg/kg AMN082 some rats were observed to develop a rigid/tremulous state within an hour of dosing, which resolved within ~3 hours of dosing. Since testing of parkinsonian behaviours was carried out a minimum of 18 hours post dosing this effect is not expected to have interfered with these measurements. However the open field testing for anxiety was performed one hour after dosing, when this effect was still present, meaning that it likely influenced the result of this test.

5.3.1.2 AMN082 did not protect against nigrostriatal degeneration

TH-positive cells in the SNc

There was no significant difference between the cell counts at the three levels of the SNc (P=0.7921; one-way RM ANOVA with Bonferroni *post-hoc*) and therefore the results were pooled before analysis.

SNc infusion of 6-OHDA caused severe loss of TH-positive cells in the SNc (Figure 66). Lesioned rats treated with vehicle had 115.0 ± 6.1 TH-positive cells in the intact SNc, with only 1.2 ± 4.7 remaining in the lesioned SNc, a reduction to 1.1 ± 4.2% of the intact side (P<0.0001; t-test).

AMN082 did not protect against the degeneration of these cells at any of the doses tested, with <4% TH-positive cells remaining in the lesioned SNc at all doses tested (2.9 ± 2.3 in the 1mg/kg-treated group, 3.5 ± 11.8% in the 5mg/kg-treated group and 3.3 ± 5.6% in the 10mg/kg-treated group). There was no significant difference between any AMN082-treated group and the vehicle-treated group (P=0.5327; Kruskal-Wallis test with Dunn's *post-hoc*).

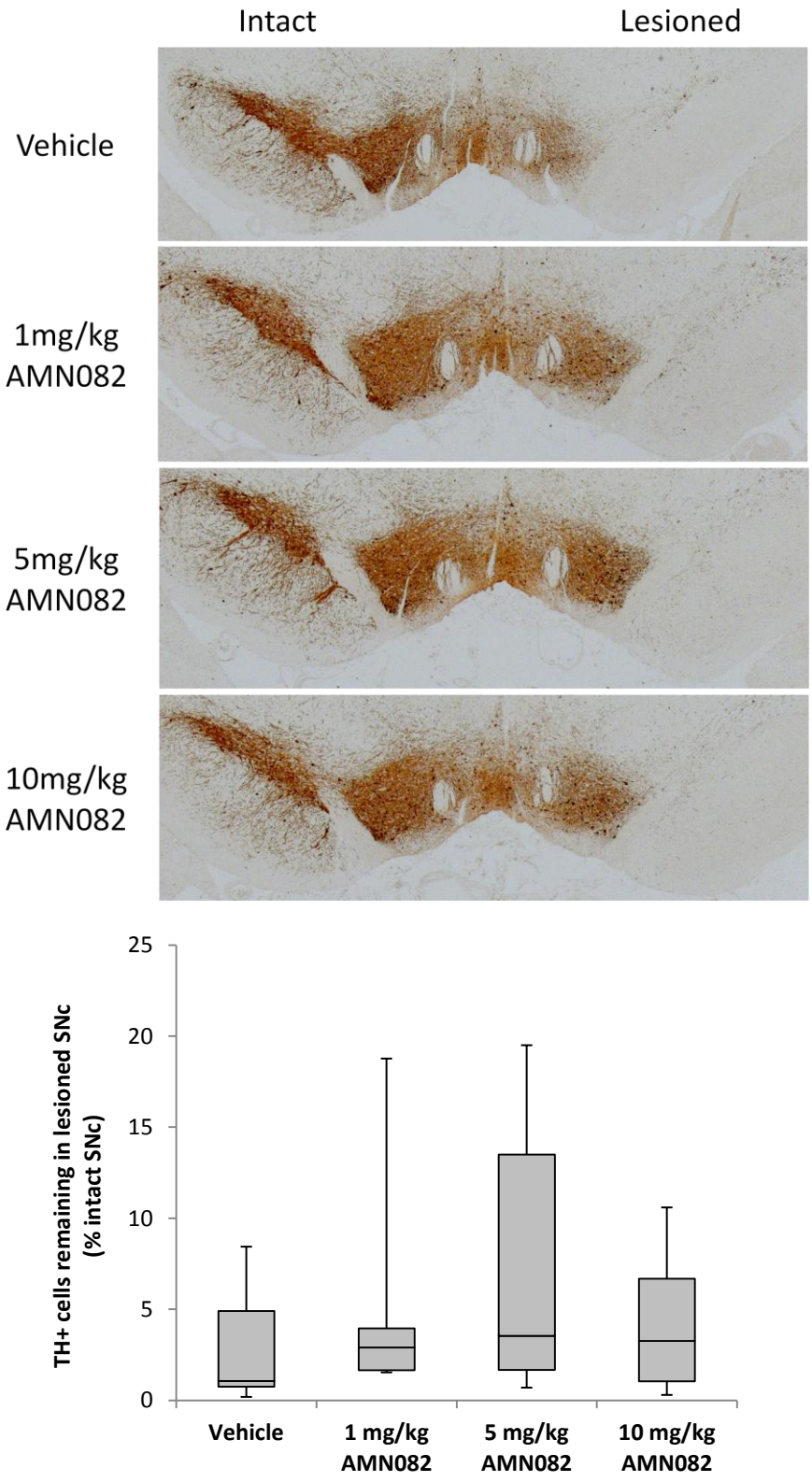

Figure 66: TH-positive cells remaining in the intact and lesioned SNc of rats with a unilateral 6-OHDA nigral lesion, following 7 days' sub-chronic treatment with vehicle or AMN082. Treatment with increasing doses of AMN082 did not provide a significant degree of neuroprotection in the SNc. Representative TH-stained nigral sections are shown in panel (a) and the number of surviving cells in the lesioned SNc as a % intact SNc is shown in graph (b). Data are presented as median ± IQR (n = 5-6 per group).

Striatal dopamine content

The striatal concentrations of dopamine and its metabolites are shown in Table 12

Table 12: Striatal concentrations of dopamine and its metabolites in the intact and lesioned striatum following a 6-OHDA nigral lesion and treatment with vehicle or AMN082. Data reported are median concentrations in ng/g (n = 5-6) **P<0.01 (Mann-Whitney U test versus intact).

	Dopamine (DA)		DOPAC		HVA	
	Intact	**Lesioned**	**Intact**	**Lesioned**	**Intact**	**Lesioned**
Vehicle	15040	6.04**	1874	277.29**	613	2.11**
1 mg/kg AMN082	13290	78.18**	2048	283.58**	903	38.12**
5 mg/kg AMN082	13134	316.65**	1978	352.87**	652	55.38**
10 mg/kg AMN082	13601	170.48**	1834	408.55**	667	39.74**

6-OHDA lesioning caused degeneration of the dopaminergic nerve terminals in the striatum, such that vehicle-treated animals with an intact striatal dopamine content of 15040 ± 2362ng/g retained only 6.0 ± 23ng/g in the lesioned striatum; 0.04 ± 0.11% of normal (Figure 67; P=0.0079; Mann-Whitney U test). DOPAC and HVA were similarly reduced (Figure 68a and Figure 68b), to only 14.78 ± 1.63% and 3.21 ± 2.41% of their respective concentrations in the intact striatum (both P<0.0001; t-tests).

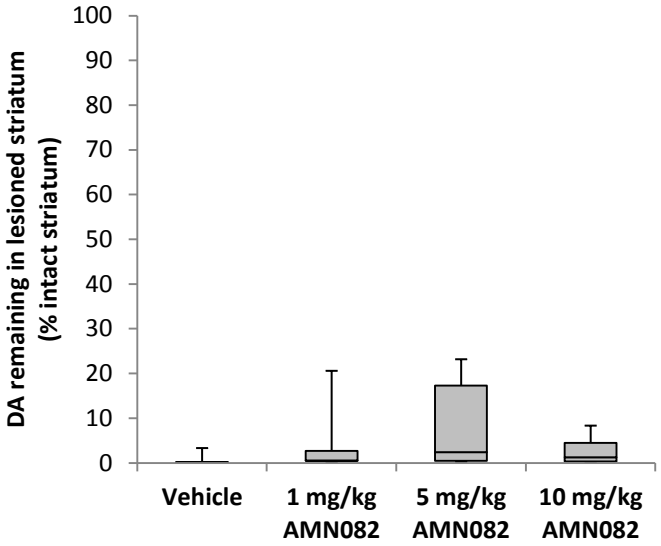

Figure 67: Striatal dopamine concentration following a unilateral nigral 6-OHDA lesion (lesioned striatum as a percent of intact striatum) and 7 days of sub-chronic treatment with AMN082 or vehicle. Treatment with AMN082 did not significantly preserve dopamine content in the lesioned striatum compared with vehicle. Data are presented as median ± IQR (n = 5-6 per group).

AMN082 did not significantly protect against loss of striatal dopamine content (P=0.2092; Kruskal-Wallis test with Dunn's *post-hoc*), with only 0.5 ± 2.2% remaining in the 1mg/kg-treated group, 2.37 ± 16.83% in the 5mg/kg-treated group and 1.24 ± 4.27% remaining in the 10mg/kg-treated group. Similarly there was no significant preservation of DOPAC (P=0.5504; one-way ANOVA with Dunnett's *post-hoc*) or HVA (P=0.3862; one-way ANOVA with Dunnett's *post-hoc*) in any treated group compared with vehicle.

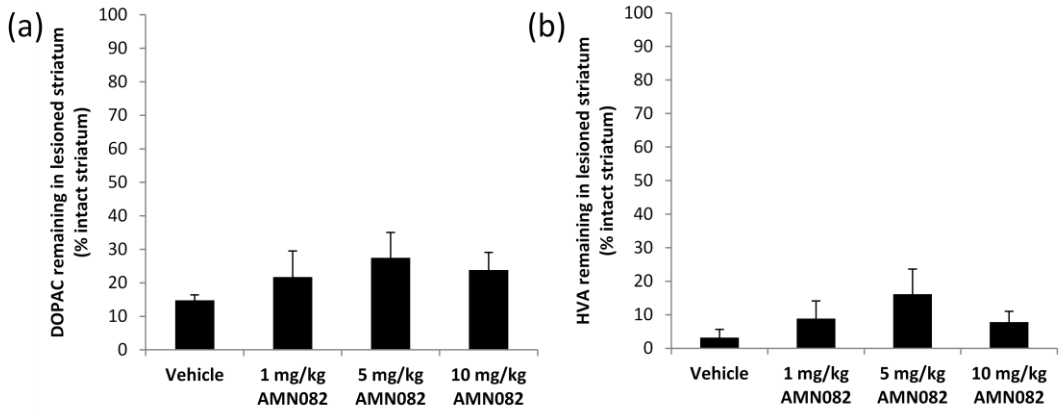

Figure 68: Striatal dopamine metabolite concentration following a unilateral nigral 6-OHDA lesion (lesioned striatum as a percent of intact striatum) and 7 days of sub-chronic treatment with AMN082 or vehicle. Treatment with AMN082 did not significantly preserve either DOPAC (a) or HVA (b) content in the lesioned striatum compared with vehicle. Data are presented as mean ± s.e.m. (n = 5-6 per group).

6-OHDA lesioning caused a large increase in dopamine turnover in vehicle-treated animals, which was increased to 41 ± 18 in the lesioned striatum compared with 0.17 ± 0.01 in the intact striatum. This is an increase to 22388 ± 9056% of the intact turnover rate, though this effect narrowly failed to reach significance due to variability within the group (P=0.0509; t-test). When the turnover rates were compared between vehicle- and AMN082-treated rats there was no significant effect of the drug on the dopamine turnover rate in the lesioned striatum (P=0.2413; Kruskal-Wallis test).

5.3.1.3 AMN082 did not show consistent preservation of functional outcomes

Cylinder test

All groups showed no overall bias in forelimb use in the cylinder test pre-lesion (Figure 69a), using each forelimb for ~50% of touches.

When tested on day 6 post-lesion, vehicle-treated rats had significantly decreased use of the contralateral forelimb post-lesion, where it was involved in only 1.7 ± 1.0% touches, compared with a baseline of 47.7 ± 1.9% touches (P<0.0001; two-way RM ANOVA with Bonferroni *post-hoc*).

AMN082-treated rats displayed a dose-dependent bell-shaped increase in use of the contralateral forelimb post-lesion (Figure 69b), with 11.3 ± 4.5% use in the 1mg/kg group, 20.6 ± 5.7% use in the 5mg/kg group and 2.7 ± 1.4% use in the 10mg/kg group. Statistical analysis revealed that there was a significant overall effect of both lesion (P<0.0001) and treatment group (P=0.0114) on the use of the contralateral forelimb in the cylinder test, with post-hoc analysis revealing a significant effect of treatment with 5mg/kg AMN082 (P<0.001; two-way RM ANOVA with Bonferroni *post-hoc*). This functional preservation was only partial and therefore still represented a significant decrease compared with pre-lesion use in this group (P=0.0021; two-way RM ANOVA with Bonferroni *post-hoc*).

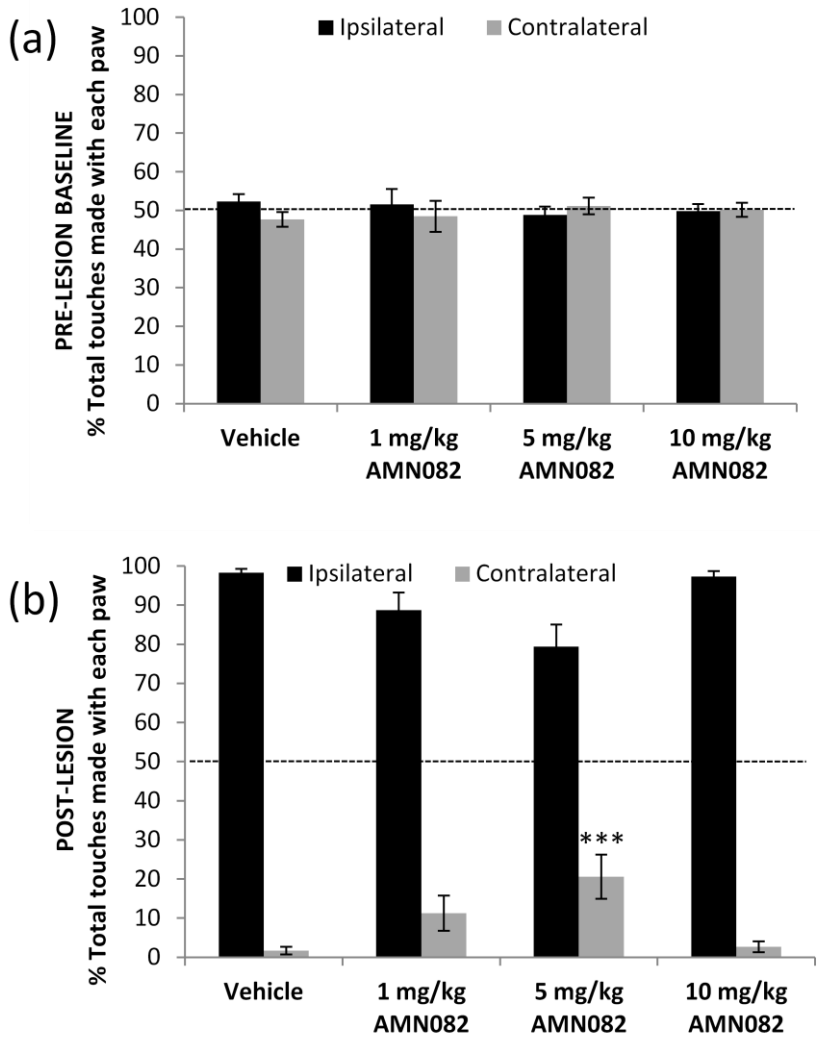

Figure 69: Cylinder test results in rats with a unilateral nigral 6-OHDA lesion following 6 days of sub-chronic treatment with AMN082 or vehicle. Pre-lesion (a) all groups showed the expected ~50% use of each of the ipsilateral and contralateral paws. Post-lesion (b) all groups showed a clear bias towards use of the ipsilateral (healthy) paw. Treatment with AMN082 at 5 mg/kg significantly increased use of the contralateral paw post-lesion compared with the vehicle treated group. Data are presented as mean ± s.e.m. (n = 5/6 per group). The dashed lines show the expected unbiased performance for each forelimb in unimpaired rats ***P<0.0001 (one-way ANOVA with Dunnett's *post-hoc*).

Adjusted steps test

Similarly to the cylinder test, vehicle-treated animals showed a deficit in contralateral stepping in both the forward direction (68.0 ± 5.3% of baseline, P=0.0022; paired t-test on no. of steps) and the reverse direction (81.5 ± 5.1% baseline, P=0.0136; paired t-test on no. of steps) when tested on day 6 post-lesion.

Unlike in the cylinder test, there was no significant effect of treatment with AMN082 in the adjusted steps test (Figure 70). Contralateral forward-stepping was reduced to 69.7 ± 9.5% of baseline in the 1mg/kg group, 67.2 ± 5.1% of baseline in the 5mg/kg group and 71.8 ± 5.0% in the 10mg/kg group (P=0.9519; one-way ANOVA with Dunnett's *post-hoc*). Contralateral reverse-stepping was reduced to 78.3 ± 2.1% baseline in the 1mg/kg group, 78.3 ± 4.1% in the 5mg/kg group and 83.2 ± 2.1% in the 10mg/kg group (P=0.7273; one-way ANOVA with Dunnett's *post-hoc*).

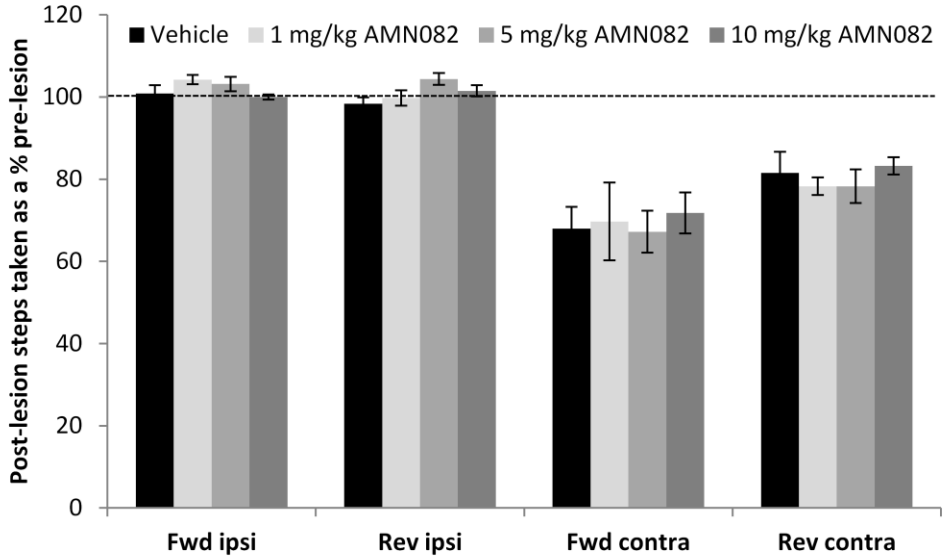

Figure 70: Adjusted steps test following 6 days of sub-chronic treatment with AMN082 or vehicle. Stepping with the ipsilateral paw was unaffected by the lesion in all groups, as expected. Stepping with the contralateral paw was impaired post-lesion, but the degree of deficit was not affected by treatment with AMN082. Fwd = forward stepping; Rev = reverse stepping; Ipsi = ipsilateral paw; Contra = contralateral paw. Data are presented as mean ± s.e.m. (n = 5-6 per group). The dashed line shows the expected unimpaired performance of 100% baseline performance.

Stepping with the ipsilateral paw was unaffected in either direction in the vehicle-treated group, as would be expected for a unilateral lesion (P>0.3330; paired t-tests on no. of steps). There was no effect of treatment on ipsilateral stepping in either the forward (P=0.2071; one-way ANOVA with Dunnett's *post-hoc*) or reverse (P=0.0596; one-way ANOVA with Dunnett's *post-hoc*) directions.

Amphetamine-induced rotational asymmetry

6-OHDA-lesioned rats treated with vehicle showed the expected ipsiversive turning in response to 2.5 mg/kg amphetamine when tested on day 12 post-lesion (5 days after the final vehicle [or AMN082] dose), with a total of 327 ± 69 turns over 90 minutes (Figure 71).

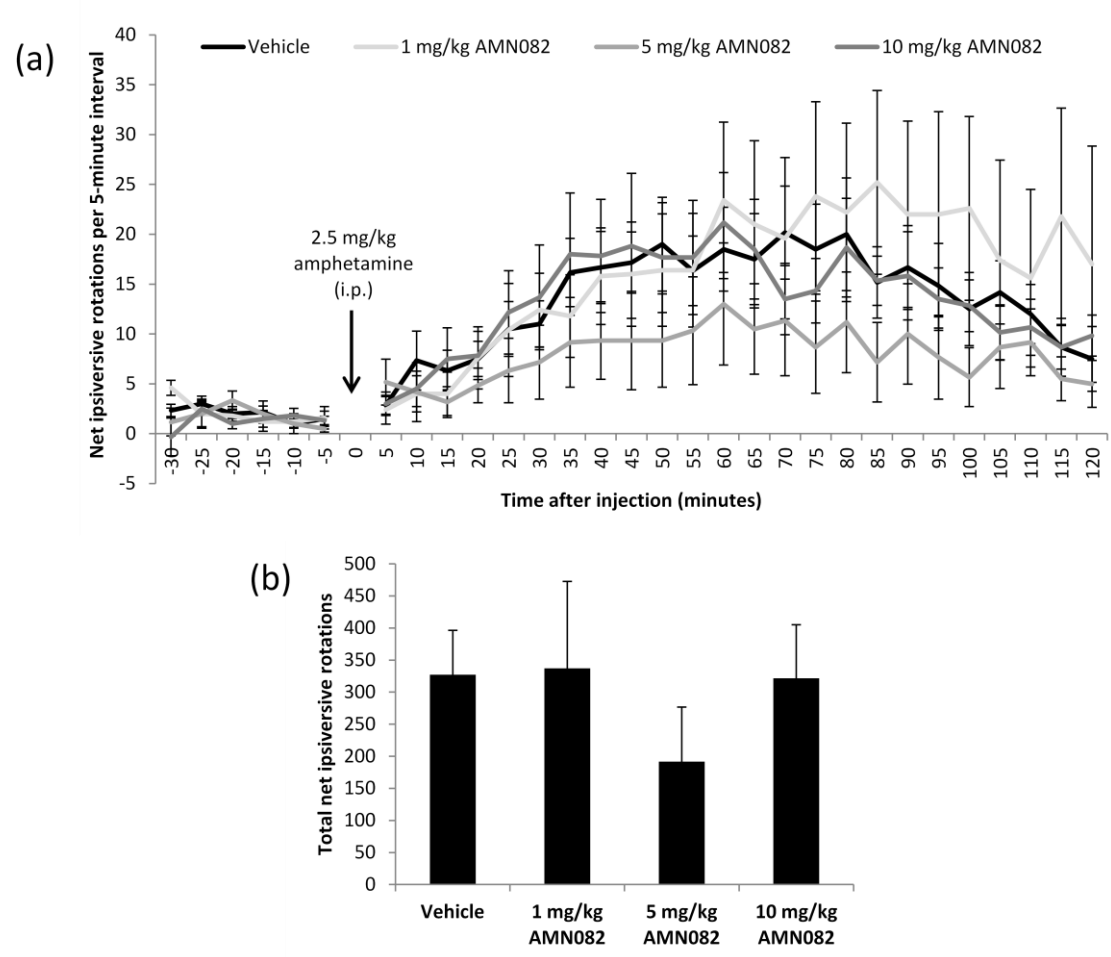

Figure 71: Amphetamine-induced rotations in rats with a unilateral nigral 6-OHDA lesion following 7 days of sub-chronic treatment with AMN082 or vehicle and 5 days of wash-out. The 120-minute time course of ipsiversive rotational response is shown in (a). The total net ipsiversive rotations are shown in (b). AMN082 treatment did not significantly reduce amphetamine-induced ipsiversive rotations. Data are presented as mean ± s.e.m. (n = 5-6 per group).

The three groups treated with AMN082 also showed net ipsiversive turning in this test, with 391 ± 152 in 1mg/kg-treated rats, 192 ± 85 in 5mg/kg-treated rats and 322 ± 84 in 10mg/kg-treated rats (Figure 71b). Despite an approximate 40% reduction in net ipsiversive turns in the 5mg/kg group compared with vehicle there was a lot of variability within all groups, therefore there was no significant effect of AMN082 on amphetamine-induced rotational asymmetry (P=0.5502; one-way ANOVA with Dunnett's *post-hoc*).

Open field test

For this test the rats were placed in the centre of the open field to start the test. This means that rats that did not move at all would score highly for % time spent in the central zone even though this could have been caused by factors other than an anxiolytic effect of

the drug, such as a sedative effect. There was one rat in the 5mg/kg AMN082 group and two rats in the 10mg/kg AMN082 group that did not move during the test, remaining exactly where they were placed, and therefore these rats were excluded from the analysis. This left n=6 for vehicle rats, n=5 for 1mg/kg AMN082 and 5mg/kg AMN082 and n=4 for 10mg/kg AMN082.

Vehicle-treated rats spent an average of 9.8 ± 2.8% of the total time in the central zone, demonstrating a clear preference for the outer zone close to the walls (Figure 72).

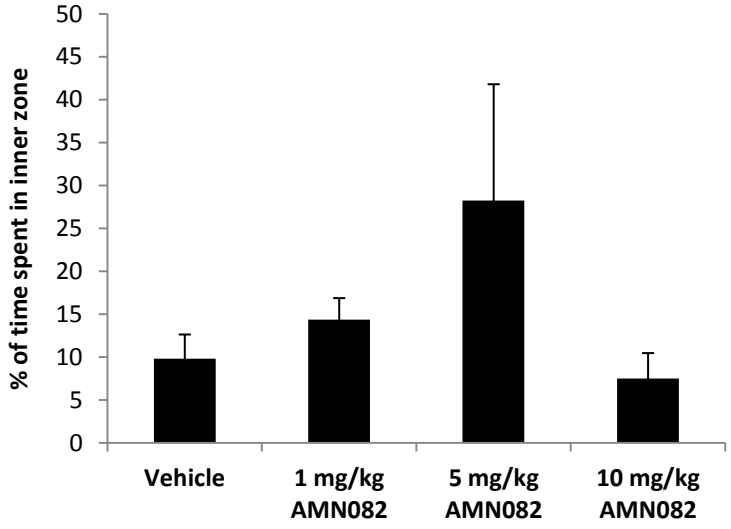

Figure 72: Time spent in the central zone of the open field following 5 days of treatment with AMN082 or vehicle (tested one hour post-dose). AMN082 did not significantly affect the percent of the testing time that was spent by rats in the central zone of the arena. Data are presented as mean ± s.e.m. (n = 5-6 per group).

AMN082 treated rats showed a bell-shaped dose-dependency regarding time spent in the central zone, which increased at 1mg/kg (14.4 ± 2.5% time in central zone), peaked at 5mg/kg (28.2 ± 13.6% time in central zone) and was lost at 10mg/kg (7.5 ± 3.0% time in central zone). This might suggest an anxiolytic effect of treatment with AMN082, however this effect was not significant (P=0.2242; one-way ANOVA with Dunnett's *post-hoc*).

The second measure of anxiety assessed was defecation during the open field testing period. However since the median number of faecal pellets produced in each group was 0-0.5 these data were not considered further.

5.3.2 Pharmacokinetic study

The pharmacokinetic study demonstrated that AMN082 is brain penetrant when administered intraperitoneally in 8% DMSO vehicle (Figure 73). Following a 10mg/kg dose, the brain C_{max} was 386.5ng/g (0.5h) and the brain $t_{1/2}$ was ~2.7 h. Plasma concentrations were also calculated, where the plasma C_{max} was 101.8ng/ml (1h) and the plasma $t_{1/2}$ was ~2.0 h.

The overall brain/plasma ratio, calculated from the AUC, was 4.76.

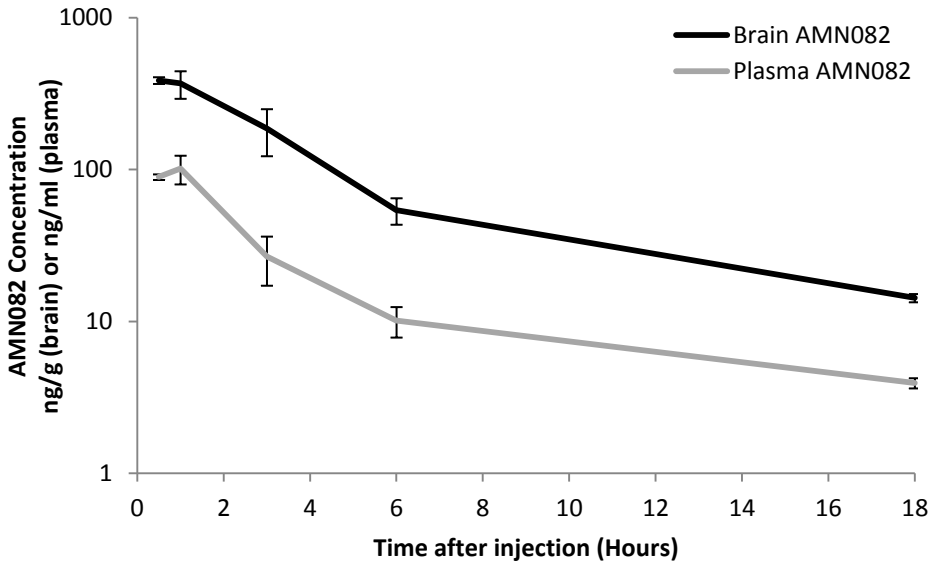

Figure 73: Brain and plasma AMN082 pharmacokinetic time course in naive rats. 10mg/kg AMN082 was administered i.p., and brain and blood samples collected at intervals. Data are presented as mean ± s.e.m. (n=4 per time point).

The concentration of Met-1, the primary metabolite of AMN082, was also measured (Figure 74). Met-1 was not detected in any of the plasma samples, but it *was* detected in brain samples. Interestingly, when shown alongside AMN082 for comparison, it is clear that the brain Met-1 levels did not change in line with those of AMN082, rather displaying a consistently low concentration of between 17.23ng/g and 32.95ng/g over the 18-hour time course, with the C_{max} occurring 6 hours after dosing.

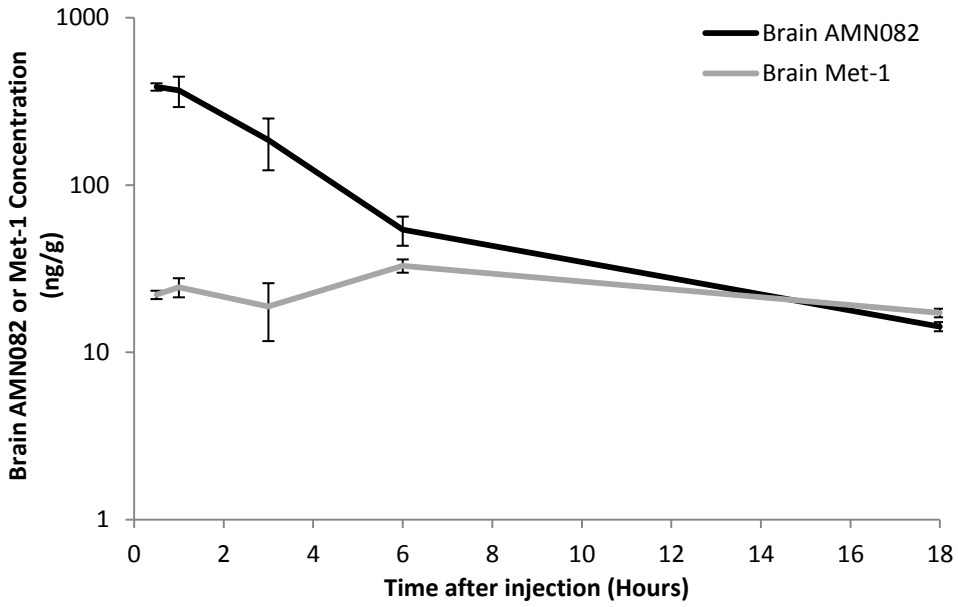

Figure 74: Brain concentrations of AMN082 and its primary metabolite Met-1 following 10mg/kg i.p. AMN082 in naive rats. Data are presented as mean ± s.e.m. (n=4 per time point).

Neither AMN082 nor Met-1 was detected in brain or plasma samples from vehicle-dosed rats (sample concentrations all BLLQ, data not shown).

5.4 Discussion

The purpose of these studies was to (1) test for a neuroprotective effect of subchronic once-daily administration of AMN082 in a rat model of PD following a 6-OHDA lesion of the SNc and (2) determine whether or not AMN082 was able to cross the BBB in rats following an intraperitoneal injection in 8% DMSO vehicle.

5.4.1 Central effects of AMN082

In an attempt to confirm a centrally-mediated effect of AMN082, an additional behavioural test was performed during the neuroprotection study itself. Given that AMN082 has widely been reported in the literature to exert anxiolytic effects in the dosing range used in the neuroprotection study, a simple measure of anxiety was undertaken 5 days post-lesion, one hour after dosing with AMN082 or vehicle. A variant of the open field test was employed to compare the time spent in the central (anxiety-inducing) vs. peripheral (safer, less anxiety-inducing) zones of a circular arena.

The open field test as performed in this study did not adequately define an anxiolytic effect of AMN082. One rat from the 5mg/kg group and two rats from the 10mg/kg group had to be excluded from the analysis due to the clear interference of drug-related side effects such as tremors and akinesia with aspects of mobility, thus affecting the movement of the rat between the central and peripheral zones. This not only left small group sizes but it is also possible that some of the rats that weren't excluded were under the influence of a less noticeable degree of these side effects and their borderline results could therefore have skewed the outcomes. Side effects such as these have been reported elsewhere following systemic doses of AMN082 exceeding 30mg/kg in rats or 10mg/kg in mice (Bahi *et al.*, 2011; Palucha *et al.*, 2007). These effects are seemingly $mGlu_7$-independent and are thought to be related to off-target effects of AMN082, especially given its reported affinity for monoaminergic transporters (Sukoff Rizzo *et al.*, 2011). This is explored in more detail below.

The anxiolytic test itself is also of questionable validity; for example it has been suggested that it may measure only a natural anxiety related to a novel situation rather than pathological anxiety (Prut *et al.*, 2003). In addition its predictive validity regarding known anti-depressant and anxiolytic compounds is doubtful, only showing effects for full agonists at $5\text{-}HT_{1A}$ or benzodiazepine receptors (Prut *et al.*, 2003), for example citalopram failed to increase time spent by rats in the central zone (Kuan *et al.*, 2008). Overall, while the reasoning behind the inclusion of this test was sound, the presence of unexpected acute

side effects of AMN082 meant that the results were not clear-cut enough to serve as proof of obtaining a central pharmacological action of AMN082, and therefore do not assist in interpretation of the neuroprotection study.

5.4.2 Neuroprotection study

Contrary to our hypothesis, the neuroprotection study did not provide any evidence for a protective effect of AMN082 at either the level of dopaminergic cell bodies in the SNc, or the level of their terminals at the striatum, using this study design. This is despite the neuroprotective effects that have recently been reported for AMN082 in neuroblastoma cell cultures against MPP^+-induced toxicity, an effect believed to reflect a reduction of both apoptosis and necrosis (Jantas *et al.*, 2014). However the protection elicited *in vitro* was lost following retinoic acid (RA)-induced differentiation of the cultured cells into a dopaminergic phenotype, suggesting that cells with a dopaminergic phenotype are not protected against MPP^+-mediated neurodegeneration. It would be interesting to test if AMN082 was protective *in vitro* against 6-OHDA in both undifferentiated and RA-differentiated cultures of this cell type.

Functionally, the results of the adjusted steps test and amphetamine-induced rotometry supported this lack of a protective effect, however there was a significant increase in use of the contralateral paw in the cylinder test in rats treated with 5mg/kg AMN082 compared with vehicle. This finding cannot be explained by any short-term pharmacological effect of AMN082 or Met-1 since the test was performed >18 hours after dosing when concentrations of both were almost back to baseline. However, the predictive validity of the cylinder test for lesion size is uncertain. Though a highly significant positive correlation between limb use asymmetry and striatal dopamine depletion has been reported in this test (Iancu *et al.*, 2005; Schallert *et al.*, 2000a) there is still a large variability in response, with 0-55% use of the contralateral forelimb reported in rats with >95% TH-positive cell loss (Iancu *et al.*, 2005). From personal experience in other experiments (e.g. AIMs induction study, section 6.3.5.1) I have seen up to 30% use of the contralateral forelimb in rats with >98% TH-positive cell loss in the lesioned SNc. This is consistent with results obtained in the cylinder test in 6-OHDA-lesioned mice, where no difference in performance was observed between mice with an intermediate (80% striatal TH loss) and a severe lesion (94% striatal TH loss) (Grealish *et al.*, 2010). Therefore it is possible that the significant effect of AMN082 seen here in the cylinder test was a false positive association arising from the variability associated with equivalent lesions in this test.

5.4.3 Neuroprotection study: general considerations

Despite the relatively small group sizes of n = 5-6, this should be sufficient to detect neuroprotection at the SNc and striatal levels with 90% power based on previous neuroprotection studies in this model (Betts *et al.*, 2012). However there are several caveats to this neuroprotection study that warrant consideration.

Firstly, the compound was only dosed once per day. While once-daily dosing has proven an effective treatment regimen for other compounds tested in this model via direct intracerebral injection (notably the $mGlu_4$ PAM VU0155041, see section 2.3.2 and Betts *et al.* 2012) we discovered from the PK profile of AMN082 that was carried out subsequent to the neuroprotection study that the drug had all but disappeared from the brain and plasma by 6 hours, with a half life in the brain of ~2.7 hours. Although the concentration of AMN082 was almost at maximal levels in the brain at the time of lesioning, it could be the case that the short duration (resulting either from rapid metabolism or receptor internalisation) and intermittent activation of $mGlu_7$ was insufficient to elicit neuroprotection. This might particularly be the case for a lesion as rapid and severe as that following intranigral infusion of 6-OHDA, as was used in this study. Possible ways around these problems could be to repeat the study using a partial lesion model, such as striatal infusion of 6-OHDA, and/or by enhancing duration of exposure to AMN082, either by more frequent injections or by continuous infusion of the drug via a mini-pump. Enhanced frequency of exposure would likely require that the drug be delivered in a different vehicle as DMSO can cause local irritation and, at higher doses, systemic toxicity.

Finally, AMN082 is reported to have a rich pharmacology (explored in more detail below) that is in contrast to its proposed use as an $mGlu_7$-specific allosteric agonist (Sukoff Rizzo *et al.*, 2011). This includes appreciable affinities for the norepinephrine transporter (NET; K_i ~1300nM) and serotonin transporter (SERT; K_i ~3000nM), which may explain its reported efficacy as an anti-depressant or anxiolytic compound. It could not only underlie some of the acute side effects noted at higher doses but may also have had unanticipated modulatory effects on signalling in the BG that might have interfered with the intended action of AMN082 on glutamate release at the subthalamonigral synapse.

5.4.4 Pharmacokinetics of AMN082

When no neuroprotective effect was observed in the main study and the proposed measure of central pharmacological action of AMN082 – the open field test for anxiety –

proved inconclusive we wanted to definitively demonstrate that AMN082 was able to cross the BBB using the dosing formulation and route employed.

The pharmacokinetic study confirmed that AMN082 was brain penetrant when administered as an intraperitoneal injection in 8% DMSO. The brain C_{max} of 386.5ng/g (t_{max} = 1h) achieved following a dose of 10mg/kg i.p. AMN082 in rats is comparable to previous PK data following 10mg/kg AMN082 i.p. in mice (Sukoff Rizzo *et al.*, 2011), which reported a brain C_{max} of ~340ng/g (t_{max} = 0.5h). On the other hand the plasma C_{max} in the current study was only 101.8ng/ml (t_{max} = 0.5h), compared with ~430ng/ml (t_{max} = 0.5h) in the mouse study. This led to a calculated brain/plasma ratio of around 4.8 in rat compared with around 1.0 in mice, suggesting that AMN082 freely crosses the BBB in both species, but possibly accumulates in the brain tissue in rats.

The brain C_{max} measured in this study was equivalent to 984.8nM, which exceeds the EC_{50} value of AMN082 at $mGlu_7$ (260nM) and is close to the reported affinity of AMN082 at other targets such as α_1-Adrenoreceptor (K_i ~1000nM) and NET (K_i ~1300nM). While this implies that $mGlu_7$ receptor stimulation would have been achieved with this highest dose, stimulation of $mGlu_7$ by AMN082 concentrations ≥500nM has been associated with robust receptor internalisation in *in vitro* studies (Pelkey *et al.*, 2007), meaning that this effect may have been self-limiting, and as such a bell-shaped dose response curve would be anticipated. The plasma C_{max} measured in this study was equivalent to 259.4nM, which is within the range where it is specific for the $mGlu_7$ receptor according to the panel of receptors tested by Sukoff-Rizzo *et al.* (2011) and Mitsukawa *et al.* (2005).

This difference in brain/plasma ratio could be a simple species difference relating to factors such as enhanced protein binding of AMN082 in rat brain compared with mouse brain, however this is unlikely between two such closely-related species and in fact brain tissue binding in rat has been shown to correlate with other rodents, dogs, monkeys and even humans (Di *et al.*, 2011). There are also several technical reasons that could also possibly account for this discrepancy. The vehicle used for dosing in the present rat study was 8% DMSO in distilled water, compared with 10% Tween-80 in distilled water for the mouse study. DMSO is an amphiphilic molecule, allowing it to solubilise relatively insoluble lipophilic/hydrophobic compounds (such as AMN082) while also being soluble in water. It is widely used in biomedical research, particularly *in vitro*, but can also be used *in vivo* to aid passage of molecules across the blood-brain barrier (BBB). Though AMN082 is lipophilic and should therefore pass easily across cell membranes and into the brain, use of DMSO as

a vehicle could have aided this process, leading to a higher accumulation of AMN082 in the brain in the present study compared with the mouse study. Alternatively one or more of the steps involved in the collection and processing of blood samples or the preparation of plasma samples for analysis could have accelerated degradation of AMN082 in these samples, while leaving the brain samples unaffected. In future studies it might be possible to spike a known concentration of a standard compound with similar properties to the drug being tested into plasma samples (blanks and/or experimental). Any degradation of this internal standard compound might be expected to reflect degradation of the drug being analysed and therefore any enhanced degradation could be accounted for in future calculations,

In addition to measuring the concentration of AMN082, the concentration of its primary metabolite, Met-1, was also measured in the collected plasma and brain samples. Met-1 was reported by Sukoff-Rizzo *et al.* to have pharmacological activity at $mGlu_7$ (EC_{50} ~6000nM, over 20-fold less potent than AMN082 itself) and a wide variety of other targets, especially the monoaminergic transporters DAT, NET and SERT (K_i ~3000, ~3000 and ~300nM respectively). In contrast to the results reported in mice, where Met-1 was detected in plasma at C_{max} 494ng/ml 30 minutes after dosing with 10mg/kg AMN082, Met-1 was not detected in the present plasma samples at any time, potentially reflecting genuinely low levels, or alternatively reflecting sample degradation as was raised as a possibility for the lower than expected concentrations of AMN082 in these plasma samples. More importantly from the point of view of the present neuroprotection study, only very low concentrations of Met-1 were detected in brain homogenates (C_{max} = 32ng/g at 6 hours, equivalent to 141.4nM – around two-fold lower than its most potent reported affinity at SERT, EC_{50} = ~300nM), equating to around half the brain concentration of AMN082 at this time-point and less than 10% of the brain C_{max} for AMN082. This is in direct contrast to the brain Met-1 concentration following AMN082 administration in mice, where even as plasma Met-1 concentrations were diminishing the brain Met-1 concentrations increased over the duration of the 5-hour study, reaching a maximum concentration of 897ng/g (3963.8nM, which is above the K_i reported for this molecule at $mGlu_7$, SERT, DAT and NET). This implies that unlike in mice, any pharmacological effect of Met-1 would be expected to be minimal compared with that of AMN082 in the present rat neuroprotection study.

One of the main caveats of the PK study was that although brain penetrance was measured by a simple brain/plasma ratio calculation there was no measurement of the free fraction of drug in the brain. This might be especially important given that the brain/plasma ratio for AMN082 was high in rat, as accumulation of a drug in the brain can imply a high degree of binding to brain tissue (Reichel, 2006). Only unbound drug (not conjugated with proteins) will be free to interact with its targets, but both bound and unbound drug will be detected using the protocol employed here. In future PK studies the free drug concentration in the brain could be determined using microdialysis, or estimated by sampling of CSF rather than whole brain, in order to get a better idea of the bioavailability of AMN082. The side effects experienced following dosing of 10mg/kg AMN082 (tremors, rigidity) certainly demonstrate that free brain concentrations of AMN082 were adequate to elicit a pharmacological effect. These side effects are thought to be $mGlu_7$-independent as they are still present in mice where the receptor has been knocked out (Palucha *et al.*, 2007), so are likely explained by off-target activity. The receptor/transporter at which AMN082 shows its next highest binding affinities after $mGlu_7$ are α_1-adrenoreceptor and NET (K_i ~1000nM at each). Though the brain C_{max}, even if it was all unbound, did not exceed this concentration, noradrenergic signalling is known to alter BG output; for example noradrenaline can alter signalling in the SNr (Berretta *et al.*, 2000) and depletion of central noradrenaline (and other monoamines) underlies the akinetic and tremulous phenotype of the reserpine model of PD (Glow, 1959). Since a rigid, akinetic parkinsonian phenotype was the exact side effect noted in this study it is therefore conceivable that a sufficient fraction of the drug was unbound in the brain to enable meaningful interaction of AMN082 with these targets.

5.5 Conclusion

The results of the PK study demonstrate that AMN082 crosses the BBB into the brain following an intraperitoneal injection, possibly accumulating in the brain, with a reasonably short half life of ~2.7 hours. The observation of side effects at higher doses also suggests that AMN082 was centrally active, though this was not shown conclusively due to the interference of these side effects in the test that was designed to test this.

During the neuroprotection study the brain concentration of AMN082 was expected to be near-maximal at the time of infusion of 6-OHDA, giving the greatest opportunity for the drug to act at this pivotal moment, however the results of the study do not provide evidence for targeting $mGlu_7$ as a means of achieving neuroprotection in PD. On the other hand, due to the severity of the lesion model used in this study, the pulsatile exposure to AMN082 and the potential off-target effects of AMN082 that may have confounded the results, a potential role for $mGlu_7$ in providing neuroprotection in this disease cannot yet be ruled out.

The discovery of $mGlu_7$ antagonists such as MMPIP (Suzuki *et al.*, 2007) may help elucidate the importance of $mGlu_7$ by establishing whether these antagonists are able to counteract the well-established protective effects brought about by broad spectrum group III agonists such as L-AP4 and L-SOP *in vivo* (Austin *et al.*, 2010; Vernon *et al.*, 2005; Vernon *et al.*, 2006). However this may not be easy since both of these group III agonists have a very low potency at $mGlu_7$ compared with $mGlu_4$ and $mGlu_8$ and would need to be applied at high concentrations that would likely cause desensitisation of the other group III receptors. Therefore new subtype-specific pharmacological activators of $mGlu_7$ would certainly be of use in continuing these investigations.

6 Targeting $mGlu_4$ as a potential antidyskinetic approach in a rat model of levodopa-induced dyskinesia

6.1 Introduction

Levodopa-induced dyskinesia (LID) was introduced in section 1.5.1 and is a major limiting factor in the use of levodopa to treat Parkinson's disease. The combination of severe dopaminergic denervation and pulsatile exposure to levodopa is believed to underlie the development of this phenomenon in patients, and as such LID can be modelled preclinically by recapitulating these aspects in rodents or primates.

6.1.1 Preclinical modelling of LID

The main dopaminergic cell loss models used for evaluation of dyskinesia are the 6-hydroxydopamine lesioned hemiparkinsonian rodent and the MPTP-treated non-human primate (NHP). Repeated exposure of these denervated animals for two or more weeks to daily levodopa plus a peripheral DOPA decarboxylase inhibitor such as benserazide or carbidopa leads to development of abnormal involuntary movements (AIMs), which can be scored according to a variety of ratings scales (Breger *et al.*, 2013; Fox *et al.*, 2012). In the rodent these AIMs manifest unilaterally as axial (twisting of the head, neck and trunk), limb (repetitive or dystonic movements involving the forepaw and/or limb) and orolingual (vacuous chewing, tongue protrusion) phenomena on the side of the body contralateral to the lesion (Cenci *et al.*, 1998; Henry *et al.*, 1998). In NHPs LID is bilaterally expressed and manifests as choreic and dystonic movements of the limbs, especially the lower limbs, and flicking of the fingers, trunk dystonias and repetitive tongue protrusion (Clarke *et al.*, 1987; Pearce *et al.*, 1995).

The NHP model more accurately reflects the human expression of dyskinesia but ethical and practical considerations mean that the rat model is a valuable tool for preclinical research. The rat AIMs model has good face validity as a model of LID, but more importantly the predictive validity of the model is also thought to be good, with compounds with known antidyskinetic efficacy in humans and primates also able to reduce AIMs expression in rodents (Dekundy *et al.*, 2007). With regard to construct validity, research suggests that several mechanisms underlying the development of LID and AIMs in these models may also be applicable to the human condition. These mechanisms are explored below.

6.1.2 Striatal mechanisms underlying dyskinesia

The role of dopamine in the striatum is to alter the response of medium spiny neurones (MSNs) in both the direct and indirect pathways to corticostriatal input. The classical model of PD involves hyperactivation of the indirect (striatopallidal) MSNs, causing a downstream inhibition of thalamocortical feedback and therefore inhibiting motor function. The classical model of LID is the opposite scenario, whereby the presence of high concentrations of exogenous dopamine causes hyperactivation of the direct (striatonigral) MSNs, which increases thalamocortical feedback and produces exaggerated motor function. Dyskinesia is therefore believed to primarily involve chronic overactivation of striatonigral MSNs (Brotchie, 2005; Santini *et al.*, 2008) and there is a wealth of evidence for a particular role of dopamine D1 receptors (D1R) in the development of LID in both patients and preclinical models (Fiorentini *et al.*, 2013; Guigoni *et al.*, 2007; Konradi *et al.*, 2004; Mela *et al.*, 2012). However this is likely a simplistic view of dyskinesia. In reality the mechanisms involved may be considerably more complex (Jenner, 2008) and a role for the indirect pathway cannot be ruled out, especially as both D1R and D2R agonists can provoke dyskinesia in primed monkeys (Blanchet *et al.*, 1993). In addition there is recent evidence that abnormal expression of the D3R in the striatum may also play an important role in the development and expression of dyskinesia (Bézard *et al.*, 2003; Cote *et al.*, 2014; Visanji *et al.*, 2009), further implicating the indirect pathway.

The striatonigral GABAergic projection is a point of convergence for, and is therefore modulated by, multiple neurotransmitter systems that have been shown to be pathologically altered in dyskinetic individuals. The major input to the BG involves release of glutamate from corticostriatal neurones, and together with dopamine and the modulatory activity of other neurotransmitters such as serotonin, this determines the activity of the output nuclei: the globus pallidus internus (GPi) and substantia nigra pars reticulata (SNr). There is evidence from animal models that this corticostriatal glutamate release is increased in LID (Nevalainen *et al.*, 2013; Robelet *et al.*, 2004), alongside alterations in expression (Hallett *et al.*, 2005; Konradi *et al.*, 2004; Ouattara *et al.*, 2011; Ouattara *et al.*, 2010; Samadi *et al.*, 2008), phosphorylation (Ba *et al.*, 2011; Kong *et al.*, 2009; Oh *et al.*, 1998) and distribution (Gardoni *et al.*, 2006; Silverdale *et al.*, 2010) of glutamate receptors, including GluN1/GluN2B NMDA receptors and metabotropic glutamate receptor 5 ($mGlu_5$), that facilitate increased signalling across this synapse. Morphological alterations indicative of increased glutamatergic transmission are also present, including decreased dendritic spine density and increased spine size in MSNs of

the direct pathway (Nishijima *et al.*, 2013). This is borne out in human LID, where abnormal glutamatergic transmission has been described in the caudate, putamen and motor cortex (Ahmed *et al.*, 2011), alongside increased putaminal expression of GluN1/GluN2B NMDA receptors (Calon *et al.*, 2003) and $mGlu_5$ (Ouattara *et al.*, 2011). Activation of extrasynaptic GluN2B-containing NMDA receptors has particularly been implicated in the development of LID (Gardoni *et al.*, 2006).

The effect of this abnormal glutamatergic transmission may be compounded by the consequences of dysregulated release of dopamine from serotonergic terminals within the striatum (Santiago *et al.*, 1998), leading to abnormal temporal activation of dopamine receptors. These receptors are expressed on striatonigral MSNs as well as in cortical dopaminergic systems, which have also been implicated in the pathophysiology of dyskinesia (Halje *et al.*, 2012). There are some reports of altered D1R expression or trafficking in LID (Guigoni *et al.*, 2007; Hurley *et al.*, 2001), but evidence suggests that the key mechanism in dyskinesia is increased functional sensitivity of these receptors (Aubert *et al.*, 2005; Bezard *et al.*, 2005; Corvol *et al.*, 2004).

Whatever the exact mechanism behind increased D1R signalling, stimulation of these receptors causes activation of the cyclic AMP (cAMP) / Protein Kinase A (PKA) / DARPP-32 (Dopamine- and cAMP-Regulated Phosphoprotein, 32KDa) / Protein phosphatase 1 (PP-1) pathway and the mitogen activated protein kinase (MAPK) pathway, which culminates in phosphorylation of extracellular signal related kinase (ERK1/2) (Neve *et al.*, 2004). This results in DNA modifications (Nicholas *et al.*, 2008; Santini *et al.*, 2009) and increased expression of transcription factors, especially ΔFosB/FosB (Andersson *et al.*, 2001), which are indicative of long-term cellular adaptations.

Both NMDA and $mGlu_5$ receptors are known to closely interact with D1R (Oh *et al.*, 1998; Oh *et al.*, 1999) and with each other (Conn *et al.*, 2005; Fiorentini *et al.*, 2008), activating common downstream mediators such as PKA and ERK1/2 (Tang *et al.*, 2000; Voulalas *et al.*, 2005). Therefore the increased expression of these receptors alongside enhanced D1R signalling will co-operate to augment striatonigral signalling in LID. In addition, activation of D1R in combination with enhanced activation of NMDA receptors by glutamate leads to long term potentiation-like phenomena, and may explain the lack of depotentiation seen in the dyskinetic versus non-dyskinetic denervated striatum (Picconi *et al.*, 2003), leading to an exaggerated response to normally irrelevant stimuli. The pathological overactivation of the direct pathway leads to GABA bursting in the SNr and GPi (Mela *et al.*, 2012), thus

disinhibiting thalamocortical feedback and leading to the hyperkinetic movements characteristic of LID.

Striatal glutamatergic and dopaminergic transmission can be modulated by several other neurotransmitters. For example, increased serotonergic innervation of the striatum along with altered expression of several 5-HT receptor subtypes (Riahi *et al.*, 2012; Riahi *et al.*, 2013) has been demonstrated in animal and human LID (Rylander *et al.*, 2010b; Zeng *et al.*, 2010). Importantly, activation of serotonin 5-HT_{1A} receptors has been shown to reduce corticostriatal glutamate release (Antonelli *et al.*, 2005; Dupre *et al.*, 2011), and also negatively regulates release of dopamine as a false neurotransmitter from serotonergic terminals (Carta *et al.*, 2007). Similarly the endocannabinoid system may play a role in LID as activation of CB_1 receptors has been shown to negatively regulate corticostriatal glutamate release (Gubellini *et al.*, 2002; Kofalvi *et al.*, 2005) and also reduce D1R-mediated responses (Martin *et al.*, 2008; Martinez *et al.*, 2012; Meschler *et al.*, 2001). Consequently, molecules such as serotonin receptor 5-HT_{1A} and 5-HT_{1B} agonists (Bezard *et al.*, 2013; Bibbiani *et al.*, 2001; Iravani *et al.*, 2006; Munoz *et al.*, 2009; Munoz *et al.*, 2008) and endocannabinoid receptor agonists (Fox *et al.*, 2002; Morgese *et al.*, 2007; Walsh *et al.*, 2010) have shown antidyskinetic efficacy in preclinical models, and also in clinical trials against human LID (Bonifati *et al.*, 1994; Sieradzan *et al.*, 2001).

6.1.3 Extrastriatal mechanisms of dyskinesia

As well as striatal alterations, there is also evidence from pharmacological studies suggesting that modulation of neurotransmission elsewhere in the BG and in areas of the cortex may also contribute to LID. Systemically active drugs could therefore produce antidyskinetic effects through actions at more than one key synapse. For example antagonists of $mGlu_5$, which are currently in clinical trials as antidyskinetic agents (Berg *et al.*, 2011; Kumar *et al.*, 2013), may exert their effects not only in the striatum but also in the subthalamic nucleus (Maranis *et al.*, 2012). Targeting of 5-HT_{1A} receptors in the subthalamic nucleus (Marin *et al.*, 2009) or primary motor cortex (Ostock *et al.*, 2011) also attenuates dyskinesia, as does activation of 5-HT_{1B} receptors (Jaunarajs *et al.*, 2009; Zhang *et al.*, 2008), which are not only present in the striatum but also on GABAergic MSNs terminating in the SNr, where their activation can inhibit GABA release (Stanford *et al.*, 1996). Alongside the striatal actions already mentioned, another potential mechanism to explain the efficacy of CB_1 agonists is potentiation of striatopallidal signalling via inhibition of GABA reuptake (Sieradzan *et al.*, 2001), which would help to rebalance a hyperactivation of striatonigral signalling. Opioid signalling, which is known to be altered in LID (Aubert *et al.*, 2007; Chen

et al., 2005a; Johansson *et al.*, 2001), can modulate transmitter release at several synapses within the BG, for example inhibition of striatopallidal GABA release (Ogura *et al.*, 2000), and inhibition of glutamate and GABA release into the SNr (Mabrouk *et al.*, 2009). Targeting several opioid receptor subtypes has shown antidyskinetic efficacy (Cox *et al.*, 2007; Henry *et al.*, 2001; Ikeda *et al.*, 2009; Koprich *et al.*, 2011), but their role is complex and the effects of opioid-targeted approaches may be dose-dependent (Mabrouk *et al.*, 2009).

6.1.4 Induction and maintenance of LID

The development or induction of dyskinesia by repeated exposure to L-DOPA involves the sensitisation of various neurotransmitter systems. This plasticity involves elements such as alterations in receptor distribution and sensitisation of downstream signalling pathways as well as morphological synaptic/dendritic alterations (explored earlier). This process of priming is thought to be facilitated by the parkinsonian state, hence the requirement for extensive nigrostriatal denervation when modelling dyskinesia in rodents or primates.

Once dyskinesia has been established, the brain seems to maintain its primed state, such that even taking an L-DOPA-free 'drug holiday' only results in a short-lived decrease in dyskinesia that is thought to be predominantly due to a transient decrease in the required therapeutic dose of L-DOPA (Feldman *et al.*, 1986; Koller *et al.*, 1981; Weiner *et al.*, 1980).

The temporal involvement of changes in these various neurotransmitter systems have not yet been fully elucidated, but can be tentatively inferred from the ability of pharmacological interventions to either inhibit the priming process and/or to suppress or reverse the expression of dyskinesia in already-primed animals.

6.1.5 Targeting glutamate as a therapeutic option for LID

As described above, modulations in glutamate signalling including altered neurotransmitter release and receptor expression and distribution are highly implicated in the development and expression of LID in both patients and preclinical models. Indeed the only therapy widely used for treatment of LID is amantadine, a low affinity non-competitive antagonist of the NMDA receptor. Despite positive results from several clinical trials (del Dotto *et al.*, 2001; Luginger *et al.*, 2000; Sawada *et al.*, 2010; Snow *et al.*, 2000) there is some disagreement as to the duration of efficacy of amantadine (Thomas *et al.*, 2004; Verhagen-Metman *et al.*, 1999; Wolf *et al.*, 2010) and therefore whether or not there is sufficient evidence to support its use for this condition (Crosby *et al.*, 2003; Elahi *et al.*, 2012). Nevertheless it is licensed by the US Food and Drug Administration for treatment of LID,

and is also included in the 2010 European Federation of Neurological Societies recommendations for management of LID (Ferreira *et al.*, 2013). In light of the support for amantadine it is perhaps not surprising that several alternative glutamate-targeted approaches have been proposed as potential antidyskinetic therapies, and these are discussed here.

AMPA: There is some evidence suggesting that blockade of AMPA receptor-mediated signalling may be effective at reducing the induction and expression of dyskinesia in preclinical animal models (Kobylecki *et al.*, 2010; Konitsiotis *et al.*, 2000; Maranis *et al.*, 2012). As yet this has not translated into the clinic, where several clinical trials have failed to report a reduction in motor complications in treated patients (Eggert *et al.*, 2010; Lees *et al.*, 2012; Rascol *et al.*, 2012).

NMDA: Enhancement of NMDA-mediated signalling plays a central role in the development and expression of LID, and as such is an obvious therapeutic target. In addition to amantadine (Dekundy *et al.*, 2007) there are several other NMDA antagonists that have been reported to have antidyskinetic efficacy in both animal models and patients. These include Dextromethorphan (Verhagen-Metman *et al.*, 1998), MK-801 (Papa *et al.*, 1995; Wu *et al.*, 2013) and LY235959 (Papa *et al.*, 1996). However due to concerns about side effects associated with long-term indiscriminate inhibition of NMDA receptors, such as cognitive deficits (Newcomer *et al.*, 2001) and possible motor side effects at effective doses (Paquette *et al.*, 2010), recent efforts have been directed at specific inhibition of NMDA receptors containing the GluN2B subunit, which have been shown to be expressed at higher levels in dyskinetic models (Hurley *et al.*, 2005) and patients (Calon *et al.*, 2003). NR2B-specific antagonists have shown antidyskinetic efficacy in preclinical models, inhibiting both the development (Hadj Tahar *et al.*, 2004; Morissette *et al.*, 2006; Wessell *et al.*, 2004) and expression of dyskinesia (Blanchet *et al.*, 1999; Wessell *et al.*, 2004). This success has translated to the clinic (Nutt *et al.*, 2008), however not without the presence of similar adverse events to those experienced with broad spectrum NMDA antagonists, including amnesia. There is also some disagreement regarding whether GluN2A or GluN2B receptor subunits are the major player in dyskinesiogenesis, with some groups reporting that GluN2B antagonists may in fact exacerbate dyskinesia under certain circumstances (Nash *et al.*, 2004; Quintana *et al.*, 2012) and that inhibition of GluN2A-containing NMDA receptors may therefore be a better therapeutic option (Gardoni *et al.*, 2012; Hallett *et al.*, 2005).

mGluR: Regarding metabotropic glutamate receptors, most interest has been directed at the group I receptor $mGlu_5$, and several antagonists at this receptor have shown antidyskinetic efficacy in rodent (Gravius *et al.*, 2008; Levandis *et al.*, 2008; Mela *et al.*, 2007) and primate (Bezard *et al.*, 2014; Grégoire *et al.*, 2011; Johnston *et al.*, 2010; Morin *et al.*, 2013; Rylander *et al.*, 2010a) models of LID, for inhibiting both dyskinesia development and expression. $mGlu_5$ antagonists have now entered clinical trials, where antidyskinetic efficacy has been reported (Berg *et al.*, 2011; Kumar *et al.*, 2013; Stocchi *et al.*, 2013), and this is extremely promising.

Within group III, at the outset of the studies reported in this chapter there was one previous published report that activation of $mGlu_4$ receptors in the rodent AIMs model can reduce the development of dyskinesia when LSP1-2111 was administered alongside L-DOPA (Lopez *et al.*, 2011) but attempts to use $mGlu_4$ agonists or PAMs to reverse established dyskinesia had been unsuccessful thus far (Le Poul *et al.*, 2012; Lopez *et al.*, 2011).

6.1.6 Considerations when testing novel antidyskinetic therapies

When testing antidyskinetic therapies preclinically or in clinical trials it is important to establish that the actions of the drug are directed only against the abnormal dyskinetic movements elicited by L-DOPA, without any inhibitory effects against the normal antiparkinsonian actions of L-DOPA.

For example several proposed antidyskinetic therapies have been found to reduce the antiparkinsonian effects of L-DOPA, meaning that at certain doses a general inhibitory effect on motor function could underlie the antidyskinetic effect observed. These include drugs targeting glutamatergic (Johnston *et al.*, 2010; Paquette *et al.*, 2010), serotonergic (Bezard *et al.*, 2013; Goetz *et al.*, 2007; Iravani *et al.*, 2006), cannabinoid (Walsh *et al.*, 2010) and opioid (Cox *et al.*, 2007) signalling.

On the other hand, a drug that can potentiate the antiparkinsonian effects of L-DOPA could minimise the development of dyskinesia by enabling the same therapeutic effect of L-DOPA to be elicited with a lower dose of L-DOPA, which in itself would be expected to reduce the incidence and/or expression of dyskinesia. These so-called L-DOPA-potentiating effects have been reported for therapies targeting glutamatergic (Grégoire *et al.*, 2011; Klockgether *et al.*, 1990; Le Poul *et al.*, 2012) and adenosine (Kanda *et al.*, 2000; Kulisevsky *et al.*, 2002; Rose *et al.*, 2006) signalling.

6.1.7 Hypothesis and aims

Dyskinesia has been shown to be inhibited by reduction of glutamatergic transmission, as demonstrated by the efficacy of antagonists of NMDA and $mGlu_5$ receptors in both preclinical models and in patients. Activation of $mGlu_4$ receptors has also been shown to reduce glutamatergic transmission at the corticostriatal synapse (Cuomo *et al.*, 2009), a key synapse implicated in the development and maintenance of dyskinesia. We therefore hypothesise that:

Activation of $mGlu_4$ receptors using positive allosteric modulators will have antidyskinetic efficacy when administered in conjunction with L-DOPA.

The aims of this set of experiments were to:

- Define several pharmacokinetic characteristics of the novel $mGlu_4$ PAMs that were to be tested in the dyskinesia studies when they are administered as an oral solution.
- Verify that we were able to model dyskinesia in rats using a combination of a medial forebrain bundle lesion and repeated exposure to L-DOPA, and characterise the development of the phenotype.
- Determine a positive control compound and dose that could suppress the expression of AIMs once established.
- Test whether established AIMs could be wholly or partially reversed using positive allosteric modulators of $mGlu_4$ in this model.
- Test whether the rotational effect of L-DOPA in this model, as a measure of antiparkinsonian efficacy, was potentiated or inhibited by $mGlu_4$ PAMs. This is especially important as targeting glutamatergic transmission has been shown to potentiate the antiparkinsonian actions of L-DOPA in some studies but to inhibit them in others.
- Test whether concurrent administration of L-DOPA with a positive allosteric modulator of $mGlu_4$ could inhibit the development of L-DOPA-induced AIMs in lesioned but L-DOPA-naive rats.

6.2 Materials and Methods

6.2.1 Compounds tested

Table 13 shows the structures of the drugs used in the AIMs studies outlined in this chapter. 8-OH-DPAT and amantadine are compounds with proven antidyskinetic efficacy in preclinical models and in human LID. AF42744 and LuAF21934 are novel $mGlu_4$ PAMs. These compounds were both tested for their ability to reverse established AIMs, and LuAF21934 was additionally tested for its ability inhibit the development of AIMs, in the rat model.

Table 13: Structures of the drugs tested for antidyskinetic efficacy in rats with L-DOPA-induced AIMs.

Structure	Name	Target
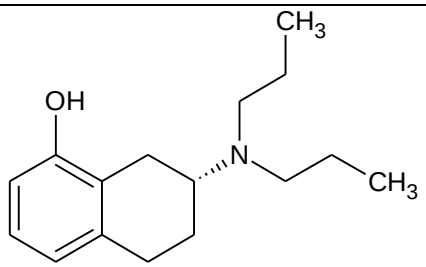	8-OH-DPAT *(R)-(+)-2-Dipropylamino-8-hydroxy-1,2,3,4-tetrahydronaphthalene*	5-HT_{1A} receptor agonist
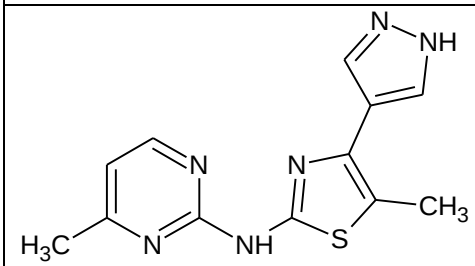	AF42744 (ADX88178) *5-Methyl-N-(4-methylpyrimidin-2-yl)-4-(1H-pyrazol-4-yl)thiazol-2-amine*	$mGlu_4$ Positive Allosteric Modulator
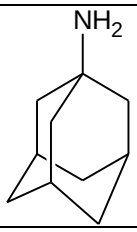	Amantadine *Adamantan-1-amine*	Weak NMDA receptor antagonist
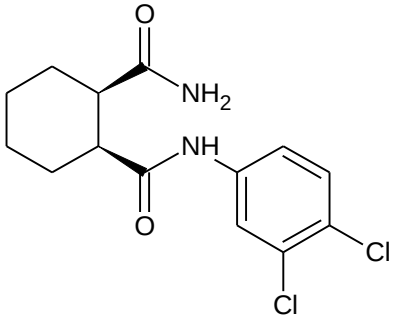	LuAF21934 *(1S, 2R)-N^1-(3,4-dichlorophenyl)-cyclohexane-1,2-dicarboxamide*	$mGlu_4$ Positive Allosteric Modulator

AF42744 (ADX88178) was developed by Addex Therapeutics and is highly potent and selective, with an EC_{50} at human $mGlu_4$ of 4nM and at rat $mGlu_4$ of 9nM (Célanire *et al.*, 2011; Le Poul *et al.*, 2012). It has been shown to potentiate the effects of L-DOPA in the adjusted stepping test in 6-OHDA-lesioned rats and in an ambulation test in MitoPark® mice, suggesting a potential antiparkinsonian action, however no reversal of established AIMs was found for doses of 0.1, 1 or 10 mg/kg (Le Poul *et al.*, 2012). Its antidyskinetic effects have not yet been tested at higher doses. In addition to $mGlu_4$, AF42744 demonstrates activity at other receptors such as $mGlu_6$ (EC_{50}>10µM), $mGlu_8$ (EC_{50} = 2.2µM) and adenosine A_1 and A_3 receptors (K_i = ~2.2µM) (Le Poul *et al.*, 2012). Of these potential off-target effects, there is some evidence that reduction of signalling at adenosine A_1 receptors attenuates AIMs in mice (Xiao *et al.*, 2011) so this could potentially come into play if concentrations were to approach 2.2 µM.

LuAF21934 was developed by Lundbeck as a more brain-penetrant variant of the Vanderbilt $mGlu_4$ PAM VU0155041 (which was used in one of the neuroprotection studies reported in Chapter 2). It has an EC_{50} of 500-636nM at human $mGlu_4$ (Bennouar *et al.*, 2013; Doller *et al.*, 2010), but its potency at rat $mGlu_4$ has not been reported. In addition to its activity at $mGlu_4$, LuAF21934 is an inhibitor of adenosine A_{2A} receptors with a K_i of 7µM. Antagonists at this receptor have been reported to inhibit the induction and expression of AIMs in primates (Bibbiani *et al.*, 2003) and in mice (Xiao *et al.*, 2006) so at certain concentrations LuAF21934 could potentially exert a dual antidyskinetic effect. However the effects of adenosine A_{2A} receptor antagonists on dyskinesia in clinical trials have been mixed (Kulisevsky *et al.*, 2002; Mizuno *et al.*, 2013) so whether any off-target effects on these receptors by LuAF21934 would be antidyskinetic is uncertain.

6.2.1.1 Drug formulation

AF42744 and LuAF21934 were synthesised, characterised and provided by Lundbeck (Copenhagen, Denmark). Both drugs were formulated in PEG-400 obtained from Sigma Aldrich (Poole, UK).

6.2.2 Other materials

6.2.2.1 Experimental materials

Drugs used for lesioning and peri-operative care, and for behavioural testing were obtained as outlined in Chapter 2 (section 2.2.2.1).

Benserazide hydrochloride and L-DOPA methyl ester hydrochloride for priming were obtained from Sigma Aldrich (Poole, UK) and were formulated in sterile saline (Aquapharm) corrected for salt weight. (R)-(+)-8-OH-DPAT hydrobromide and amantadine hydrochloride were also obtained from Sigma Aldrich (Poole, UK) and were formulated in sterile saline (Aquapharm) uncorrected for salt weight.

6.2.2.2 Analytical materials

Perfusions: Phosphate buffered saline (PBS) and 10% buffered formalin were obtained from Sigma Aldrich (Poole, UK). 4% paraformaldehyde was obtained from Pioneer Research Chemicals.

HPLC for striatal dopamine: Dopamine content was analysed by High Performance Liquid Chromatography (HPLC) at King's College London. The materials used were as described in section 2.2.3.2.

TH immunohistochemistry: The tyrosine hydroxylase (TH) immunohistochemistry materials used were as described in section 2.2.3.2.

UPLC-MS/MS for PK studies: Brain and plasma samples for the PK studies were analysed by Ultra-high Performance Liquid Chromatography with tandem Mass Spectrometry (UPLC-MS/MS) at Lundbeck (Copenhagen, Denmark). 2-propanol, acetonitrile (ACN), ammonium hydroxide, dimethylsulfoxide (DMSO) and formic acid used for brain and plasma sample preparation and UPLC-MS/MS were obtained from Sigma Aldrich (Poole, UK or St. Louis, MO).

6.2.3 Pharmacokinetic testing of LuAF21934, AF42744 and Amantadine

All procedures were performed in accordance with the U.K. Animals (Scientific Procedures) Act, 1986.

Several PK studies were carried out:

- (PK1) a plasma time course of LuAF21934 and AF42744 in naive rats.
- (PK2) a single 2-hour time plasma and brain point for both LuAF21934 and AF42744 at the end of the AIMs reversal study to determine the brain/plasma ratio.
- (PK3) a single 90-minute plasma and brain time point for 40mg/kg amantadine in naive rats.

PK1 was carried out at H. Lundbeck A/S (Copenhagen, Denmark). PK2 and PK3 were carried out at King's College London.

6.2.3.1 Drug formulation and dosing

For LuAF21934 and AF42744 studies (PK1 and PK2), solutions of 10mg/kg or 30mg/kg were formulated in PEG-400 (5ml/kg for PK1, 3ml/kg for PK2) and administered by oral gavage (n=3 per dose per time point) to male Sprague-Dawley rats within an hour of formulation. For PK1, blood samples were collected at 5 minutes, 20 minutes, 1, 2, 4 and 6 hours after dosing. For PK2, blood and brain samples were collected 2 hours after dosing.

For the amantadine brain/plasma ratio study (PK3), a single solution of 40mg/kg amantadine.HCl was made up as a 1ml/kg solution in sterile saline. It was administered as a single subcutaneous injection and blood and brain samples were collected 90 minutes after dosing.

6.2.3.2 Sample collection

PK1: Serial blood samples (~200µl/time point) were collected from the tail vein into EDTA-coated tubes. Blood samples were centrifuged at 3300 x g for 10 minutes at 4°C to separate the cells from the plasma, and the plasma was removed and snap-frozen on dry ice to await analysis.

PK2 and PK3: Rats were deeply anaesthetised with isoflurane and a blood sample withdrawn by cardiac puncture and placed into a Lithium-heparin coated tube (Sarstedt). Blood samples were centrifuged at 2000 x g for 10 minutes at room temperature to separate the cells from the plasma, and the plasma was removed and snap-frozen on dry

ice to await analysis. Immediately following cardiac puncture, rats were decapitated and the brain was removed from the skull, weighed and snap-frozen on dry ice to await analysis.

6.2.3.3 Bioanalysis

Plasma samples for all studies were prepared for analysis at Lundbeck (Copenhagen, Denmark). Brain samples for PK2 were prepared at Lundbeck. Brain samples for PK3 were prepared at King's College London 24 hours after collection using an identical protocol. All brain and plasma samples were analysed by UPLC-MS/MS at Lundbeck.

Brain sample preparation: Brains were homogenised in 4 volumes of homogenisation buffer comprising a 5:3:2 v/v/v ratio of HPLC water, 2-propanol and DMSO. Homogenates were centrifuged at 2700xg for 20 minutes at 4°C and the resulting supernatant removed into a 96-well plate for analysis.

Plasma sample preparation: 25µl plasma samples were protein-precipitated with 150µl ACN containing 5ng/ml internal standard (Lundbeck compound LuAE90074). Samples were centrifuged at 6200 x g for 20 minutes at 4°C and 100µl supernatant removed. This supernatant was diluted 1:1 with 100µl water containing either 0.1% ammonium hydroxide (for LuAF21934 analysis) or 0.1% formic acid (for AF42744 and amantadine analysis).

Analysis by UPLC-MS/MS: Drug concentrations were determined using UPLC-MS/MS. For all analytes, gradient UPLC was carried out, with a phase 1 to phase 2 transition time of 3 minutes. Mobile phase 1 consisted of water with 0.1% ammonium hydroxide (for analysis of LuAF21934) or 0.1% formic acid (for analysis of AF42744 or amantadine); mobile phase 2 consisted of ACN with 0.1% ammonium hydroxide (for analysis of LuAF21934) or 0.1% formic acid (for analysis of AF42744 or amantadine). Different analytical columns were used for each analyte: for analysis of LuAF21934 an Acquity UPLC BEH Phenyl column 1.7µm, 2.1 x 30mm (Waters, MA) was used, for analysis of AF42744, a C18SB HSS 1.8µm, 30mm x 2.1mm column (Waters, MA) was used and for analysis of amantadine a C8 BEH 1.7µm, 50mm x 2.1mm column (Waters, MA) was used. Detection was performed using a Sciex-API 4000 MS (Applied Biosystems, NL) using electrospray with positive ionization mode.

For all analytes, the limit of detection was 1ng/ml in plasma and 5ng/g in brain. The peak area correlated linearly with the plasma and brain concentration of the analytes in the range of 1-1000ng/ml plasma and 5–5000ng/g brain (corrected for dilution). If the

plasma/brain sample drug concentration was above 1000ng/ml or 5000ng/g, the sample was diluted appropriately in blank plasma/blank brain homogenate before repeat analysis.

6.2.4 General methods: AIMs studies

All procedures were performed in accordance with the U.K. Animals (Scientific Procedures) Act, 1986.

6.2.4.1 MFB Lesioning

Male Sprague-Dawley rats (270-300g, Harlan, UK) were maintained in a temperature- and humidity-controlled environment with a 12-hour light-dark cycle and *ad libitum* access to chow and tap water.

Following baseline cylinder and adjusted steps measurements (described in section 2.2.3.3), rats were lesioned in the left MFB. 12.5µg 6-OHDA.HCl in 2.5µl 0.2% ascorbate in 0.9% saline was infused into the MFB at -2.6mm AP, +2.0mm ML and -8.8mm DV from bregma (Figure 75) at a rate of 0.5µl/min using a 25G injection needle. Where used, sham animals received an infusion of the vehicle only. Following infusion the injection needle was allowed to remain in place for a further 5 minutes to prevent reflux. Rats were pre-treated 30 minutes before lesioning with 5mg/kg pargyline and 25mg/kg desipramine (i.p.) to inhibit extracellular metabolism of 6-OHDA by monoamine oxidase B and to block the norepinephrine transporter to ensure selective uptake of the toxin into dopaminergic cells respectively. Peri-operative and post-operative care was provided as described previously in Chapter 2.

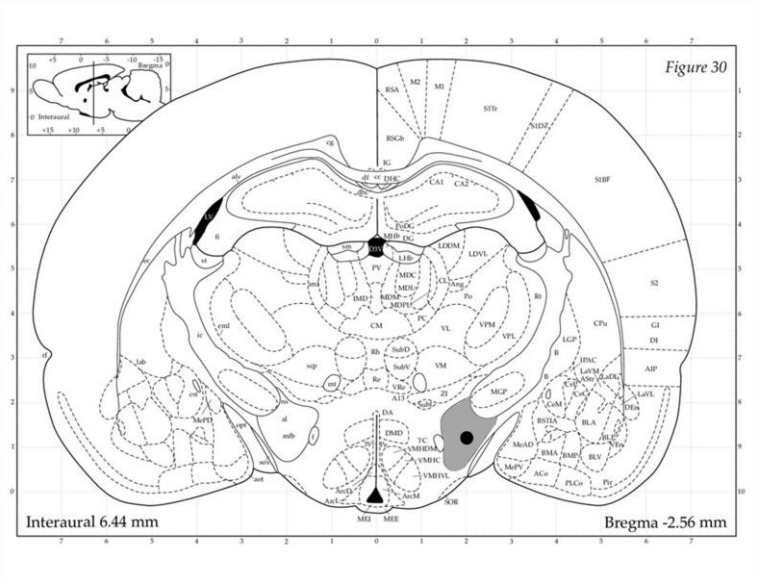

Figure 75: Approximate co-ordinates for 6-OHDA infusion for the MFB lesions. The anteroposterior level shown is 2.56mm posterior of Bregma, whereas the co-ordinates employed were 2.6mm posterior of Bregma, however the positioning of the MFB is comparable. The coronal diagram was obtained from The Rat Brain in Stereotaxic Coordinates (Paxinos *et al.*, 1998). The grey shaded region is the MFB and the black spot represents the positioning of the tip of the infusion needle.

6.2.4.2 Behavioural assessment

After 2 weeks' recovery time, the extent of the lesion was assessed using the cylinder test, adjusted steps test (exploratory study only) and apomorphine- or amphetamine-induced rotations. These tests are briefly described below, but can be found in more detail in section 2.2.3.3.

For the cylinder test (Schallert *et al.*, 2000a) rats were placed in a clear Perspex cylinder of 21cm diameter and 34cm height and video-recorded for 5 minutes. Supporting paw touches during exploratory rearing were scored as ipsi, contra or both paws. Percentage use of each paw was compared between groups.

In the adjusted steps test (Olsson *et al.*, 1995) rats were held such that they were resting their weight on a single forepaw on the edge of a table. The rat was then moved along a 90cm distance over 5 seconds and the number of adjusting steps taken was counted in triplicate for each paw in both the forehand and backhand directions. Post-lesion performance (number of steps) is expressed as a percentage of pre-lesion performance for both the ipsilateral and contralateral paws.

Apomorphine- or amphetamine-induced rotations were measured automatically in enclosed rotometer chambers, where rats are tethered to a rotational encoder that monitors turning in both directions. Following 30 minutes' habituation, rats received a subcutaneous dose of 0.5mg/kg apomorphine or an intraperitoneal dose of 2.5mg/kg amphetamine and their induced rotation was recorded for 120 minutes thereafter using RotoRat software (MedAssociates Inc).

6.2.4.3 Assessment of AIMs

In all experiments, AIMs were assessed at intervals during the priming period. Where applicable AIMs were also assessed following stable establishment of dyskinesia, for example for testing of putative antidyskinetic compounds. The details of the timings of assessments within each study are shown in the relevant methods sections.

Within each testing session, AIMs were assessed according to the criteria first described by Cenci et al. (Cenci *et al.*, 1998) and later modified by Winkler et al. (Winkler *et al.*, 2002). Rats were placed in a clear Perspex cylinder 40cm high and 40cm in diameter. After a baseline period of 30 minutes to acclimatise to the equipment, rats were scored for their baseline AIMs expression. Following the administration of L-DOPA, rats were scored for a period of one minute out of every 20 to follow the time course of the expression of L-

DOPA-induced AIMs. Rats were generally scored for 180 minutes after L-DOPA administration. In some instances, for example when testing L-DOPA alongside amantadine, the rats had not returned to baseline by 180 minutes so in this instance scoring was continued every 20 minutes until they returned to baseline.

Scores during each 1-minute recording period were allocated for both duration and severity of the three AIMs subtypes; axial, forelimb and orolingual, and were defined thus:

Duration (from Cenci et al. 1998)

Score	**0**	**1**	**2**	**3**	**4**
Duration (all subtypes)	Absent	Occasional <50% time	Frequent > 50% time	Continuous but **can** be interrupted by sensory stimuli	Continuous and **cannot** be interrupted by sensory stimuli

Severity (from Winkler et al. 2002)

Score	**0**	**1**	**2**	**3**	**4**
Axial	Absent	Consistent lateral deviation of the head & neck >30°	Consistent lateral deviation of the head & neck 30°<x<60°	Lateral deviation/torsion of head, neck & upper trunk >60°	Torsion of head, neck & trunk causing loss of balance
Forelimb	Absent	Low amplitude movements involving the paw	Low amplitude movements involving the paw and distal limb	Movements involving the paw, distal and proximal limb	Vigorous or ballistic movements of large amplitude involving the whole limb and shoulder
Orolingual	Absent	Vacuous chewing	Tongue protrusion	-	-

Sensory stimuli used to interrupt the rats comprised a sharp double tap with a pen on the top and side of the Perspex cylinder close to the rat's position. An example of a rat displaying AIMs is shown in Figure 76.

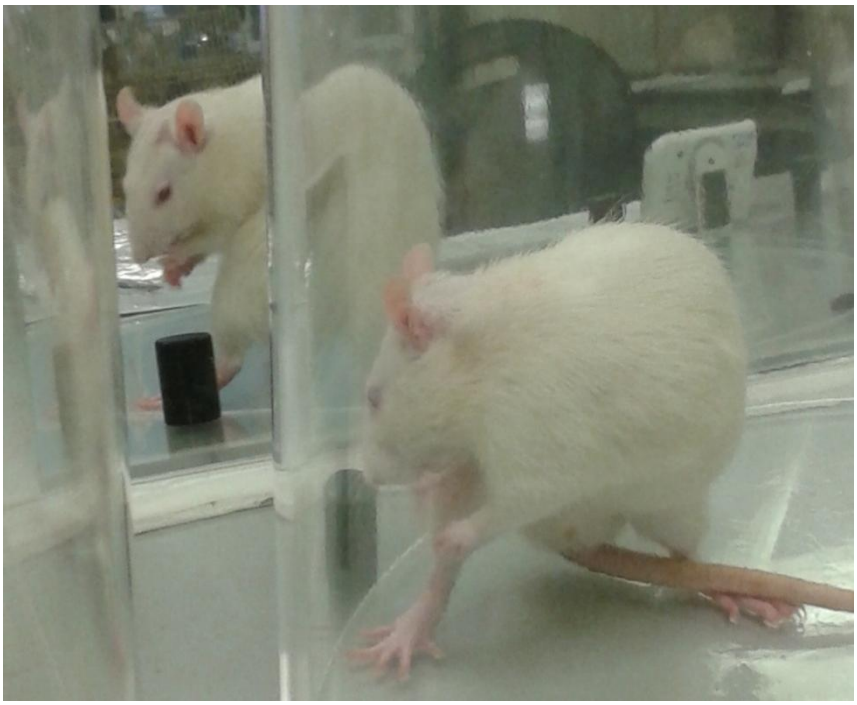

Figure 76: A rat displaying AIMs following a MFB lesion and 21 days of daily administration of 6.25mg/kg L-DOPA + 15 mg/kg benserazide. The axial twisting away from the side of the lesion can clearly be seen, along with a slightly open mouth from the chewing motion of orolingual AIMs. Although not visible from this picture, the right forelimb makes circling or stirring movements.

The theoretical maximum score that could be obtained by any rat over a 3-hour scoring period was 360, comprising a maximum 144 for the axial subtype (max duration 4 x max severity 4 x 9 time points), a maximum of 144 for the limb subtype (max duration 4 x max severity 4 x 9 time points) and a maximum of 72 for the orolingual subtype (max duration 4 x max severity 2 x 9 time points). Within any given time point the maximum score that could be obtained was 40.

6.2.4.4 Blinding

Exploratory study: Scoring of AIMs in the presence of known antidyskinetic compounds was not blinded.

Reversal study: Scoring of AIMs during the antidyskinetics testing on weeks 6 and 8 was blinded. LuAF21934 or AF42744 and vehicle solutions were formulated daily by the

experimenter to maintain consistency, and the vials were then blinded by another person such that they were labelled A, B and C. Scoring of AIMs during testing with amantadine was also performed blinded, with the amantadine and vehicle solutions prepared by the experimenter, which were then relabelled A and B by another person.

Induction study: Scoring of AIMs during the induction study was performed blinded. As for the reversal study, vehicle and LuAF21934 solutions were formulated daily by the experimenter to maintain consistency, and the vials were then blinded by another person such that they were labelled A, B and C.

6.2.5 Methods specific to Exploratory Study

Figure 77 shows the plan for the AIMs exploratory study.

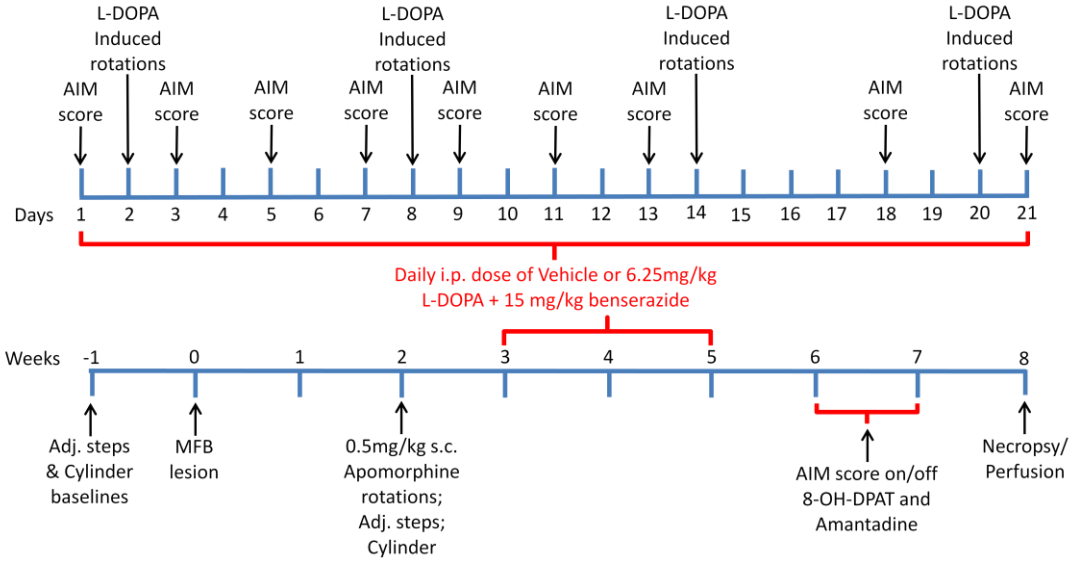

Figure 77: Study plan for the AIMs exploratory study. The weekly time-line is shown in the lower section of the diagram and a break-down of the AIMs scoring during the 3-week priming period is shown in the upper section of the diagram. Following baseline testing rats underwent sham or 6-OHDA lesioning of the MFB. Post-lesion behavioural measures were taken after at least 2 weeks' recovery and lesioned rats were divided into 2 groups with equal behavioural readouts. Thereafter all rats underwent 21 days of once-daily dosing with vehicle (1ml/kg saline) or L-DOPA; sham rats received L-DOPA (n = 5), lesioned rats received L-DOPA (n = 9) or vehicle (n = 10). AIMs scoring and L-DOPA induced rotations were measured at intervals during this time (upper section of the diagram, daily time-line). During weeks 7 and 8, at the end of the priming period, all rats underwent AIMs reversal testing with known antidyskinetic compounds using a randomised crossover design. Rats were perfused 4 days following the last dose of L-DOPA/vehicle.

6.2.5.1 Surgery – Week 0

Rats received either a 6-OHDA (n=19) or sham (n=5) unilateral lesion of the MFB.

6.2.5.2 Lesion assessment – Week 2

Lesion assessment in this study was carried out by measuring apomorphine-induced rotations, the cylinder test and the adjusted steps test between 2 and 3 weeks after lesioning. Lesioned rats with >6 net contraversive rotations per minute at peak, along with clear deficits in contralateral forelimb use, were taken forward to the L-DOPA priming phase.

6.2.5.3 Induction of AIMs (priming) – Weeks 3-5

Three days after behavioural testing, a group of rats with complete lesions (n=9) began daily treatment (between 10:30 and 11:00) with 6.25mg/kg L-DOPA + 15mg/kg benserazide

(i.p.) to induce abnormal involuntary movements (AIMs). A second group of lesioned rats were treated with vehicle (1ml/kg saline; n=10) to provide a control group for the effect of the L-DOPA, and the sham-lesioned group (n=5) was treated daily with L-DOPA + benserazide to provide a control for the effect of lesion on the response to treatment.

The severity and duration of AIMs were assessed on alternating days, following the ratings scale described earlier in section 6.2.4.3, to build a time course of the development of L-DOPA-induced dyskinesia in this model.

In addition to scoring AIMs, the development of contraversive turning in response to L-DOPA/vehicle was also measured on days 2, 8, 14 and 20 of the priming period. Rats were habituated to the automated rotometer chambers for 30 minutes before receiving their usual daily dose of L-DOPA or vehicle, after which their rotational response was measured over the course of 180 minutes.

6.2.5.4 Reversal with known antidyskinetic drugs – Weeks 6-7

Following 21 days of priming, the ability of 8-OH-DPAT (0.6mg/kg s.c) and amantadine (40mg/kg s.c.) to suppress L-DOPA-induced AIMs in these primed animals was tested in a crossover design with a minimum of 3 days' wash-out between tests.

6.2.5.5 Necropsy – Week 8

At least 3 days after final exposure to L-DOPA/vehicle, rats were terminally anaesthetised with sodium pentobarbital (600mg/kg i.p.) and the upper half of the body perfused transcardially with 0.9% saline followed by 4% paraformaldehyde (~200ml per rat). The heads were removed and post-fixed for 24 hours in 4% PFA.

In order to wash out the excess paraformaldehyde and prepare the brains for magnetic resonance imaging (MRI) the heads were immersed in PBS with 0.05% sodium azide at 4°C for 3 weeks, with the solution changed at least twice per week. This MRI analysis is still ongoing at the time of writing and does not form part of the body of work in this thesis.

6.2.5.6 Statistical analysis

All statistics analyses were carried out using GraphPad Prism version 5.

Pre- and post-lesion performance in the cylinder test was compared between sham- and 6-OHDA-lesioned groups using a two-way repeated-measured (RM) ANOVA with Bonferroni *post-hoc* test. Post-lesion adjusted steps performance, expressed as a percent of pre-lesion baseline performance, was compared between groups using a t-test. Net contraversive

rotations over 90 minutes following injection with apomorphine was also compared between groups using a t-test.

When the 6-OHDA-lesioned group (n = 19) was divided between priming treatments (6-OHDA/L-DOPA, n = 9; 6-OHDA/saline, n = 10), post-lesion performance in the cylinder test, adjusted steps test and apomorphine-induced rotational asymmetry was compared between these subdivided groups using t-tests.

The development of AIMs was compared between groups by comparing the AIMs scores over time using a two-way RM ANOVA with Bonferroni *post-hoc* test. Within the 6-OHDA/L-DOPA group the change in AIMs scores over the 21-day priming period was compared using a one-way RM ANOVA with Bonferroni *post-hoc* test.

Rotational response to L-DOPA was compared between groups and between testing days using a two-way RM ANOVA with Bonferroni *post-hoc* test.

Analysis of the effects of the antidyskinetic agents in the 6-OHDA-lesioned L-DOPA-treated group comprised a one-way RM ANOVA with Dunnett's *post-hoc* performed on the total overall AIMs scores recorded after L-DOPA dosing. No statistical analysis was possible on Sham/L-DOPA or 6-OHDA/saline groups due to all rats in these groups scoring zero throughout.

In all tests, comparisons were considered significant where $P<0.05$.

6.2.6 Methods specific to AIMs Reversal Study

Figure 78 shows the study plan for the entire AIMs reversal study. Further detail is given regarding the breakdown of the 4 weeks of antidyskinetics testing and the 2 weeks of L-DOPA sparing both in the text and in Figure 79 and Figure 80.

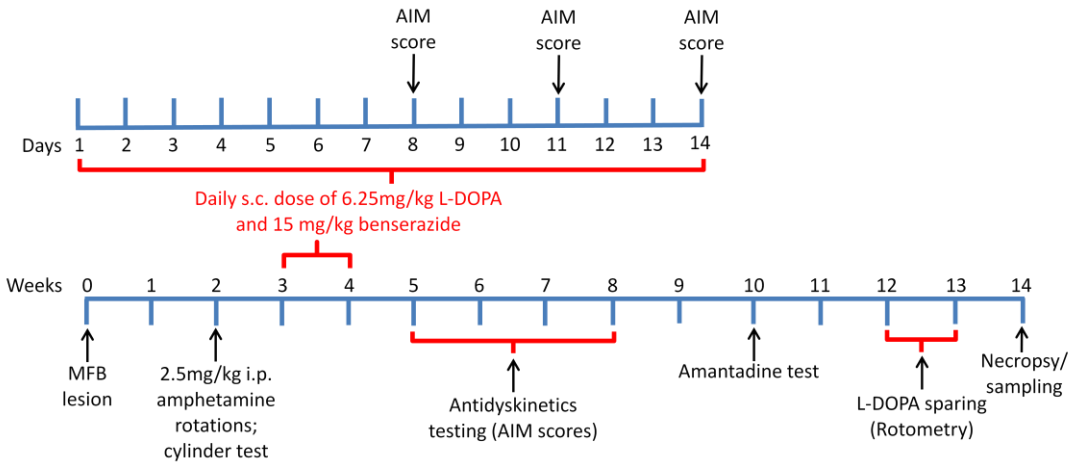

Figure 78: Study plan for the AIMs reversal study. The week-by-week plan is shown in the lower part of the diagram, with further details on the 2-weekpriming period in the upper part of the diagram. Rats underwent 6-OHDA lesioning of the MFB at week 0 and after a minimum of 2 weeks' recovery were tested for their rotational response to amphetamine. The 14 rats with the greatest rotational asymmetry that also showed a clear ipsilateral bias in the cylinder test were then primed for 14 days with once-daily injection of L-DOPA/benserazide. The 10 rats with the most concordant AIMs scores at day 14 of priming were taken forward to test the acute and sub-chronic antidyskinetic efficacies of two $mGlu_4$ PAMs (see Figure 79 for further details) and the positive control drug amantadine. The same rats were also used to test for L-DOPA sparing effects of these drugs (see Figure 80 for further details). From week 6 to week 13 all rats received a minimum of 3 doses of L-DOPA+benserazide per week to maintain a dyskinetic state.

6.2.6.1 Surgery – Week 0

All rats underwent a unilateral 6-OHDA lesion of the MFB (n=16).

6.2.6.2 Lesion assessment – Week 2

Lesion assessment in this study was carried out by measuring amphetamine-induced rotations, with post-lesion paw use also assessed as a secondary measure using the cylinder test. The 14 best responders to amphetamine were taken forward to the priming phase.

6.2.6.3 Induction of AIMs (priming) – Weeks 3-4

Three days after behavioural testing, the 14 rats that had shown the greatest number of rotations in response to amphetamine and showed a strong bias towards ipsilateral paw

use in the cylinder test began daily L-DOPA treatment to prime for dyskinesia. Rats received a subcutaneous injection of 6.25mg/kg L-DOPA + 15mg/kg benserazide in 1ml/kg 0.9% saline daily for 14 days to induce AIMs. This change from the intraperitoneal dosing protocol in the exploratory study was in response to a paper describing dose failure episodes when using the i.p. route (Lindgren *et al.*, 2007). The severity and duration of AIMs were assessed after 8, 11 and 14 days' treatment following the ratings scale described earlier to verify that the AIMs scores had stabilised. The 10 rats with the most similar and stable scores were moved into the drug testing phase of the experiment.

6.2.6.4 Reversal of established dyskinesia – Weeks 5-8

AIMs reversal testing was carried out for LuAF21934 and AF42744 as shown in Figure 79. LuAF21934 was solubilised in PEG-400 to give doses of 10 and 30mg/kg at a volume of 5ml/kg. Testing of AF42744 was identical to LuAF21934, except that the dosing volume was reduced to 3ml/kg. This was to limit the volume of PEG-400 ingested by the rats as it was causing moderate diarrhoea during the sub-chronic dosing phase of the experiment.

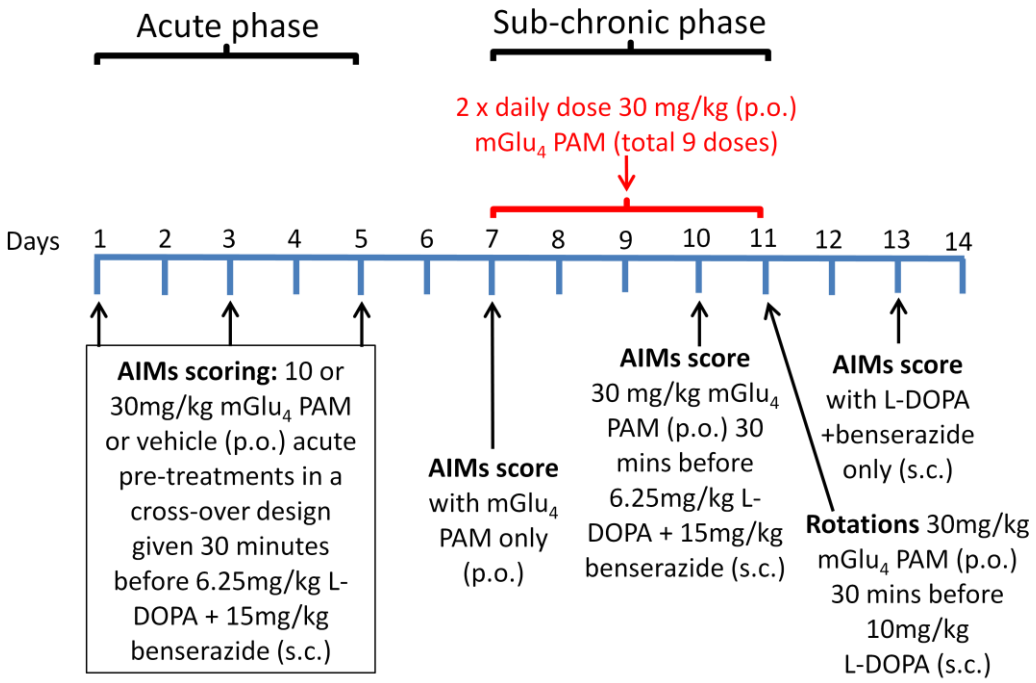

Figure 79: The 14-day AIMs reversal testing plan that was applied to each $mGlu_4$ PAM consecutively: LuAF21934 during weeks 5-6 and AF42744 during weeks 7-8. On days 1, 3 and 5 rats received vehicle or 10 or 30mg/kg drug in a randomised cross-over design 30 minutes prior to L-DOPA+benserazide to test for AIMs reversal effects of acute doses of $mGlu_4$ PAMs. From day 7-10 rats received a twice-daily dose of 30mg/kg $mGlu_4$ PAM (08:00 and 19:00) and AIMs were scored once for the $mGlu_4$ PAM alone (day 7) and once with L-DOPA+benserazide (day 10). Rotations in response to a high dose (10mg/kg) L-DOPA were tested 30 minutes after the single dose of $mGlu_4$ PAM on day 11. On day 13, following 48 hours' drug washout, AIMs were scored using the usual L-DOPA+benserazide dose to check whether or not sub-chronic $mGlu_4$ PAM administration had any long-lasting effects on AIMs expression.

For both $mGlu_4$ PAMs, the same rats were used (n = 10). For acute testing on days 1, 3 and 5, rats were administered $mGlu_4$ PAM (10 or 30mg/kg) or vehicle by oral gavage 30 minutes before injection with 6.25mg/kg L-DOPA + 15mg/kg benserazide and the AIMs scored by an experimenter blinded to the drug treatments. Each rat received both doses of $mGlu_4$ PAM and vehicle in a crossover design with 48 hours wash-out between tests. For the subchronic dose testing, rats were administered 30mg/kg $mGlu_4$ PAM twice daily for 9 doses (08:00 and 19:00), from day 7 to 11. AIMs were scored on day 7 after $mGlu_4$ PAM alone (to check for dyskinesiogenic effects of the $mGlu_4$ PAMs themselves) and on day 10 alongside 6.25mg/kg L-DOPA + 15mg/kg benserazide, administered 30 minutes after drug (to check for reversal of L-DOPA-induced AIMs by sub-chronic exposure to $mGlu_4$ PAM).

In order to assess whether $mGlu_4$ PAMs had a detrimental effect on the antiparkinsonian effects of L-DOPA, L-DOPA-induced rotations were measured on day 11 in the rotometers in rats given 30mg/kg $mGlu_4$ PAM 30 minutes prior to 10mg/kg L-DOPA + 15mg/kg benserazide. Rotations were assessed in the same way as for the amphetamine testing but recording for 4 hours.

Drug-free AIMs were scored following a further 48 hours' wash-out to verify that subchronic exposure to drug has not altered the subjects' usual response to 6.25mg/kg L-DOPA + 15mg/kg benserazide.

In total, rats received 6 doses of L-DOPA+benserazide over each 14-day testing period, which is sufficient to maintain the dyskinetic phenotype.

The ability of the weak NMDA antagonist amantadine to suppress AIMs expression was also tested as a positive control in week 10 of the study (Figure 78). Animals received 40 mg/kg amantadine hydrochloride or vehicle (1ml/kg 0.9% saline s.c.) 30 minutes prior to 6.25mg/kg L-DOPA + 15mg/kg benserazide and AIMs were scored as usual. Amantadine and saline treatments were randomised and the tests were performed 72 hours apart to allow for wash-out of amantadine, which has a long half life (known to be ~15h in humans following an oral dose; NOVARTIS-Pharmaceuticals, 2011).

6.2.6.5 L-DOPA sparing – Weeks 12-13

L-DOPA sparing was assessed during weeks 12-13 of this study, using the same rats (n = 10) as had previously been used for the acute and sub-chronic reversal studies. The rotational response of these rats to a low dose of L-DOPA (5mg/kg L-DOPA + 15mg/kg benserazide) was tested in the presence of vehicle, 30mg/kg LuAF21934 and 30mg/kg AF42744 (Figure

80). As before, the $mGlu_4$ PAMs or vehicle (3ml/kg PEG-400) were administered by oral gavage 30 minutes prior to L-DOPA or vehicle (1 ml/kg 0.9% saline) and the rotational response recorded for 3 hours in the automated rotometers.

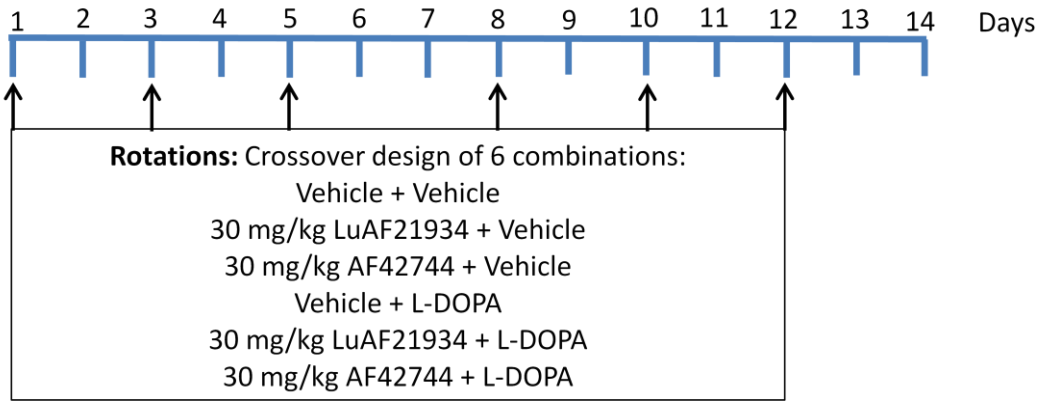

Figure 80: L-DOPA sparing experimental plan for testing both $mGlu_4$ PAMs for their ability to inhibit or enhance the rotational response of primed rats to a low dose (5mg/kg) L-DOPA. 10 rats received an acute oral dose of vehicle, 30mg/kg LuAF21934 or 30mg/kg AF42744 30 minutes prior to a subcutaneous dose of L-DOPA or saline vehicle. The rotational response was recorded in automated rotometers for 180 minutes. All tests were carried out in a crossover design with a minimum of 48 hours' wash-out in between.

6.2.6.6 Necropsy – Week 14

Rats were given a final dose of either 30mg/kg LuAF21934 (n=5) or 30mg/kg AF42744 (n=5) 2 hours prior to sacrifice, and the blood and part of the brain prepared for analysis of drug concentrations as described earlier (PK2). On this occasion the whole brain was not taken, only part of the cerebellum.

Following cardiac puncture the brain was removed and cut in a brain matrix. The striatum was dissected out, weighed and snap-frozen on dry ice in preparation for HPLC analysis of dopamine levels. A block containing the midbrain was immersion-fixed in 10% buffered formalin for additional analysis of the lesion size by TH-positive cell counts, should this have been necessary. The hindbrain/cerebellum was snap-frozen on dry ice for analysis of drug concentration.

6.2.6.7 Dopamine HPLC

The success of the MFB lesion was verified *post mortem* by analysis of striatal dopamine concentrations by HPLC at King's College London. The method of analysis has been described earlier in this thesis in Chapter 4 (section 4.2.4.2).

6.2.6.8 Statistical analysis

In the reversal studies, the overall AIMs scores were compared between vehicle and $mGlu_4$ PAM-treated tests (both acute and sub-chronic administration) using a one-way RM ANOVA with a Dunnett's *post-hoc* for comparison of $mGlu_4$ PAM-treated scores with vehicle scores. A paired t-test was used to verify that the AIMs score at the end of the fortnight of $mGlu_4$ PAM testing was not different from the day 14 AIMs score (end of priming phase).

The effect of the antidyskinetic agent amantadine was analysed by a paired t-test comparing the total AIMs score after amantadine with the total AIMs score after vehicle.

For the rotational studies including L-DOPA sparing, the total net number of contraversive turns made in response to L-DOPA was compared between vehicle and $mGlu_4$ PAMs using a one-way RM ANOVA with Dunnett's *post-hoc*.

In all tests, results were considered significant where $P<0.05$.

6.2.7 Methods specific to AIMs Induction Study

Figure 81 shows the study plan for testing the efficacy of the $mGlu_4$ PAM LuAF21934 at inhibiting the onset of AIMs.

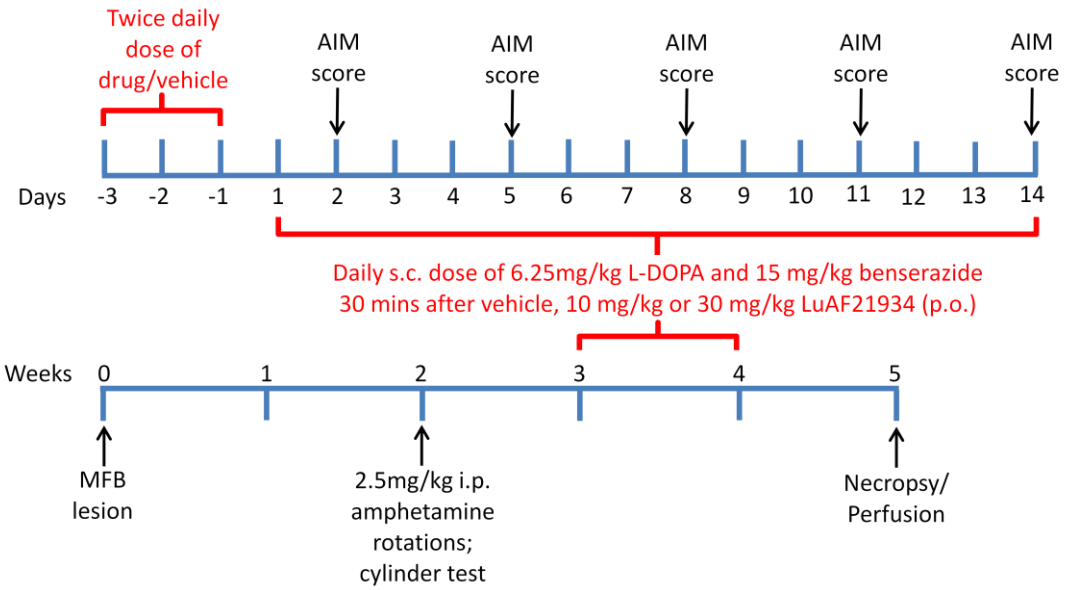

Figure 81: Study plan to test inhibition of AIMs induction by an $mGlu_4$ PAM. The week-by-week study time-line is shown in the lower part of the diagram and a more detailed breakdown of the 14-day priming period is shown in the upper part of the diagram. Rats underwent 6-OHDA lesioning of the MFB at week 0 and following at least 2 weeks' recovery the extent of lesioning was verified by analysis of amphetamine-induced rotational asymmetry and limb use bias in the cylinder test. Rats were divided into 3 groups of equal post-lesion behavioural ability. Each group received 2 daily oral doses of vehicle, 10mg/kg or 30mg/kg LuAF21934 for three days and then one daily oral dose of vehicle or drug for a further 14 days. For the 14 days of once-daily dosing, the dose of drug or vehicle was followed 30 minutes later by a subcutaneous injection of L-DOPA/benserazide. AIMs were scored at intervals within this L-DOPA priming period. 72 hours after the final dose of drug/vehicle + L-DOPA, rats were perfused and the brains removed for analysis.

6.2.7.1 Surgery – Week 0

All rats underwent a unilateral 6-OHDA lesion of the MFB (n = 24).

6.2.7.2 Assessment of lesion – Week 2

Lesion size was assessed before the experimental phase using the cylinder test and amphetamine-induced rotations to establish whether or not the lesion was successful. The 21 rats with the highest degree of asymmetry in response to 2.5mg/kg i.p. amphetamine, and verified by reduced use of the contralateral forepaw in the cylinder test, were stratified into 3 groups of n=7 based on net rotational asymmetry. This stratification was performed blinded to the eventual treatment that each group would receive.

6.2.7.3 Induction of AIMs – Weeks 3-4

All rats had 3 days of twice-daily treatment with vehicle, 10mg/kg or 30mg/kg Lu AF21934, administered p.o. at a volume of 2ml/kg. Thereafter they received a single daily treatment with vehicle or drug, followed 30 minutes later by a subcutaneous injection of 6.25mg/kg L-DOPA + 15mg/kg benserazide, for a total of 14 days. This priming period was chosen because the exploratory study outlined earlier had shown that AIMs scores had stabilised by this time point. AIMs were scored at intervals within this induction period at days 2, 5, 8, 11 and 14 by an experimenter blinded to the treatments received by each group.

6.2.7.4 Necropsy – Week 5

At least 3 days after final exposure to L-DOPA, rats were terminally anaesthetised with sodium pentobarbital (600mg/kg i.p.) and the upper half of the body perfused transcardially with PBS followed by 10% buffered formalin. The brains were removed from the skull and post-fixed for a minimum of 24 hours before being cut in a brain matrix. A coronal block containing the midbrain was processed and embedded for histological analysis of the lesion size by TH staining of nigral cells. A coronal block containing the striatum was saved in formalin in case of later analysis of striatal markers of dyskinesia.

6.2.7.5 Tyrosine Hydroxylase immunohistochemistry

Lesion size was verified post-mortem by counting the number of TH-positive cells remaining in the lesioned SNc, expressed as a percentage of the number of TH-positive cells remaining in the intact SNc. Rats with <95% lesion were discarded from the analysis on the basis that their chance of developing levodopa-induced AIMs was reduced.

Coronal sections were cut through the SN at 7µm and mounted on SuperFrost Plus® slides. Sections at -5.3mm from bregma, where the medial terminal nucleus fully bisects the SNc from the VTA, were stained, imaged and analysed as described in section 2.2.3.2. Counts were made in triplicate on three adjacent sections and the mean percentage cells remaining calculated.

6.2.7.6 Statistical analysis

TH-positive cells remaining in the lesioned SNc, expressed as a percent of TH-positive cells in the intact SNc, were compared using a one-way ANOVA with Dunnett's *post-hoc* test.

The number of rats developing AIMs was compared between the vehicle-treated group and LuAF21934-treated groups using a Fisher's exact test.

The total score for overall AIMs, the individual AIMs subtypes, and the duration and severity scores they comprised were compared using two-way repeated measures ANOVAs with Bonferroni *post-hoc* tests.

In all tests, results were considered significant where $P<0.05$.

6.3 Results

6.3.1 Pharmacokinetic study

6.3.1.1 PK1 – Plasma time course of LuAF21934 and AF42744

The plasma profile of LuAF21934 was already shown in Chapter 4 in relation to the LuAF21934 neuroprotection study. The C_{max} of LuAF21934 was 869 ± 202ng/ml following a 10mg/kg dose and 4733 ± 758ng/ml following a 30mg/kg dose, both attained 1 hour after dosing. The $t_{1/2}$ was 1.4 ± 0.1 hours following 10mg/kg and 0.8 ± 0.1 hours following 30mg/kg.

The plasma profile of AF42744 is shown in Figure 82. The C_{max} for AF42744 was 1355 ± 388 following a 10mg/kg dose and 5407 ± 517 following a 30mg/kg dose, attained between 0.5 and 1 hour post-dose. The $t_{1/2}$ was 1.2 ± 0.3 hours following 10mg/kg and 2.7 ± 0.8 hours following 30mg/kg.

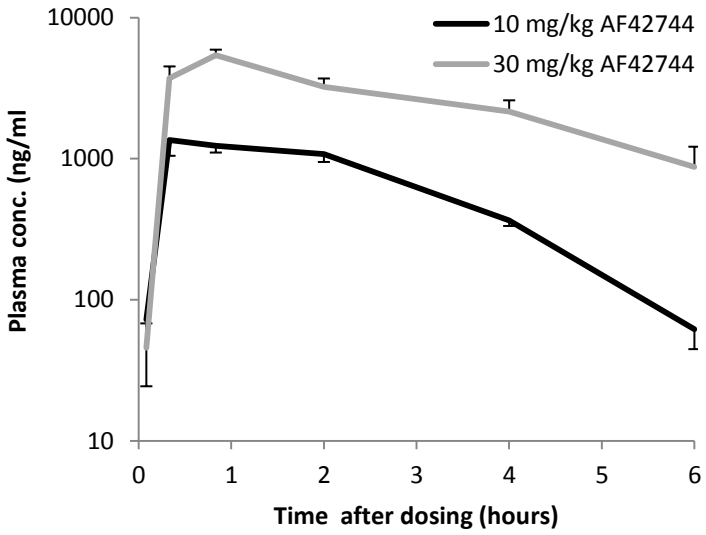

Figure 82: Plasma profiles in naive rats following an oral dose of 10mg/kg or 30mg/kg AF42744. Serial blood samples were taken from the cannulated tail veins of naive rats following an oral dose of 10mg/kg or 30mg/kg AF42744. Data are expressed as mean ± s.e.m. (n = 3 per dose).

Since t_{max} for both drugs is ~1hr, the pre-treatment time of 30 minutes prior to L-DOPA adopted in subsequent studies ensure that maximum plasma drug levels coincide with maximal striatal L-DOPA concentration (Carta *et al.*, 2006).

6.3.1.2 PK2 – Brain/plasma ratio LuAF21934 and AF42744 after 2 hours

2-hour brain and plasma concentrations were analysed following an acute oral dose of 30mg/kg LuAF21934 (n = 5) or 30mg/kg AF42744 (n = 5). These samples were collected at the end of the AIMs reversal study and stored at -80°C for 6 months before analysis.

LuAF21934

2 hours after a 30mg/kg dose, the plasma concentration of LuAF21934 was 2186 ± 225ng/ml and the brain concentration was 1196 ± 179ng/g, giving a brain/plasma ratio of 0.55. This is comparable with the brain/plasma ratio of 0.66 calculated in the LuAF21934 PK-B study reported in Chapter 4, however the absolute brain and plasma concentrations obtained in PK2 were approximately 66% less than the absolute brain and plasma concentrations obtained in PK-B. This is likely due to the long-term storage of these samples before processing.

AF42744

No AF42744 was detected in 2 of the 5 brain samples collected in PK3, despite plasma concentrations being comparable in these rats to the other 3 rats in the study.

If these rats are included, the plasma concentration of AF42744 measured 2 hours after a single oral dose of 30mg/kg AF42744 is 1046 ± 365ng/ml and the brain concentration is 297 ± 181ng/g, giving a brain/plasma ratio of 0.28.

If the rats whose brains had undetectable concentrations of AF42744 are excluded, the plasma concentration is 683 ± 339ng/ml and the brain concentration is 495 ± 244ng/g, giving a brain/plasma ratio of 0.74.

As for the LuAF21934 samples in this study, these samples also likely underwent a degree of degradation. For example the 2-hour plasma concentration was between 683 and 1046ng/ml compared with 3223ng/ml at the same time point in PK1. However the brain/plasma ratio calculated for AF42744 may be close to the real value, as was found to be the case for LuAF21934 in this study.

6.3.1.3 PK3 – Brain/plasma ratio of amantadine after 90 minutes

Since amantadine is a known antidyskinetic agent and had shown efficacy in the AIMs studies, we wanted to ascertain the brain and plasma concentrations at the time point that corresponded with the start of the maximal L-DOPA effect. L-DOPA effect is maximal around 60 minutes after administration, so given the 30 minute pre-treatment time allowed for amantadine this meant taking brain/plasma ratios 90 minutes after dosing with

amantadine. According to previous studies, free brain concentrations are expected to be maximal following a systemic injection between 60 and 80 minutes (Kornhuber *et al.*, 1995) so this PK study approximates the maximal brain exposure.

We found that 90 minutes after a subcutaneous dose of 40mg/kg amantadine, the plasma concentration was 2513 ± 145ng/ml and the brain concentration was 23633 ± 1885ng/g, giving a brain/plasma ratio at this time point of 9.40.

6.3.3 Levodopa-induced AIMs exploratory study

6.3.3.1 MFB lesioning led to measurable behavioural impairments

Before priming, the success of the MFB lesion was assessed using the cylinder test, adjusted steps test and apomorphine-induced rotational asymmetry.

Cylinder test

Rats with 6-OHDA MFB lesions showed significantly impaired use of the contralateral forepaw in the cylinder test (Figure 83), with a reduction in use from 49 ± 1% of total touches pre-lesion to 6 ± 1% post-lesion (P<0.001; two-way RM ANOVA with Bonferroni *post-hoc*). Sham-lesioned animals retained normal use of the contralateral paw after surgery with 53 ± 1% contralateral touches, compared with 51 ± 2% at baseline (P=0.4826; two-way RM ANOVA with Bonferroni *post-hoc*).

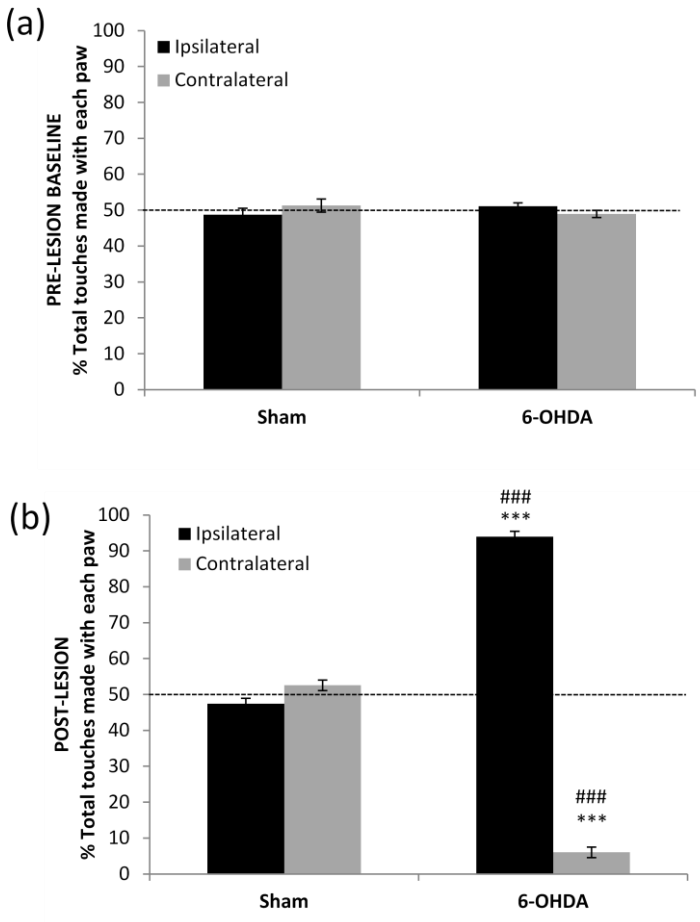

Figure 83: Performance of Sham- and 6-OHDA-lesioned rats in the cylinder test. The dotted lines show the expected unbiased use for an intact rat. Graph (a) shows pre-lesion use of ipsilateral and contralateral paws. Graph (b) shows the effect of a sham of 6-OHDA lesion on paw use, with a clear bias towards the ipsilateral paw in 6-OHDA-lesioned rats. Data are presented as mean ± s.e.m. (n = 5 for sham group, n = 19 for 6-OHDA group) ***P<0.001 versus 6-OHDA pre-lesion ###P<0.001 versus sham post-lesion (two-way RM ANOVA with Bonferroni *post-hoc*).

Adjusted steps test

A similar impairment was noted in the adjusted steps test (Figure 84). 6-OHDA-lesioned animals showed a significant reduction in contralateral paw stepping post-lesion in both the forward (50 ± 1% of baseline number of steps taken) and reverse (71 ± 1% of baseline number of steps taken) directions compared with sham-lesioned animals, where contralateral paw stepping was preserved at 101 ± 1% baseline in the forward direction and 100±1% in the reverse direction (P<0.0001; t-tests). Ipsilateral paw function was preserved in both groups in both directions.

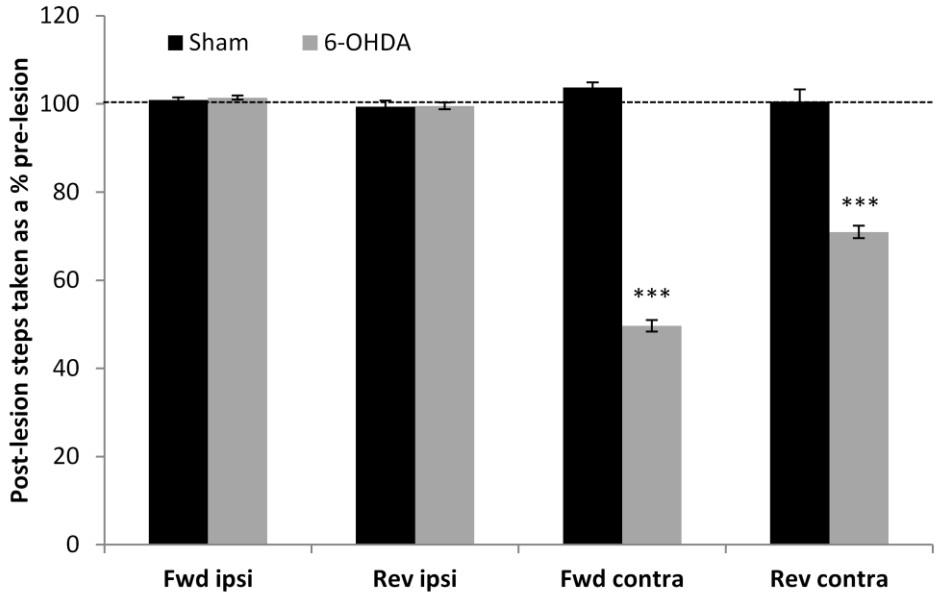

Figure 84: Adjusted steps test performance in sham- and 6-OHDA-lesioned rats. The dotted line shows the expected percentage of pre-lesion steps that an intact rat would be expected to take post-lesion. Both sham- and 6-OHDA-lesioned rats' ipsilateral paws had unimpaired function in the forward and reverse directions. Sham-lesioned rats also showed no impairment in use of the contralateral paw in either direction, in contrast to 6-OHDA-lesioned rats, which showed a significant reduction in contralateral paw function in both the forward and reverse directions. Data are presented as mean ± s.e.m. (n = 5 for sham group, n = 19 for 6-OHDA group) ***P<0.0001 versus Sham (t-test).

Apomorphine-induced rotational asymmetry

6-OHDA-lesioned rats also showed significantly increased contraversive rotations in response to apomorphine compared with sham-lesioned rats (Figure 85), with on average 382 ± 32 net contraversive rotations over 90 minutes compared with 10 ± 10 respectively (P<0.0001; t-test).

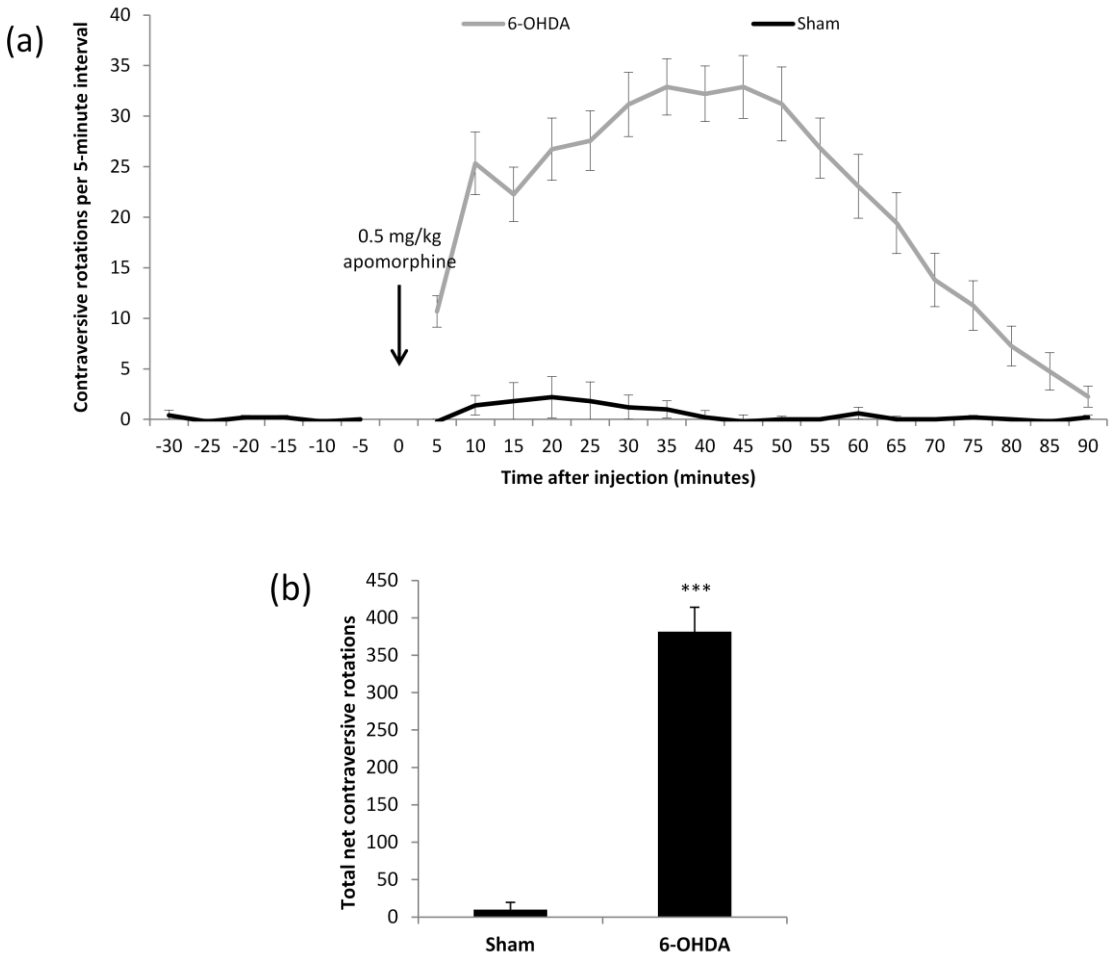

Figure 85: Rotational response of sham- and 6-OHDA-lesioned rats in response to 0.5mg/kg apomorphine. Graph (a) shows the time course of the rotational response. The total net contraversive rotations over the 90-minute testing period are quantified in (b). Data are presented as mean ± s.e.m. (n = 5 for sham group, n = 19 for 6-OHDA group) ***P<0.001 versus Sham (t-test).

Lesioned animals were subsequently assigned to L-DOPA-treated and saline-treated subgroups, ensuring that there was no significant difference between their post-lesion scores for the cylinder test (P=0.9050; t-test), adjusted steps test (P>0.3810; t-test) or apomorphine-induced rotational asymmetry (P=0.8956; t-test).

6.3.3.2 Repeated exposure of lesioned rats to L-DOPA led to the development of AIMs

During the 21-day priming period, half of lesioned rats were treated daily with 6.25mg/kg L-DOPA + 15mg/kg benserazide i.p. (n = 9; 6-OHDA/L-DOPA) and the other half were treated daily with saline vehicle i.p. (n = 10; 6-OHDA/saline). Sham-lesioned rats were treated daily with an identical dose of L-DOPA and benserazide i.p. (n = 5; Sham/L-DOPA).

The scores obtained over the priming period for 6-OHDA/L-DOPA rats are shown in Figure 86, both as an overall score and divided into the three AIMs subtypes. At the first injection, some rats in the 6-OHDA/L-DOPA group were already displaying axial and limb AIMs, in accordance with previous studies (Winkler *et al.*, 2002). AIMs expression tended to level off after the first week of L-DOPA priming, with no significant difference between AIMs scores between days 5 and 21 ($P>0.05$; one-way RM ANOVA with Bonferroni *post-hoc*), with a mean score on day 21 of 173 ± 13. In addition, all AIMs subtypes – axial, forelimb and orolingual – developed and stabilised at similar rates, with no change between scores from day 3 onwards, day 7 onwards and day 5 onwards respectively (one-way RM ANOVAs with Bonferroni *post-hoc* tests).

By the end of the 21-day priming phase eight of the nine rats in the 6-OHDA/L-DOPA group displayed axial, forelimb and orolingual AIMs with a duration score of at least 3 for each subtype, classing them as severely dyskinetic. The ninth rat attained duration scores of at least 2 for each subtype, indicative of a more moderate dyskinetic phenotype. The overall incidence of dyskinesia in this group was therefore 100%.

6-OHDA/Saline rats did not display any signs of dyskinesia (scores of zero for duration and severity throughout) over the duration of the 21 days of dosing, indicating that the lesion alone was insufficient to cause development of this phenotype (data not shown). Similarly, Sham/L-DOPA rats did not display any signs of dyskinesia (scores of zero for duration and severity throughout), indicating that repeated L-DOPA treatment was insufficient to cause dyskinesia in the absence of a nigrostriatal lesion over the 21-day period tested (data not shown). There was a significant difference between AIMs scores in the 6-OHDA/L-DOPA group and the scores in the 6-OHDA/saline and Sham/L-DOPA groups (effect of treatment $P<0.0001$; two-way RM ANOVA with Bonferroni *post-hoc*).

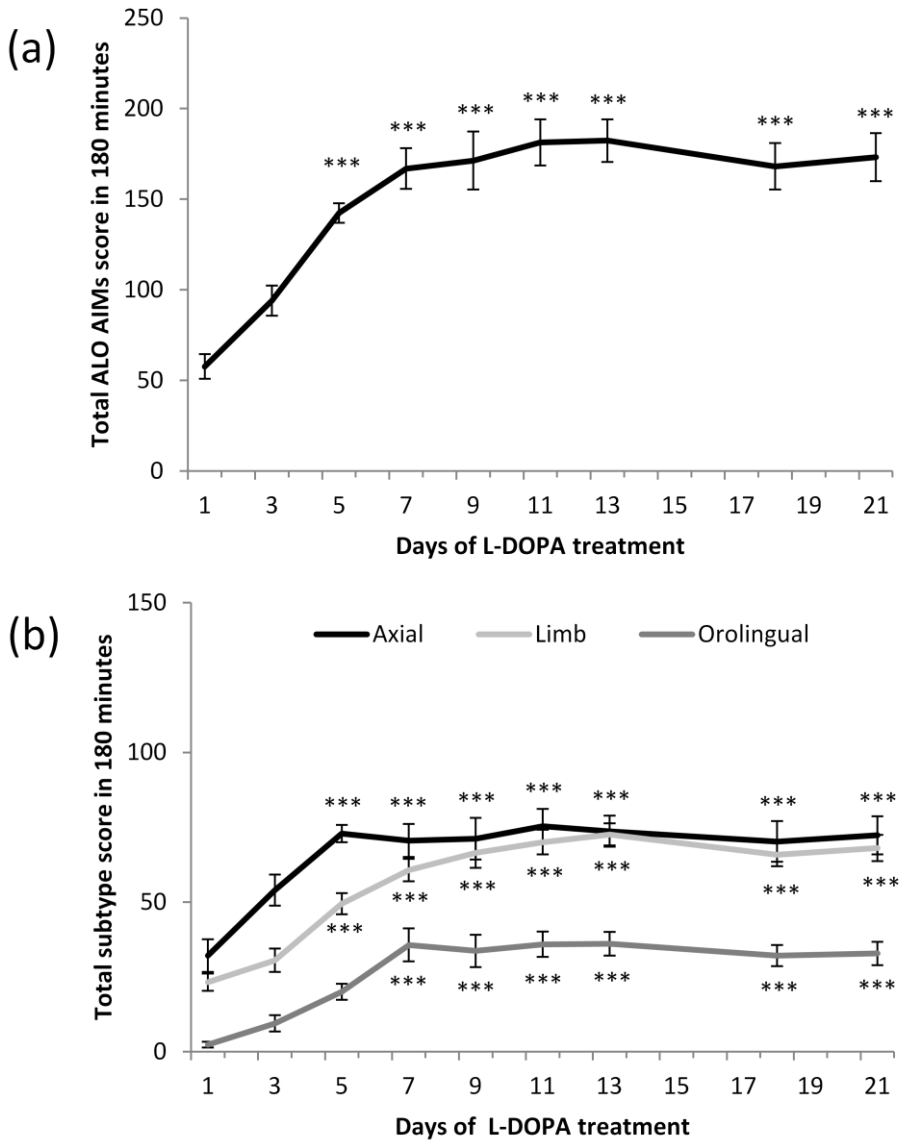

Figure 86: AIMs scores over the course of 21 days of priming in 6-OHDA/L-DOPA rats. Graph (a) shows the total score obtained over 180 minutes following L-DOPA administration. Graph (b) shows the individual scores obtained per AIMs subtype. Data are presented as mean ± s.e.m. (n = 9) ***P<0.0001 versus corresponding score on day 1 (one-way RM ANOVA with Bonferroni *post-hoc*).

6.3.3.3 AIMs expression followed a 3-hour time course

Dyskinetic 6-OHDA/L-DOPA rats started to express dyskinesia within 20 minutes of L-DOPA injection, with the severity and duration peaking between around 40 and 100 minutes. After this time the score decreased at a similar rate as it increased, with rats returning to baseline by 180 minutes after the L-DOPA was injected. All AIMs subtypes increased and decreased at similar rates to one another. An example time course from day 21 is shown for these rats in Figure 87 for overall AIMs and also the individual subtypes.

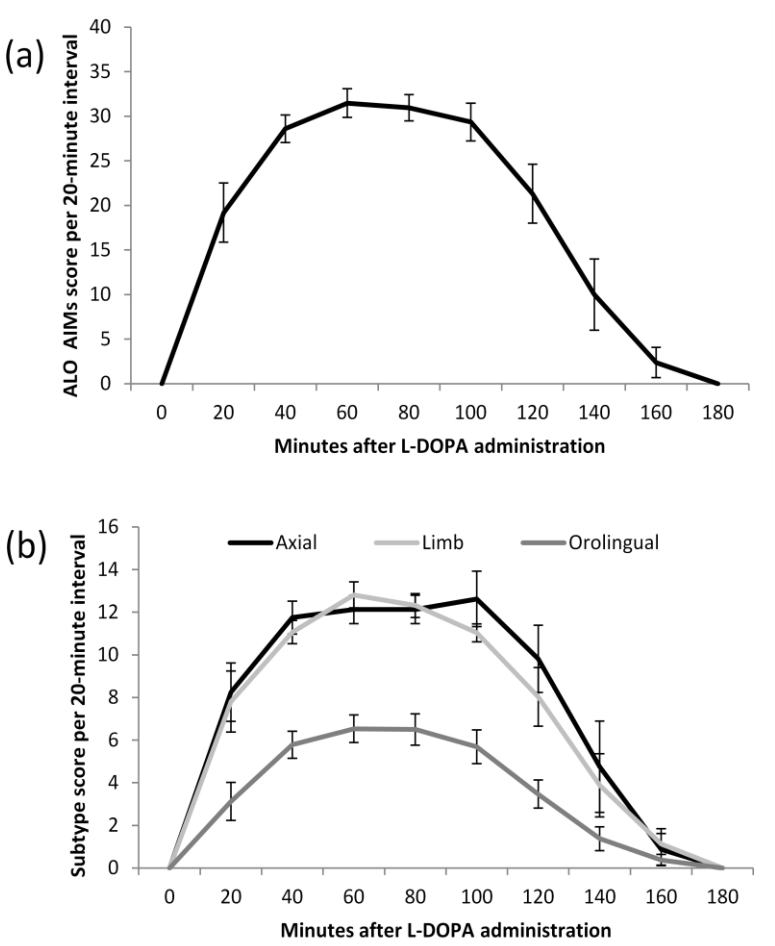

Figure 87: AIMs scores over 180 minutes following L-DOPA dosing on day 21 in 6-OHDA/L-DOPA rats. Graph (a) shows the overall AIMs scores at each time point. Graph (b) shows the individual scores obtained per AIMs subtype. Data are presented as mean ± s.e.m. (n = 9).

6.3.3.4 L-DOPA induced contraversive rotations

The rotational response of all rats was measured at intervals throughout the L-DOPA/saline priming period (Figure 88). The pattern of rotational development closely reflected the development of AIMs in the 6-OHDA/L-DOPA treated group, and the lack of any development of marked rotational asymmetry in the Sham/L-DOPA group or the 6-OHDA/Saline group also reflect the fact that no rats in either of these groups displayed AIMs at any point during the 21 days of priming.

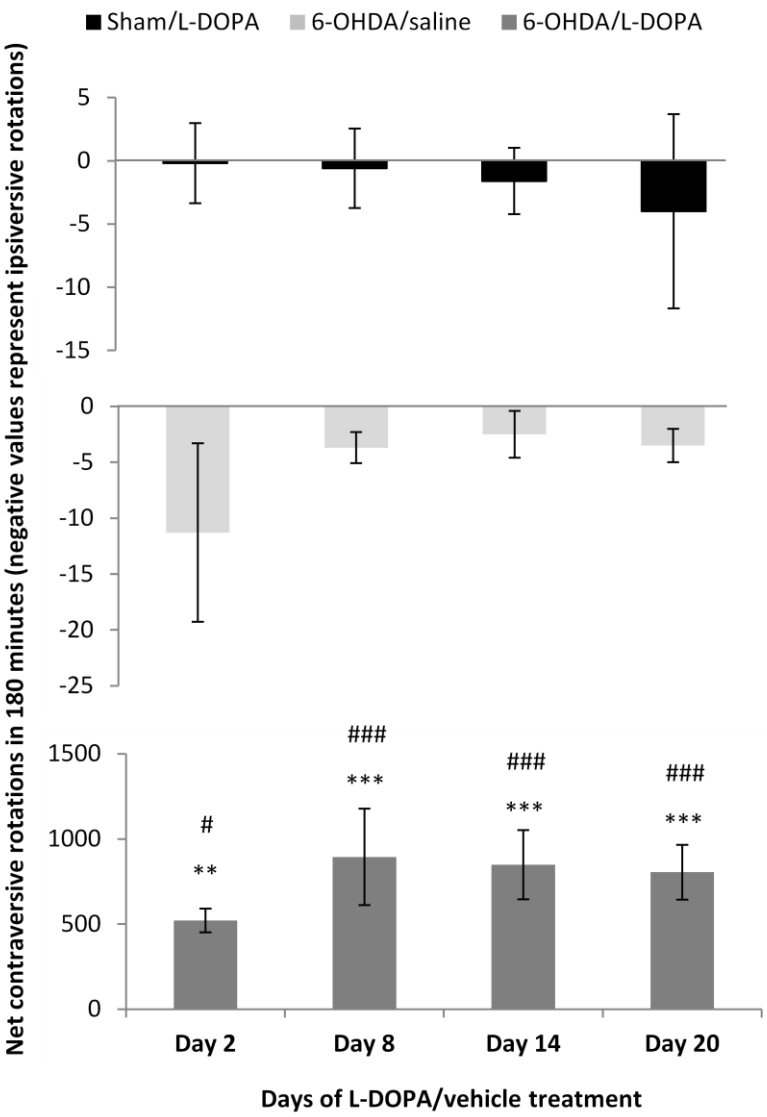

Figure 88: Development of a rotational response following L-DOPA or saline injection during the priming period. Data are presented as mean ± s.e.m. (n = 5-10) ** P<0.01, *** P<0.001 versus 6-OHDA/saline; # P<0.05, ## P<0.01, ### P<0.001 versus Sham/L-DOPA (two-way RM ANOVA with Bonferroni *post-hoc*).

All statistical values quoted below were calculated using a two-way RM ANOVA with Bonferroni *post-hoc* analysis.

On day 2 the 6-OHDA/L-DOPA group displayed a mean asymmetry of 520 ± 70 net contraversive turns in response to L-DOPA, which was significantly higher than the 6-OHDA/Saline group (-11 ± 8; P<0.01) and the Sham/L-DOPA group (-0.2 ± 3.2; P=0.05).

On day 8 the 6-OHDA/L-DOPA group displayed a mean asymmetry of 894 ± 293 net contraversive turns in response to L-DOPA, which was significantly higher than the 6-OHDA/Saline group (-3.7 ± 1.4; P<0.001) and the Sham/L-DOPA group (-0.6 ± 3.1; P<0.001).

On day 14 the 6-OHDA/L-DOPA group displayed a mean asymmetry of 848 ± 204 net contraversive turns in response to L-DOPA, which was significantly higher than the 6-OHDA/saline group (-2.5 ± 2.1; P<0.001) and the Sham/L-DOPA group (-1.6 ± 2.6; P<0.001).

On day 20 the 6-OHDA/L-DOPA group displayed a mean asymmetry of 805 ± 161 net contraversive turns in response to L-DOPA, which was significantly higher than the 6-OHDA/saline group (-3.5 ± 1.5; P<0.001) and the Sham/L-DOPA group (-4 ± 8; P<0.001).

There were no significant differences in rotational asymmetry between the Sham/L-DOPA and the 6-OHDA/Saline group on any day (P>0.05).

There was no significant effect of time on rotational response to L-DOPA/saline in any group (P>0.05).

6.3.3.5 AIMs could be reversed by 8-OH-DPAT or amantadine

Two drugs with known antidyskinetic properties were tested in all rats to test their efficacy at suppressing AIMs in this model (Figure 89), and for any dyskinesiogenic effects they may exert in non-dyskinetic rats.

In dyskinetic rats (6-OHDA/L-DOPA), 0.6mg/kg 8-OH-DPAT completely abolished AIMs expression for 160 minutes after dosing. Thereafter rats experienced a 100-minute period during which they expressed AIMs of mild to moderate severity (duration scores 1-2) before returning to baseline. The overall AIMs score over the 260-minute testing period was reduced from 179 ± 14 to 30 ± 11, an 85% reduction that was statistically significant (P<0.001; one-way RM ANOVA with Dunnett's *post-hoc*). AIMs scores were reduced in all subtype areas compared with vehicle treatment; axial from 75 ± 7 to 12 ± 5, limb from 70 ± 6 to 13 ± 5 and orolingual from 33 ± 3 to 5 ± 2 (all P<0.001; one-way RM ANOVAs with Dunnett's *post-hoc* tests).

8-OH-DPAT did not show any dyskinesiogenic effects in either of the two non-dyskinetic groups (Sham/L-DOPA and 6-OHDA/Saline). However at this dose all rats in all three groups were observed to alternately pad their forepaws and to adopt a flat body posture for around one hour after 8-OH-DPAT injection. This is indicative of inhibition of serotonergic signalling leading to the development of serotonin-dependent stereotypies. However the presence of this side effect does not explain the entire duration of AIMs suppression exerted by 8-OH-DPAT in the 6-OHDA/L-DOPA group and therefore is not responsible for the antidyskinetic action of this drug.

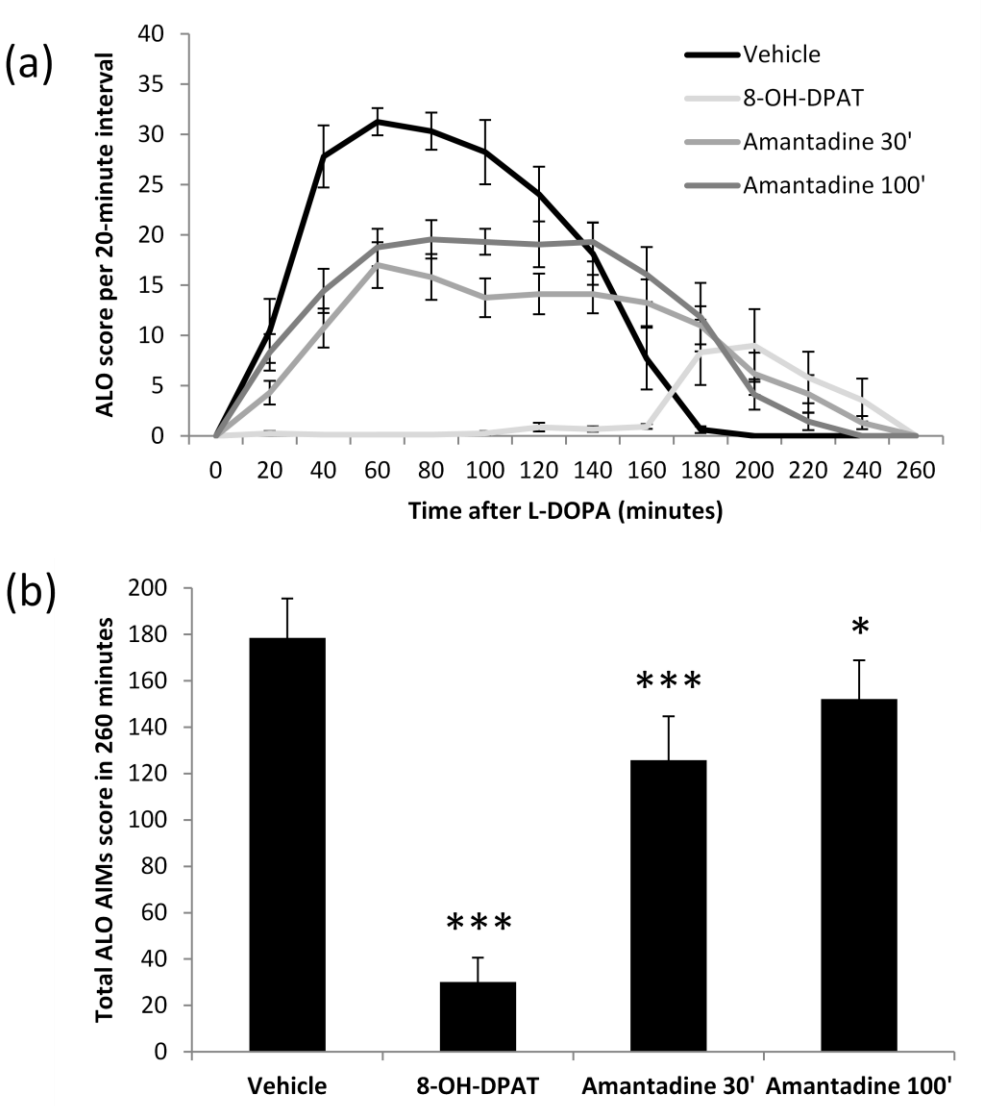

Figure 89: Effect of pre-treatment with known antidyskinetics on total AIMs scores in 6-OHDA/L-DOPA rats. AIMs were scored after administration of L-DOPA following pre-treatment with the known antidyskinetic agents 8-OH-DPAT and amantadine. The time course of AIMs scoring is shown in graph (a) and the overall AIMs score over 260 minutes is compared in graph (b). The numbers after amantadine denote the pre-treatment time in minutes. 8-OH-DPAT was administered immediately before L-DOPA. Data are presented as mean ± s.e.m. (n = 9) *P<0.05, ***P<0.001 compared with vehicle (one-way RM ANOVA with Dunnett's *post-hoc*).

In dyskinetic rats (6-OHDA/L-DOPA group), 40mg/kg amantadine reduced the expression of AIMs by 30 ± 4.7% and 14 ± 4.5% when administered 30- and 100-minutes prior to L-DOPA respectively. Both of these were statistically significant reductions from the vehicle score of 179 ± 14 with the 30-minute pre-treatment time giving a more marked reduction: 126 ± 16 (P<0.001; one-way RM ANOVA with Dunnett's *post-hoc*) versus 152 ± 15 (P<0.05; one-way

RM ANOVA with Dunnett's *post-hoc*) for the 100-minute pre-treatment time. The reduction in AIMs score following 30-minute pre-treatment with amantadine was significant for all AIMs subtypes when compared using a one-way RM ANOVA with Dunnett's *post-hoc*; axial scores were reduced from 75 ± 7 to 56 ± 8 ($P<0.001$), limb from 70 ± 6 to 56 ± 9 ($P<0.05$) and orolingual from 33 ± 3 to 14 ± 2 ($P<0.001$).

Similarly to 8-OH-DPAT, amantadine did not show any dyskinesiogenic effects in either of the two non-dyskinetic groups, and no side effects of treatment were noted in any rat.

6.3.4 Reversal of established L-DOPA-induced dyskinesia

6.3.4.1 Lesioned rats displayed functional deficits

Rats were assessed using the cylinder test and amphetamine-induced rotations to establish whether or not the lesion was successful. In the cylinder test all but one rat showed a clear bias towards using the ipsilateral paw versus the contralateral paw. This rat, with 49.32% contralateral touches, was eliminated from the study before the priming stage along with another with 30.77% contralateral touches.

The mean use of the contralateral paw among the remaining rats that were taken forward for priming was 12.57 ± 1.87% of total touches. When assessed for amphetamine-induced rotations, the rats that were taken forward for priming had a mean net rotational asymmetry over the 120 minute testing period of 230 ± 38 ipsiversive rotations.

The lesser post-lesion behavioural deficit in the cylinder test in this study compared with the exploratory study, where mean use of the contralateral paw was 6 ± 1%, might suggest that the lesion severity was also reduced. However when striatal dopamine content was assessed by HPLC in the final rats used in this study the dopamine concentration in the lesioned striatum was <1% of the dopamine concentration in the intact striatum, indicating a successful and complete nigrostriatal lesion (data not shown).

6.3.4.2 AIMs developed over 14 days of priming

At the end of the 14-day priming phase, 13 of the 14 rats treated with L-DOPA displayed axial, forelimb and orolingual AIMs with a duration score of at least 3, classing them as severely dyskinetic. The 10 rats with the most similar and consistent expression of AIMs were chosen for the acute reversal testing; these rats scored a mean of 180 ± 7 on day 14, comprising 76 ± 4 total axial score, 69 ± 3 total forelimb score and 35 ± 3 total orolingual score. A plot of the development of AIMs in the 10 rats used in the reversal testing is shown in Figure 90. There was no significant difference between scores on days 8, 11 and 14 with respect to overall score (P=0.2844; one-way RM ANOVA with Bonferroni *post-hoc*), axial subtype (P=0.9727; one-way RM ANOVA with Bonferroni *post-hoc*), limb subtype (P=0.1869; one-way RM ANOVA with Bonferroni *post-hoc*) or orolingual subtype (P=0.1041; one-way RM ANOVA with Bonferroni *post-hoc*), showing that AIMs scores had stabilised.

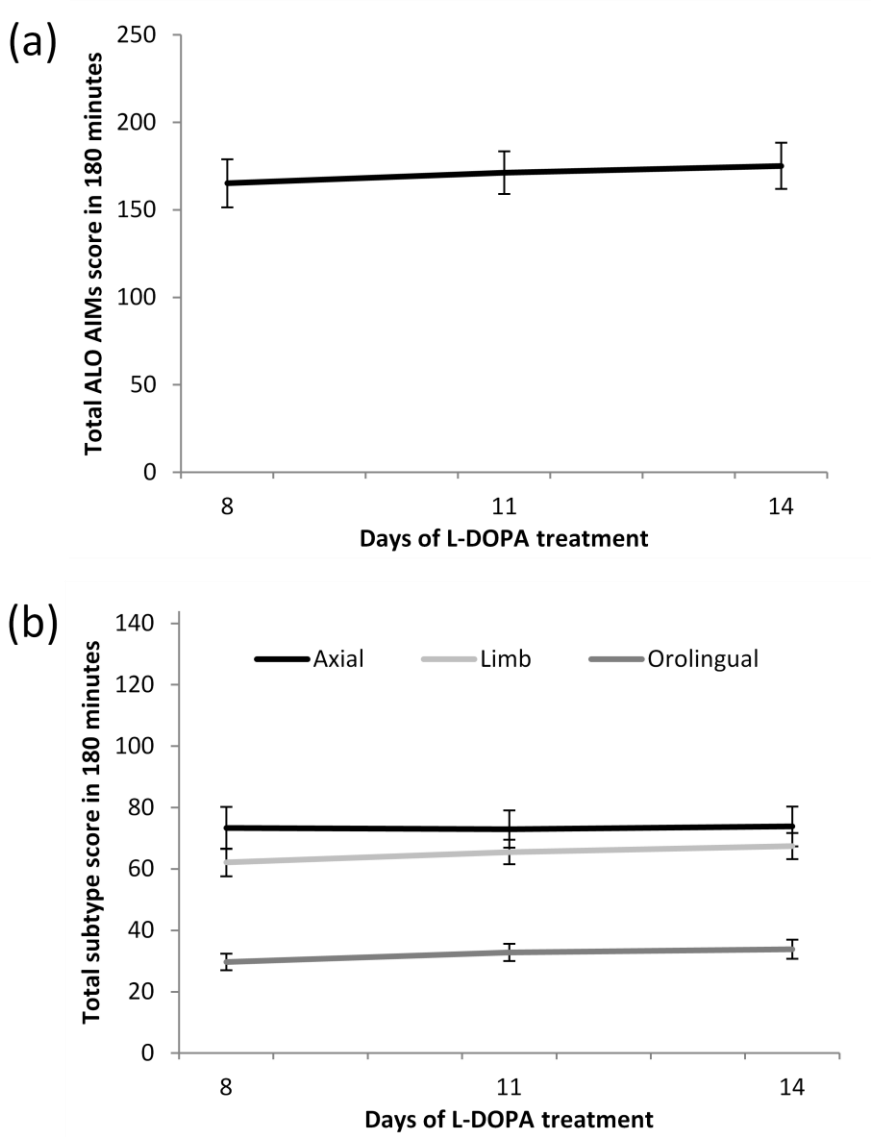

Figure 90: Stabilisation of AIMs scores during L-DOPA priming period. Mean total scores (a) and subtype-specific scores (b) over the last 6 days of L-DOPA priming of the 10 rats that were used for the AIMs reversal and L-DOPA sparing tests. Data are displayed as mean ± s.e.m. (n = 10).

6.3.4.3 mGlu$_4$ PAMs did not reverse expression of AIMs

LuAF21934: The time course of L-DOPA-induced AIMs following L-DOPA administration after 30 minute pre-treatment with 10mg/kg or 30mg/kg LuAF21934 or vehicle is shown in Figure 91. The mean total AIMs score with vehicle treatment was 184 ± 8. There was no significant effect of acute treatment with 10mg/kg LuAF21934 or 30mg/kg LuAF21934 alongside L-DOPA, which resulted in total AIMs scores of 179 ± 5 and 184 ± 8 respectively (P=0.6857; one-way RM ANOVA with Dunnett's *post-hoc*). When the AIMs components were analysed separately there was no effect of treatment at either dose on axial (P=0.5912; one-way RM ANOVA with Dunnett's *post-hoc*), forelimb (P=0.9209; one-way RM

ANOVA with Dunnett's *post-hoc*) or orolingual (P=0.3024; one-way ANOVA with Dunnett's *post-hoc*) scores.

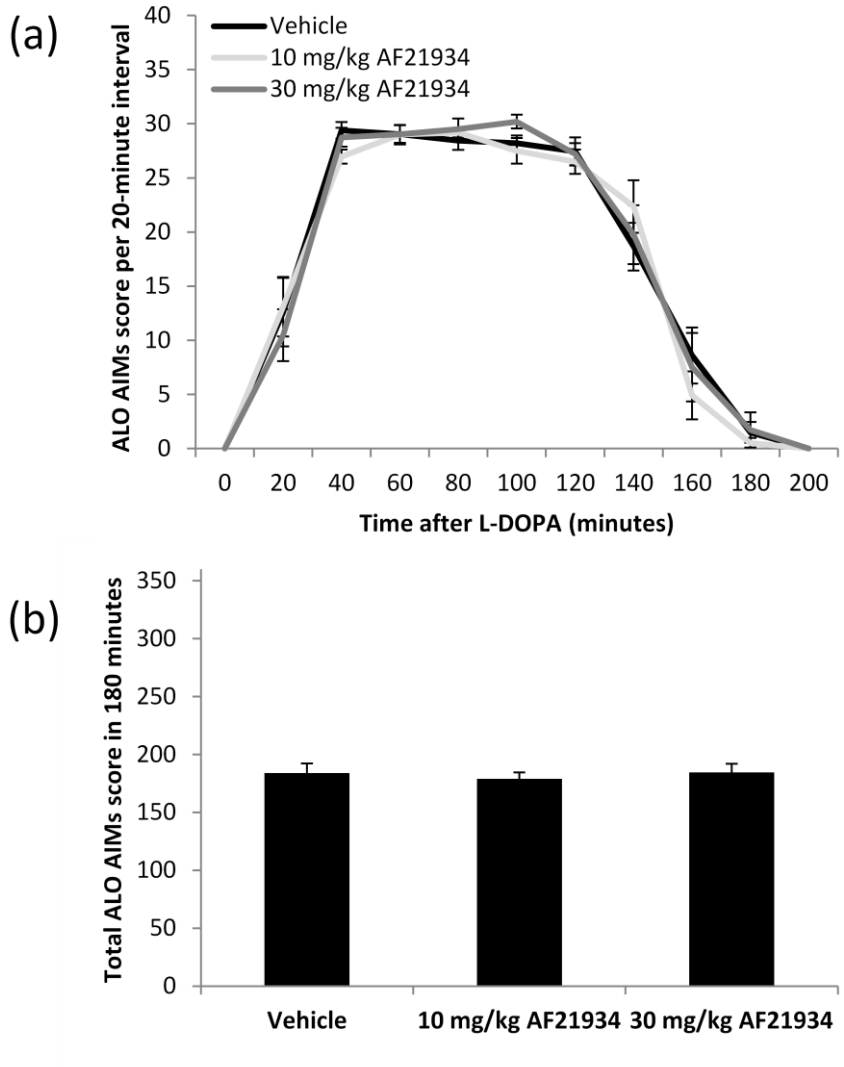

Figure 91: AIMs scores after L-DOPA following 30-minute acute pre-treatment with LuAF21934. Neither dose of LuAF21934 altered AIMs expression scores compared with vehicle. Data are displayed as mean ± s.e.m. (n = 10).

AF42744: The time course of L-DOPA-induced AIMs in the presence of 10mg/kg or 30mg/kg AF42744 or vehicle is shown in Figure 92. The mean total AIMs score with vehicle treatment was 173 ± 6. There was no significant effect of acute treatment with 10mg/kg or 30mg/kg AF42744 (P=0.4190; one-way RM ANOVA with Dunnett's *post-hoc*). When the AIMs components were analysed separately there was no effect of treatment at either dose on axial (P=0.3082; one-way RM ANOVA with Dunnett's *post-hoc*), forelimb

(P=0.1872; one-way RM ANOVA with Dunnett's *post-hoc*) or orolingual (P=0.3743; one-way RM ANOVA with Dunnett's *post-hoc*) scores.

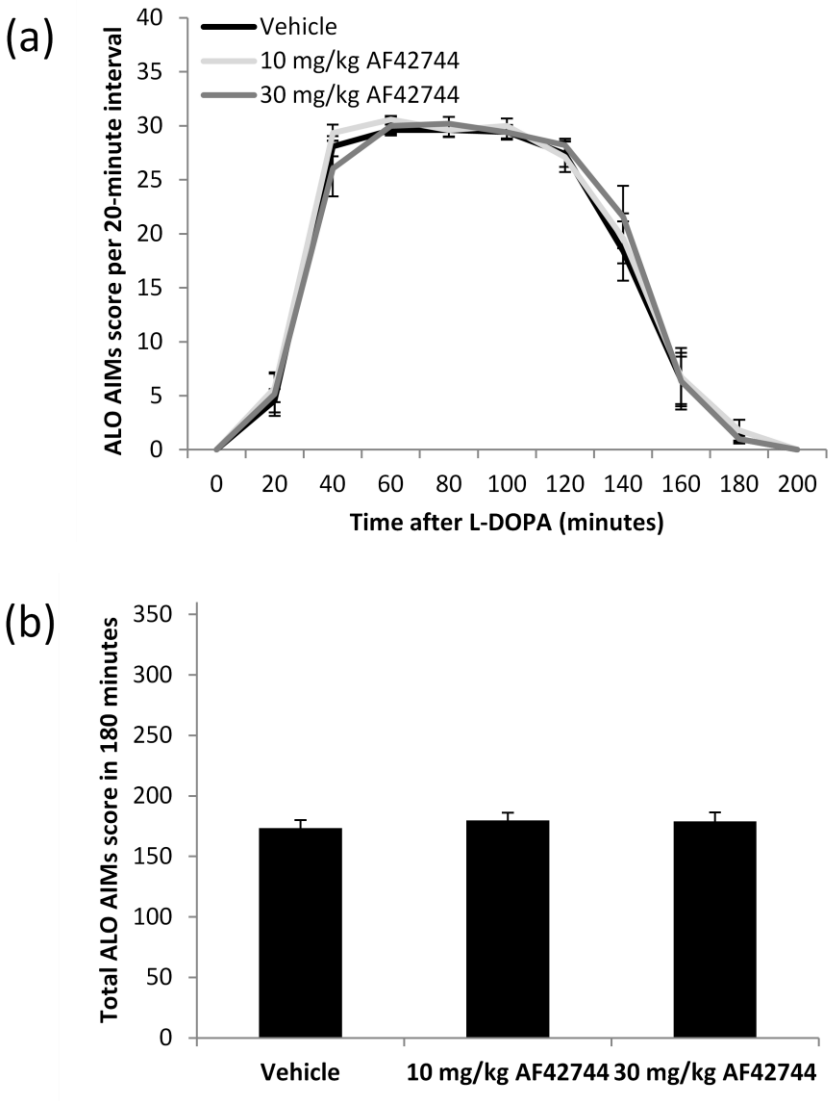

Figure 92: AIMs scores after L-DOPA following 30-minute acute pre-treatment with AF42744. Neither dose of AF42744 altered AIMs expression scores compared with vehicle. Data are displayed as mean ± s.e.m. (n = 10).

When acute treatment failed to give an effect, a sub-chronic dosing regime was tested. Rats received 30mg/kg LuAF21934 or AF42744 twice a day at ~12h intervals for 5 days, with L-DOPA-induced AIMs scored starting 30 minutes after the morning drug dose on the fourth day. The results of the AIMs scores are shown in Figure 93, relative to the scores obtained when these rats received an acute dose of vehicle.

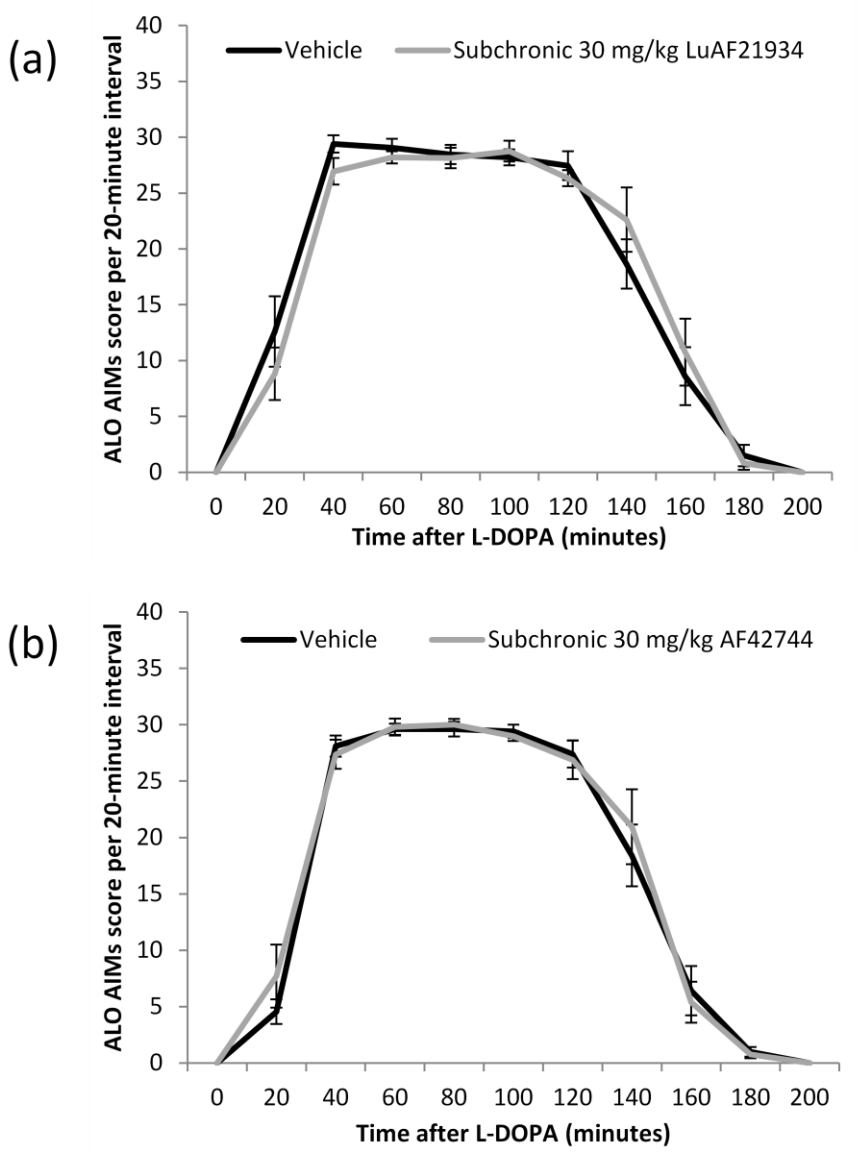

Figure 93: Time course of L-DOPA response following sub-chronic administration of $mGlu_4$ PAMs. There was no AIMs suppressing effect of 3.5-day twice-daily dosing with either 30mg/kg LuAF21934 (a) or 30mg/kg AF42744 (b) compared with the response 30 minutes after dosing with vehicle. L-DOPA was administered 30 minutes after the preceding drug/vehicle dose. Data are presented as mean ± s.e.m. (n = 9 (a) or n = 10 (b)).

Neither LuAF21934 nor AF42744 had a significant effect on the overall AIMs score when dosed sub-chronically in this manner. LuAF21934-treated rats had a total AIMs score of 181 ± 8 compared with 184 ± 8 when pre-treated with vehicle (P=0.6857; part of the one-way RM ANOVA above), and showed no significant change within the subtype scores (data not shown). AF42744-treated rats had a total AIMs score of 178 ± 7 compared with 173 ± 6 when pre-treated with vehicle (P=0.4190; part of the one-way RM ANOVA above), and similarly showed no significant change within subtype scores (data not shown).

Sub-chronic treatment with LuAF21934 or AF42744 did not have any lasting effects on normal AIMs expression, such that there was no difference in total AIMs score when rats were re-tested on day 13 (see Figure 79) compared with their scores on day 14 of the priming period (P>0.4534; paired t-tests, data not shown).

6.3.4.4 Amantadine significantly reversed expression of AIMs

Since neither novel compound reversed the AIMs expressed by these animals, rats were administered 40mg/kg amantadine.HCl 30 minutes prior to L-DOPA as a positive control. Results from the exploratory study indicated that this should reduce the AIMs scores of severely dyskinetic rats by around 30%. On this occasion the overall AIMs score was reduced by 42 ± 4%, from 180 ± 7 to 106 ± 10 (Figure 94). This represented a significant inhibition of AIMs expression (P<0.0001; paired t-test). Within the AIMs subtypes, amantadine treatment reduced the axial dyskinesia score by 37 ± 6%, the forelimb score by 40 ± 4% and the orolingual score by 54 ± 4% (all P<0.0001; paired t-tests).

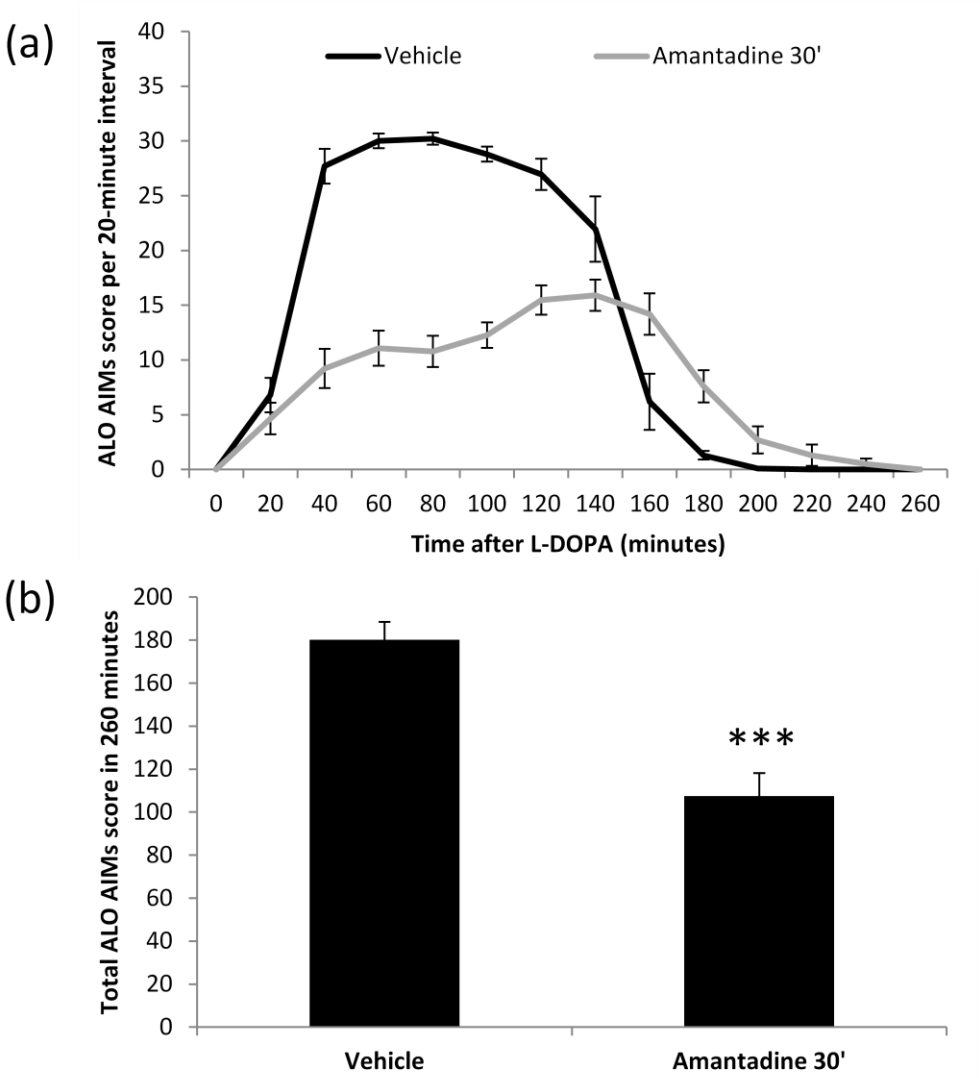

Figure 94: AIMs expression was suppressible by pre-treatment with amantadine. AIMs in the rats used for testing the antidyskinetic potential of LuAF21934 and AF42744 were suppressible by 30-minute pre-treatment with 40mg/kg amantadine. Data are expressed as mean ± s.e.m. (n = 10) ***P<0.0001 versus AIMs following vehicle treatment (paired t-test).

6.3.4.5 mGlu$_4$ PAMs did not affect the rotational response to L-DOPA

In order to examine whether or not LuAF21934 or AF42744 could potentiate the effects of L-DOPA and therefore act as L-DOPA sparing agents, 30mg/kg doses of each drug were tested acutely for their ability to potentiate the rotational response to a sub-maximal dose of L-DOPA.

The total number of net contraversive rotations was measured in rats for 180 minutes following a dose of 5mg/kg L-DOPA + 15mg/kg benserazide (Figure 95). 30 minutes before L-DOPA administration, rats received an oral dose of either vehicle, 30mg/kg LuAF21934 or 30mg/kg AF42744. Neither AF21934 nor AF42744 altered the rotational response of these

primed rats to L-DOPA compared with vehicle (LuAF21934 311 ± 79 turns, AF42744 442 ± 103 turns both versus vehicle 317 ± 45 turns; P=0.1821; one-way RM ANOVA with Dunnett's *post-hoc*).

Neither drug elicited any rotational response in the absence of L-DOPA (Drug/saline vs. Vehicle/saline P>0.405; paired t-tests) and saline elicited a significantly reduced rotational response in all groups compared with the corresponding response to 5mg/kg L-DOPA (P<0.0001; paired t-tests).

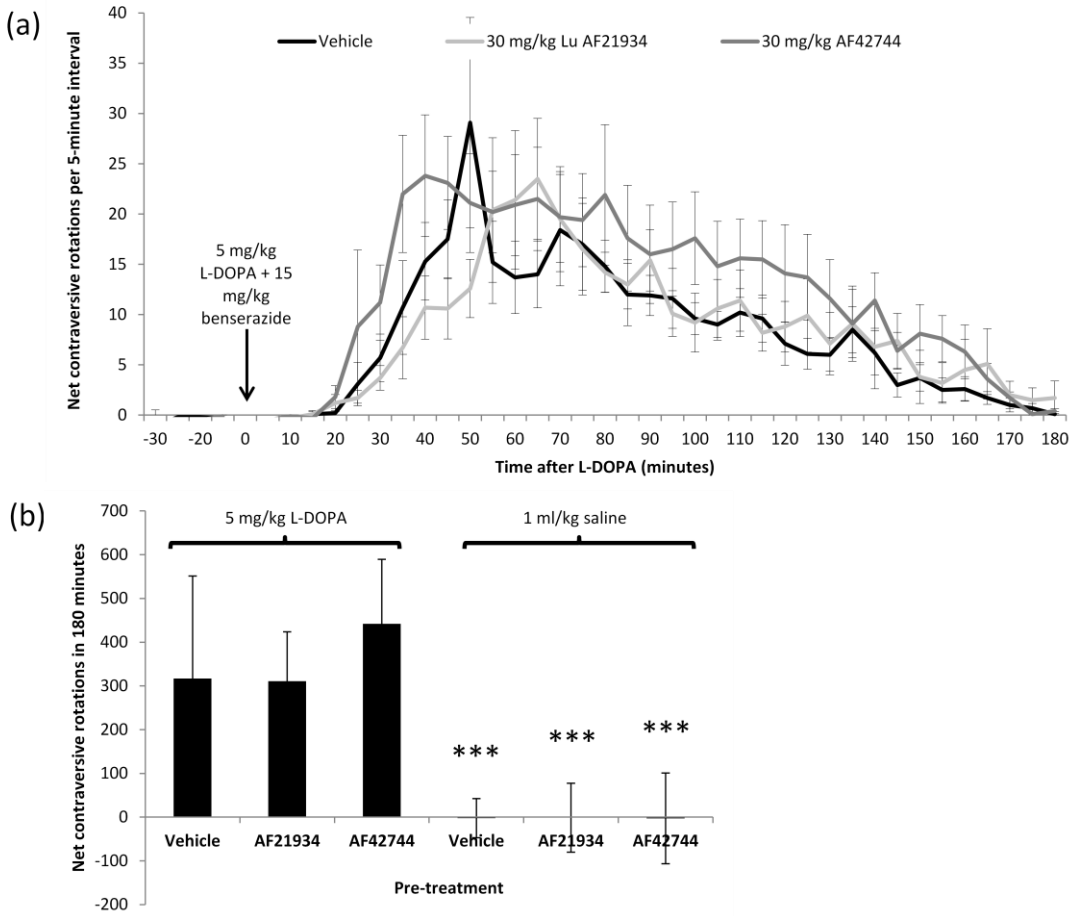

Figure 95: Rotations in response to low-dose L-DOPA following pre-treatment with $mGlu_4$ PAMs. Graph (a) shows the time course of rotations induced by 5mg/kg L-DOPA following 30-minute pre-treatment (p.o.) with Vehicle or 30mg/kg LuAF21934 or 30mg/kg AF42744. (b) Quantification of net contraversive rotations over 180 minutes after injection with either L-DOPA or saline vehicle following the aforementioned pre-treatments. Data are displayed as mean ± s.e.m. (n = 10) ***P<0.001 versus corresponding treatment with L-DOPA (paired t-tests).

In order to check that the $mGlu_4$ PAMs did not worsen the normal antiparkinsonian response to L-DOPA, the number of net contraversive rotations was also measured on the

fifth day of sub-chronic treatment, this time against a high dose of L-DOPA (10mg/kg + 15mg/kg benserazide) and for a period of 240 minutes (Figure 96). This rotational response was compared with the rotational response elicited by the same dose of L-DOPA following an acute (rather than sub-chronic) dose of vehicle.

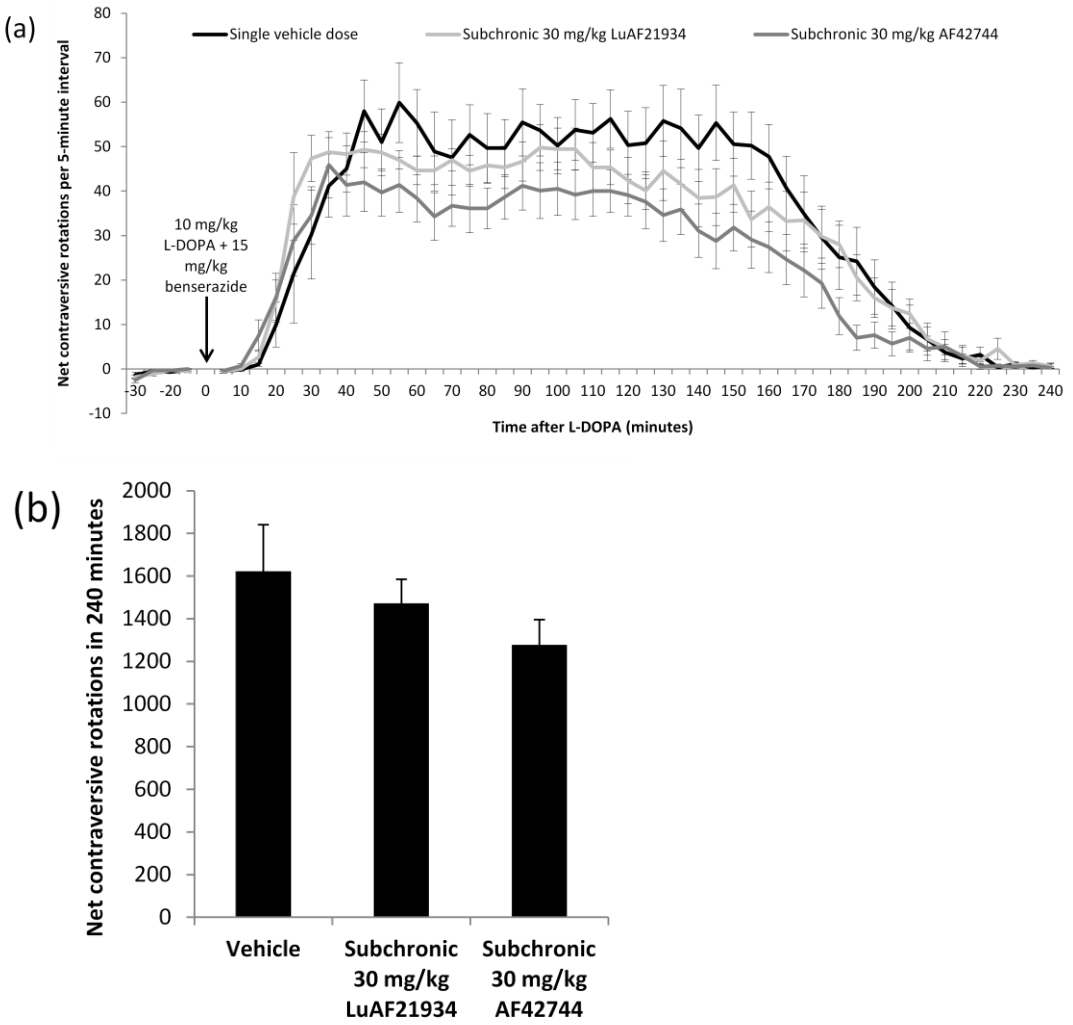

Figure 96: Rotations in response to high L-DOPA following sub-chronic pre-treatment with $mGlu_4$ PAMs. Graph (a) shows the time course of rotations induced by 10mg/kg L-DOPA following 30-minute pre-treatment with Vehicle, 30mg/kg LuAF21934 or 30mg/kg AF42744. (b) Quantification of net contraversive rotations over 240 minutes. Data are displayed as mean ± s.e.m. (n = 10).

Vehicle-pretreated L-DOPA-injected rats had a mean net rotational asymmetry of 1493 ± 234 contraversive turns in 240 minutes, compared with 1472 ± 113 when pre-treated with 30mg/kg LuAF21934 and 1175 ± 147 when pre-treated with 30mg/kg AF42744. Net rotational asymmetry in response to 10mg/kg L-DOPA was therefore not significantly affected by sub-chronic pre-treatment with 30mg/kg LuAF21934 or AF42744 compared

with vehicle (P=0.2407; one-way RM ANOVA with Dunnett's *post-hoc*). Although not a direct comparison, the results of this experiment also point to the fact that neither LuAF21934 nor AF42744 affects the rotational response of these rats to an L-DOPA challenge.

Thus while the $mGlu_4$ PAMs tested did not offer any L-DOPA sparing capacity alongside a low dose of L-DOPA, neither did they suppress the rotational response to a high dose of L-DOPA. Therefore treatment with $mGlu_4$ PAMs does not suppress the antiparkinsonian action of L-DOPA.

6.3.5 Inhibition of induction of L-DOPA-induced dyskinesia

6.3.5.1 Lesioned rats displayed functional deficits

Lesioned rats were assessed using the cylinder test and amphetamine-induced rotations to establish whether or not the lesion was successful. The mean number of net ipsiversive rotations over 120 minutes was 222 ± 38, ranging between 13 and 534. Amphetamine-induced rotations are known to be variable, therefore the additional measure of contraversive paw use in the cylinder test was used to help decide which rats to include and which to exclude. Two rats with 51 and 60% use of the contralateral paw were deemed to have an incomplete lesion and were excluded from the rest of the study. The remaining 21 rats were stratified by their net amphetamine-induced rotational response to give three groups (n = 7 each) of equal chance of developing AIMs in response to L-DOPA priming. There were no differences between groups with respect to amphetamine-induced rotations (P=0.9938; one-way ANOVA with Bonferroni *post-hoc*) or contralateral paw use in the cylinder test (P=0.6769; one-way ANOVA with Bonferroni *post-hoc*).

6.3.5.2 6-OHDA lesioning caused a severe loss of TH-positive cells in the SNc

At the end of the experiment the lesion success was verified by quantification of tyrosine hydroxylase-immunopositive cells in the substantia nigra. MFB lesions are expected to result in >98% loss of TH-positive cells in the SNc. One rat from the vehicle group was excluded at this stage as it had only 88% cell loss, leaving n=6 in this group, but n=7 in both the 10 mg/kg and 30 mg/kg treatment groups. An example of the cell loss obtained in these rats is shown in Figure 97, together with quantification of the data.

When post-lesion amphetamine-induced rotations and cylinder contralateral paw use were reanalysed with this rat removed there were still no significant differences between groups with respect to either parameter (P=0.9654 and P=0.7827 respectively; one-way ANOVAs with Bonferroni *post-hoc* tests).

There were no significant differences between groups with respect to intact SNc cell number (P=0.9326; one-way ANOVA with Bonferroni *post-hoc*), lesioned SNc cell number (P=0.1127; one-way ANOVA with Bonferroni *post-hoc*) or the overall % cells remaining in the lesioned side (P=0.1055; one-way ANOVA with Bonferroni *post-hoc*).

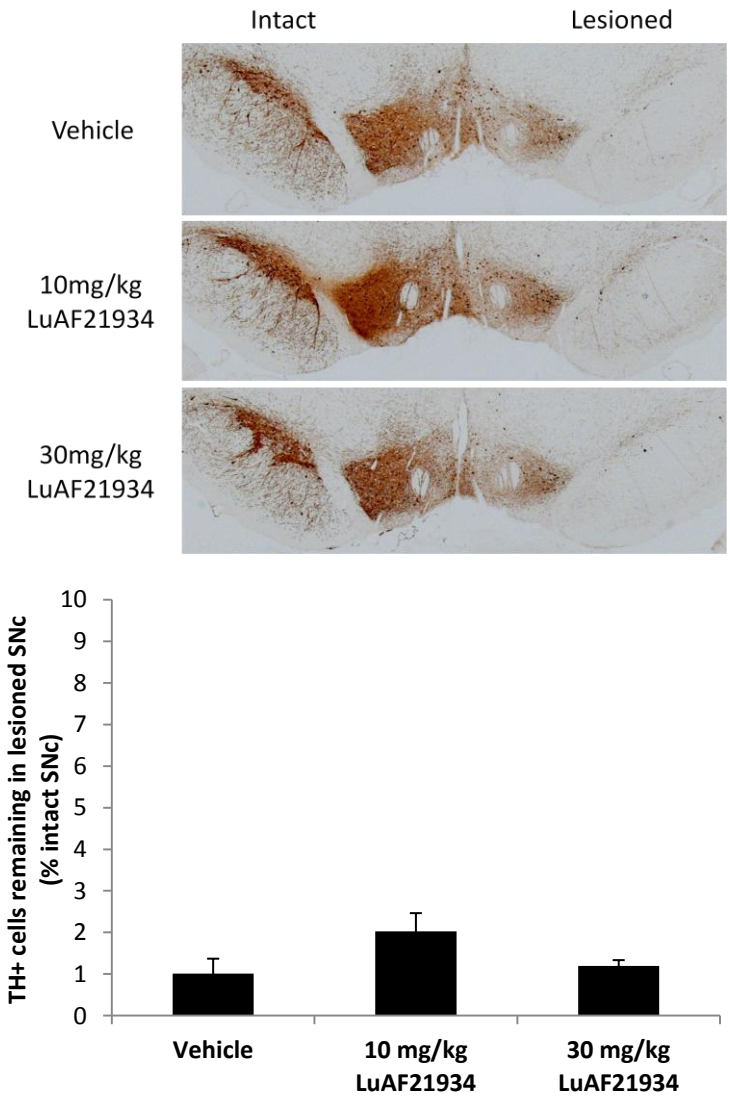

Figure 97: Verification of lesion size for the AIMs induction study. The upper panel shows images of typical cell loss patterns in each group in the AIMs induction study. The graph below shows the cells remaining in the lesioned SNc as a percent of those counted in the intact SNc. There was no difference between treatment groups with regard to the degree of cell-loss induced by the lesion, and therefore the risk of developing AIMs in response to repeated exposure to L-DOPA is expected to be similar. Data are presented as mean ± s.e.m. (n = 6-7 per group).

6.3.5.3 Incidence of dyskinesia was not reduced by LuAF21934

Rats were defined as having developed dyskinesia where the duration scores for all AIMs subtypes was >1 (Lundblad *et al.*, 2002). Early in the study, on day 2, there was a suggestion that rats treated with 30mg/kg LuAF21934 might be developing AIMs more slowly than vehicle-treated rats (Figure 98a), however this was not statistically significant (P=0.266; Fisher's exact test). From day 5 onwards the number of rats in each group that was considered to be dyskinetic was stable (Figure 98b). 5 out of 6 rats in the vehicle group developed dyskinesia by the end of the 14-day L-DOPA priming period. This was not

significantly different to the incidence of dyskinesia at day 14 in rats treated with 10mg/kg LuAF21934 (7 out of 7 rats; P=0.462) or in rats treated with 30mg/kg LuAF21934 (6 out of 7 rats; P=1.000).

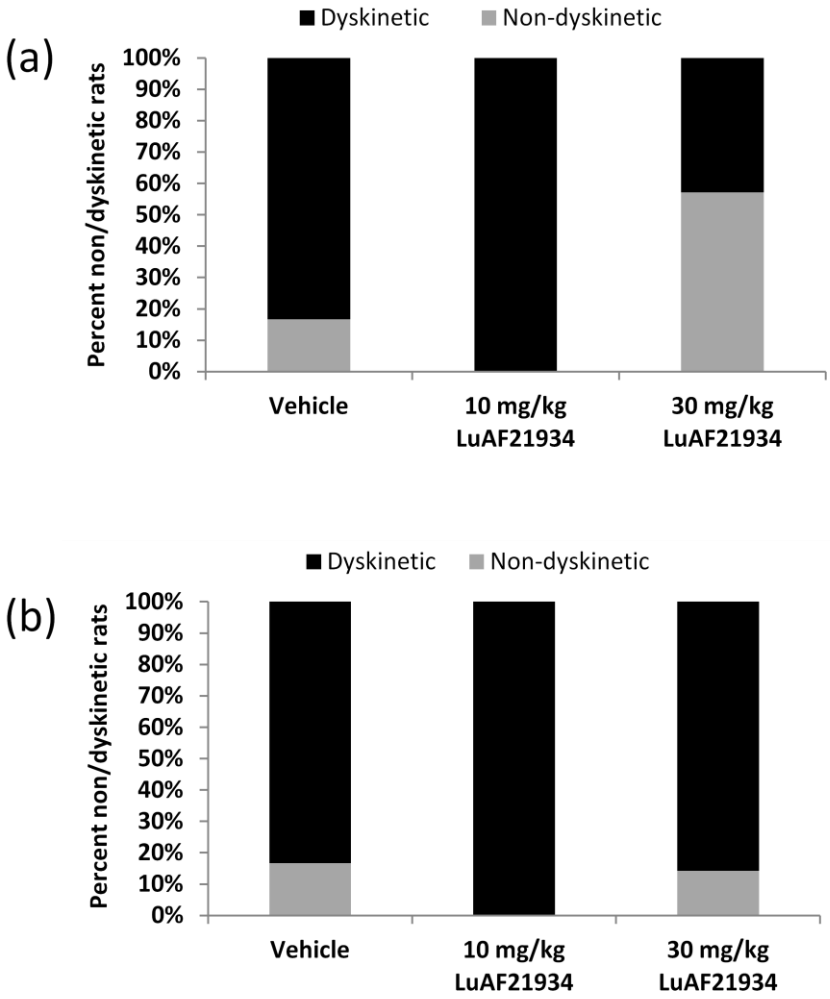

Figure 98: Incidence of dyskinesia in rats treated for 14 days with L-DOPA, with or without LuAF21934. Once-daily L-DOPA was administered 30 minutes after pre-treatment with either vehicle, 10mg/kg LuAF21934 or 30mg/kg LuAF21934. (a) shows the incidence of dyskinesia on day 2 of treatment and (b) shows the incidence of dyskinesia on days 5, 8, 11 and 14 (identical results for all days). Data are displayed as percentages of each group.

6.3.5.4 Severity of dyskinesia was not reduced by LuAF21934

The severity of dyskinesia between groups was assessed by comparing the scores of all rats that were considered to have developed dyskinesia, as defined in the methods. Comparing the development of overall dyskinesia (total score for all subtypes, duration x severity), there was an effect of time (P<0.0001) but not of treatment (P=0.5364). When the AIMs subtypes (total score for duration x severity) were assessed between groups this effect of

time was maintained (P<0.0001) but there was still no effect of treatment (axial P=0.469; limb P=0.435; orolingual P=0.703). These data are shown in Figure 99.

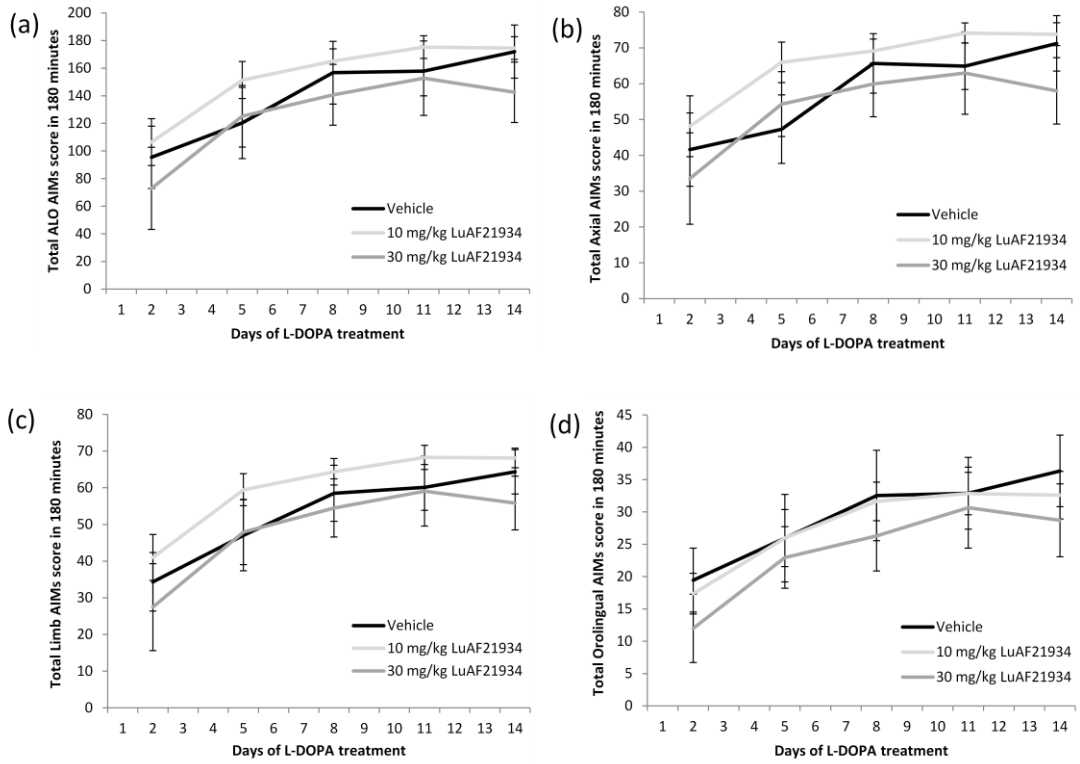

Figure 99: Time course showing the development of AIMs with or without LuAF21934. Time courses are shown for (a) total AIMs, (b) axial AIMs, (c) limb AIMs and (d) orolingual AIMs in rats that developed dyskinesia following 14 days of treatment with L-DOPA in combination with either vehicle, 10mg/kg LuAF21934 or 30mg/kg LuAF21934. Data are displayed as mean ± s.e.m. (n = 5-7 per group). While there was a significant effect of time on total AIMs and total subtype scores, there was no effect of treatment on any of these parameters.

The significant effect of time on AIMs scores was expected, since in the exploratory study reported earlier in this chapter we saw that the scores for all AIMs subtypes increase over the course of the first few days of the priming period, stabilising after 5-7 doses of L-DOPA.

Total AIMs and AIMs subtype scores were then compared for duration score or for severity score independently. For total AIMs where was still no effect of treatment on either parameter (P<0.0001 for the effect of time, P>0.439 for the effect of treatment). Neither was any effect of treatment found for the individual duration or severity scores for the AIMs subtypes. Table 14 shows the results of all the individual analyses performed.

Table 14: AIMs development over 14 days of L-DOPA priming with or without LuAF21934. The development of total AIMs and AIMs subtypes were compared between groups for dyskinetic rats (Two-way ANOVAs with Bonferroni *post-hoc*). These scores were further divided into duration and severity scores to test for an effect of treatment on these finer parameters. No effect of treatment was found. D x S = duration x severity score

	ALO total (D x S)	**ALO Duration**	**ALO Severity**	**Axial total (D x S)**	**Axial Duration**	**Axial Severity**
Time effect	P<0.0001	P<0.0001	P<0.0001	P<0.0001	P<0.0001	P<0.0001
Treatment effect	P=0.5364	P=0.4397	P=0.5623	P=0.4689	P=0.4541	P=0.6224
	Limb total (D x S)	**Limb Duration**	**Limb Severity**	**Orolingual total (D x S)**	**Orolingual Duration**	**Orolingual Severity**
Time effect	P<0.0001	P<0.0001	P<0.0001	P<0.0001	P<0.0001	P<0.0001
Treatment effect	P=0.4347	P=0.3403	P=0.3798	P=0.7033	P=0.5272	P=0.6137

6.4 Discussion

The purpose of the studies in this chapter was to investigate the potential of $mGlu_4$ positive allosteric modulators to suppress the expression of established L-DOPA-induced AIMs in rats, or to inhibit the development of AIMs in denervated rats when administered alongside L-DOPA during priming. In order to design these experiments we firstly investigated the pharmacokinetics of the $mGlu_4$ PAMs that were tested in order to choose a suitable pre-treatment time, and secondly we carried out an exploratory study to characterise the development of AIMs in rats with an MFB lesion using our chosen protocol of once-daily administration of 6.25 mg/kg L-DOPA (+ 15 mg/kg benserazide), including identification of a positive control compound for AIMs suppression.

6.4.1 Pharmacokinetics of tested compounds

The pharmacokinetics studies carried out demonstrated that oral dosing of LuAF21934 and AF42744 gave maximum plasma exposures within 1 hour of dosing, followed by 1-3 hours of reasonable plasma exposure (at least ½ C_{max}). This led us to administer both drugs 30 minutes prior to L-DOPA dosing so that the drug C_{max} was coincident with the striatal C_{max} of L-DOPA (Carta *et al.*, 2006), and was at a good concentration for the subsequent 1-2 hours during which time L-DOPA-induced AIMs are expressed.

LuAF21934: As reported in Chapter 4, there are no published reports of the pharmacokinetic profile of LuAF21934 following oral administration, however Bennouar et al (2013) reported the 1-hour brain and plasma concentrations following a subcutaneous dose of 10mg/kg LuAF21934 in hydroxypropyl-β-cyclodextrin. This resulted in a brain concentration of 2422ng/g, and a plasma concentration of 2763ng/ml; a brain/plasma ratio of 0.88. The results of PK1 suggest that for the same dose given orally, the plasma C_{max} is considerably diminished to 869ng/ml, likely reflecting a combination of a slower rate of absorption from the intestinal tract compared with the subcutaneous space and loss of drug via first-pass metabolism in the liver. From the PK study that was reported in Chapter 4 (PK-B), the brain C_{max} was 3963 ± 585ng/g at 1 hour following a 30mg/kg dose and the plasma C_{max} was 6060 ± 721ng/ml at the same time point, giving a brain/plasma ratio of 0.65. Though slightly lower than that described by Bennouar et al. it is comparable and suggests that a good proportion of the circulating drug crosses the BBB.

Results from slice electrophysiology demonstrated a significant effect of LuAF21934 at the synapse of key interest with respect to LID, the corticostriatal synapse. LuAF21934 was able to inhibit corticostriatal excitatory post-synaptic currents (EPSCs) (Bennouar *et al.*, 2013;

Gubellini *et al.*, 2014), requiring a bath concentration of at least 1μM – interestingly the reported EC_{50} concentration of LuAF21934, 500nM, had no significant inhibitory effect on EPSCs in either of these studies.

1μM LuAF21934 is the equivalent of 315.2ng/ml in plasma (315.2ng/g in brain). The brain C_{max} measured for this compound in Chapter 4 was 3963ng/g, attained 1 hour following the 30mg/kg dose, which is over 10-fold higher than this threshold. However the free fraction of LuAF21934 in rat brain homogenate has been measured at 3% of the total concentration (Bennouar *et al.*, 2013). This means that LuAF21934 was present in the brain at a free concentration of around 119ng/g at 1 hour after the highest dose that was used in these studies, which at ~0.38μM is below both the EC_{50} at $mGlu_4$ (0.5μM) and the threshold for inhibition of corticostriatal EPSCs according to the electrophysiological studies that have been previously performed (1μM). Nonetheless LuAF21934 is known to exert a pharmacological effect in the haloperidol model of catalepsy when total brain concentration is ≥400ng/g (Bennouar *et al.*, 2013), and the brain C_{max} obtained for LuAF21934 in the PK study in Chapter 4 was 10-fold higher than this. Therefore even if overall free brain concentrations of LuAF21934 are low, it is still possible that local free brain concentrations of LuAF21934 may be sufficient to activate target receptors in certain brain regions, or that the *in vivo* potency of LuAF21934 is higher than that measured *in vitro*; a discrepancy between the *in vitro* potency and the *in vivo* pharmacological efficacy of LuAF21934 would not be unexpected given that the correlation between these parameters is not always strong (Gleeson *et al.*, 2011). Overall, we are therefore confident that LuAF21934 had every opportunity to display any antidyskinetic efficacy in the AIMs reversal and induction studies.

AF42744: A full plasma profile following oral dose of 10mg/kg and 30mg/kg AF42744 has been reported previously, with plasma C_{max} values of 613 and 3230ng/ml respectively and a half life of 2.9 hours after an oral dose (Célanire *et al.*, 2011; Le Poul *et al.*, 2012). Whereas the $t_{1/2}$ obtained in PK1 for AF42744 (2.8 hours) was comparable with the previously reported value, the plasma C_{max} values obtained were approximately 2-fold higher at 1355ng/ml and 5407ng/ml for 10 and 30mg/kg oral doses respectively. This could reflect the differing vehicles used, as Le Poul *et al.* administered AF42744 as a suspension in carboxymethylcellulose, perhaps limiting the bioavailability compared with administration of a drug that has been fully solubilised in PEG-400 as in the case of PK1. Brain concentrations were not reported in this paper, but CSF concentrations (which more

closely reflect free concentrations of drug in the brain) were measured at plasma t_{max} as 150nM following 10mg/kg and 1014nM following 30mg/kg AF42744.

The 2-hour brain/plasma ratio in the samples collected for AF42744 in PK2 was calculated to be 0.74, which is comparable to previous in-house data collected at Lundbeck where the brain/plasma ratio was ~1.0 following a subcutaneous dose. However the lower-than-expected absolute concentrations measured in these samples suggest that the extended period of storage in the -80°C freezer between collection and analysis (6 months) led to a degree of sample degradation. When the plasma and brain samples for PK2 were analysed for LuAF21934, lower than expected drug concentrations were also detected in these samples compared with the plasma and brain samples collected at this time point in a previous PK study (PK-B, reported in Chapter 4). Nonetheless, the rates of degradation in brain and plasma samples for LuAF21934 seem to have been roughly equivalent, meaning that the brain/plasma ratio was not significantly different in PK2 (0.55) compared with the Chapter 4 PK-B study (0.66). This suggests that the brain/plasma ratio measured for AF42744 in PK2 (0.74) may also be close to the true value despite the fact that the absolute plasma and brain concentrations are lower than might be expected. Having said that, the possible brain/plasma ratios that can be calculated depending on whether or not the rats whose brains had undetectable AF42744 concentrations are included are very different from each other. The only way to resolve this issue would be to repeat the study, preparing the brain homogenates 24 hours after collection as in the PK-B study in Chapter 4. For the purposes of the rest of this discussion I will assume the brain/plasma ratio of 0.74 is the true value, in order to assess the best possible scenario.

No electrophysiological data has been reported for AF42744 at the corticostriatal synapse of key interest here, or indeed at any BG synapse but its potency at rat $mGlu_4$ is higher than LuAF21934 (EC_{50} = 9.1nM AF42744 compared with 500nM for LuAF21934). Therefore it might be expected that a 50-fold lower concentration of this drug in the brain (i.e. 20nM) would have comparable effects on corticostriatal transmission to those found for 1µM LuAF21934 (Bennouar *et al.*, 2013). 20nM AF42744 is equivalent to 5.45ng/ml in plasma (5.45ng/g in brain). The plasma C_{max} measured for this drug was far above this threshold after both 10 and 30mg/kg doses, but more importantly the brain/plasma ratio was 0.74, equating to approximately 1003ng/g and 4001ng/g in the brain at t_{max} respectively. The unbound fraction of AF42744 in the brain has been determined at 1% (internal data, Lundbeck), leaving unbound brain concentrations following 10mg/kg and 30mg/kg

AF42744 of 10.3ng/g and 40.1ng/g respectively. These are the equivalent of 37.8nM and 147.3nM, which are 5- to 10-fold lower than the 150nM and 1014nM CSF concentrations measured by another group following oral administration of 10 and 30mg/kg AF42744 (Le Poul *et al.*, 2012), however CSF concentrations are only an estimate of the free drug concentration in the brain, generally within 3-fold of each other (Friden *et al.*, 2009; Liu *et al.*, 2009), so this would suggest that our estimated values are not unreasonable. More importantly, the free brain concentrations in our best case scenario are above the 20nM concentration calculated above to have a similar potency to a 1µM concentration of LuAF21934, and also exceed the EC_{50} of AF42744 at rat $mGlu_4$ (9.1nM).

We would therefore expect that the doses of AF42744 used in the dyskinesia reversal study would result in sufficient free brain concentrations to activate $mGlu_4$, which is supported by the finding that 3, 10 and 30mg/kg AF42744 are effective against haloperidol-induced catalepsy in the rat (Le Poul *et al.*, 2012). These free brain concentrations should not be sufficient to interact with other known targets of AF42744, for example adenosine A_1, adenosine A_3 and $mGlu_8$ receptors (EC_{50} all ~2.2µM), meaning that any effects are expected to be mediated by selective activation of $mGlu_4$.

Amantadine: Given that amantadine is currently prescribed in patients with LID, we wanted to use this drug as a positive control for the reversal of dyskinesia in the rat AIMs model. Based on similar pre-treatment times in previous published research (Breger *et al.*, 2013) we decided that in our AIMs experiments we would administer amantadine 30 minutes prior to L-DOPA, and therefore we wanted to ascertain the brain concentration of amantadine close to the time of its peak effect (when AIMs expression is maximal), which is 60 minutes following L-DOPA injection and therefore 90 minutes after amantadine injection. Following a subcutaneous dose of 40mg/kg amantadine, the measured brain concentration was 23,633ng/g, equivalent to 156.25µM. The brain/plasma ratio was 9.40, which is comparable with the ratio of 9.9 obtained in mice following oral doses of amantadine (Kooijmans *et al.*, 2012), suggesting that amantadine is actively transported across the BBB by a Na^+ and Cl^--dependent transporter in both species. The fraction of amantadine that is unbound in the brain is 23.3% (Summerfield *et al.*, 2007), equivalent to 5506.5ng/g or 36.4µM in our PK3 study. This is a slightly higher than both the *in vitro* potency of amantadine on striatal NMDA receptors (IC_{50} = 12.4µM; Parsons *et al.*, 1996) and the free brain concentration of amantadine measured by microdialysis in rats following a comparable dose (11µM; Kornhuber *et al.*, 1995). Nevertheless this free concentration is

only an indirect estimate, and as such it is not unreasonable to assume that the real free brain concentration of amantadine measured in our study is likely not dissimilar to either the IC_{50} value or the concentrations measured directly in previous studies. Therefore the brain concentration of amantadine after 90 minutes in our PK3 study is broadly in line with previous data and also implies that if administered 30 minutes prior to L-DOPA, amantadine will be present in the brain in the range at which NMDA receptor transmission is effectively inhibited at the time when the pharmacological effect of L-DOPA is maximal.

6.4.2 General considerations for PK studies

The main limitation in the way in which these PK studies were carried out is that only total brain and plasma concentrations were measured. This means that calculations of the free brain concentrations are indirect, relying on the applicability of brain binding data that was collected *in vitro* to the *in vivo* situation. To avoid this issue, future PK studies might involve microdialysis in relevant brain areas (e.g. the striatum for dyskinesia studies) in order to accurately measure the drug concentration in the extracellular space.

In addition, we had some discrepancies in the brain concentrations for both LuAF21934 and AF42744 measured in PK2 compared with those that would be expected based on the PK data for LuAF21934 reported in Chapter 4. The underlying reasons for this are unknown, but could relate to issues of stability during storage and shipping. The influence of storage on drug levels was clearly demonstrated by the fact that both brain and plasma samples in PK3 had around 67% reduced LuAF21934 content when samples were stored for 6 months, compared with when they were analysed within a week. Therefore any fluctuations in storage conditions or temperatures that affected the brain samples in PK2 could account for these differences.

6.4.3 Exploratory study

6.4.3.1 Induction of AIMs

The results of this study confirmed that using a combination of a 6-OHDA lesion of the MFB and a 21-day daily treatment regimen with L-DOPA it was possible to successfully induce AIMs in rats. Either the 6-OHDA lesion alone (with vehicle-treatment during the priming period) or L-DOPA treatment alone (in rats with a sham lesion and therefore an intact nigrostriatal pathway) was insufficient to induce dyskinesia, demonstrating that the combination of both is necessary for this phenomenon to occur. The AIMs expressed in 6-OHDA/L-DOPA rats included axial, forelimb and orolingual manifestations that increased at comparable rates upon initiation of priming, reaching maximal severity by day 11 of

treatment. Only one of the nine rats treated with L-DOPA failed to express AIMs of all subtypes with a duration score of 3 or 4, therefore the incidence of severe dyskinesia is high when using this protocol, and is comparable to a previous report regarding both the incidence and severity of dyskinesia obtained (Winkler *et al.*, 2002).

6.4.3.2 Suppression of AIMs

In agreement with previous reports in the rodent model, dyskinetic behaviours evoked by repeated exposure to L-DOPA were suppressible by inhibition of serotonergic signalling by 8-OH-DPAT (Carta *et al.*, 2007; Dupre *et al.*, 2011; Iderberg *et al.*, 2013) or glutamatergic signalling by amantadine (Bido *et al.*, 2011; Breger *et al.*, 2013; Dekundy *et al.*, 2007; Lundblad *et al.*, 2002). Activators of 5-HT_{1A} receptors are mainly thought to decrease dyskinesia by reducing release of dopamine from serotonergic terminals that have aberrantly taken up and converted L-DOPA (Kannari *et al.*, 1991), but there is evidence that they may also reduce striatal glutamate release (Dupre *et al.*, 2013). The side effects noted with the dose of 8-OH-DPAT tested, whereby rats exhibited a flat body posture with bilateral forepaw padding, are qualitatively and temporally similar to those reported in previous rat studies (Dourish *et al.*, 1985; Goodwin *et al.*, 1987), and also reflect a previous report in the macaque model of LID where immobility and abnormal body posture coincided with reduced dyskinesia expression with this dose (Iravani *et al.*, 2006).

It is of particular interest from the point of view of this thesis that amantadine, a weak NMDA receptor inhibitor, significantly suppressed AIMs expression to a degree that was similar to that reported in humans (Luginger *et al.*, 2000). The brain concentration of amantadine measured at inhibition of peak L-DOPA effect was 156.25µM, of which 36.4µM is predicted to be bioavailable. As stated earlier, though this estimated free brain concentration is a little higher than previous data, it is close to the range of the effective free brain concentrations (6-21µM) previously reported in rats (Kornhuber *et al.*, 1995). This lends support to the idea of enhanced glutamatergic signalling as a mechanism behind the expression of this phenomenon. The antidyskinetic mechanism of action of amantadine is thought to mainly result from its inhibitory action on NMDA receptors (Paquette *et al.*, 2012) located on MSNs of the direct pathway, thereby inhibiting striatonigral activation (Bido *et al.*, 2011). However amantadine has a rich pharmacology that is proposed to include enhancement of dopamine synthesis and release (Heikkila *et al.*, 1972) and sensitisation of striatal dopamine receptors (Gianutsos *et al.*, 1985), so part of this effect could be attributable to alterations in activity in dopaminergic neurotransmitter systems. However based on the affinity of ligand used by Gianutsos *et al.* at the different dopamine

receptor subtypes, the enhanced binding reported after long-term administration of amantadine is likely attributable to D2-like receptors, whose activation would in fact decrease signalling in the indirect pathway, further unbalancing BG activation in favour of the direct pathway, therefore this action is unlikely to play a role in the acute antidyskinetic actions of amantadine.

6.4.3.3 Rotational behaviour

Rotational behaviour is not adequately defined in terms of dyskinesia. Several studies in unilaterally-lesioned PD models have measured the contraversive rotations induced by L-DOPA as a measure of its antiparkinsonian efficacy, and have reported various 'L-DOPA sparing' treatments that potentiate the rotations induced by a sub-threshold dose of L-DOPA (Lindén *et al.*, 1988; Rose *et al.*, 2006). However while rotation in non-primed rats following administration of L-DOPA may represent an antiparkinsonian effect, the significance of L-DOPA-induced rotation in primed rats is uncertain, especially as it has been suggested that rotation in primed animals is predominantly a consequence of axial dyskinesia, such that a twisted rat will automatically rotate in the direction in which it is facing (Konitsiotis *et al.*, 2006). In order to address the question of whether turning in L-DOPA primed animals still reflects the antiparkinsonian effect of L-DOPA or whether is it part of the dyskinetic phenomenon, the effects of known antidyskinetic compounds on L-DOPA-induced rotation in dyskinetic animals have been tested. However the results are not yet definitive; while on one hand some studies have found that L-DOPA-induced turning is *not reduced* by known antidyskinetic drugs (e.g. Lundblad *et al.*, 2002), others have found that antidyskinetic drugs *do reduce* contraversive turning (e.g. Henry *et al.*, 1998).

In the study reported here, L-DOPA-induced rotational behaviour in lesioned rats increased between days 2 and 8 but stabilised thereafter, in parallel with the axial subscore and indeed the development of total AIMs. This would certainly seem to support the theory that rotation is driven by axial twisting in dyskinetic rats, and if true would have an obvious confounding effect on the interpretation of this data in relation to the antiparkinsonian efficacy of L-DOPA. However since the effects of 8-OH-DPAT or amantadine on rotational behaviour were not tested in this study it is therefore impossible to say for sure whether the rotational asymmetry measured was indicative of the antiparkinsonian action of L-DOPA or to the development of axial AIMs. In future, measurement of rotational AIMs with these known antidyskinetic agents would help to inform us on whether or not L-DOPA-induced rotation is driven predominantly by axial AIMs in our hands.

Regardless of the lack of clarity as to the significance of rotations in this model, overall the exploratory study served well to validate the establishment of L-DOPA-induced AIMs in this laboratory and to confirm that the behavioural outcomes were certainly sensitive enough to pick up a suppression of dyskinesia with the known antidyskinetic compounds 8-OH-DPAT and amantadine.

6.4.4 Reversal study

In order to suppress the expression of established dyskinesia a drug would need to sufficiently reduce the abnormal basal ganglia transmission elicited by repeated exposure to L-DOPA. The critical glutamatergic synapse involved in this priming process is believed to be the corticostriatal synapse, specifically onto striatonigral neurones.

Neither of the $mGlu_4$ PAMs tested in this study was able to reduce the expression of established severe dyskinesia in rats at the doses tested. There are no previous publications regarding testing of LuAF21934 for reversal, however the results obtained for AF42744 were in line with the single published report thus far using this compound, where rat AIMs expression was not reversed using acute doses of 0.1, 1 or 10mg/kg AF42744 (Le Poul *et al.*, 2012). To my knowledge no other $mGlu_4$ PAMs have been tested for their ability to reverse established AIMs expression, but the $mGlu_4$ orthosteric agonist LSP1-2111 also failed reverse established AIMs in mice (Lopez *et al.*, 2011) in agreement with our results.

The fact that amantadine was able to suppress AIMs in this study demonstrates that inhibition of glutamatergic transmission in these rats represented a valid dyskinetic strategy. This is supported by a wealth of evidence for antidyskinetic efficacy using molecules targeting post-synaptically expressed glutamate receptors, notably NMDA and $mGlu_5$ receptors, as detailed in the introduction to this chapter. Indeed one of the drugs tested in our study, LuAF21934, has been shown to inhibit corticostriatal glutamatergic excitatory post-synaptic currents (EPSCs) in brain slices from naive rats (Bennouar et al., 2013; Gubellini et al., 2014). There is no data published as yet to show that LuAF21934 retains its ability to reduce corticostriatal glutamatergic EPSCs in 6-OHDA lesioned and/or dyskinetic rats, but this would help to identify whether or not an $mGlu_4$ PAM would also modulate signalling under these circumstances. It could be the case that the sensitisation of MSNs thought to underlie the development of dyskinesia is simply too robust to be significantly affected by a positive allosteric modulator, which may only exert a subtle effect on glutamate release that has already been shown to be overactive in the dyskinetic rat striatum (Dupre *et al.*, 2011; Nevalainen *et al.*, 2013).

An alternative possibility is that the net effect of the presence of LuAF21934 or AF42744 at all basal ganglia synapses, as would be obtained following systemic dosing, was small. Since $mGlu_4$ receptors are present and functional at multiple glutamatergic and GABAergic synapses in this system (detailed elsewhere in this thesis), their simultaneous activation at all locations could exert opposing effects and cancel each other out (Cuomo *et al.*, 2009; Gubellini *et al.*, 2014; Marino *et al.*, 2003; Valenti *et al.*, 2005). For example $mGlu_4$ mRNA has been localised to the striatum, GP and STN (Messenger *et al.*, 2002; Testa *et al.*, 1994), and $mGlu_4$ receptor protein to the GP, SNr and EPN (Bradley *et al.*, 1999b; Bradley *et al.*, 1999c; Broadstock *et al.*, 2012; Corti *et al.*, 2002), so activation of $mGlu_4$ could reduce signalling in the indirect pathway. This might counteract the antidyskinetic action of decreased activation in the direct pathway elicited by reduction of glutamate release from corticostriatal neurones.

Finally it is also possible that the drugs were not present at sufficient concentrations at the relevant brain regions to affect neurotransmission. While our projected free brain concentration of AF42744 (see earlier) would suggest that this drug is present in the brain at sufficient concentrations to selectively activate $mGlu_4$, this was not the case for LuAF21934. Based on the PK study reported in Chapter 4 and internal Lundbeck studies into drug binding in brain homogenates, we estimate that at the highest dose given, 30mg/kg, LuAF21934 was present in the brain at a free concentration of around 377nM. This is around two thirds of the EC_{50} concentration of LuAF21934 at $mGlu_4$ (~500nM) and could mean that there is insufficient bioavailable drug to give meaningful activation of these receptors. It is also only a third of the concentration that was required to inhibit corticostriatal EPSCs *in vitro* (1μM; Bennouar *et al.*, 2013). However, the translatability between *in vitro* measures of potency and *in vivo* average brain free concentrations is unclear. It is possible that LuAF21934 is not homogenously distributed in the brain and could therefore be present in sufficient local concentrations to activate $mGlu_4$ receptors in certain regions. Certainly the total brain concentrations measured in our PK studies (C_{max} = 3963ng/g) are comparable if not higher than other studies into the antiparkinsonian actions of LuAF21934 where a definite pharmacological effect has been found (e.g. 400-2500ng/g at the time of peak effect in the haloperidol model; Bennouar *et al.*, 2013).

Thus targeting $mGlu_4$ receptors with PAMs is not an efficacious way of reversing or suppressing established dyskinesia. In addition, since the completion of this study in rats a similar study has been carried out in MPTP-treated marmosets, where doses of 3mg/kg and

10mg/kg LuAF21934 administered p.o. immediately before 8mg/kg L-DOPA + 10mg/kg benserazide failed to reduce the expression of established dyskinesia (unpublished data, M. Jackson *et al.* 2014). This is perhaps not surprising given the many striatal signalling alterations that are involved in the development of dyskinesia, meaning that a subtle alteration in corticostriatal glutamate release is likely insufficient to meaningfully reduce activation of the sensitised post-synaptic striatonigral neurone. Indeed the only effective glutamatergic therapies that have been reported in the literature to inhibit expression of established dyskinesia target post-synaptic AMPA, NMDA or group I mGlu receptors that are known to be involved with D1 receptor signalling (see sections 6.1.2 to 6.1.5), and thus directly inhibit activation of these neurones, whereas agonists or PAMs of the predominantly pre-synaptic group II or group III mGlu receptors, which seek to reduce activation of the post-synaptic neurone indirectly by inhibiting presynaptic neurotransmitter release, have so far failed to reproduce this effect (Le Poul *et al.*, 2012; Lopez *et al.*, 2011; Rylander *et al.*, 2009).

6.4.5 L-DOPA sparing/potentiation

This test was carried out to ascertain whether $mGlu_4$ PAMs could act as L-DOPA potentiators, and also to rule out any inhibitory effects of these PAMs on the antiparkinsonian actions of L-DOPA. However as discussed earlier, the significance of rotational behaviour in this model is not well-defined. It is likely that even if L-DOPA-induced rotations in dyskinetic rats partly reflect the antiparkinsonian actions of L-DOPA, they will be confounded by the strong influence that axial AIMs are believed to play in also promoting contraversive turning (Konitsiotis *et al.*, 2006).

If one were to suppose that L-DOPA-induced rotational asymmetry is representative of the antiparkinsonian effect of L-DOPA then the results of the L-DOPA potentiation study would suggest that neither LuAF21934 nor AF42744 potentiate, or indeed inhibit, this antiparkinsonian action. Alternatively if one were to suppose that rotational asymmetry reflects the degree of overall or axial dyskinesia elicited by L-DOPA, then these rotometry results would suggest that neither drug suppressed nor exacerbated overall AIMs, or axial subtype AIMs. This reflects the data collected earlier in this study regarding the lack of effect of an acute dose of either LuAF21934 or AF42744 on the duration or severity of overall or axial AIMs.

Therefore the interpretation of these results could be that $mGlu_4$ PAMs do not potentiate or inhibit the antiparkinsonian actions of L-DOPA, or that $mGlu_4$ PAMs do not improve or

worsen axial AIMs, or indeed that both conclusions are correct if both mechanisms contribute to the overall rotational response. Meanwhile in a recent marmoset study where we assessed the ability of LuAF21934 to reverse established dyskinesia, we found that this drug had no detrimental or L-DOPA potentiating effects with regard to the antiparkinsonian actions of L-DOPA in this model. This supports the results of the rat study in finding no overall effect in either direction.

L-DOPA potentiation/sparing activity has previously been reported for both drugs tested in this study (Bennouar *et al.*, 2013; Le Poul *et al.*, 2012), and similarly for other $mGlu_4$ PAMs such as VU0364770 (Jones *et al.*, 2012), however notably these results were obtained using behavioural tests such as the cylinder and adjusted steps tests rather than L-DOPA-induced rotational asymmetry. The failure of LuAF21934 and AF42744 to potentiate L-DOPA-induced rotations in our experiments is in contrast to a recent study showing that a different $mGlu_4$ PAM, TAS-4, dose-dependently potentiates L-DOPA-induced turning in lesioned rats (Dube *et al.*, 2014). However it is important to note that in all the studies of L-DOPA sparing activity mentioned above, the rats were lesioned but had either not undergone L-DOPA priming or were primed but had not developed dyskinesia. It is therefore difficult to tell to what extent the L-DOPA-induced rotation measured in our study, where all rats were severe dyskinetic, was reflective of the antiparkinsonian effects of L-DOPA and to what extent it was reflective of the dyskinesiogenic effects of L-DOPA. Since no other tests of the antiparkinsonian actions of L-DOPA, such as the cylinder test or rotarod, were performed on our rats under the influence of either LuAF21934 or AF42744 there is no further information to support or discount the validity of the rotometry results regarding L-DOPA sparing. Nevertheless what can be concluded is that the $mGlu_4$ PAMs tested did not have a detrimental effect on L-DOPA-evoked rotation when administered alongside either a high dose or a low dose of L-DOPA.

Testing of LuAF21934 and AF42744 for L-DOPA sparing/potentiation in non-primed rats or in primed but non-dyskinetic rats would help to inform us on the potential of these compounds to reduce the development of dyskinesia by virtue of a reduction in the required dose of L-DOPA.

6.4.6 AIMs induction study

Building on the previous study, where we tested the ability of $mGlu_4$ PAMs to reverse established dyskinesia, in this study we set out to determine whether an $mGlu_4$ PAM could inhibit the induction of AIMs when administered alongside L-DOPA in rats that had been

lesioned but were L-DOPA naive. LuAF21934 or vehicle was given 30 minutes before injection of L-DOPA, once daily for 14 days, and AIMs were scored at intervals during this priming period on days 2, 5, 8, 11 and 14. However as was the case for AIMs reversal, no significant effect of treatment with LuAF21934 was noted on the development of AIMs in treated groups compared with vehicle. There was a hint that the highest dose of LuAF21934 delayed the onset of AIMs early on in the study, however this effect was lost at all later time points.

The failure of LuAF21934 to prevent the induction of AIMs in my study is in contrast to a recent report using the same compound, where coadministration of 30mg/kg LuAF21934 with L-DOPA significantly reduced the incidence of dyskinesia in denervated rats (Bennouar *et al.*, 2013), though the early hint of reduced incidence in my induction study at this same dose might suggest that it partially reflected these previous results. Similarly to the Bennouar *et al.* study, all rats in my induction study that did develop AIMs did so with comparable severity regardless of treatment group, suggesting that once priming has occurred, treatment with LuAF21934 does not suppress the severity or expression of AIMs.

One potential explanation for the different outcomes in these studies could lie in the different dosing protocols employed; twice daily i.p. co-injection of L-DOPA plus LuAF21934 in the Bennouar study, once daily s.c. L-DOPA 30 minutes after p.o. LuAF21934 in the present study. Intraperitoneal dosing may have resulted in higher drug exposure due to bypassing primary metabolism in the liver and avoiding variability in gastrointestinal absorption, though with no brain concentrations reported after i.p. dosing this cannot be known for sure. Certainly the plasma C_{max} reported in the Bennouar paper following a 10 mg/kg s.c. dose of LuAF21934 is over 3 times that obtained following a 10 mg/kg oral dose in our PK1 study; 2763 ng/ml versus 869 ng/ml, suggesting that these factors significantly influence drug bioavailability and maximum exposures.

Alternative explanations for the lack of significant inhibition of AIMs development in this study are that LuAF21934 was not present at the correct synapses at sufficient concentrations to alter neurotransmitter release, or that any reduced signalling obtained was either insufficient to significantly affect downstream signalling in sensitised striatonigral MSNs or was counteracted by effects of the drug elsewhere in the basal ganglia. These possibilities were discussed in more detail in relation to the AIMs reversal study.

The inability of LuAF21934 administration to inhibit AIMs development is in contrast not only to the Bennouar (2013) study but also to results using other PAMs or agonists targeting $mGlu_4$. For example the allosteric agonist LSP1-2111 attenuated AIMs development when administered alongside L-DOPA in mice (Lopez *et al.*, 2011) and a very recent publication reported that the $mGlu_4$ PAM TAS-4 inhibited AIMs development when administered alongside L-DOPA in rats (Dube *et al.*, 2014), though in this case it might be explained by the administration of a lower concentration of L-DOPA in TAS-4 treated groups compared with vehicle groups, as TAS-4 was also demonstrated to have L-DOPA sparing properties.

6.5 Conclusion

The ability of amantadine to suppress the expression of AIMs in these studies demonstrate that targeting glutamatergic transmission is a valid antidyskinetic strategy in this model, as it is in human LID.

Our findings that LuAF21934 and AF42744 do not have antidyskinetic efficacy where AIMs are already established do not support the use of these drugs in existing dyskinesia, in accordance with existing work. Since brain penetrance of these compounds was confirmed at concentrations that have been shown by others to be pharmacologically active in PD models, the likely reason for the lack of success of these reversal studies is that any effect on glutamatergic transmission was insufficient to be clinically effective in the already sensitised, dyskinetic state.

The L-DOPA sparing potential of LuAF21934 and AF42744 was not confirmed in the rotational study despite being reported by other groups, however due to the possible confounding effects of axial dyskinesia in measuring this outcome it would be useful to re-test this parameter in non-dyskinetic animals. Nevertheless the early results from a recent marmoset study support the lack of an effect of LuAF21934 on the antiparkinsonian actions of L-DOPA.

The hint of an ability of 30mg/kg LuAF21934 to delay the onset of AIMs in rats reflects previous research where this compound partly inhibited the development of AIMs when given alongside L-DOPA. However the lack of a significant effect means that the results are not conclusive, and warrants further work into the ability of this compound to delay or prevent AIMs onset, perhaps incorporating different dosing regimens or varying doses of L-DOPA.

7 General Discussion and Conclusions

The search for new treatments for Parkinson's disease is necessary to tackle the continuing decline in patients' motor function and quality of life that is not adequately controlled by currently available therapies. There is much interest in targeting glutamatergic signalling in the context of this disease as a means to alleviate the symptoms, provide neuroprotection and also prevent or suppress the treatment-related side effects, but as yet the only antiglutamatergic drug that is regularly prescribed in PD or L-DOPA-induced dyskinesia (LID) is amantadine, a weak NMDA receptor antagonist. The move towards more subtle manipulation of glutamate signalling by avoiding direct targeting of ionotropic glutamate receptors in favour of modulating their activity and decreasing neurotransmitter release probability led to a great research effort focused on G-protein coupled metabotropic glutamate receptors.

Group III mGlu receptors are predominantly presynaptically located on glutamate and GABA terminals where their activation inhibits adenylate cyclase activity and Ca^{2+} channels, reducing the probability of neurotransmitter release. They are activated by endogenous glutamate and due to their localisation in and around the presynaptic active zone they provide feedback inhibition of release in situations where glutamate is at sufficient concentration to begin to 'overspill' the synaptic cleft. Enhancing or manipulating their activation should therefore be useful in the circumstances of pathologically increased glutamate release such as is encountered at the subthalamonigral synapse in the indirect pathway in PD. Additionally, since global reduction of glutamatergic signalling is also beneficial in LID, likely by reducing corticostriatal input to the hyperactive direct pathway, targeting group III mGlu receptors to reduce glutamate release at this synapse might also be expected to have an antidyskinetic effect.

The general aims of this thesis were therefore to use allosteric activators of group III mGlu receptors, predominantly $mGlu_4$ but also $mGlu_7$, to address two of the principal unmet clinical needs in Parkinson's disease; ongoing neurodegeneration and levodopa-induced dyskinesia.

7.1 Neuroprotection

Neuroprotection is one of the key goals in PD research, since preventing the loss of further dopaminergic neurones after diagnosis would theoretically halt the decline in motor function and also reduce the risk of development of LID, which is increased as the number of dopaminergic terminals in the striatum diminishes. We hypothesised that activation of

these group III mGlu receptor subtypes would provide protection against 6-OHDA-induced neurodegeneration in the rat.

7.1.1 $mGlu_4$

The results described in Chapter 2 demonstrate that neuroprotection can indeed be achieved in rats with a full unilateral nigral 6-OHDA lesion by sub-chronic supranigral infusion of the $mGlu_4$ PAM VU0155041, in support of our hypothesis. Though the protection provided was not full, neuronal survival and striatal dopamine concentration were both approaching 40% in the best-responding group. Given that PD symptoms appear in patients when around 60% of dopaminergic cells are lost (i.e. 40% survive) this degree of protection is potentially clinically relevant. In support of this, the group with the greatest degree of protection also showed significant preservation of motor function as assessed by several behavioural tests. Interestingly this PAM showed a bell-shaped dose response profile, which is unexpected given that PAMs are not expected to cause receptor desensitisation unlike their agonist counterparts. In this case the loss of a therapeutic effect at high concentrations suggests that at these doses VU0155041 is acting as an agonist, as has been reported for this compound at high concentrations. This agonist activity could cause receptor desensitisation and thereby limit the efficacy of the agent. Overall though, these results strongly support the idea that a meaningful degree of neuroprotection can be provided in this model by selective activation of $mGlu_4$. On the other hand the lack of neuroprotection afforded in this model by a different $mGlu_4$ PAM, Compound 11, highlights the likelihood that this protective effect is highly influenced by the individual characteristics of the different allosteric modulators. This might include aspects such as the *in vivo* clearance rate, concentration-dependent PAM/agonist activity and the recently described differential efficacy regarding the activation of $mGlu_2/mGlu_4$ receptor heterodimers, which adds an additional layer of complexity that must be considered in future preclinical and especially clinical situations. Therefore in addition to finding $mGlu_4$ PAMs with favourable pharmacokinetic profiles and good selectivity and potency, in the light of the loss of efficacy of VU0155041 at higher concentrations it is also clear that it will be crucial to identify an efficacious dose range for those PAMs that also exhibit agonist activity that avoids loss of the therapeutic effect.

Though we did not investigate the mechanisms involved within the neuroprotection experiments themselves, our hypothesis was based on the notion that local activation of presynaptic $mGlu_4$ receptors at the subthalamonigral synapse would normalise the enhanced glutamate release into the SNc that is associated with nigral cell loss in this

model, thereby inhibiting excitotoxic neurodegeneration. Whilst we predicted therefore that we would see a VU0155041-mediated inhibition of glutamate release into the SNc, the results of the microdialysis studies reported in Chapter 3 do not support this. In fact our results suggest that in intact rats, both broad spectrum activation of group III mGlu receptors with L-AP4 and positive allosteric modulation of $mGlu_4$ with VU0155041 preferentially inhibit GABA release, with a concomitant *increase* in glutamate release. We propose that the increase in glutamate release is a secondary effect of group III mGlu heteroreceptor-mediated reduction of GABA release. This could potentially be driven by disinhibition of nigrosubthalamic dopaminergic signalling, which is known to increase activity of STN neurones (Cragg *et al.*, 2004; Paladini *et al.*, 1999), and/or by reduction of direct GABA-mediated inhibitory control of subthalamic terminals (Hatzipetros *et al.*, 2006). While this inhibition of GABA release and augmentation of glutamate release in the SNc might be expected to promote excitotoxic cell loss, and therefore would caution against use of group III mGlu receptor activation in PD, when L-AP4 was tested in the fully 6-OHDA lesioned SNc these potentially detrimental effects were lost, such that no significant alterations were seen in KCl-evoked release of either glutamate or GABA in the presence of the agonist compared with control. While this still does not support reduction of subthalamonigral glutamate release as the mechanism behind L-AP4 or VU0155041-mediated neuroprotection it at least suggests that in the dopamine depleted situation these treatments would not be expected to enhance excitotoxicity. In the absence of support for a reduction of glutamate release it is possible that alternative neuroprotective mechanisms that have been attributed to selective $mGlu_4$ activation, such as attenuation of inflammation, underlie the neuroprotection seen in the 6-OHDA-lesioned rat when treated with supranigrally with VU0155041. For example there is evidence that activation of $mGlu_4$ in mixed glial/neuronal cultures exerts a neuroprotective effect, which is supported by reduced production of inflammatory markers *in vitro* (Besong *et al.*, 2002; Maj *et al.*, 2003). This is further supported by the observation of a similar anti-inflammatory effect following intranigral delivery of VU0155041 in a previous study in this lab (Betts *et al.*, 2012).

Having successfully demonstrated neuroprotection following local intracerebral administration of an $mGlu_4$ PAM the next step was to investigate if a similar effect could be obtained following sub-chronic systemic administration of a brain penetrant $mGlu_4$ PAM. For this we used LuAF21934, which is structurally similar to VU0155041 and has a similar potency at $mGlu_4$ but which has improved BBB penetrance. Before commencing the neuroprotection study we confirmed that we could achieve good brain concentrations

following oral administration of LuAF21934 in solution. Initial analysis of the results suggested that LuAF21934 had not provided functional neuroprotection in this model at either of the doses tested, with no improvements in nigrostriatal integrity at the nigral or striatal levels and, consistently, no functional improvements in any behavioural tests. However whilst carrying out additional analysis of inflammatory markers in these rats we observed that around two thirds of rats across all groups in this study had some degree of physical damage in the SNc. The cause of this physical damage is unknown, as it was not restricted to rats within a single lesioning day or treatment group, however this might well have proven insurmountable from the point of view of neuroprotection and thus the neuroprotective potential of sub-chronic systemic treatment with LuAF21934 against a nigral 6-OHDA lesion cannot be unequivocally deduced from this experiment. Another possibility behind the failure of this study to reveal a protective effect is that the lesion was simply too severe, since even in those rats with no evident physical damage there was no suggestion of a protective effect of treatment with LuAF21934. Given the previous report of successful protection against MPTP-induced degeneration in mice that were treated systemically with PHCCC (Battaglia *et al.*, 2006) it seems that it is worth pursuing this line of investigation. Ideally the compounds tested should not have the selectivity issues of PHCCC, which has partial antagonist activity at $mGlu_{1b}$ that could also account for the neuroprotective effect, as has been demonstrated for other $mGlu_1$ antagonists, (e.g. Vernon *et al.*, 2007). First steps might include repeating the LuAF21934 experiment in a partial 6-OHDA lesion model (with the toxin infused in either the MFB or striatum to avoid physical damage to the SNc) or in the MPTP mouse model as carried out by Battaglia *et al.* (2006) for comparison with PHCCC. If the lack of a protective effect in this study is indeed a real negative result then it raises questions as to whether the actions of an $mGlu_4$ PAM elsewhere in the BG or brain might counteract its effects at the subthalamonigral synapse. This might be first assessed using a PAM with proven neuroprotective activity in this model, such as VU0155041, administered i.c.v. This would be a good step back from local SNc administration to more general activation of $mGlu_4$ receptors in the brain, but will negate the problems that this compound demonstrates in penetrating the blood-brain barrier.

7.1.2 $mGlu_7$

In contrast to $mGlu_4$ (at least when administered supranigrally), selective activation of $mGlu_7$ does not currently seem to be a promising strategy for providing neuroprotection in PD models. As reported in Chapter 5 the allosteric agonist AMN082 failed to provide

neuroprotection or functional improvements in rats with a nigral 6-OHDA lesion, despite achieving good brain levels that were pharmacologically significant judging by the side effects seen at high doses. In addition, in contrast to the LuAF21934 neuroprotection study, no physical damage was evident in the SNc of these animals, suggesting that this was not a factor in the failure of AMN082 to protect against 6-OHDA-induced neurodegeneration. This does not rule out the possibility, however, that the lesion was too severe to allow time for AMN082 to exert any protective effects and similarly to the LuAF21934 study in hindsight this study might have been better conducted in a partial lesion model. Nevertheless previous studies performed in this lab (Betts *et al.*, unpublished) failed to show a protective effect when AMN082 was administered supranigrally in this model, therefore there is not the same discrepancy between local versus systemic neuroprotective efficacy that we have found for activation of $mGlu_{4,}$ making the negative outcome of the AMN082 study more likely to be a real effect.

Aside from the concerns related to the model, the tool compound used also has limitations that might easily have affected the outcome of this study. AMN082 is not only an allosteric agonist, raising the possibility that $mGlu_7$ receptors were rapidly desensitised/internalised upon ligand binding, but it also has multiple off-target effects, some of which we believe we observed in this study. It is therefore impossible to tell exactly what other pharmacological interactions might have interfered with or counteracted the actions of this compound on $mGlu_7$ receptors. In addition we saw from the experiments in Chapter 2 that different ligands can have different neuroprotective efficacies *in vivo* despite similar *in vitro* profiles, therefore it cannot be ruled out that a different $mGlu_7$-specific allosteric modulator might be protective in this model. The potential of $mGlu_7$ as a therapeutic target in PD therefore remains uncertain pending the development of more selective $mGlu_7$ agonists or positive allosteric modulators, and likely also needs to be tested in a partial lesion model to more closely reflect the clinical situation and allow the compound the time to exert its effects.

7.2 Levodopa-Induced Dyskinesia

One of the major limiting factors in the use of dopamine replacement strategies, and in particular the dopamine precursor L-DOPA, is the development over time of abnormal involuntary movements. This process involves multiple alterations in synaptic functioning, especially in the striatum, and once established is seemingly irreversible such that any future exposure to L-DOPA will elicit dyskinesia. Current treatment options are limited to a

reduction of the dose of L-DOPA, which can mean that patients' motor dysfunction is not adequately controlled, or the antiglutamatergic drug amantadine. There is a clear need for alternative antidyskinetic compounds, either to suppress dyskinesia in those who have already developed the side effect or to take alongside L-DOPA to prevent its occurrence in people who have not. We hypothesised that due to the well-known antidyskinetic effects of amantadine, positive allosteric modulation of $mGlu_4$ might be another antiglutamatergic strategy that might prove worthwhile in the treatment or prevention of LID.

With regard to their use in LID, the experimental results presented in Chapter 6 do not support the use of $mGlu_4$ PAMs as antidyskinetic agents for the suppression of existing dyskinesia. Since our pharmacokinetic studies showed that both LuAF21934 and AF42744 were brain penetrant and were present throughout the duration of action of L-DOPA it is probable that the subtle modulatory effect afforded by targeting $mGlu_4$ receptors is simply inadequate to overcome the seemingly irreversible plasticity that underlies the development and maintenance of LID. This is concordant with previous publications where neither the $mGlu_4$ PAM AF42744 (ADX88178) nor the $mGlu_4$ agonist LSP1-2111 were able to diminish the expression of established dyskinesia in the rodent AIMs model (Le Poul *et al.*, 2012; Lopez *et al.*, 2011), and therefore the weight of evidence is against the usefulness of this approach. Further to this, recent experiments that we carried out in collaboration with Lundbeck and the Salvage lab at King's found that LuAF21934 showed no antidyskinetic efficacy in the MPTP-treated L-DOPA-primed marmoset, which would certainly suggest that this approach is not worth pursuing further.

On a positive note, while the L-DOPA-induced rotations might not have been the most accurate reflection of the antiparkinsonian effects of L-DOPA in our rodent experiment considering the possible confounding effects of axial AIMs, neither LuAF21934 nor AF42744 inhibited this aspect of the L-DOPA response in rats. Furthermore LuAF21934 did not detrimentally affect the L-DOPA-induced improvements in locomotor and motor disability scores in the marmosets when tested. Unlike previous reports using these compounds we found no significant evidence in support of a beneficial L-DOPA potentiating effect of either of these compounds in rats or of LuAF21934 in marmosets. Nevertheless these results suggest that even if they do not act as L-DOPA potentiators, $mGlu_4$ PAMs at least do not interfere with the therapeutic effects of L-DOPA in these models. This is an important finding as any agent that compromised the efficacy of L-DOPA would certainly not be considered further as a potential therapeutic agent against any aspect of PD, whether that

might be motor symptoms, LID or non-motor symptoms. Therefore this class of agents as a whole is still worthwhile investigating for these indications.

When LuAF21934 was tested for its ability to prevent the development of dyskinesia when administered alongside L-DOPA in *de novo* treated 6-OHDA-lesioned rats there was no significant antidyskinetic effect, though there was a trend towards a delayed development of abnormal movements in the group treated with 30mg/kg LuAF21934. It would be interesting to look more closely at this by repeating the experiment in a larger group of animals, particularly in light of the reports in the literature of inhibition of induction of rodent AIMs with coadministration of allosteric modulators or agonists of $mGlu_4$ alongside L-DOPA (Bennouar *et al.*, 2013; Lopez *et al.*, 2011). Possible reasons for the lack of success in my experiment when compared with the positive results of these two studies include the different dosing route used and the type of ligand. Bennouar *et al.* (2013) also used LuAF21934 at the same doses as in my study, however the drug was dosed intraperitoneally and therefore reached higher maximal plasma concentrations (and thus likely higher maximal brain concentrations) compared with my study where the drug was given as an oral dose. Lopez *et al.* (2011) used an allosteric agonist of $mGlu_4$ rather than a PAM, and the increased activation of receptors that might be expected to result from this approach may have proved important in eliciting the antidyskinetic effect. The fact that more than one study using more than one different ligand has shown positive results in the reduction of dyskinesia development supports further studies into the efficacy of this approach. The use of allosteric agonists instead of PAMs might prove to be important in some circumstances where a more powerful activation of mGlu receptors seems to be required, provided that receptor desensitisation can be avoided.

Even if $mGlu_4$ PAMs do not show consistent effects in reducing the development of LID against a stable experimentally defined dose of L-DOPA, several of these compounds have shown L-DOPA potentiating actions in previous reports (Bennouar *et al.*, 2013; Le Poul *et al.*, 2012). This raises the possibility that they might still be indirectly efficacious at reducing the development of LID by reducing the necessary therapeutic dose of L-DOPA, as was recently demonstrated for the novel $mGlu_4$ PAM TAS-4 in the rodent AIMs model (Dube *et al.*, 2014).

7.3 Non-motor symptoms

Though not addressed in this thesis, activation of group III mGlu receptors might also be beneficial with regard to the treatment of several of the non-motor symptoms that are

regularly experienced by PD patients alongside their motor disabilities. These include depression, anxiety, pain and autonomic dysfunction as detailed below.

Activation of group III mGlu receptors in general with ACPT-I, or selective activation of $mGlu_4$ with LuAF21934 or LSP1-2111, has shown anxiolytic and antidepressant effects in rodents (Slawinska *et al.*, 2013; Tatarczyñska *et al.*, 2002; Wierońska *et al.*, 2010). Similar effects have been seen using the selective $mGlu_7$ agonist AMN082 in models of depression (Palucha *et al.*, 2007) and the selective $mGlu_8$ agonist DCPG in models of learned fear (Schmid *et al.*, 2006).

In addition to this, broad spectrum group III agonists (ACPT-I and L-AP4), $mGlu_4$ PAMs (PHCCC and VU0155041) and the $mGlu_7$ allosteric agonist AMN082 have shown efficacy in various rodent models of pain, including neuropathic and inflammatory pain (Chen *et al.*, 2005b; Dolan *et al.*, 2009; Goudet *et al.*, 2008; Wang *et al.*, 2011).

With respect to autonomic dysfunction, activation of $mGlu_7$ (Julio-Pieper *et al.*, 2010) and $mGlu_8$ (Tong *et al.*, 2003) have been shown to increase faecal water content and colonic motility respectively, which could have implications for treatment of constipation that is often experienced by PD patients and can affect absorption of medication.

These results raise the possibility that targeting this group of receptors as a whole or subtype-selectively could not only improve the symptoms and possibly delay the neurodegeneration associated with PD (depending on the route of administration) but could also help address some of the non-motor symptoms that are commonly experienced by patients and which limit their quality of life.

7.4 Final thoughts

Overall the work presented in this thesis supports the continued examination of $mGlu_4$ as a target for neuroprotection in PD and sets the scene for future experiments that will advance this area of research. The unexpected results of the microdialysis studies highlight the requirement for further investigation into the protective mechanisms involved in the *in vivo* neuroprotective effects of supranigral injection of $mGlu_4$ PAMs, perhaps by testing for these protective effects in rats that have been depleted of microglia (Elmore *et al.*, 2014) or using inhibitors of pathways that may be initiated by $mGlu_4$ activation such as MAPK (Jiang *et al.*, 2006). In addition to this, due to the inconclusive nature of the systemic LuAF21934 neuroprotection study, a repeat of this study using this same compound or another

systemically active $mGlu_4$ PAM but in a model with a partial lesion would be a worthwhile next step.

$mGlu_7$ seems less likely to prove a useful target in the near future given the lack of selective ligands that have been developed to target this receptor subtype, however the potential benefits of targeting this receptor in PD cannot be ruled out on the basis of this one compound. Studies using $mGlu_7$-specific antagonists to counteract the effects of either broad spectrum group III agonists or AMN082 might help to discriminate between $mGlu_7$-mediated effects and those mediated by other group III subtypes or off-target effects to elucidate whether this receptor warrants further investigation in the context of PD.

On the topic of LID, while $mGlu_4$ PAMs do not show potential regarding suppression of the expression of established dyskinesia they may show some promise as inhibitors of dyskinesiogenesis. However this effect is more variable than that obtained when postsynaptic glutamate receptors such as NMDA receptors and $mGlu_5$ are targeted and therefore these two receptor types are likely to be more actively pursued as targets for both suppression and inhibition of development of dyskinesia in the near future. One very important finding from the dyskinesia studies in rats and marmosets was a confirmation that $mGlu_4$ PAMs do not appear to interfere with the antiparkinsonian actions of L-DOPA, which paves the way for use of this class of agents in any aspect of Parkinson's disease for which it may be beneficial.

In conclusion, although the results reported in this thesis are largely negative they have helped to shed light on several aspects of this field of research, including which mechanisms may or may not be involved in the neuroprotective effects of local activation of $mGlu_4$ receptors and the lack of detrimental interactions of $mGlu_4$ PAMs on the therapeutic efficacy of L-DOPA. They pave the way for future studies into the antidyskinesiogenic efficacy of $mGlu_4$ receptor activation and the neuroprotective efficacy of widespread targeting of $mGlu_4$ and $mGlu_7$ receptors using more clinically relevant models.

8 References

Abraham S, Soundararajan CC, Vivekanandhan S, Behari M (2005). Erythrocyte antioxidant enzymes in Parkinson's disease. *Indian J. Med. Res.* **121:** 111-115.

Addy C, Assaid C, Hreniuk D, Stroh M, Xu Y, Herring WJ*, et al.* (2009). Single-dose administration of MK-0657, an NR2B-selective NMDA antagonist, does not result in clinically meaningful improvement in motor function in patients with moderate Parkinson's disease. *J. Clin. Pharmacol.* **49**(7)**:** 856-864.

Aguirre JA, Kehr J, Yoshitake T, Liu FL, Rivera A, Fernandez-Espinola S*, et al.* (2005). Protection but maintained dysfunction of nigral dopaminergic nerve cell bodies and striatal dopaminergic terminals in MPTP-lesioned mice after acute treatment with the mGluR5 antagonist MPEP. *Brain Res.* **1033**(2)**:** 216-220.

Ahlskog JE, Muenter MD (2001). Frequency of levodopa-related dyskinesias and motor fluctuations as estimated from the cumulative literature. *Mov. Disord.* **16**(3)**:** 448-458.

Ahmed I, Bose SK, Pavese N, Ramlackhansingh A, Turkheimer F, Hotton G*, et al.* (2011). Glutamate NMDA receptor dysregulation in Parkinson's disease with dyskinesias. *Brain* **134**(4)**:** 979-986.

Alam M, Danysz W, Schmidt WJ, Dekundy A (2009). Effects of glutamate and alpha2-noradrenergic receptor antagonists on the development of neurotoxicity produced by chronic rotenone in rats. *Toxicol. Appl. Pharmacol.* **240**(2)**:** 198-207.

Alam ZI, Daniel SE, Lees AJ, David C. Marsden, Jenner P, Halliwell B (1997). A generalised increase in protein carbonyls in the brain in Parkinson's but not incidental Lewy Body Disease. *J. Neurochem.* **69:** 1326-1329.

Albers DS, Weiss SW, Iadarola MJ, Standaert DG (1999). Immunohistochemical localization of N-methyl-d-aspartate and α-amino-3-hydroxy-5-methyl-4-isoxazolepropionate receptor subunits in the substantia nigra pars compacta of the rat. *Neuroscience* **89**(1)**:** 209-220.

Albin RL, Young AB, Penney JB (1989). The functional anatomy of basal ganglia disorders. *Trends Neurosci.* **12**(10)**:** 366-375.

Alvarez L, Macias R, Pavon N, Lopez G, Rodriguez-Oroz MC, Rodriguez R*, et al.* (2009). Therapeutic efficacy of unilateral subthalamotomy in Parkinson's disease: results in 89 patients followed for up to 36 months. *J. Neurol. Neurosurg. Psychiatry* **80**(9)**:** 979-985.

Ambani LM, Woert MHV, Murphy S (1975). Brain peroxidase and catalase in Parkinson disease. *Arch. Neurol.* **32:** 114-118.

Ambrosi G, Armentero MT, Levandis G, Bramanti P, Nappi G, Blandini F (2010). Effects of early and delayed treatment with an mGluR5 antagonist on motor impairment, nigrostriatal damage and neuroinflammation in a rodent model of Parkinson's disease. *Brain Res. Bull.* **82**(1-2)**:** 29-38.

Ammari R, Bioulac B, Garcia L, Hammond C (2011). The subthalamic nucleus becomes a generator of bursts in the dopamine-depleted state. Its high frequency stimulation dramatically weakens transmission to the globus pallidus. *Front. Sys. Neurosci.* **5:** 43.

Anderson VC, Burchiel KJ, Hogarth P, Favre J, Hammerstad JP (2005). Pallidal vs subthalamic nucleus deep brain stimulation in Parkinson disease. *Arch. Neurol.* **62**(4)**:** 554-560.

Andersson M, Konradi C, Cenci MA (2001). cAMP response element-binding protein is required for dopamine-dependent gene expression in the intact but not the dopamine-denervated striatum. *J. Neurosci.* **21**(24)**:** 9930-9943.

Anglade P, Mouatt-Prigent A, Agid Y, Hirsch EC (1996). Synaptic plasticity in the caudate nucleus of patients with Parkinson's disease. *Neurodegeneration* **5:** 121-128.

Antal M, Beneduce BM, Regehr WG (2014). The substantia nigra conveys target-dependent excitatory and inhibitory outputs from the basal ganglia to the thalamus. *J. Neurosci.* **34**(23)**:** 8032-8042.

Antonelli T, Fuxe K, Tomasini MC, Bartoszyk GD, Seyfried CA, Tanganelli S*, et al.* (2005). Effects of sarizotan on the corticostriatal glutamate pathways. *Synapse* **58**(3)**:** 193-199.

Antonini A, Tolosa E, Mizuno Y, Yamamoto M, Poewe WH (2009). A reassessment of risks and benefits of dopamine agonists in Parkinson's disease. *Lancet Neurol.* **8:** 929-937.

Ariano MA, Grissell AE, Littlejohn FC, Buchanan TM, Elsworth JD, Collier TJ*, et al.* (2005). Partial dopamine loss enhances activated caspase-3 activity: differential outcomes in striatal projection systems. *J. Neurosci. Res.* **82**(3)**:** 387-396.

Armentero MT, Fancellu R, Nappi G, Bramanti P, Blandini F (2006). Prolonged blockade of NMDA or mGluR5 glutamate receptors reduces nigrostriatal degeneration while inducing selective metabolic changes in the basal ganglia circuitry in a rodent model of Parkinson's disease. *Neurobiol. Dis.* **22**(1)**:** 1-9.

Assous M, Had-Aissouni L, Gubellini P, Melon C, Nafia I, Salin P*, et al.* (2014). Progressive Parkinsonism by acute dysfunction of excitatory amino acid transporters in the rat substantia nigra. *Neurobiol. Dis.* **65:** 69-81.

Aubert I, Guigoni C, Hakansson K, Li Q, Dovero S, Barthe N*, et al.* (2005). Increased D1 dopamine receptor signaling in levodopa-induced dyskinesia. *Ann. Neurol.* **57**(1)**:** 17-26.

Aubert I, Guigoni C, Li Q, Dovero S, Bioulac BH, Gross CE*, et al.* (2007). Enhanced preproenkephalin-B-derived opioid transmission in striatum and subthalamic nucleus converges upon globus pallidus internalis in L-3,4-dihydroxyphenylalanine-induced dyskinesia. *Biol. Psychiatry* **61**(7)**:** 836-844.

Austin PJ, Betts MJ, Broadstock M, O'Neill MJ, Mitchell SN, Duty S (2010). Symptomatic and neuroprotective effects following activation of nigral group III metabotropic glutamate receptors in rodent models of Parkinson's disease. *Br. J. Pharmacol.* **160**(7)**:** 1741-1753.

Ba M, Kong M, Yu G, Sun X, Liu Z, Wang X (2011). GluR1 phosphorylation and persistent expression of levodopa-induced motor response alterations in the hemi-parkinsonian rat. *Neurochem. Res.* **36**(6)**:** 1135-1144.

Bahi A, Fizia K, Dietz M, Gasparini F, Flor PJ (2011). Pharmacological modulation of mGluR7 with AMN082 and MMPIP exerts specific influences on alcohol consumption and preference in rats. *Addict. Biol.* **17**(2)**:** 235-247.

Baluchnejadmojarad T, Roghani M (2004). Evaluation of functional asymmetry in rats with dose-dependent lesions of dopaminergic nigrostriatal system using elevated body swing test. *Physiol. Behav.* **82**(2-3)**:** 369-373.

Bannai S, Kitamura E (1980). Transport interaction of L-Cystine and L-Glutamate in human diploid fibroblasts in culture. *J. Biol. Chem.* **255**(6)**:** 2372-2376.

Barbeau A (1969). L-Dopa therapy in Parkinson's disease. A critical review of nine years' experience. *Can. Med. Assoc. J.* **101**(13)**:** 59-68.

Barnéoud P, Descombris E, Aubin N, Abrous DN (2001). Evaluation of simple and complex sensorimotor behaviours in rats with a partial lesion of the dopaminergic nigrostriatal system. *Eur. J. Neurosci.* **12:** 322-336.

Baron MS, Vitek JL, Bakay RAE, Green J, Kaneoke Y, Hashimoto T*, et al.* (1996). Treatment of advanced Parkinson's disease by posterior GPi pallidotomy: 1-year results of a pilot study. *Ann. Neurol.* **40:** 355-366.

Baron MS, Wichmann T, Ma D, DeLong MR (2002). Effects of transient focal inactivation of the basal ganglia in parkinsonian primates. *J. Neurosci.* **22**(2)**:** 592-599.

Basma AN, Morris EJ, Nicklas WJ, Geller HM (1995). L-dopa cytotoxicity to PC12 cells in culture is via its autoxidation. *J. Neurochem.* **64**(2)**:** 825-832.

Basso DM, Beattie MS, Bresnahan JC (1995). A sensitive and reliable locomotor rating scale for open field testing in rats. *J. Neurotrauma* **12**(1)**:** 1-21.

Battaglia G, Busceti CL, Molinaro G, Biagioni F, Storto M, Fornai F*, et al.* (2004). Endogenous activation of mGlu5 metabotropic glutamate receptors contributes to the development of nigro-striatal damage induced by 1-methyl-4-phenyl-1,2,3,6-tetrahydropyridine in mice. *J. Neurosci.* **24**(4)**:** 828-835.

Battaglia G, Busceti CL, Molinaro G, Biagioni F, Traficante A, Nicoletti F*, et al.* (2006). Pharmacological activation of mGlu4 metabotropic glutamate receptors reduces nigrostriatal degeneration in mice treated with 1-methyl-4-phenyl-1,2,3,6-tetrahydropyridine. *J. Neurosci.* **26**(27)**:** 7222-7229.

Battaglia G, Busceti CL, Pontarelli F, Biagioni F, Fornai F, Paparelli A*, et al.* (2003). Protective role of group-II metabotropic glutamate receptors against nigro-striatal degeneration induced by 1-methyl-4-phenyl-1,2,3,6-tetrahydropyridine in mice. *Neuropharmacology* **45**(2)**:** 155-166.

Battaglia G, Molinaro G, Riozzi B, Storto M, Busceti CL, Spinsanti P*, et al.* (2009). Activation of mGlu3 receptors stimulates the production of GDNF in striatal neurons. *PLoS One* **4**(8)**:** e6591.

Bédard PJ, Di Paolo T, Falardeau P, Boucher R (1986). Chronic treatment with L-DOPA, but not bromocriptine induces dyskinesia in MPTP-parkinsonian monkeys. Correlation with [3H]spiperone binding. *Brain Res.* **379**(2)**:** 294-299.

Belluzzi E, Bisaglia M, Lazzarini E, Tabares LC, Beltramini M, Bubacco L (2012). Human SOD2 modification by dopamine quinones affects enzymatic activity by promoting its aggregation: possible implications for Parkinson's disease. *PLoS One* **7**(6)**:** e38026.

Benabid AL, Chabardes S, Mitrofanis J, Pollak P (2009). Deep brain stimulation of the subthalamic nucleus for the treatment of Parkinson’s disease. *Lancet Neurol.* **8:** 67-81.

Benabid AL, Pollak P, Hoffmann D, Gervason C, Hommel M, Perret JE*, et al.* (1991). Long-term suppression of tremor by chronic stimulation of the ventral intermediate thalamic nucleus. *Lancet* **337**(8738)**:** 403-406.

Benazzouz A, Gross C, Féger J, Boraud T, Bioulac B (1993). Reversal of rigidity and improvement in motor performance by subthalamic high-frequency stimulation in MPTP-treated monkeys. *Eur. J. Neurosci.* **5**(4)**:** 382-389.

Bennouar K-E, Uberti MA, Melon C, Bacolod MD, Jimenez HN, Cajina M*, et al.* (2013). Synergy between L-DOPA and a novel positive allosteric modulator of metabotropic

glutamate receptor 4: implications for Parkinson's disease treatment and dyskinesia. *Neuropharmacology* **66:** 158-169.

Berg D, Godau J, Trenkwalder C, Eggert K, Csoti I, Storch A*, et al.* (2011). AFQ056 treatment of levodopa-induced dyskinesias: Results of 2 randomized controlled trials. *Mov. Disord.* **26**(7)**:** 1243-1250.

Bergles DE, Diamond JS, Jahr CE (1999). Clearance of glutamate inside the synapse and beyond. *Curr. Opin. Neurobiol.* **9:** 293-298.

Bergman H, Wichmann T, DeLong MR (1990). Reversal of experimental parkinsonism by lesions of the subthalamic nucleus. *Science* **249:** 1436-1438.

Bergman H, Wichmann T, Karmon B, DeLong MR (1994a). The primate subthalamic nucleus. II. Neuronal activity in the MPTP model of parkinsonism. *J. Neurophysiol.* **72**(2).

Bergman H, Wichmann T, Karmon B, DeLong MR (1994b). The primate subthalamic nucleus. II. Neuronal activity in the MPTP model of parkinsonism. *J. Neurophysiol.* **72**(2)**:** 507-520.

Berretta N, Bernardi G, Mercuri NB (2000). Alpha1-adrenoreceptor-mediated excitation of substantia nigra pars reticulata neurons. *Neuroscience* **98**(3)**:** 599-604.

Berretta N, Freestone PS, Guatteo E, de Castro D, Geracitano R, Bernardi G*, et al.* (2005). Acute effects of 6-hydroxydopamine on dopaminergic neurons of the rat substantia nigra pars compacta in vitro. *Neurotoxicology* **26**(5)**:** 869-881.

Bertran-Gonzalez J, Herve D, Girault JA, Valjent E (2010). What is the degree of segregation between striatonigral and striatopallidal projections? *Front. Neuroanat.* **4:** pii 136.

Besong G, Battaglia G, D'Onofrio M, Marco RD, Ngomba RT, Storto M*, et al.* (2002). Activation of group III metabotropic glutamate receptors inhibits the production of RANTES in glial cell cultures. *J. Neurosci.* **22**(13)**:** 5403-5411.

Betarbet R, Greenamyre JT (2004). Regulation of dopamine receptor and neuropeptide expression in the basal ganglia of monkeys treated with MPTP. *Exp. Neurol.* **189**(2)**:** 393-403.

Betarbet R, Sherer TB, MacKenzie G, Garcia-Osuna M, Panov AV, Greenamyre JT (2000). Chronic systemic pesticide exposure reproduces features of Parkinson's disease. *Nat. Neurosci.* **3**(12)**:** 1301-1306.

Betts MJ, O'Neill MJ, Duty S (2012). Allosteric modulation of the group III mGlu4 receptor provides functional neuroprotection in the 6-hydroxydopamine rat model of Parkinson's disease. *Br. J. Pharmacol.* **166**(8)**:** 2317-2330.

Beurrier C, Bioulac B, Audin J, Hammond C (2001). High-frequency stimulation produces a transient blockade of voltage-gated currents in subthalamic neurons. *J. Neurophysiol.* **85**(4)**:** 1351-1356.

Beurrier C, Lopez S, Revy D, Selvam C, Goudet C, Lherondel M*, et al.* (2009). Electrophysiological and behavioral evidence that modulation of metabotropic glutamate receptor 4 with a new agonist reverses experimental parkinsonism. *FASEB J.* **23**(10)**:** 3619-3628.

Bézard E, Ferry S, Mach U, Stark H, Leriche L, Boraud T*, et al.* (2003). Attenuation of levodopa-induced dyskinesia by normalizing dopamine D3 receptor function. *Nat. Med.* **9**(6)**:** 762-767.

Bezard E, Gross CE, Qin L, Gurevich VV, Benovic JL, Gurevich EV (2005). L-DOPA reverses the MPTP-induced elevation of the arrestin2 and GRK6 expression and enhanced ERK activation in monkey brain. *Neurobiol. Dis.* **18**(2)**:** 323-335.

Bezard E, Pioli EY, Li Q, Girard F, Mutel V, Keywood C*, et al.* (2014). The mGluR5 negative allosteric modulator dipraglurant reduces dyskinesia in the MPTP macaque model. *Mov. Disord.* **29**(8)**:** 1074-1079.

Bezard E, Tronci E, Pioli EY, Li Q, Porras G, Bjorklund A*, et al.* (2013). Study of the antidyskinetic effect of eltoprazine in animal models of levodopa-induced dyskinesia. *Mov. Disord.* **28**(8)**:** 1088-1096.

Bianchi L, Galeffi F, Bolam JP, Della Corte L (2003). The effect of 6-hydroxydopamine lesions on the release of amino acids in the direct and indirect pathways of the basal ganglia: a dual microdialysis probe analysis. *Eur. J. Neurosci.* **18**(4)**:** 856-868.

Bibbiani F, Oh JD, Chase TN (2001). Serotonin 5-HT1A agonist improves motor complications in rodent and primate parkinsonian models. *Neurology* **57:** 1829-1834.

Bibbiani F, Oh JD, Petzer JP, Castagnoli N, Chen JF, Schwarzschild MA*, et al.* (2003). A2A antagonist prevents dopamine agonist-induced motor complications in animal models of Parkinson's disease. *Exp. Neurol.* **184**(1)**:** 285-294.

Bichler Z, Lim HC, Zeng L, Tan EK (2013). Non-motor and motor features in LRRK2 transgenic mice. *PLoS One* **8**(7)**:** e70249.

Bido S, Marti M, Morari M (2011). Amantadine attenuates levodopa-induced dyskinesia in mice and rats preventing the accompanying rise in nigral GABA levels. *J. Neurochem.* **118**(6)**:** 1043-1055.

Billings LM, Marshall JF (2004). Glutamic acid decarboxylase 67 mRNA regulation in two globus pallidus neuron populations by dopamine and the subthalamic nucleus. *J. Neurosci.* **24**(12)**:** 3094-3103.

Bischoff S, Barhanin J, Bettler B, Mulle C, Heinemann S (1997). Spatial distribution of kainate receptor subunit mRNA in the mouse basal ganglia and ventral mesencephalon. *J. Comp. Neurol.* **379:** 541-562.

Blanchet P, Bedard PJ, Britton DR, Kebabian JW (1993). Differential effect of selective D-1 and D-2 dopamine receptor agonists on levodopa-induced dyskinesia in 1-methyl-4-phenyl1,2,3,6-tetrahydropyridine-exposed monkeys. *J. Pharmacol. Exp. Ther.* **267**(1)**:** 275-279.

Blanchet PJ, Konitsiotis S, Whittemore ER, Zhou ZL, Woodward RM, Chase TN (1999). Differing effects of N-methyl-D-aspartate receptor subtype selective antagonists on dyskinesias in levodopa-treated 1-methyl-4-phenyl-tetrahydropyridine monkeys. *J. Pharmacol. Exp. Ther.* **290**(3)**:** 1034-1040.

Blandini F (2000). Functional changes of the basal ganglia circuitry in Parkinson's disease. *Prog. Neurobiol.* **62**(1)**:** 63-88.

Blandini F, Garcia-Osuna M, Greenamyre JT (1997). Subthalamic ablation reverses changes in basal ganglia oxidative metabolism and motor response to apomorphine induced by nigrostriatal lesion in rats. *Eur. J. Neurosci.* **9:** 1407-1413.

Blandini F, Levandis G, Bazzini E, Nappi G, Armentero MT (2007). Time-course of nigrostriatal damage, basal ganglia metabolic changes and behavioural alterations following intrastriatal injection of 6-hydroxydopamine in the rat: new clues from an old model. *Eur. J. Neurosci.* **25**(2)**:** 397-405.

Blandini F, Nappi G, Greenamyre JT (2001). Subthalamic infusion of an NMDA antagonist prevents basal ganglia metabolic changes and nigral degeneration in a rodent model of Parkinson’s disease. *Ann. Neurol.* **49**(4)**:** 525-529.

Blume SR, Cass DK, Tseng KY (2009). Stepping test in mice: a reliable approach in determining forelimb akinesia in MPTP-induced Parkinsonism. *Exp. Neurol.* **219**(1)**:** 208-211.

Bogenpohl J, Galvan A, Hu X, Wichmann T, Smith Y (2012). Metabotropic glutamate receptor 4 in the basal ganglia of parkinsonian monkeys: Ultrastructural localization and

electrophysiological effects of activation in the striatopallidal complex. *Neuropharmacology* **66:** 242-252.

Boka G, Anglade P, Wallach D, Javoy-Agid F, Agid Y, Hirsch EC (1994). Immunocytochemical analysis of tumor necrosis factor and its receptors in Parkinson's disease. *Neurosci. Lett.* **172:** 151-154.

Bolam JP, Hanley JJ, Booth PAC, Bevan MD (2000). Synaptic organisation of the basal ganglia. *J. Anat.* **196:** 527-542.

Bonci A, Grillner P, Siniscalchi A, Mercuri NB, Bernardi G (1997). Glutamate metabotropic receptor agonists depress excitatory and inhibitory transmission on rat mesencephalic principal neurons. *Eur. J. Neurosci.* **9:** 2359-2369.

Bonifati V (2014). Genetics of Parkinson's disease – state of the art, 2013. *Parkinsonism Relat. Disord.* **20:** S23-S28.

Bonifati V, Fabrizio E, Cipriani R, Vanacore N, Meco G (1994). Buspirone in levodopa-induced dyskinesias. *Clin. Neuropharmacol.* **17**(1)**:** 73-72.

Boraud T, Bezard E, Bioulac B, Gross C (1996). High frequency stimulation of the internal Globus Pallidus (GPi) simultaneously improves parkinsonian symptoms and reduces the firing frequency of GPi neurons in the MPTP-treated monkey. *Neurosci. Lett.* **215**(1)**:** 17-20.

Bosch C, Mailly P, Degos B, Deniau JM, Venance L (2012). Preservation of the hyperdirect pathway of basal ganglia in a rodent brain slice. *Neuroscience* **215:** 31-41.

Bostan AC, Strick PL (2010). The cerebellum and basal ganglia are interconnected. *Neuropsychol. Rev.* **20**(3)**:** 261-270.

Bové J, Zhou C, Jackson-Lewis V, Taylor J, Chu Y, Rideout HJ*, et al.* (2006). Proteasome inhibition and Parkinson's disease modeling. *Ann. Neurol.* **60**(2)**:** 260-264.

Boyes J, Bolam JP (2003). The subcellular localization of $GABA_B$ receptor subunits in the rat substantia nigra. *Eur. J. Neurosci.* **18:** 3279-3293.

Braak H, Del Tredici K (2008). Cortico-basal ganglia-cortical circuitry in Parkinson's disease reconsidered. *Exp. Neurol.* **212**(1)**:** 226-229.

Braak H, Del Tredici K, Bratzke H, Hamm-Clement J, Sandmann-Keil D, Rub U (2002). Staging of the intracerebral inclusion body pathology associated with idiopathic Parkinson's disease (preclinical and clinical stages). *J. Neurol.* **249**(0)**:** 1-1.

Braak H, Tredici KD, Rüb U, de Vos RAI, Jansen Steur ENH, Braak E (2003). Staging of brain pathology related to sporadic Parkinson's disease. *Neurobiol. Aging* **24**(2)**:** 197-211.

Bracci E, Centonze D, Bernardi G, Calabresi P (2002). Dopamine excites fast-spiking interneurons in the striatum. *J. Neurophysiol.* **87**(4)**:** 2190-2194.

Bradley SR, Marino MJ, Wittmann M, Rouse ST, Awad H, Levey AI*, et al.* (2000). Activation of group II metabotropic glutamate receptors inhibits synaptic excitation of the substantia nigra pars reticulata. *J. Neurosci.* **20**(9)**:** 3085-3094.

Bradley SR, Marino MJ, Wittmann M, Rouse ST, Levey AI, Conn PJ (1999a). Physiological roles of presynaptically localized type 2, 3 and 7 metabotropic glutamate receptors in rat basal ganglia. In: *SfN*. Miami, Florida.

Bradley SR, Rees HD, Yi H, Levey AI, Conn PJ (1998). Distribution and developmental regulation of metabotropic glutamate receptor 7a in rat brain. *J. Neurochem.* **71**(2)**:** 636-645.

Bradley SR, Standaert DG, Levey AI, Conn PJ (1999b). Distribution of group III mGluRs in rat basal ganglia with subtype-specific antibodies. *Ann. N. Y. Acad. Sci.* **868**(1)**:** 531-534.

Bradley SR, Standaert DG, Rhodes KJ, Rees HD, Testa CM, Levey AI*, et al.* (1999c). Immunohistochemical localization of subtype 4a metabotropic glutamate receptors in the rat and mouse basal ganglia. *J. Comp. Neurol.* **407:** 33-46.

Branchi I, D'Andrea I, Armida M, Cassano T, Pezzola A, Potenza RL*, et al.* (2008). Nonmotor symptoms in Parkinson's disease: investigating early-phase onset of behavioral dysfunction in the 6-hydroxydopamine-lesioned rat model. *J. Neurosci. Res.* **86**(9)**:** 2050-2061.

Breger LS, Dunnett SB, Lane EL (2013). Comparison of rating scales used to evaluate L-DOPA-induced dyskinesia in the 6-OHDA lesioned rat. *Neurobiol. Dis.* **50:** 142-150.

Breit S, Lessmann L, Benazzouz A, Schulz JB (2005). Unilateral lesion of the pedunculopontine nucleus induces hyperactivity in the subthalamic nucleus and substantia nigra in the rat. *Eur. J. Neurosci.* **22**(9)**:** 2283-2294.

Breit S, Lessmann L, Unterbrink D, Popa RC, Gasser T, Schulz JB (2006). Lesion of the pedunculopontine nucleus reverses hyperactivity of the subthalamic nucleus and substantia nigra pars reticulata in a 6-hydroxydopamine rat model. *Eur. J. Neurosci.* **24**(8)**:** 2275-2282.

Brenner M, Haass A, Jacobi P, Schimrigk K (1989). Amantadine sulphate in treating Parkinson's disease: clinical effects, psychometric tests and serum concentrations. *J. Neurol.* **236:** 153-156.

Breysse N, Baunez C, Spooren W, Gasparini F, Amalric M (2002). Chronic but not acute treatment with a metabotropic glutamate 5 receptor antagonist reverses the akinetic deficits in a rat model of parkinsonism. *J. Neurosci.* **22**(13)**:** 5669-5678.

Broadstock M, Austin P, Betts M, Duty S (2012). Antiparkinsonian potential of targeting group III metabotropic glutamate receptor subtypes in the rodent substantia nigra pars reticulata. *Br. J. Pharmacol.* **165**(4b)**:** 1034-1045.

Broom L, Marinova-Mutafchieva L, Sadeghian M, Davis JB, Medhurst AD, Dexter DT (2011). Neuroprotection by the selective iNOS inhibitor GW274150 in a model of Parkinson disease. *Free Radical Biol. Med.* **50**(5)**:** 633-640.

Brotchie JM (2005). Nondopaminergic mechanisms in levodopa-induced dyskinesia. *Mov. Disord.* **20**(8)**:** 919-931.

Brothwell SLC, Barber JL, Monaghan DT, Jane DE, Gibb AJ, Jones S (2008). NR2B- and NR2D-containing synaptic NMDA receptors in developing rat substantia nigra pars compacta dopaminergic neurones. *J. Physiol.* **586:** 739-750.

Brouillet E, Beal MF (1993). NMDA antagonists partially protect against MPTP induced neurotoxicity in mice. *Neuroreport* **4**(4)**:** 387-390.

Brundin P, Barker RA, Parmar M (2010). Neural grafting in Parkinson's disease: problems and possibilities. *Prog. Brain Res.* **184:** 265-294.

Brunenberg EJ, Moeskops P, Backes WH, Pollo C, Cammoun L, Vilanova A*, et al.* (2012). Structural and resting state functional connectivity of the subthalamic nucleus: identification of motor STN parts and the hyperdirect pathway. *PLoS One* **7**(6)**:** e39061.

Bruno V, Battaglia G, Ksiazek I, Putten Hvd, Catania MV, Giuffrida R*, et al.* (2000). Selective activation of mGlu4 metabotropic glutamate receptors is protective against excitotoxic neuronal death. *J. Neurosci.* **20**(17)**:** 6413-6420.

Bruno V, Sureda FX, Storto M, Casabona G, Caruso A, Knopfel T*, et al.* (1997). The neuroprotective activity of group-II metabotropic glutamate receptors requires new protein synthesis and involves a glial-neuronal signaling. *J. Neurosci.* **17**(6)**:** 1891-1897.

Brusa L, Orlacchio A, Stefani A, Galati S, Pierantozzi M, Iani C*, et al.* (2013). A controlled release form of madopar in parkinsonian patients with advanced disease and marked fluctuations in motor performance. *Funct. Neurol.* **28**(2)**:** 101-105.

Bungay PM, Newton-Vinson P, Isele W, Garris PA, Justice JB (2003). Microdialysis of dopamine interpreted with quantitative model incorporating probe implantation trauma. *J. Neurochem.* **86**(4)**:** 932-946.

Burda JE, Sofroniew MV (2014). Reactive gliosis and the multicellular response to CNS damage and disease. *Neuron* **81**(2)**:** 229-248.

Burman JL, Yu S, Poole AC, Decal RB, Pallanck L (2012). Analysis of neural subtypes reveals selective mitochondrial dysfunction in dopaminergic neurons from parkin mutants. *Proc. Natl. Acad. Sci. U. S. A.* **109**(26)**:** 10438-10443.

Burnashev N, Schoepfer R, Monyer H, Ruppersberg JP, Günther W, Seeburg PH*, et al.* (1992). Control by asparagine residues of calcium permeability and magnesium blockade in the NMDA receptor. *Science* **257**(5075)**:** 1415-1419.

Burnashev N, Zhou Z, Neher E, Sakmann B (1995). Fractional calcium currents through recombinant GluR channels of the NMDA, AMPA and kainate receptor subtypes. *J. Physiol.* **485**(2)**:** 403-418.

Burns RS, Chiueh CC, Markey SP, Ebert MH, Jacobowitz DM, Kopin IJ (1983). A primate model of parkinsonism: Selective destruction of dopaminergic neurons in the pars compacta of the substantia nigra by N-methyl-4-phenyl-1,2,3,6-tetrahydropyridine. *Proc. Natl. Acad. Sci. U. S. A.* **80:** 4546-4550.

Bywood PT, Johnson SM (2003). Mitochondrial complex inhibitors preferentially damage substantia nigra dopamine neurons in rat brain slices. *Exp. Neurol.* **179**(1)**:** 47-59.

Caccia C, Maj R, Calabresi M, Maestroni S, Faravelli L, Curatolo L*, et al.* (2006). Safinamide: from molecular targets to a new anti-Parkinson drug. *Neurology* **67**(7 (Supp 2))**:** S18-S23.

Cadet JL, Katz M, Jackson-Lewis V, Fahn S (1989). Vitamin E attenuates the toxic effects of intrastriatal injection of 6-hydroxydopamine (6-OHDA) in rats: behavioral and biochemical evidence. *Brain Res.* **476:** 10-15.

Cain SM, Meadows HJ, Dunlop J, Bushell TJ (2008). mGlu4 potentiation of K(2P)2.1 is dependant on C-terminal dephosphorylation. *Mol. Cell. Neurosci.* **37**(1)**:** 32-39.

Calò M, Iannöne M, Passafaro M, Nisticò G (1990). Selective vulnerability of hippocampal CA3 neurones after microinfusion of paraquat into the rat substantia nigra or into the ventral tegmental area. *J. Comp. Pathol.* **103**(1)**:** 73-78.

Calon F, Rajput AH, Hornykiewicz O, Bedard PJ, Di Paolo T (2003). Levodopa-induced motor complications are associated with alterations of glutamate receptors in Parkinson's disease. *Neurobiol. Dis.* **14**(3)**:** 404-416.

Campbell GA, Eckardt MJ, Weight FF (1985). Dopaminergic mechanisms in subthalamic nucleus of rat: analysis using horseradish peroxidase and microiontophoresis. *Brain Res.* **333:** 261-270.

Canet-Aviles RM, Wilson MA, Miller DW, Ahmad R, McLendon C, Bandyopadhyay S*, et al.* (2004). The Parkinson's disease protein DJ-1 is neuroprotective due to cysteine-sulfinic acid-driven mitochondrial localization. *Proc. Natl. Acad. Sci. U. S. A.* **101**(24)**:** 9103-9108.

Cannella M, Motolese M, Bucci D, Molinaro G, Gradini R, Bruno V*, et al.* (2012). Early increase in the transcript of mGlu4 receptors in the striatum of mice treated with MPTP or haloperidol In: *SfN*. New Orleans.

Cannon JR, Tapias V, Na HM, Honick AS, Drolet RE, Greenamyre JT (2009). A highly reproducible rotenone model of Parkinson's disease. *Neurobiol. Dis.* **34**(2)**:** 279-290.

Canteras NS, Shammah-Lagnado SJ, Silva BA, Ricardo JA (1990). Afferent connections of the subthalamic nucleus: a combined retrograde and anterograde horseradish peroxidase study in the rat. *Brain Res.* **513**(1)**:** 43-59.

Carey RJ (1992). Factors in amphetamine-induced contralateral rotation in the unilateral 6-OHDA lesion rat model during the first-week postoperative: implications for neuropathology and neural grafting. *Brain Res.* **570**(1-2)**:** 11-20.

Carlsson A, Lindqvist M, Magnusson T (1957). 3,4-dihydroxyphenylalanine and 5-hydroxytryptophan as reserpine antagonists. *Nature* **180:** 1200.

Carlsson M, Carlsson A (1988). The NMDA antagonist MK-801 causes marked locomotor stimulation in monoamine-depleted mice. *J. Neural Transm.* **75:** 221-226.

Carman LS, Gage FH, Shults CW (1991). Partial lesion of the substantia nigra: relation between extent of lesion and rotational behavior. *Brain Res.* **553:** 275-283.

Carta M, Carlsson T, Kirik D, Bjorklund A (2007). Dopamine released from 5-HT terminals is the cause of L-DOPA-induced dyskinesia in parkinsonian rats. *Brain* **130**(Pt 7)**:** 1819-1833.

Carta M, Lindgren HS, Lundblad M, Stancampiano R, Fadda F, Cenci MA (2006). Role of striatal L-DOPA in the production of dyskinesia in 6-hydroxydopamine lesioned rats. *J. Neurochem.* **96**(6)**:** 1718-1727.

Cartmell J, Schoepp DD (2000). Regulation of neurotransmitter release by metabotropic glutamate receptors. *J. Neurochem.* **75**(3)**:** 889-907.

Carvalho GA, Nikkhah G (2001). Subthalamic nucleus lesions are neuroprotective against terminal 6-OHDA-induced striatal lesions and restore postural balancing reactions. *Exp. Neurol.* **171**(2)**:** 405-417.

Casas S, García S, Cabrera R, Nanfaro F, Escudero C, Yunes R (2011). Progesterone prevents depression-like behavior in a model of Parkinson's disease induced by 6-hydroxydopamine in male rats. *Pharmacol. Biochem. Behav.* **99**(4)**:** 614-618.

Célanire S, Boléa C, Brückner S, Liverton N, Charvin D, Hess F*, et al.* (2011). Discovery and characterization of novel metabotropic glutamate receptor 4 (mGluR4) positive allosteric modulators. In: *7th International Meeting on Metabotropic Glutamate Receptors (October 2-7, 2011).* Taormina.

Cenci MA, Lee CS, Bjorklund A (1998). L-DOPA-induced dyskinesia in the rat is associated with striatal overexpression of prodynorphin- and glutamic acid decarboxylase mRNA. *Eur. J. Neurosci.* **10**(8)**:** 2694-2706.

Cenci MA, Whishaw IQ, Schallert T (2002). Animal models of neurological deficits: how relevant is the rat? *Nat. Rev. Neurosci.* **3**(7)**:** 574-579.

Chan H, Paur H, Vernon AC, Zabarsky V, Datla KP, Croucher MJ*, et al.* (2010). Neuroprotection and functional recovery associated with decreased microglial activation following selective activation of mGluR2/3 receptors in a rodent model of Parkinson's disease. *Parkinsons Dis.* **2010:** ID 190450.

Chan HH, Kumar S, Zhuo L (2013). Neuroprotective and behavioural assessments of an imidazolium compound (DBZIM) in a rat model of Parkinson's disease induced by 6-OHDA. *Eur. J. Pharmacol.* **715**(1-3)**:** 405-413.

Chang J-W, Wachtel SR, Young D, Kang U-J (1999). Biochemical and anatomical characterization of forepaw adjusting steps in rat models of Parkinson's disease: studies on medial forebrain bundle and striatal lesions. *Neuroscience* **8**(2)**:** 617-628.

Chang X, Lu W, Dou T, Wang X, Lou D, Sun X*, et al.* (2013). Paraquat inhibits cell viability via enhanced oxidative stress and apoptosis in human neural progenitor cells. *Chem.-Biol. Interact.* **206**(2)**:** 248-255.

Chang YC, Kim H-W, Rapoport SI, Rao JS (2008). Chronic NMDA administration increases neuroinflammatory markers in rat frontal cortex: cross-talk between excitotoxicity and neuroinflammation. *Neurochem. Res.* **33**(11)**:** 2318-2323.

Chapuis S, Ouchchane L, Metz O, Gerbaud L, Durif F (2005). Impact of the motor complications of Parkinson's disease on the quality of life. *Mov. Disord.* **20**(2)**:** 224-230.

Chatha BT, Bernard V, Streit P, Bolam JP (2000). Synaptic localization of ionotropic glutamate receptors in the rat substantia nigra. *Neuroscience* **101**(4)**:** 1037-1051.

Chaudhuri KR, Healy DG, Schapira AHV (2006). Non-motor symptoms of Parkinson's disease: diagnosis and management. *Lancet Neurol.* **5**(3)**:** 235-245.

Chavis P, Shinozaki H, Bockaert J, Fagnil L (1994). The metabotropic glutamate receptor types 2/3 inhibit L-type calcium channels via a pertussis toxin-sensitive G-protein in cultured cerebellar granule cells. *J. Neurosci.* **14**(11)**:** 7067-7076.

Chen L, Huang L-YM (1992). Protein kinase C reduces Mg2+ block of NMDA-receptor channels as a mechanism of modulation. *Nature* **356:** 521-523.

Chen L, Liu J, Ali U, Gui Z-H, Wang Y, Wang T*, et al.* (2012). Blockade of mGluR5 reverses abnormal firing of subthalamic nucleus neurons in 6-hydroxydopamine partially lesioned rats. *Chin J. Physiol.* **54**(5)**:** 303-309.

Chen L, Togasaki DM, Langston JW, Di Monte DA, Quik M (2005a). Enhanced striatal opioid receptor-mediated G-protein activation in L-DOPA-treated dyskinetic monkeys. *Neuroscience* **132**(2)**:** 409-420.

Chen SR, Pan HL (2005b). Distinct roles of group III metabotropic glutamate receptors in control of nociception and dorsal horn neurons in normal and nerve-injured Rats. *J. Pharmacol. Exp. Ther.* **312**(1)**:** 120-126.

Chesselet M-F, Richter F (2011). Modelling of Parkinson's disease in mice. *Lancet Neurol.* **10**(12)**:** 1108-1118.

Chevalier G, Deniau JM (1990). Disinhibition as a basic process in the expression of striatal functions. *Trends Neurosci.* **13**(7)**:** 277-280.

Chiba K, Trevor A, Castagnoli N (1984). Metabolism of the neurotoxic tertiary amine, MPTP, by brain monoamine oxidase. *Biochem. Biophys. Res. Commun.* **120**(2)**:** 574-578.

Chuang S-C, Bianchi R, Wong RKS (2000). Group I mGluR activation turns on a voltage-gated inward current in hippocampal pyramidal cells. *J. Neurophysiol.* **83**(5)**:** 2844-2853.

Chung EK, Chen LW, Chan YS, Yung KK (2008). Downregulation of glial glutamate transporters after dopamine denervation in the striatum of 6-hydroxydopamine-lesioned rats. *J. Comp. Neurol.* **511**(4)**:** 421-437.

Ciccarelli R, Di Iorio P, Bruno V, Battaglia G, D'Alimonte I, D'Onofrio M*, et al.* (1999). Activation of A(1) adenosine or mGlu3 metabotropic glutamate receptors enhances the release of nerve growth factor and S-100beta protein from cultured astrocytes. *Glia* **27**(3)**:** 275-281.

Clarke CE, Sambrook MA, Mitchell IJ, Crossman AR (1987). Levodopa-induced dyskinesia and response fluctuations in primates rendered parkinsonian with 1-methyl-4-phenyl-1,2,3,6-tetrahydropyridine (MPTP). *J. Neurol. Sci.* **78:** 273-280.

Clarke RJ, Glasgow NG, Johnson JW (2013). Mechanistic and structural determinants of NMDA receptor voltage-dependent gating and slow Mg2+ unblock. *J. Neurosci.* **33**(9)**:** 4140-4150.

Çoban A, Hanagasi HA, Karamursel S, Barlas O (2009). Comparison of unilateral pallidotomy and subthalamotomy findings in advanced idiopathic Parkinson's disease. *Br. J. Neurosurg.* **23**(1)**:** 23-29.

Cohen G, Heikkila RE (1974). The generation of hydrogen peroxide, superoxide radical, and hydroxyl radical by 6-hydroxydopamine, dialuric acid, and related cytotoxic agents. *J. Biol. Chem.* **249**(8)**:** 2447-2452.

Colucci M, Cervio M, Faniglione M, De Angelis S, Pajoro M, Levandis G*, et al.* (2012). Intestinal dysmotility and enteric neurochemical changes in a Parkinson's disease rat model. *Auton. Neurosci.* **169**(2)**:** 77-86.

Congar P, Leinekugel X, Ben-Ari Y, Crépel V (1997). A long-lasting calcium-activated nonselective cationic current is generated by synaptic stimulation or exogenous activation of group I metabotropic glutamate receptors in CA1 pyramidal neurons. *J. Neurosci.* **17**(14)**:** 5366-5379.

Conn JP, Pin JP (1997). Pharmacology and functions of metabotropic glutamate receptors. *Annu. Rev. Pharmacol. Toxicol.* **37:** 205-237.

Conn PJ, Battaglia G, Marino MJ, Nicoletti F (2005). Metabotropic glutamate receptors in the basal ganglia motor circuit. *Nat. Rev. Neurosci.* **6**(10)**:** 787-798.

Cookson MR (2012). Cellular effects of LRRK2 mutations. *Biochem. Soc. Trans.* **40**(5)**:** 1070-1073.

Coon S, Stark A, Peterson E, Gloi A, Kortsha G, Pounds J*, et al.* (2006). Whole-body lifetime occupational lead exposure and risk of Parkinson's disease. *Environ. Health Perspect.* **114**(12)**:** 1872-1876.

Corti C, Aldegheri L, Somogyi P, Ferraguti F (2002). Distribution and synaptic localisation of the metabotropic glutamate receptor 4 (mGluR4) in the rodent CNS. *Neuroscience* **110**(3)**:** 403-420.

Corti C, Battaglia G, Molinaro G, Riozzi B, Pittaluga A, Corsi M*, et al.* (2007). The use of knock-out mice unravels distinct roles for mGlu2 and mGlu3 metabotropic glutamate receptors in mechanisms of neurodegeneration/neuroprotection. *J. Neurosci.* **27**(31)**:** 8297-8308.

Corvol JC, Muriel MP, Valjent E, Feger J, Hanoun N, Girault JA*, et al.* (2004). Persistent increase in olfactory type G-protein alpha subunit levels may underlie D1 receptor functional hypersensitivity in Parkinson disease. *J. Neurosci.* **24**(31)**:** 7007-7014.

Costa G, Abin-Carriquiry JA, Dajas F (2001). Nicotine prevents striatal dopamine loss produced by 6-hydroxydopamine lesion in the substantia nigra. *Brain Res.* **888:** 336-342.

Cote SR, Chitravanshi VC, Bleickardt C, Sapru HN, Kuzhikandathil EV (2014). Overexpression of the dopamine D3 receptor in the rat dorsal striatum induces dyskinetic behaviors. *Behav. Brain Res.* **263:** 46-50.

Cotzias GC, Papavasilou PS, Gellene R (1969). Modification of Parkinsonism - chronic treatment with L-DOPA. *New Engl. J. Med.* **280**(7)**:** 337-345.

Cox H, Togasaki DM, Chen L, Langston JW, Di Monte DA, Quik M (2007). The selective kappa-opioid receptor agonist U50,488 reduces L-dopa-induced dyskinesias but worsens parkinsonism in MPTP-treated primates. *Exp. Neurol.* **205**(1)**:** 101-107.

Cragg SJ, Baufreton J, Xue Y, Bolam JP, Bevan MD (2004). Synaptic release of dopamine in the subthalamic nucleus. *Eur. J. Neurosci.* **20**(7)**:** 1788-1802.

Crosby NJ, Deane K, Clarke CE (2003). Amantadine in Parkinson’s disease. *Cochrane Database Syst. Rev.*(1)**:** CD003468.

Cui L, Kim YR, Kim HY, Lee SC, Shin HS, Szabo G*, et al.* (2011). Modulation of synaptic transmission from primary afferents to spinal substantia gelatinosa neurons by group III mGluRs in GAD65-EGFP transgenic mice. *J. Neurophysiol.* **105**(3)**:** 1102-1111.

Cuomo D, Martella G, Barabino E, Platania P, Vita D, Madeo G*, et al.* (2009). Metabotropic glutamate receptor subtype 4 selectively modulates both glutamate and GABA transmission in the striatum: implications for Parkinson's disease treatment. *J. Neurochem.* **109**(4)**:** 1096-1105.

Da Cunha C, Wietzikoski EC, Ferro MM, Martinez GR, Vital MA, Hipolide D*, et al.* (2008). Hemiparkinsonian rats rotate toward the side with the weaker dopaminergic neurotransmission. *Behav. Brain Res.* **189**(2)**:** 364-372.

Danysz W, Gossel M, Zajaczkowski W, Dill D, Quack G (1994). Are NMDA antagonistic properties relevant for antiparkinsonian-like activity in rats? - Case of amantadine and memantine. *J. Neural Transm.* **7:** 155-166.

Datla KP, Blunt SB, Dexter DT (2001). Chronic L-DOPA administration is not toxic to the remaining dopaminergic nigrostriatal neurons, but instead may promote their functional recovery, in rats with partial 6-OHDA or $FeCl_3$ nigrostriatal lesions. *Mov. Disord.* **16**(3)**:** 424-434.

Davis GC, Williams AC, Markey SP, Ebert MH, Caine ED, Reichert CM*, et al.* (1979). Chronic Parkinsonism secondary to intravenous injection of meperidine analogues. *Psychiatry Res.* **1:** 249-254.

Dawson L, Chadha A, Megalou M, Duty S (2000). The group II metabotropic glutamate receptor agonist, DCG-IV, alleviates akinesia following intranigral or intraventricular administration in the reserpine-treated rat. *Br. J. Pharmacol.* **129**(3)**:** 541-546.

Dawson TM, Dawson VL (2010). The role of parkin in familial and sporadic Parkinson's disease. *Mov. Disord.* **25 Suppl 1:** S32-39.

Day M, Wang Z, Ding J, An X, Ingham CA, Shering AF*, et al.* (2006). Selective elimination of glutamatergic synapses on striatopallidal neurons in Parkinson disease models. *Nat. Neurosci.* **9**(2)**:** 251-259.

DBS For Parkinson's Disease Study Group (2001). Deep-brain stimulation of the subthalamic nucleus or the pars interna of the globus pallidus in Parkinson's disease. *New Engl. J. Med.* **345**(13)**:** 956-963.

de Araujo DP, De Sousa CN, Araujo PV, Menezes CE, Sousa Rodrigues FT, Escudeiro SS*, et al.* (2013). Behavioral and neurochemical effects of alpha-lipoic acid in the model of Parkinson's disease induced by unilateral stereotaxic injection of 6-OHDA in rat. *Evid. Based Complement. Altern. Med.* **2013:** 571378.

de Rijk MC, Launer LJ, Berger K, Breteler MMB, Dartigues J-F, Baldereschi M*, et al.* (2000). Prevalence of Parkinson's disease in Europe: A collaborative study of population-based cohorts. *Neurology* **54**(11(Supp. 5))**:** S21-S23.

de Rover M, Meye FJ, Ramakers GM (2008). Presynaptic metabotropic glutamate receptors regulate glutamatergic input to dopamine neurons in the ventral tegmental area. *Neuroscience* **154**(4)**:** 1318-1323.

de Souza Silva MA, Muller CP, Huston JP (2007). Microdialysis in the brain of anaesthetized vs. freely moving animals. In: Westerink BHC, Cremers TIFH (ed)^(eds). *Handbook of Microdialysis: Methods, Applications and Perspectives*, 1 edn: Elsevier Academic Press. p^pp.

Decressac M, Mattsson B, Bjorklund A (2012). Comparison of the behavioural and histological characteristics of the 6-OHDA and alpha-synuclein rat models of Parkinson's disease. *Exp. Neurol.* **235**(1)**:** 306-315.

Dejean C, Gross CE, Bioulac B, Boraud T (2008). Dynamic changes in the cortex-basal ganglia network after dopamine depletion in the rat. *J. Neurophysiol.* **100**(1)**:** 385-396.

Dekundy A, Lundblad M, Danysz W, Cenci MA (2007). Modulation of L-DOPA-induced abnormal involuntary movements by clinically tested compounds: further validation of the rat dyskinesia model. *Behav. Brain Res.* **179**(1)**:** 76-89.

Dekundy A, Pietraszek M, Schaefer D, Cenci MA, Danysz W (2006). Effects of group I metabotropic glutamate receptors blockade in experimental models of Parkinson's disease. *Brain Res. Bull.* **69**(3)**:** 318-326.

Del Arco A, Segovia G, Fuxe K, Mora F (2003). Changes in dialysate concentrations of glutamate and GABA in the brain: an index of volume transmission mediated actions? *J. Neurochem.* **85**(1)**:** 23-33.

del Dotto P, Pavese N, Gambaccini G, Bernardini S, Metman LV, Chase TN*, et al.* (2001). Intravenous amantadine improves levadopa-induced dyskinesias: an acute double-blind placebo-controlled study. *Mov. Disord.* **16**(3)**:** 515-520.

Denes L, Szilágyi G, Gál A, Nagy Z (2006). Talampanel a non-competitive AMPA-antagonist attenuates caspase-3 dependent apoptosis in mouse brain after transient focal cerebral ischemia. *Brain Res. Bull.* **70**(3)**:** 260-262.

Deniau J-M, Degos B, Bosch C, Maurice N (2010). Deep brain stimulation mechanisms: beyond the concept of local functional inhibition. *Eur. J. Neurosci.* **32**(7)**:** 1080-1091.

Dexter DT, Carter CJ, Wells FR, Javoy-Agid F, Agid Y, Lees A*, et al.* (1989). Basal lipid peroxidation in substantia nigra is increased in Parkinson's disease. *J. Neurochem.* **52**(2)**:** 381-389.

Dexter DT, Statton SA, Whitmore C, Freinbichler W, Weinberger P, Tipton KF*, et al.* (2010). Clinically available iron chelators induce neuroprotection in the 6-OHDA model of Parkinson's disease after peripheral administration. *J. Neural Transm.* **118**(2)**:** 223-231.

Di Giorgio AM, Hou Y, Zhao X, Zhang B, Lyeth BG, Russell MJ (2008). Dimethyl sulfoxide provides neuroprotection in a traumatic brain injury model. *Restor. Neurol. Neurosci.* **26**(6)**:** 501-507.

Di L, Umland JP, Chang G, Huang Y, Lin Z, Scott DO*, et al.* (2011). Species independence in brain tissue binding using brain homogenates. *Drug Metab. Dispos.* **39**(7)**:** 1270-1277.

Di Liberto V, Bonomo A, Frinchi M, Belluardo N, Mudo G (2010). Group II metabotropic glutamate receptor activation by agonist LY379268 treatment increases the expression of brain derived neurotrophic factor in the mouse brain. *Neuroscience* **165**(3)**:** 863-873.

Dickson DW, Fujishiro H, Orr C, DelleDonne A, Josephs KA, Frigerio R*, et al.* (2009). Neuropathology of non-motor features of Parkinson disease. *Parkinsonism Relat. Disord.* **15**(S3)**:** S1-S5.

Dolan S, Gunn MD, Biddlestone L, Nolan AM (2009). The selective metabotropic glutamate receptor 7 allosteric agonist AMN082 inhibits inflammatory pain-induced and incision-induced hypersensitivity in rat. *Behav. Pharmacol.* **20**(7)**:** 596-604.

Dolleman-van der Weel MJ, Nijssen A, Steinbusch HWM (1993). Morphological and behavioral drawbacks of fetal dopaminergic grafts, prelabeled with *Phaseolus vulgaris* leucoagglutinin. *Exp. Neurol.* **122:** 260-272.

Doller D, Hong SP, Uberti MA, Nerio MT, Brodbeck RM, Breysse N*, et al.* (2010). LuAF21934, a brain penetrant $mGluR_4$ receptor positive allosteric modulator tool compound. In: *SfN*. San Diego.

Domin H, Golembiowska K, Jantas D, Kaminska K, Zieba B, Smialowska M (2014). Group III mGlu receptor agonist, ACPT-I, exerts potential neuroprotective effects in vitro and in vivo. *Neurotox. Res.* **26**(1)**:** 99-113.

Doty RL (2012). Olfactory dysfunction in Parkinson disease. *Nat. Rev. Neurol.* **8**(6)**:** 329-339.

Doumazane E, Scholler P, Zwier JM, Trinquet E, Rondard P, Pin JP (2011). A new approach to analyze cell surface protein complexes reveals specific heterodimeric metabotropic glutamate receptors. *FASEB J.* **25**(1)**:** 66-77.

Dourish CT, Hutson PH, Curzon G (1985). Low doses of the putative serotonin agonist 8-hydroxy-2-(di-n-propylamino) tetralin (8-OH-DPAT) elicit feeding in the rat. *Psychopharmacology* **86:** 197-204.

Dube A, Chaudhary S, Mengawade T, Upasani CD (2014). Therapeutic potential of metabotropic glutamate receptor 4-positive allosteric modulator TAS-4 in rodent models of movement disorders. *J. Neurol. Sci.*

Dupre KB, Ostock CY, Eskow Jaunarajs KL, Button T, Savage LM, Wolf W*, et al.* (2011). Local modulation of striatal glutamate efflux by serotonin 1A receptor stimulation in dyskinetic, hemiparkinsonian rats. *Exp. Neurol.* **229**(2)**:** 288-299.

Dupre KB, Ostock CY, George JA, Eskow Jaunarajs KL, Hueston CM, Bishop C (2013). Effects of 5-HT1A receptor stimulation on D1 receptor agonist-induced striatonigral activity and dyskinesia in hemiparkinsonian rats. *ACS Chem. Neurosci.* **4**(5)**:** 747-760.

Dusonchet J, Kochubey O, Stafa K, Young SM, Jr., Zufferey R, Moore DJ*, et al.* (2011). A rat model of progressive nigral neurodegeneration induced by the Parkinson's disease-associated G2019S mutation in LRRK2. *J. Neurosci.* **31**(3)**:** 907-912.

Duty S, Jenner P (2011). Animal models of Parkinson's disease: a source of novel treatments and clues to the cause of the disease. *Br. J. Pharmacol.* **164**(4)**:** 1357-1391.

Duval C, Panisset M, Strafella AP, Sadikot AF (2006). The impact of ventrolateral thalamotomy on tremor and voluntary motor behavior in patients with Parkinson's disease. *Exp. Brain Res.* **170**(2)**:** 160-171.

Duvoisin RM, Pfankuch T, Wilson JM, Grabell J, Chhajlani V, Brown DG*, et al.* (2010). Acute pharmacological modulation of mGluR8 reduces measures of anxiety. *Behav. Brain Res.* **212**(2)**:** 168-173.

Dvorzhak A, Gertler C, Harnack D, Grantyn R (2013). High frequency stimulation of the subthalamic nucleus leads to presynaptic GABA(B)-dependent depression of subthalamo-nigral afferents. *PLoS One* **8**(12)**:** e82191.

East SP, Bamford S, Dietz MGA, Eickmeier C, Flegg A, Ferger B*, et al.* (2010). An orally bioavailable positive allosteric modulator of the mGlu4 receptor with efficacy in an animal model of motor dysfunction. *Bioorg. Med. Chem. Lett.* **20**(16)**:** 4901-4905.

Eggert K, Squillacote D, Barone P, Dodel R, Katzenschlager R, Emre M*, et al.* (2010). Safety and efficacy of perampanel in advanced Parkinson's disease: a randomized, placebo-controlled study. *Mov. Disord.* **25**(7)**:** 896-905.

Ekstrand MI, Terzioglu M, Galter D, Zhu S, Hofstetter C, Lindqvist E*, et al.* (2007). Progressive parkinsonism in mice with respiratory-chain-deficient dopamine neurons. *Proc. Natl. Acad. Sci. U. S. A.* **104**(4)**:** 1325-1330.

Elahi B, Phielipp N, Chen R (2012). N-Methyl-D-Aspartate antagonists in levodopa-induced dyskinesia: a meta-analysis. *Can. J. Neurol. Sci.* **39:** 365-372.

Elkon H, Melamed E, Offen D (2004). Oxidative stress, induced by 6-hydroxydopamine, reduces proteasome activities in PC12 cells. Implications for the pathogenesis of Parkinson's disease. *J. Mol. Neurosci.* **24:** 387-400.

Elmore MRP, Najafi AR, Koike MA, Dagher NN, Spangenberg EE, Rice RA*, et al.* (2014). Colony-Stimulating Factor 1 receptor signaling is necessary for microglia viability, unmasking a microglia progenitor cell in the adult brain. *Neuron* **82**(2)**:** 380-397.

Engers DW, Lindsley CW (2012). Allosteric modulation of class C GPCRs: a novel approach for the treatment of CNS disorders. *Drug Discov. Today* **10**(2)**:** e269-e276.

Enz R (2007). The trick of the tail: protein-protein interactions of metabotropic glutamate receptors. *Bioessays* **29**(1)**:** 60-73.

Ercal N, Gurer-Orhan H, Aykin-Burns N (1991). Toxic metals and oxidative stress part 1: mechanisms involved in metal-induced oxidative damage. *Curr. Top. Med. Chem.* **1:** 529-539.

Erdo F, Berzsenyi P, Andrási F (2005). The AMPA-antagonist talampanel is neuroprotective in rodent models of focal cerebral ischemia. *Brain Res. Bull.* **66**(1)**:** 43-49.

Fabbrini G, Brotchie JM, Grandas F, Nomoto M, Goetz CG (2007). Levodopa-induced dyskinesias. *Mov. Disord.* **22**(10)**:** 1379-1389; quiz 1523.

Fahn S (1991). An open trial of high-dosage antioxidants in early Parkinson's disease. *Am. J. Clin. Nutr.* **53:** 380S-382S.

Fahn SS (2004). Levodopa and the progression of Parkinson's disease. *New Engl. J. Med.* **351:** 2498-2508.

Fallarino F, Volpi C, Fazio F, Notartomaso S, Vacca C, Busceti C*, et al.* (2010). Metabotropic glutamate receptor-4 modulates adaptive immunity and restrains neuroinflammation. *Nat. Med.* **16**(8)**:** 897-902.

Fan KY, Baufreton J, Surmeier DJ, Chan CS, Bevan MD (2012). Proliferation of external globus pallidus-subthalamic nucleus synapses following degeneration of midbrain dopamine neurons. *J. Neurosci.* **32**(40)**:** 13718-13728.

Fang F, Wirdefeldt K, Jacks A, Kamel F, Ye W, Chen H (2012). CNS infections, sepsis and risk of Parkinson's disease. *Int. J. Epidemiol.* **41**(4)**:** 1042-1049.

Fang X, Sugiyama K, Akamine S, Namba H (2006). The stepping test and its learning process in different degrees of unilateral striatal lesions by 6-hydroxydopamine in rats. *Neurosci. Res.* **55**(4)**:** 403-409.

Fazio F, Lionetto L, Molinaro G, Bertrand HO, Acher F, Ngomba RT*, et al.* (2012). Cinnabarinic acid, an endogenous metabolite of the kynurenine pathway, activates type 4 metabotropic glutamate receptors. *Mol. Pharmacol.* **81**(5)**:** 643-656.

Feldman RG, Kaye JA, Lannon MC (1986). Parkinson's disease: follow-up after "Drug Holiday". *J. Clin. Pharmacol.* **26:** 662-667.

Felix-Ortiz AC, Beyeler A, Seo C, Leppla CA, Wildes CP, Tye KM (2013). BLA to vHPC inputs modulate anxiety-related behaviors. *Neuron* **79**(4)**:** 658-664.

Fernandez-Suarez D, Celorrio M, Lanciego JL, Franco R, Maria S. Aymerich P (2012). Loss of parvalbumin-positive neurons from the globus pallidus in animal models of Parkinson disease. *J. Neuropathol. Exp. Neurol.* **71**(11)**:** 973-982.

Ferrarese C, Zoia C, Pecora N, Piolti R, Frigo M, Bianchi G*, et al.* (1999). Reduced platelet glutamate uptake in Parkinson's disease. *J. Neural Transm.* **106:** 685-692.

Ferreira JJ, Katzenschlager R, Bloem BR, Bonuccelli U, Burn D, Deuschl G*, et al.* (2013). Summary of the recommendations of the EFNS/MDS-ES review on therapeutic management of Parkinson's disease. *Eur. J. Neurol.* **20**(1)**:** 5-15.

Fillion M, Tremblay L (1991). Abnormal spontaneous activity of globus pallidus neurons in monkeys with MPTP-induced parkinsonism. *Brain Res.* **547:** 142-151.

Finlay C, Duty S (2014). Therapeutic potential of targeting glutamate receptors in Parkinson's disease. *J. Neural Transm.* **121**(8)**:** 861-880.

Fiorentini C, Busi C, Spano P, Missale C (2008). Role of receptor heterodimers in the development of L-dopa-induced dyskinesias in the 6-hydroxydopamine rat model of Parkinson's disease. *Parkinsonism Relat. Disord.* **14**(Suppl 2)**:** S159-164.

Fiorentini C, Savoia P, Savoldi D, Barbon A, Missale C (2013). Persistent activation of the D1R/Shp-2/Erk1/2 pathway in l-DOPA-induced dyskinesia in the 6-hydroxy-dopamine rat model of Parkinson's disease. *Neurobiol. Dis.* **54:** 339-348.

Flor PJ, Acher FC (2012). Orthosteric versus allosteric GPCR activation: The great challenge of group-III mGluRs. *Biochem. Pharmacol.* **84**(4)**:** 414-424.

Follett KA, Weaver FM, Stern M, Hur K, Harris CL, Luo P*, et al.* (2010). Pallidal versus subthalamic deep-brain stimulation for Parkinson's disease. *New Engl. J. Med.* **362**(22)**:** 2077-2091.

Fonnum F, Storm-Mathisen J, Divac I (1981). Biochemical evidence for glutamate as neurotransmitter in corticostriatal and corticothalamic fibres in rat brain. *Neuroscience* **6**(5)**:** 863-873.

Fornai F, Lenzi P, Gesi M, Ferrucci M, Lazzeri G, Busceti CL*, et al.* (2003). Fine structure and biochemical mechanisms underlying nigrostriatal inclusions and cell death after proteasome inhibition. *J. Neurosci.* **23**(26)**:** 8955-8966.

Fornai F, Schluter OM, Lenzi P, Gesi M, Ruffoli R, Ferrucci M*, et al.* (2005). Parkinson-like syndrome induced by continuous MPTP infusion: convergent roles of the ubiquitin-proteasome system and alpha-synuclein. *Proc. Natl. Acad. Sci. U. S. A.* **102**(9)**:** 3413-3418.

Forno LS, Langston JW, DeLanney LE, Irwin I, Ricaurte GA (1986). Locus ceruleus lesions and eosinophilic inclusions in MPTP-treated monkeys. *Ann. Neurol.* **20**(4)**:** 449-455.

Forsberg M, Lehtonen M, Heikkinen M, Savolainen J, Jarvinen T, Mannisto PT (2003). Pharmacokinetics and pharmacodynamics of entacapone and tolcapone after acute and repeated administration: a comparative study in the rat. *J. Pharmacol. Exp. Ther.* **304**(2): 498-506.

Fox SH, Henry B, Hill M, Crossman A, Brotchie J (2002). Stimulation of cannabinoid receptors reduces levodopa-induced dyskinesia in the MPTP-lesioned nonhuman primate model of Parkinson's disease. *Mov. Disord.* **17**(6)**:** 1180-1187.

Fox SH, Johnston TH, Li Q, Brotchie J, Bezard E (2012). A critique of available scales and presentation of the non-human primate dyskinesia rating scale. *Mov. Disord.* **27**(11)**:** 1373-1378.

Francardo V, Recchia A, Popovic N, Andersson D, Nissbrandt H, Cenci MA (2011). Impact of the lesion procedure on the profiles of motor impairment and molecular responsiveness to L-DOPA in the 6-hydroxydopamine mouse model of Parkinson's disease. *Neurobiol. Dis.* **42**(3)**:** 327-340.

Freed CR, Greene PE, Breeze RE, Tsai WY, DuMouchel W, Kao R*, et al.* (2001). Transplantation of embryonic dopamine neurons for severe Parkinson's disease. *New Engl. J. Med.* **344**(10)**:** 710-719.

Friden M, Winiwarter S, Jerndal G, Bengtsson O, Wan H, Bredberg U*, et al.* (2009). Structure-brain exposure relationships in rat and human using a novel data set of unbound drug concentrations in brain interstitial and cerebrospinal fluids. *J. Med. Chem.* **52**(20)**:** 6233-6243.

Friedman JH (1989). Progressive parkinsonism in boxers. *South. Med. J.* **82**(5)**:** 543-546.

Friehs GM, Ojakangas CL, Pachatz P, Schröttner O, Ott E, Pendl G (1995). Thalamotomy and caudatotomy with the Gamma Knife as a treatment for parkinsonism with a comment on lesion sizes. *Stereotact. Funct. Neurosurg.* **64**(Supplement 1)**:** 209-221.

Fujiyama F, Stephenson FA, Bolam JP (2002). Synaptic localization of GABAA receptor subunits in the substantia nigra of the rat: effects of quinolinic acid lesions of the striatum. *Eur. J. Neurosci.* **15:** 1961-1975.

Fukushima T, Tan X, Luo Y, Kanda H (2010). Relationship between blood levels of heavy metals and Parkinson's disease in China. *Neuroepidemiology* **34**(1)**:** 18-24.

Gainetdinov RR, Fumagalli F, Jones SR, Caron MG (1997). Dopamine transporter is required for in vivo MPTP neurotoxicity: evidence from mice lacking the transporter. *J. Neurochem.* **69:** 1322-1325.

Galter D, Pernold K, Yoshitake T, Lindqvist E, Hoffer B, Kehr J*, et al.* (2010). MitoPark mice mirror the slow progression of key symptoms and L-DOPA response in Parkinson's disease. *Genes Brain Behav.* **9**(2)**:** 173-181.

Gao HM, Zhang F, Zhou H, Kam W, Wilson B, Hong JS (2011). Neuroinflammation and alpha-synuclein dysfunction potentiate each other, driving chronic progression of neurodegeneration in a mouse model of Parkinson's disease. *Environ. Health Perspect.* **119**(6)**:** 807-814.

Garcia PS, Kolesky SE, Jenkins A (2010). General anesthetic actions on $GABA_A$ receptors. *Curr. Neuropharmacol.* **8:** 2-9.

Gardoni F, Picconi B, Ghiglieri V, Polli F, Bagetta V, Bernardi G*, et al.* (2006). A critical interaction between NR2B and MAGUK in L-DOPA induced dyskinesia. *J. Neurosci.* **26**(11)**:** 2914-2922.

Gardoni F, Sgobio C, Pendolino V, Calabresi P, Di Luca M, Picconi B (2012). Targeting NR2A-containing NMDA receptors reduces L-DOPA-induced dyskinesias. *Neurobiol. Aging* **33**(9)**:** 2138-2144.

Garrido M, Tereshchenko Y, Zhevtsova Z, Taschenberger G, Bähr M, Kügler S (2010). Glutathione depletion and overproduction both initiate degeneration of nigral dopaminergic neurons. *Acta Neuropathol. (Berl).* **121**(4)**:** 475-485.

Gasparini F, Bruno V, Battaglia G, Lukic S, Leonhardt T, Inderbitzin W*, et al.* (1999). (R,S)-4-phosphonophenylglycine, a potent and selective group III metabotropic glutamate receptor agonist, is anticonvulsive and neuroprotective *in vivo*. *J. Pharmacol. Exp. Ther.* **289**(3)**:** 1678-1687.

Gee CE, Benquet P, Gerber U (2002). Group I metabotropic glutamate receptors activate a calcium-sensitive transient receptor potential-like conductance in rat hippocampus. *J. Physiol.* **546:** 655-664.

Gentsch C, Lichtsteiner M, Feer H (1987). Open field and elevated plus-maze" a behavioural comparison between spontaneously hypertensive (SHR) and Wistar-Kyoto (WKY) rats and the effects of chlordiazepoxide. *Behav. Brain Res.* **25:** 101-107.

Gerber U, Gee C, Benquet P (2007). Metabotropic glutamate receptors: intracellular signaling pathways. *Curr. Opin. Pharm.* **7**(1)**:** 56-61.

Gerfen CR, Engber TM, Mahan LC, Susel Z, Chase TN, Monsma FJ*, et al.* (1990). D1 and D2 dopamine receptor-regulated gene expression of striatonigral and striatopallidal neurons. *Science* **250**(4986)**:** 1429-1432.

Gerfen CR, McGinty JF, Young WS (1991). Dopamine differentially regulates dynorphin, substance P, and enkephalin expression in striatal neurons: in situ hybridization histochemical analysis. *J. Neurosci.* **11**(4)**:** 1016-1031.

Ghika J, Gachoud JP, Gasser U (1997). Clinical efficacy and tolerability of a new levodopa/benserazide dual-release formulation in parkinsonian patients. *Clin. Neuropharmacol.* **22**(2)**:** 130-139.

GHR (2014). Genetics Home Reference http://ghr.nlm.nih.gov Vol. 2014.

Gianutsos G, Chute S, Dunn JP (1985). Pharmacoloical changes in dopaminergic systems induced by long-term administration of amantadine. *Eur. J. Pharmacol.* **110:** 357-361.

Gillies A, Willshaw D, Li Z (2002). Subthalamic-pallidal interactions are critical in determining normal and abnormal functioning of the basal ganglia. *Proc. Biol. Sci.* **269**(1491)**:** 545-551.

Glajch KE, Fleming SM, Surmeier DJ, Osten P (2012). Sensorimotor assessment of the unilateral 6-hydroxydopamine mouse model of Parkinson's disease. *Behav. Brain Res.* **230**(2)**:** 309-316.

Gleeson MP, Hersey A, Montanari D, Overington J (2011). Probing the links between in vitro potency, ADMET and physicochemical parameters. *Nat. Rev. Drug Discov.* **10**(3)**:** 197-208.

Glick SD, Dong N, Keller RW, Carlson JN (1994). Estimating extracellular concentrations of dopamine and 3,4-dihydroxyphenylacetic acid in nucleus accumbens and striatum using microdialysis: relationships between *in vitro* and *in vivo* recoveries. *J. Neurochem.* **62**(5)**:** 2017-2021.

Glow PH (1959). Some aspects of the effects of acute reserpine treatment on behavior. *J. Neurol. Neurosurg. Psychiatry* **22:** 11-32.

Godwin-Austen RB, Tomlinson EB, Frears CC, Kok HWL (1969). Effects of L-DOPA in Parkinson's disease. *Lancet* **294**(7613)**:** 165-168.

Goetz CG, Damier P, Hicking C, Laska E, Muller T, Olanow CW*, et al.* (2007). Sarizotan as a treatment for dyskinesias in Parkinson's disease: a double-blind placebo-controlled trial. *Mov. Disord.* **22**(2)**:** 179-186.

Goldman SM, Tanner CM, Oakes D, Bhudhikanok GS, Gupta A, Langston JW (2006). Head injury and Parkinson's disease risk in twins. *Ann. Neurol.* **60**(1)**:** 65-72.

Gomeza J, Joly C, Kuhn R, Knopfel T, Bockaert J, Pin J-P (1996). The second intracellular loop of metabotropic glutamate receptor 1 cooperates with the other intracellular domains to control coupling to G-proteins. *J. Biol. Chem.* **271**(4)**:** 2199-2205.

Good PF, Hsu A, Werner P, Perl DP, Olanow CW (1998). Protein nitration in Parkinson's disease. *J. Neuropathol. Exp. Neurol.* **57**(4)**:** 338-342.

Goodwin GM, Souza RJD, Green AR (1987). Attenuation by electroconvulsive shock and antidepressant drugs of the 5-HT1A receptor-mediated hypothermia and serotonin syndrome produced by 8-OH-DPAT in the rat. *Psychopharmacology* **91:** 500-505.

Gorell JM, Rybicki BA, Johnson CC, Peterson EL (1999). Smoking and Parkinson's disease: a dose-response relationship. *Neurology* **52**(1)**:** 115-119.

Goudet C, Chapuy E, Alloui A, Acher F, Pin JP, Eschalier A (2008). Group III metabotropic glutamate receptors inhibit hyperalgesia in animal models of inflammation and neuropathic pain. *Pain* **137**(1)**:** 112-124.

Gravius A, Dekundy A, Nagel J, More L, Pietraszek M, Danysz W (2008). Investigation on tolerance development to subchronic blockade of mGluR5 in models of learning, anxiety, and levodopa-induced dyskinesia in rats. *J. Neural Transm.* **115**(12)**:** 1609-1619.

Grealish S, Mattsson B, Draxler P, Björklund A (2010). Characterisation of behavioural and neurodegenerative changes induced by intranigral 6-hydroxydopamine lesions in a mouse model of Parkinson's disease. *Eur. J. Neurosci.* **31**(12)**:** 2266-2278.

Grealish S, Xie L, Kelly M, Dowd E (2008). Unilateral axonal or terminal injection of 6-hydroxydopamine causes rapid-onset nigrostriatal degeneration and contralateral motor impairments in the rat. *Brain Res. Bull.* **77**(5)**:** 312-319.

Greco B, Lopez S, van der Putten H, Flor PJ, Amalric M (2010). Metabotropic glutamate 7 receptor subtype modulates motor symptoms in rodent models of Parkinson's disease. *J. Pharmacol. Exp. Ther.* **332**(3)**:** 1064-1071.

Greenamyre JT (2001). Glutamatergic influences on the basal ganglia. *Clin. Neuropharmacol.* **24**(2)**:** 65-70.

Grégoire L, Morin N, Ouattara B, Gasparini F, Bilbe G, Johns D*, et al.* (2011). The acute antiparkinsonian and antidyskinetic effect of AFQ056, a novel metabotropic glutamate receptor type 5 antagonist, in L-DOPA-treated parkinsonian monkeys. *Parkinsonism Relat. Disord.* **17**(4)**:** 270-276.

Groc L, Bard L, Choquet D (2009). Surface trafficking of N-methyl-D-aspartate receptors: physiological and pathological perspectives. *Neuroscience* **158**(1)**:** 4-18.

Groenewegen HJ, Berendse HW (1994). The specificity of the 'nonspecific' midline and intralaminar thalamic nuclei. *Trends Neurosci.* **17**(2)**:** 52-57.

Grunewald A, Voges L, Rakovic A, Kasten M, Vandebona H, Hemmelmann C*, et al.* (2010). Mutant Parkin impairs mitochondrial function and morphology in human fibroblasts. *PLoS One* **5**(9)**:** e12962.

Gu B (2003). A unilateral 6-hydroxydopamine lesion decreases the expression of metabotropic glutamate receptors in rat substantia nigra. *Neurosci. Lett.* **351**(3)**:** 186-190.

Guatteo E, Mercuri NB, Bernardi G, Knöpfel T (1999). Group I metabotropic glutamate receptors mediate an inward current in rat substantia nigra dopamine neurons that is independent from calcium mobilization. *J. Neurophysiol.* **82**(4)**:** 1974-1981.

Gubellini P, Melon C, Dale E, Doller D, Kerkerian-Le Goff L (2014). Distinct effects of mGlu4 receptor positive allosteric modulators at corticostriatal vs. striatopallidal synapses may differentially contribute to their antiparkinsonian action. *Neuropharmacology* **85:** 166-177.

Gubellini P, Picconi B, Bari M, Battista N, Calabresi P, Centonze D*, et al.* (2002). Experimental Parkinsonism alters endocannabinoid degradation: implications for striatal glutamatergic transmission. *J. Neurosci.* **22**(16)**:** 6900-6907.

Guigoni C, Doudnikoff E, Li Q, Bloch B, Bezard E (2007). Altered D(1) dopamine receptor trafficking in parkinsonian and dyskinetic non-human primates. *Neurobiol. Dis.* **26**(2)**:** 452-463.

Guimarães-Souza EM, Calaza KC (2012). Selective activation of group III metabotropic glutamate receptor subtypes produces different patterns of γ-aminobutyric acid immunoreactivity and glutamate release in the retina. *J. Neurosci. Res.* **90**(12)**:** 2349-2361.

Gurevich EV, Tesmer JJG, Mushegian A, Gurevich VV (2012). G protein-coupled receptor kinases: more than just kinases and not only for GPCRs. *Pharmacol. Ther.* **133**(1)**:** 40-69.

Gurevich T, Balash Y, Merims D, Peretz C, Herman T, Hausdorff JM*, et al.* (2014). Effect of rivastigmine on mobility of patients with higher-level gait disorder: a pilot exploratory study. *Drugs in R&D* **14**(2)**:** 57-62.

Guridi J, Herrero MT, Luquin MR, Guillen J, Ruberg M, Laguna J*, et al.* (1996). Subthalamotomy in parkinsonian monkeys. Behavioural and biochemical analysis. *Brain* **119:** 1717-1727.

Guyenet PG, Aghajanian GK (1978). Antidromic identification of dopaminergic and other output neurons of the rat substantia nigra. *Brain Res.* **150**(69-84).

Haas RH, Nasirian F, Nakano K, Ward D, Pay M, Hill R*, et al.* (1995). Low platelet mitochondrial complex I and complex II/III activity in early untreated Parkinson's disease. *Ann. Neurol.* **37:** 714-722.

Haas SJ, Beckmann S, Petrov S, Andressen C, Wree A, Schmitt O (2007). Transplantation of immortalized mesencephalic progenitors (CSM14.1 cells) into the neonatal parkinsonian rat caudate putamen. *J. Neurosci. Res.* **85**(4)**:** 778-786.

Haber S, McFarland NR (2001). The place of the thalamus in frontal cortical-basal ganglia circuits. *Neuroscientist* **7**(4)**:** 315-324.

Hadj Tahar A, Gregoire L, Darre A, Belanger N, Meltzer L, Bedard PJ (2004). Effect of a selective glutamate antagonist on L-dopa-induced dyskinesias in drug-naive parkinsonian monkeys. *Neurobiol. Dis.* **15**(2)**:** 171-176.

Halje P, Tamte M, Richter U, Mohammed M, Cenci MA, Petersson P (2012). Levodopa-induced dyskinesia is strongly associated with resonant cortical oscillations. *J. Neurosci.* **32**(47)**:** 16541-16551.

Hallett PJ, Dunah AW, Ravenscroft P, Zhou S, Bezard E, Crossman AR*, et al.* (2005). Alterations of striatal NMDA receptor subunits associated with the development of dyskinesia in the MPTP-lesioned primate model of Parkinson's disease. *Neuropharmacology* **48**(4)**:** 503-516.

Hammond C, Ammari R, Bioulac B, Garcia L (2008). Latest view on the mechanism of action of deep brain stimulation. *Mov. Disord.* **23**(15)**:** 2111-2121.

Hanrott K, Murray TK, Orfali Z, Ward M, Finlay C, O'Neill MJ*, et al.* (2008). Differential activation of PKC delta in the substantia nigra of rats following striatal or nigral 6-hydroxydopamine lesions. *Eur. J. Neurosci.* **27**(5)**:** 1086-1096.

Hara K, Harris RA (2002). The anesthetic mechanism of Urethane: the effects on neurotransmitter-gated ion channels. *Anesth. Analg.* **94:** 313-318.

Hardingham GE, Bading H (2010). Synaptic versus extrasynaptic NMDA receptor signalling: implications for neurodegenerative disorders. *Nat. Rev. Neurosci.* **11**(10)**:** 682-696.

Harvey BK, Wang Y, Hoffer BJ (2008). Transgenic rodent models of Parkinson's disease. *Acta Neurochir. (Wien).* **101**(Supplement)**:** 89-92.

Hashimoto T, Elder CM, Okun MS, Patrick SK, Vitek JL (2003). Stimulation of the subthalamic nucleus changes the firing pattern of pallidal neurons. *J. Neurosci.* **23**(5)**:** 1916-1923.

Hassani O-K, Mouroux M, Féger J (1996). Increased subthalamic neuronal activity after nigral dopaminergic lesion independent of disinhibition via the globus pallidus. *Neuroscience* **72**(1)**:** 105-115.

Hassani OK, François C, Yelnik J, Féger J (1997). Evidence for a dopaminergic innervation of the subthalamic nucleus in the rat. *Brain Res.* **749**(1)**:** 88-94.

Hastings TG (2009). The role of dopamine oxidation in mitochondrial dysfunction: implications for Parkinson's disease. *J. Bioenerg. Biomembr.* **41**(6)**:** 469-472.

Hatzipetros T, Yamamoto BK (2006). Dopaminergic and GABAergic modulation of glutamate release from rat subthalamic nucleus efferents to the substantia nigra. *Brain Res.* **1076**(1)**:** 60-67.

Hauber W, Lutz S (1999). Dopamine D1 or D2 receptor blockade in the globus pallidus produces akinesia in the rat. *Behav. Brain Res.* **106**(1-2)**:** 143-150.

Hauber W, Schmidt WJ (1990). The NMDA antagonist dizocilpine (MK-801) reverses haloperidol-induced movement initiation deficits. *Behav. Brain Res.* **40:** 161-166.

He Y, Lee T, Leong SK (2000). 6-Hydroxydopamine induced apoptosis of dopaminergic cells in the rat substantia nigra. *Brain Res.* **858:** 163-166.

Hefti F, Melamed E, Wurtman RJ (1980). Partial lesions of the dopaminergic nigrostriatal system in rat brain: biochemical characterization. *Brain Res.* **195**(1)**:** 123-137.

Heikkila RE, Cohen G (1972). Evaluation of amantadine as a releasing agent or uptake blocker for H^3-dopamine in rat brain slices. *Eur. J. Pharmacol.* **20:** 156-160.

Henderson EJ, Lord SR, Close JC, Lawrence AD, Whone A, Ben-Shlomo Y (2013). The ReSPonD trial--rivastigmine to stabilise gait in Parkinson's disease a phase II, randomised, double blind, placebo controlled trial to evaluate the effect of rivastigmine on gait in patients with Parkinson's disease who have fallen. *BMC Neurol.* **13**(188).

Henning J, Strauss U, Wree A, Gimsa J, Rolfs A, Benecke R*, et al.* (2008). Differential astroglial activation in 6-hydroxydopamine models of Parkinson's disease. *Neurosci. Res.* **62**(4)**:** 246-253.

Henry B, Crossman AR, Brotchie JM (1998). Characterization of enhanced behavioral responses to L-DOPA following repeated administration in the 6-hydroxydopamine-lesioned rat model of Parkinson's disease. *Exp. Neurol.* **151:** 334-352.

Henry B, Crossman AR, Brotchie JM (1999). Effect of repeated L-DOPA, bromocriptine, or lisuride administration on preproenkephalin-A and preproenkephalin-B mRNA levels in the striatum of the 6-hydroxydopamine-lesioned rat. *Exp. Neurol.* **155:** 204-220.

Henry B, Fox SH, Crossman AR, Brotchie JM (2001). Mu- and delta-opioid receptor antagonists reduce levodopa-induced dyskinesia in the MPTP-lesioned primate model of Parkinson's disease. *Exp. Neurol.* **171**(1)**:** 139-146.

Hermans E, Challiss RAJ (2001). Structural, signalling and regulatory properties of the group I metabotropic glutamate receptors : prototypic family C G-protein-coupled receptors. *Biochem. J.* **359:** 464-484.

Hernán MA, Zhang SM, Rueda-deCastro AM, Colditz GA, Speizer FE, Ascherio A (2001). Cigarette smoking and the incidence of Parkinson's disease in two prospective studies. *Ann. Neurol.* **50**(6)**:** 780-786.

Hernandez-Lopez S, Bargas J, Surmeier DJ, Reyes A, Galarraga E (1997). D1 receptor activation enhances evoked discharge in neostriatal medium spiny neurons by modulating an L-type Ca^{2+} conductance. *J. Neurosci.* **17**(9)**:** 3334-3342.

Hernandez-Lopez S, Tkatch T, Perez-Garci E, Galarraga E, Bargas J, Hamm H*, et al.* (2000). D2 dopamine receptors in striatal medium spiny neurons reduce L-type Ca^{2+} currents and excitability via a novel PLCb1–IP3–Calcineurin-signaling cascade. *J. Neurosci.* **20**(24)**:** 8987-8995.

Herrera-Marschitz M, Meana JJ, O'Connor WT, Goiny M, Reid MS, Ungerstedt U (1992). Neuronal dependence of extracellular dopamine, acetylcholine, glutamate, aspartate and gamma-aminobutyric acid (GABA) measured simultaneously from rat neostriatum using in vivo microdialysis: reciprocal interactions. *Amino Acids* **2:** 157-179.

Herrera-Marschitz M, You Z-B, Goiny M, Meana JJ, Silveira R, Godukhin OV*, et al.* (1996). On the origin of extracellular glutamate levels monitored in the basal ganglia of the rat by *in vivo* microdialysis. *J. Neurochem.* **66**(4)**:** 1726-1735.

Hilker R, Portman AT, Voges J, Staal MJ, Burghaus L, van Laar T*, et al.* (2005). Disease progression continues in patients with advanced Parkinson´s disease and effective subthalamic nucleus stimulation. *J. Neurol. Neurosurg. Psychiatry* **76**(9)**:** 1217-1221.

Hillegaart V, Ahlenius S, Magnusson O, Fowler CJ (1986). Repeated testing of rats markedly enhances the duration of effects induced by haloperidol on treadmill locomotion, catalepsy, and a conditioned avoidance response. *Pharmacol. Biochem. Behav.* **27:** 159-164.

Hoglinger GU, Féger J, Prigent A, Michel PP, Parain K, Champy P*, et al.* (2003). Chronic systemic complex I inhibition induces a hypokinetic multisystem degeneration in rats. *J. Neurochem.* **84:** 491-502.

Hoglinger GU, Oertel WH, Hirsch EC (2006). The rotenone model of parkinsonism – the five years inspection. *J. Neural Transm.* **70:** 269-272.

Holloway RG, Shoulson I, Fahn S, Kieburtz K, Lang A, Marek K*, et al.* (2004). Pramipexole vs levodopa as initial treatment for Parkinson disease: a 4-year randomized controlled trial. *Arch. Neurol.* **61**(7)**:** 1044-1053.

Holt AB, Netoff TI (2014). Origins and suppression of oscillations in a computational model of Parkinson's disease. *J. Comput. Neurosci. [Epub ahead of print]*

Hsieh M-H, Ho S-C, Yeh K-Y, Pawlak CR, Chang H-M, Ho Y-J*, et al.* (2012). Blockade of metabotropic glutamate receptors inhibits cognition and neurodegeneration in an MPTP-induced Parkinson's disease rat model. *Pharmacol. Biochem. Behav.* **102**(1)**:** 64-71.

Huettner JE (2003). Kainate receptors and synaptic transmission. *Prog. Neurobiol.* **70**(5)**:** 387-407.

Hunot S, Dugas N, Faucheux B, Hartmann A, Tardieu M, Debré P*, et al.* (1999). FceRII/CD23 is expressed in Parkinson's disease and induces, in vitro, production of nitric oxide and Tumor Necrosis Factor-a in glial cells. *J. Neurosci.* **19**(9)**:** 3440-3447.

Hurley MJ, Jackson MJ, Smith LA, Rose S, Jenner P (2005). Immunoautoradiographic analysis of NMDA receptor subunits and associated postsynaptic density proteins in the brain of dyskinetic MPTP-treated common marmosets. *Eur. J. Neurosci.* **21**(12)**:** 3240-3250.

Hurley MJ, Mash DC, Jenner P (2001). Dopamine D1 receptor expression in human basal ganglia and changes in Parkinson's disease. *Mol. Brain Res.* **87:** 271-279.

Iacovelli L, Bruno V, Salvatore L, Melchiorri D, Gradini R, Caricasole A*, et al.* (2002). Native group-III metabotropic glutamate receptors are coupled to the mitogen-activated protein kinase/phosphatidylinositol-3-kinase pathways. *J. Neurochem.* **82:** 216-223.

Iancu R, Mohapel P, Brundin P, Paul G (2005). Behavioral characterization of a unilateral 6-OHDA-lesion model of Parkinson's disease in mice. *Behav. Brain Res.* **162**(1)**:** 1-10.

Ibanez-Sandoval O, Hernandez A, Floran B, Galarraga E, Tapia D, Valdiosera R*, et al.* (2006). Control of the subthalamic innervation of substantia nigra pars reticulata by D1 and D2 dopamine receptors. *J. Neurophysiol.* **95**(3)**:** 1800-1811.

Iczkiewicz J, Broom L, Cooper JD, Wong AM, Rose S, Jenner P (2010). The RGD-containing peptide fragment of osteopontin protects tyrosine hydroxylase positive cells against toxic insult in primary ventral mesencephalic cultures and in the rat substantia nigra. *J. Neurochem.* **114**(6)**:** 1792-1804.

Iderberg H, Rylander D, Bimpisidis Z, Cenci MA (2013). Modulating mGluR5 and 5-HT1A/1B receptors to treat l-DOPA-induced dyskinesia: Effects of combined treatment and possible mechanisms of action. *Exp. Neurol.* **250C:** 116-124.

Ikeda K, Yoshikawa S, Kurokawa T, Yuzawa N, Nakao K, Mochizuki H (2009). TRK-820, a selective kappa opioid receptor agonist, could effectively ameliorate L-DOPA-induced dyskinesia symptoms in a rat model of Parkinson's disease. *Eur. J. Pharmacol.* **620**(1-3)**:** 42-48.

Ikeda SR, Lovinger DM, McCool BA, Lewis DL (1995). Heterologous expression of metabotropic glutamate receptors in adult rat sympathetic neurons: subtype-specific coupling to ion channels. *Neuron* **14:** 1029-1038.

Imamura K, Hishikawa N, Sawada M, Nagatsu T, Yoshida M, Hashizume Y (2003). Distribution of major histocompatibility complex class II-positive microglia and cytokine profile of Parkinson's disease brains. *Acta Neuropathol.* **106**(6)**:** 518-526.

Ingham CA, Hood SH, Maldegem Bv, Weenink A, Arbuthnott GW (1993). Morphological changes in the rat neostriatum after unilateral 6-hydroxydopamine injections into the nigrostriatal pathway. *Exp. Brain Res.* **93:** 17-27.

Iravani MM, Tayarani-Binazir K, Chu WB, Jackson MJ, Jenner P (2006). In 1-methyl-4-phenyl-1,2,3,6-tetrahydropyridine-treated primates, the selective 5-hydroxytryptamine 1a agonist (R)-(+)-8-OHDPAT inhibits levodopa-induced dyskinesia but only with increased motor disability. *J. Pharmacol. Exp. Ther.* **319**(3)**:** 1225-1234.

Isaacson JS, Solis JM, Nicoll RA (1993). Local and diffuse synaptic actions of GABA in the hippocampus. *Neuron* **10:** 165-175.

Ismayilova N, Verkhratsky A, Dascombe MJ (2006). Changes in mGlu5 receptor expression in the basal ganglia of reserpinised rats. *Eur. J. Pharmacol.* **545**(2-3)**:** 134-141.

Jackson-Lewis V, Przedborski S (2007). Protocol for the MPTP mouse model of Parkinson's disease. *Nat. Protoc.* **2**(1)**:** 141-151.

Jana S, Sinha M, Chanda D, Roy T, Banerjee K, Munshi S*, et al.* (2011). Mitochondrial dysfunction mediated by quinone oxidation products of dopamine: Implications in dopamine cytotoxicity and pathogenesis of Parkinson's disease. *Biochim. Biophys. Acta* **1812**(6)**:** 663-673.

Jantas D, Greda A, Golda S, Korostynski M, Grygier B, Roman A*, et al.* (2014). Neuroprotective effects of metabotropic glutamate receptor group II and III activators against MPP(+)-induced cell death in human neuroblastoma SH-SY5Y cells : The impact of cell differentiation state. *Neuropharmacology* **83:** 36-53.

Jaunarajs KL, Dupre KB, Steiniger A, Kliioueva A, Moore A, Kelly C*, et al.* (2009). Serotonin 1B receptor stimulation reduces D1 receptor agonist-induced dyskinesia. *Neuroreport* **20**(14)**:** 1265-1269.

Javitch JA, D'Amato RJ, Strittmatter SM, Snyder SH (1985). Parkinsonism-inducing neurotoxin, N-methyl-4-phenyl-1,2,3,6-tetrahydropyridine: uptake of the metabolite N-methyl-4-phenylpyridine by dopamine neurons explains selective toxicity. *Proc. Natl. Acad. Sci. U. S. A.* **82:** 2173-2177.

Jenner P (2008). Molecular mechanisms of L-DOPA-induced dyskinesia. *Nat. Rev. Neurosci.* **9**(9)**:** 665-677.

Jensen N, Dupont E, Hansen E, Mikkelsen B, Mikkelsen BO (1988). A controlled release form of Madopar in Parkinsonian patients with advanced disease and marked fluctuations in motor performance. *Acta Neurol. Scand.* **77:** 422-425.

Jeon BS, Jackson-Lewis V, Burke RE (1995). 6-hydroxydopamine lesion of the rat substantia nigra: time course and morphology of cell death. *Neurodegeneration* **4:** 131-137.

Jian M, Staines WA, Iadarola MJ, Robertson GS (1993). Destruction of the nigrostriatal pathway increases Fos-like immunoreactivity predominantly in striatopallidal neurons. *Brain Res. Mol. Brain Res.* **19**(1-2)**:** 156-160.

Jiang Q, Yan Z, Feng J (2006). Activation of group III metabotropic glutamate receptors attenuates rotenone toxicity on dopaminergic neurons through a microtubule-dependent mechanism. *J. Neurosci.* **26**(16)**:** 4318-4328.

Jin CM, Yang YJ, Huang HS, Kai M, Lee MK (2010). Mechanisms of L-DOPA-induced cytotoxicity in rat adrenal pheochromocytoma cells: implication of oxidative stress-related kinases and cyclic AMP. *Neuroscience* **170**(2)**:** 390-398.

Johansen TH, Drejer J, Wätjen F, Nielsen EØ (1993). A novel non-NMDA receptor antagonist shows selective displacement of low-affinity [3H]kainate binding. *Eur. J. Pharmacol. (Mol. Pharmacol)* **246**(3)**:** 195-204.

Johansson PA, Andersson M, Andersson KE, Cenci MA (2001). Alterations in cortical and basal ganglia levels of opioid receptor binding in a rat model of l-DOPA-induced dyskinesia. *Neurobiol. Dis.* **8**(2)**:** 220-239.

Johnson KA, Jones CK, Marvanova M, Tantawy MN, Baldwin RM, Conn PJ (2008). (S)-3,4-DCPG has antiparkinsonian effects in chronic models of Parkinson's disease. In: *International Meeting on Metabotropic Glutamate Receptors*. Taormina, Sicily.

Johnston TH, Fox SH, McIldowie MJ, Piggott MJ, Brotchie JM (2010). Reduction of L-DOPA-induced dyskinesia by the selective metabotropic glutamate receptor 5 antagonist 3-[(2-Methyl-1,3-thiazol-4-yl)ethynyl]pyridine in the 1-methyl-4-phenyl-1,2,3,6-tetrahydropyridine-lesioned macaque model of Parkinson's disease. *J. Pharmacol. Exp. Ther.* **333**(3)**:** 865-873.

Johnston TH, Lee J, Gomez-Ramirez J, Fox SH, Brotchie JM (2005). A simple rodent assay for the *in vivo* identification of agents with potential to reduce levodopa-induced dyskinesia in Parkinson's disease. *Exp. Neurol.* **191**(2)**:** 243-250.

Jones CK, Bubser M, Thompson AD, Dickerson JW, Turle-Lorenzo N, Amalric M*, et al.* (2012). The metabotropic glutamate receptor 4-positive allosteric modulator VU0364770 produces efficacy alone and in combination with L-DOPA or an adenosine 2A antagonist in preclinical rodent models of Parkinson's disease. *J. Pharmacol. Exp. Ther.* **340**(2)**:** 404-421.

Jones S, Gibb AJ (2005). Functional NR2B- and NR2D-containing NMDA receptor channels in rat substantia nigra dopaminergic neurones. *J. Physiol.* **569:** 209-221.

Julio-Pieper M, Hyland NP, Bravo JA, Dinan TG, Cryan JF (2010). A novel role for the metabotropic glutamate receptor-7: modulation of faecal water content and colonic electrolyte transport in the mouse. *Br. J. Pharmacol.* **160**(2)**:** 367-375.

Kadoguchi N, Kimoto H, Yano R, Kato H, Araki T (2008). Failure of acute administration with proteasome inhibitor to provide a model of Parkinson's disease in mice. *Metab. Brain Dis.* **23**(2)**:** 147-154.

Kalinichev M, Rouillier M, Girard F, Royer-Urios I, Bournique B, Finn T*, et al.* (2013). ADX71743, a potent and selective negative allosteric modulator of metabotropic glutamate receptor 7: in vitro and in vivo characterization. *J. Pharmacol. Exp. Ther.* **344**(3)**:** 624-636.

Kalra J, Rajput AH, Mantha SV, Prasad K (1992). Serum antioxidant enzyme activity in Parkinson' s disease. *Mol. Cell. Biochem.* **110:** 165-168.

Kamel F, Tanner C, Umbach D, Hoppin J, Alavanja M, Blair A*, et al.* (2007). Pesticide exposure and self-reported Parkinson's disease in the agricultural health study. *Am. J. Epidemiol.* **165**(4)**:** 364-374.

Kammermeier PJ (2012). Functional and pharmacological characteristics of metabotropic glutamate receptors 2/4 heterodimers. *Mol. Pharmacol.* **82**(3)**:** 438-447.

Kanazawa I, Marshall GR, Kelly JS (1976). Afferents to the rat substantia nigra studied with horseradish peroxidase, with special reference to fibres from the subthalamic nucleus. *Brain Res.* **115**(3)**:** 485-491.

Kanda T, Jackson MJ, Smith LA, Pearce RK, Nakamura J, Kase H*, et al.* (2000). Combined use of the adenosine A(2A) antagonist KW-6002 with L-DOPA or with selective D1 or D2 dopamine agonists increases antiparkinsonian activity but not dyskinesia in MPTP-treated monkeys. *Exp. Neurol.* **162**(2)**:** 321-327.

Kang G, Lowery MM (2013). Interaction of oscillations, and their suppression via deep brain stimulation, in a model of the cortico-basal ganglia network. *IEEE Trans. Neural Syst. Rehab. Eng.* **21**(2)**:** 244-253.

Kannari K, Yamato H, Shen H, Tomiyama M, Suda T, Matsunaga M (1991). Activation of 5-HT_{1A} but not 5-HT_{1B} receptors attenuates an increase in extracellular dopamine derived from exogenously administered l-DOPA in the striatum with nigrostriatal denervation. *J. Neurochem.* **76:** 1346-1353.

Kanthasamy AG, Kanthasamy A, Matsumoto RR, Vu TQ, Truong DD (1997). Neuroprotective effects of the strychnine-insensitive glycine site NMDA antagonist (R)-HA-966 in an experimental model of Parkinson's disease. *Brain Res.* **759**(1)**:** 1-8.

Keeney PM, Xie J, Capaldi RA, Bennett JP, Jr. (2006). Parkinson's disease brain mitochondrial complex I has oxidatively damaged subunits and is functionally impaired and misassembled. *J. Neurosci.* **26**(19)**:** 5256-5264.

Kehoe LA, Bernardinelli Y, Muller D (2013). GluN3A: an NMDA receptor subunit with exquisite properties and functions. *Neural Plas.* **2013:** Article 145387.

Kelsey JE, Mague SD, Pijanowski RS, Harris RC, Kleckner NW, Matthews RT (2004). NMDA receptor antagonists ameliorate the stepping deficits produced by unilateral medial forebrain bundle injections of 6-OHDA in rats. *Psychopharmacology* **175**(2)**:** 179-188.

Kendrick KM (1989). Use of microdialysis in neuroendocrinology. *Methods Enzymol.* **168:** 182-205.

Kew JN, Kemp JA (2005). Ionotropic and metabotropic glutamate receptor structure and pharmacology. *Psychopharmacology* **179**(1)**:** 4-29.

Kikuchi Y, Yasuhara T, Agari T, Kondo A, Kuramoto S, Kameda M*, et al.* (2011). Urinary 8-OHdG elevations in a partial lesion rat model of Parkinson's disease correlate with behavioral symptoms and nigrostriatal dopaminergic depletion. *J. Cell. Physiol.* **226**(5)**:** 1390-1398.

Kim DY, Kim SH, Choi HB, Min C, Gwag BJ (2001). High abundance of GluR1 mRNA and reduced Q/R editing of GluR2 mRNA in individual NADPH-diaphorase neurons. *Mol. Cell. Neurosci.* **17**(6)**:** 1025-1033.

Kim RH, Smith PD, Aleyasin H, Hayley S, Mount MP, Pownall S*, et al.* (2005). Hypersensitivity of DJ-1-deficient mice to 1-methyl-4-phenyl-1,2,3,6-tetrahydropyrindine (MPTP) and oxidative stress. *Proc. Natl. Acad. Sci. U. S. A.* **102**(14)**:** 5215-5220.

Kim W-G, Mohney RP, Wilson B, Jeohn G-H, Liu B, Hong J-S (2000). Regional difference in susceptibility to lipopolysaccharide-induced neurotoxicity in the rat brain: role of microglia. *J. Neurosci.* **20**(16)**:** 6309-6316.

Kinoshita A, Shigemoto R, Ohishi H, Putten Hvd, Mizuno N (1998). Immunohistochemical localization of metabotropic glutamate receptors, mGluR7a and mGluR7b, in the central nervous system of the adult rat and mouse: a light and electron microscopic study. *J. Comp. Neurol.* **393:** 332-352.

Kinzie JM, Saugstad JA, Westbrook GL, Segerson TP (1995). Distribution of metabotropic glutamate receptor 7 messenger RNA in the developing and adult rat brain. *Neuroscience* **69**(1)**:** 167-176.

Kipfer S, Stephan MA, Schupbach WMM, Ballinari P, Kaelin-Lang A (2011). Resting tremor in Parkinson disease: a negative predictor of levodopa-induced dyskinesia. *Arch. Neurol.* **68**(8)**:** 1037-1039.

Kirik D, Georgievska B, Rosenblad C, Bjorklund A (2001). Delayed infusion of GDNF promotes recovery of motor function in the partial lesion model of Parkinson's disease. *Eur. J. Neurosci.* **13:** 1589-1599.

Kirik D, Rosenblad C, Bjorklund A (1998). Characterization of behavioral and neurodegenerative changes following partial lesions of the nigrostriatal dopamine system induced by intrastriatal 6-hydroxydopamine in the rat. *Exp. Neurol.* **152:** 259-277.

Kirik D, Rosenblad C, Bjorklund A, Mandel RJ (2000). Long-term rAAV-mediated gene transfer of GDNF in the rat Parkinson's model: intrastriatal but not intranigral transduction promotes functional regeneration in the lesioned nigrostriatal system. *J. Neurosci.* **20**(12)**:** 4686-4700.

Kirik D, Rosenblad C, Burger C, Lundberg C, Johansen TE, Muzyczka N*, et al.* (2002). Parkinson-like neurodegeneration induced by targeted overexpression of alpha-synuclein in the nigrostriatal system. *J. Neurosci.* **22**(7)**:** 2780-2791.

Kish SJ, Morito K, Hornykiewicz O (1985). Glutathione peroxidase activity in Parkinson's disease brain. *Neurosci. Lett.* **58:** 343-346.

Kitada T, Tong Y, Gautier CA, Shen J (2009). Absence of nigral degeneration in aged parkin/DJ-1/PINK1 triple knockout mice. *J. Neurochem.* **111**(3)**:** 696-702.

Klockgether T, Turski L (1990). NMDA antagonists potentiate antiparkinsonian actions of L-DOPA in monoamine-depleted rats. *Ann. Neurol.* **28:** 539-546.

Klockgether T, Turski L, Honore T, Zhang ZM, Gash DM, Kurlan R*, et al.* (1991). The AMPA receptor antagonist NBQX has antiparkinsonian effects in monoamine-depleted rats and MPTP-treated monkeys. *Ann. Neurol.* **30**(5)**:** 717-723.

Kobylecki C, Cenci MA, Crossman AR, Ravenscroft P (2010). Calcium-permeable AMPA receptors are involved in the induction and expression of l-DOPA-induced dyskinesia in Parkinson's disease. *J. Neurochem.* **114**(2)**:** 499-511.

Kofalvi A, Rodrigues RJ, Ledent C, Mackie K, Vizi ES, Cunha RA*, et al.* (2005). Involvement of cannabinoid receptors in the regulation of neurotransmitter release in the rodent striatum: a combined immunochemical and pharmacological analysis. *J. Neurosci.* **25**(11)**:** 2874-2884.

Kohutnicka M, Lewandowska E, Kurkowska-Jastrzebska I, Członkowski A, Członkowska A (1998). Microglial and astrocytic involvement in a murine model of Parkinson's disease induced by 1-methyl-4-phenyl-1,2,3,6-tetrahydropyridine (MPTP). *Immunopharmacology* **39:** 167-180.

Koller WC, Weiner WJ, Perlik S, Nausieda PA, Goetz CG, Klawans HL (1981). Complications of chronic levodopa therapy. *Neurology* **31**(4).

Kolyaduke OV, Hughes RN (2013). Increased anxiety-related behavior in male and female adult rats following early and late adolescent exposure to 3,4-methylenedioxymethamphetamine (MDMA). *Pharmacol. Biochem. Behav.* **103**(4)**:** 742-749.

Kong M, Ba M, Song L, Liu Z (2009). Comparative effects of acute or chronic administration of levodopa to 6-OHDA-lesioned rats on the expression and phosphorylation of N-methyl-D-aspartate receptor NR1 subunits in the striatum. *Neurochem. Res.* **34**(8)**:** 1513-1521.

Konieczny J, Czarnecka A, Lenda T, Kamińska K, Lorenc-Koci E (2014). Chronic L-DOPA treatment attenuates behavioral and biochemical deficits induced by unilateral lactacystin administration into the rat substantia nigra. *Behav. Brain Res.* **261:** 79-88.

Konieczny J, Lenda T (2013). Contribution of the mGluR7 receptor to antiparkinsonian-like effects in rats: a behavioral study with the selective agonist AMN082. *Pharmacol. Rep.* **65:** 1194-1203.

Konieczny J, Wardas J, Kuter K, Pilc A, Ossowska K (2007). The influence of group III metabotropic glutamate receptor stimulation by (1S,3R,4S)-1-aminocyclo-pentane-1,3,4-tricarboxylic acid on the parkinsonian-like akinesia and striatal proenkephalin and prodynorphin mRNA expression in rats. *Neuroscience* **145**(2)**:** 611-620.

Konitsiotis S, Blanchet PJ, Verhagen L, Lamers E, Chase TN (2000). AMPA receptor blockade improves levodopa-induced dyskinesia in MPTP monkeys. *Neurology* **54**(8)**:** 1589-1595.

Konitsiotis S, Tsironis C (2006). Levodopa-induced dyskinesia and rotational behavior in hemiparkinsonian rats: independent features or components of the same phenomenon? *Behav. Brain Res.* **170**(2)**:** 337-341.

Konradi C, Westin JE, Carta M, Eaton ME, Kuter K, Dekundy A*, et al.* (2004). Transcriptome analysis in a rat model of L-DOPA-induced dyskinesia. *Neurobiol. Dis.* **17**(2)**:** 219-236.

Kooijmans SA, Senyschyn D, Mezhiselvam MM, Morizzi J, Charman SA, Weksler B*, et al.* (2012). The involvement of a Na(+)- and Cl(-)-dependent transporter in the brain uptake of amantadine and rimantadine. *Mol. Pharm.* **9**(4)**:** 883-893.

Koprich JB, Fox SH, Johnston TH, Goodman A, Le Bourdonnec B, Dolle RE*, et al.* (2011). The selective mu-opioid receptor antagonist ADL5510 reduces levodopa-induced dyskinesia without affecting antiparkinsonian action in MPTP-lesioned macaque model of Parkinson's disease. *Mov. Disord.* **26**(7)**:** 1225-1233.

Kordower JH, Kanaan NM, Chu Y, Suresh Babu R, Stansell J, Terpstra BT*, et al.* (2006). Failure of proteasome inhibitor administration to provide a model of Parkinson's disease in rats and monkeys. *Ann. Neurol.* **60**(2)**:** 264-268.

Kordower JH, Olanow CW, Dodiya HB, Chu Y, Beach TG, Adler CH*, et al.* (2013). Disease duration and the integrity of the nigrostriatal system in Parkinson's disease. *Brain* **136**(Pt 8)**:** 2419-2431.

Kornhuber J, Quack G, Danysz W, Jellinger K, Danielczyk W, Gsell W*, et al.* (1995). Therapeutic brain concentration of the NMDA receptor antagonist amantadine. *Neuropharmacology* **34**(7)**:** 713-721.

Kosinski CM, Risso Bradley S, Conn PJ, Levey AI, Landwehrmeyer GB, Penney JB, Jr.*, et al.* (1999). Localization of metabotropic glutamate receptor 7 mRNA and mGluR7a protein in the rat basal ganglia. *J. Comp. Neurol.* **415**(2)**:** 266-284.

Krack P, Batir A, Van Blercom N, Chabardes S, Fraix V, Ardouin C*, et al.* (2003). Five-year follow-up of bilateral stimulation of the subthalamic nucleus in advanced Parkinson's disease. *New Engl. J. Med.* **349**(20)**:** 1925-1934.

Kreiss DS, Mastropietro CW, Rawji SS, Walters JR (1997). The response of subthalamic nucleus neurons to dopamine receptor stimulation in a rodent model of Parkinson's disease. *J. Neurosci.* **17**(17)**:** 6807-6819.

Krystal JH, Perry EB, Gueorguieva R, Belger A, Madonick SH, Abi-Dargham A*, et al.* (2005). Comparative and interactive human psychopharmacologic effects of ketamine and amphetamine: implications for glutamatergic and dopaminergic model psychoses and cognitive function. *Arch. Gen. Psychiatry* **62**(9)**:** 985-994.

Kuan WL, Zhao JW, Barker RA (2008). The role of anxiety in the development of levodopa-induced dyskinesias in an animal model of Parkinson's disease, and the effect of chronic treatment with the selective serotonin reuptake inhibitor citalopram. *Psychopharmacology* **197**(2)**:** 279-293.

Kucheryanu VG, Kryzhanvskii GN (2000). Effect of glutamate and antagonists of N-Methyl-D-Aspartate receptors on experimental Parkinsonian syndrome in rats. *Bull. Exp. Biol. Med.* **130**(7)**:** 20-23.

Kudo T, Loh DH, Truong D, Wu Y, Colwell CS (2011). Circadian dysfunction in a mouse model of Parkinson's disease. *Exp. Neurol.* **232:** 66-75.

Kühn AA, Kupsch A, Schneider GH, Brown P (2006). Reduction in subthalamic 8–35 Hz oscillatory activity correlates with clinical improvement in Parkinson's disease. *Eur. J. Neurosci.* **23:** 1956-1960.

Kühn AA, Tsui A, Aziz T, Ray N, Brücke C, Kupsch A*, et al.* (2008). Pathological synchronisation in the subthalamic nucleus of patients with Parkinson's disease relates to both bradykinesia and rigidity. *Exp. Neurol.* **215**(2)**:** 380-387.

Kulisevsky J, Barbanoj M, Gironell A, Antonijoan R, Casas M, Pascual–Sedano B (2002). A double-blind crossover, placebo-controlled study of the adenosine A2A antagonist theophylline in Parkinson's disease. *Clin. Neuropharmacol.* **25**(1)**:** 25-31.

Kumar R, Hauser RA, Mostillo J, Dronamraju N, Graf A, Merschhemke M*, et al.* (2013). Mavoglurant (AFQ056) in combination with increased levodopa dosages in Parkinson's disease patients. *Int. J. Neurosci.*

Kunishima N, Shimada Y, Tsuji Y, Sato T, Yamamoto M, Kumasaka T*, et al.* (2000). Structural basis of glutamate recognition by a dimeric metabotropic glutamate receptor. *Nature* **407**(6807)**:** 971-977.

Kupsch A, Schmidt W, Gizatullina Z, Debska-Vielhaber G, Voges J, Striggow F*, et al.* (2014). 6-Hydroxydopamine impairs mitochondrial function in the rat model of Parkinson's disease: respirometric, histological, and behavioral analyses. *J. Neural Transm. [Epub ahead of print]*

Labandeira-Garcia JL, Rozas G, Lopez-Martin E, Liste I, Guerra MJ (1996). Time course of striatal changes induced by 6-hydroxydopamine lesion of the nigrostriatal pathway, as

studied by combined evaluation of rotational behaviour and striatal Fos expression. *Exp. Brain Res.* **108**(1)**:** 69-84.

Lada MW, Vickroy TW, Kennedy RT (1998). Evidence for neuronal origin and metabotropic receptor-mediated regulation of extracellular glutamate and aspartate in rat striatum *in vivo* following electrical stimulation of the prefrontal cortex. *J. Neurochem.* **70:** 617-625.

Lafon-Cazal M, Viennois G, Kuhn R, Malitschek B, Pin JP, Shigemoto R*, et al.* (1999). mGluR7-like receptor and GABA(B) receptor activation enhance neurotoxic effects of N-methyl-D-aspartate in cultured mouse striatal GABAergic neurones. *Neuropharmacology* **38**(10)**:** 1631-1640.

Lange KW, Loschmann PA, Sofic E, Burg M, Horowski R, Kalveram KT*, et al.* (1993). The competitive NMDA antagonist CPP protects substantia nigra neurons from MPTP-induced degeneration in primates. *Naunyn-Schmiedeberg's Arch. Pharmacol.* **348**(6)**:** 586-592.

Langston J, Ballard P, Tetrud J, I I (1983a). Chronic Parkinsonism in humans due to a product of meperidine-analog synthesis. *Science* **219**(4587)**:** 979-980.

Langston JW, Forno LS, Rebert CS, Irwin I (1983b). Selective nigral toxicity after systemic administration of 1-methyl-4-phenyl-1,2,5,6-tetrahydropyrine (MPTP) in the squirrel monkey. *Brain Res.* **292**(2)**:** 390-394.

Lapointe N, St-Hilaire M, Martinoli M-G, Blanchet J, Gould P, Rouillard C*, et al.* (2004). Rotenone induces non-specific central nervous system and systemic toxicity. *FASEB J.* **18**(6)**:** 717-719.

Larsen M, Langmoen IA (1998). The effect of volatile anaesthetics on synaptic release and uptake of glutamate. *Toxicol. Lett.* **100-101:** 59-64.

Le Poul E, Bolea C, Girard F, Poli S, Charvin D, Campo B*, et al.* (2012). A potent and selective metabotropic glutamate receptor 4 positive allosteric modulator improves movement in rodent models of Parkinson's disease. *J. Pharmacol. Exp. Ther.* **343**(1)**:** 167-177.

Leaver KR, Allbutt HN, Creber NJ, Kassiou M, Henderson JM (2008). Neuroprotective effects of a selective N-methyl-d-aspartate NR2B receptor antagonist in the 6-hydroxydopamine rat model of Parkinson's disease. *Clin. Exp. Pharmacol. Physiol.* **35**(11)**:** 1388-1394.

Lee JJ, Jane DE, Croucher MJ (2003). Anticonvulsant dicarboxyphenylglycines differentially modulate excitatory amino acid release in the rat cerebral cortex. *Brain Res.* **977**(1)**:** 119-123.

Lees A, Fahn S, Eggert KM, Jankovic J, Lang A, Micheli F*, et al.* (2012). Perampanel, an AMPA antagonist, found to have no benefit in reducing "off" time in Parkinson's disease. *Mov. Disord.* **27**(2)**:** 284-288.

Lees AJ (2008). Evidence-based efficacy comparison of tolcapone and entacapone as adjunctive therapy in Parkinson's disease. *CNS Neurosci. Ther.* **14**(1): 83-93

Lees AJ, Hardy J, Revesz T (2009). Parkinson's disease. *Lancet* **373**(9680)**:** 2055-2066.

Lei W, Jiao Y, Del Mar N, Reiner A (2004). Evidence for differential cortical input to direct pathway versus indirect pathway striatal projection neurons in rats. *J. Neurosci.* **24**(38)**:** 8289-8299.

Leroy E, Boyer R, Auburger G, Leube B, Ulm G, Mezey E*, et al.* (1998). The ubiquitin pathway in Parkinson's disease. *Nature* **395:** 451-452.

Lesage F, Terrenoire C, Romey G, Lazdunski M (2000). Human TREK2, a 2P domain mechano-sensitive K+ channel with multiple regulations by polyunsaturated fatty acids, lysophospholipids, and Gs, Gi, and Gq protein-coupled receptors. *J. Biol. Chem.* **275:** 28398-28405.

Levandis G, Bazzini E, Armentero MT, Nappi G, Blandini F (2008). Systemic administration of an mGluR5 antagonist, but not unilateral subthalamic lesion, counteracts l-DOPA-induced dyskinesias in a rodent model of Parkinson's disease. *Neurobiol. Dis.* **29**(1)**:** 161-168.

Li X, Gardner E, Xi Z (2008). The metabotropic glutamate receptor 7 (mGluR7) allosteric agonist AMN082 modulates nucleus accumbens GABA and glutamate, but not dopamine, in rats. *Neuropharmacology* **54**(3)**:** 542-551.

Li X, Li J, Gardner EL, Xi Z-X (2010a). Activation of mGluR7s inhibits cocaine-induced reinstatement of drug-seeking behavior by a nucleus accumbens glutamate-mGluR2/3 mechanism in rats. *J. Neurochem.* **114**(5)**:** 1368-1380.

Li X, Redus L, Chen C, Martinez PA, Strong R, Li S*, et al.* (2013). Cognitive dysfunction precedes the onset of motor symptoms in the MitoPark mouse model of Parkinson's disease. *PLoS One* **8**(8)**:** e71341.

Li XH, Wang JY, Gao G, Chang JY, Woodward DJ, Luo F (2010b). High-frequency stimulation of the subthalamic nucleus restores neural and behavioral functions during reaction time task in a rat model of Parkinson's disease. *J. Neurosci. Res.* **88**(7)**:** 1510-1521.

Li Y, Liu W, Oo TF, Wang L, Tang Y, Jackson-Lewis V*, et al.* (2009). Mutant LRRK2(R1441G) BAC transgenic mice recapitulate cardinal features of Parkinson's disease. *Nat. Neurosci.* **12**(7)**:** 826-828.

Liebsch G, Montkowski A, Holsboer F, Landgraf R (1998). Behavioural profiles of two Wistar rat lines selectively bred for high or low anxiety-related behaviour. *Behav. Brain Res.* **94:** 301-310.

Lim KL (2010). Non-mammalian animal models of Parkinson's disease for drug discovery. *Exp. Opin. Drug Discov.* **5**(2)**:** 165-176.

Limousin P, Pollak P, Benazzouz A, Hoffmann D, Bas J-FL, Perret JE*, et al.* (1995). Effect on parkinsonian signs and symptoms of bilateral subthalamic nucleus stimulation. *Lancet* **345**(8942)**:** 91-95.

Lindén I-B, Nissinen E, Etemadzadeh E, Kaakkola S, Mannisto P, Pohto P (1988). Favorable effect of Catechol-O-Methyltransferase inhibition by OR-462 in experimental models of Parkinson's disease. *J. Pharmacol. Exp. Ther.* **247**(1)**:** 289-293.

Lindgren HS, Andersson DR, Lagerkvist S, Nissbrandt H, Cenci MA (2010). L-DOPA-induced dopamine efflux in the striatum and the substantia nigra in a rat model of Parkinson's disease: temporal and quantitative relationship to the expression of dyskinesia. *J. Neurochem.* **112**(6)**:** 1465-1476.

Lindgren HS, Rylander D, Ohlin KE, Lundblad M, Cenci MA (2007). The "motor complication syndrome" in rats with 6-OHDA lesions treated chronically with L-DOPA: relation to dose and route of administration. *Behav. Brain Res.* **177**(1)**:** 150-159.

Lindner MD, Cain CK, Plone MA, Frydel BR, Blaney TJ, Emerich DF*, et al.* (1999). Incomplete nigrostriatal dopaminergic cell loss and partial reductions in striatal dopamine produce akinesia, rigidity, tremor and cognitive deficits in middle-aged rats. *Behav. Brain Res.* **102**(1-2)**:** 1-16.

Liu B, Gao H-M, Hong J-S (2003). Parkinson's disease and exposure to infectious agents and pesticides and the occurrence of brain injuries: role of neuroinflammation. *Environ. Health Perspect.* **111:** 1065-1073.

Liu X, Van Natta K, Yeo H, Vilenski O, Weller PE, Worboys PD*, et al.* (2009). Unbound drug concentration in brain homogenate and cerebral spinal fluid at steady state as a surrogate for unbound concentration in brain interstitial fluid. *Drug Metab. Dispos.* **37**(4)**:** 787-793.

López-Lozano JJ, Bravo G, Brera B, Millán I, Dargallo J, Salmeán J*, et al.* (1997). Long-term improvement in patients with severe Parkinson's disease after implantation of fetal ventral mesencephalic tissue in a cavity of the caudate nucleus: 5-year follow up in 10 patients. *J. Neurosurg.* **86**(6)**:** 931-942.

Lopez S, Bonito-Oliva A, Pallottino S, Acher F, Fisone G (2011). Activation of metabotropic glutamate 4 receptors decreases L-DOPA-induced dyskinesia in a mouse model of Parkinson's disease. *J. Parkinsons Dis.* **1**(4)**:** 339-346.

Lopez S, Jouve L, Turle-Lorenzo N, Kerkerian-LeGoff L, Salin P, Amalric M (2012). Antiparkinsonian action of a selective group III mGlu receptor agonist is associated with reversal of subthalamonigral overactivity. *Neurobiol. Dis.* **46**(1)**:** 69-77.

Lopez S, Turle-Lorenzo N, Acher F, De Leonibus E, Mele A, Amalric M (2007). Targeting group III metabotropic glutamate receptors produces complex behavioral effects in rodent models of Parkinson's disease. *J. Neurosci.* **27**(25)**:** 6701-6711.

Lorenc-Koci E, Lenda T, Antkiewicz-Michaluk L, Wardas J, Domin H, Smialowska M*, et al.* (2011). Different effects of intranigral and intrastriatal administration of the proteasome inhibitor lactacystin on typical neurochemical and histological markers of Parkinson's disease in rats. *Neurochem. Int.* **58**(7)**:** 839-849.

Lorrain DS, Schaffhauser H, Campbell UC, Baccei CS, Correa LD, Rowe B*, et al.* (2003). Group II mGlu receptor activation suppresses norepinephrine release in the ventral hippocampus and locomotor responses to acute ketamine challenge. *Neuropsychopharmacology* **28**(9)**:** 1622-1632.

Loschmann PA, De Groote C, Smith L, Wullner U, Fischer G, Kemp JA*, et al.* (2004). Antiparkinsonian activity of Ro 25-6981, a NR2B subunit specific NMDA receptor antagonist, in animal models of Parkinson's disease. *Exp. Neurol.* **187**(1)**:** 86-93.

Loschmann PA, Lange KW, Kunow M, Rettig KJ, Jahnig P, Honore T*, et al.* (1991). Synergism of the AMPA-antagonist NBQX and the NMDA-antagonist CPP with L-dopa in models of Parkinson's disease. *J. Neural Transm.* **3**(3)**:** 203-213.

Lozano AM, Lang AE, Galvez-Jimenez N, Miyasaki J, Duff J, Hutchison WD*, et al.* (1995). Effect of GPi pallidotomy on motor function in Parkinson's disease. *Lancet* **346**(8987)**:** 1383-1387.

Luginger E, Wenning GK, Bosch S, Poewe W (2000). Beneficial effects of amantadine on L-DOPA-induced dyskinesias in Parkinson's disease. *Mov. Disord.* **15**(5)**:** 873-878.

Luk KC, Lee VMY (2014). Modeling Lewy pathology propagation in Parkinson's disease. *Parkinsonism Relat. Disord.* **20:** S85-S87.

Lundblad M, Andersson M, Winkler C, Kirik D, Wierup N, Cenci MA (2002). Pharmacological validation of behavioural measures of akinesia and dyskinesia in a rat model of Parkinson's disease. *Eur. J. Neurosci.* **15**(1)**:** 120-132.

Luquin MR, Obeso JA, Laguna J, Guillen J, Martinez-Lage JM (1993). The AMPA receptor antagonist NBQX does not alter the motor response induced by selective dopamine agonists in MPTP-treated monkeys. *Eur. J. Pharmacol.* **235**(2-3)**:** 297-300.

Ma Y, Tang C, Chaly T, Greene P, Breeze R, Fahn S*, et al.* (2010). Dopamine cell implantation in Parkinson's disease: long-term clinical and (18)F-FDOPA PET outcomes. *J. Nucl. Med.* **51**(1)**:** 7-15.

Mabrouk OS, Marti M, Salvadori S, Morari M (2009). The novel delta opioid receptor agonist UFP-512 dually modulates motor activity in hemiparkinsonian rats via control of the nigro-thalamic pathway. *Neuroscience* **164**(2)**:** 360-369.

MacDermott AB, Dale N (1986). Receptors, ion channels and synaptic potentials underlying the integrative actions of excitatory amino acids. *Trends Neurosci.* **10**(7)**:** 280-284.

MacInnes N, Duty S (2008). Group III metabotropic glutamate receptors act as hetero-receptors modulating evoked GABA release in the globus pallidus *in vivo*. *Eur. J. Pharmacol.* **580**(1-2)**:** 95-99.

MacInnes N, Messenger MJ, Duty S (2004). Activation of group III metabotropic glutamate receptors in selected regions of the basal ganglia alleviates akinesia in the reserpine-treated rat. *Br. J. Pharmacol.* **141**(1)**:** 15-22.

MacIver MB, Mikulec AA, Amagasu SM, Monroe FA (1996). Volatile anesthetics depress glutamate transmission via presynaptic actions. *Anesthesiology* **85**(4)**:** 823-834.

Maesawa S, Kaneoke Y, Kajita Y, Usui N, Misawa N, Nakayama A*, et al.* (2004). Long-term stimulation of the subthalamic nucleus in hemiparkinsonian rats: neuroprotection of dopaminergic neurons. *J. Neurosurg.* **100:** 679-687.

Maggos C (2012). Addex Reports Positive Top Line Phase IIa Data for Dipraglurant in Parkinson's Disease Levodopa-Induced Dyskinesia (PD-LID). http://www.addextherapeutics.com/investors/press-releases/news-details/article/addex-reports-positive-top-line-phase-iia-data-for-dipraglurant-in-parkinsons-disease-levodopa-indu/: Addex Therapeutics.

Maia S, Arlicot N, Vierron E, Bodard S, Vergote J, Guilloteau D*, et al.* (2012). Longitudinal and parallel monitoring of neuroinflammation and neurodegeneration in a 6-hydroxydopamine rat model of Parkinson's disease. *Synapse* **66**(7)**:** 573-583.

Maj M, Bruno V, Dragic Z, Yamamoto R, Battaglia G, Inderbitzin W*, et al.* (2003). (−)-PHCCC, a positive allosteric modulator of mGluR4: characterization, mechanism of action, and neuroprotection. *Neuropharmacology* **45**(7)**:** 895-906.

Maler L, Fibiger HC, McGeer PL (1973). Demonstration of the nigrostriatal projection by silver staining after nigral injections of 6-hydroxydopamine. *Exp. Neurol.* **40:** 505-515.

Mallet N, Ballion B, Le Moine C, Gonon F (2006). Cortical inputs and GABA interneurons imbalance projection neurons in the striatum of parkinsonian rats. *J. Neurosci.* **26**(14)**:** 3875-3884.

Malmlöf T, Rylander D, Alken R-G, Schneider F, Svensson TH, Cenci MA*, et al.* (2010). Deuterium substitutions in the L-DOPA molecule improve its anti-akinetic potency without increasing dyskinesias. *Exp. Neurol.* **225**(2)**:** 408-415.

Manning-Boğ AB, Reaney SH, Chou VP, Johnston LC, McCormack AL, Johnston J*, et al.* (2006). Lack of nigrostriatal pathology in a rat model of proteasome inhibition. *Ann. Neurol.* **60**(2)**:** 256-260.

Mao L-M, Guo M-L, Jin D-Z, Fibuch EE, Choe ES, Wang JQ (2011). Post-translational modification biology of glutamate receptors and drug addiction. *Front. Neuroanat.* **5**(19).

Maranis S, Stamatis D, Tsironis C, Konitsiotis S (2012). Investigation of the antidyskinetic site of action of metabotropic and ionotropic glutamate receptor antagonists. Intracerebral infusions in 6-hydroxydopamine-lesioned rats with levodopa-induced dyskinesia. *Eur. J. Pharmacol.* **683**(1-3)**:** 71-77.

Marey-Semper I, Gelman M, Levi-Strauss M (1995). A selective toxicity toward cultured mesencephalic dopaminergic neurons is induced by the synergistic effects of energetic metabolism impairment and NMDA receptor activation. *J. Neurosci.* **15**(9)**:** 5912-5918.

Marin C, Aguilar E, Rodriguez-Oroz MC, Bartoszyk GD, Obeso JA (2009). Local administration of sarizotan into the subthalamic nucleus attenuates levodopa-induced dyskinesias in 6-OHDA-lesioned rats. *Psychopharmacology* **204**(2)**:** 241-250.

Marino MJ, Williams DL, Jr., O'Brien JA, Valenti O, McDonald TP, Clements MK*, et al.* (2003). Allosteric modulation of group III metabotropic glutamate receptor 4: a potential approach to Parkinson's disease treatment. *Proc. Natl. Acad. Sci. U. S. A.* **100**(23)**:** 13668-13673.

Marinova-Mutafchieva L, Sadeghian M, Broom L, Davis JB, Medhurst AD, Dexter DT (2009). Relationship between microglial activation and dopaminergic neuronal loss in the substantia nigra: a time course study in a 6-hydroxydopamine model of Parkinson's disease. *J. Neurochem.* **110**(3)**:** 966-975.

Marongiu R, Spencer B, Crews L, Adame A, Patrick C, Trejo M*, et al.* (2009). Mutant Pink1 induces mitochondrial dysfunction in a neuronal cell model of Parkinson's disease by disturbing calcium flux. *J. Neurochem.* **108**(6)**:** 1561-1574.

Martin AB, Fernandez-Espejo E, Ferrer B, Gorriti MA, Bilbao A, Navarro M*, et al.* (2008). Expression and function of CB1 receptor in the rat striatum: localization and effects on D1 and D2 dopamine receptor-mediated motor behaviors. *Neuropsychopharmacology* **33**(7)**:** 1667-1679.

Martín R, Torres M, Sánchez-Prieto J (2007). mGluR7 inhibits glutamate release through a PKC-independent decrease in the activity of P/Q-type Ca2+ channels and by diminishing cAMP in hippocampal nerve terminals. *Eur. J. Neurosci.* **26**(2)**:** 312-322.

Martinez-Martin P (2011). The importance of non-motor disturbances to quality of life in Parkinson's disease. *J. Neurol. Sci.* **310**(1-2)**:** 12-16.

Martinez A, Macheda T, Morgese MG, Trabace L, Giuffrida A (2012). The cannabinoid agonist WIN55212-2 decreases L-DOPA-induced PKA activation and dyskinetic behavior in 6-OHDA-treated rats. *Neurosci. Res.* **72**(3)**:** 236-242.

Masuda-Suzukake M, Nonaka T, Hosokawa M, Oikawa T, Arai T, Akiyama H*, et al.* (2013). Prion-like spreading of pathological alpha-synuclein in brain. *Brain* **136**(Pt 4)**:** 1128-1138.

Matarredona ER, Santiago M, Venero JL, Cano J, Machado A (2001). Group II metabotropic glutamate receptor activation protects striatal dopaminergic nerve terminals against MPP+-induced neurotoxicity along with brain-derived neurotrophic factor induction. *J. Neurochem.* **76**(2)**:** 351-360.

Matsui T, Kita H (2003). Activation of group III metabotropic glutamate receptors presynaptically reduces both GABAergic and glutamatergic transmission in the rat globus pallidus. *Neuroscience* **122:** 727-737.

McAllister K (1996). The competitive NMDA receptor antagonist SDZ 220-581 reverses haloperidol-induced catalepsy in rats. *Eur. J. Pharmacol.* **314:** 307-311.

McCarter SJ, St Louis EK, Boeve BF (2012). REM sleep behavior disorder and REM sleep without atonia as an early manifestation of degenerative neurological disease. *Curr. Neurol. Neurosci. Rep.* **12**(2)**:** 182-192.

McCool BA, Pin J-P, Brust PF, Harpold MM, Lovinger DM (1996). Functional coupling of rat group II metabotropic glutamate receptors to an omega-conotoxin GVIA-sensitive calcium channel in human embryonic kidney 293 cells. *Mol. Pharmacol.* **50:** 912-922.

McCormack AL, Thiruchelvam M, Manning-Bog AB, Thiffault C, Langston JW, Cory-Slechta DA*, et al.* (2002). Environmental risk factors and Parkinson's disease: selective degeneration of nigral dopaminergic neurons caused by the herbicide Paraquat. *Neurobiol. Dis.* **10**(2)**:** 119-127.

McDowell K, Chesselet MF (2012). Animal models of the non-motor features of Parkinson's disease. *Neurobiol. Dis.* **46**(3)**:** 597-606.

McFarland NR, Haber SN (2002). Thalamic relay nuclei of the basal ganglia form both reciprocal and nonreciprocal cortical connections, linking multiple frontal cortical areas. *J. Neurosci.* **22**(18)**:** 8117-8132.

McGeer PL, Itagaki S, Boyes BE, McGeer EG (1988). Reactive microglia are positive for HLA-DR in the substantia nigra of Parkinson's and Alzheimer's disease brains. *Neurology* **38**(8)**:** 1285-1291.

McGeer PL, McGeer EG (2004). Inflammation and neurodegeneration in Parkinson's disease. *Parkinsonism Relat. Disord.* **10:** S3-S7.

McGeorge AJ, Faull RLM (1989). The organization of the projection from the cerebral cortex to the striatum in the rat. *Neuroscience* **29**(3)**:** 503-537.

McMullan SM, Phanavanh B, Li GG, Barger SW (2012). Metabotropic glutamate receptors inhibit microglial glutamate release. *ASN Neuro.* **4**(5).

McNaught KS, Perl DP, Brownell AL, Olanow CW (2004). Systemic exposure to proteasome inhibitors causes a progressive model of Parkinson's disease. *Ann. Neurol.* **56**(1)**:** 149-162.

McNaught KSP, Belizaire R, Isacson O, Jenner P, Olanow CW (2003). Altered proteasomal function in sporadic Parkinson's disease. *Exp. Neurol.* **179**(1)**:** 38-46.

McNaught KSP, Jenner P (2001). Proteasomal function is impaired in substantia nigra in Parkinson's disease. *Neurosci. Lett.* **297:** 191-194.

McNaught KSP, Olanow CW (2006). Proteasome inhibitor–induced model of Parkinson's disease. *Ann. Neurol.* **60**(2)**:** 243-247.

Mela F, Marti M, Bido S, Cenci MA, Morari M (2012). In vivo evidence for a differential contribution of striatal and nigral D1 and D2 receptors to L-DOPA induced dyskinesia and the accompanying surge of nigral amino acid levels. *Neurobiol. Dis.* **45**(1)**:** 573-582.

Mela F, Marti M, Dekundy A, Danysz W, Morari M, Cenci MA (2007). Antagonism of metabotropic glutamate receptor type 5 attenuates l-DOPA-induced dyskinesia and its molecular and neurochemical correlates in a rat model of Parkinson's disease. *J. Neurochem.* **101**(2)**:** 483-497.

Meschler JP, Howlett AC (2001). Signal transduction interactions between CB1 cannabinoid and dopamine receptors in the rat and monkey striatum. *Neuropharmacology* **40:** 918-926.

Messenger MJ, Dawson LG, Duty S (2002). Changes in metabotropic glutamate receptor 1-8 gene expression in the rodent basal ganglia motor loop following lesion of the nigrostriatal tract. *Neuropharmacology* **43**(2)**:** 261-271.

Millán C, Luján R, Shigemoto R, Sánchez-Prieto J (2002). Subtype-specific expression of group III metabotropic glutamate receptors and Ca2+ channels in single nerve terminals. *J. Biol. Chem.* **277**(49)**:** 47796-47803.

Mintz I, Hammond C, Féger J (1986a). Excitatory effect of iontophoretically applied dopamine on identified neurons of the rat subthalamic nucleus. *Brain Res.* **375**(172-175).

Mintz M, Douglas RJ, Tomer R, de Villiers AS, Kellaway L (1986b). Transient contralateral rotation following unilateral substantia nigra lesion reflects susceptibility of the nigrostriatal system to exhaustion by amphetamine. *Life Sci.* **39**(1)**:** 69-76.

Mirza B, Hadberg H, Thomsen P, Moos T (2000). The absence of reactive astrocytosis is indicative of a unique inflammatory process in Parkinson's disease. *Neuroscience* **95**(2)**:** 425-432.

Mitchell SJ, Silver RA (2000). Glutamate spillover suppresses inhibition by activating presynaptic mGluRs. *Nature* **404:** 498-502.

Mitsukawa K, Yamamoto R, Ofner S, Nozulak J, Pescott O, Lukic S*, et al.* (2005). A selective metabotropic glutamate receptor 7 agonist: activation of receptor signaling via an allosteric site modulates stress parameters *in vivo*. *Proc. Natl. Acad. Sci. U. S. A.* **102**(51)**:** 18712-18717.

Miwa H, Kubo T, Suzuki A, Nishi K, Kondo T (2005). Retrograde dopaminergic neuron degeneration following intrastriatal proteasome inhibition. *Neurosci. Lett.* **380**(1-2)**:** 93-98.

Miyazaki H, Nakamura Y, Arai T, Kataoka K (1997). Increase of glutamate uptake in astrocytes: a possible mechanism of action of volatile anesthetics. *Anesthesiology* **86**(6)**:** 1359-1366.

Mizuno Y, Kondo T (2013). Adenosine A2A receptor antagonist istradefylline reduces daily OFF time in Parkinson's disease. *Mov. Disord.* **28**(8)**:** 1138-1141.

Mogi M, Harada M, Narabayashi H, Inagaki H, Minami M, Nagatsu T (1996). Interleukin (IL)-lb, IL-2, IL-4, IL-6 and transforming growth factor-a levels are elevated in ventricular

cerebrospinal fluid in juvenile parkinsonism and Parkinson's disease. *Neurosci. Lett.* **211:** 13-16.

Moisoi N, Fedele V, Edwards J, Martinsa LM (2014). Loss of PINK1 enhances neurodegeneration in a mouse model of Parkinson's disease triggered by mitochondrial stress. *Neuropharmacology* **77**(100)**:** 350-357.

Montoya CP, Campbell-Hope LJ, Pemberton KD, Dunnett SB (1991). The "staircase test" a measure of independent forelimb reaching and grasping abilities in rats. *J. Neurosci. Methods* **36:** 219-228.

Moran RJ, Mallet N, Litvak V, Dolan RJ, Magill PJ, Friston KJ*, et al.* (2011). Alterations in brain connectivity underlying Beta oscillations in parkinsonism. *PLoS Comp. Biol.* **7**(8)**:** e1002124.

Moreau C, Delval A, Tiffreau V, Defebvre L, Dujardin K, Duhamel A*, et al.* (2013). Memantine for axial signs in Parkinson's disease: a randomised, double-blind, placebo-controlled pilot study. *J. Neurol. Neurosurg. Psychiatry* **84**(5)**:** 552-555.

Morgese MG, Cassano T, Cuomo V, Giuffrida A (2007). Anti-dyskinetic effects of cannabinoids in a rat model of Parkinson's disease: role of CB(1) and TRPV1 receptors. *Exp. Neurol.* **208**(1)**:** 110-119.

Morin N, Grégoire L, Morissette M, Desrayaud S, Gomez-Mancilla B, Gasparini F*, et al.* (2013). MPEP, an mGlu5 receptor antagonist, reduces the development of l-DOPA-induced motor complications in *de novo* parkinsonian monkeys: biochemical correlates. *Neuropharmacology* **66:** 355-364.

Morissette M, Dridi M, Calon F, Hadj Tahar A, Meltzer LT, Bedard PJ*, et al.* (2006). Prevention of levodopa-induced dyskinesias by a selective NR1A/2B N-methyl-D-aspartate receptor antagonist in parkinsonian monkeys: implication of preproenkephalin. *Mov. Disord.* **21**(1)**:** 9-17.

Mukhida K, Baker KA, D. Sadi, Mendez I (2001). Enhancement of sensorimotor behavioral recovery in hemiparkinsonian rats with intrastriatal, intranigral, and intrasubthalamic nucleus dopaminergic transplants. *J. Neurosci.* **21**(10)**:** 3521-3530.

Munoz A, Carlsson T, Tronci E, Kirik D, Bjorklund A, Carta M (2009). Serotonin neuron-dependent and -independent reduction of dyskinesia by 5-HT1A and 5-HT1B receptor agonists in the rat Parkinson model. *Exp. Neurol.* **219**(1)**:** 298-307.

Munoz A, Li Q, Gardoni F, Marcello E, Qin C, Carlsson T*, et al.* (2008). Combined 5-HT1A and 5-HT1B receptor agonists for the treatment of L-DOPA-induced dyskinesia. *Brain* **131**(Pt 12)**:** 3380-3394.

Murray HE, Pillai AV, McArthur SR, Razvi N, Datla KP, Dexter DT*, et al.* (2003a). Dose- and sex-dependent effects of the neurotoxin 6-hydroxydopamine on the nigrostriatal dopaminergic pathway of adult rats: differential actions of estrogen in males and females. *Neuroscience* **116:** 213-222.

Murray TK, Messenger MJ, Ward MA, Woodhouse S, Osborne DJ, Duty S*, et al.* (2002). Evaluation of the mGluR2/3 agonist LY379268 in rodent models of Parkinson's disease. *Pharmacol. Biochem. Behav.* **73**(2)**:** 455-466.

Murray TK, Whalley K, Robinson CS, Ward MA, Hicks CA, Lodge D*, et al.* (2003b). LY503430, a novel alpha-amino-3-hydroxy-5-methylisoxazole-4-propionic acid receptor potentiator with functional, neuroprotective and neurotrophic effects in rodent models of Parkinson's disease. *J. Pharmacol. Exp. Ther.* **306**(2)**:** 752-762.

Myllyla VV, Sotaniemi KA, Vuorinen JA, Heinonen EH (1993). Selegiline in de novo parkinsonian patients: the Finnish study. *Mov. Disord.* **8**(1)**:** S41-S44.

Mytilineou C, McNaught KS, Shashidharan P, Yabut J, Baptiste RJ, Parnandi A*, et al.* (2004). Inhibition of proteasome activity sensitizes dopamine neurons to protein alterations and oxidative stress. *J. Neural Transm.* **111**(10-11)**:** 1237-1251.

Naito A, Kita H (1994). The cortico-nigral projection in the rat: an anterograde tracing study with biotinylated dextran amine. *Brain Res.* **637**(1-2)**:** 317-322.

Nakajima Y, Iwakabe H, Akazawa C, Nawa H, Shigemoto R, Mizuno N*, et al.* (1993). Molecular characterization of a novel retinal metabotropic glutamate receptor mGluR6 with a high agonist selectivity for L-2-amino-4-phosphonobutyrate. *J. Biol. Chem.* **268**(16)**:** 11868-11873.

Nambu A, Takada M, Inase M, Tokuno H (1996). Dual somatotopical representations in the primate subthalamic nucleus: evidence for ordered but reversed body-map transformations from the primary motor cortex and the supplementary motor area. *J. Neurosci.* **16**(8)**:** 2671-2683.

Narendra D, Walker JE, Youle R (2012). Mitochondrial quality control mediated by PINK1 and Parkin: links to parkinsonism. *Cold Spring Harb. Perspect. Biol.* **4**(11)**:** pii: a011338.

Nash JE, Fox SH, Henry B, Hill MP, Peggs D, McGuire S*, et al.* (2000). Antiparkinsonian actions of ifenprodil in the MPTP-lesioned marmoset model of Parkinson's disease. *Exp. Neurol.* **165**(1)**:** 136-142.

Nash JE, Hill MP, Brotchie JM (1999). Antiparkinsonian actions of blockade of NR2B-containing NMDA receptors in the reserpine-treated rat. *Exp. Neurol.* **155:** 42-48.

Nash JE, Ravenscroft P, McGuire S, Crossman AR, Menniti FS, Brotchie JM (2004). The NR2B-selective NMDA receptor antagonist CP-101,606 exacerbates L-DOPA-induced dyskinesia and provides mild potentiation of anti-parkinsonian effects of L-DOPA in the MPTP-lesioned marmoset model of Parkinson's disease. *Exp. Neurol.* **188**(2)**:** 471-479.

Neuhaus JF, Baris OR, Hess S, Moser N, Schroder H, Chinta SJ*, et al.* (2014). Catecholamine metabolism drives generation of mitochondrial DNA deletions in dopaminergic neurons. *Brain* **137**(Pt 2)**:** 354-365.

Nevalainen N, Lundblad M, Gerhardt GA, Stromberg I (2013). Striatal glutamate release in L-DOPA-induced dyskinetic animals. *PLoS One* **8**(2)**:** e55706.

Neve KA, Seamans JK, Trantham-Davidson H (2004). Dopamine receptor signaling. *J. Recept. Signal Transduct. Res.* **24**(3)**:** 165-205.

Newcomer JW, Krystal JH (2001). NMDA receptor regulation of memory and behavior in humans. *Hippocampus* **11:** 529-542.

Ni Z, Gao D, Bouali-Benazzouz R, Benabid A-L, Benazzouz A (2001). Effect of microiontophoretic application of dopamine on subthalamic nucleus neuronal activity in normal rats and in rats with unilateral lesion of the nigrostriatal pathway. *Eur. J. Neurosci.* **14:** 373-3811.

Nicholas AP, Lubin FD, Hallett PJ, Vattem P, Ravenscroft P, Bezard E*, et al.* (2008). Striatal histone modifications in models of levodopa-induced dyskinesia. *J. Neurochem.* **106**(1)**:** 486-494.

Nicholson C, Rice ME (1986). The migration of substances in the neuronal microenvironment. *Ann. N. Y. Acad. Sci.* **481:** 55-71.

Nicklas WJ, Vyas I, Heikkila RE (1985). Inhibition of NADH-linked oxidation in brain mitochondria by 1-methyl-4-phenyl pyridine, a metabolite of the neurotoxin 1-methyl-4-phenyl-1,2,3,6-tetrahydropyridine. *Life Sci.* **36:** 2503-2508.

Nishi A, Kuroiwa M, Shuto T (2011). Mechanisms for the modulation of dopamine D1 receptor signaling in striatal neurons. *Front. Neuroanat.* **5:** 43.

Nishijima H, Arai A, Kimura T, Mori F, Yamada J, Migita K*, et al.* (2013). Drebrin immunoreactivity in the striatum of a rat model of levodopa-induced dyskinesia. *Neuropathology* **33**(4)**:** 391-396.

Niswender CM, Conn PJ (2010). Metabotropic glutamate receptors: physiology, pharmacology, and disease. *Annu. Rev. Pharmacol. Toxicol.* **50**(1)**:** 295-322.

Niswender CM, Johnson KA, Luo Q, Ayala JE, Kim C, Conn PJ*, et al.* (2008a). A novel assay of Gi/o-linked G protein-coupled receptor coupling to potassium channels provides new insights into the pharmacology of the group III metabotropic glutamate receptors. *Mol. Pharmacol.* **73**(4)**:** 1213-1224.

Niswender CM, Johnson KA, Weaver CD, Jones CK, Xiang Z, Luo Q*, et al.* (2008b). Discovery, characterization, and antiparkinsonian effect of novel positive allosteric modulators of metabotropic glutamate receptor 4. *Mol. Pharmacol.* **74**(5)**:** 1345-1358.

Noorian AR, Rha J, Annerino DM, Bernhard D, Taylor GM, Greene JG (2012). Alpha-synuclein transgenic mice display age-related slowing of gastrointestinal motility associated with transgene expression in the vagal system. *Neurobiol. Dis.* **48**(1)**:** 1-19.

NOVARTIS-Pharmaceuticals (2011). SYMMETREL® (amantadine hydrochloride). www.novartis.com.au/PI_PDF/sym.pdf.

Nutt JG, Gunzler SA, Kirchhoff T, Hogarth P, Weaver JL, Krams M*, et al.* (2008). Effects of a NR2B selective NMDA glutamate antagonist, CP-101,606, on dyskinesia and Parkinsonism. *Mov. Disord.* **23**(13)**:** 1860-1866.

Nyholm D, Askmark H, Gomes–Trolin C, Knutson T, Lennernas H, Nystrom C*, et al.* (2003). Optimizing levodopa pharmacokinetics: intestinal infusion versus oral sustained-release tablets. *Clin. Neuropharmacol.* **26**(3)**:** 156-163.

O'Connor RM, Cryan JF (2013). The effects of mGlu(7) receptor modulation in behavioural models sensitive to antidepressant action in two mouse strains. *Behav. Pharmacol.* **24**(2)**:** 105-113.

O'Neill MJ, Murray TK, Whalley K, Ward MA, Hicks CA, Woodhouse S*, et al.* (2004). Neurotrophic actions of the novel AMPA receptor potentiator, LY404187, in rodent models of Parkinson's disease. *Eur. J. Pharmacol.* **486**(2)**:** 163-174.

O'Neill MJ, Bogaert L, Hicks CA, Bond A, Ward MA, Ebinger G*, et al.* (2000). LY377770, a novel iGlu5 kainate receptor antagonist with neuroprotective effects in global and focal cerebral ischaemia. *Neuropharmacology* **39:** 1575-1588.

Obeso JA, Marin C, Rodriguez-Oroz C, Blesa J, Benitez-Temino B, Mena-Segovia J*, et al.* (2008). The basal ganglia in Parkinson's disease: current concepts and unexplained observations. *Ann. Neurol.* **64**(Suppl 2)**:** S30-46.

Obrenovitch TP, Urenjak J, Zilkha E, Jay TM (2000). Excitotoxicity in neurological disorders - the glutamate paradox. *Int. J. Dev. Neurosci.* **18:** 281-287.

Ochi M, Shiozaki S, Kase H (2004). Adenosine A(2A) receptor-mediated modulation of GABA and glutamate release in the output regions of the basal ganglia in a rodent model of Parkinson's disease. *Neuroscience* **127**(1)**:** 223-231.

Ogura M, Kita H (2000). Dynorphin exerts both postsynaptic and presynaptic effects in the globus pallidus of the rat. *Am. J. Physiol.* **83**(6)**:** 3366-3376.

Oh JD, Russell D, Vaughan CL, Chase TN (1998). Enhanced tyrosine phosphorylation of striatal NMDA receptor subunits: effect of dopaminergic denervation and L-DOPA administration. *Brain Res.* **813**(1)**:** 150-159.

Oh JD, Vaughan CL, Chase TN (1999). Effect of dopamine denervation and dopamine agonist administration on serine phosphorylation of striatal NMDA receptor subunits. *Brain Res.* **821:** 433-442.

Ohishi H, Akazawa C, Shigemoto R, Nakanishi S, Mizuno N (1995). Distributions of the mRNAs for L-2-amino-4-phosphonobutyrate-sensitive metabotropic glutamate receptors, mGluR4 and mGluR7, in the rat brain. *J. Comp. Neurol.* **360:** 555-570.

Ohishi H, Shigemoto R, Nakanishi S, Mizuno N (1993a). Distribution of the messenger RNA for a metabotropic glutamate receptor, mGluR2, in the central nervous system of the rat. *Neuroscience* **53**(4)**:** 1009-1018.

Ohishi H, Shigemoto R, Nakanishi S, Mizuno N (1993b). Distribution of the mRNA for a metabotropic glutamate receptor (mGluR3) in the rat brain: an in situ hybridization study. *J. Comp. Neurol.* **335:** 252-266.

Olanow CW, Perl DP, DeMartino GN, McNaught KSP (2004). Lewy-body formation is an aggresome-related process: a hypothesis. *Lancet Neurol.* **3**(8)**:** 496-503.

Oldham WM, Hamm HE (2008). Heterotrimeric G protein activation by G-protein-coupled receptors. *Nat. Rev. Mol. Cell Biol.* **9**(1)**:** 60-71.

Oliveri RL, Annesi G, Zappia M, Civitelli D, Montesanti R, Branca D*, et al.* (1999). Dopamine D2 receptor gene polymorphism and the risk of levodopa-induced dyskinesias in PD. *Neurology* **53**(7)**:** 1425-1430.

Olsson M, Nikkhah G, Bentlage C, Bjorklund A (1995). Forelimb akinesia in the rat Parkinson model: differential effects of dopamine agonists and nigral transplants as assessed by a new stepping test. *J. Neurosci.* **15**(5 Pt 2)**:** 3863-3875.

Omura S, Fujimoto T, Otoguro K, Matsuzaki K, Moriguchi R, Tanaka H*, et al.* (1991). Lactacystin, a novel microbial metabolite, induces neuritogenesis of neuroblastoma cells. *J. Antibiot.* **44**(1)**:** 113-116.

Orieux G, Francois C, Féger J, Hirsch EC (2002). Consequences of dopaminergic denervation on the metabolic activity of the cortical neurons projecting to the subthalamic nucleus in the rat. *J. Neurosci.* **22**(19)**:** 8762-8770.

Ossola B, Schendzielorz N, Chen SH, Bird GS, Tuominen RK, Mannisto PT*, et al.* (2011). Amantadine protects dopamine neurons by a dual action: reducing activation of microglia and inducing expression of GDNF in astroglia [corrected]. *Neuropharmacology* **61**(4)**:** 574-582.

Ossowska K, Konieczny J, Wardas J, Pietraszek M, Kuter K, Wolfarth S*, et al.* (2007). An influence of ligands of metabotropic glutamate receptor subtypes on parkinsonian-like symptoms and the striatopallidal pathway in rats. *Amino Acids* **32**(2)**:** 179-188.

Ossowska K, Konieczny J, Wolfarth S, Wieronska J, Pilc A (2001). Blockade of the metabotropic glutamate receptor subtype 5 (mGluR5) produces antiparkinsonian-like effects in rats. *Neuropharmacology* **41**(4)**:** 413-420.

Østergaard K, Sunde NA (2006). Evolution of Parkinson's disease during 4 years of bilateral deep brain stimulation of the subthalamic nucleus. *Mov. Disord.* **21**(5)**:** 624-631.

Ostock CY, Dupre KB, Jaunarajs KL, Walters H, George J, Krolewski D*, et al.* (2011). Role of the primary motor cortex in L-DOPA-induced dyskinesia and its modulation by 5-HT1A receptor stimulation. *Neuropharmacology* **61**(4)**:** 753-760.

Ouattara B, Gregoire L, Morissette M, Gasparini F, Vranesic I, Bilbe G*, et al.* (2011). Metabotropic glutamate receptor type 5 in levodopa-induced motor complications. *Neurobiol. Aging* **32**(7)**:** 1286-1295.

Ouattara B, Hoyer D, Gregoire L, Morissette M, Gasparini F, Gomez-Mancilla B*, et al.* (2010). Changes of AMPA receptors in MPTP monkeys with levodopa-induced dyskinesias. *Neuroscience* **167**(4)**:** 1160-1167.

Paillé V, Henry V, Lescaudron L, Brachet P, Damier P (2007). Rat model of Parkinson's disease with bilateral motor abnormalities, reversible with levodopa, and dyskinesias. *Mov. Disord.* **22**(4)**:** 533-539.

Pakhotin P, Bracci E (2007). Cholinergic interneurons control the excitatory input to the striatum. *J. Neurosci.* **27**(2)**:** 391-400.

Paladini CA, Celada P, Tepper JM (1999). Striatal, pallidal, and pars reticulata evoked inhibition of nigrostriatal dopaminergic neurons is mediated by $GABA_A$ receptors *in vivo*. *Neuroscience* **89**(3)**:** 799-812.

Palucha-Poniewiera A, Pilc A (2013). A selective mGlu7 receptor antagonist MMPIP reversed antidepressant-like effects of AMN082 in rats. *Behav. Brain Res.* **238:** 109-112.

Palucha A, Klak K, Branski P, van der Putten H, Flor PJ, Pilc A (2007). Activation of the mGlu7 receptor elicits antidepressant-like effects in mice. *Psychopharmacology (Berl).* **194**(4)**:** 555-562.

Pan HS, Walters JR (1988). Unilateral lesion of the nigrostriatal pathway decreases the firing rate and alters the firing pattern of globus pallidus neurons in the rat. *Synapse* **2:** 650-656.

Papa SM, Boldry RC, Engber TM, Kask AM, Chase TN (1995). Reversal of levodopa-induced motor fluctuations in experimental parkinsonism by NMDA receptor blockade. *Brain Res.* **701**(1-2)**:** 13-18.

Papa SM, Chase TN (1996). Levodopa-induced dyskinesias improved by a glutamate antgonist in Parkinsonian monkeys. *Ann. Neurol.* **39:** 574-578.

Papathanou M, van der Laan R, Jenner P, Rose S, McCreary AC (2012). Levodopa infusion does not decrease the onset of abnormal involuntary movements in Parkinsonian rats. *Mov. Disord.* **28**(8)**:** 1072-1079.

Paquette MA, Anderson AM, Lewis JR, Meshul CK, Johnson SW, Paul Berger S (2010). MK-801 inhibits L-DOPA-induced abnormal involuntary movements only at doses that worsen parkinsonism. *Neuropharmacology* **58**(7)**:** 1002-1008.

Paquette MA, Martinez AA, Macheda T, Meshul CK, Johnson SW, Berger SP*, et al.* (2012). Anti-dyskinetic mechanisms of amantadine and dextromethorphan in the 6-OHDA rat model of Parkinson's disease: role of NMDA vs. 5-HT1A receptors. *Eur. J. Neurosci.* **36**(9)**:** 3224-3234.

Parent A, Hazrati L-N (1995a). Functional anatomy of the basal ganglia I. The cortico-basal ganglia-thalamo-corticalloop. *Brain Res. Rev.* **20:** 91-127.

Parent A, Hazrati L-N (1995b). Functional anatomy of the basal ganglia. II. The place of subthalamic nucleus and external pallidum in basal ganglia circuitry. *Brain Res. Rev.* **20:** 128-154.

Parent A, Parent M, Charara A (1999). Glutamatergic inputs to midbrain dopaminergic neurons in primates. *Parkinsonism Relat. Disord.* **5**(4)**:** 193-201.

Parker WD, Boyson SJ, Parks JK (1989). Abnormalities of the electron transport chain in idiopathic Parkinson's disease. *Ann. Neurol.* **26:** 719-723.

Parkinson J (2002 (orig. 1817)). Neuropsychiatry classics: An essay on the shaking palsy. *J. Neuropsychiatry Clin. Neurosci.* **14**(2)**:** 223-236; discussion 222.

ParkinsonStudyGroup (2002). Dopamine transporter brain imaging to assess the effects of pramipexole vs levodopa on Parkinson disease progression. *JAMA* **287**(13)**:** 1653-1661.

Parkkinen L, O'Sullivan SS, Kuoppamäki M, Collins C, Kallis C, Holton JL*, et al.* (2011). Does levodopa accelerate the pathologic process in Parkinson disease brain? *Neurology* **77**(15)**:** 1420-1426.

Parsons CG, Panchenko VA, Pinchenko V, Tsyndrenko AY, Krishtal A (1996). Comparative patch-clamp studies with freshly dissociated rat hippocampal and striatal neurons on the NMDA receptor antagonistic effects of amantadine and memantine. *Eur. J. Neurosci.* **8:** 446-454.

Paxinos G, Watson C (1998). *The Rat Brain in Stereotaxic Coordinates*. Fourth edition edn. Academic Press.

Peace RKB, Banerji T, Jenner P, Marsden CD (1998). De novo administration of ropinirole and bromocriptine induces less dyskinesia than L-Dopa in the MPTP-treated marmoset. *Mov. Disord.* **13**(2)**:** 234-241.

Pearce RKB, Jackson M, Smith L, Jenner P, Marsden CD (1995). Chronic L-DOPA administration induces dyskinesias in the 1-methyl-4-phenyl-1,2,3,6-tetrahydropyridine-treated common marmoset (Callithrix jacchus). *Mov. Disord.* **10**(6)**:** 731-740.

Pearce RKB, Owen A, Daniel S, Jenner P, Marsden CD (1997). Alterations in the distribution of glutathione in the substantia nigra in Parkinson's disease. *J. Neural Transm.* **104:** 661-677.

Péchevis M, Clarke CE, Vieregge P, Khoshnood B, Deschaseaux-Voinet C, Berdeaux G*, et al.* (2005). Effects of dyskinesias in Parkinson's disease on quality of life and health-related costs: a prospective European study. *Eur. J. Neurol.* **12:** 956-963.

Pei W, Huang Z, Wang C, Han Y, Park JS, Niu L (2009). Flip and flop: a molecular determinant for AMPA receptor channel opening. *Biochemistry (Mosc).* **48**(17)**:** 3767-3777.

Pelkey KA, Yuan X, Lavezzari G, Roche KW, McBain CJ (2007). mGluR7 undergoes rapid internalization in response to activation by the allosteric agonist AMN082. *Neuropharmacology* **52**(1)**:** 108-117.

Perreault ML, Hasbi A, O'Dowd BF, George SR (2011). The dopamine d1-d2 receptor heteromer in striatal medium spiny neurons: evidence for a third distinct neuronal pathway in Basal Ganglia. *Front. Neuroanat.* **5:** 31.

Petralia RS, Wang Y-X, Niedzielski AS, Wenthold RJ (1996). The metabotropic glutamate receptors, MGLUR2 and MGLUR3, show unique postsynaptic, presynaptic and glial localizations. *Neuroscience* **71**(4)**:** 949-976.

Piallat B, Benazzouz A, Benabid AL (1996). Subthalamic nucleus lesion in rats prevents dopaminergic nigral neuron degeneration after striatal 6-OHDA injection: behavioural and immunohistochemical studies. *Eur. J. Neurosci.* **8:** 1408-1414.

Picconi B, Centonze D, Hakansson K, Bernardi G, Greengard P, Fisone G*, et al.* (2003). Loss of bidirectional striatal synaptic plasticity in L-DOPA-induced dyskinesia. *Nat. Neurosci.* **6**(5)**:** 501-506.

Picconi B, Pisani A, Centonze D, Battaglia G, Storto M, Nicoletti F*, et al.* (2002). Striatal metabotropic glutamate receptor function following experimental parkinsonism and chronic levodopa treatment. *Brain* **125**(Pt 12)**:** 2635-2645.

Pinter MM, Birk M, Helscher RJ, Binder H (1999). Short-term effect of amantadine sulphate on motor performance and reaction time in patients with idiopathic Parkinson's disease. *J. Neural Transm.* **106**(7-8)**:** 711-724.

Pisani A, Calabresi P, Centonze D, Bernardi G (1997). Activation of group III metabotropic glutamate receptors depresses glutamatergic transmission at corticostriatal synapse. *Neuropharmacology* **36**(6)**:** 845-851.

Plowey ED, Johnson JW, Steer E, Zhu W, Eisenberg DA, Valentino NM*, et al.* (2014). Mutant LRRK2 enhances glutamatergic synapse activity and evokes excitotoxic dendrite degeneration. *Biochim. Biophys. Acta* **1842**(9)**:** 1596-1603.

Politis M, Wu K, Loane C, Brooks DJ, Kiferle L, Turkheimer FE*, et al.* (2014). Serotonergic mechanisms responsible for levodopa-induced dyskinesias in Parkinson's disease patients. *J. Clin. Invest.* **124**(3)**:** 1340-1349.

Prediger RD, Matheus FC, Schwarzbold ML, Lima MM, Vital MA (2012). Anxiety in Parkinson's disease: a critical review of experimental and clinical studies. *Neuropharmacology* **62**(1)**:** 115-124.

Priyadarshi A, Khuder SA, Schaub EA, Priyadarshi SS (2001). Environmental risk factors and Parkinson's disease: a metaanalysis. *Environ. Res.* **86**(2)**:** 122-127.

Prut L, Belzung C (2003). The open field as a paradigm to measure the effects of drugs on anxiety-like behaviors: a review. *Eur. J. Pharmacol.* **463**(1-3)**:** 3-33.

Przedborski S, Levivier M, Jiang H, Ferreira M, Jackson-Lewis V, Donaldson D*, et al.* (1995). Dose-dependent lesions of the dopaminergic nigrostriatal pathway induced by intrastriatal injectionof 6-hydroxydopamine. *Neuroscience* **67**(3)**:** 631-647.

Quik M, Wonnacott S (2011). a6b2* and a4b2* nicotinic acetylcholine receptors as drug targets for Parkinson's disease. *Pharmacol. Rev.* **63**(4)**:** 938-966.

Quintana A, Sgambato-Faure V, Savasta M (2012). Effects of L-DOPA and STN-HFS dyskinesiogenic treatments on NR2B regulation in basal ganglia in the rat model of Parkinson's disease. *Neurobiol. Dis.* **48**(3)**:** 379-390.

Rabey JM, Burns RS (2008). Neurochemistry. In: Factor SA, Weiner WJ (ed)^(eds). *Parkinson's disease: diagnosis and clinical management*, 2 edn: Demos Medical Publishing. p^pp.

Rajput AH (2001). Levodopa prolongs life expectancy and is non-toxic to substantia nigra. *Parkinsonism Relat. Disord.* **8:** 95-100.

Rascol O (2000). Medical treatment of levodopa-induced dyskinesias. *Ann. Neurol.* **47**(4 Suppl 1)**:** S179-S188.

Rascol O, Barone P, Behari M, Emre M, Giladi N, Olanow CW*, et al.* (2012). Perampanel in Parkinson disease fluctuations: a double-blind randomized trial with placebo and Entacapone. *Clin. Neuropharmacol.* **35**(1)**:** 15-20.

Rascol O, Brooks DJ, Korczyn AD, Deyn PDd, Clarke CE, Lang AE (2000). A five-year study of the incidence of dyskinesia in patients with early Parkinson's disease who were treated with Ropinirole of Levodopa. *New Engl. J. Med.* **342:** 1484-1491.

Rasola A, Bernardi P (2011). Mitochondrial permeability transition in Ca(2+)-dependent apoptosis and necrosis. *Cell Calcium* **50**(3)**:** 222-233.

Ray NJ, Jenkinson N, Wang S, Holland P, Brittain JS, Joint C*, et al.* (2008). Local field potential beta activity in the subthalamic nucleus of patients with Parkinson's disease is associated with improvements in bradykinesia after dopamine and deep brain stimulation. *Exp. Neurol.* **213:** 108-113.

Raz A, Vaadia E, Bergman H (2000). Firing patterns and correlations of pontaneous discharge of pallidal neurons in the normal and the tremulous 1-methyl-4-phenyl-1,2,3,6-tetrahydropyridine vervet model of parkinsonism. *J. Neurosci.* **20**(22)**:** 8559-8571.

Reichel A (2006). The role of blood-brain barrier studies in the pharmaceutical industry. *Curr. Drug Metab.* **7:** 183-203.

Reinheckel T, Sitte N, Ullrich O, Kuckelkorn U, Davies KJA, Grune T (1998). Comparative resistance of the 20S and 26S proteasome to oxidative stress. *Biochem. J.* **335:** 637-642.

Remple MS, Bradenham CH, Kao CC, Charles PD, Neimat JS, Konrad PE (2011). Subthalamic nucleus neuronal firing rate increases with Parkinson's disease progression. *Mov. Disord.* **26**(9)**:** 1657-1662.

Ren W, Palazzo E, Maione S, Neugebauer V (2011). Differential effects of mGluR7 and mGluR8 activation on pain-related synaptic activity in the amygdala. *Neuropharmacology* **61**(8)**:** 1334-1344.

Riahi G, Morissette M, Levesque D, Rouillard C, Samadi P, Parent M*, et al.* (2012). Effect of chronic l-DOPA treatment on 5-HT(1A) receptors in parkinsonian monkey brain. *Neurochem. Int.* **61**(7)**:** 1160-1171.

Riahi G, Morissette M, Samadi P, Parent M, Di Paolo T (2013). Basal ganglia serotonin 1B receptors in parkinsonian monkeys with L-DOPA- induced dyskinesia. *Biochem. Pharmacol.* **86**(7)**:** 970-978.

Rideout HJ, Lang-Rollin IC, Savalle M, Stefanis L (2005). Dopaminergic neurons in rat ventral midbrain cultures undergo selective apoptosis and form inclusions, but do not up-regulate iHSP70, following proteasomal inhibition. *J. Neurochem.* **93**(5)**:** 1304-1313.

Rideout HJ, Larsen KE, Sulzer D, Stefanis L (2001). Proteasomal inhibition leads to formation of ubiquitin/alpha-synuclein-immunoreactive inclusions in PC12 cells. *J. Neurochem.* **78**(4)**:** 899-908.

Rieck M, Schumacher-Schuh AF, Altmann V, Francisconi CL, Fagundes PT, Monte TL*, et al.* (2012). DRD2 haplotype is associated with dyskinesia induced by levodopa therapy in Parkinson's disease patients. *Pharmacogenomics* **13**(15)**:** 1701-1710.

Riederer P, Sofic E, Rausch W-D, Schmidt B, Reynolds GP, Jellinger K*, et al.* (1989). Transition metals, ferritin, glutathione, and ascorbic acid in Parkinsonian brains. *J. Neurochem.* **52:** 515-520.

Riederer P, Wuketich S (1976). Time course of nigrostriatal degeneration in Parkinson's disease. *J. Neural Transm.* **38:** 277-301.

Riquelme E, Abarca J, Campusano JM, Bustos G (2012). An NR2B-dependent decrease in the expression of trkB receptors precedes the disappearance of dopaminergic cells in substantia nigra in a rat model of presymptomatic Parkinson's disease. *Parkinsons Dis.* **2012:** 129605.

Robbins MJ, Starr KR, Honey A, Soffin EM, Rourke C, Jones GA*, et al.* (2007). Evaluation of the mGlu8 receptor as a putative therapeutic target in schizophrenia. *Brain Res.* **1152:** 215-227.

Robelet S, Melon C, Guillet B, Salin P, Kerkerian-Le Goff L (2004). Chronic L-DOPA treatment increases extracellular glutamate levels and GLT1 expression in the basal ganglia in a rat model of Parkinson's disease. *Eur. J. Neurosci.* **20**(5)**:** 1255-1266.

Robertson RG, Clarke CA, Boyce S, Sambrook MA, Crossman AR (1990). The role of striatopallidal neurones utilizing gamma-aminobutyric acid in the pathophysiology of MPTP-induced parkinsonism in the primate: evidence from [3H]flunitrazepam autoradiography. *Brain Res.* **531**(1-2)**:** 95-104.

Robinson TE, Noordhoorn M, Chan EM, Mocsary Z, Camp DM, Whishaw IQ (1994). Relationship between asymmetries in striatal dopamine release and the direction of amphetamine-induced rotation during the first week following a unilateral 6-OHDA lesion of the substantia nigra. *Synapse* **17**(1)**:** 16-25.

Rodriguez-Oroz MC, Moro E, Krack P (2012). Long-term outcomes of surgical therapies for Parkinson's disease. *Mov. Disord.* **27**(14)**:** 1718-1728.

Roedter A, Winkler C, Samii M, Walter GF, Brandis A, Nikkhah G (2001). Comparison of unilateral and bilateral intrastriatal 6-hydroxydopamine-induced axon terminal lesions: evidence for interhemispheric functional coupling of the two nigrostriatal pathways. *J. Comp. Neurol.* **432:** 217-229.

Romano C, Yang WL, O'Malley KL (1996). Metabotropic glutamate receptor 5 is a disulfide-linked dimer. *J. Biol. Chem.* **271**(45)**:** 28612-28616.

Rose S, Jackson MJ, Smith LA, Stockwell K, Johnson L, Carminati P*, et al.* (2006). The novel adenosine A2a receptor antagonist ST1535 potentiates the effects of a threshold dose of L-DOPA in MPTP treated common marmosets. *Eur. J. Pharmacol.* **546**(1-3)**:** 82-87.

Rosenmund C, Stern-Bach Y, Stevens CF (1998). The tetrameric structure of a glutamate receptor channel. *Science* **280**(5369)**:** 1596-1599.

Rozas G, Guerra MJ, Labandeira-Garcia JL (1997). An automated rotarod method for quantitative drug-free evaluation of overall motor deficits in rat models of parkinsonism. *Brain Res. Protoc.* **2:** 75-84.

Rutherford EC, Pomerleau F, Huettl P, Strömberg I, Gerhardt GA (2007). Chronic second-by-second measures of L-glutamate in the central nervous system of freely moving rats. *J. Neurochem.* **102**(3)**:** 712-722.

Rybicki BA, Johnson CC, Uman J, Gorell JM (1993). Parkinson's disease mortality and the industrial use of heavy metals in Michigan. *Mov. Disord.* **8**(1)**:** 87-92.

Rylander D, Iderberg H, Li Q, Dekundy A, Zhang J, Li H*, et al.* (2010a). A mGluR5 antagonist under clinical development improves L-DOPA-induced dyskinesia in parkinsonian rats and monkeys. *Neurobiol. Dis.* **39**(3)**:** 352-361.

Rylander D, Parent M, O'Sullivan SS, Dovero S, Lees AJ, Bezard E*, et al.* (2010b). Maladaptive plasticity of serotonin axon terminals in levodopa-induced dyskinesia. *Ann. Neurol.* **68**(5)**:** 619-628.

Rylander D, Recchia A, Mela F, Dekundy A, Danysz W, Cenci MA (2009). Pharmacological modulation of glutamate transmission in a rat model of L-DOPA-induced dyskinesia: effects on motor behavior and striatal nuclear signaling. *J. Pharmacol. Exp. Ther.* **330**(1)**:** 227-235.

Saggu H, Cooksey J, Dexter D, Wells FR, Lees A, Jenner P*, et al.* (1989). A selective increase in particulate superoxide dismutase activity in parkinsonian substantia nigra. *J. Neurochem.* **53:** 692-697.

Salt TE, Eaton SA (1995). Distinct presynaptic metabotropic receptors for l-AP4 and CCG1 on GABAergic terminals: Pharmacological evidence using novel α-methyl derivative mGluR antagonists, MAP4 and MCCG, in the rat thalamus in vivo. *Neuroscience* **65**(1)**:** 5-13.

Samadi P, Gregoire L, Morissette M, Calon F, Hadj Tahar A, Dridi M*, et al.* (2008). mGluR5 metabotropic glutamate receptors and dyskinesias in MPTP monkeys. *Neurobiol. Aging* **29**(7)**:** 1040-1051.

Sanberg PR (1980). Haloperidol-induced catalepsy is mediated by post-synaptic dopamine receptors. *Nature* **284:** 472-473.

Sanchez-Iglesias S, Rey P, Mendez-Alvarez E, Labandeira-Garcia JL, Soto-Otero R (2007). Time-course of brain oxidative damage caused by intrastriatal administration of 6-hydroxydopamine in a rat model of Parkinson's disease. *Neurochem. Res.* **32**(1)**:** 99-105.

Saner A, Thoenen H (1970). Model experiments on the molecular mechanism of action of 6-hydroxydopamine. *Mol. Pharmacol.* **7**(147-154).

Sanmartín-Suárez C, Soto-Otero R, Sánchez-Sellero I, Méndez-Álvarez E (2011). Antioxidant properties of dimethyl sulfoxide and its viability as a solvent in the evaluation of neuroprotective antioxidants. *J. Pharmacol. Toxicol. Methods* **63**(2)**:** 209-215.

Sano H, Chiken S, Hikida T, Kobayashi K, Nambu A (2013). Signals through the striatopallidal indirect pathway stop movements by phasic excitation in the substantia nigra. *J. Neurosci.* **33**(17)**:** 7583-7594.

Santiago M, Matarredona ER, Machado A, Cano J (1998). Influence of serotoninergic drugs on in vivo dopamine extracellular output in rat striatum. *J. Neurosci. Res.* **52:** 591-598.

Santini E, Alcacer C, Cacciatore S, Heiman M, Herve D, Greengard P*, et al.* (2009). L-DOPA activates ERK signaling and phosphorylates histone H3 in the striatonigral medium spiny neurons of hemiparkinsonian mice. *J. Neurochem.* **108**(3)**:** 621-633.

Santini E, Valjent E, Fisone G (2008). Parkinson's disease: levodopa-induced dyskinesia and signal transduction. *FEBS J.* **275**(7)**:** 1392-1399.

Sanz-Clemente A, Nicoll RA, Roche KW (2013). Diversity in NMDA receptor composition: many regulators, many consequences. *Neuroscientist* **19**(1)**:** 62-75.

Saravanan KS, Sindhu KM, Mohanakumar KP (2005). Acute intranigral infusion of rotenone in rats causes progressive biochemical lesions in the striatum similar to Parkinson's disease. *Brain Res.* **1049**(2)**:** 147-155.

Saugstad JA, Kinzie JM, Shinohara MM, Segerson TP, Westbrook GL (1997). Cloning and expression of rat metabotropic glutamate receptor 8 reveals a distinct pharmacological profile. *Mol. Pharmacol.* **51:** 119-125.

Sawada H, Oeda T, Kuno S, Nomoto M, Yamamoto K, Yamamoto M*, et al.* (2010). Amantadine for dyskinesias in Parkinson's disease: a randomized controlled trial. *PLoS One* **5**(12)**:** e15298.

Scanziani M, Salin PA, Vogt KE, Malenka RC, Nicoll RA (1997). Use-dependent increases in glutamate concentration activate presynaptic metabotropic glutamate receptors. *Nature* **385:** 630-634.

Schallert T, Fleming SM, Leasure JL, Tillerson JL, Bland ST (2000a). CNS plasticity and assessment of forelimb sensorimotor outcome in unilateral rat models of stroke, cortical ablation, parkinsonism and spinal cord injury. *Neuropharmacology* **39**(5)**:** 777-787.

Schallert T, Tillerson JL (2000b). Intervention strategies for degeneration of dopamine neurons in Parkinsonism: optimizing behavioural assessment of outcome. In: Emerich DF, Dean RL, Sanberg PR (ed)^(eds). *Central Nervous System Diseases.* , edn: Humana Press. p^pp 131-151.

Schapira AH, Cleeter MW, Muddle JR, Workman JM, Cooper JM, King RH (2006). Proteasomal inhibition causes loss of nigral tyrosine hydroxylase neurons. *Ann. Neurol.* **60**(2)**:** 253-255.

Schapira AHV, Cooper JM, Dexter D, Clark JB, Jenner P, Marsden CD (1990). Mitochondrial complex I deficiency in Parkinson's disease. *J. Neurochem.* **54:** 823-827.

Schell GR, Strick PL (1984). The origin of thalamic inputs to the arcuate premotor and supplementary motor areas. *J. Neurosci.* **4**(2)**:** 539-560.

Schmid S, Fendt M (2006). Effects of the mGluR8 agonist (S)-3,4-DCPG in the lateral amygdala on acquisition/expression of fear-potentiated startle, synaptic transmission, and plasticity. *Neuropharmacology* **50**(2)**:** 154-164.

Schmidt N, Ferger B (2001). Neurochemical findings in the MPTP model of Parkinson's disease. *J. Neural Transm.* **108:** 1263-1282.

Schrag A, Schelosky L, Scholz U, Poewe W (1999). Reduction of parkinsonian signs in patients With Parkinson's disease by dopaminergic versus anticholinergic single-dose challenges. *Mov. Disord.* **14**(2)**:** 252-255.

Schwab RS, England AC, Poskanzer DC, Young RR (1969). Amantadine in the treatment of Parkinson's disease. *JAMA* **208**(7)**:** 1168-1170.

Sedelis M, Schwarting RKW, Huston JP (2001). Behavioral phenotyping of the MPTP mouse model of Parkinson's disease. *Behav. Brain Res.* **125:** 109-122.

Sherer TB, Kim J-H, Betarbet R, Greenamyre JT (2003). Subcutaneous rotenone exposure causes highly selective dopaminergic degeneration and α-synuclein aggregation. *Exp. Neurol.* **179**(1)**:** 9-16.

Sherer TB, Richardson JR, Testa CM, Seo BB, Panov AV, Yagi T*, et al.* (2007). Mechanism of toxicity of pesticides acting at complex I: relevance to environmental etiologies of Parkinson's disease. *J. Neurochem.* **100**(6)**:** 1469-1479.

Shigemoto R, Kinoshita A, Wada E, Nomura S, Ohishi H, Takada M*, et al.* (1997). Differential presynaptic localization of metabotropic glutamate receptor subtypes in the rat hippocampus. *J. Neurosci.* **17**(19)**:** 7503-7522.

Shults CW, Oakes D, Kieburtz K, Beal MF, Haas R, Plumb S*, et al.* (2002). Effects of coenzyme Q10 in early Parkinson's disease: evidence of slowing of the functional decline. *Arch. Neurol.* **59**(10)**:** 1541-1550.

Sian J, Dexter DT, Lees AJ, Daniel S, Agid Y, Javoy-Agid F*, et al.* (1994). Alterations in glutathione levels Parkinson's disease and other neurodegenerative disorders affecting basal ganglia. *Ann. Neurol.* **36:** 348-355.

Sieradzan KA, Fox SH, Hill M, Dick JPR, Crossman AR, Brotchie JM (2001). Cannabinoids reduce levodopa-induced dyskinesia in Parkinson's disease: A pilot study. *Neurology* **57:** 2108-2111.

Silverdale MA, Kobylecki C, Hallett PJ, Li Q, Dunah AW, Ravenscroft P*, et al.* (2010). Synaptic recruitment of AMPA glutamate receptor subunits in levodopa-induced dyskinesia in the MPTP-lesioned nonhuman primate. *Synapse* **64**(2)**:** 177-180.

Simonyi A, Miller LA, Sun GY (2000). Region-specific decline in the expression of metabotropic glutamate receptor 7 mRNA in rat brain during aging. *Mol. Brain Res.* **82:** 101-106.

Sindhu KM, Saravanan KS, Mohanakumar KP (2005). Behavioral differences in a rotenone-induced hemiparkinsonian rat model developed following intranigral or median forebrain bundle infusion. *Brain Res.* **1051**(1-2)**:** 25-34.

Slawinska A, Wieronska JM, Stachowicz K, Palucha-Poniewiera A, Uberti MA, Bacolod MA*, et al.* (2013). Anxiolytic- but not antidepressant-like activity of Lu AF21934, a novel, selective positive allosteric modulator of the mGlu(4) receptor. *Neuropharmacology* **66:** 225-235.

Sleeman IJ, Boshoff EL, Duty S (2012). Fibroblast growth factor-20 protects against dopamine neuron loss in vitro and provides functional protection in the 6-hydroxydopamine-lesioned rat model of Parkinson's disease. *Neuropharmacology* **63**(7)**:** 1268-1277.

Smith AD, Olson RJ, Justice JB (1992). Quantitative microdialysis of dopamine in the striatum: effect of circadian variation. *J. Neurosci. Methods* **44**(1)**:** 33-41.

Smith ER, Hadidian Z, Mason MM (1967). The single- and repeated-dose toxiticy of dimethyl sulfoxide. *Ann. N. Y. Acad. Sci.* **141**(1)**:** 96-109.

Smith Y, Bolam JP (1989). Neurons of the substantia nigra reticulata receive a dense GABA-containing input from the globus pallidus in the rat. *Brain Res.* **493**(1)**:** 160-167.

Smith Y, Kieval JZ (2000). Anatomy of the dopamine system in the basal ganglia. *Trends Neurosci.* **23**(10 (Supp))**:** S28-S33.

Smith Y, Villalba RM, Raju DV (2009). Striatal spine plasticity in Parkinson's disease: pathological or not? *Parkinsonism Relat. Disord.* **15**(Supp 3)**:** S156-S161.

Snow BJ, Macdonald L, Mcauley D, Wallis W (2000). The effect of amantadine on levodopa-induced dyskinesias in Parkinson's disease: a double-blind, placebo-controlled study. *Clin. Neuropharmacol.* **23**(2)**:** 82-85.

Soghomonian JJ, Laprade N (1997). Glutamate decarboxylase (GAD67 and GAD65) gene expression is increased in a subpopulation of neurons in the putamen of Parkinsonian monkeys. *Synapse* **27**(2)**:** 122-132.

Soto-Otero R, Mendez-Alvarez E, Hermida-Ameijeiras A, Munoz-Patino AM, Labandeira-Garcia JL (2010). Autoxidation and neurotoxicity of 6-hydroxydopamine in the presence of some antioxidants: potential implication in relation to the pathogenesis of Parkinson's disease. *J. Neurochem.* **74:** 1605-1612.

Spatola M, Wider C (2014). Genetics of Parkinson's disease: the yield. *Parkinsonism Relat. Disord.* **20:** S35-S38.

Spillantini MG, Schmidt ML, Lee VM-Y, Trojanowski JQ, Jakes R, Goedert M (1997). a-Synuclein in Lewy bodies. *Nature* **388:** 839-840.

Staal RG, Hogan KA, Liang CL, German DC, Sonsalla PK (2000). In vitro studies of striatal vesicles containing the vesicular monoamine transporter (VMAT2): rat versus mouse differences in sequestration of 1-methyl-4-phenylpyridinium. *J. Pharmacol. Exp. Ther.* **293**(2)**:** 329-335.

Stamford JA (1990). Fast cyclic voltammetry: measuring transmitter release in 'real time'. *J. Neurosci. Methods* **34**(1-3)**:** 67-72.

Stanford IM, Lacey MG (1996). Differential actions of serotonin, mediated by 5-HT_{1B} and 5-HT_{2C} receptors, on GABA-mediated synaptic input to rat substantia nigra pars reticulata neurons *in vitro*. *J. Neurosci.* **16**(23)**:** 7566-7573.

Stark DT, Bazan NG (2011). Synaptic and extrasynaptic NMDA receptors differentially modulate neuronal cyclooxygenase-2 function, lipid peroxidation, and neuroprotection. *J. Neurosci.* **31**(39)**:** 13710-13721.

Steece-Collier K, Chambers LK, Jaw-Tsai SS, Menniti FS, Greenamyre JT (2000). Antiparkinsonian actions of CP-101,606, an antagonist of NR2B subunit-containing N-methyl-d-aspartate receptors. *Exp. Neurol.* **163**(1)**:** 239-243.

Stefani A, Fedele E, Galati S, Pepicelli O, Frasca S, Pierantozzi M*, et al.* (2005). Subthalamic stimulation activates internal pallidus: evidence from cGMP microdialysis in PD patients. *Ann. Neurol.* **57**(3)**:** 448-452.

Stefani A, Spadoni F, Bernardi G (1999). Group III metabotropic glutamate receptor agonists modulate high voltage-activated Ca2+ currents in pyramidal neurons of the adult rat. *Exp. Brain Res.* **119**(2)**:** 237-244.

Stephens B, Mueller AJ, Shering AF, Hood SH, Taggart P, Arbuthnott GW*, et al.* (2005). Evidence of a breakdown of corticostriatal connections in Parkinson's disease. *Neuroscience* **132**(3)**:** 741-754.

Stocchi F (2009). The therapeutic concept of continuous dopaminergic stimulation (CDS) in the treatment of Parkinson's disease. *Parkinsonism Relat. Disord.* **15**(S3)**:** S68-S71.

Stocchi F, Arnold G, Onofrj M, Kwiecinski H, Szczudlik A, Thomas A*, et al.* (2004). Improvement of motor function in early Parkinson disease by safinamide. *Neurology* **63**(4)**:** 746-748.

Stocchi F, Borgohain R, Onofrj M, Schapira AHV, Bhatt M, Lucini V*, et al.* (2012). A randomized, double-blind, placebo-controlled trial of safinamide as add-on therapy in early Parkinson's disease patients. *Mov. Disord.* **27**(1)**:** 106-112.

Stocchi F, Rascol O, Destee A, Hattori N, Hauser RA, Lang AE*, et al.* (2013). AFQ056 in Parkinson patients with levodopa-induced dyskinesia: 13-week, randomized, dose-finding study. *Mov. Disord.* **28**(13)**:** 1838-1846.

Strong JA, Dalvi A, Revilla FJ, Sahay A, Samaha FJ, Welge JA*, et al.* (2006). Genotype and smoking history affect risk of levodopa-induced dyskinesias in Parkinson's disease. *Mov. Disord.* **21**(5)**:** 654-659.

Sukoff Rizzo SJ, Leonard SK, Gilbert A, Dollings P, Smith DL, Zhang MY*, et al.* (2011). The metabotropic glutamate receptor 7 allosteric modulator AMN082: a monoaminergic agent in disguise? *J. Pharmacol. Exp. Ther.* **388**(1)**:** 345-352.

Summa M, Di Prisco S, Grilli M, Usai C, Marchi M, Pittaluga A (2013). Presynaptic mGlu7 receptors control GABA release in mouse hippocampus. *Neuropharmacology* **66:** 215-224.

Summerfield SG, Read K, Begley DJ, Obradovic T, Hidalgo IJ, Coggon S*, et al.* (2007). Central nervous system drug disposition: the relationship between in situ brain permeability and brain free fraction. *J. Pharmacol. Exp. Ther.* **322**(1)**:** 205-213.

Sun W, Sugiyama K, Asakawa T, Ito-Yamashita T, Namba H (2013). Behavioral performance at early (4 weeks) and later (6 months) stages in rats with unilateral medial forebrain bundle and striatal 6-hydroxydopamine lesions. *Neurol. Med. Chir. (Tokyo).* **53:** 7-11.

Surmeier DJ, Ding J, Day M, Wang Z, Shen W (2007). D1 and D2 dopamine-receptor modulation of striatal glutamatergic signaling in striatal medium spiny neurons. *Trends Neurosci.* **30**(5)**:** 228-235.

Surmeier DJ, Guzman JN, Sanchez J, Schumacker PT (2012). Physiological phenotype and vulnerability in Parkinson's disease. *Cold Spring Harb. Perspect. Med.* **2**(7)**:** a009290.

Suzuki G, Tsukamoto N, Fushiki H, Kawagishi A, Nakamura M, Kurihara H*, et al.* (2007). *In vitro* pharmacological characterization of novel isoxazolopyridone derivatives as allosteric metabotropic glutamate receptor 7 antagonists. *J. Pharmacol. Exp. Ther.* **323**(1)**:** 147-156.

Swerdlow RH, Parks JK, Miller SW, Tuttle JB, Trimmer PA, Sheehan JP*, et al.* (1996). Origin and functional consequences of the complex I defect in Parkinson's disease. *Ann. Neurol.* **40:** 663-671.

Szydlowska K, Kaminska B, Baude A, Parsons CG, Danysz W (2007). Neuroprotective activity of selective mGlu1 and mGlu5 antagonists in vitro and in vivo. *Eur. J. Pharmacol.* **554**(1)**:** 18-29.

Tachibana Y, Iwamuro H, Kita H, Takada M, Nambu A (2011). Subthalamo-pallidal interactions underlying parkinsonian neuronal oscillations in the primate basal ganglia. *Eur. J. Neurosci.* **34**(9)**:** 1470-1484.

Tai C-H, Pan M-K, Lin JJ, Huang C-S, Yang Y-C, Kuo C-C (2012). Subthalamic discharges as a causal determinant of parkinsonian motor deficits. *Ann. Neurol.* **72**(3)**:** 464-476.

Tanabe Y, Nomura A, Maw M, Shigemoto R, Mizuno N, Nakanishi S (1993). Signal transduction, pharmacological properties, and expression patterns of two rat metabotropic glutamate receptors, mGluR3 and mGluR4. *J. Neurosci.* **13**(4)**:** 1372-1378.

Tanaka C, Nishizuka Y (1994). The protein kinase C family for neuronal signaling. *Annu. Rev. Neurosci.* **17:** 551-567.

Tanaka H, Kannari K, Maeda T, Tomiyama M, Suda T, Matsunaga M (1999). Role of serotonergic neurons in L-DOPA derived extracellular dopamine in the striatum of 6-OHDA-lesioned rats. *Neuroreport* **10:** 631-634.

Tang F-M, Sun Y-F, Wang R, Ding Y-M, Zhang G-Y, Jin G-Z (2000). Dopamine-glutamate interaction in rat striatal slices: changes of CCDPK II, PKA and LDH activity by receptor-mediated mechanisms. *Acta Pharmacol. Sin.* **21**(2)**:** 145-150.

Tang FR, Lee WL (2001). Expression of the group II and III metabotropic glutamate receptors in the hippocampus of patients with mesial temporal lobe epilepsy. *J. Neurocytol.* **30**(2)**:** 137-143.

Tatarczyñska E, Palucha A, Szewczyk B, Chojnacka-Wójcik E, Wieroñska J, Pilc A (2002). Anxiolytic and antidepressant-like effects of group III metabotropic glutamate agonist (1S,3R,4S)-1-aminocyclopentane-1,3,4-tricarboxylic acid (ACPT-I) in rats. *Pol. J. Pharmacol.* **54:** 707-710.

Tatton NA, Kish SJ (1997). In situ detection of apoptotic nuclei in the substantia nigra compacta of 1-methyl-4-phenyl-1,2,3,6-tetrahydropyridine-treated mice using terminal deoxynucleotidyl transferase labelling and acridine orange staining. *Neuroscience* **77**(4)**:** 1037-1048.

Taylor DL, Diemel LT, Pocock JM (2003). Activation of microglial group III metabotropic glutamate receptors protects neurons against microglial neurotoxicity. *J. Neurosci.* **23**(6)**:** 2150-2160.

Taylor TN, Caudle WM, Shepherd KR, Noorian A, Jackson CR, Iuvone PM*, et al.* (2009). Nonmotor symptoms of Parkinson's disease revealed in an animal model with reduced monoamine storage capacity. *J. Neurosci.* **29**(25)**:** 8103-8113.

Teismann P, Tieu K, Cohen O, Choi D-K, Wu DC, Marks D*, et al.* (2003). Pathogenic role of glial cells in Parkinson's disease. *Mov. Disord.* **18**(2)**:** 121-129.

Temel Y, Visser-Vandewalle V, Kaplan S, Kozan R, Daemen MA, Blokland A*, et al.* (2006). Protection of nigral cell death by bilateral subthalamic nucleus stimulation. *Brain Res.* **1120**(1)**:** 100-105.

Tepper JM, Koos T, Wilson CJ (2004). GABAergic microcircuits in the neostriatum. *Trends Neurosci.* **27**(11)**:** 662-669.

Testa CM, Standaert DG, Young AB, Penney JB (1994). Metabotropic glutamate receptor mRNA expression in the basal ganglia of the rat. *J. Neurosci.* **14**(5)**:** 3005-3018.

Thiruchelvam M, McCormack A, Richfield EK, Baggs RB, Tank AW, Di Monte DA*, et al.* (2003). Age-related irreversible progressive nigrostriatal dopaminergic neurotoxicity in the paraquat and maneb model of the Parkinson's disease phenotype. *Eur. J. Neurosci.* **18**(3)**:** 589-600.

Thomas A, Iacono D, Luciano AL, Armellino K, Iorio AD, Onofrj M (2004). Duration of amantadine benefit on dyskinesia of severe Parkinson's disease. *J. Neurol. Neurosurg. Psychiatry* **75:** 141-143.

Thomas J, Wang J, Takubo H, Sheng J, Jesus Sd, Bankiewicz KS (1994). A 6-hydroxydopamine-induced hemiparkinsonian rat model: further biochemical and behavioral characterisation. *Exp. Neurol.* **126:** 159-167.

Tian Y, Lei T, Yang Z, Zhang T (2012). Urethane suppresses hippocampal CA1 neuron excitability via changes in presynaptic glutamate release and in potassium channel activity. *Brain Res. Bull.* **87**(4-5)**:** 420-426.

Tian Y, Liu Y, Chen X, Kang Q, Zhang J, Shi Q*, et al.* (2010). AMN082 promotes the proliferation and differentiation of neural progenitor cells with influence on phosphorylation of MAPK signaling pathways. *Neurochem. Int.* **57**(1)**:** 8-15.

Tichelaar W, Safferling M, Keinänen K, Stark H, Madden DR (2004). The three-dimensional structure of an ionotropic glutamate receptor reveals a dimer-of-dimers assembly. *J. Mol. Biol.* **344**(2)**:** 435-442.

Tong Q, Kirchgessner AL (2003). Localization and function of metabotropic glutamate receptor 8 in the enteric nervous system. *Am. J. Physio. Gastrointest. Liver Physiol.* **285**(5)**:** G992-G1003.

Tong Y, Pisani A, Martella G, Karouani M, Yamaguchi H, Pothos EN*, et al.* (2009). R1441C mutation in LRRK2 impairs dopaminergic neurotransmission in mice. *Proc. Natl. Acad. Sci. U. S. A.* **106**(34)**:** 14622-14627.

Trombley PQ, Westbrook GL (1992). L-AP4 inhibits calcium currents and synaptic transmission via a G-protein-coupled glutamate receptor. *J. Neurosci.* **12**(6)**:** 2043-2050.

Truong L, Allbutt H, Kassiou M, Henderson JM (2006). Developing a preclinical model of Parkinson's disease: a study of behaviour in rats with graded 6-OHDA lesions. *Behav. Brain Res.* **169**(1)**:** 1-9.

Tseng KY, Kargieman L, Gacio S, Riquelme LA, Murer MG (2005). Consequences of partial and severe dopaminergic lesion on basal ganglia oscillatory activity and akinesia. *Eur. J. Neurosci.* **22**(10)**:** 2579-2586.

Turner JP, Salt TE (1999). Group III metabotropic glutamate receptors control corticothalamic synaptic transmission in the rat thalamus in vitro. *J. Physiol.* **519:** 481-491.

Turski L, Bressler K, Rettig KJ, Loschmann PA, Wachtel H (1991). Protection of substantia nigra from MPP+ neurotoxicity by N-methyl-D-aspartate antagonists. *Nature* **349**(6308)**:** 414-418.

Twelves D, Perkins KSM, Counsell C (2003). Systematic review of incidence studies of Parkinson's disease. *Mov. Disord.* **18**(1)**:** 19-31.

Ugolini A, Large CH, Corsi M (2008). AMN082, an allosteric mGluR7 agonist that inhibits afferent glutamatergic transmission in rat basolateral amygdala. *Neuropharmacology* **55**(4)**:** 532-536.

Um JW, Park HJ, Song J, Jeon I, Lee G, Lee PH*, et al.* (2010). Formation of parkin aggregates and enhanced PINK1 accumulation during the pathogenesis of Parkinson's disease. *Biochem. Biophys. Res. Commun.* **393**(4)**:** 824-828.

Ungerstedt U (1968). 6-hydroxydopamine induced degeneration of central monoamine neurons. *Eur. J. Pharmacol.* **5:** 107-110.

Ungerstedt U (1971a). Adipsia and aphagia after 6-hydroxydopamine induced degeneration of the nigro-striatal dopamine system. *Acta Physiol. Scand.* **367:** 95-122.

Ungerstedt U (1971b). Striatal dopamine release after amphetamine or nerve degeneration revealed by rotational behaviour. *Acta Physiol. Scand. Suppl.* **367:** 49-68.

Uversky VN, Li J, Bower K, Fink AL (2002). Synergistic effects of pesticides and metals on the fibrillation of a-synuclein: implications for Parkinson's disease. *Neurotoxicology* **23:** 527-536.

Uversky VN, Li J, Fink AL (2001). Pesticides directly accelerate the rate of alpha-synuclein fibril formation: a possible factor in Parkinson's disease. *FEBS Lett.* **500**(3)**:** 105-108.

Valenti O, Mannaioni G, Seabrook GR, Conn PJ, Marino MJ (2005). Group III metabotropic glutamate-receptor-mediated modulation of excitatory transmission in rodent substantia nigra *pars compacta* dopamine neurons. *J. Pharmacol. Exp. Ther.* **313**(3)**:** 1296-1304.

Valenti O, Marino MJ, Wittmann M, Lis E, DiLella AG, Kinney GG*, et al.* (2003). Group III metabotropic glutamate receptor-mediated modulation of the striatopallidal synapse. *J. Neurosci.* **23**(18)**:** 7218-7226.

van Oosten RV, Cools AR (2002). Differential effects of a small, unilateral, 6-hydroxydopamine-induced nigral lesion on behavior in high and low responders to novelty. *Exp. Neurol.* **173**(2)**:** 245-255.

Vera G, Tapia R (2012). Activation of group III metabotropic glutamate receptors by endogenous glutamate protects against glutamate-mediated excitotoxicity in the hippocampus *in vivo*. *J. Neurosci. Res.* **90**(5)**:** 1055-1066.

Verhagen-Metman L, Dotto Pd, LePool K, Konitsiotis S, Fang J, Chase TN (1999). Amantadine for levodopa-induced dyskinesias: a one year follow-up study. *Arch. Neurol.* **56:** 1383-1386.

Verhagen-Metman L, Dotto PD, R. Natte M, Munckhof Pvd, Chase TN (1998). Dextromethorphan improves levodopa-induced dyskinesias in Parkinson's disease. *Neurology* **51:** 203-206.

Verhave PS, Jongsma MJ, Van den Berg RM, Vis JC, Vanwersch RA, Smit AB*, et al.* (2011). REM sleep behavior disorder in the marmoset MPTP model of early Parkinson disease. *Sleep* **34**(8)**:** 1119-1125.

Vernon AC, Palmer S, Datla KP, Zbarsky V, Croucher MJ, Dexter DT (2005). Neuroprotective effects of metabotropic glutamate receptor ligands in a 6-hydroxydopamine rodent model of Parkinson's disease. *Eur. J. Neurosci.* **22**(7)**:** 1799-1806.

Vernon AC, Smith EJ, Stevanato L, Modo M (2011). Selective activation of metabotropic glutamate receptor 7 induces inhibition of cellular proliferation and promotes astrocyte differentiation of ventral mesencephalon human neural stem/progenitor cells. *Neurochem. Int.* **59**(3)**:** 421-431.

Vernon AC, Zbarsky V, Datla KP, Croucher MJ, Dexter DT (2007). Subtype selective antagonism of substantia nigra pars compacta group I metabotropic glutamate receptors protects the nigrostriatal system against 6-hydroxydopamine toxicity in vivo. *J. Neurochem.* **103**(3)**:** 1075-1091.

Vernon AC, Zbarsky V, Datla KP, Dexter DT, Croucher MJ (2006). Selective activation of group III metabotropic glutamate receptors by L-(+)-2-amino-4-phosphonobutryic acid protects the nigrostriatal system against 6-hydroxydopamine toxicity *in vivo*. *J. Pharmacol. Exp. Ther.* **320**(1)**:** 397-409.

Visanji NP, Fox SH, Johnston T, Reyes G, Millan MJ, Brotchie JM (2009). Dopamine D3 receptor stimulation underlies the development of L-DOPA-induced dyskinesia in animal models of Parkinson's disease. *Neurobiol. Dis.* **35**(2)**:** 184-192.

Visser-Vandewalle V, van der Linden C, Temel Y, Celik H, Ackermans L, Spincemaille G*, et al.* (2005). Long-term effects of bilateral subthalamic nucleus stimulation in advanced Parkinson's disease: a four year follow-up study. *Parkinsonism Relat. Disord.* **11**(3)**:** 157-165.

Vlajinac H, Dzoljic E, Maksimovic J, Marinkovic J, Sipetic S, Kostic V (2013). Infections as a risk factor for Parkinson's disease: a case-control study. *Int. J. Neurosci.* **123**(5)**:** 329-332.

Voulalas PJ, Holtzclaw L, Wolstenholme J, Russell JT, Hyman SE (2005). Metabotropic glutamate receptors and dopamine receptors cooperate to enhance extracellular signal-regulated kinase phosphorylation in striatal neurons. *J. Neurosci.* **25**(15)**:** 3763-3773.

Vu TC, Nutt JG, Holford NH (2012). Progression of motor and nonmotor features of Parkinson's disease and their response to treatment. *Br. J. Clin. Pharmacol.* **74**(2)**:** 267-283.

Wachtel H, Kunow M, Löschmann PA (1992). NBQX (6-nitro-sulfamoyl-benzo-quinoxaline-dione) and CPP (3-carboxy-piperazin-propyl phosphonic acid) potentiate dopamine agonist induced rotations in substantia nigra lesioned rat. *Neurosci. Lett.* **142**(2)**:** 179-182.

Wallace BA, Ashkan K, Heise CE, Foote KD, Torres N, Mitrofanis J*, et al.* (2007). Survival of midbrain dopaminergic cells after lesion or deep brain stimulation of the subthalamic nucleus in MPTP-treated monkeys. *Brain* **130**(8)**:** 2129-2145.

Walsh RN, Cummins RA (1976). The open field test: a critical review. *Psychol. Bull.* **83:** 482-504.

Walsh S, Finn DP, Dowd E (2011). Time-course of nigrostriatal neurodegeneration and neuroinflammation in the 6-hydroxydopamine-induced axonal and terminal lesion models of Parkinson's disease in the rat. *Neuroscience* **175:** 251-261.

Walsh S, Gorman AM, Finn DP, Dowd E (2010). The effects of cannabinoid drugs on abnormal involuntary movements in dyskinetic and non-dyskinetic 6-hydroxydopamine lesioned rats. *Brain Res.* **1363:** 40-48.

Wang H, Jiang W, Yang R, Li Y (2011). Spinal metabotropic glutamate receptor 4 is involved in neuropathic pain. *Neuroreport* **22**(5)**:** 244-248.

Wang J, Jiang H, Xie J-X (2004). Time dependent effects of 6-OHDA lesions on iron level and neuronal loss in rat nigrostriatal system. *Neurochem. Res.* **29**(12)**:** 2239-2243.

Wang JQ, Arora A, Yang L, Parelkar NK, Zhang G, Liu X*, et al.* (2005). Phosphorylation of AMPA receptors: mechanisms and synaptic plasticity. *Mol. Neurobiol.* **32**(3)**:** 237-249.

Wang WY, Wang H, Luo Y, Jia LJ, Zhao JN, Zhang HH*, et al.* (2012a). The effects of metabotropic glutamate receptor 7 allosteric agonist N,N'-dibenzhydrylethane-1,2-diamine dihydrochloride on developmental sevoflurane neurotoxicity: role of extracellular signal-regulated kinase 1 and 2 mitogen-activated protein kinase signaling pathway. *Neuroscience* **205:** 167-177.

Wang X, Yan MH, Fujioka H, Liu J, Wilson-Delfosse A, Chen SG*, et al.* (2012b). LRRK2 regulates mitochondrial dynamics and function through direct interaction with DLP1. *Hum. Mol. Genet.* **21**(9)**:** 1931-1944.

Wang XF, Li S, Chou AP, Bronstein JM (2006). Inhibitory effects of pesticides on proteasome activity: implication in Parkinson's disease. *Neurobiol. Dis.* **23**(1)**:** 198-205.

Weinberger M, Mahant N, Hutchison WD, Lozano AM, Moro E, Hodaie M*, et al.* (2006). Beta oscillatory activity in the subthalamic nucleus and its relation to dopaminergic response in Parkinson's disease. *J. Neurophysiol.* **96**(6)**:** 3248-3256.

Weiner WJ, Koller WC, Perlik S, Nausieda PA, Klawans HL (1980). Drug holiday and management of Parkinson disease. *Neurology* **31**(12).

Wessell RH, Ahmed SM, Menniti FS, Dunbar GL, Chase TN, Oh JD (2004). NR2B selective NMDA receptor antagonist CP-101,606 prevents levodopa-induced motor response alterations in hemi-parkinsonian rats. *Neuropharmacology* **47**(2)**:** 184-194.

West AR, Grace AA (2002). Opposite influences of endogenous dopamine D1 and D2 receptor activation on activity states and electrophysiological properties of striatal neurons: studies combining *in vivo* intracellular recordings and reverse microdialysis. *J. Neurosci.* **22**(1)**:** 294-304.

Westerink BHC, Rea K, Oldenziel WH, Cremers TIFH (2007). Microdialysis of glutamate and GABA in the brain: analysis and interpretation. In: Westerink BHC, Cremers TIFH (ed)^(eds). *Handbook of Microdialysis: Methods, Applications and Perspectives*, 1 edn: Elsevier Academic Press. p^pp.

Westphalen RI, Hemmings HCJ (2005). Volatile anesthetic effects on glutamate versus GABA release from isolated rat cortical nerve terminals: basal release. *J. Pharmacol. Exp. Ther.* **316**(1)**:** 208-215.

Whone AL, Watts RL, Stoessl AJ, Davis M, Reske S, Nahmias C*, et al.* (2003). Slower progression of Parkinson's disease with ropinirole versus levodopa: the REAL-PET study. *Ann. Neurol.* **54:** 93-101.

Wichmann T, Bergman H, DeLong MR (1994). The primate subthalamic nucleus. III. changes in motor behavior and neuronal activity in the internal pallidum induced by subthalamic inactivation in the MPTP model of Parkinsonism. *J. Neurophysiol.* **72**(2)**:** 521-530.

Wichmann T, Dostrovsky JO (2011). Pathological basal ganglia activity in movement disorders. *Neuroscience* **198:** 232-244.

Wierońska JM, Stachowicz K, Acher F, Lech T, Pilc A (2011). Opposing efficacy of group III mGlu receptor activators, LSP1-2111 and AMN082, in animal models of positive symptoms of schizophrenia. *Psychopharmacology* **220**(3)**:** 481-494.

Wierońska JM, Stachowicz K, Pałucha-Poniewiera A, Acher F, Brański P, Pilc A (2010). Metabotropic glutamate receptor 4 novel agonist LSP1-2111 with anxiolytic, but not antidepressant-like activity, mediated by serotonergic and GABAergic systems. *Neuropharmacology* **59**(7-8)**:** 627-634.

Wigmore MA, Lacey MG (1998). Metabotropic glutamate receptors depress glutamate-mediated synaptic input to rat midbrain dopamine neurones *in vitro*. *Br. J. Pharmacol.* **123:** 667-674.

Williams C, Dexter DT (2010). Neuroprotective and behavioural effects of (S)-3,4-dicarboxyphenylglycine in the Lactacystin model of Parkinson's disease. In: *Parkinson's UK*. York UK.

Windels F, Bruet N, Poupard A, Urbain N, Chouvet G, Feuerstein C*, et al.* (2000). Effects of hugh-frequency stimulation of subthalamic nucleus on extracellular glutamate and GABA in substantia nigra and glubus pallidus in the normal rat. *Eur. J. Neurosci.* **12:** 4141-4146.

Winkler C, Kirik D, Björklund A, Cenci MA (2002). L-DOPA-induced dyskinesia in the intrastriatal 6-hydroxydopamine model of Parkinson's disease: relation to motor and cellular parameters of nigrostriatal function. *Neurobiol. Dis.* **10**(2)**:** 165-186.

Wittmann M, Marino MJ, Bradley SR, Conn PJ (2001). Activation of group III mGluRs inhibits GABAergic and glutamatergic transmission in the substantia nigra pars reticulata. *J. Neurophysiol.* **85:** 1960-1968.

Wittmann M, Marino MJ, Conn PJ (2002). Dopamine modulates the function of group II and group III metabotropic glutamate receptors in the substantia nigra pars reticulata. *J. Pharmacol. Exp. Ther.* **302**(2)**:** 433-441.

Wolf E, Seppi K, Katzenschlager R, Hochschorner G, Ransmayr G, Schwingenschuh P*, et al.* (2010). Long-term antidyskinetic efficacy of amantadine in Parkinson's disease. *Mov. Disord.* **25**(10)**:** 1357-1363.

Wright AK, Atherton JF, Norrie L, Arbuthnott GW (2004). Death of dopaminergic neurones in the rat substantia nigra can be induced by damage to globus pallidus. *Eur. J. Neurosci.* **20**(7)**:** 1737-1744.

Wu N, Song L, Yang X, Yuan W, Liu Z (2013). NMDA receptor regulation of levodopa-induced behavior and changes in striatal G protein-coupled receptor kinase 6 and beta-arrestin-1 expression in parkinsonian rats. *Clin. Interv. Aging* **8:** 347-352.

Wullner U, Standaert DG, Testa CM, Penney JB, Young AB (1997). Differential expression of kainate receptors in the basal ganglia of the developing and adult rat brain. *Brain Res.* **768:** 215-223.

Xi ZX, Baker DA, Shen H, Carson DS, Kalivas PW (2002). Group II metabotropic glutamate receptors modulate extracellular glutamate in the nucleus accumbens. *J. Pharmacol. Exp. Ther.* **300**(1)**:** 162-171.

Xiao D, Bastia E, Xu YH, Benn CL, Cha JH, Peterson TS*, et al.* (2006). Forebrain adenosine A2A receptors contribute to L-3,4-dihydroxyphenylalanine-induced dyskinesia in hemiparkinsonian mice. *J. Neurosci.* **26**(52)**:** 13548-13555.

Xiao D, Cassin JJ, Healy B, Burdett TC, Chen JF, Fredholm BB*, et al.* (2011). Deletion of adenosine A(1) or A((2)A) receptors reduces L-3,4-dihydroxyphenylalanine-induced dyskinesia in a model of Parkinson's disease. *Brain Res.* **1367:** 310-318.

Xie W, Li X, Li C, Zhu W, Jankovic J, Le W (2010). Proteasome inhibition modeling nigral neuron degeneration in Parkinson's disease. *J. Neurochem.* **115**(1)**:** 188-199.

Xiong H, Wang D, Chen L, Choo YS, Ma H, Tang C*, et al.* (2009). Parkin, PINK1, and DJ-1 form a ubiquitin E3 ligase complex promoting unfolded protein degradation. *J. Clin. Invest.* **119**(3)**:** 650-660.

Xu J, Kurup P, Zhang Y, Goebel-Goody SM, Wu PH, Hawasli AH*, et al.* (2009). Extrasynaptic NMDA receptors couple preferentially to excitotoxicity via calpain-mediated cleavage of STEP. *J. Neurosci.* **29**(29)**:** 9330-9343.

Yang X, Chen Y, Hong X, Wu N, Song L, Yuan W*, et al.* (2012a). Levodopa/benserazide microspheres reduced levodopa-induced dyskinesia by downregulating phosphorylated GluR1 expression in 6-OHDA-lesioned rats. *Drug Des. Devel. Ther.* **6:** 341-347.

Yang X, Zheng R, Cai Y, Liao M, Yuan W, Liu Z (2012b). Controlled-release levodopa methyl ester/benserazide-loaded nanoparticles ameliorate levodopa-induced dyskinesia in rats *Int. J. Nanomed.* **7:** 2077-2086.

Yao HH, Ding JH, Zhou F, Wang F, Hu LF, Sun T*, et al.* (2005). Enhancement of glutamate uptake mediates the neuroprotection exerted by activating group II or III metabotropic glutamate receptors on astrocytes. *J. Neurochem.* **92**(4)**:** 948-961.

Yin S, Noetzel MJ, Johnson KA, Zamorano R, Jalan-Sakrikar N, Gregory KJ*, et al.* (2014). Selective actions of novel allosteric modulators reveal functional heteromers of metabotropic glutamate receptors in the CNS. *J. Neurosci.* **34**(1)**:** 79-94.

Yokoyama T, Sugiyama K, Nishizawa S, Tanaka T, Yokota N, Ohta S*, et al.* (1998). Neural activity of the subthalamic nucleus in Parkinson's disease patients. *Acta Neurochir. (Wien).* **140:** 1287-1291.

Yoritaka A, Hattori N, Uchida K, Tanake M, Stadtman ER, Mizuno Y (1996). Immunohistochemical detection of 4-hydroxynonenal protein adducts in Parkinson disease. *Proc. Natl. Acad. Sci. U. S. A.* **93:** 2696-2701.

Yu T-S, Wang S-D, Liu J-C, Yin H-S (2001). Changes in the gene expression of $GABA_A$ receptor a1 and a2 subunits and metabotropic glutamate receptor 5 in the basal ganglia of the rats with unilateral 6-hydroxydopamine lesion and embryonic mesencephalic grafts. *Exp. Neurol.* **168:** 231-241.

Yuan H, Sarre S, Ebinger G, Michotte Y (2005). Histological, behavioural and neurochemical evaluation of medial forebrain bundle and striatal 6-OHDA lesions as rat models of Parkinson's disease. *J. Neurosci. Methods* **144**(1)**:** 35-45.

Zamponi GW, Currie KPM (2013). Regulation of CaV2 calcium channels by G protein coupled receptors. *Biochim. Biophys. Acta* **1828:** 1629-1643.

Zeng BY, Bukhatwa S, Hikima A, Rose S, Jenner P (2006). Reproducible nigral cell loss after systemic proteasomal inhibitor administration to rats. *Ann. Neurol.* **60**(2)**:** 248-252.

Zeng BY, Iravani MM, Jackson MJ, Rose S, Parent A, Jenner P (2010). Morphological changes in serotoninergic neurites in the striatum and globus pallidus in levodopa primed MPTP treated common marmosets with dyskinesia. *Neurobiol. Dis.* **40**(3)**:** 599-607.

Zhang G-C, Vu K, Parelkar NK, Mao L-M, Stanford IM, Fibuch EE*, et al.* (2009). Acute administration of cocaine reduces metabotropic glutamate receptor 8 protein expression in the rat striatum in vivo. *Neurosci. Lett.* **449**(3)**:** 224-227.

Zhang H, Sulzer D (2003). Glutamate spillover in the striatum depresses dopaminergic transmission by activating group I metabotropic glutamate receptors. *J. Neurosci.* **23**(33)**:** 10585-10592.

Zhang J, Perry G, Smith MA, Robertson D, Olson SJ, Graham DG*, et al.* (1999). Parkinson's disease is associated with oxidative damage to cytoplasmic DNA and RNA in substantia nigra neurons. *Am. J. Pathol.* **154**(5)**:** 1423-1429.

Zhang X, Andren PE, Greengard P, Svenningsson P (2008). Evidence for a role of the 5-HT1B receptor and its adaptor protein, p11, in L-DOPA treatment of an animal model of Parkinsonism. *Proc. Natl. Acad. Sci. U. S. A.* **105**(6)**:** 2163-2168.

Zhou F, Yao HH, Wu JY, Yang YJ, Ding JH, Zhang J*, et al.* (2006). Activation of Group II/III metabotropic glutamate receptors attenuates LPS-induced astroglial neurotoxicity via promoting glutamate uptake. *J. Neurosci. Res.* **84**(2)**:** 268-277.

Zhou H, Huang C, Tong J, Hong WC, Liu Y-J, Xia X-G (2011). Temporal expression of mutant LRRK2 in adult rats impairs dopamine reuptake. *Int. J. Biol. Sci.* **7**(6)**:** 753-761.

Zhu Z-T, Shen K-Z, Johnson SW (2002). Pharmacological identification of inward current evoked by dopamine in rat subthalamic neurons in vitro. *Neuropharmacology* **42**(6)**:** 772-781.

Zuddas A, Vaglini F, Fornai F, Fascetti F, Saginario A, Corsini GU (1992). Pharmacologic modulation of MPTP toxicity: MK 801 in prevention of dopaminergic cell death in monkeys and mice. *Ann. N. Y. Acad. Sci.* **648:** 268-271.